The Role of Complement and Complement Regulators in Peripheral Nerve and Neuromuscular Disorders

Jayne L. Chamberlain-Banoub

A thesis submitted to Cardiff University in Candidature for the Degree of Doctor of Philosophy

Department of Medical Biochemistry & Immunology,
School of Medicine,
Cardiff University,
CARDIFF
Wales

November 2005

ProQuest LLC
789 East Eisenhower Parkway
P.O. Box 1346
Ann Arbor, MI 48106-1346

Acknowledgements

First and foremost, I would like to thank my supervisors Paul and Claire for their support and guidance during this project, and especially for the faith and confidence they have shown in me. I am eternally grateful to them for making me into a scientist.

I would also like to thank Masashi Mizuno for his patience and help throughout the project, and for providing me and the lab with constant entertainment, not forgetting the infamous 'sperm dance', and our trip to Raglan abattoir. Also, a big thank you to Natalie 'the calculator' Hepburn for always being willing to help, and for being a great ally in the battle for a PhD.

Thanks also to Philippe Gasque, and his never-ending supply of antibodies, and for asking questions at EVERY lab meeting and seminar.

Also, to Mark Griffiths, for being Mark, my ally in BSU, for teaching me animal techniques, and for being totally approachable and always encouraging.

I would also like to thank Kristina Elward, in whom I have gained a lifelong friend, for providing me with friendship, kindness and support, at any hour of the day. Thanks a million matey. To Miriam also, who is a good friend, and who has shown that she is a big softie under that tough exterior.

A special thank you to Jim Neal for always encouraging me, and for his unending enthusiasm for this project. Also thanks to Anwen Williams for her incredible animal expertise and encouragement.

To Debbie, Roy, Katrina, Sally and Keith, and all the staff in BSU, I could not have done this without your help.

To Liz Harmer, for not trying to talk me out of giving up the PhD, and always being on hand to help.

To others that have contributed to this project; Paula Longhi, Emily Mathey, Ian Gray, Konrad Beck, Daniel Kirschner, Chris Linington, Neil Robertson, Ruth, Louise and Geoff at Medical Microscopy Services, Erdem Tuzun, Vanda Lennon, Angela Vincent, staff in the histology labs, UWCM, and everyone in Medical Biochemistry & Immunology.

To Eryl Liddell, without whom, I would never have had the confidence to do a PhD.

And to all the animals, who so bravely gave their lives in the pursuit of science.

Thank you to my mum, dad and Joanne, for their love and encouragement that knows no bounds.

And to Hany, for his constant love, support and encouragement, hugs, smiles and technical support, always willing to listen, and who now knows all about C6, EANs, EAMGs and Complements. I couldn't have done it without you, and wouldn't have wanted to.

This work was funded by the Medical Research Council and GlaxoSmithKline.

For Hany,

Then, Now and Always

For Mum, Dad and Sis Blis,
Diolch

For Miss Laurie Warren,
Rest in Peace

Publications

Presented in abstract form

10th Meeting on Complement in Human Disease, Heidelberg, Germany, September 2005
(Oral & Poster presentation)

Experimental autoimmune myasthenia gravis in the rat is dependent on membrane attack complex formation

British Society of Immunology, Harrogate, UK, December 2004 (Poster presentation) & Annual Postgraduate Day, Cardiff University, UK, November 2004 (Oral presentation)

Can the Rat Peripheral Nervous System take a Complement?

Abbreviations used in the thesis

ACh	acetylcholine
nAChR	acetylcholine receptor
ADCC	antibody-dependent cellular cytotoxicity
AIDP	acute inflammatory demyelinating polyneuropathy
AMAN	acute motor axonal neuropathy
AMSAN	acute motor and sensory neuropathy
AP	alternative Pathway
APC	antigen presenting cell
AT	adoptive transfer
BNB	blood nerve barrier
BPNM	bovine peripheral nerve myelin
BSA	bovine serum albumin
BSE	bovine spongiform encephalopathy
BSU	biomedical services unit
BuTx	bungarotoxin
C	Complement
C1inh	C1 inhibitor
C4bp	C4 binding protein
CAMs	cellular adhesion molecules
cDNA	complementary DNA
CFD	complement fixation diluent
CIDP	chronic inflammatory demyelinating polyneuropathy
CMT	Charcot-Marie-Tooth neuropathy
CMV	cytomegalovirus
CNPase	2',3'-cyclic nucleotide-3'-phosphohydrolase
CNS	central nervous system
CP	classical Pathway
CR	complement receptors
CRegs	complement regulators
CR1	complement receptor 1
CSF	cerebrospinal fluid
Cry	CR1-related gene Y
CTLA-4	cytotoxic T lymphocyte-associated antigen-4
CV	column volume
CVF	cobra venom factor
Cx-32	connexin 32
DAF	decay accelerating factor
DEPC	diethylpyrocarbonate
DMEM	Dulbecco's modified eagle's medium
DTT	dithiothreitol
E	erythrocytes
EA	antibody-coated erythrocytes
EAE	experimental autoimmune encephalomyelitis
EAN	experimental autoimmune neuritis
EAMG	experimental autoimmune myasthenia gravis
EBV	Epstein-Barr Virus
EC	extracellular
ECACC	European Collection of Cell Cultures
EDTA	ethylene diamine tetra-acetic acid
ELISA	enzyme-linked immunosorbent assay
EN	endoneurium
ENU	ethylnitrosourea
EPN	epineurium
fB	factor B
FCA	Freund's complete adjuvant

FCM	flow cytometry media
FCS	foetal calf serum
fD	factor D
fI	factor I
FDC	follicular dendritic cell
GBS	Guillain-Barré Syndrome
GFAP	glial fibrillary acidic protein
gpE	guinea pig erythrocytes
GPI	glycophosphatodylinositol
H&E	haematoxylin and eosin
HIV	human immunodeficiency virus
HRPO	horseradish peroxidase
IC	immune complex
ICAM	intercellular adhesion molecule
Ig	immunoglobulin
i.p.	intra-peritoneal
IPTG	isopropyl-1-thio-β-galactopyanoside
i.v.	intra-venous
LB	Luria-Bertani
LHR	long homologous repeat
LFB	luxol fast blue
LPS	lipopolysaccharide
mAb	monoclonal antibody
MAC	membrane attack complex
MACS	magnetic cell sorting
MAG	myelin-associated glycoprotein
MASP	MBL-associated serine protease
MBL	mannan-binding lectin pathway
MBP	myelin basic protein
MCP	membrane cofactor protein
MCS	multiple cloning site
MCV	motor conduction velocity
MFS	Miller-Fisher Syndrome
MG	myasthenia gravis
MHC	major histocompatibility complex
MIR	main immunogenic region
MOG	myelin oligodendrocyte glycoprotein
MMP	matrix metalloproteinases
MS	multiple sclerosis
MuSK	muscle-specific receptor protein kinase
NCV	nerve conduction velocity
NMJ	neuromuscular junction
P2	myelin protein 2
pAb	polyclonal antibody
PCR	polymerase chain reaction
p.i.	post-induction
PN	perineurium
PNM	peripheral nerve myelin
PO	myelin protein zero
PNS	peripheral nervous system
PMP22	peripheral myelin protein 22
PNH	paroxysmal nocturnal haemoglobinuria
PNR	peripheral nerve roots
PT	pertussis toxin
RCA	regulators of complement activation
rPE	recombinant phycoerythrin
rPO-EC	recombinant PO-extracellular domain

RSNH	rat sciatic nerve homogenate
RT-PCR	reverse transcription polymerase chain reaction
RyR	ryanodine receptor
s.c.	sub-cutaneous
SCR	short consensus repeat
sCR1	soluble complement receptor 1
SDS-PAGE	sodium dodecyl sulphate-polyacrylamide gel electrophoresis
SN	sciatic nerve
SSNH	sheep sciatic nerve homogenate
STP	serine, threonine, proline-rich
TAE	Tris/acetate/EDTA
TM	transmembrane
UWCM	University of Wales College of Medicine
VSV	Varicella Zoster Virus

Suppliers and Company Addresses

AbCam	Cambridge, UK
Agar Scientific	Stanstead, Essex, UK
Amersham Pharmacia Biotech	St. Alban's, UK
Amicon Bioseparations	Millipore, Watford, UK
BDH	Lutterworth, UK
Bioline	London, UK
BioRad	Hemel Hempstead, UK
Biotecx	Houston, Texas, USA
Becton Dickinson	Oxford, UK
Caltag	Botolph Claydon, UK
Charles River	Kent, UK
DAKO	Ely, Cambridge, UK
ECACC	Porton Down, UK
Fisher Scientific	Loughborough, UK
Hoefer Scientific Instruments	Newcastle-under-Lyme, UK
Invitrogen Coropration	Paisley, UK
Jackson ImmunoResearch Laboratories, Inc	Luton, UK
Kodak	Hemel Hempstead, UK
Leica Microsystems	Cambridge, UK
Molecular Probes	via Invitrogen Corporation, Paisley, UK
Miltenyi Biotech	Bisely, Surrey, UK
New England Biolabs	Hitchin, UK
Qiagen	Dorking, UK
Raymond A. Lamb	Eastbourne, UK
Serotec	Oxford, UK
Sigma Chemical Company	Poole, UK
Surgipath, Europe	Peterborough, UK
Vector Laboratories	Peterborough, UK

Summary

This thesis describes the evaluation of the role of Complement (C) and C regulators (CRegs) in experimental models of peripheral neuropathy and neuromuscular disease. Although a role for C in mediating peripheral neuropathy has previously been demonstrated in Guillain-Barré Syndrome (GBS) and its well characterised animal model Experimnetal Autoimmune Neuritis (EAN), evaluation of the role of individual components is lacking. C activation has also been widely implicated in the pathology seen in myasthenia gravis (MG) and its associated animal model Experimental Autoimmune Myasthenia Gravis (EAMG), although the precise effectors are uncertain.

Evaluation of the extent of protection conferred by CRegs in the peripheral nervous system (PNS), and the ability of the myelin-producing Schwann cell to synthesize C components was a vital first step in determining the susceptibility of the system to C attack, and for providing a method of targeting key C-related molecules for further study *in vivo*. This work demonstrated that the PNS is well protected from membrane attack complex (MAC) attack, with high expression of the terminal pathway regulator, CD59. Crry was also highly expressed, while CD55 had a limited expression, suggesting a possible alternative role for this protein. CD46 was not expressed in the PNS.

Testing the susceptibility of C and CReg deficient and knockout animals to induction of EAN and EAMG would enable further clarification of the role of individual C components to disease pathogenesis. For EAN, various antigens derived from myelin protein zero (P0) were generated to induce disease in rodents. Using this panel of antigens, specific, reproducible EAN was not achieved, and the possible reasons for this are discussed.

C activation at the neuromuscular junction (NMJ) contributes to pathology in MG, although the precise role of the MAC is unclear. EAMG was used to test the susceptibility of wildtype rats versus rats deficient in the terminal pathway component C6, to disease induction. Wildtype rats demonstrated severe weakness following induction of passively transferred EAMG, while C6 deficient rats were completely protected, demonstrated by protection against clinical disease, reduction in acetylcholine receptor (nAChR) loss, absence of inflammatory infiltrates and lack of C9 deposition. Reconstitution of human C6 to the C6 deficient rats resulted in increased disease. Soluble and fusion protein forms of CRegs, and a novel C5 inhibitor were also tested for their ability to abrogate disease in this model. Preliminary studies of EAMG induction in CReg knockout mice revealed that a lack of CD55 and CD59 markedly enhanced disease, although this remains to be confirmed.

In conclusion, this work demonstrates:

1 The potential susceptibility of the PNS to C-mediated pathology
2 The difficulties in inducing EAN in rodents using published protocols
3 That MAC is the major drive to NMJ destruction in EAMG

CRegs tested in EAMG hold promise for treatment of inflammatory disease, and analysis of the role of CRegs in EAMG in the mouse may shed new light on the precise effectors mediating disease pathogenesis.

Table of Contents

Abbreviations 6

Suppliers and Company Addresses 9

Summary 10

Chapter 1 Introduction 17

1 Introduction

1.1 Overview of the C system

1.1.1 Activation of C

1.1.1.1 The Classical Pathway 17

1.1.1.2 The Mannan-Binding Lectin Pathway 23

1.1.1.3 The Alternative Pathway 23

1.1.1.4 Central elements 24

1.1.1.5 The Terminal Pathway 24

1.1.1.6 C biosynthesis 25

1.2 Physiological Roles of C

1.2.1 Opsonisation of pathogens 26

1.2.2 Immune complex clearance 27

1.3 C Regulatory (CReg) proteins 28

1.3.1 Serpins 28

1.3.2 RCA gene cluster proteins 29

1.3.3 Fluid phase RCA regulators 29

1.3.4 Membrane-bound RCA regulators 33

1.3.5 Ly-6 superfamily CRegs 40

1.3.6 Fluid phase regulation of the terminal pathway 43

1.4 Complement and Autoimmunity 44

1.5 The Peripheral Nervous System (PNS) 45

1.5.1 The Structure of the PNS 45

1.5.2 Structure of myelin 45

1.5.3 Myelin proteins in the PNS 48

1.6 Peripheral Neuropathy 51

1.6.1 Neuropathies associated with IgM antibodies 51

1.6.2 Guillain-Barré Syndrome (GBS) 51
1.6.2.1 Spectrum of GBS phenotype 53
1.6.2.2 Pathogenesis of GBS 53
1.6.2.3 Molecular mimicry and anti-ganglioside antibodies 57

1.7 Animal models of peripheral neuropathy 57
1.7.1 Experimental Autoimmune Neuritis (EAN) 59
1.7.1.1 Disease mechanisms in EAN 59

1.8 C in Peripheral Neuropathy 63

1.8.1 GBS 63
1.8.1.1 Human studies 63
1.8.1.2 Studies in animal models 64
1.8.1.3 *In vitro* studies 65

1.9 Summary and Project Aim 66

2 Myasthenia Gravis (MG) 67
2.1 Background 67
2.2 The Action Potential 67
2.3 Acetylcholine Receptors (nAChR) 67
2.4 Clinical characteristics of MG 70
2.5 Epidemiology 72
2.6 Pathophysiology of MG 73
2.7 Animal models of MG 75
2.7.1 Experimental Autoimmune Myasthenia Gravis (EAMG) 75
2.8 C in MG 76
2.8.1 Human studies 77
2.8.2 Animal studies 78
2.8.3 *In vitro* studies 78
2.9 Summary and Project Aims 79
3 Overall Project Aims 79

Chapter 2 Characterisation of the susceptibility of the rat PNS to C attack 80

1 Introduction 80

2 Materials and Methods 82

2.1 Rat Schwann cell lines 82

2.2 Cell culture 83

2.3 Analysis of membrane-bound CReg expression on rat Schwann cell lines by single colour flow cytometry 83

2.4 Analysis of membrane-bound CReg expression by Western blotting 84

2.5 RT-PCR for detection of mRNA for membrane-bound CRegs and C components on rat Schwann cell lines 90

2.6 Immunostaining of rat Schwann cell lines, primary Schwann cell cultures and rat sciatic nerve sections 96

2.7 Discussion 110

Chapter 3 Generations of antigens for induction of EAN 114

1 Introduction 114

2 Materials and Methods 117

2.1 Synthesis of peptides derived from myelin protein zero (PO) 117

2.2 Cloning, expression, purification & refolding of the extracellular domain of human Myelin Protein Zero (PO-EC) 118

2.2.1 Cloning of cDNA for PO-EC domain into pQE9 vector 118

2.2.2 Preparative PCR 121

2.2.3 Restriction digest of pQE9-mMOG to release mMOG sequence 124

2.2.4 Generation of 'sticky ends' on PO-EC domain sequence by double digest with BamH1 and HindIII restriction enzymes 125

2.2.5 'Sticky end' ligation of PO-EC domain and pQE9 vector 125

2.2.6 Sequencing of positive clones 128

2.2.7 Transformation of M15pREP4 *E. coli* 129

2.2.8 Expression, purification and refolding of PO-EC domain 131

2.2.9 Purification and solid phase refolding of PO-EC domain 131

2.2.10 Characterisation of refolded PO-EC domain 133

2.2.11 Non-refolding protocol for PO-EC domain expression and purification 136

2.2.12 Characterisation of non-refolded PO-EC domain 138

2.2.13 Circular Dichroism (CD) spectrum analysis of refolded versus non-refolded PO-EC domain 141
2.2.14 Other myelin antigens 145

3 Discussion 145

Chapter 4
Part 1 The Rat as a target species for EAN 149

1 Introduction 149
2 Materials and Methods 150
2.1 Animals 150
2.2 Collection and processing of tissues for immunohistochemical analysis 151
2.2.1 Paraffin wax embedded sections for light microscopy 151
2.3 Collection and processing of tissues for electron microscopy (EM) 152
2.4 Disease assessment 153

3 Optimisation of EAN induction in the Rat 154
3.1 Induction of EAN in PVG/c rats using PO peptide 180-199 via footpad versus base of tail injection route 154
3.2 Induction of EAN in PVG/c rats using bacterially expressed, refolded PO-extracellular domain (rPO-EC): Footpad versus base of tail injection route 159
3.3 Experimental Modifications 163
3.4 Induction of EAN using C-amidated PO peptide 180-199 using Lewis rats 165
3.5 Induction of EAN using rPO-EC (non-refolded, non-washed versus washed) in Lewis rats 168
3.6 Analysis of the T and B cell responses to the rPO-EC in the Lewis rat 172
3.7 Induction of EAN using sheep sciatic nerve homogenate (SSNH) 182
3.8 Induction of EAN using rat sciatic nerve homogenate (RSNH) in the Lewis rat 184
3.9 Induction of EAN using bovine peripheral nerve myelin (BPNM) in Lewis rats 192

4 Summary and Discussion 195

Chapter 4
Part 2 The Mouse as a target species for EAN 197

1 Introduction 197

2 Materials and Methods **199**

3 Optimisation of EAN in the mouse **199**

3.1 Induction of EAN in C57Bl/6 mice using PO peptide 180-199 199

3.2 Induction of EAN in *Cd59a* -/- mice with PO peptide 180-199 202

3.3 Induction of EAN in C57Bl/6 mice using PO peptide 180-199-amide 206

3.4 Induction of EAN using PO peptide 106-125 in C57Bl/6 versus *Cd59a* -/- mice 209

3.5 Induction of EAN in C57Bl/6 and *Cd59a* knockout mice using non-refolded rPO-EC 212

3.6 Induction of EAN in C57Bl/6 mice using rat sciatic nerve homogenate (RSNH) 216

4 Summary & Discussion **219**

Chapter 5

Part 1

Passive transfer Experimental Autoimmune Myasthenia Gravis (EAMG) in the Lewis rat **222**

1 Introduction **222**

2 Materials and Methods **223**

3 Optimisation of passive transfer EAMG in the rat **224**

3.1 Purification of rat anti-nAChR mAb35 from tissue culture supernatant 224

3.2 Optimisation of dose of mAb35 required to induce EAMG in the Lewis rat 228

4 EAMG in the Rat is dependent on Membrane Attack Complex (MAC) formation **230**

4.1 Aim 230

4.2 Generation of C6 deficient Lewis rats 230

4.3 Induction protocol 230

4.4 Results 231

4.5 Analysis of CReg expression following EAMG induction 240

4.6 Reconstitution of human C6 247

4.7 Results 248

5 Testing of efficacy of anti-C therapy in passive transfer EAMG in the rat **254**

5.1 Aim 254

5.2 Materials and Methods 255
5.3 Results 256
5.4 Discussion 273

Chapter 5
Part 2
Preliminary optimisation of passive transfer EAMG in the mouse 274

1 Introduction 274
2 *Daf1/Cd59a-/-* mice are more susceptible to passively induced EAMG than their single knockout counterparts 277
2.1 Materials and Methods 277
2.2 Results 277
2.3 Discussion 283

Chapter 6 General Discussion, Future Work and Conclusions 286

1 Project Aim 286
1.1 C in GBS 286
1.2 C and MG 295
1.3 Conclusions 298

Chapter 7 References 300

Chapter 1
Introduction

1 The Complement (C) System

The C pathway was discovered as a heat-labile component of normal plasma, able to augment opsonisation of bacteria by antibody and enhance killing of invading pathogens. However, it was only during the 1960s that the multi-component nature of complement was realised, and individual components were isolated and characterised.

It consists of an array of 12 plasma proteins, activated in a sequential, self-perpetuating manner, resulting in opsonisation of target surfaces, generation of anaphylatoxins, immune complex formation and cell lysis (Janeway, Travers et al. 2001).

C activation may be triggered both via the innate and adaptive arms of the immune system; innately via pattern recognition molecules (the MBL pathway), directly by certain foreign surfaces (Alternative Pathway, AP) or via immune complex formation (Classical Pathway, CP). All three pathways feed into a common central element involving cleavage of C3 and C5. A final common pathway exists (Terminal Pathway) where penetration of the target surface by the membrane attack complex (MAC) results in lysis.

Individuals deficient in C components dramatically exemplify the importance of C in normal immune function with recurrent and severe bacterial infections, as well as immune complex (IC) disease.

Since the C activation pathways are proteolytic cascades and as such, have enormous potential for amplification, nature has evolved a battery of regulators acting at several points along the cascade.

In autoimmune disease however, C may be activated inappropriately and overwhelm the protection offered by such regulators, leading to tissue damage. C has been implicated in a wide variety of autoimmune disease, including peripheral neuropathies, and neuromuscular conduction disorders. Guillain-Barré Syndrome (GBS) and Myasthenia Gravis (MG) are two examples of such diseases. The role of C in peripheral neuropathies and neuromuscular disease will be the subject of this thesis.

1.1 Overview of the C System

1.1.1 Activation of C

1.1.1.1 The Classical Pathway (Figure 1a)

C1 is a large multimolecular protein complex comprising a single molecule of Clq and two molecules each of Cls and Clr ($C1q:r_2:s_2$). These are associated non-covalently and act in a calcium-dependent manner to initiate the classical pathway by binding of C1q to an activator, e.g. aggregated or immune complex-bound IgG or IgM antibody on target surfaces. Clq is composed of 6 globular heads joined to a common stem by long filamentous domains (likened

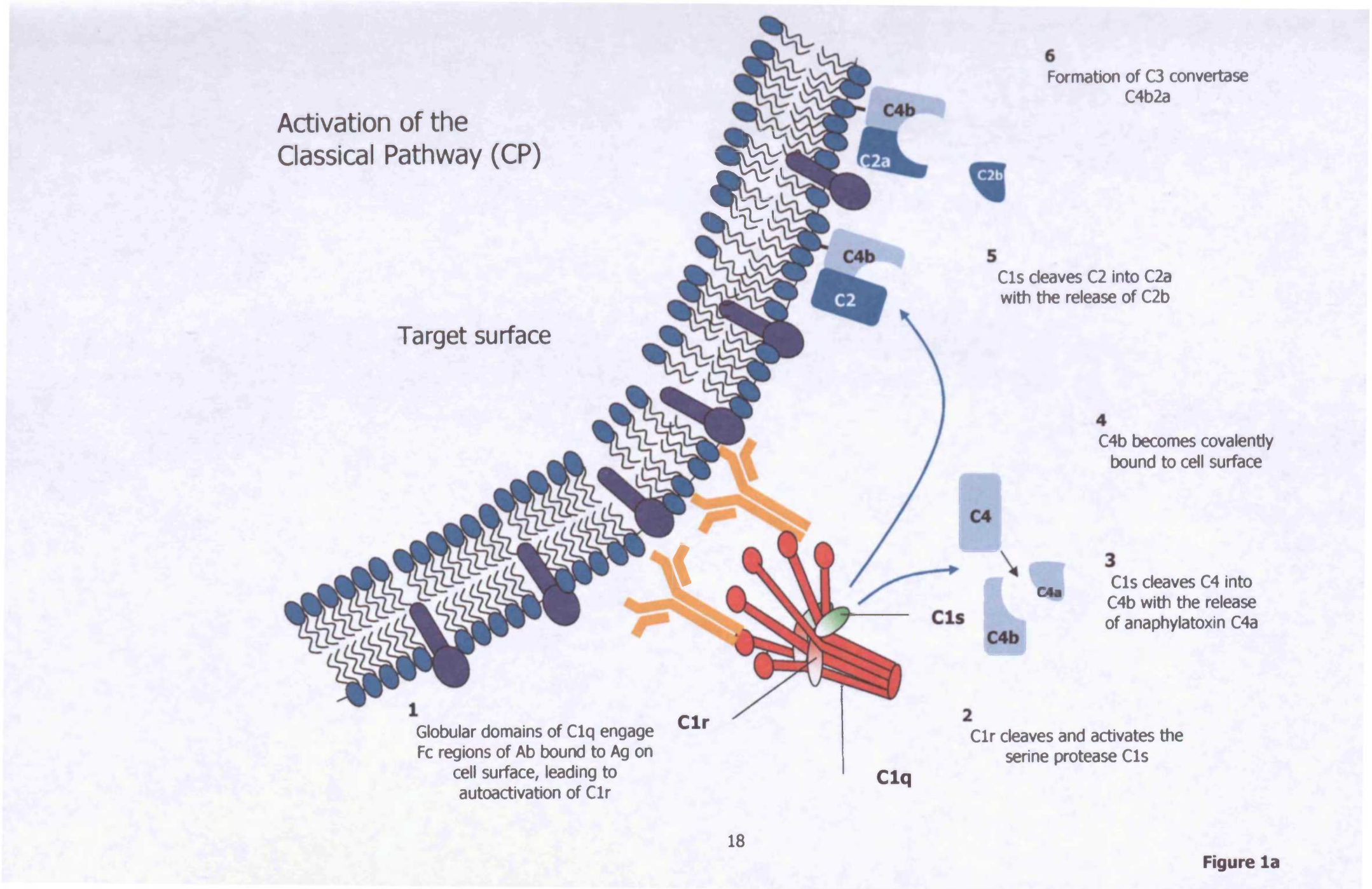
Activation of the
Classical Pathway (CP)
Target surface
6
Formation of C3 convertase
C4b2a
C4b
C2a
C2b
5
C1s cleaves C2 into C2a
with the release of C2b
C4b
C2
4
C4b becomes covalently
bound to cell surface
C4
3
C1s cleaves C4 into
C4b with the release
of anaphylatoxin C4a
C4a
C4b
C1s
1
Globular domains of C1q engage
Fc regions of Ab bound to Ag on
cell surface, leading to
autoactivation of C1r
C1r
2
C1r cleaves and activates the
serine protease C1s
C1q

Figure 1a

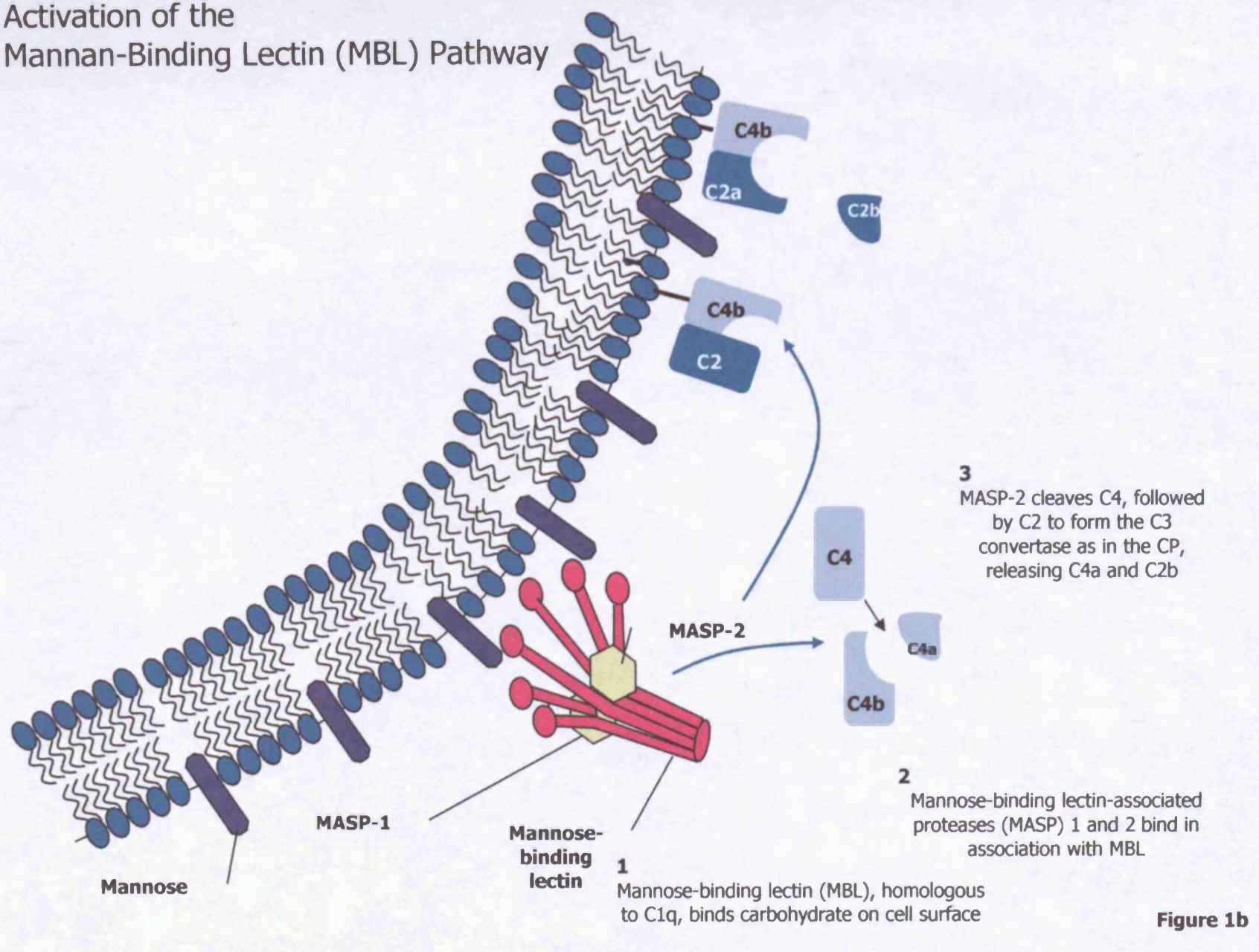
Activation of the
Mannan-Binding Lectin (MBL) Pathway
C4b
C2a
C2b
C4b
C2
3
MASP-2 cleaves C4, followed by C2 to form the C3 convertase as in the CP, releasing C4a and C2b
C4
MASP-2
C4a
C4b
2
Mannose-binding lectin-associated proteases (MASP) 1 and 2 bind in association with MBL
MASP-1
Mannose-binding lectin
Mannose
1
Mannose-binding lectin (MBL), homologous to C1q, binds carbohydrate on cell surface

Figure 1b

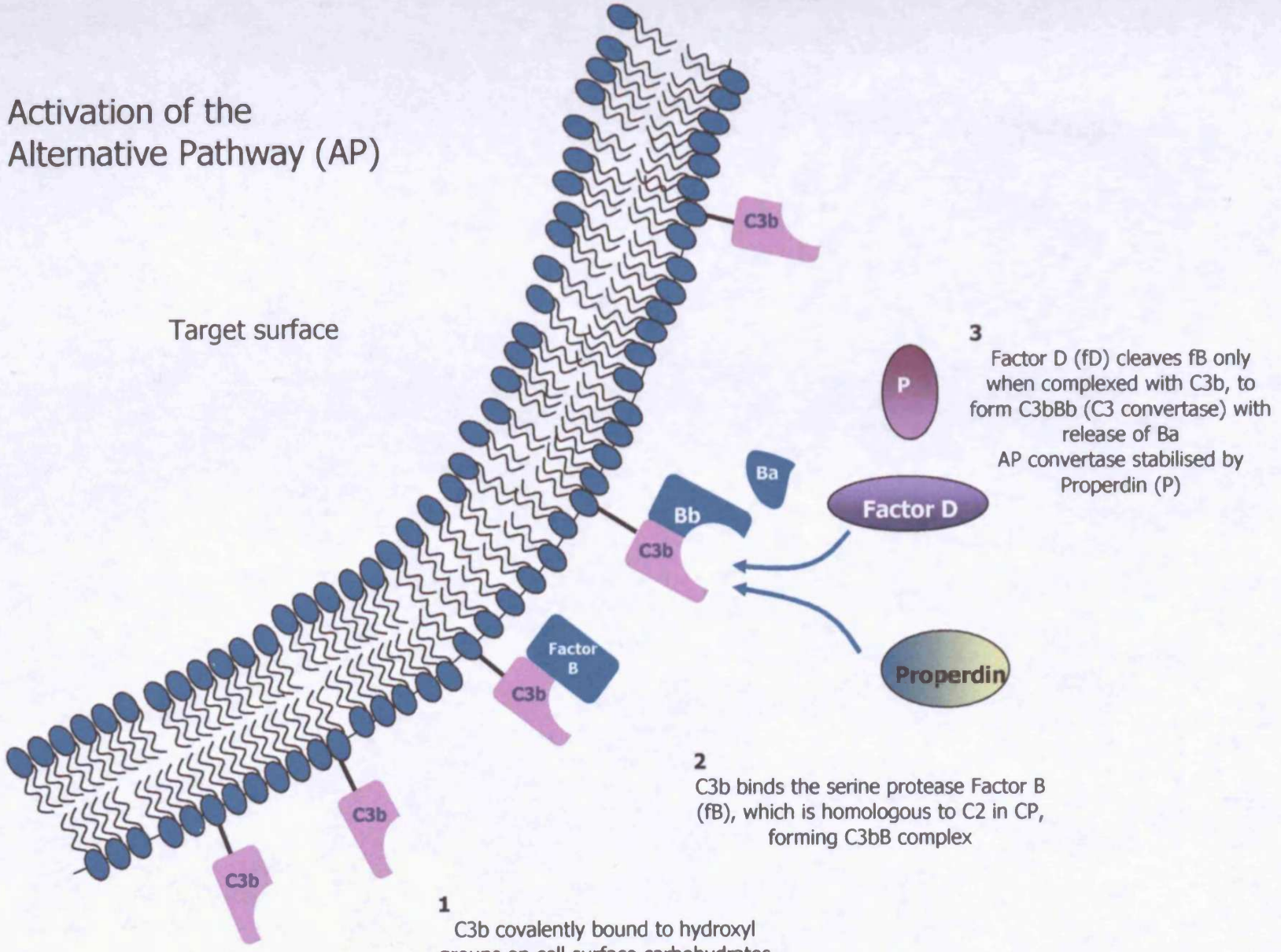
Activation of the
Alternative Pathway (AP)
Target surface
C3b
C3b
C3b
C3b
Factor
B
C3b
Bb
Ba
P
Factor D
Properdin
3
Factor D (fD) cleaves fB only when complexed with C3b, to form C3bBb (C3 convertase) with release of Ba
AP convertase stabilised by Properdin (P)
2
C3b binds the serine protease Factor B (fB), which is homologous to C2 in CP, forming C3bB complex
1
C3b covalently bound to hydroxyl groups on cell surface carbohydrates and proteins.
Activated by low grade cleavage or hydrolysis of C3 in plasma

Figure 1c

Central Elements of the C Cascade

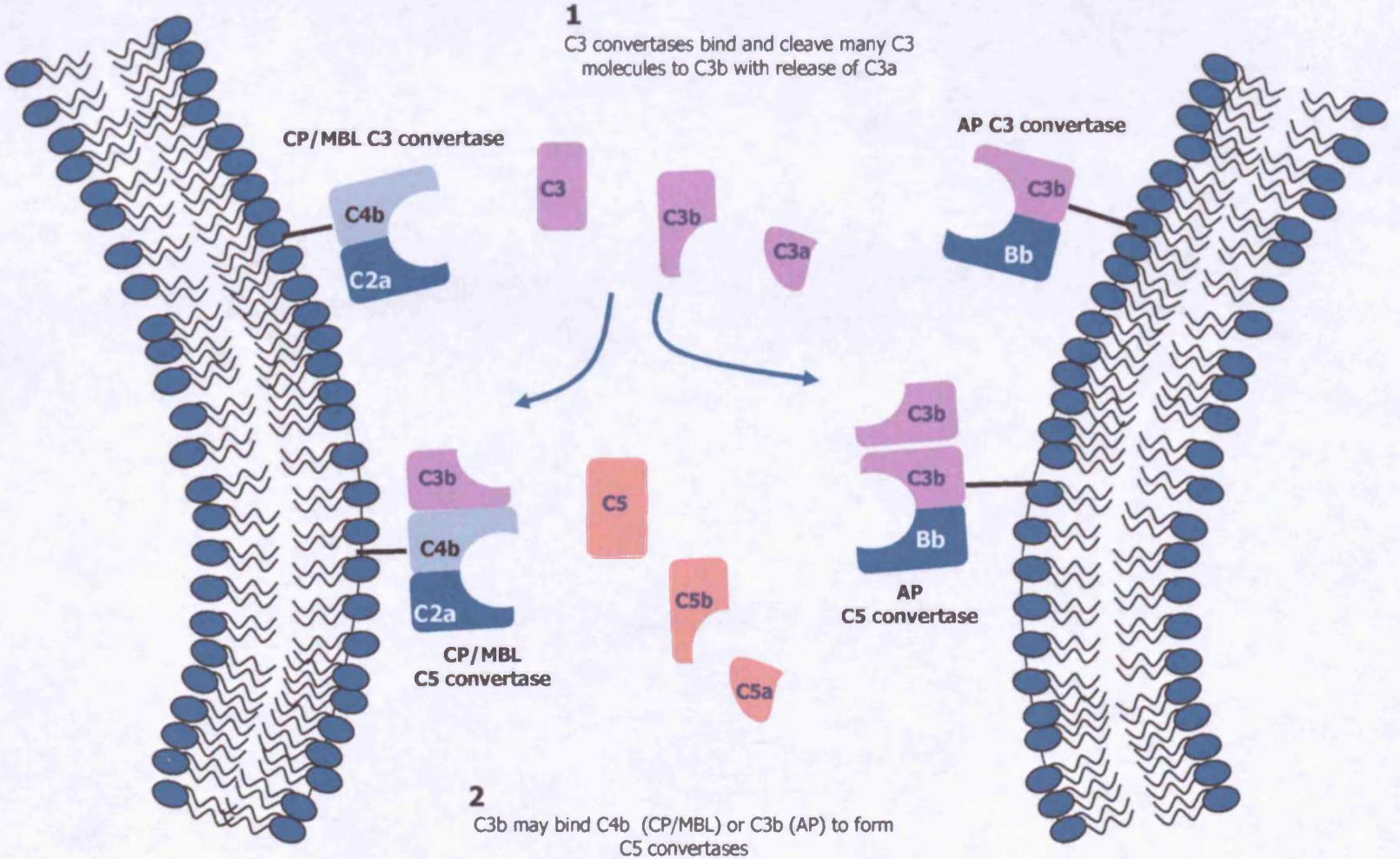

Figure 1d

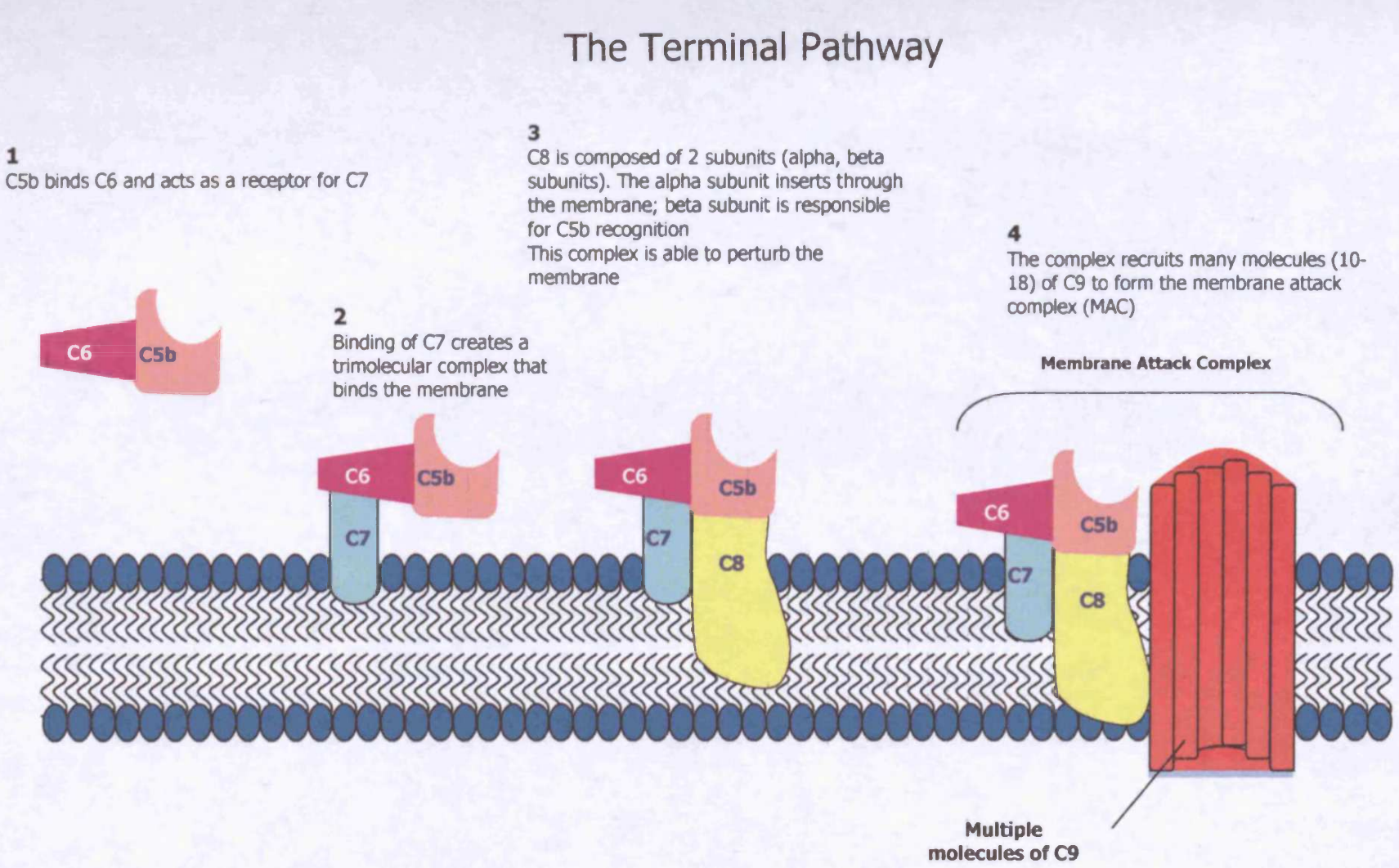

Figure 1 The C cascade

C may be activated by any of 3 pathways depending on the nature of the target cell; the Classical Pathway (CP) is activated by binding of C1 complex to antibody bound to an antigen on the surface of the target cell, the Mannan-Binding Lectin Pathway (MBL) is activated by binding of MBL-MASP complex to mannose arrays on the surface of a bacterial cell, and the Alternative Pathway (AP), which is activated by low grade cleavage of C3 in plasma, depositing C3b on carbohydrates and proteins via their hydroxyl groups. All pathways lead to the formation of a C3 convertase enzyme.
All three pathways converge in the central element of the cascade, the cleavage of C3, which leads to formation of the C5 convertase. Binding of C5b to C6 initiates the Terminal Pathway which culminates in the formation of the membrane attack complex (MAC). Adapted from (Walport 2001).

to a bunch of tulips held together by the stems) (Perkins and Nealis 1989). Although Clq possesses no enzymatic activity, simultaneous engagement of the globular domains of Clq to the Fc portion of activating antibodies induces a conformational change in Clq, resulting in auto-activation of the pro enzyme component Clr. The active site in Clr is exposed, leading to activation of the serine protease component, Cls (Bansal and Malaviya 1984). This enzymatically cleaves and activates the next component of the CP, C4.

C4 is a large plasma protein consisting of disulphide bonded α, β and γ chains (Bolotin, Morris et al. 1977). C4 is cleaved by Cls at the amino terminus of its α-chain, releasing a small anaphylatoxin, C4a and a larger reactive protein, C4b. The reactive thioester group within the α-chain of C4b, buried in a hydrophobic pocket in the native molecule but exposed by the action of C1s, forms covalent amide or ester bonds with exposed amino or hydroxyl groups on the activating surface. This now provides the receptor for C2. If C4b does not rapidly form a bond with these groups, the thioester bond is cleaved by hydrolysis, irreversibly inactivating C4b and preventing it attaching to host cells by diffusion (Isenman 1983).

C2 exists as a heat-sensitive, single-chain proenzyme within plasma (Kerr 1981). In the presence of magnesium ions, it is recruited by membrane-bound C4b via its amino terminus, and presented for cleavage by Cls in a neighbouring C1 complex (Horiuchi, Macon et al. 1989). Cleavage yields a 30kDa product, C2b, which has no enzymatic activity but may remain weakly associated with the larger product C2a (70kDa). C2a forms the first enzymatic complex, the classical pathway C3 convertase (C4b2a), and is entirely responsible for the enzymatic activity, whilst C4b provides a 'tether' to the activating surface (Nagasawa, Kobayashi et al. 1985).

1.1.1.2 The Mannan Binding Lectin (MBL) Pathway (Figure 1b)

The MBL pathway is the most recently discovered of the C activation pathways, and provides an innate mechanism of C activation. MBL is structurally similar to C1q, possessing an N-terminal collagenous region attached to a C-terminal lectin domain. The collagenous regions associate to form a triple helix, and 2-6 of these subunits further associate to produce the MBL multimer. MBL binds mannose or N-acetylglucosamine (GlcNAc) found on bacteria, yeast and viruses, in a calcium-dependent manner. C activation occurs via MBL-associated serine proteases (MASP 1 and 2), which bear structural homology to C1r and C1s. When complexed MBL-MASP binds the target surface; the serine protease cleaves C4 and C2, generating the C3 convertase (Thiel, Vorup-Jensen et al. 1997).

1.1.1.3 The Alternative Pathway (Figure 1c)

The AP was discovered by Pillemer in 1954 (Pillemer, Blum et al. 1954), and provides an antibody independent route for C activation as well as a route for amplification of both the CP and MBL pathways. As well as C3, three further components characterise this pathway, namely factor B (fB), a single chain 93kDa plasma protein with sequence identity with C2 (Curman,

Sandberg-Tragardh et al. 1977); factor D (fD, adipsin), a 26kDa serine protease found in its active form in plasma; and properdin, whose basic unit comprises a 53kDa monomer (Volanakis, Schrohenloher et al. 1977). Properdin acts to stabilise the C3 convertase by extending its half-life 3/4-fold (Fearon, Austen et al. 1974). The mechanism of activation of the AP involves C3b, either in the fluid phase, or bound to an activating surface, binding to fB in a magnesium-dependent manner. fB is rendered susceptible to cleavage by fD, producing two fragments, Ba (30kDa), and Bb (60kDa). Bb has an exposed serine protease domain enabling it to form the C3 convertase of the AP (C3bBb) (Lambris and Muller-Eberhard 1984). The C5 convertase of the AP is merely an extension of the C3 convertase in that it binds another molecule of C3b (C3bBbC3b), which forms the receptor for C5.

For direct initiation of the AP, C3 may undergo conversion to a C3b-like molecule termed C3(H_20) via small nucleophiles such as water. They attack the thioester and hydrolyse it. The resulting conformational change is sufficient to enable binding to fB, and subsequent fD cleavage. This fluid phase C3(H_20)Bb complex can cleave C3 allowing C3b deposition on nearby surfaces. Such action is termed 'tickover' activation and occurs constantly, resulting in C3b deposition on self cells (Pangburn, Schreiber et al. 1981); however C3b is rapidly degraded by membrane bound C regulators.

1.1.1.4 Central elements (Figure 1d)

C3 is central to all activation pathways, and the most highly abundant C component in serum (1-2mg/ml). It consists of two disulphide-linked chains, α and β, and again is synthesised as a precursor molecule and cleaved intracellularly before secretion. C3 binds non-covalently to C2a in the C3 convertase, and is cleaved in the α-chain, releasing C3a, an anaphylatoxin, and C3b. C3b, as in C4b, has a reactive thioester group, and demonstrates binding sites for several C receptors and regulatory proteins. Binding of C3b to the C3 convertase culminates in the formation of the C5 convertase. It may also bind adjacent membranes, and is implicated in phagocytic cell interactions (Levine and Dodds 1990).

C5 exists as a two-chain plasma protein with structural homology to C3 and C4, suggesting a common ancestor. However, it has no reactive thioester group, and thus cannot bind directly to surfaces. C5 binds into the C5 convertase and is cleaved into C5b with the release of C5a (Cooper and Muller-Eberhard 1970).

1.1.1.5 The Terminal Pathway (Figure 1e)

A series of highly homologous, hydrophilic plasma proteins constitute the terminal pathway, termed C6 (Chakravarti and Muller-Eberhard 1988), C7, C8 α,β, and C9. C5b initiates the assembly of terminal pathway components and subsequent insertion into the membrane. C5b binds C6. Binding of C7 to C5b-6 induces a conformational change, exposing a hydrophobic binding site on C7, which inserts into the membrane, but does not perturb the membrane

(Preissner, Podack et al. 1985). The subsequent component of the MAC is C8, a complex molecule consisting of three subunits; α (65kDa), β (65kDa) and γ (22kDa), which are products of different genes. Binding of C8 is the beginning of the end for the target cell. The β subunit of C8 binds C5b in the complex, allowing the hydrophobic portion of C8 (α, γ) to further insert into the membrane (Tamura, Shimada et al. 1972), and recruit C9 molecules. C9, in its native state, exists as a globular and hydrophilic molecule, but upon binding C8α, it becomes elongated, and inserts through the membrane, exacerbating disruption of the membrane. Polymerisation of 10-18 molecules of C9 generates the lytic pore or membrane attack complex (MAC). Disruption of the membrane leads to loss of cellular homeostasis, disruption of the proton gradient, and eventual destruction (Stanley 1989).

Contrary to the dramatic nature of the MAC, individuals deficient in its components are only associated with an increased susceptibility to *Neisseria* infection. Thus clearly, other roles of C such as opsonisation and inflammatory actions are more important for host defence (Dragon-Durey, Freemeaux-Bacchu et al. 2003).

The lytic mechanism is analogous to that utilised by cytotoxic T lymphocytes, and its effector molecule, perforin (Young, Liu et al. 1986).

1.1.1.6 C biosynthesis

Normal human plasma contains components of the CP, AP and terminal pathways of C at concentrations ranging from 2μg/ml (fD) to as high as 2mg/ml (C3). Although the liver, specifically hepatocytes, have classically been regarded as primarily responsible for their synthesis, no C1q, fD or properdin expression has been detected within any cell type contained within that tissue. Plasma C1q has however been shown to be produced by epithelial cells, fibroblasts, and cells of the monocyte/macrophage lineage (Tenner and Volkin 1986). The primary source of plasma fD is the adipocyte (Choy, Rosen et al. 1992), while plasma properdin is derived mainly from monocytes and macrophages (Maves and Weiler 1993). However, more recently, properdin expression was demonstrated in shear stress-exposed endothelial cells (EC), and authors suggest that this site provides the primary source of plasma properdin (Bongrazio, Pries et al. 2003). C biosynthesis at extrahepatic sites remote from plasma C may be important in protection of tissues against inflammation and infection, but may also contribute to tissue injury (Table 1).

Cells within the CNS are capable of generating a complete, functional C system, with the major source being astrocytes. Other brain cell types likely contribute to this production, notably microglia (Morgan, Gasque et al. 1997). However, work involving C component expression in the PNS is limited, and has previously focussed on the expression of CRegs (Vedeler, Ulvestad et al. 1994) (Koski, Estep et al. 1996). One study, (de Jonge, van Schaik et al. 2004) suggested high expression of CP and AP C components; however, the validity of the results can be

questioned since the authors also claim that properdin was expressed in the nerve *and* liver. No properdin expression has ever been detected in the liver.

Localisation	CP	AP	Terminal Pathway
Liver: Hepatocyte	C1r/s, C4, C2	C3, fB	C5-C9
Blood cells: T cells		C3	C5
B cells		C3	C5
monocytes	C1q, r/s, C4, C2	C3, fB, fD, properdin	C5-C9
platelets			C5-C9
neutrophils		C3	C6, C7
Macrophages	C1q, r/s, C4, C2	C3, fB, fD, properdin	C5-C9
Fibroblasts	C1q, r/s, C4, C2	C3, fB	C5-C9
Endothelial cells	C1s, C2	C3, fB	
Epithelial cells	C1q, C1r/s, C4, C2	C3, fB	C5
Lung, macrophage+epithelial	C1q, C4, C2	C3, fB, fD	C5
Kidney, epithelial	C4	C3	
Skin, keratinocyte+fibroblast		C3, fB	
Intestine, epithelial	C4	C3, fB	
Skin, muscle, myoblast		C3, fB, fD, properdin	
Fat tissue, adipocyte		C3, fB, fD	
Synovial tissue	C1q/r/s, C2, C4	C3, fB, fD	C5, C6, C7, C9
Brain: Astrocytes	C1q, C1r/s, C2, C4	C3, fB, fD	C5-C9
Microglia	C1q, C1r/s, C2, C4	C3, fB, fD	C5-C9
Genital tract		C3	

Table 1 C Component localisation (excluding CRegs)
Modified from (Morgan and Gasque 1997)

1.2 Physiological Roles of C

1.2.1 Opsonisation of pathogens: C-tagging & bacterial killing

One of the most important functions of C is to facilitate uptake and destruction of pathogens by phagocytes via recognition by C receptors (CR) expressed on the surface of phagocytic cells. CRs bind pathogens opsonised by C components, e.g. CR1 binds C3b and C4b (Klickstein, Bartow et al. 1988). Table 2 displays examples of CR characterised to date.

Bacteria are generally resistant to C-mediated attack on account of their thick cell wall and peptidoglycan capsule. One exception to this is the gram-negative bacteria, in particular *Neisseria* species, which are MAC-sensitive.

To counter the inherent lytic resistance of bacterial species, C has evolved the role of opsonisation. This refers to the extensive coating of invading pathogens with C3 breakdown products C3b, iC3b and C3d, marking them for destruction by phagocytic cells expressing CR1, CR2 and CR3. C is initially activated on these cells via all 3 activation pathways, and promotes the inflammatory response by production of C3a and C5a. These act as both anaphylatoxins to promote vasodilation and vascular permeability via release of vasoactive amines, and as chemotactic agents for phagocytes. C4a is also produced although its function remains unclear (Hugli, Gerard et al. 1981). The inflammatory response is further amplified by increased oxygen radical formation coupled with increased cytokine and arachidonic acid metabolites (Kirshfink 2001).

Receptor	Specificity	Functions	Cell types
CR1 (CD35)	C3b, C4b	Promotes C3b and C4b decay Stimulates phagocytosis Erythrocyte transport of immune complexes	Erythrocytes, macrophages, monocytes, PMNL, B cells, FDC
CR2 (CD21)	C3d, iC3b, C3dg, EBV	Part of B-cell co-receptor EBV receptor	B cells, FDC
CR3 (CD11b, CD18)	iC3b	Stimulates phagocytosis	Macrophages, monocytes, PMNL, FDC
CR4 (gp150, 95, CD11c, CD18)	iC3b	Stimulates phagocytosis	Macrophages, monocytes, PMNL, dendritic cells
C5a receptor C3a receptor	C5a C3a	Binding of C5a/ C3a activates G protein	Endothelial cells, mast cells, phagocytes

Table 2

Examples of CRs identified to date, their ligands, their function, and their distribution

Taken from (Janeway, Travers et al. 2001)

1.2.2 Immune complex clearance

ICs are formed from aggregated antibody and antigen in the plasma. As more molecules are recruited to the 'lattice', the CP is activated, and the IC is opsonised with C fragments. This

action effectively renders the large insoluble complex soluble by disaggregation. It also effects CR1 binding on erythrocytes and this promotes IC transport and subsequent clearance by tissue macrophages (Petersen, Baatrup et al. 1985).
In addition, follicular dendritic cells (FDCs) are capable of binding IC-bound C3b, facilitating interaction with B and T lymphocytes, and promoting the cell-mediated immune response. Recent evidence indicates a further role for C3 in providing a second signal following antigen binding to initiate proliferation and antibody production (Fearon 1995).

1.3 C Regulatory (CReg) Proteins

The importance of regulation within the complement system is indicated by the fact that there are almost as many regulators as there are actual C components, acting at several points along the cascade.
The activation pathways of C are proteolytic cascades, akin to the blood coagulation system, and as such have enormous potential for amplification. With C continually activated at a low level in serum, amplification of even a very small stimulus would rapidly cause local damage, as well as rendering the individual C deficient, in the absence of regulation.
Nature has therefore evolved a battery of CReg proteins, which function either by inactivation of the convertases within the activation pathways, or by interfering with MAC formation.
CReg belong to three structurally and functionally distinct protein families:

1 **Serine protease inhibitors** (Serpins), e.g. C1 inhibitor

2 **Regulators of C activation (RCA) gene cluster proteins**, e.g. CD55, CD46, Crry, CR1, factor H (fH), C4-binding protein (C4bp), functioning as decay accelerators or as cofactors for Factor I

3 **Ly-6 superfamily**, e.g. CD59 (Harris and Morgan 2004)

1.3.1 Serpins

1.3.1.1 C1 inhibitor (C1inh); fluid phase CP reg

C1inh was discovered in 1957 by Ratnoff and Lepow as a plasma component capable of C1 inactivation (Ratnoff and Lepow 1957). As a member of the SERPIN family, it is composed of a single chain with a conserved 380aa domain responsible for its function. C1inh reversibly binds to native C1 to prevent auto-activation, and also interacts with C1r and C1s, promoting their dissociation from cell-bound C1q. The resulting fluid phase complex of C1r, C1s and 2 molecules of C1inh is stable and may be detected in plasma after C1 activation (Harrison 1983).

1.3.2 RCA gene cluster proteins

The RCA gene cluster is located on the short arm of chromosome 1 and contains genes encoding for CReg sharing a structural motif called a short consensus repeat (SCR). Each SCR consists of approximately 60-70 amino acids folded into a compact globular domain via 2 disulphide bridges. Their function centres on interaction with the activation products of C3 and/or C4, either by decay-acceleration of convertase enzymes, or Factor I-mediated cofactor activity (Harris and Morgan 1999).

1.3.2.1 Decay-acceleration

Such regulators function by promoting rapid dissociation of the convertases from either CP or AP activation pathways by competing for binding to the convertase (Figure 2a). Regulators possessing this function are CR1, CD55 and C4bp for the CP convertases, and CR1, Factor H and CD55 for the AP convertases (Hourcade, Mitchell et al. 2002).

1.3.2.2 Cofactor activity

Convertase formation may be prevented by cleaving C3b to an inactive form designated iC3b. This is achieved by the plasma protease Factor I, in conjunction with a C3b-binding protein, e.g. CR1, CD46, CD55 (Seya, Okada et al. 1990), (Figure 2b).

1.3.2.3 Factor I (fI)

Human fI is a regulatory serine protease synthesised primarily in the liver and by monocytes. It is a heterodimer of 88kDa consisting of a non-catalytic heavy chain (50kDa), and a catalytic light chain (38kDa) bound by a single disulphide bond. fI is capable of cleaving three peptide bonds in the alpha chain of C3b, and two bonds in the alpha chain of C4b, thereby inactivating them, in the presence of cofactors, fH, C4bp, CR1 and MCP (Tsiftsoglou, Willis et al. 2005). Mouse fI demonstrates an overall conservation of primary structure and domain organisation to human fI; however, a species-specific divergent sequence exists, which differs in length, organisation and number of repeated sub-regions in xenopus, human, mouse and chicken (Minta, Wong et al. 1996). Rat fI was cloned more recently, and shows overall homology of 85% to the mouse protein, and 69% to the human protein (Schlaf, Rothermel et al. 1999).

1.3.3 Fluid-phase RCA regulators

1.3.3.1 C4-binding protein (C4bp)

C4bp is a large protein composed of multiple disulphide-linked subunits, capable of regulating the CP convertases by decay-acceleration and fI-mediated cofactor activity. The most common isoform has 7α chains containing 8 SCRs, and 1β chain containing 3 SCRs (α7β1) covalently linked at the carboxy- terminal by disulphide bonded cysteine residues (Figure 3a). C4bp acts in

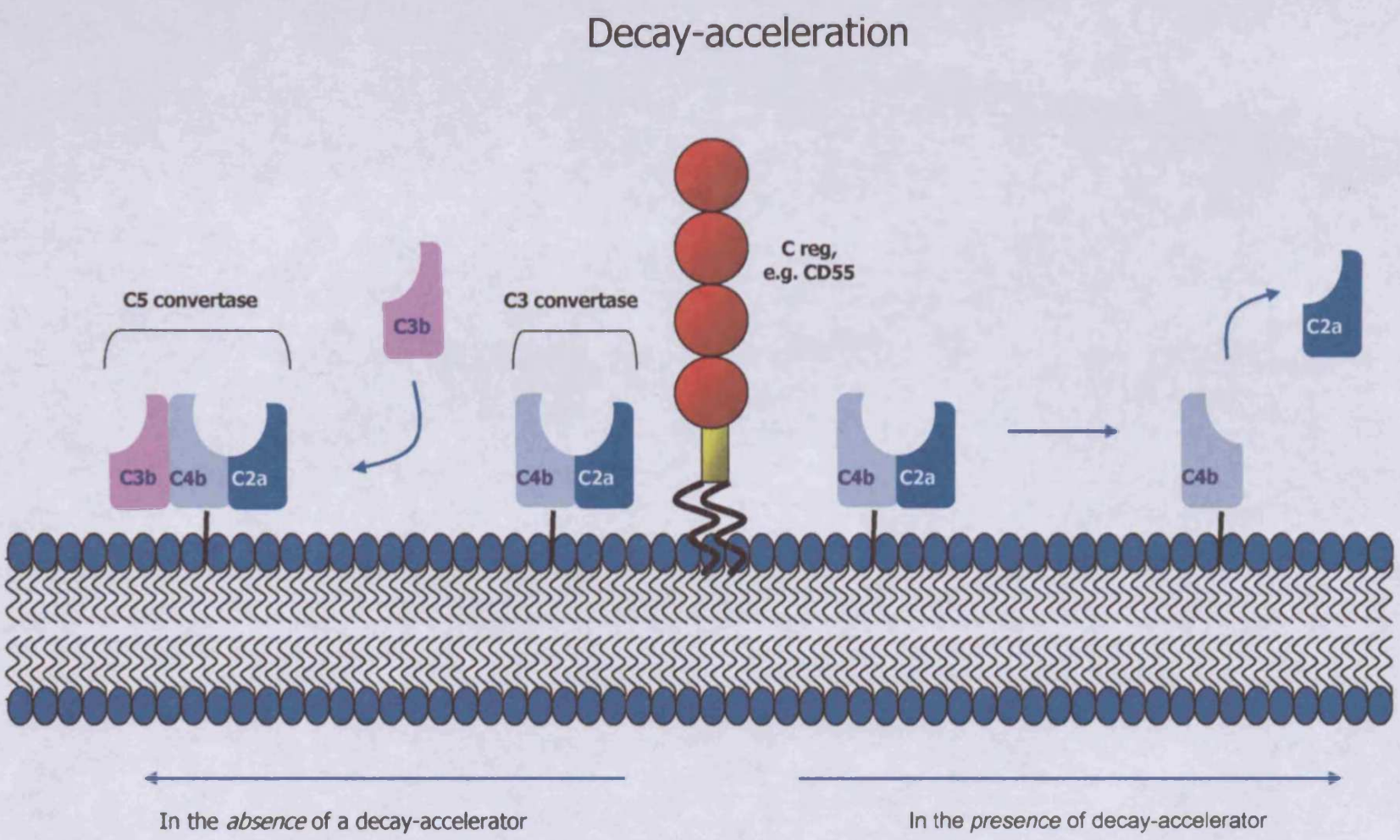

Figure 2a The basis of the decay-accelerating activity of C regs
In the absence of decay-acceleration, a C3 convertase may bind C3b, and become a functional C5 convertase, and proceed along the C casacde. However, regulators which act to accelerate the decay of the C3/C5 convertases bind, and dissociate the serine protease domain of the convertase, thus removing its catalytic potential.

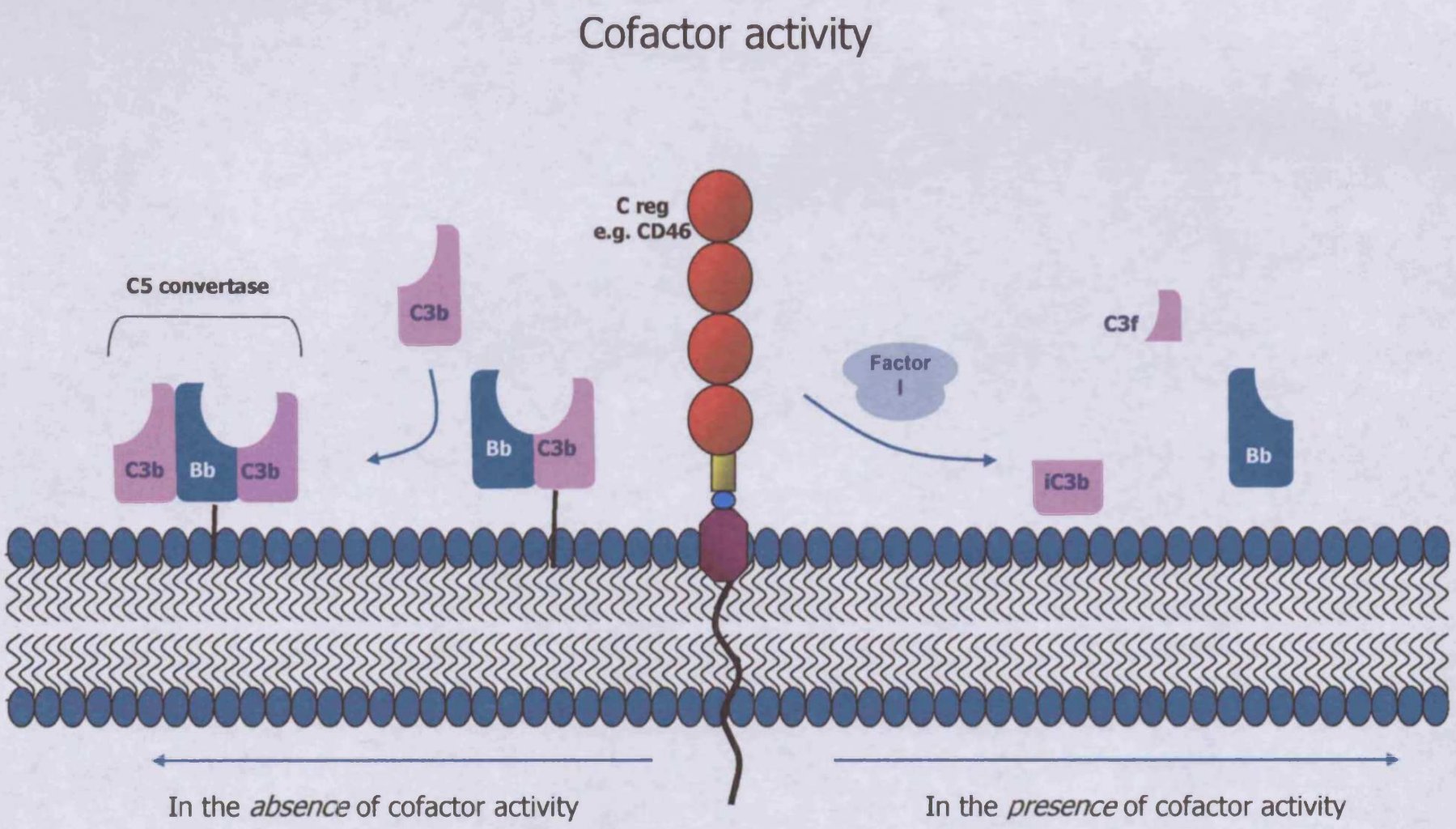

Figure 2b The basis of cofactor activity

C3 and C5 may be inactivated by the serine protease Factor I, but only in the presence of a cofactor. C regs such as CD46 provide this cofactor, and thus promote Factor I-mediated cleavage of C3b (or C4b), into iC3b and C3f, releasing the serine protease of the convertase, e.g. Bb. Although iC3b can no longer participate in the active convertase, it remains attached to the target surface to act as an opsonin.

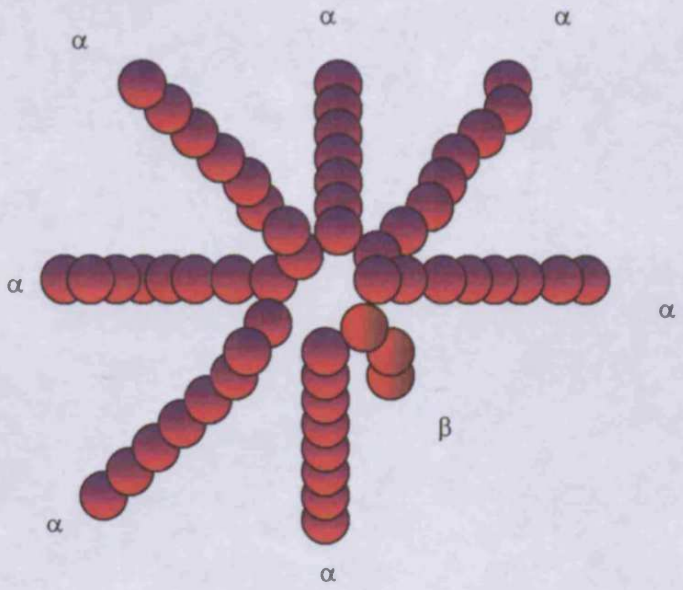

Figure 3a Structure of the most common isoform of C4bp, α7β1

C4bp is a member of the RCA family, and is capable of decay acceleration of the CP convertases in addition to fI-mediated cofactor activity. The most common isoform, depicted here, contains 8 chains, with 7α-chains containing 8 SCRs, and 1β chain containing 3SCRs, linked at their carboxy termini by disulphide bonds.

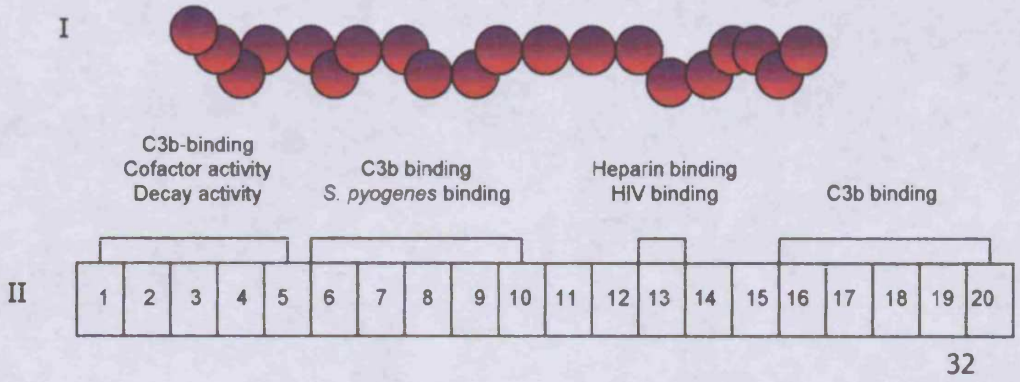

Figure 3b Domain structure of Factor H

A member of the RCA family, fH is composed entirely of 20 SCR domains, giving the molecule a high degree of flexibility (I). Numerous binding sites exist within fH for C3b (II, 1-10, 16-20). SCRs 1-5 are responsible for the decay-accelerating and cofactor activity (Harris and Morgan 1999). Numerous pathogens have evolved capability for sequestering of fH to prevent C activation and opsonisation on their surface by the host e.g. Streptococcus pyogenes (Harris and Morgan 2004)

the CP to regulate the C3 and C5 convertases by accelerating the decay of, and inhibiting association of the convertase subunits. It also functions as a cofactor for fI mediated cleavage of C4b into iC4b and further into C4c and C4d (Ziccardi, Dahlback et al. 1984).
Murine C4bp is closely related to human C4bp sharing 51% homology at the amino acid level. Although it consists of multiple SCR domains, murine α chains consist of only 6 SCRs, and are non-covalently associated at their carboxy termini. In addition, the β chain, responsible for Protein S interaction in humans, is present as a pseudogene in mice (Kristensen, Ogata et al. 1987). The rat homologue is found in a complex with Protein S in serum and shares high homology to human C4bp in both α and β chains (Hillarp, Wiklund et al. 1997).

1.3.3.2 Factor H (fH)

fH is the predominant soluble regulatory molecule of the C system, and is composed of a single chain highly glycosylated protein of 150kDa, composed entirely of 20 SCR domains, giving the molecule a high degree of flexibility (Figure 3b). fH regulates the convertases by decay acceleration by binding to C3b and promoting the dissociation of the serine protease Bb. In addition, fH is able to bind C3b and prevent the binding of fB thus inhibiting the formation of the convertase in the first instance. fH also possesses co-factor activity. When bound to C3b, it acts as a cofactor for the serine protease Factor I, promoting the release of C3f and the formation of inactive C3b (iC3b) (Kristensen, Wetsel et al. 1986). Factor H-like proteins also exist, for example, factor H-like protein 1 (FHL-1) is composed of 7 SCRs that are identical in sequence to the 7 amino terminal SCRs of Factor H (Kuhn, Skerka et al. 1995).
Murine fH shares high structural conservation with the human analogue. It also comprises several distinct molecular forms analogous to fH-like molecules (FHL) and fH-related molecules (FHR) molecules in humans (Vik, Munoz-Canoves et al. 1990). Rat fH has recently been cloned using degenerate primers to conserved regions of the human and mouse sequences, and shown to have 63% identity to the human protein, and 82% homology to the murine protein (Demberg, Pollok-Kopp et al. 2002).

1.3.4 Membrane-bound RCA regulators

1.3.4.1 Decay-accelerating factor (DAF, CD55)

A glycophosphatidyl-inositol (GPI)-anchored glycoprotein of 70-80kDa, CD55 contains 4 SCRs followed by a heavily glycosylated region rich in Serine, Threonine and Proline residues (STP), which is essential to project the functional domains away from the

membrane, and to prevent non-specific proteolysis at the membrane (Caras, Davitz et al. 1987) (Figure 4).

CD55 primarily functions to enhance the decay of the C3 and C5 convertases of the CP and AP. CD55 binds to preformed C4b2a or C3bBb and promotes the dissociation of C2a or Bb respectively. Evidence suggests that CD55 functions most efficiently on pre-formed convertase complexes (Apparent dissociation constants (appKa) C3 convertase = $910nM^{-1}$, C3b = $45nM^{-1}$)(Nicholson-Weller and Wang 1994).

CD55 also possesses functions in addition to C regulation. For example, CD55 may also function as a ligand for CD97, a seven-span TM receptor, which is immediately expressed on leucocytes during activation, implying a novel adhesion pathway (Hamman, Vogel et al. 1996).

In humans, CD55 is uniformly expressed as a GPI-anchored form; however, murine CD55 is encoded by two separate genes, *Daf1* and *Daf2*, coding for a GPI-anchored form and a transmembrane (TM) form. Exons coding for both the GPI and TM forms are present in both genes, thus both genes can give rise to both forms of mouse CD55 by alternative splicing. Alternative splicing may also give rise to a putative secretory form. GPI-CD55 was found to be present in all tissues in relative abundance, whereas TM-CD55 was abundant only in testis and weakly in lymphoid tissue (Miwa, Okada et al. 2000; Lin, Fukuoka et al. 2001).

Rat CD55 is encoded by a single gene, giving rise to two membrane forms (GPI and TM) by alternative splicing (Miwa, Okada et al. 2000). A further putative secretory form was identified in our laboratory (Hinchliffe, Spiller et al. 1998). The expression of isoforms varies between tissues, with GPI present in all tissues, and TM being testis-specific (Miwa, Okada et al. 2000). Work examining the species restriction of human and rodent analogues of CD55 in terms of C-inhibitory activity, demonstrated that all three analogues were capable of inhibiting human, rat and mouse C (Harris, Spiller et al. 2000).

1.3.4.2 Membrane co-factor protein (MCP, CD46)

CD46 is a widely distributed 60kDa transmembrane protein, which complements but does not replicate the activity of CD55. Its acts as a cofactor for fI-mediated cleavage of C3b or C4b thereby irreversibly inactivating the convertases (Lublin, Liszewski et al. 1988). It is composed of 4 SCR domains followed by a highly glycosylated STP region attached to the membrane via a transmembrane linkage (Figure 4). CD46 can express 3 different STP regions, A, B and C by alternative splicing, as well as 2 different cytoplasmic tails, CYT-1 (16aa) and CYT-2 (23aa) (Post, Liszewski et al. 1991).

CD46 is widely distributed on all human cells and tissues with the exception of erythrocytes. It is particularly highly expressed on sperm, in the genital tract and within seminal plasma

(Harris and Morgan 1999). The high expression of CD46 on sperm, and the finding that it is localised specifically to the inner acrosomal membrane, and comes to the surface only after the acrosomal reaction has led to the hypothesis that CD46 is involved in mediating sperm-egg interactions (Anderson, Abbott et al. 1993).

Rat CD46 is encoded by a single gene, although several isoforms may arise via alternative splicing. The most prevalent isoform corresponds to the STP-rich C type of human CD46. The domain structure of rat CD46 is composed of 4 SCRs followed by an STP region, TM segment and cytoplasmic tail, and preferentially expressed in the testis, although expression can be detected in a range of other tissues by RT-PCR (Miwa, Nonaka et al. 1998; Mead, Hinchliffe et al. 1999). Murine MCP shows 77% identity to rat CD46 at the amino acid level, and is also preferentially expressed in testis (Miwa, Nonaka et al. 1998).

The restricted expression of CD46 in rodents suggests a unique role for CD46 in reproduction and fertilisation, and has been the focus of studies in our laboratory. Following generation of a monoclonal antibody (mAb) to rat CD46, analysis of CD46 distribution revealed that CD46 expression was indeed restricted to the testis in sexually-mature rats, and was expressed only by spermatozoa and their precursors, spermatids. Such expression was absent from prepubertal rats, and embryos. As in humans, CD46 was found in the inner acrosomal membrane, and exposed only following acrosome reaction; acrosome-reacted spermatozoa were capable of binding methylamine-reacted, i.e. activated C3 on a plastic surface (Mizuno, Harris et al. 2004). Subsequent studies involved identification of stages of seminal tubule epithelium in the rat, which is important in spermatogenesis. Early expression of CD46 suggests a role in spermatogenesis or acrosomal maturation (Mizuno, Harris et al. 2005). Studies are being conducted to further define the role of CD46 in reproduction.

Figure 4

Structure of membrane-bound RCA CRegs

All regulators in this group are closely related in terms of their structure. All contain SCR domains.

CD55/DAF contains 4 SCRs followed by an STP-rich region, and in humans, is anchored to the membrane by a GPI tail. However, TM and secretory forms have been identified in rats and mice.

CD46/MCP is composed of 4 SCRs, followed by a highly glycosylated STP region. There are 5 O-linked glycosylation sites in this region. CD46 is capable of 3 differentially spliced STP regions A, B and C. It is anchored to the membrane via a TM domain, and also has a cytoplasmic tail, of which there are 2 forms. SCRs 2-4 hold CD46's regulatory activity, while SCR 1 and 2 make up the measles virus receptor motif; SCR 2 has an N-linked glycosylation site. A short region of unknown function also exists.

Crry is a regulator possessing both decay-accelerating and cofactor activity for the CP and AP convertases, which is only expressed in rodents. Mice have a 5 SCR form, while 2 forms exist in the rat; 6 and 7 SCR forms. Crry is anchored to the membrane by a TM domain in all species, and has a cytoplasmic tail. Rat Crry has N-linked glycosylation sites on SCRs 4 and 5 in both the 6 and 7 SCR forms.

CR1 contains 30 SCR domains, arranged in 4 groups of 7 SCRs each, termed long homologous repeats (LHRs), and is anchored to the membrane via a TM domain. It also contains a cytoplasmic tail, and exhibits both decay-accelerating and cofactor activity (Harris and Morgan 1999)

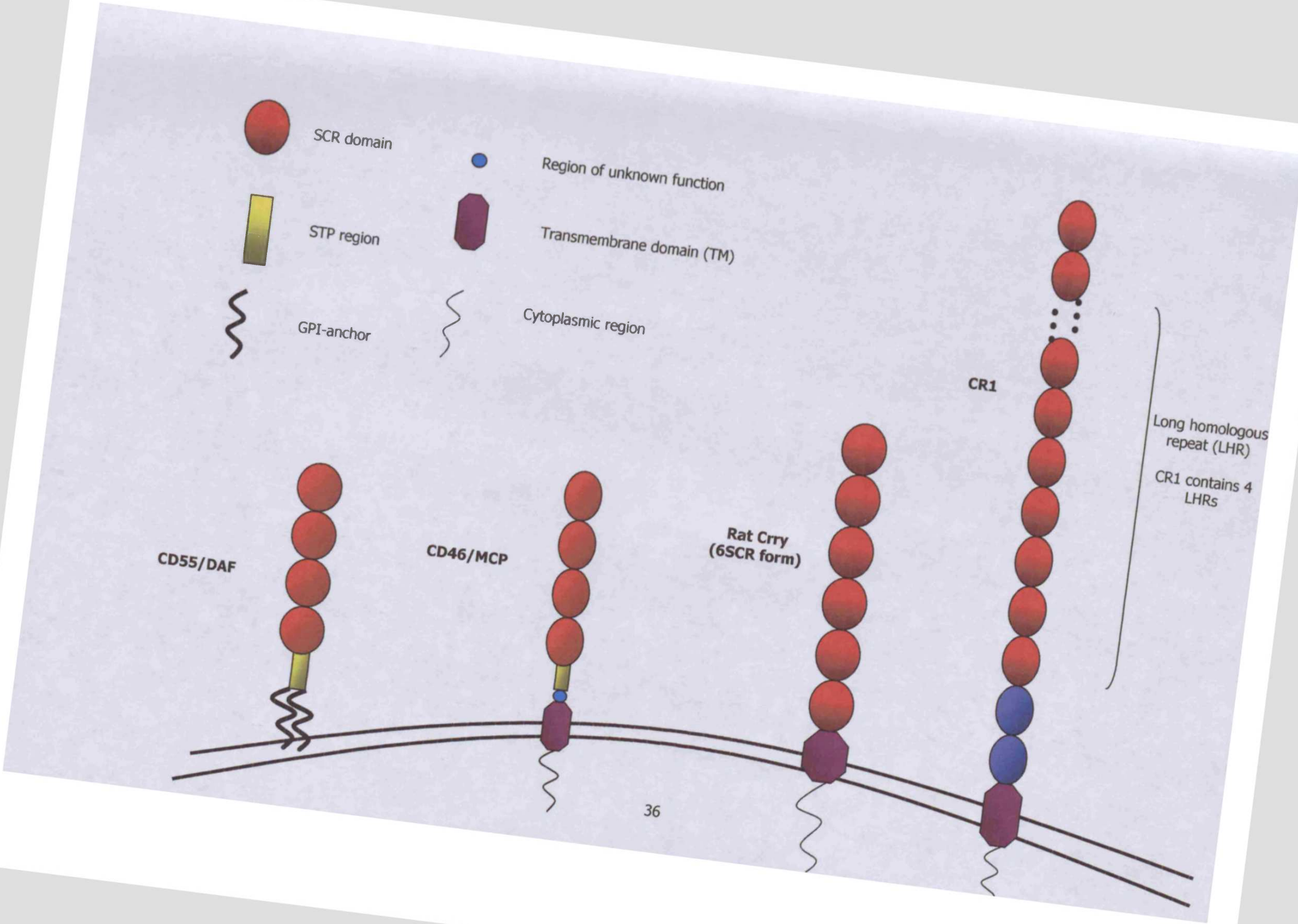
SCR domain
Region of unknown function
STP region
Transmembrane domain (TM)
GPI-anchor
Cytoplasmic region
CR1
Long homologous repeat (LHR)
CR1 contains 4 LHRs
CD55/DAF
CD46/MCP
Rat Crry (6SCR form)

1.3.4.3 Complement receptor 1 (CR1, C3b receptor, CD35)

CR1 is a multifunctional 200kDa transmembrane protein exhibiting both decay accelerating and co-factor activity. In humans, its main allelic form is composed of 30 SCR repeats, arranged into 4 sets of 7 SCRs termed long homologous repeats (LHRs) A, B, C and D where inter-LHR homology extends to 65-90%, and 2 membrane-proximal SCRs. CR1 also possesses a transmembrane domain and a cytoplasmic tail (Wong 1990) (Figure 4). A putative secretory form may be found in plasma (30ng/ml), probably as a result of enzymatic cleavage from the surface of leucocytes. An increase in plasma soluble CR1 is seen in liver disease, renal failure and in synovial fluids of patients with inflammatory joint disease (Yoon and Fearon 1985).

Human CR1 is expressed on B cells, FDCs, erythrocytes, polymorphonuclear cells and phagocytic macrophages (Janeway, Travers et al. 2001). CR1 encompasses the functions of both CD55 and CD46 by acting as a decay-accelerating factor and a cofactor for fI mediated cleavage of C3b and C4b. The binding sites for C3b and C4b are located in the first 3 SCRs of the first 3 LHRs. It is also responsible for the cleavage of iC3b into C3c and C3dg (Medicus, Melamed et al. 1983). Its major physiological action lies in immune complex (IC) processing, where ICs are coated with opsonins C3b, C4b or C1q, and are bound to CR1 on erythrocyte membranes. fI mediated cleavage of C3b for example, and subsequent formation of iC3b results in release of the IC. This is a dynamic event with the rapid 'on-off' binding mechanism facilitating transfer to tissue macrophages in the spleen and liver (Yokoyama and Waxman 1994).

An antibody-based approach was applied to the identification of murine CR1, which yielded two proteins; 190kDa (murine CR1, 21 SCRs) and 150kDa (murine CR2, 15 SCRs) (Molina, Kinoshita et al. 1990). Subsequent cloning revealed that CR1 and CR2, encoded on separate genes in man, are derived from the same gene (*mCr2*) located on the RCA cluster on chromosome 1 in mice. Mouse CR1 is expressed primarily on B cells and FDCs, but not on erythrocytes or platelets (Molina, Wong et al. 1992).

A putative CR1 analogue in rats has been identified on platelets, neutrophils and splenocytes, (Quigg, Galishoff et al. 1993), found to be a 200kDa C3b-binding protein distinct from CR1 (Quigg and Holers 1995).

CR1 provided a focus in the development of anti-C therapeutics, and to date, remains the only one to have been tested in humans. Soluble CR1 (sCR1) comprises the entire extracellular domain of CR1 (30 SCRs), and inhibits formation of C3 and C5 convertases (Yeh, Marsh et al. 1991). sCR1 has subsequently been tested extensively in a variety of animal models, e.g. hyperacute allograft rejection (Pruitt and Bollinger 1991), ischemia

reperfusion (Hill, Lindsay et al. 1992), experimental autoimmune encephalomyelitis (EAE) (Piddlesden, Storch et al. 1994), experimental autoimmune myasthenia gravis (EAMG) (Piddlesden, Jiang et al. 1996), experimental autoimmune neuritis (EAN) (Vrisendorp, Flynn et al. 1997), and more recently in clinical trials in high risk cardiac surgery patients requiring cardiopulmonary bypass (Lazar, Bokesch et al. 2004).

1.3.4.4 CR-1 related gene Y (Crry, 5I2 antigen)

Crry is a unique and powerful complement regulatory protein exclusive to rodents. It possesses both decay-accelerating and cofactor activity. Crry was first identified in mice through studies on mouse CR1. A 65kDa protein was isolated from a mouse spleen cell membrane preparation using a polyclonal antibody to human CR1, and termed p65 (Wong and Fearon 1985). Later, the same group identified genes relating to human CR1 in the mouse by cDNA library screening, one of which coded for a 5 SCR protein (Aegerter-Shaw, Cole et al. 1987). Complement regulatory activity was further demonstrated by transfection of the cDNA into K562 cells, where a reduction in CP-mediated C3 deposition was seen (Molina, Wong et al. 1992). Murine Crry was also shown to possess both decay accelerating and cofactor activity, and was originally thought to encompass both the functions of CD55 and CD46 (Kim, Kinoshita et al. 1995). Mouse Crry is known to possess decay accelerating activity for the C3 convertase of the CP, and to a lesser extent, the AP. The relative importance of Crry in the mouse is dramatically exemplified by observations that Crry-deficient mice die *in utero* due to severe C deposition and leucocyte infiltration on placental tissue. Breeding to C3-/- mice rescued Crry-/- mice from this lethality (Xu and Mao 2000)

Rat Crry was discovered through studies using rat glomerular epithelial cells and anti-human CR1 antibodies, which identified a 70kDa protein presumed to be rat Crry (Quigg, Galishoff et al. 1993). In addition, a Japanese group had identified a monoclonal antibody (5I2) capable of enhancing the susceptibility of rat erythrocytes to C-mediated lysis. The antigen ran as a doublet by SDS-PAGE of 55 and 65kDa, and subsequent peptide sequencing revealed significant homology to mouse Crry (Takisawa, Okada et al. 1994). Two isoforms of rat Crry exist: a 6 SCR form (Sakurada, Seno et al. 1994), and a 7 SCR form, essentially a duplication of SCR 6 thought to extend the function of the molecule (Quigg, Lo et al. 1995).

Rat Crry inhibits both the CP and the AP. Function blocking experiments in the rat using a mAb resulted in hypotension, increased vascular permeability, leucocytopaenia and thrombocytopaenia (Matsuo, Ichida et al. 1994). In addition, mAb blocking of Crry following LPS priming in rats led to lethal shock, which was rescued by CVF treatment, or by sCR1 treatment (Mizuno, Nishikawa et al. 2002).

Both mouse and rat Crry are abundantly expressed on all circulating cells, epithelia and most tissues. Since Crry is so powerful in its complement-regulatory activities, an alternative

role is suggested for CD55 and CD46 in rodents, which have limited and tissue-specific distribution (Harris and Morgan 1999).

1.3.5 Ly-6 superfamily CReg

1.3.5.1 CD59 (protectin, H19, MAC inhibitory factor, membrane inhibitor of reactive lysis (MIRL))

CD59 is a small (19kDa) highly glycosylated GPI-anchored protein capable of inhibiting MAC formation by preventing C9 incorporation (Figure 5). It is the sole membrane regulator of the terminal pathway (Davies, Simmons et al. 1989), and its role in maintaining homeostasis is dramatically exemplified in the acquired haematological disorder paroxysmal noctural haemoglobinuria (PNH), where the lack of GPI-anchored proteins sensitises erythrocytes to autologous C-mediated lysis and activation, leading to haemolytic anaemia and thrombosis. Although lack of CD55 would also contribute to this phenotype, studies on isolated deficiency of CD59 demonstrated haemolysis and thrombosis (Yamashina, Ueda et al. 1990). CD59 is widely expressed on all circulating cells in humans, endothelia, epithelia and on organs. It is also found in urine (1-4μg/ml and lacks the GPI-anchor), amniotic fluid, seminal plasma, breast milk (associated with lipid and retains GPI-anchor), and cerebrospinal fluid (Watts, Dankerts et al. 1990).

CD59 belongs to the Ly6 family of proteins characterised by evolutionary conservation of the arrangement of disulphide bridges (Philbrick, Palfree et al. 1990). Other members of the family include the mouse protein Ly6, and the urokinase-plasminogen activator receptor (UPAR). This complex cysteine-rich structure has also been found in snake venom toxins such as Bungarotoxin (Miwa, Ibanez-Tallon et al. 1999). Evidence that these proteins belong to the same family comes from the similarity of the organisation of the genes encoding them. The coding region consists of an exon coding for most of the leader peptide sequence, a short exon encoding the first one–third of the protein, and a third longer exon coding for the remaining protein (Sawada, Ohashi et al. 1990). The mature CD59 protein is composed of a single 77aa chain containing 10 cysteine residues which form 5 intra-chain disulphide bonds, essential for function. The signal peptide is removed concurrent with addition of the GPI-anchor. All proteins share a canonical structure consisting of a central hydrophobic core with three finger-like loops held by disulphide bridges extending from it. A fourth loop is also present, although is always small and the distal cysteine is always followed by an arginine. CD59 is unique within the Ly6 superfamily in that it contains a helical structure in the third and largest loop (Petranka, Zhao et al. 1996). CD59 binds to the

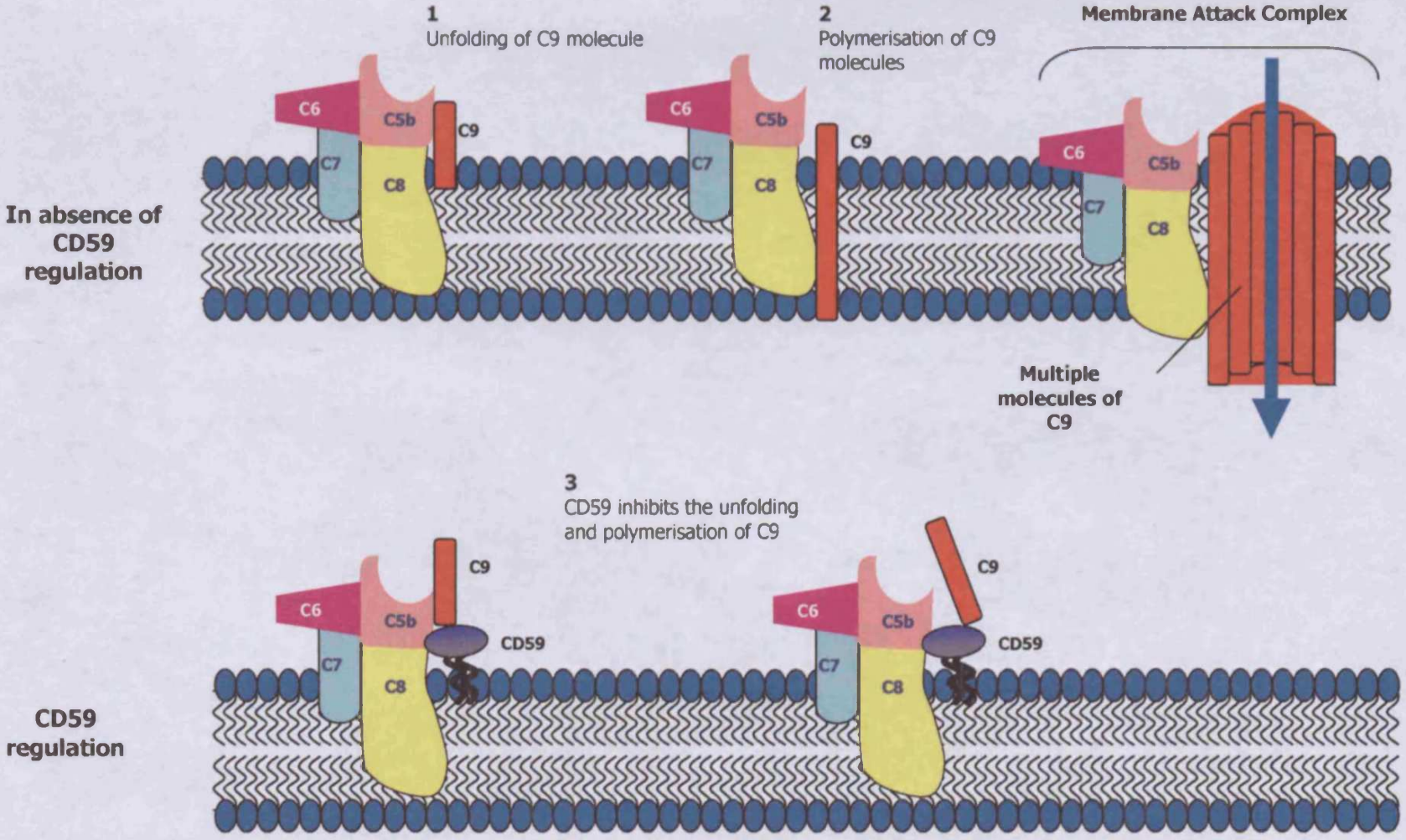

Figure 5 The basis of terminal pathway inhibitory activity of CD59
In the absence of regulation, normal unfolding and polymerisation of C9 molecule following binding of C5b-8 proceeds to complete the MAC (top panel). CD59 is a small GPI-anchored molecule capable of inhibiting unfolding and polymerisation of C9, thus inhibiting MAC formation (bottom panel).

α chain of C8 in the C5b-8 complex, and although a molecule of C9 is able to bind to C5b8-CD59 complex, further incorporation is prevented by CD59 binding to the carboxy-terminal domain of C9. Limited perturbation of the target membrane therefore occurs, but further MAC assembly is inhibited. Roles for CD59, distinct from C regulation have been suggested; in mediating natural killer cell cytotoxicity (Omidvar, Wang et al. 2005), enhancing fibroblast proliferation (Donev, Baalasubramanian et al. 2005), and down-modulation of CD4+ T cell activity (Longhi, Sivasankar et al. 2005).

The rat analogue of CD59 was isolated from erythrocyte membranes in 1992. Rat CD59 was partially purified by column chromatography and used to generate mAbs to be used for further affinity purification. The 21kDa protein obtained demonstrated inhibition of CVF-mediated reactive lysis of guinea pig erythrocytes (gpE) by rat C (Hughes, Piddlesden et al. 1992). Rat CD59 shared only 44% homology with human CD59 at the amino acid level, although it did share 5 disulphide bonds (Rushmere, Harrison et al. 1994). No species specificity for C inhibition was exhibited, and natural and recombinant forms of protein have been shown to be capable of inhibiting human C (Rushmere, Tomlinson et al. 1997).

The mouse analogue was isolated from a mouse kidney cDNA library using the rat CD59 coding region as a probe. Mouse CD59 is 22-24kDa, and is widely expressed (Powell, Marchbank et al. 1997). Targeted deletion of the mouse CD59 gene resulted in a paroxysmal nocturnal haemoglobinuria (PNH)-like phenotype, with erythrocytes from the CD59-deleted mice more susceptible to C-mediated lysis than heterozygotes or wild-type mice, in addition to evidence for spontaneous intravascular haemolysis (Holt, Botto et al. 2001). This phenotype was mild compared to that seen in humans with CD59 deficiency; however, in contrast to humans, mice also express the powerful CReg Crry, and thus its presence most likely explains this mild phenotype. The discovery of two genes coding for CD59 in the mouse, added a level of complexity that was absent from all other species tested. The two genes, designated *cd59a* and *cd59b* were found to be 63% identical, and initial analysis suggested that distribution of CD59b was restricted to the testis (Qian, Qin et al. 2000). This data was confirmed in studies performed in our laboratory using the CD59a knockout mice, which showed that expression of CD59b was indeed restricted to the testis (Harris, Hanna et al. 2003).

However, later studies by Qin and co workers on the analysis of distribution of the two forms stated that both genes were widely expressed in all tissues examined (Qin, Miwa et al. 2001). Further to this work, the same authors generated a mouse deficient in *cd59b*. The mice exhibited a severe PNH-like phenotype, with a progressive loss of fertility, and the authors concluded that mCD59b is the key CReg in mice (Qin, Krumrei et al. 2003). Work completed in our laboratory, using new specific reagents contradicted this evidence, and demonstrated conclusively that CD59b is detectable only in testis and in trace amounts in

bone marrow and erythrocytes, and was only capable of inhibiting C-mediated lysis in the absence or blocking of CD59a. CD59a is therefore the primary regulator of MAC in the mouse (Baalasubramanian, Harris et al. 2004).

1.3.6 Fluid phase regulation of the terminal pathway

The C system has evolved a neat way of regulating the terminal pathway itself; the C5b-7 complex is able to dissociate from the membrane, and attach to adjacent membranes. However, if C8 binds the fluid phase complex, the labile binding site of the complex is masked, and the complex is unable to attach to the target membrane. It is only when C8 binds to membrane-associated C5b-7 that the MAC may form.

In addition to this regulation, other fluid phase inhibitors are available to bind the C5b-7 complex, S-protein and Clusterin.

1.3.6.1 S-Protein

S-Protein is an 80kDa adhesive glycoprotein composed of two disulphide-linked chains, capable of inhibiting the formation of the MAC by binding C5b-7 in the fluid phase. It is composed of a single polypeptide chain of 478 residues; the mature protein contains several domains. An RGD domain within residues 45-47 is responsible for the adhesive properties. S protein functions by binding the C5b-7 complex to form the non-lytic sC5b-7. This masks the transient hydrophobic membrane-binding site in fluid phase C5b-7 (Dahlback and Podack 1985). Another mechanism for inhibition has been proposed involving S-Protein inhibition of C9 polymerisation, thus MAC formation. Although these proteins are highly conserved between species, there have been no specific studies to address this. However, S-Protein deleted mice appear normal with no evidence of inappropriate C activation (Zheng, Saunders et al. 1995).

1.3.6.2 Clusterin

Clusterin is a heterodimeric serum glycoprotein capable of many functions including C inhibition and cholesterol transport. Clusterin is composed of 2 non-identical subunits, α and β, of the same molecular weight (40kDa), which are heavily glycosylated. Clusterin inhibits C5b-6-initiated C haemolysis (Kirszbaum, Sharpe et al. 1989), but may also have a potential role in reproduction, being present at 2-15mg/ml in seminal plasma, compared with just 35-105µg/ml in serum. Normal sperm do not express clusterin, but abnormal sperm stain strongly and are prone to aggregation (O'Bryan, Baker et al. 1990).

1.4 Complement and Autoimmunity

Autoimmune disease occurs when specific adaptive immune responses are directed towards self-antigens. Usually, when this response is directed against a pathogen, the pathogen is subsequently eliminated; however, these same effector mechanisms are usually unable to completely eliminate the antigen when the antigen is self, thus perpetuating a sustained inflammatory response. The consequence is chronic inflammation to tissues which may prove lethal (Janeway, Travers et al. 2001).

Autoimmunity is thought to be triggered in much the same way as an adaptive immune response, i.e. initiated by activation of antigen-specific T cells, which may cause damage directly or indirectly. Cytotoxic T cells and macrophage activation by T_H1 cells have the potential for extensive tissue damage. In addition, inappropriate activation of T cell help to B cells may initiate pathogenic B cells responses and subsequent C activation via the CP (Maurer and Gold 2002). The degenerate nature of the T and B cell repertoire which allows them to recognise an almost unlimited number of antigens is often viewed as a double-edged sword since it is this large repertoire that carries the potential for recognition of self-antigens. Most high affinity anti-self receptors are deleted during development, but some low affinity receptors may remain. The trigger for autoimmunity remains unknown, although evidence clearly suggests a role for environmental and genetic factors (Janeway, Travers et al. 2001).

When activated inappropriately, such as in autoimmunity, C can be a potent mediator of tissue damage and inflammation. C activation and subsequent pathogenesis has been implicated in a variety of autoimmune disease. Two such examples are the demyelinating peripheral neuropathy Guillain-Barré Syndrome (GBS), and the neuromuscular conduction disorder Myasthenia Gravis (MG), which will be the focus of this thesis. The next section will concentrate on GBS, and give an overview of the Peripheral Nervous System (PNS) followed by an outline of GBS, the role of C in mediating this disease, and the use of animal models. The subsequent section will focus on MG, and provide an overview of muscle function and contraction, the role of C in mediating disease and the use of animal models.

1.5 The PNS

The PNS is the part of the nervous system consisting of everything but the brain and spinal cord. It is composed of neurons and supporting cells connecting the central nervous system (CNS) to the rest of the body.

1.5.1 The Structure of the PNS

Neurons are perfectly adapted for the function of receiving, conducting and transmitting signals. They are extremely elongated, consisting of a cell body capable of receiving signals, with a number of long, thin processes radiating from it, together with a long axon to conduct the signals away from the cell body and toward distant targets. In addition, numerous branching dendrites extend from the cell body, rather like antennae, providing a larger surface area to receive signals (Figure 6).

Axons of many vertebrate neurons are surrounded by an insulating myelin sheath, enabling the axon to greatly increase the rate at which it conducts an action potential. The importance of myelination is exemplified by the demyelinating disorders multiple sclerosis (MS) and GBS, both of which lead to destruction, either permanent or temporary of the propagation of nerve impulses in the central nervous system (CNS) and PNS respectively.

1.5.2 Structure of myelin

Myelin itself is synthesized by glial cells; in the PNS, these are called Schwann cells (oligodendrocytes in the CNS). These cells wrap layer upon layer of their own plasma membrane in a tight spiral around the axon, thereby ensuring complete insulation, and no leakage of current (Figure 7). This insulating sheath is periodically interrupted by nodes of Ranvier, where the majority of the sodium channels are located. The system is designed such that a depolarisation event at the membrane of one node is immediately conducted to the next node, thus an action potential is propagated by so called 'saltatory conduction' (jumping from node to node). This mode of conduction is not only rapid, but it also conserves metabolic energy since the excitation is confined to the nodes of Ranvier (Alberts, Bray et al. 1994). Myelin integrity is essential for the proper functioning of the nervous system and the rapid conduction of neural signals. Many diseases affecting the PNS do so via damage to myelin (Mathers 1985).

Schwann cells are most intimately associated with peripheral axons, and are derived from the embryonic neural crest. Generally, single Schwann cells are responsible for the myelination or ensheathing of only one axon. However, each axon may be myelinated by multiple Schwann cells. When an axon is encircled by one layer of Schwann cell cytoplasm and membrane, it is said to be ensheathed; however, an axon may be encircled with multiple layers of Schwann cell membranes, and thus the cytoplasm between these layers is

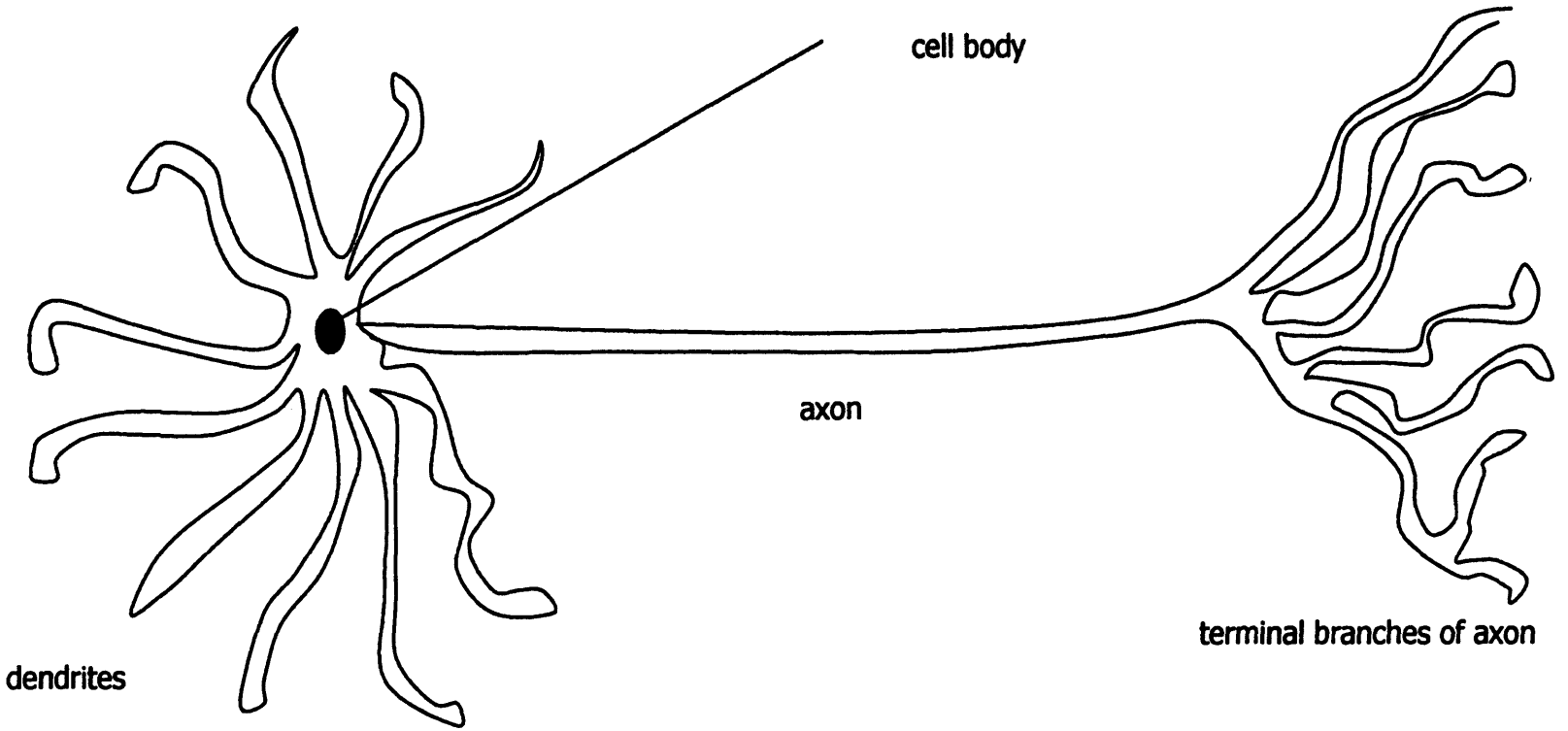

Figure 6 Schematic diagram of a typical vertebrate neuron

Neurons have an elongated structure, composed of a cell body with dendrites radiating from it, a long axon so as to enable conduction of signals to distant targets, together with terminal branches, all of which demonstrate its suitability to perform the functions of signal reception, conduction and transmission.

Adapted from (Alberts, Bray et al. 1994)

I

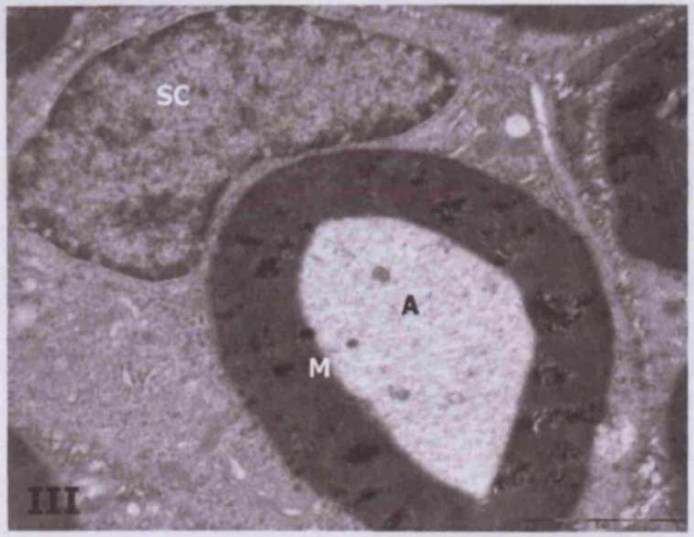

III

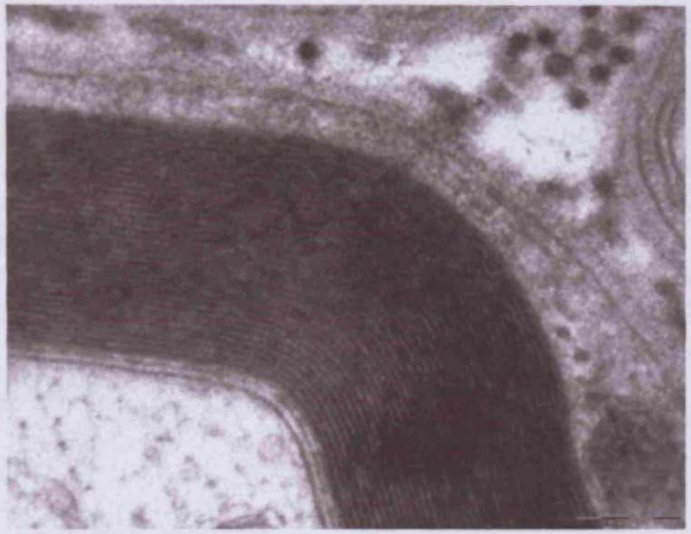

II

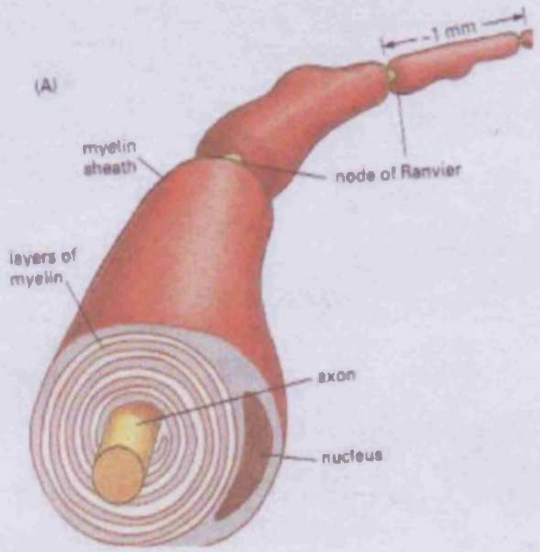

Figure 7

Schwann cells are responsible for myelination of PNS axons

Panel I shows a section of rat sciatic nerve under an electron microscope (EM), with a Schwann cell (SC) surrounding an axon (A) surrounded by layers of myelin (M) (panel I, scale bar = 2μm). Schwann cells wrap layer upon layer of their own cytoplasm around an axon to provide an insulating layer which will allow faster nerve conduction (schematic, panel II). High power EM analysis allows visualisation of the individual layers of myelin laid down by the Schwann cell forming tight insulation around the axon (panel III, scale bar = 200nm)

Electron micrographs are author's own. Panel II was taken from (Alberts, Bray et al. 1994).

squeezed out, and forms concentric layers of myelin around the shaft of the axon. These axons are said to be myelinated. Exterior to the Schwann cell layer is the basal lamina composed of collagen, and functions to exclude large molecules. Outside the basal lamina is the innermost of three layers of connective tissue, the endoneurium that surrounds individual axons. In the majority of peripheral nerves, individual axons collect into discrete bundles or fasicles, and are surrounded by perineurium. Several fasicles grouped together comprise the peripheral nerve, with the connective tissue surrounding the entire structure called the epineurium (Midroni and Bilbao 1995) (Figure 8).

1.5.3 Myelin proteins in the PNS (Figure 9)

1.5.3.1 Myelin Protein Zero (MPZ, PO)

PO is the major integral protein of the PNS in higher vertebrates. It accounts for more than 50% of PNS myelin proteins (Kursula 2001). It plays a critical role in myelin formation and maintenance of membrane packing in the internodal region of the myelin sheath. Its importance is dramatically exemplified by the severe hypomyelination and myelin degeneration observed through the disruption of the PO gene in mice (Giese, Martini et al. 1992), and in the knockout mouse (Martini, Zielasek et al. 1995). In addition, several peripheral neuropathies correlate with mutations and deletions in the human PO gene (Warner, Hilz et al. 1996). PO is an adhesion molecule of the functionally diverse immunoglobulin superfamily, and its extracellular domain contains a single immunoglobulin loop and carries a HNK-1 carbohydrate motif. The cytoplasmic domain by contrast holds a basic charge, and functions to hoid the cytoplasmic leaflets of myelin together by electrostatic interactions with membrane lipids (Kursula 2001). The human PO sequence shares 97% homology with the rat sequence; the only differences being in 3 residues in the extracellular domain. In its native form, PO is N-glycosylated at Asn93, and molecular modelling studies have demonstrated that the carbohydrate may function to maintain the orientation of PO extracellular domain at the membrane surface (Wells, Saavedra et al. 1993). Studies on the crystal structure of PO extracellular domain indicate that the domain forms homotetramers, which function, in opposing myelin membranes, to form and maintain compact myelin (Kursula 2001).

1.5.3.2 Peripheral myelin protein 22 (PMP-22)

PMP-22 is a 22kDa transmembrane protein expressed on Schwann cell and by compact myelin, and constitutes between 2-10% of total peripheral nerve myelin (Snipes, Suter et al. 1992). Tandem duplication of chromosome 17 within the gene for PMP-22 is responsible for hereditary motor and sensory neuropathy type 1a (HMSN 1a) (Matsunami, Smith et al. 1992), as well as point mutations within the gene (Valentijn, Bolhuis et al. 1992). The exact

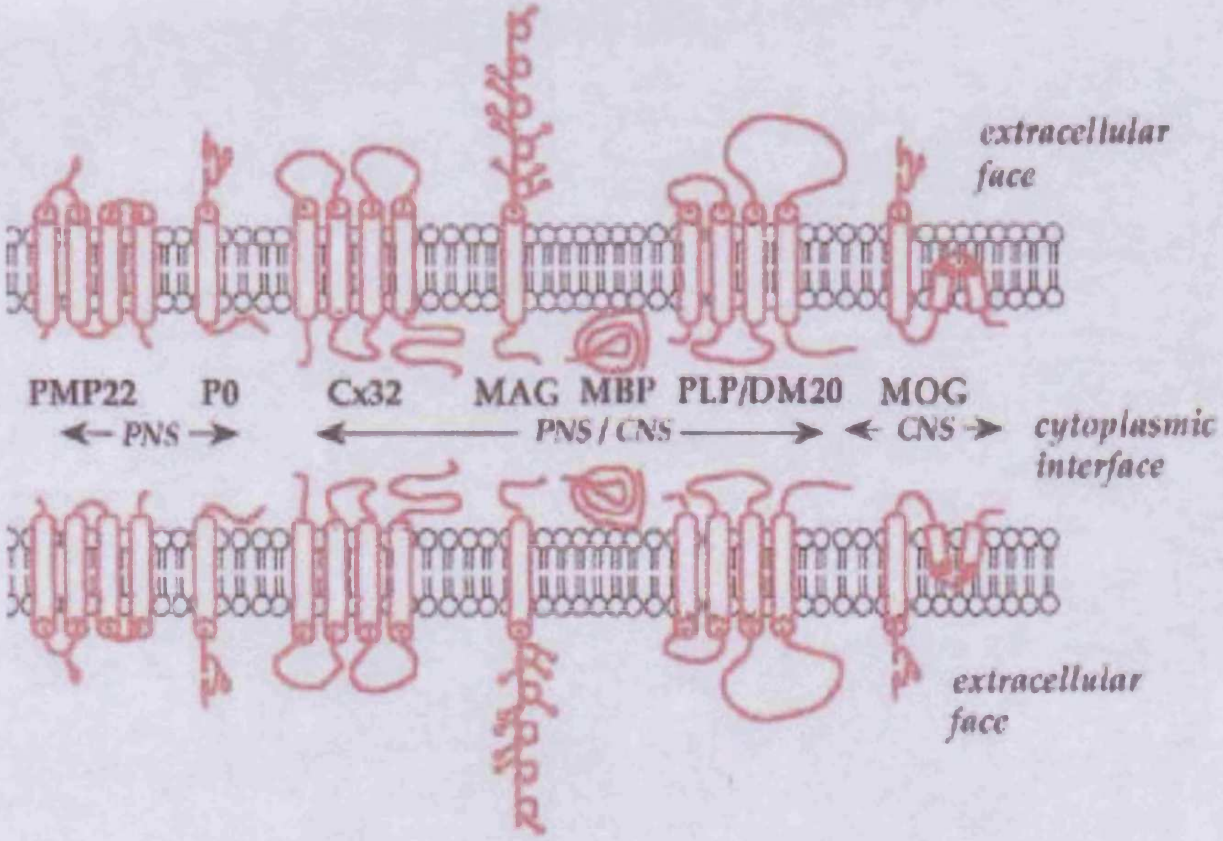

Figure 9 Structure and composition of myelin proteins in the PNS and CNS

PNS myelin contains proteins, such as PMP22 and PO, which are found exclusively in the PNS; others, e.g. Cx32, and MBP are found both in the PNS and the CNS, while MOG is exclusive to the CNS. All proteins have an extracellular domain, a transmembrane region, and various cytoplasmic tails, with the exception of MBP.

Taken from (Baumann and Pham-Dinh 2001)

function of the protein within myelin is poorly understood, although rats over expressing a transgene for PMP-22 exhibit a hypomyelinating peripheral neuropathy (Sereda, Griffiths et al. 1996). Studies have hinted at a role for PMP-22 in Schwann cell-axon adhesion (Snipes, Suter et al. 1992), intercellular signalling (Snipes, Suter et al. 1993), and in the control of Schwann cell growth cycle (Zoidl, Blass-Kampmann et al. 1995).

1.5.3.3 Myelin Protein 2 (P2)

P2 is a 14.8kDa highly basic cytosolic protein found on the cytoplasmic side of compact myelin (Trapp, Dubois-Dalcq et al. 1984). Its function lies in binding of fatty acids, particularly oleic acid, retinoic acid and retinol. Possible roles for this protein include fatty acid targeting to metabolic pathways, and maintenance of intracellular fatty acid pools (Jones, Bergfors et al. 1988).

1.5.3.4 Myelin basic protein (MBP)

MBP is a highly basic protein found at the cytoplasmic surfaces of compact myelin membranes, and accounts for between 5-15% of peripheral nerve myelin (Kursula 2001). MBP comprises a family of proteins containing many isoforms coded by alternative transcripts from the MBP gene. Of particular note here, the 17 and 25kDa isoforms in humans are expressed during myelinogenesis, and re-expressed during chronic lesions in MS; their expression correlates with remyelination. Post-translational modifications may occur in MBP including amino terminal acetylation, phosphorylation and methylation (Baumann and Pham-Dinh 2001). Its strong positive charge suggests a role complimentary to that of PO in myelin compaction via electrostatic interactions with the cell membrane (Kursula 2001).

1.5.3.5 Myelin-associated glycoprotein (MAG)

MAG constitutes only 0.1% of total protein in myelin within the PNS, and like the other proteins, has a high degree of glycosylation. Two isoforms exist; large MAG (L-MAG, 72kDa) and small MAG (S-MAG, 67kDa) which arise by alternative splicing. MAG proteins have a membrane-spanning domain and extracellular portion closely resembling immunoglobulin domains (Baumann and Pham-Dinh 2001). MAG function has been studied by generating MAG knockout mice. Of particular relevance to the PNS is the study involving L-MAG mutants, where mice expressed a truncated form of L-MAG while S-MAG expression was unaffected. PNS axons and myelin did not degenerate in contrast to the peripheral neuropathy observed in total MAG knockout animals. This suggests that S-MAG alone is sufficient to maintain PNS integrity (Fujita, Kemper et al. 1998).

1.5.3.6 Connexin 32 (CX-32)

Connexins are the basic subunit from which gap junctions are derived. Gap junctions themselves are responsible for the exchange of small molecules (less than 1kDa) between cells, and provide a mechanism for the propagation of signalling molecules and metabolites. Connexins are highly conserved, and 15 isoforms have been identified in rodents to date. They consist of a 4-transmembrane domain, two extracellular loops, 1 intracellular loop and cytoplasmic N- and C- termini (Martin, Steggles et al. 2000). Recently, CX32 was localised to paranodal loops and Schmidt-Lanterman incisures of myelinating Schwann cells, where gap junctions are thought to be located enabling uni- and bi-directional transport of small molecules, possibly to regulate or facilitate myelin compaction (Meier, Dermietzel et al. 2004).

Mutations in genes encoding peripheral nerve proteins result in various neuropathies. For example, deletion of Ser34 within the extracellular domain of PO gene results in Charcot-Marie-Tooth disease type 1B (CMT1B) (Kulkens, Bolhuis et al. 1993), while duplication of the PMP-22 gene results in a demyelinating CMT phenotype. Patients with Cx32 mutations showed intermediate slowing of motor conduction velocity (MCV), predominantly axonal features and relatively mild demyelinating pathology (Hattori, Yamamoto et al. 2003).

1.6 Peripheral Neuropathy

Peripheral neuropathy is the pathology that results from a failure of the nerves to carry information to and from the brain and spinal cord. In the broadest sense, it refers to a scope of clinical syndromes affecting a variety of peripheral nerve cells and fibres, including motor, sensory, and autonomic fibres. Nerve damage may occur through inflammatory or infectious disease, e.g. GBS; hereditary disorder, e.g. CMT disease; systemic or metabolic disorders, e.g. diabetic neuropathy; and exposure to toxic compounds or neuropathy secondary to drugs.

1.6.1 Neuropathies associated with IgM monoclonal antibodies (M-proteins)

Monoclonal expansion of B cells and plasma cells results in the secretion of large amounts of monoclonal immunoglobulin or paraproteins known as monoclonal gammopathy. They may be polymers, monomers or fragments of immunoglobulin detectable by a narrow discrete spike (M protein) by electrophoresis. About 60% of paraproteins are due to multiple myeloma (MM). Of relevance to this study is that some patients with monoclonal gammopathy have an associated peripheral neuropathy. Neuropathy-associated monoclonal IgM gammopathies are usually non-malignant. The M protein binds to peripheral nerve proteins such as myelin-associated glycoprotein (MAG), sulfoglucuronyl paragloboside (SGPG) or sulfoglucuronyl lactosaminyl paragloboside (SGLPG) (Latov 1995). Of particular

relevance to this project is that P0-specific IgM producing monoclonal B cell lines have previously been established from patients with peripheral neuropathy associated with monoclonal gammopathy (Kvarnstrom, Sidorova et al. 2002), demonstrating the potential of P0 to act as a neuritogen.

This is a clear example of an antibody-mediated disease, and as such, C is likely to be involved in its pathogenesis. Previous studies demonstrated that intraneural injection of serum from patients with IgM M-protein that reacted with myelin-associated glycoprotein (MAG) into feline sciatic nerve resulted in C deposition on the myelin sheath, and subsequent demyelination (Hays, Latov et al. 1987). Passive transfer of serum from a patient with IgM-gamma-anti-sulfatide into newborn rabbits resulted in demyelinating lesions similar to those observed in the donor, with C deposition demonstrated on the peripheral nerve (Nardelli, Bassi et al. 1996).

1.6.2 GBS

GBS is a transient immune-mediated demyelinating disorder of the PNS. First described in 1916 by Guillain, Barré, and Strohl, GBS was a syndrome characterised by 'motor difficulty, abolition of deep tendon reflexes with preservation of cutaneous reflexes, parathesias without demonstrable objective sensory loss, pain on deep palpation of large muscles, minor modifications in electrical reactions of nerve and muscle, and increased albumin in the CSF' (Guillain, Barre et al. 1916). Following this, numerous reports appeared in the literature; German and French observers found that an inflammatory element with mononuclear cell infiltration was present within some autopsy nerve samples (Pette and Kornyey 1930) , (Alajouanine, Thurel et al. 1936). Haymaker and Kernohan performed a study of fatal GBS cases during World War I, recognised that the disorder was demyelinating, and believed lymphocytes to play a repair role (Haymaker and Kernohan 1949). In a landmark study, Prineas in 1972 analysed the ultra structural changes in the nerves of GBS patients, identifying a role for activated phagocytes in the mechanism of demyelination (Prineas 1972). Prineas further clarified the pathological features of GBS in 1981 (Prineas 1981). GBS is considered to be a post-infectious disease, and evidence comes from studies such as those undertaken in the Netherlands, where infections with *Campylobacter jejuni (C. jejuni)*, cytomegalovirus (CMV), Epstein-Barr virus (EBV) and *Mycoplasma pneumoniae (M. pneumoniae)* were shown to be significantly associated with GBS (Jacobs, Rothbarth et al. 1998). In addition, a Norwegian study reported that 60% of patients with GBS had preceeding respiratory infection, and 10% had gastrointestinal infections prior to GBS onset (Vedeler, Wik et al. 1997). Other infections implicated are leprosy, diphtheria, HIV, Lyme borreliosis, poliomyelitis and herpes zoster (Vedeler 2000).

1.6.1.1 Spectrum of GBS phenotype

GBS is characterised by a rapid onset symmetrical limb weakness, loss of tendon reflexes, absent or mild sensory signs, and variable autonomic dysfunctions (Hahn 1998). Weakness may occur acutely, i.e. within days, or sub-acutely over a period of a month. Upon reaching a plateau level, spontaneous resolution of paralysis may occur.

GBS does not refer to one disease; rather it includes several distinct subtypes which can be classified according to pathological and electrodiagnostic features (Table 2). The clinical-pathological spectrum of GBS extends from classical acute inflammatory demyelinating polyneuropathy (AIDP), to the various axonal forms; acute motor sensory axonal neuropathy (AMSAN), i.e. with sensory involvement, acute motor axonal neuropathy (AMAN), without sensory involvement, and clinical variants such as Miller-Fisher syndrome (MFS) (Hartung, Kieseier et al. 2001). Although complete and accurate epidemiological studies have been limited due to the absence of a definitive diagnostic test, population-based surveys attempting to document the annual incidence of GBS have been conducted in various countries worldwide and generally are in agreement on a rate of 1 to 4 per 100,000 persons (Hahn 1998). The most frequent pattern of GBS in Europe and North America is AIDP, whilst in China for example; the axonal patterns are prevalent (Vedeler 2000).

As many as two thirds of GBS patients report a preceding infectious illness, thus GBS is considered a post-infectious disease. Epidemiological studies show a slight increase in the number in young adults and also in the elderly, correlating with an increased risk of infections such as CMV and *C. jejuni*. In fact, *C. jejuni* has been recognised as the single most frequent preceding pathogen for GBS, including that in MFS (Hahn 1998).

1.6.1.2 Pathogenesis of GBS

There is general agreement that GBS is an immune-mediated disease. The immune reaction may be directed towards the Schwann-cell surface membrane or the myelin sheath, whereupon it results in the more common inflammatory demyelinating neuropathy (85% of cases), or the axon causing the acute axonal form (15% of cases) (Hahn 1998).

Classically, it was believed that macrophages, in the presence of lymphocytes, penetrate the basement membrane around intact nerve fibres and displace the Schwann cell membrane from the myelin sheath. 'Stripping' of the myelin sheath and dissolution of the myelin is performed by these macrophages, which may attack the myelin at the node of Ranvier. The association with macrophages and the finding that in the animal model, Experimental Allergic Neuritis (EAN), disease could be transferred by sensitised lymphocytes, led researchers to believe EAN was a cell-mediated immune response (Astrom and Waksman 1962). Further, ultrastructural studies have confirmed the presence of macrophages in the

GBS subtype	Clinical features	Epidemiology	Antecedent illness	Laboratory features	Histology	Pathogenesis
Acute inflammatory demyelinating polyneuropathy **(AIDP)**	Progressive weakness Numbness and tingling of lower limbs ascends to arms, trunk, head and neck Onset 2-4 weeks	1-4 per 100,000	Acute illness 1-3 wks prior to onset e.g. *C. jejuni* Cytomegalovirus EBV	Elevated CSF protein Anti-ganglioside Ab correlate with *C. jejuni* infection (molecular mimicry)	Perivascular mononuclear cell infiltrate (macrophage, lymphocytes) Nodes of Ranvier most susceptible Increased MMP-7, 9 around blood vessels in epineurium and endoneurium Increased MMP-9 in serum C-activation products on Schwann cells	T cell activation (sIL-2 R, IFN-γ in serum) Passive transfer of AIDP serum into animals results in C-dependent demyelination and conduction block Autoantibodies binds Schwann cells, activate C; recruit further inflammatory cells
Acute motor and sensory axonal neuropathy **(AMSAN)**	Rapidly progressive and severe generalised weakness Opthalmoplegia Difficulty swallowing – ventilator Sensations reduced Complete areflexia Autonomic dysfunction Onset 2-3 days Slow, incomplete recovery	Very rare	*C. jejuni*	Elevated CSF protein Anti-GM1 antibodies Evidence of *C. jejuni* infection	Performed early to aid diagnosis No demyelination or lymphocytic infiltrates Axonal degeneration in ventral and dorsal root and peripheral nerves Macrophage in periaxonal space	Immune-mediated attack on axon probably due to gangliosides GM-1 and GM1a on nodal axolemma C-activation on nodal axolemma Recruitment of macrophage Axonal degeneration

GBS subtype	Clinical features	Epidemiology	Antecedent illness	Laboratory features	Histology	Pathogenesis
Acute motor axonal neuropathy **(AMAN)**	Rapid onset of generalised weakness, particularly distal muscles Cranial nerve deficits, respiratory failure Absent sensory signs Autonomic dysfunction Recovery often within 1 year but residual limb weakness common Recurrence reported	High incidence in Northern China	GI infection *C. jejuni* in 30-85% patients	Elevated CSF protein Evidence of *C. jejuni* infection Anti-GM1 and anti-GD1a antibodies commonly detected	Nodal gaps lengthened at nodes of Ranvier (nerve fibre otherwise normal) IgG and C activation products on nodal and internodal axolemma of motor fibres Macrophages over nodes of Ranvier recruited via C analphylatoxin release, penetrate nodal gap into periaxonal gap. Severe cases exhibit axonal degeneration	Immune-mediated attack on nodal axolemma. Antibody binding to nodal axolemma +/- C activation leads to conduction block Axonal degeneration in presence of C activation,
Miller Fisher Syndrome **(MFS)**	Ataxia Areflexia Ophalmoplegia Double vision Facial weakness Dysphagia Dysarthria (speech disorder) Recovery begins approx. 2 weeks after onset; full recovery seen within 3-5 months	2:1 male predominance Mean age of onset 40 years	In Japan, higher frequency in Spring; 25% of GBS cases in Japan are MFS cf 1% of GBS in USA	Elevated CSF protein Evidence of *C. jejuni* infection Anti-GQ1b antibodies	Demyelination Mild inflammatory infiltrates in cranial nerves Infiltrates also in sensory ganglia of peripheral nerves	Oculomotor fibres and sensory ganglion enriched with GQ1b. Suggested molecular mimicry following *C. jejuni* infection Passive transfer of serum from MFS patient; anti-GQ1b antibodies binds NMJ in C-mediated process leading to massive quantal release of acetylcholine which blocks neuromuscular transmission.

GBS subtype	Clinical features	Epidemiology	Antecedent illness	Laboratory features	Histology	Pathogenesis
Chronic Inflammatory Demyelinating Polyradiculoneuropathy **(CIDP)**	Relapsing/ progressive course 'chronic GBS' Symptoms progressive over 2 months Analogous to MS, but limited to PNS Symmetrical proximal and distal weakness Motor and sensory involvement Areflexia Hyporeflexia 'Dropped head syndrome' 3-5% of patients show evidence of CNS demyelination	Adults 40-60 years	20-30% of patients	Elevated CSF protein in 80-95% of patients Monoclonal gammopathy Anti-GM-1, PO and P2 antibodies detected	Peripheral nerve and nerve root affected (occasional CNS involvement) Segmental demyelination and remyelination BUT multifocal so not evident in all cases Decrease in myelinated fibres Onion bulb formation Inflammatory infiltrates, Schwann cell proliferation Increased MMP-2, 9	Autoimmune Improvement after IVIg treatment suggests role for C and other humoral factors Activation of macrophages; penetration and engulfment of myelin Blocking of ion channels by auto antibodies in absence of demyelination

Table 2

Summary of the various subtypes of GBS listing clinical features, epidemiology, preceding illnesses, laboratory features, histological findings, and pathogenesis of disease (Fisher 1956), (Fross and Daube 1987), (McCombe, Pollard et al. 1987), (Asbury and Thomas 1995), (Plomp, Molenaar et al. 1999), (O' Leary and Willison 2000).

basal lamina and their subsequent penetration and ingestion of myelin lamellae (Prineas 1972), (Prineas 1981). The macrophages have Fc receptors enabling direct attachment to myelin-bound antibodies or Schwann cell antigens (Hughes, Atkinson et al. 1992b).

The current paradigm for the immune mechanism leading to the pathogenesis of GBS is that it is triggered by an initial infection leading to recognition of a specific auto-antigen by auto-reactive T cells, together with the simultaneous delivery of co-stimulatory molecules on the surface of antigen presenting cells such as macrophages. Activated T lymphocytes are permitted across the blood-nerve barrier (BNB) and into the PNS, assisted by chemokines, cellular adhesion molecules (CAMs) and matrix metalloproteinases (MMPs). Within the PNS, activated T lymphocytes can further activate macrophages leading to production of cytokines, release of toxic mediators, e.g. nitric oxide, MMPs and proinflammatory cytokines such as TNF-α or IFN-γ. Antibodies produced by B lymphocytes also contribute to demyelination and axonal damage via processes of antibody-dependent cellular cytotoxicity (ADCC), blocking of epitopes involved in nerve conduction and activation of C (Hartung, Willison et al. 2002). A summary flow chart simplifies this sequence of events (Figure 10).

1.6.1.3 Molecular mimicry and anti-ganglioside antibodies

Gangliosides are a group of sialic acid-containing glycosphingolipids found in the surface membranes of nerve cells. They are highly expressed in nervous tissues and are implicated in numerous biological functions.

The majority of patients with GBS subsequent to *C. jejuni* enteritis have IgG antibody to ganglioside GM1, while MFS patients have IgG antibody to GQ1b ganglioside. Studies in 1997 demonstrated the existence of molecular mimicry between the gangliosides above and lipopolysaccharide of *C. jejuni* isolated from a GBS and MFS patient. This 'molecular mimicry' between infectious agents and gangliosides is suggested to account for the production of anti- ganglioside auto-antibodies and development of peripheral neuropathy (Yuki 1997).

1.7 Animal models of peripheral neuropathy

A limited understanding into the human disease has been gained from biopsy material and other *ex-vivo* analysis. However, animal models offer the possibility to study the intricate interaction of genetic and immunological factors. They provide a rational basis to gain understanding of the pathogenesis of peripheral neuropathy, and provide a platform for new therapeutic strategies in treating human inflammatory neuropathies.

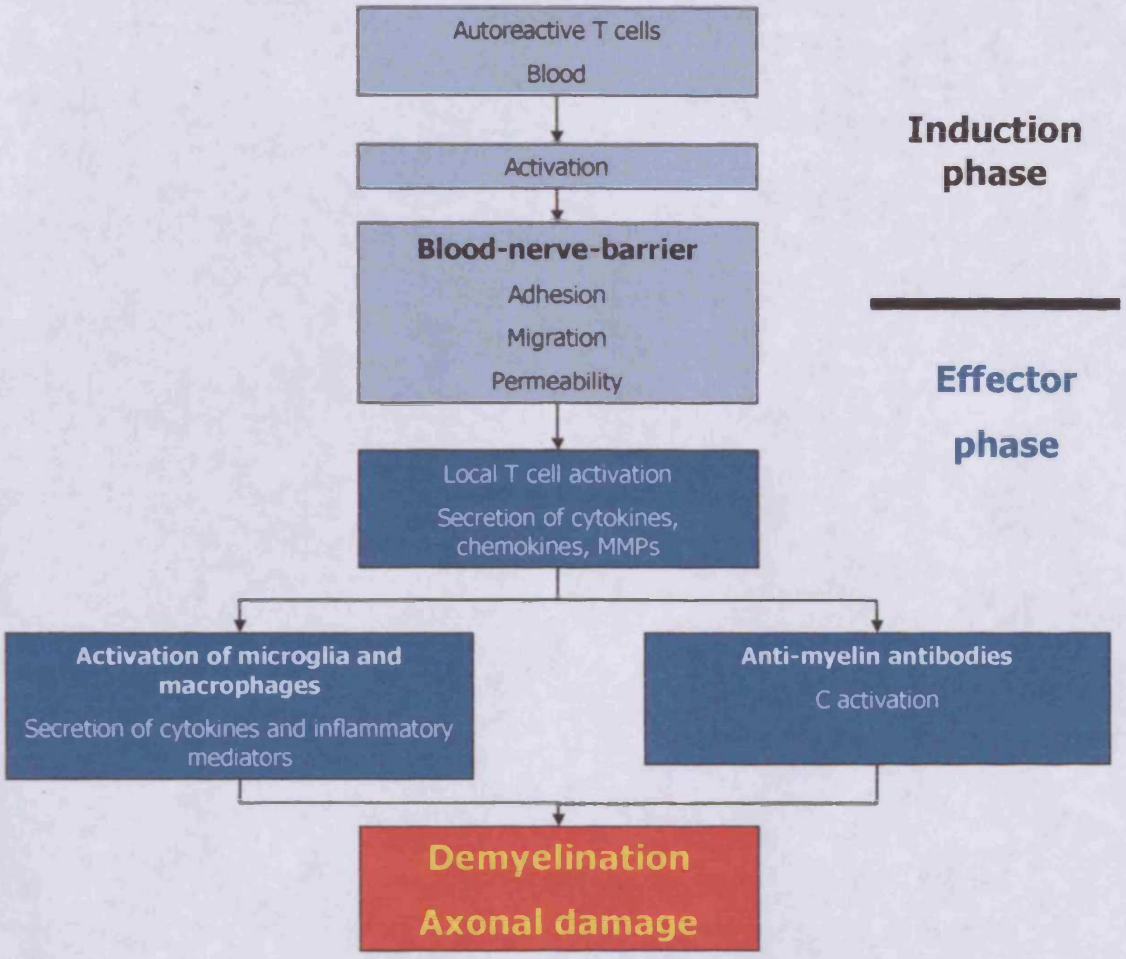

Figure 10 Summary chart of pathogenesis of immune-mediated neuropathies

Immune-mediated neuropathies follow a biphasic disease course, with an induction phase followed by an effector phase. Within the induction phase, autoreactive T cells in the blood become activated, and cross the blood nerve barrier; within the effector phase, local T cell activation, in association with secretion of cytokines, chemokines and matrix metalloproteinases (MMPs), leads to activation of microglia and macrophage. B cell involvement results in the generation of anti-myelin antibodies leading to C activation. Both of these mechanisms lead to demyelination and axonal damage.

Modified from (Maurer and Gold 2002)

1.7.1 Experimental Autoimmune Neuritis (EAN)

Preliminary work in the development of EAN was described by Waksman and Adams, where inoculation of rabbits with homogenised PNS tissue induced chronic EAN (Waksman and Adams 1955). EAN has subsequently been actively induced in susceptible strains of various species by immunisation with various PNS antigens combined with Freunds Complete Adjuvant (FCA), chronically induced using galactocerebrosides, and by adoptive transfer of T cell lines reactive to peripheral myelin proteins.

1.7.1.1 Disease mechanisms in EAN: Modelling acute EAN

The generation of auto-aggressive T cell lines produced a wider understanding of the immune mechanisms at play in peripheral neuropathy. T cell lines (CD4+) reactive with P2 were established *in vitro,* transferred intravenously into the rat, and were found to transfer disease (Linington, Izumo et al. 1984). This provided the first demonstration that acute EAN was a CD4+ T cell dependent, MHC restricted disease. Detailed pathology was subsequently published using this model, demonstrating almost complete restriction of histological changes to the PNS. Lesions developed from day 4 p.i., and were composed of oedema, cellular infiltrates (both mononuclear and granulocytes), demyelination and axonal degeneration. Such changes were most severe in the sciatic nerve and lumbrosacral nerve roots (Izumo, Linington et al. 1985). Additionally, electrophysiological examination of rats injected with these P2-specific T cell lines revealed nerve conduction failure and conduction slowing in the peripheral nerves and roots starting 72 hours following T cell transfer (Heininger, Stoll et al. 1986). Together, these studies defined the minimum requirement for disease induction as a CD4+, MHC class II restricted PNS–specific T cell response.

Susceptibility to EAN has been shown to differ widely between different inbred strains of rat (Zhu, Zou et al. 1998), underlining the influence of genetic factors. MHC polymorphisms are one factor that can influence genetic susceptibility to EAN (de Graaf, Wallstrom et al. 2004). T cells recognise cell-bound antigen is association with MHC molecules, known as MHC restriction. Antigen processing involves the degradation of antigen into peptide fragments; only a minority of these fragments are able to bind a particular MHC molecule. The relative importance of different amino acids within a defined epitope can be investigated by amino acid substitutions at different sites; such studies have enabled conclusions as to which amino acids contact the MHC and which contact the TCR. The peptide-binding site on the MHC molecule has a plethora of pockets, clefts, ridges, intrusions and depressions. Its precise topology depends largely on the nature of the amino acids within the groove, and therefore varies form one haplotype to another. Peptide binding depends also on the nature of the amino acid side chains, and their complementarity within the MHC molecule's binding groove. Three-dimensional analysis of MHC class II molecules has revealed a clear picture of

the peptide residing in the binding groove. The cleft incorporates a number of binding pockets; however, in MHC class II molecules, the cleft is not closed at each end, therefore the peptides extend out of the sides of the groove. Consistent with this observation is the fact that peptides eluted from MHC class II molecules tend to be longer than their MHC class I counterparts (approximately 15aa) (Roitt, Brostoff et al. 1998).

Single amino acid substitutions within a peptide sequence in the context of MHC molecules have profound effects on the T cell repertoire. A study by de Graaf and colleagues investigated the influence of antigen and MHC class II molecules on the T cell repertoire *in vivo* using the rat EAE model. Investigators examined the effect of immunising either MBP 63-88 (rat) or MBP 63-88 (guinea pig) which differ in the core region of the peptide binding site at position 79 (threonine to serine), and of altering the MHC by immunising MHC congenic LEW (RT1(1)) and LEW.1.W (RT1u) in the development of EAE in the rat. Results demonstrated that only MBP63-88 (guinea pig) in the context of RT1 haplotype in the Lewis rat lead to a strong expansion of activated T cells in the CNS. This small substitution therefore had a strong influence on the encephalitogenic potential of the peptide, and therefore the number of T cells infiltrating the CNS (de Graaf, Berne et al. 2005). Thus even minor changes in the side chains of amino acids within an autoantigen can dramatically alter TCR avidity for some MHC class II peptide complexes.

With respect to the EAN model, Linington and co-workers demonstrated that alternate PNS myelin proteins were capable of inducing disease. Two distinct T cell epitopes were identified in the PO protein; peptide 56-71 located in the extracellular Ig-like domain of PO, and 180-199 located within the cytoplasmic carboxyterminal domain of PO. AT of CD4+ T cells specific for these peptides were capable of inducing disease. Immunologic properties of both peptides *in vivo* was very different; while PO 180-199 was immunodominant in animals immunised with purified PO, no response to peptide 56-71 was detected suggesting that the epitope was cryptic (Linington, Lassman et al. 1992). Due to the post-infectious nature of GBS, research into the possiblity of molecular mimicry of viral antigens to epitopes on PO was examined. Absolute sequence homology involving 5 or more consecutive amino acids was demonstrated between PO and sequences within Epstein-Barr virus (EBV), cytomegalovirus (CMV), Varicella zoster virus (VZV) and human immunodeficiency virus (HIV) (Adelmann and Linington 1992). More recently, AT of P2-specific T cell lines into newborn, 3 day old, and adult Lewis rats has been used to test age-dependence of disease initiation. Results showed only minor nerve fibre degeneration in newborn rats but clinical disease in neonates associated with an inflammatory response (Pilartz, Jess et al. 2002). AT-EAN has also been used to assess the accumulation of Ig across the BNB. Ig accumulation was maximal during neurological deficit, and declined before onset of recovery (Hadden, Gregson et al. 2002).

Although EAN is a T cell mediated disease, a potential role for C and pathogenic antibodies has been demonstrated by many groups. Exacerbation of EAN was demonstrated by immunisation of systemic anti-myelin concurrent with AT of P2-specific T cells. The authors suggested that neural antigen-specific T cells breach the blood-nerve-barrier (BNB), facilitating access of demyelinating antibodies to the peripheral nerve (Spies, Pollard et al. 1995). Subsequently, systemic C depletion has been shown to reduce inflammation and demyelination in EAN in the rat (Jung, Toyka et al. 1995), (Vrisendorp, Flynn et al. 1995; Vrisendorp, Flynn et al. 1997), (Vrisendorp, Flynn et al. 1998).

1.7.1.2 Modelling chronic forms of GBS (CIDP)

Chronic EAN has been induced by the immunisation of rabbits with galactocerebroside, as a model of progressive CIDP. IgG antibodies to galactocerebroside were detected in serum, and IgG deposits were detected in spinal roots long before onset of clinical disease. This mimics human CIDP since disease is progressive over a period of two months. This also underscores the pathogenic contribution of circulating auto-antibodies in the induction of demyelinating lesions. T cell infiltration was absent even in the presence of high titres of antibody, although macrophages were present. Passive transfer of antiserum from diseased rabbits was able to induce demyelination in recipient rat peripheral nerve (Heininger, Stoll et al. 1986).

Attempts have also been made to model relapsing CIDP in the Lewis rat by repeated transfer of P2-specific T cell lines. Each transfer resulted in a relapse accompanied by weight loss, and hind limb paralysis, followed by a recovery. Multiple transfers resulted in incomplete recovery, leaving a neurological deficit during remission. During the active phase of disease, massive inflammation within the PNS was associated with nerve fibre destruction and Wallerian degeneration, i.e. the separation of a part of an axon from the neuronal cell body resulting in the degeneration of the distal axonal segment. Selective primary demyelination was associated with remyelination in a minority of affected nerve fibres, and some CNS involvement was evident (Lassman, Fierz et al. 1991).

1.7.1.3 Modelling axonal forms of GBS (AMAN, AMSAN)

Yuki and co-workers (Yuki, Yamada et al. 2001) recently established a model of an axonal form of GBS by immunisation of rabbits with bovine brain ganglioside. Following sensitisation, all rabbits developed high titres of anti-GM1 antibodies, acute flaccid limb weakness associated with a monophasic disease course. Histological analysis demonstrated a predominant Wallerian-like degeneration in the absence of lymphocytic infiltration and demyelination. In addition, IgG deposits were localised to the axons of anterior roots. GM1

was found to be present on axons, and sensitisation with purified GM1 proved conclusively that it was GM1 acting as the immunogen (Yuki, Yamada et al. 2001).

1.7.1.4 Modelling inherited peripheral neuropathies

Inherited peripheral neuropathies are caused by various genetic defects in peripheral nerve proteins, for example, PO, PMP-22 and Cx32. Both spontaneous and engineered rodent mutants are available with mutations similar to those found in humans. The pathological changes observed in these animals closely mimic the changes in humans. Back-crossing a PO deficient mouse (heterozygote, showing symptoms of CMT-1B) with a RAG knockout (deficient in functional T lymphocytes) led to alleviation of the demyelinating phenotype, suggesting a role for T lymphocytes in genetically determined demyelination (Schmid, Stienekemeier et al. 2000).

1.7.1.5 Modelling GBS in the Mouse

Mice present a conundrum in terms of inducing disease. The advantage of generating models of disease in mice is the availability of numerous genetic mutants; however, mice are well known to be relatively resistant to induction.

In 1985, Taylor and Hughes reported neurological deficit in SJL/JOrlCrl (SJL) mice following injection with bovine myelin or myelin-derived P2 protein. Other inbred strains (Balb/C, CBA and C57Bl/6) were relatively resistant to disease induction (Taylor and Hughes 1985). Subsequent experiments on SJL mice found that the mice only suffered subclinical damage to the peripheral nerve myelin, while electrophysical abnormalities were predominant (Dieperink, O'Neill et al. 1991).

More recent work has focussed on the combined manipulation of the immune system using pertussis toxin in the presence or absence of murine recombinant interleukin-12 (mrIL-12) as an adjuvant. Together with bovine peripheral nerve myelin, SJL mice developed severe consistent signs of EAN. Those mice additionally receiving mrIL-12 demonstrated a prolonged disease course. Histological analysis of the caudae equinae and sciatic nerve revealed severe demyelination, remyelination and evidence of mononuclear cell infiltration (Calida, Kremlev et al. 2000).

The C57Bl/6 strain of mouse is widely used as the background for genetic mutants (knockouts and transgenics), thus reproducible EAN in such mice would be particularly useful. The first study demonstrating induction of disease in such mice was from a Swedish group using a complex induction procedure. In this experiment, wild type C57Bl/6, CD4-/-, CD8-/- and CD4/CD8-/- mice were injected with bovine peripheral nerve myelin (BPNM)-primed donor lymph node cells that had been stimulated *in vitro* with BPNM P2 protein peptide 57-81, derived from syngeneic recipients. These animals were further challenged

with BPNM, FCA and pertussis toxin (PT). EAN was most severe after transfer from CD4/CD8-/- to corresponding naïve animals than from any other group. Lack of CD4+ and CD8+ T cell did not completely prevent autoimmune disease initiation (Zhu, Nennesmo et al. 1999). Subsequently, the same group described the induction of EAN in C57Bl/6 mice by active immunisation of the immunodominant PO peptide 180-199 in combination with FCA with added *M. tuberculosis*, and PT. In addition, they tested the effectiveness of BPNM. Results demonstrated that 43% of mice showed clinical signs when injected with peptide only, increasing to 94% when PT was used in combination. Interestingly, the male mice failed to respond to BPNM, while female mice were resistant to disease regardless of the induction procedure (Zou, Ljunggren et al. 2000). In 2001, Zhu and co-workers demonstrated that further manipulation of the immune response by blocking cytotoxic T lymphocyte-associated antigen-4 (CTLA-4) while immunising with PO peptide 180-199 enhanced the severity of EAN in resistant mice, resulting in augmented cellular infiltration and demyelination in sciatic nerves. This provided a means of breaking the relative tolerance to peripheral autoantigen PO in resistant C57Bl/6 mice (Zhu, Zou et al. 2001).

With regard to murine AT-EAN, reports exist of disease induction in Balb/C mice using MBP-specific T cell clones (Abromson-Leeman, Bronson et al. 1995). This has limited relevance for studying PNS autoimmunity since MBP-reactive T cell clones may well cross-react with CNS MBP and initiate an EAE phenotype.

It is clear that owing to the complexity and heterogeneity of GBS, no single animal model would be able to encompass all of the pathogenic changes in all forms of GBS. However, this panel of animal models provides a valuable tool with which to investigate the individual mechanisms at play in the pathogenesis of the different forms of EAN, and systems in which to test various therapeutic interventions.

1.8 C in peripheral neuropathy

1.8.1 Guillain-Barré Syndrome (GBS)

1.8.1.1 Human studies

A role for C in the pathogenesis of GBS was first described in 1981 by Nyland et al, who undertook immunological characterisation of sural nerve biopsies of GBS patients and demonstrated the presence of C3 deposition within the endoneurium of 4/8 GBS patients. IgG deposits were also detected along the myelin sheaths of patients (Nyland, Matre et al. 1981). Detection of C-fixing anti-peripheral nerve myelin antibodies in serum of patients with acute monophasic GBS serum by Koski and co-workers in 1985 (Koski, Vanguri et al. 1985a), was later found to correlate with activation products of terminal C cascade activation in serum, CSF and peripheral nerve (Sanders, Koski et al. 1986), (Koski, Sanders

et al. 1987). Koski also demonstrated that human myelin can activate C via the alternative pathway (Koski, Vanguri et al. 1985). C activation products C3a and C5a were found in CSF of patients with acute monophasic GBS (Hartung, Schwenke et al. 1987). Further studies to elucidate the nature of autoantibodies in GBS demonstrated the presence of C fixing antibodies to peripheral nerve myelin (PNM) in the serum of patients with GBS. Anti-PNM Ab was detected in 53 from 56 patients, and titres were elevated above normal controls and disease controls, e.g. patients with systemic lupus erythematosus (SLE), rheumatoid arthritis (RA) and multiple sclerosis (MS). As expected, anti-PNM Ab titre correlated with clinical course. Furthermore, clearance of these Ab correlated with increased muscle strength and pulmonary vital capacity (Koski 1990). More recent work has concentrated on dissecting the role of humoral and cellular immune responses in GBS. A group in Austria studied archival autopsy data from 11 subjects who died between day 1-8 post-disease onset and demonstrated a primary demyelinating pathology in the majority of cases. Deposits of C9neo antigen on degenerating myelin sheaths were detected, as well as increased CD59 expression, although this did not correlate with duration of disease or presence of C9neo. Interestingly, CD8+ positive lymphocytes and upregulation of MHC I molecules on Schwann cells and myelin sheaths were detected in cases of more than 4 weeks duration, suggesting a putative role for CD8+ in myelin damage in subacute stages of GBS (Wanschitz, Maier et al. 2003).

1.8.1.2 Studies in animal models

The first study of the role of C in mediating disease in animal models of GBS was performed in 1984, where deposition of IgG and C3 was demonstrated in the blood vessel walls surrounding peripheral nerves in rats showing clinical signs of EAN (Koh, Nakano et al. 1984). Conclusive evidence for a role for C in the pathogenesis of peripheral neuropathy was delivered by a study in 1987 by Feasby and co-workers, where depletion of C using CVF suppressed Lewis rat EAN induced by immunisation with myelin. CVF given at day 9 post-disease induction delayed onset by 2-3 days, and CVF given at days 9 and 12 delayed onset by 4-5 days. This correlated with less demyelination in lumbar nerve roots as compared to control rats (Feasby, Gilbert et al. 1987). Subsequent to this, a German group documented the presence of the MAC on the surface of Schwann cells and their associated myelin sheaths during EAN in female Lewis rats, and this deposition was found to precede overt demyelination in the model suggesting a pathogenic role for the terminal pathway of C in the initiation of myelin damage (Stoll, Schmidt et al. 1991). A more detailed study involving CVF-mediated C depletion in Lewis rat EAN was performed in 1995. C depletion markedly reduced the clinical manifestations of the disease, in addition to the inflammatory infiltrate and demyelination in rats immunised with a limited concentration of peripheral nerve

myelin. The effect was in part due to reduced recruitment of myelin-reactive macrophages, as a result of inhibition of C5a generation or down-regulation of CR3 following massive release of C3 fragments (Vrisendorp, Flynn et al. 1995). This was also the case in AT-EAN (Vrisendorp, Flynn et al. 1998). A study of the effect of sCR1 on EAN in the Lewis rat was conducted in 1995 by Jung and colleagues, in which EAN was significantly suppressed by sCR1 treatment. None of the treated rats progressed to ataxia or paraparesis but only one was completely protected from disease. sCR1 treated animals exhibited faster nerve conduction and no demyelination and axonal degeneration when compared to non-treated animals (Jung, Toyka et al. 1995). More recently, Willison's group in Glasgow demonstrated that anti-ganglioside antibodies are capable of diffusing into de-sheathed nerves, binding to nodes of Ranvier and fixing C in an *in vitro* model without any physical deterioration, but this model has limited use due to the short term viability of sciatic nerve *in vitro* (Paparounas, O'Hanlon et al. 1999). The same group has generated a murine model of neuropathy, which mimics some of the features of MFS, mediated by anti-ganglioside GQ1b antibodies binding at the neuromuscular junction (NMJ), and blocking neurotransmitter release. Recent work focused on exposing the NMJ both *in vivo* and *in vitro* to an anti-disialoside antibody in the presence of intact and C deficient sera. Immuno-electron microscopy allowed visualisation of antibody deposits on both neuronal and perisynaptic Schwann cells. At both sites, the damage indicators correlated with MAC deposition. In CD59a-/- mice, these effects were exacerbated suggesting a dysregulation of MAC (Halstead, O'Hanlon et al. 2004).

1.8.1.3 *In vitro* studies

Indirect evidence for a role for C in mediating neuropathy was reported in 1982 by the demonstration that isolated CNS myelin was capable of activating the classical pathway of C *in vitro* in the absence of antibody (Vanguri, Koski et al. 1982). A subsequent study involving sera from GBS patients showed that heat inactivation of the sera severely reduced demyelination and cellular changes to organ cultures, which was restored upon addition of a fresh source of C (Bradbury, Aparicio et al. 1984).

Other studies have focussed on the expression of CR within the PNS. CR1 was localised to human peripheral nerve in 1988, and it was suggested that CR1 expression may be of significance in the pathogenesis of demyelinating neuropathies by trapping C3b-containing immune complexes. Alternatively, the regulatory activity of CR1 may function to limit the damage caused by C on peripheral nerves (Vedeler and Matre 1988). Further work on characterising CR1 on peripheral nerve established that myelinated nerves express a functionally active form of CR1 whereas unmyelinated nerves have a non-functional form thought to be due to differences in glycosylation (Vedeler, Matre et al. 1989).

Studies involving the interplay between macrophages and C components in degenerating nerves using a co-culture system of rat dorsal root ganglia and peritoneal macrophages, demonstrated the requirement of C opsonisation in myelin ingestion by macrophages. Macrophages co-cultured with degenerating nerves were unable to invade nerves in the presence of C3 deficient serum (Bruck and Friede 1991). Subsequent studies by the same group examined the role of activated C components during demyelination *in vitro*, using the co-culture system. Detection of MAC *in vitro* was associated with morphological changes to the myelin sheath in terms of decompaction and myelin splitting, followed by macrophage attack resulting in demyelination, while the axon remained unaffected (Bruck, Bruck et al. 1995).

Studies reflecting the expression of CD59 in normal human nervous tissue were described in 1994. CD59 was shown to be expressed on human Schwann cells, neurons and endothelial cells in the PNS, and on Schwann cells *in vitro*. CD59 was also detected in CSF of healthy subjects (Vedeler, Ulvestad et al. 1994). Subsequent work on characterising CReg molecules on human myelin and glial cells demonstrated the presence of CD55, CD46 and CD59 on Schwann cells derived from human sural nerve (Koski, Estep et al. 1996).

Work from our laboratory in 1996 demonstrated the function of rat CD59 in C-dependent lysis of rat Schwann cells. Antibody-sensitised sciatic nerve Schwann cells of 2 day old rats were shown to be significantly more susceptible to C-mediated lysis than Schwann cells isolated form 6 day old rats, and correlated with expression of rat CD59 (Sawant-Mane, Piddlesden et al. 1996). Further studies on rat CD59 during active EAN in Lewis rats suggest that expression of CD59 on Schwann cells is enhanced during demyelination and axonal degeneration, probably as a result of MAC deposition on Schwann cells at days 7-11 post immunisation prior to overt demyelination (Vedeler, Conti et al. 1999).

1.9 Summary and Project Aim

A role for C in mediating this disease has clearly been established. C deposition (C3, MAC) has been observed on peripheral nerves of GBS patients, and this has been mirrored in the animal model. C activation products have also been detected in serum, CSF and on peripheral nerves in GBS patients. The animal model has served to substantiate this evidence; C depletion markedly suppressed EAN, and reduced inflammatory infiltration. Anti-C therapy conferred some protection against EAN, and a dependence on C was observed for blocking neuromuscular transmission in an animal model of MFS. Limited studies have been performed on expression of C components, receptors and regulators in the PNS; in humans, CR1, CD46, CD55 and CD59 were expressed on sural nerves, and some upregulation of CD59 was observed during active EAN in the rat.

A comprehensive study on the expression of individual components of the C system in the PNS, and in their role in mediating disease however is lacking. It is the aim of this study to fully evaluate C component and regulator expression in the PNS in the rat, and apply this to the human situation. Further, it is my aim to dissect out the role of the individual C components in mediating disease by optimising methods of EAN disease induction, and then assessing the susceptibility of various C deficient and knockout animals available in-house. This will help to target future therapeutics to areas of the cascade critical to disease progression.

2 Myasthenia gravis (MG)

2.1 Background

MG literally translated means grave muscle weakness, and has been recognised since 1672, when Thomas Willis described a woman with dysarthria (speech disorders caused by weakness, paralysis, slowness, or sensory loss in the muscle groups responsible for speech) (cited by Vincent, Palace et al. 2001). In the majority of patients, this weakness is caused by auto-antibodies specific for the nicotinic acetylcholine receptor (nAChR), located at the post-synaptic region of the NMJ. Such antibodies reduce the number of functional nAChR causing impaired neuromuscular transmission leading to muscle weakness.

2.2 The Action Potential

To fully appreciate the function of the nAChR in neurotransmission, it is necessary to understand the nature of the action potential. When the nerve impulse reaches the nerve terminal, acetylcholine (ACh) molecules are released from the presynaptic vesicles. ACh binds the acetylcholine receptor (nAChR) on the peaks of the post-synaptic folds, causing an allosteric change in the conformation of the pentameric structure of the nAChR, forcing the ion channel to open, and allow positively charged sodium ions to enter the muscle fibre endplate. This depolarises the endplate, and if enough of these depolarisations occur, an action potential is generated, which travels along the muscle fibre ultimately causing muscle contraction (Figure 11).

2.3 nAChRs

nAChR can be classified into 2 main types; muscarinic and nicotinic according to the selectivity of the agonists muscarine and nicotine respectively (Figure 12). Although ACh stimulates each type of response, pharmacologically and physiologically distinct responses are produced by each type of receptor. Nicotinic responses are of fast onset, short duration and excitatory in nature, while muscarinic responses are slower, may produce excitation or inhibition and involve second messenger systems, rather than direct opening of an ion

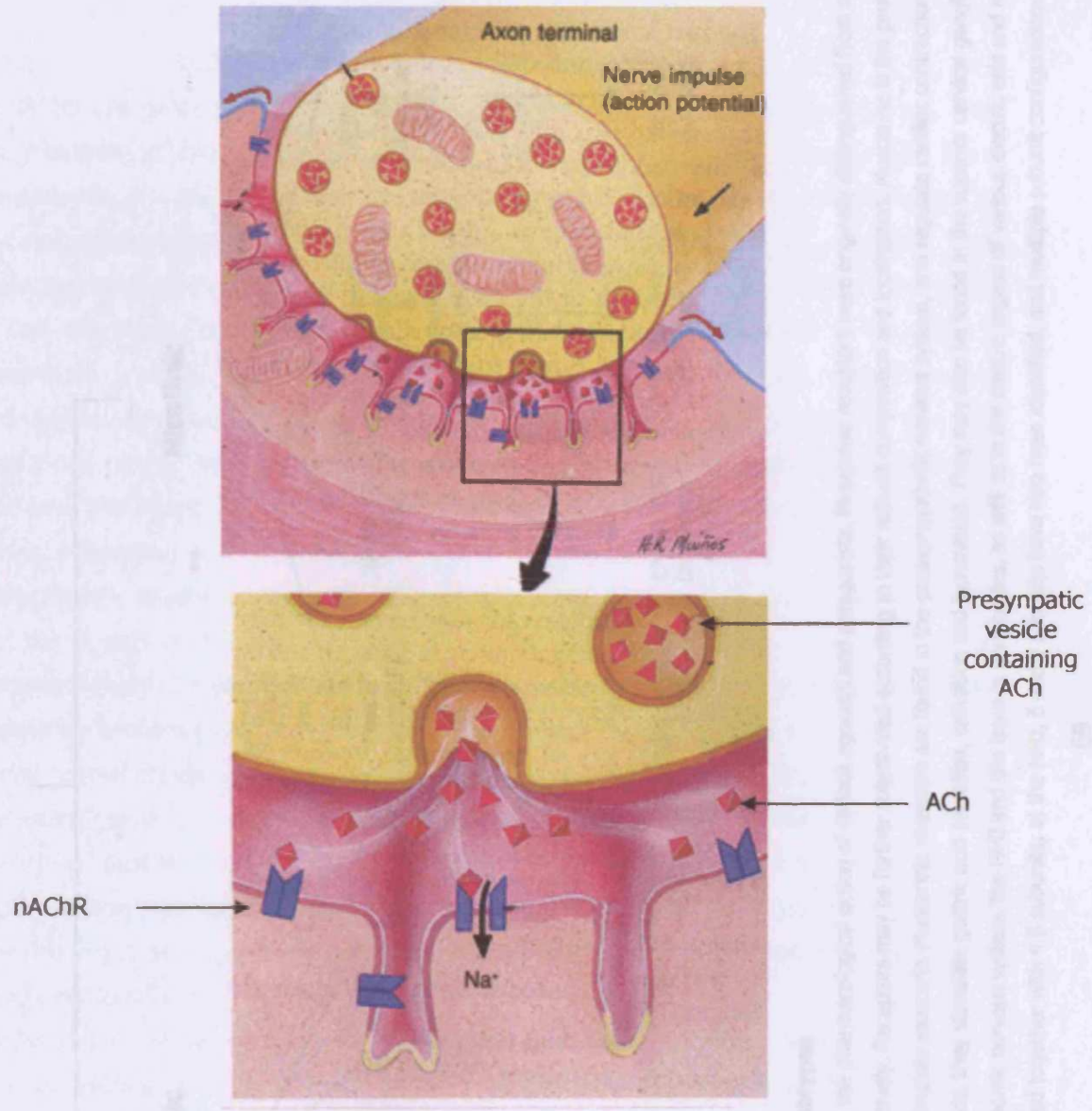

Figure 11 The Action Potential

When the nerve impulse reaches the nerve terminal, ACh molecules are released from the presynaptic vesicles. ACh (pink) binds the nAChR on the peaks of the post-synaptic folds, causing an allosteric change in the conformation of the pentameric structure of the nAChR, forcing the ion channel to open, and allow positively charged sodium ions to enter the muscle fibre endplate. This depolarises the endplate, and if enough of these depolarisations occur, an action potential is generated, which travels along the muscle fibre ultimately causing muscle contraction.

Modified from (Alberts, Bray et al. 1994)

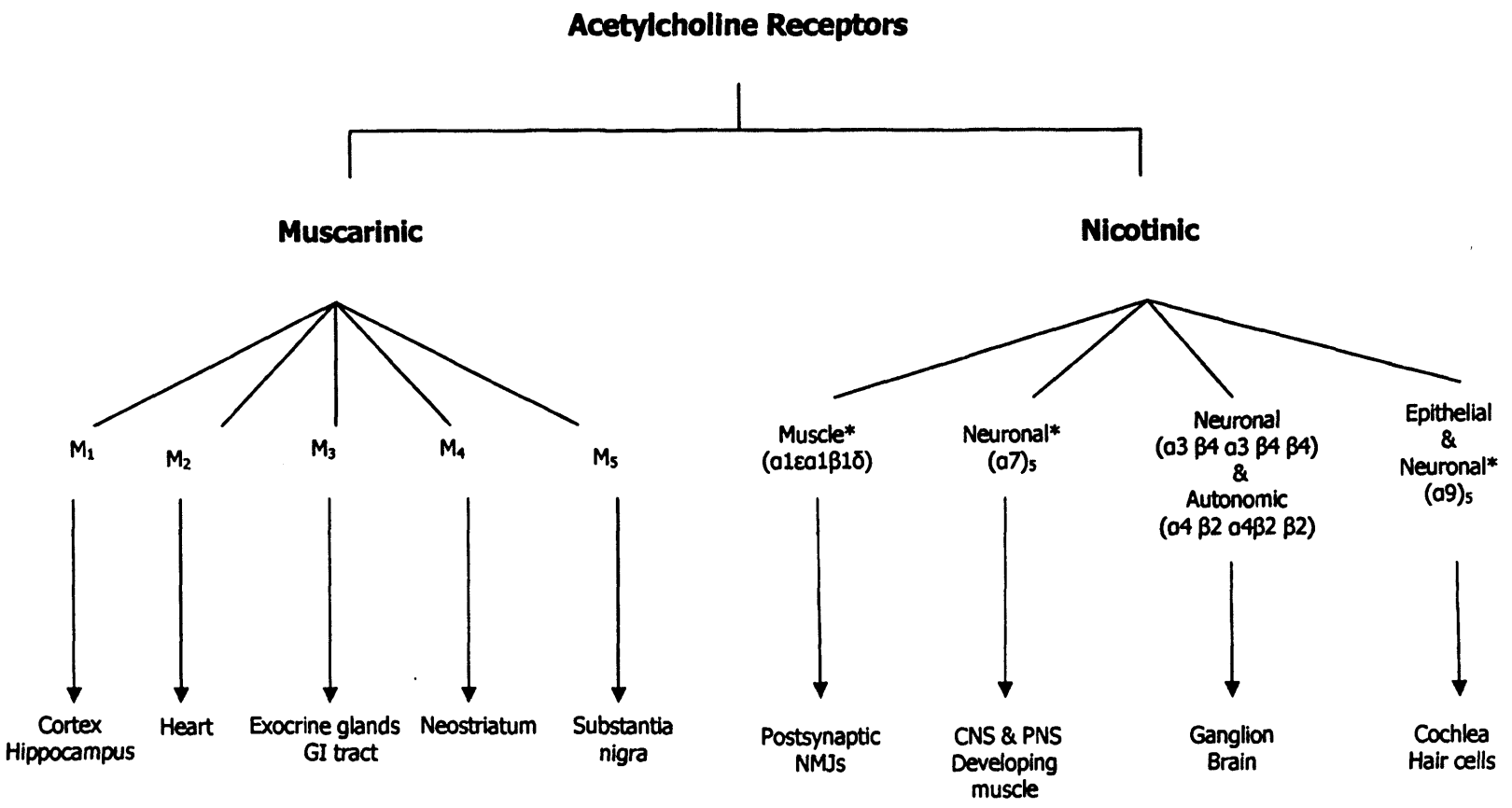

Figure 12 The major types of nAChR, and their subtypes

nAChR may be classified into muscarinic and nicotinic based on the pharmacological action of various agonists and antagonists. Muscarinic receptors were originally distinguished from nicotinic receptors by the selectivity of the agonists muscarine and nicotine respectively. Receptors may be further sub-divided according to their subunit composition and localisation. Muscarine is the prototypical muscarinic agonist and derives from the fly agaric mushroom *Amanita muscaria*. Muscarinic receptors are found in the parasympathetic nervous system, and regulate cardiac contractions in smooth muscle, gut motility and bronchial constriction; in exocrine glands, they stimulate gastric acid secretion, salivation and lacrimation. They may also be found in the superior cervical ganglion, and throughout the brain. Nicotinic receptors are found in the autonomic nervous system, the NMJ and the brain in vertebrates, as well as in the electric organs of various electric eels and rays. The nicotinic receptor consists of 5 subunits; nine α subunits have been cloned together with 4 β subunits; at the NMJ, δ and γ subunits have also been identified, and multiple subunit configurations are possible.

* α-bungarotoxin-sensitive

Adapted from (Watling 1998), (Lindstrom 2000).

channel. They are typically G-protein coupled receptors and mediate their responses by activating a cascade of intracellular pathways (Watling 1998).

2.3.1 nAChR

All nAChR are pentamers, with subunits clustered around a central receptor channel. They are members of the superfamily of ligand-gated ion channels, and mediate fast signal transmission at synapses (Lindstrom 2000). The nAChR is a 250kDa transmitter-gated ion channel glycoprotein, arranged in a barrel-like conformation around a central pore, projecting through the NMJ membrane. In adult innervated muscle, the nAChR is composed of two α-subunits, one β-subunit, a δ-subunit and a ε-subunit, whereas in immature or denervated muscle, a γ-subunit substitutes for the ε-subunit. Each subunit has 4 hydrophobic domains suggesting that they traverse the muscle membrane 4 times, with both the N- and C- terminus located extracellularly. All subunits have been fully sequenced, and bear significant homology to each other, even though they are encoded by separate genes, suggesting a common ancestor. Each α subunit has one binding site for ACh located extracellularly around amino acids 192 and 193 at the interfaces of the α- and δ-subunits and the α- and ε- /γ- subunits (Figure 13). In the resting state, the ion channel is closed. Upon binding of 2 molecules of ACh, the nAChR twists slightly (similar to a Chinese purse), transiently opening the channel to allow cations to pass (Lindstrom 2003).

Under normal conditions, nAChR are clustered at the peaks of folds of the NMJ, adjacent to the motor nerve ACh release site. Such clustering is dependent on the interaction of several anchoring proteins, rapsyn, agrin, utrophin, dystroglycan and muscle-specific receptor protein kinase (MuSK). The importance of MuSK has recently been highlighted, since it has been shown to be a target for auto-antibodies in patients with nAChR antibody negative MG (Hoch, McConville et al. 2001).

nAChR in the postsynaptic membrane of muscle are part of enormous synapses containing tens of millions of nAChRs, since the NMJ is specifically designed with the capability of amplifying small currents involved in the action potential. An excess of ACh is released at the pre-synaptic membrane directly onto an excess of nAChR. Despite this obvious redundancy, neuromuscular transmission is still susceptible to attack by toxins, for example, α-bungarotoxin from the snake *Bungarus multicinctus*; by man-made toxins such as nerve gases, as well as genetic and autoimmune diseases (Lindstrom 2003).

2.4 Clinical characteristics of MG

MG characteristically presents either acutely or sub-acutely, as a painless weakness that worsens upon exertion. Although the pattern of disease is variable between individuals, it frequently presents with drooping of the upper eyelid (ptosis) and double vision (diplopia)

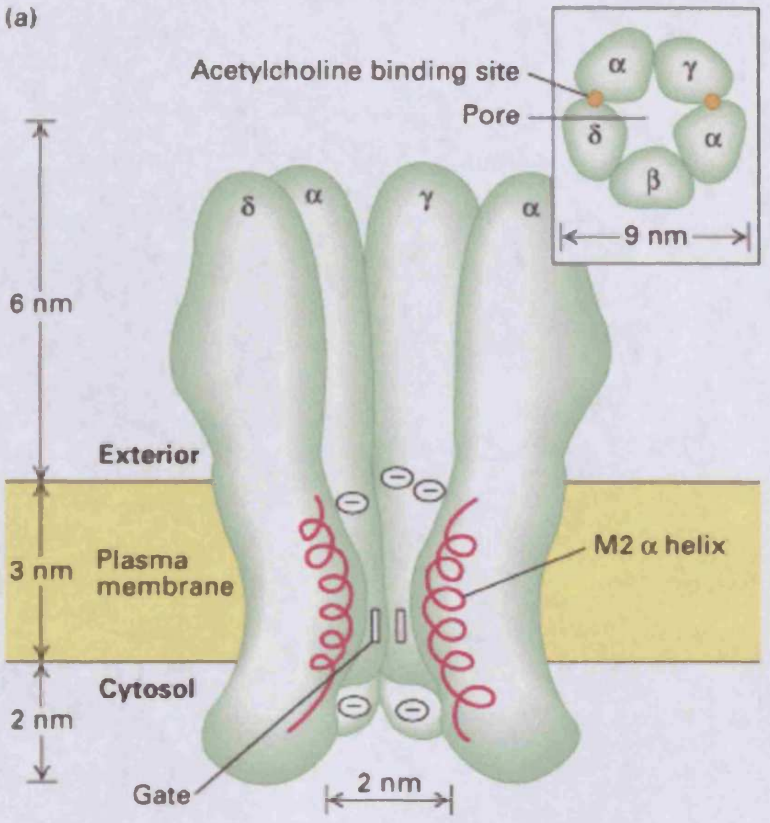

Figure 13 The Nicotininc Muscle Acetylcholine Receptor (nAChR)

The nAChR is a pentameric structure composed of 2α, β, γ and δ subunits arranged in a barrel-like configuration around a central ion pore. Binding of ACh causes an allosteric change in the configuration of the subunits, causing the ion pore to open and allow the inward flow of positive sodium ions, as described previously.

Taken from (Alberts, Bray et al. 1994)

caused by the involvement of extraocular muscles. Further involvement of bulbar and facial muscles cause reduced facial expression, speech, chewing and swallowing difficulties. In addition, neck weakness leads to head droop. Respiratory muscle weakness is considered life-threatening, and weakness can remain localised to one muscle group, for example ocular MG, or may spread to affect other skeletal muscles to give a generalised MG (Oosterhuis 1989).

2.5 Epidemiology

The annual incidence of MG is between 0.25 and 2 people per 100,000, with a bimodal frequency; those presenting with early onset MG (before age 40), and those presenting with late onset MG (after age 60). Numbers presenting with early onset MG have a bias towards females, most are positive for anti-nAChR antibodies and have an enlarged thymus. Statistical analysis has proven that cases of late onset MG are on the increase, with a bias towards males; although the thymus gland is not enlarged, there appears to be an association with HLA B7 and DR2. (Vincent, Palace et al. 2001). In the majority of cases, no specific cause can be identified. However, there is evidence of genetic involvement as a predisposing factor to development of disease by as yet unidentified environmental factors. Patients with early and late onset MG have different HLA associations (Compston, Vincent et al. 1980). For example, in China, up to 30% of patients with juvenile MG present with ocular myasthenia associated with HLA-BW46 (Hawkins, Chan-Lui et al. 1984).

Thymic abnormalities exist in the majority of cases of MG, with simple hyperplasia found in 60-70% of patients and coinciding thymoma in another 10-15%. The connection of thymic abnormalities to MG points to the thymus as a possible origin of the autoimmune process, although no definite pathophysiology has been determined (Vincent, Palace et al. 2001). Auto-antibodies present in the sera of these patients often have high affinity and specificity for intact conformation of the antigen. Others may be directed against cell surface antigens and be directly pathogenic, whilst others may be against intracellular antigens not accessible to the antibodies. Thymomas often generate large numbers of T cells sensitised to self-epitopes in the thymoma. Current hypotheses suggest that both cytotoxic T cells and helper T cells have the capability to be induced against specific peptides in the thymomas, and then move to the periphery where they can persist. At some point, cytotoxic T cells may recognise epitopes presented by muscle, following a small inflammatory stimulus or tissue damage and up-regulation of MHC class I. Such cytotoxicity results in release of inflammatory mediators, and presentation by MHC class II antigen positive presenting cells, including antigen-specific B cells, which may account for the characteristic high titres of autoantibody; only those directed against cell surface antigens will be pathogenic (Vincent and Willcox 1999).

2.6 Pathophysiology of MG

The pathogenic role of antibodies in MG was first realised in the 1970s, by the finding that plasma exchange leads to a dramatic, albeit transient improvement in muscle function, by removing pathogenic circulating antibodies (Newsom-Davis, Pinching et al. 1978). A study in 1977 demonstrated that passive transfer of IgG from MG patients into mice resulted in a reduction in amplitude of miniature end-plate potentials (m.e.p.p.s) by decreasing the sensitivity of the postsynaptic membrane to ACh, or reduction in numbers of nAChR at the NMJ (Toyka, Drachman et al. 1977). To confirm that antibodies were indeed against the nAChR, mice were immunised with purified nAChR, and demonstrated clinical symptoms related to MG (Patrick and Lindstrom 1973). In addition, passive transfer of monoclonal antibodies to the nAChR were capable of producing clinical weakness in laboratory animals, without blocking binding of ACh to its receptor (Lennon and Lambert 1980).

The immune response in MG impairs neuromuscular transmission by several mechanisms. Antibodies bound to the nAChR target the postsynaptic membrane for C activation, and subsequent MAC-mediated lysis. The detrimental effect is two-fold; firstly, this causes loss of the nAChRs themselves, and secondly C-mediated damage disrupts the folded architecture of the post-synaptic membrane, leaving a larger space between ACh release from the pre-synaptic membrane, and nAChR, thereby slowing down neuromuscular transmission. Antibodies may also cross-link the nAChR, and increase their rate of internalisation. Auto-antibodies generally target the main immunogenic region (MIR) of the nAChR which is located at the extracellular face of the nAChR. It is the structure of the receptor that provides the basis of the pathological significance of the MIR (Figure 14) (Lindstrom 2003). MG is generally caused by antibodies against the nAChR, but may also be caused by antibodies against other muscle proteins, for example titin and ryanodine receptor (RyR). These antibodies are usually associated with patients with thymoma and late-onset MG, may correlate with disease severity and show a cross-striational staining pattern on skeletal and heart muscle sections (Romi, Skeie et al. 2005). The majority of anti-titin and anti-RyR antibodies from MG patients are also capable of activating C (Romi, Skeie et al. 2000). A subgroup of MG patients is described as nAChR negative, but is indistinguishable clinically from antibody positive MG patients. In 2001, Hoch and colleagues demonstrated the presence of antibodies to a muscle-specific receptor tyrosine kinase (MuSK) in these patients (Hoch, McConville et al. 2001). Further work has demonstrated that antibodies against MuSK are directed towards the extracellular domain, and are capable of inhibiting agrin-induced nAChR clustering in muscle myotubes (Vincent, McConville et al. 2004).

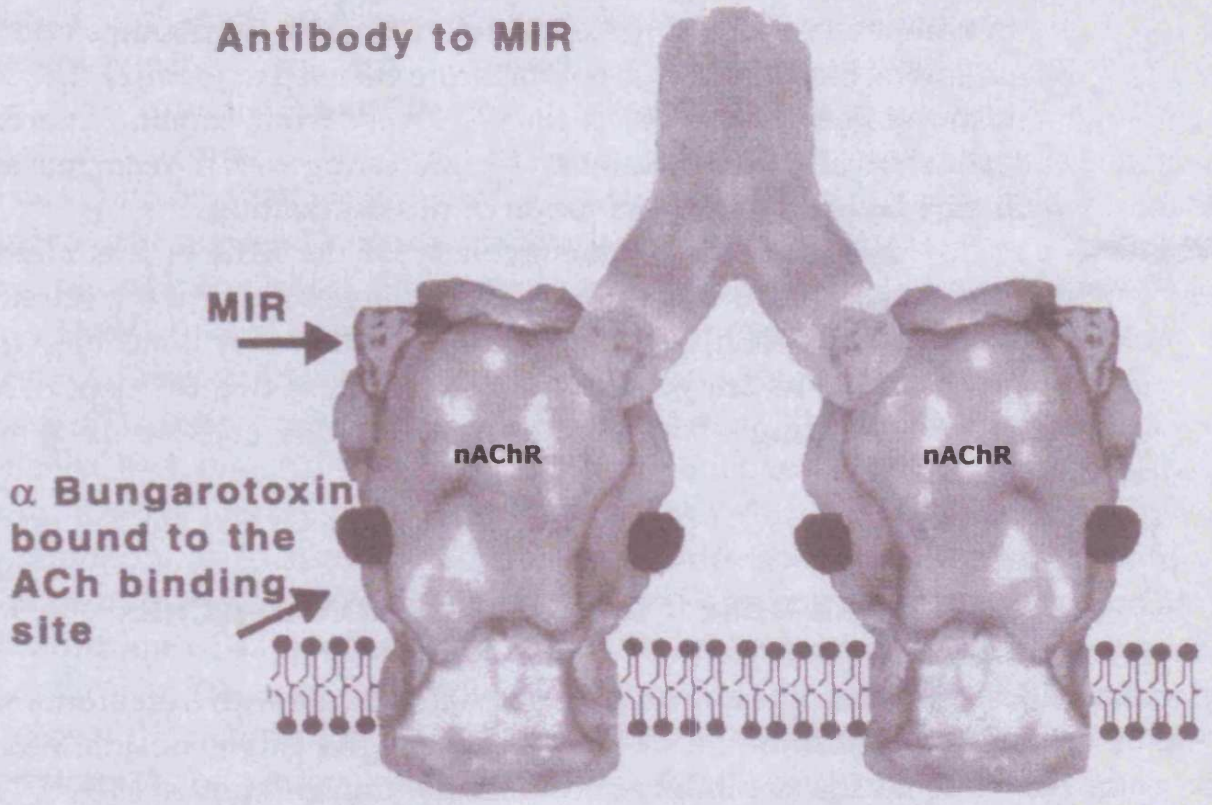

Figure 14

Structural basis of the pathological significance of the main immunogenic region (MIR)

The structure of the MIR accounts for many of the pathological features seen in MG. Since the MIR is located at the extracellular face of the nAChR, and the nAChRs are clustered together within the postsynaptic membrane, this permits many anti-nAChR antibodies to bind, and fix C at those surfaces. In addition, since the MIR is angled away from the central axis of the nAChR, it would be impossible to cross-link the MIR on the same nAChR; however, it is possible to cross-link adjacent nAChR and induce antigenic modulation.

Although auto-antibodies bind the MIR, they bind at sites distinct from the ACh binding site, and thus do not interfere with the nAChR function. It is this property which allows nAChR to be identified in immunodiagnostic assays, using α-bungarotoxin.

Taken from (Lindstrom 2003)

2.7 Animal models of MG

2.7.1 Experimental Autoimmune Myasthenia Gravis (EAMG)

2.7.1.1 Active immunisation

MG can be induced in susceptible strains of animals by immunisation with nAChR isolated from the electric organ of *Torpedo californica (T. californica)* and *Electrophorus electricus (E. electricus).* This was first performed in 1973 by immunisation of rabbits with nAChR in FCA (Patrick and Lindstrom 1973). Lennon and co-workers expanded this work by immunisation of rats and guinea pigs with nAChR from electric organs as above. Both species developed EAMG in a dose related manner, and the detection of antibodies to syngeneic rat muscle nAChR in the serum of these animals provided evidence for autoimmunity as a pathogenic mechanism in MG (Lennon, Lindstrom et al. 1975). Further to this work, Lindstrom and co-workers demonstrated that immunisation of rats with syngeneic nAChR or electric organ nAChR resulted in EAMG. Antibodies to nAChR were found in serum of animals immunised, as well as bound to muscle nAChR, corresponding to a large decrease in numbers of nAChR, and phagocytic infiltration (Lindstrom, Einarson et al. 1976).

2.7.1.2 Passive transfer

Lindstrom et al also described a passive transfer model of EAMG (Lindstrom, Engel et al. 1976). Serum from actively induced EAMG rats was passively transferred to naïve rats, and the disturbances at the NMJ were similar to those observed in actively immunised rats. Phagocytic infiltration was also evident suggesting that such cells are not nAChR-sensitised cells, but non-specific macrophages responding to antibody bound to nAChR in the postsynaptic membrane and local C-mediated membrane damage (Lindstrom, Engel et al. 1976). This work was extended to include localisation of IgG and C3 at the NMJ during passive transfer EAMG (Engel, Sakakibara et al. 1979). It was also demonstrated during this time, that passive transfer of IgG from MG serum was capable of inducing EAMG in mice. Mice showed reduced amplitudes of minature endplate potentials (m.e.p.p.s) and reduced numbers of nAChRs at NMJs (Toyka, Drachman et al. 1975).

Further, monoclonal antibodies raised in rats against nAChR purified from the electric organ of *T. californica* (McAb1, 2 and 3) were capable of inducing disease in mice, rats and guinea pigs. McAb2 and 3 bound extensively to nAChR in skeletal muscle in all species tested, and total nAChR in these muscles was reduced. Passive transfer into rats and guinea pigs induced clinical, electrophysical and biochemical evidence of EAMG. However, mice did not show any signs of clinical weakness, although their m.e.p.p. amplitude was reduced by 50%; this reflects their large safety factor of neuromuscular transmission (Lennon and Lambert 1980). In 1981, Lindstrom and colleagues generated 40 monoclonal antibodies in the rat to the nAChR of *E. electricus* in order to map the surface structure of the nAChR.

Twenty three of these antibodies were directed at the MIR of the nAChR (Tzartos, Rand et al. 1981). Four of these antibodies were used to induce EAMG in rats, with remarkable efficiency; within 2 days the rats became moribund, and nAChR content was decreased to about 50% of normal (Tzartos, Hochschwender et al. 1987). One of the antibodies, mAb35, derived from the TIB175 hybridoma, has been used extensively to induce EAMG in rats (Graus, Verschurren et al. 1993; Piddlesden, Jiang et al. 1996; Hoedemaekers, Graus et al. 1997; Hoedemaekers, Bessereau et al. 2001). It has a high affinity for native receptors, and the alpha subunit in particular. It binds the MIR, and thus does not block binding of ACh, leaving receptor function intact (American Type Culture Collection information sheet, TIB175). This will be the method of choice for disease induction for the studies described in this thesis.

2.8 C in MG

The role of C was first realised in the 1960s with an observation of changes in serum C activity in patients with MG (Nastuk, Plescia et al. 1960). Since then, a wealth of literature on the role of C in disease pathogenesis has been published.

2.8.1 Human studies

Following the realisation in the 1960s of a role of C in mediating disease, subsequent studies revealed C deposition at the motor endplate in patients with generalised MG. Firstly, IgG and C3 deposits were localised (Engel, Lambert et al. 1977), followed closely by C9 deposits (Sahashi, Engel et al. 1978), and C5b-9 (Fazekas, Komoly et al. 1986), (Engel and Arahata 1987). This was also the case in patients with ocular MG having minimal serum anti-nAChR antibodies (Tsujihata, Yoshimura et al. 1989). C activation products such as C3c were detected in MG patients, and appeared to correlate with disease severity (Kamolvarin, Hemachudha et al. 1991). A brief study into expression of CR1 showed that CR1 expression remained unaffected in MG patients (Vedeler, Gilhus et al. 1990). A cell-mediated mechanism for tissue damage was eliminated following the realisation that inflammatory cell infiltration present in MG muscle was at topographically distinct locations from the NMJ, and thus could not play a direct role in tissue damage (Nakano and Engel 1993). C deposition capacity of MG serum was also tested by measurement of C3 deposition on sensitised targets, and revealed increased uptake compared to controls (Basta, Illa et al. 1996). With the finding that auto-antibodies, other than those against the nAChR, were present in a subset of patients, their ability to activate C was tested. The majority of anti-titin and anti-RyR antibodies were found to be capable of activating C, and some correlation between antibody titre and clinical improvement was observed (Romi, Skeie et al. 2000). Most

recently, increased C consumption has been detected in MG patients with high anti-nAChR antibodies (Romi, Kristoffersen et al. 2005).

2.8.2 Animal studies

2.8.2.1 Active immunisation

As with the data regarding MG patients, C deposition has also been observed in animals actively induced for EAMG. IgG and C3 were first observed in 1978 (Sahashi, Engel et al. 1978), while CVF treatment inhibited development of EAMG in the rat (Lennon, Seybold et al. 1978). More recently, actively induced EAMG has been used in the context of various knockout and deficient animals. For example, a reduction in actively induced EAMG was observed in IL-6 deficient mice, which was associated with reduced germinal centre formation and C3 production (Deng, Goluszko et al. 2002). C5-deficient mice were protected from actively induced EAMG despite having equivalent concentrations of anti-nAChR antibodies in their serum (Christadoss 1988). In addition, C3-/- and C4-/- mice were resistant to actively induced EAMG, with heterozygotes displaying intermediate susceptibility (Tuzun, Scott et al. 2003).

2.8.2.2 Passive transfer

As for actively induced disease, the classical studies confirmed the presence of C deposition at the NMJ in passively induced EAMG in the rat (Engel, Sakakibara et al. 1979), and CVF treatment also inhibited development of EAMG (Lennon, Seybold et al. 1978) (Tsujihata, Satoh et al. 2003). The only study to specifically address the role of the terminal pathway in mediating disease blocked C6 activity in rats using polyclonal antiserum. Investigators observed complete protection from the clinical manifestations of disease (Biesecker and Gomez 1989). Treatment of EAMG rats with sCR1 also delayed onset and reduced the severity of clinical manifestations of disease (Piddlesden, Jiang et al. 1996). Treatment of passively induced EAMG in the rat with papain, to specifically cleave the Fc portion of possible C activating antibodies resulted in reduced clinical manifestations of EAMG and promoted rapid recovery (Poulas, Tsouloufis et al. 2000). As for the actively induced disease, knockout animals have been exploited with this immunisation procedure; lack of regulation of C activation in CD55-/- *(Daf1-/-)* mice resulted in increased susceptibility to EAMG induction (Lin, Kaminski et al. 2002); decreased levels of mRNA coding for membrane-bound CRegs CD55, CD59 and Crry were found in extraocular muscles in EAMG mice, providing a possible explanation for the increased susceptibility of these muscles to pathological changes (Kaminski, Li et al. 2004).

2.8.3 *In vitro* studies

Due to relative ease of diagnosis of MG patients, and the availability of a reliable animal model, *in vitro* studies have been limited. Two studies however have been reported. Heat inactivated MG patient serum showed myotoxicity in a rat myotube culture only in the presence of C-sufficient serum (Childs, Harrison et al. 1985). Sublytic terminal pathway attack on myotubes *in vitro* decreased expression of mRNAs encoding muscle-specific proteins, e.g. α-subunit of nAChR (Lang, Badea et al. 1997).

2.9 Summary and Project Aims

As for GBS, a role for C in mediating MG has clearly been established previously. C deposition has been observed at the NMJ of MG patients and in actively and passively induced EAMG. Anti-nAChR, titin and RyR antibodies have been shown to be capable of activation of C. Numerous studies have been performed in the animal model; C depletion inhibited both actively and passively induced EAMG. Limited studies into the efficacy of anti-C therapeutics have been performed using sCR1, and were shown to confer a degree of protection against passively induced EAMG onset and progression. Knockout and deficient C3, C4 and C5 mice have been shown to be protected from actively induced EAMG, whereas mice deficient in CReg CD55 showed an increased susceptibility to disease.

Limited studies into the role of the terminal pathway in mediating disease have been considered. Blocking of C6 using polyclonal antisera abrogated disease, but the system would have introduced numerous immune complexes, which may mask some of the effects. Rat deficient in C component C6 are now available, and provide a unique opportunity to reinforce data for a specific role of the terminal pathway. In addition, our laboratory has generated CD59a-/- mice, allowing further studies into the importance of regulation within the terminal pathway in preventing progression of EAMG.

Following successful 'proof of concept' using first generation anti-C therapeutics, such as sCR1, the way has been paved for so-called 'second generation' therapies. Reagents are being developed in our laboratory to circumvent undesirable characteristics of existing reagents such as short half-life, high cost, and immunogenicity. An animal model to test the efficacy of such therapies would be extremely beneficial. EAMG provides an excellent opportunity for such testing due to the dependence of C in mediating disease.

3 Overall Project Aims

- Characterisation of the C system (C components and CReg) in the rat PNS using Schwann cell lines, Schwann cell primary cultures and whole sciatic nerve as model systems
- Establish EAN as an animal model of GBS in rats and mice, and test the susceptibility of various C deficient and knockout animals to disease induction
- Generation of antigens derived from PO to optimise EAN induction including peptides, bacterial expression of the extracellular domain of PO (PO-EC), whole PNS tissue homogenates and purified myelin
- Establish passive transfer EAMG as an animal model of MG in rats and mice, and test the dependence of the MAC for disease induction and progression using C6 deficient rats
- Utilise EAMG in the rat to test the efficacy of various anti-C therapeutics
- Analyse the susceptibility of CReg knockout mice to passive transfer EAMG

Chapter 2

Characterisation of the susceptibility of the rat PNS to C attack

1 Introduction

1.1 C in the PNS

GBS is a transient, immune-mediated, demyelinating disorder of the PNS. The immune reaction may be directed towards the Schwann cell membrane, or the myelin sheath, where it results in the more common inflammatory demyelinating neuropathy; or alternatively towards the axon causing the acute axonal form (Hahn 1998). The current paradigm for disease pathogenesis is that disease is triggered by an initial infection leading to recognition of a specific autoantigen by auto-reactive T cells. Activated T cells transit across the blood-nerve barrier (BNB) and into the PNS, assisted by chemokines, cellular adhesion molecules (CAMs) and matrix metalloproteinases (MMPs). Further activation of macrophages results in production of pro-inflammatory cytokines. Antibodies, either auto-reactive or locally produced by B cells contribute to demyelination and axonal damage via C activation, antibody-dependent cellular cytotoxicity (ADCC) or blocking of epitopes involved in nerve conduction (Hartung, Willison et al. 2002).

Numerous studies have demonstrated the presence of C activation and terminal pathway components within peripheral nerve biopsies and sera of GBS patients (Nyland, Matre et al. 1981), (Koski, Vanguri et al. 1985a), (Sanders, Koski et al. 1986), (Koski, Sanders et al. 1987), (Hartung, Schwenke et al. 1987), (Wanschitz, Maier et al. 2003). There is also evidence that C activation has a pathogenic role in the animal model of GBS, Experimental Autoimmune Neuritis (EAN). Systemic C depletion by CVF markedly reduced the clinical manifestations of the disease (Feasby, Gilbert et al. 1987), (Vrisendorp, Flynn et al. 1997). In addition, soluble CR1 treatment significantly suppressed the demyelinating phenotype of Lewis rat EAN (Jung, Toyka et al. 1995). The MAC has also been demonstrated on the surface of Schwann cells, and their associated myelin sheaths during EAN, and found to precede overt demyelination, suggesting a pathogenic role for C in initiation of myelin damage (Stoll, Schmidt et al. 1991). Further studies have demonstrated the role of C opsonisation of myelin in myelin ingestion by macrophages in degenerating nerves using a co-culture system (Bruck and Friede 1991). Further they suggest that detection of MAC *in vitro* was associated with morphological changes within the myelin sheath, followed by

macrophage attack and demyelination without axonal damage (Bruck, Bruck et al. 1995). C dependence in pathology has also been demonstrated in an *ex vivo* mouse diaphragm model of a variant of GBS, MFS, in which anti-ganglioside antibody GQ1b from MFS patients induces muscle block (Jacobs, Bullens et al. 2002). Further work utilising this model has demonstrated antibody deposits on both perisynaptic and neuronal Schwann cells which correlate with MAC deposition (Halstead, O'Hanlon et al. 2004). In addition, GBS sera containing anti-ganglioside antibodies have been shown to cause neuronal cell lysis via a C-dependent mechanism (Zhang, Lopez et al. 2004).

1.2 C regulation

The majority of nucleated cells protect themselves from C attack by the activities of intrinsic membrane regulatory proteins (CReg). Within the human system, CD55 and CD46 function to prevent C3b deposition on self tissues by accelerating decay of the convertases spanning the classical and alternative pathway, or by acting as a cofactor for fI-mediated cleavage of the convertases respectively. CD59 regulates the formation of the MAC by binding C8 and preventing C9 polymerisation. In rodents, Crry is a unique and powerful CReg possessing both decay-accelerating and co-factor activity.

Work involving C regulation in the PNS is limited. However, study of the human PNS by serial analysis of gene expression (SAGE) established that classical pathway C components were expressed in axons, whereas CD59 was expressed in the perineurium. The work also suggested that local production of C may participate in the clearance of myelin in disease, and facilitate nerve regeneration, while the presence of CReg in the perineurium is protective against C attack (de Jonge, van Schaik et al. 2004). In the rat, work from our laboratory demonstrated the function of rat CD59 in C-dependent lysis of rat Schwann cells (Sawant-Mane 1996) and further work on rat CD59 during EAN suggested an up-regulation of CD59 on Schwann cells during demyelination (Vedeler, 1999). However, a comprehensive study of the expression of CReg in the rat PNS is lacking, and will be the focus of this chapter.

1.3 Chapter Aim

Here we investigate expression of membrane CRegs CD55, CD46, CD59 and Crry on rat Schwann cell lines, primary rat Schwann cells and whole peripheral nerves by immunostaining, RT-PCR, flow cytometry and Western blotting, to demonstrate their potential importance in limiting C-mediated damage during inflammation. Evaluation of the capability of rat Schwann cell lines to express mRNA for C components spanning the entire C cascade was also investigated.

2 Materials and Methods

All chemicals unless otherwise stated were from Sigma Aldrich Chemical Company, (Gillingham, UK).

2.1 Rat Schwann cell lines

Established clonal cell lines capable of retaining differentiated function have provided investigators with functionally and genetically homogeneous viable cell populations in sufficient quantities for most applications. Cell lines have advantages over primary culture in their ease of preparation, and their ability to continuously proliferate *in vitro*. However, in general, cell lines have this property since they have been transformed into tumour lines, either by culture of actual clinical tumours, or by chemical or viral transformation. As such, they may retain few of their *in vivo* characteristics.

2.1.2 RN22

Rat Schwann cell lines were obtained from the European Collection of Cell Cultures (ECACC). RN22 (ECACC No. 93011414) is designated an immature rat Schwann cell with a bipolar, stellate morphology. In the original work, four clonal lines were established in culture from a transplantable tumour of cervical nerve root induced transplacentally with ethylnitrosourea (ENU) within an inbred rat strain (BD-1X). Briefly, 80mg/kg ENU was injected IV into a pregnant inbred BD-1X rat. At 15 days gestation all offspring developed neurogenic tumours, and the tumour used in the development of these lines was derived from a second passage transplant of a primary cervical root tumour. Following dispersion of the tissue, cultures were maintained in 10% (v/v) horse serum, 2.5% (v/v) FCS. Morphologically distinct cells were separated using their varying rates of detachment in the presence of Viokase (enzymatic digestion, now use trypsin-EDTA). Clonal cell lines were established by repeated single cell platings. RN22 displayed synthesis of nervous system protein S100, and a high specific activity of 2',3'-cyclic nucleotide-3'-phosphohydrolase (CNPase), an enzyme present in very high levels in brain and peripheral nerve (Pfeiffer and Wechsler 1972).

2.1.3 RT4-D6P2T

RT4 (ECACC No. 93011415) is also designated an immature rat Schwann cell derived from the ethylnitrosourea-induced tumour line D6 of the rat peripheral nervous system. RT4 cells have a bipolar morphology and are reported to de-differentiate after 10 passages. The original work describes a clonal stem cell line (RT4-AC) of a rat peripheral neurotumour, which is capable of differentiating in culture to produce morphologically and functionally

distinct cell types. RT4-AC showed both neuronal and glial properties, and gave rise to 3 morphologically and biochemically distinct cell types. Of these, RT4-B and RT4-E had neuronal properties whereas RT4-D displayed glial characteristics (S100 production, negative voltage-dependent sodium influx and high tumourigenicity (Tomozawa and Sueoka 1978). The RT4-D line was further subcloned to give rise to four morphologically related but biochemically distinct clones (D6P1, D6P2, D6P3, D6P4). D6P2 was taken for further analysis since it has the highest level of sulphatide synthesis, and from this D6P2T was derived (Bansal and Pfeiffer 1987).

RT4-D6P2T has been used extensively as a model system for myelin gene transcription studies. Evidence from work by Hai and colleagues demonstrated that primary Schwann cells express myelin proteins at similar levels to RT4-D6P2T, and suggest that primary cultures are not necessarily better than cell lines as model systems (Hai, Muja et al. 2002).

2.2 Cell culture

Unless otherwise stated, all tissue culture reagents were obtained from Invitrogen Life Technologies, Paisley, UK. For culture of both cell lines, Dulbecco's Modified Eagles Medium (DMEM) was supplemented with 5% (v/v) foetal calf serum (FCS, heat inactivated), 2mM L-glutamine and 1mM sodium pyruvate (DMEM-F5).

2.2.1 Sub-culture of rat Schwann cell lines

Both RN22 and RT4 are adherent cell lines, and were sub-cultured by washing three times in sterile saline, and incubating in 1ml trypsin-EDTA with agitation until cells detached from the flask. Cells were harvested into medium, pelleted at 1000g and transferred to fresh medium at 1/10 dilution.

2.3 Analysis of membrane-bound CReg expression on rat Schwann cell lines by single colour flow cytometry

2.3.1 Methods

Rat Schwann cell lines in passage 1-4 were washed three times in flow cytometry medium (FCM, 10% (w/v) BSA, 15mM EDTA, 0.1% (w/v) sodium azide in PBS) and resuspended at 10^6 cells/ml. Cells (100µl) were transferred to a 96 well round bottomed plate, and centrifuged at 450g for 3 minutes. For the purposes of a positive control, whole rat blood was collected into heparin (12-30U/ml blood), and a 0.1% (v/v) suspension composed of mainly erythrocytes (E) was washed in FCM by centrifuging at 1800g for 3 minutes. 100µl of cells were used per well. Following centrifugation, one of the following antibodies was added to the pellet: mouse anti-rat CD59 (6D1), mouse anti-rat CD55 (RDIII7), mouse anti-rat Crry

(TLD1C11), mouse anti-rat CD46 (MM1) each at 10μg/ml were added in a total volume of 100μl including a buffer only control for secondary antibody cross-reactivity, and incubated for 40 minutes at 4^0C. After washing three times in FCM by centrifuging at 450g for 3 minutes, pelleted cells were resuspended in 100μl of a 1/100 dilution of goat anti-mouse-Ig-recombinant phycoerythrin (rPE)-conjugated secondary antibody (DAKO Cat No. R0480), and incubated for a further 40 minutes at 4^0C in the dark. Cells were washed three times and analysed on a FACScalibur (Becton Dickinson, Oxford, UK). Data were imported to WinMDI for analysis.

2.3.2 Results

Both lines displayed high relative expression of CD59 and Crry in comparison with rat erythrocytes (Figure 1). While RT4 displayed no surface expression of CD55, RN22 was weakly positive for the regulator. Neither line demonstrated expression of CD46. Rat E were used as a positive control for CD59, CD55 and Crry expression. Since rat CD46 is testis-specific, antibody staining was confirmed on rat sperm by immunocytochemistry (Figure 1, panel D).

2.4 Analysis of membrane-bound CReg expression by Western blotting

Western blotting was employed to confirm flow cytometry expression profiles of CReg on rat Schwann cell lines. Rat CD59 was immunoprecipitated in order to obtain a clear band by Western blotting.

Rat E ghosts were used as a positive control for regulators CD55, CD59 and Crry. Rat testis lysate was used as a positive control for CD46.

2.4.1 Methods

2.4.1.1 Preparation of rat Schwann cell lysates

Two confluent T-80cm^3 tissue culture flasks of each cell line were harvested in FCM containing 15mM EDTA, centrifuged at 450g for 3 minutes, and resuspended in 750μl of cell lysis buffer (PBS, 3% (v/v) NP40, 0.5mM PMSF, 10mM EDTA, 0.05% (w/v) SDS). The lysate was incubated for 1 hour on ice, and then centrifuged at 20,000g in a refrigerated microfuge for 10 minutes. The supernatant was used for Western blotting. Using this method, there was some difficulty in obtaining a clear blot for rat CD59, even though flow cytometry showed that it was highly expressed. Rat CD59 was therefore immunoprecipitated from lysates as described below.

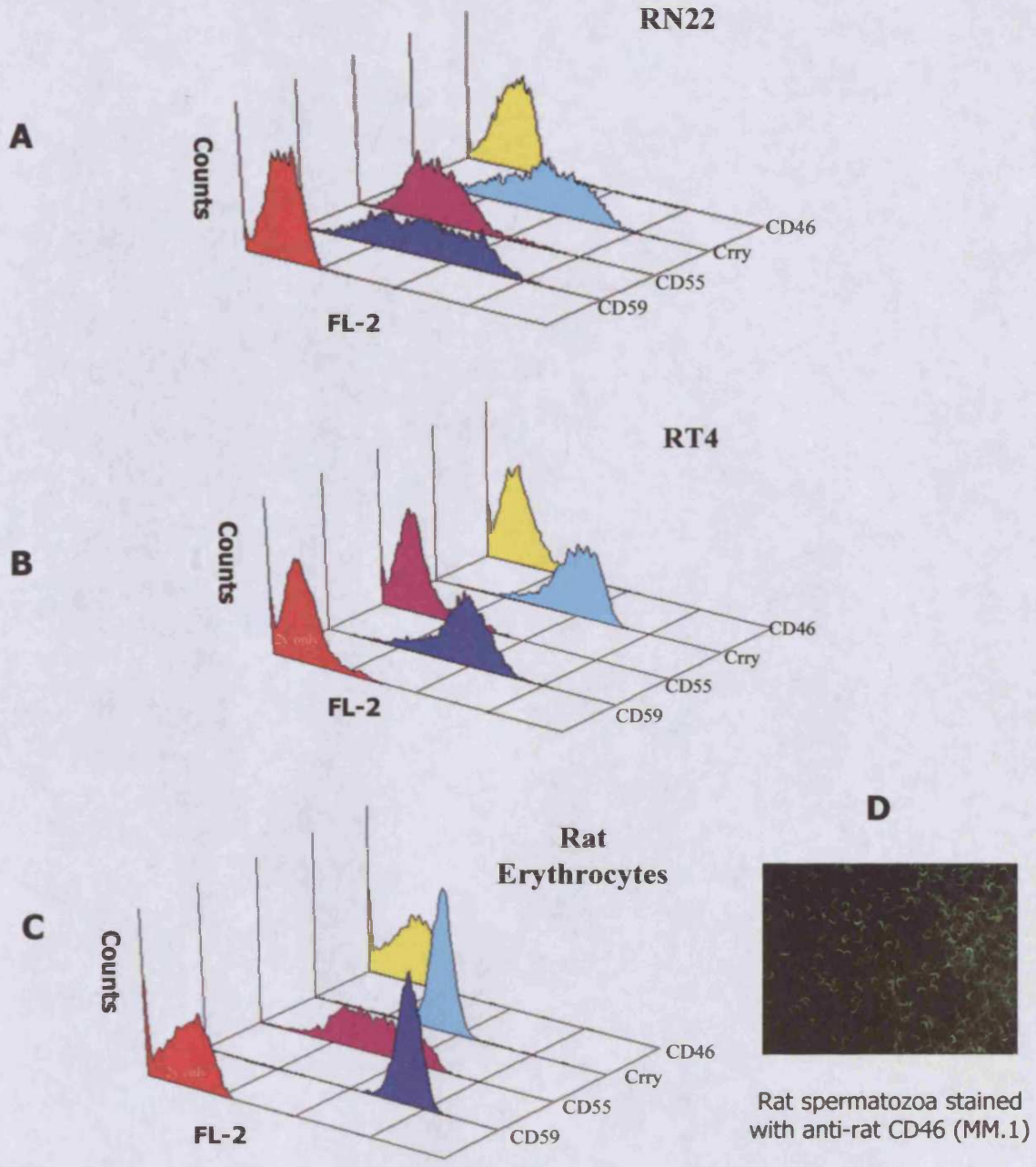

Figure 1

Single colour flow cytometry analysis of membrane bound CReg expression on rat Schwann cells

Rat Schwann cell lines RN22 (A), RT4 (B) and rat E (C) were harvested, and stained for membrane-bound C regs as described previously. Briefly, cells were incubated with 10µg/ml of mouse anti-rat CD55 (RDIII7), mouse anti-rat CD59 (6D1), mouse-anti-rat Crry (TLD1C11) and mouse anti-rat CD46 (MM.1), for 40 minutes at 4^0C, and processed as described using rPE-conjugated secondary antibodies. Rat E were used as a positive control for CD55, CD59 and Crry. Due to the restricted nature of CD46 expression, anti-rat CD46 antibody integrity was confirmed by ICC staining of rat spermatozoa (D). All cells were analysed on a FACSalibur using the FL-2 channel. The result shown above represents mean values obtained from 4 replicates.

2.4.1.2 Immunoprecipitation of rat CD59 from rat Schwann cell lysates

Cell lysates were prepared as described previously. Following centrifugation, the supernatant was incubated with 10µg of mouse anti-rat CD59 (6D1) for 1 hour at 4^0C, followed by 100µl of Protein A sepharose beads, (Amersham Pharmacia, UK) and incubated overnight at 4^0C. The sepharose was washed once in PBS, 0.1% (v/v) NP40, a further four times in PBS, 0.1% NP40 (v/v), 0.5M NaCl, and once more in PBS, 0.1% (v/v) NP40. Following centrifugation at 1000g in a microfuge, the sepharose beads were resuspended in 100µl of non-reducing sample loading buffer, and boiled for 5 minutes. The sample was centrifuged briefly to pellet the beads, and the supernatant was loaded onto the gel at 20µl/well.

2.4.1.3 Preparation of E ghosts

Whole rat blood was collected into heparin (approx. 50-100 U/ml blood). Rat E were washed three times in PBS at room temperature by centrifugation at 1800g for 5 minutes. All subsequent manipulations were performed at 4^0C or on ice. The resulting pellet was resuspended in ice-cold E lysis buffer (5mM sodium phosphate, pH 7.4, 2mM EDTA, 1mM benzamidine, 1mM PMSF, 0.02% (v/v) sodium azide) at a ratio of 10 volumes of lysis buffer: 1 volume packed rat E. The suspension became clear immediately, and was centrifuged at 18,000g for 20 minutes in a refrigerated microfuge. E ghosts form a cloudy layer on top of any remaining non-lysed E, and were carefully removed and washed five times in E lysis buffer until almost white in colour, and stored at -80^0C until use.

Rat E ghost lysates (RtE lysate) were prepared by resuspending at a ratio of 1 volume of ghosts: 5 volumes of cell lysis buffer and incubating for 1 hour on ice.

2.4.1.4 Preparation of testis lysate

Testes were obtained fresh from euthanized rats. The tissue was finely minced, suspended in 3ml cell lysis buffer per testis, and incubated for 60 minutes on ice. Insoluble debris was removed by centrifugation at 15,000g for 15 minutes at 4^0C, and the supernatant was stored at -80^0C until use.

2.4.2 Sodium dodecyl sulphate-polyacrylamide gel electrophoresis (SDS-PAGE)

Rat Schwann cell lysates were prepared as described. Schwann cell lysate (15µl) was mixed with 5µl PBS and 20µl of 1X non-reducing sample loading buffer (5X sample buffer: 0.313M Tris-HCl, pH 6.8, 10% (w/v) SDS, 0.05% (v/v) bromophenol blue, 50% (v/v) glycerol), and boiled for 5 minutes. Sample (20µl/lane) was loaded onto an appropriate percentage SDS-PAGE gel with suitable positive control samples selected for each regulator (Table 1). Rat testis lysate was prepared as described. Testis lysate (5µl) was diluted in 20µl PBS, and

mixed with 25µl of non-reducing sample buffer; 10µl/lane was loaded onto the gel. Gels were electrophoresed at 30mA per gel until the dye front reached the bottom of the gel. Following electrophoresis, the gel was soaked in transfer buffer (0.192 M glycine, 25 mM Tris, 20% (v/v) methanol, pH 8.3). The gel was assembled into a cassette (sponge, filter paper, gel, membrane, filter paper, sponge), ensuring no air bubbles remained. The cassette was placed into a blotting tank filled with transfer buffer, with the membrane closest to the anode, and transferred at constant 100V for 1 hour using a running water cooler.

The membrane was transferred to a universal container containing PBS-milk (5% (w/v)) to block excess protein binding sites, and incubated for 30 minutes at room temperature. Mouse anti-rat CD59 (6D1), CD55 (RDIII7), Crry (TLD1C11) or CD46 (MM.1) were added to a solution of PBS-milk at 10µg/ml and incubated for 1 hour at room temperature on a roller. Following three washes in PBS, 0.1% (v/v) Tween, anti-mouse-immunoglobulin (Ig)-HRPO conjugate (BioRad, UK) was added at 1/1000 dilution in PBS-milk, and incubated for 1 hour at room temperature on a roller. After three further washes in PBS-Tween, the blot was placed between two sheets of polythene, sealed around three edges and incubated for 5 minutes with SuperSignal reagent (Pierce) according to the manufacturer's instructions. Following removal of excess substrate, the polythene was completely sealed and exposed to X-OMAT UV-film (Kodak). The film was developed in a Compact X2 developer.

CReg	**Molecular weight**	**Percentage running gel**	**Positive control**
Rat CD59	18-25kDa	12.5%	Rat E ghosts
Rat CD55 (GPI, TM, Sec)	62-74kDa	10%	Rat E ghosts
Rat Crry (6 SCR, 7 SCR)	55, 65kDa	10%	Rat E ghosts
Rat CD46	40kDa	10%	Rat testis lysate

Table 1

Summary table of CReg identifying correct percentage running gel for molecular weight of protein, and selection of appropriate positive control samples

2.4.2 Results

CD55 was not detected by Western blotting on rat Schwann cell line lysates, although the rat E ghost lysate revealed a band of approximately 60kDa corresponding to rat CD55 (Figure 2a, panel I). In contrast, rat Crry was detected in both cell lines, and in the positive

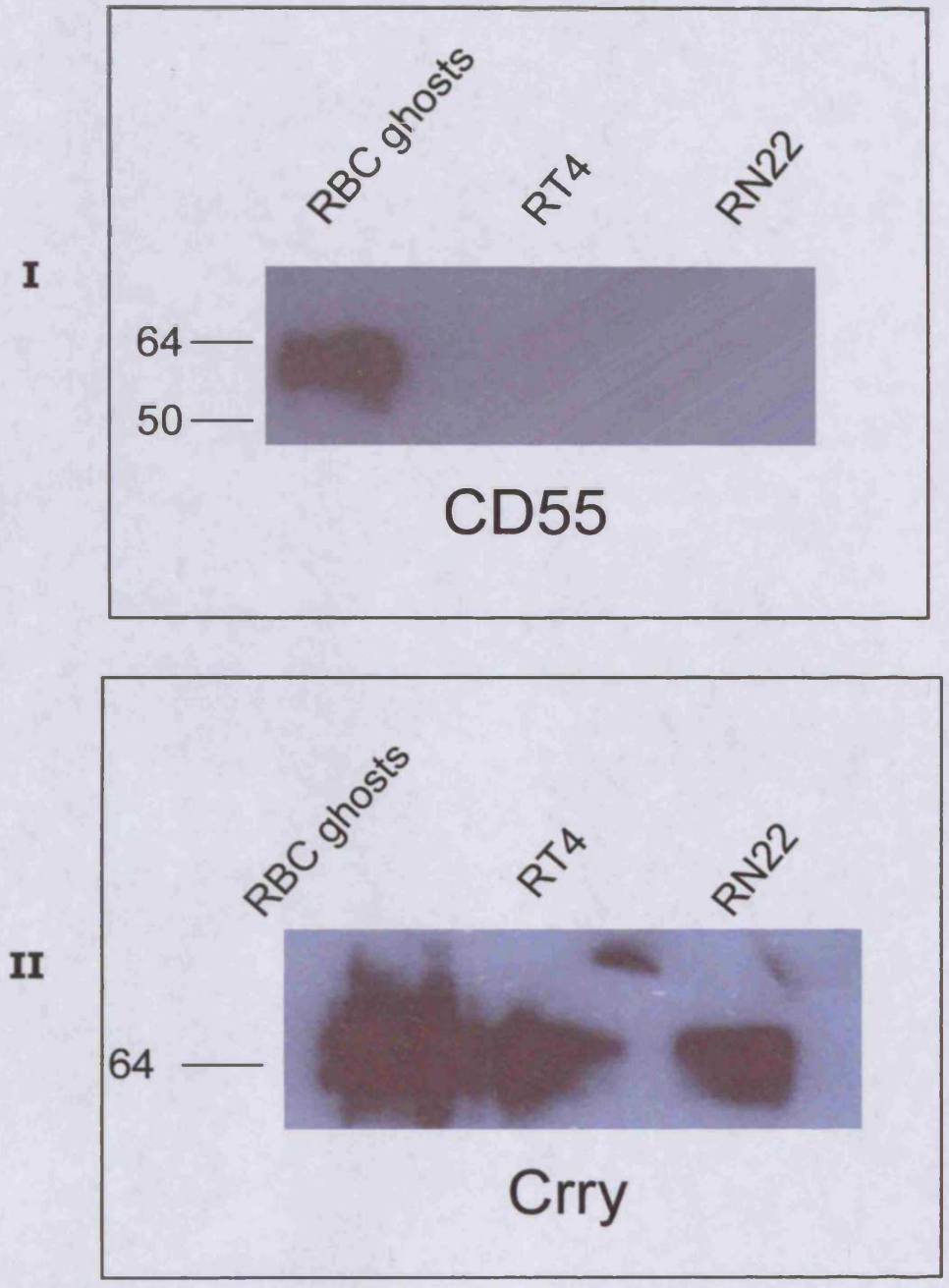

Figure 2a

Detection of CD55 and Crry by SDS-PAGE and Western blotting of rat Schwann cell line lysates

Rat Schwann cell lysates were prepared as described previously. Briefly, 2 confluent T-80cm^3 flasks were harvested, and lysed in 750µl cell lysis buffer for 1 hour on ice. Resulting supernatants were loaded onto appropriate percentage SDS-PAGE gels, and electrophoresed. Gels were transferred onto nitrocellulose using published methods. Blots were probed with mouse anti-rat CD55 (RDIII7, panel I) or mouse anti-rat Crry (TLD1C11, panel II). Rat E ghosts were used as a positive control for blots for CD55 and Crry.

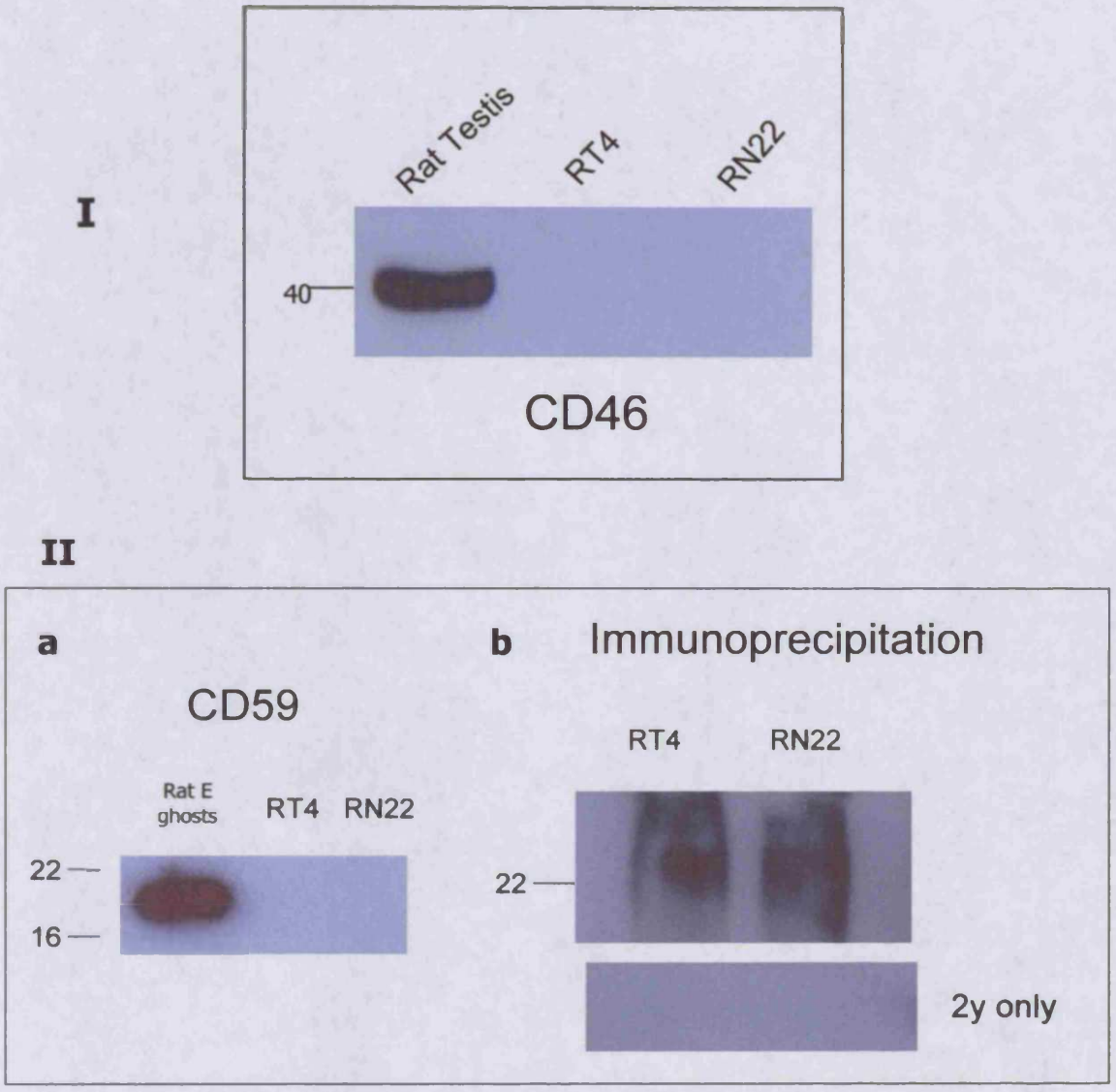

Figure 2b

Detection of CD46 and CD59 by SDS-PAGE and Western blotting of rat Schwann cell lysates

Cell lysates were prepared as described previously. Blots were probed with mouse anti-rat CD46 (MM.1, panel I), and following immunoprecipitation, with mouse anti-rat CD59 (6D1, panel II). Rat testis lysate was used as a positive control for CD46, and rat E ghosts were used as a positive control for CD59.

control corresponding to approximately 65kDa (Figure 2a, panel II). No bands were detected for CD46 in the cell lines as expected. Rat testis lysate was used as a positive control for CD46 and revealed a band of approximately 40kDa corresponding to rat CD46 (Figure 2b, panel I).

Rat E ghost lysates were used as a positive control for CD59, and revealed a band of approximately 20kDa. On initial blotting using standard methods, no bands were detected for CD59 in RN22 or RT4 (Figure 2b, panel II, section a), but upon immunoprecipitation as described, broad bands were visible corresponding to approximately 20kDa (Figure 2b, panel II, section b).

2.5 Reverse transcription polymerase chain reaction (RT-PCR) for detection of mRNA for membrane-bound CReg and C components on rat Schwann cell lines

In order to understand the susceptibility of RN22 and RT4-D6P2T to C attack, it was necessary to confirm mRNA expression for the membrane-bound CRegs to verify flow cytometry and Western blotting results, and to determine their capability to express C components. Chart 1 shows a flow chart summarising the steps involved in an RT-PCR reaction. cDNA from rat testis was used as a source of template for membrane-bound CRegs, while cDNA from rat liver was used for C components.

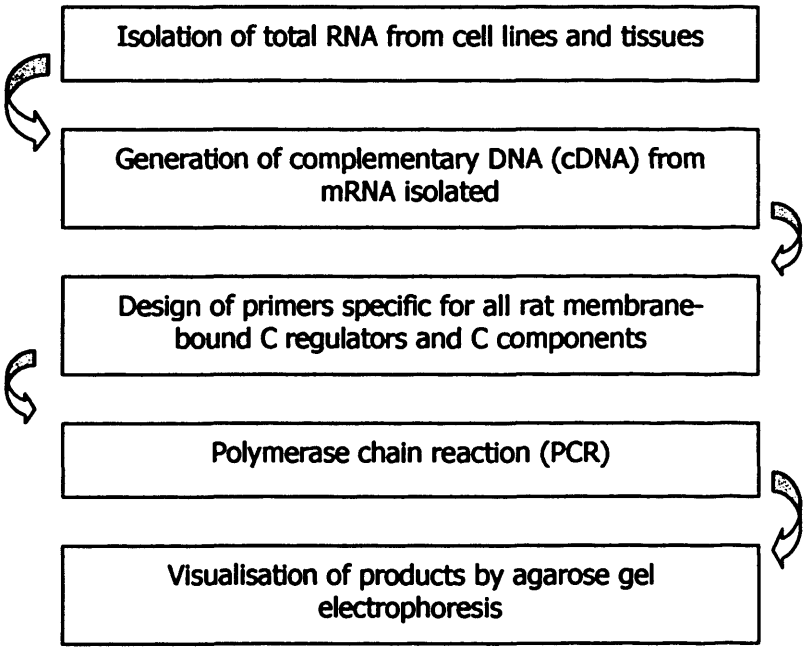

Chart 1 **Flow chart summary of RT-PCR protocol**

2.5.1 Method: RNA isolation

All equipment used was pre-treated with 0.1% (w/v) diethylpyrocarbonate (DEPC) to remove RNAse contamination.

2.5.1.1 Total RNA purification: Tissues

Total RNA was purified from rat liver and rat testis as positive controls for RT-PCR using Ultraspec RNA isolation medium (Biotecx Laboratories, Texas, USA) containing guanidine salts and urea as rapid denaturants, and phenol for RNA extraction. Upon euthanasia of an adult male Lewis rat, tissues of interest (1cm^3 from each tissue) were quickly removed from the rat and homogenised into 1ml Ultraspec medium. Following incubation on ice to permit dissociation of nucleoprotein complexes for 30 minutes, chloroform (0.2ml per 1ml Ultraspec used) was added and vigorously mixed for 15 seconds. The tube was further incubated on ice for 5 minutes and centrifuged at 22,000g for 15min at 4^{0}C. The upper aqueous phase was transferred to a fresh microcentrifuge tube and an equal volume of isopropanol was added. Following mixing, the solution was incubated on ice for 10min, and a precipitate was pelleted by centrifugation at 22,000g for 15min. The pellet was washed twice in 70% (v/v) Ethanol in DEPC-water by centrifuging at 6000g for 5 minutes, and finally resuspended in 50-100µl DEPC-treated water. RNA concentration was obtained using the RNA command and measuring absorbance at 260nm on a GeneQuant spectrophotometer (Amersham Biosciences, UK).

2.5.1.2 Total RNA purification: Cell lines

Confluent T-80cm^3 flasks of RN22 and RT4-D6P2T cells were washed three times with sterile 0.9% (w/v) saline. For adherent cells, FCM containing 2mM EDTA was used to lift cells which were centrifuged at 450g for 3 minutes. The resulting pellet was homogenised into 1ml of Ultraspec RNA isolation medium, and RNA was isolated as detailed above.

2.5.2 Preparation of complementary DNA (cDNA) by reverse transcription (RT)

A standard RT protocol was performed as follows. Random hexamers (2µl, PdN6, stock concentration 0.5mg/ml, Bioline), 1.5µl 25mM dNTPs (Bioline), 6µl 5X first strand buffer, 3µl dithiothreitol (DTT, stock concentration 0.5M), 1.5µg total RNA, DEPC-treated water to make final volume of 30µl, 1.5µl Superscript™ II Reverse Transcriptase (Invitrogen Life Technologies). The components, excluding Superscript were mixed, and the following temperature changes employed (Table 2).

Temperature	Duration	Action
65^0C	10 minutes	RNA denaturation
Ice	10 minutes	RNA condensation to prevent re-annealing and reformation of secondary structures
Add Superscript		65^0C would denature enzyme
25^0C	10 minutes	Random hexamer annealing
42^0C	2 hours	cDNA elongation
99^0C	1 minute	RT denaturation
Ice	20 minutes	Storage; final storage at -20^0C

Table 2

Summary of temperature changes and their consequence during an RT reaction

Sequences were obtained from Entrez Pubmed, and primer sequences were derived using MS-DOS program OLIGO or using Custom OligoPerfect primer design software (Invitrogen Life Technologies). Forward and reverse primers were designed of approximately 20bp corresponding to rat membrane-bound CRegs CD55, CD59, Crry and CD46. In addition, primers were also designed to correspond to C components from all aspects of the cascade. For the Classical Pathway (CP), primers were designed for rat C1q-beta subunit and rat C2. Since the sequence for rat Factor B (fB) was not known, the sequence for mouse fB was utilised to design primers relating to the Alternative Pathway (AP). C3 and C5 primers were created, covering the central C component, and the beginning of the Terminal Pathway (Table 3).

2.5.4 Polymerase chain reaction (PCR)

The protocol for 'hot-start' PCR for DNA amplification was as follows. Reaction buffer (5µl of 10X stock, Bioline), 1µl 50mM Mg^{2+}, 10µl 1mM dNTPs (Bioline), 2µl of forward and reverse primers from 10pmol/µl stock, 3µl cDNA, DEPC-treated water to give final reaction volume of 50µl (Bioline, 1U/µl). The reaction was mixed, overlaid with mineral oil and heated to 94^0C for 2 minutes in a PCR block (Hybaid Omnigene). Taq polymerase was added (1µl, Bioline), and thermal cycling was started, consisting of a denaturation step at 94^0C for 90 seconds (s) followed by primer annealing at 50-64^0C (dependent on primer set utilised) for 45s and extension at 72^0C for 2 minutes (optimal temperature for Taq polymerase). A total of 30 cycles were performed followed by a final extension step at 72^0C for 10min.

Primer ID	NCBI UID*	Sequence FWD	Sequence REV	Expected product size (bp)
Membrane-bound CReg				
Rat CD55	3873188	AATGCCACGCCAAACTCGGGT	CCCAGTCCACAGCATTCCCCG	511
Rat CD59	6978634	CGAAACTGGCGCAGGCAAGAA	CCGCCTGGCAGCATCTGTATT	343
Rat Crry	550510	CGCTCTAGAGAGCGCTGTGAGGG	CGCGGATCCTATCACTTGTTCACACACAGG	1100
Rat CD46	9506882	GCCCTTCTGTTTCTGCTGTC	AATAGCATGCTCGGTCCAAC	568
C Components				
Rat C1q-beta	9506432	TGCTGCTCCTGGGTTTGCTCC	TTCTGCATGCGGTCTCGGTCG	529
Rat C2	26449161	CAACGGGCAGTGGCAGACACC	TCCGACCCACTCCACACTCCG	429
Mouse Factor B	6996918	TCTCTGAGTCTCTGTGGCAT	TTGGGGTCAGCATAGGGA	658
Rat C3	8393023	TCAACTTCCACCTGCGCACGG	GGCTTGGCGCACTCAGGATCT	535
Rat C5	34853896	GGAGTGGCTTCATTTGTGGT	CACCATGTCAAGGGACACAG	744

* refers to unique identification (UID) number on nucleotide function of NCBI Entrez Pubmed

Table 3

Summary of primers designed against membrane-bound C reg, and a variety of C components spanning the entire C cascade. Forward and reverse sequences are given, in addition to the expected PCR product length

2.5.5 Agarose gel electrophoresis visualisation of PCR products

Agarose (1% w/v) was melted in 1x TAE buffer (40 mM Tris, 20 mM acetic acid, 1 mM EDTA, pH 8.0) in a microwave with regular mixing, cooled to approximately 50^0C, ethidium bromide added to a final concentration of 100ng/ml and the solution poured into a casting tray containing a well-forming comb. The agarose was allowed to set, the well-comb

removed, the gel placed in an electrophoresis tank and covered with 1xTAE buffer. At least 100ng of each DNA sample was mixed with $1/10^{th}$ volume of gel loading buffer and pipetted into individual wells. At least one well contained a DNA ladder to enable accurate sizing of DNA fragments. The gel tank was connected to a power supply and electrophoresed at constant voltage (80V) until adequate separation of DNA was achieved. Gels were visualised under UV illumination and images captured with a digital camera using the Bio-Rad Gel Documentation system.

2.5.6 Results

Both RN22 and RT4-D6P2T express mRNA for membrane-bound CRegs CD59, Crry and CD46. Only RN22 expressed mRNA for CD55. Both lines are limited in expression of actual C components, with the exception of C2 within the classical pathway (CP). As positive controls for all RT-PCR reactions, rat testis cDNA was used for CReg, with rat liver cDNA used for C components. pQE9-PO vector containing the sequence for the extracellular domain of PO (refer Chapter 3) was used as a positive control for PO PCR as a marker of myelinating Schwann cells (Figure 3). These results confirm the data obtained from flow cytometry and Western blot analysis. Surprisingly, mRNA for CD46 was detected in both cell lines, although no protein expression was detected by flow cytometry and Western blotting. However, mRNA for CD46 has previously been detected in tissues distinct from reproductive organs (Mead, Hinchliffe et al. 1999).

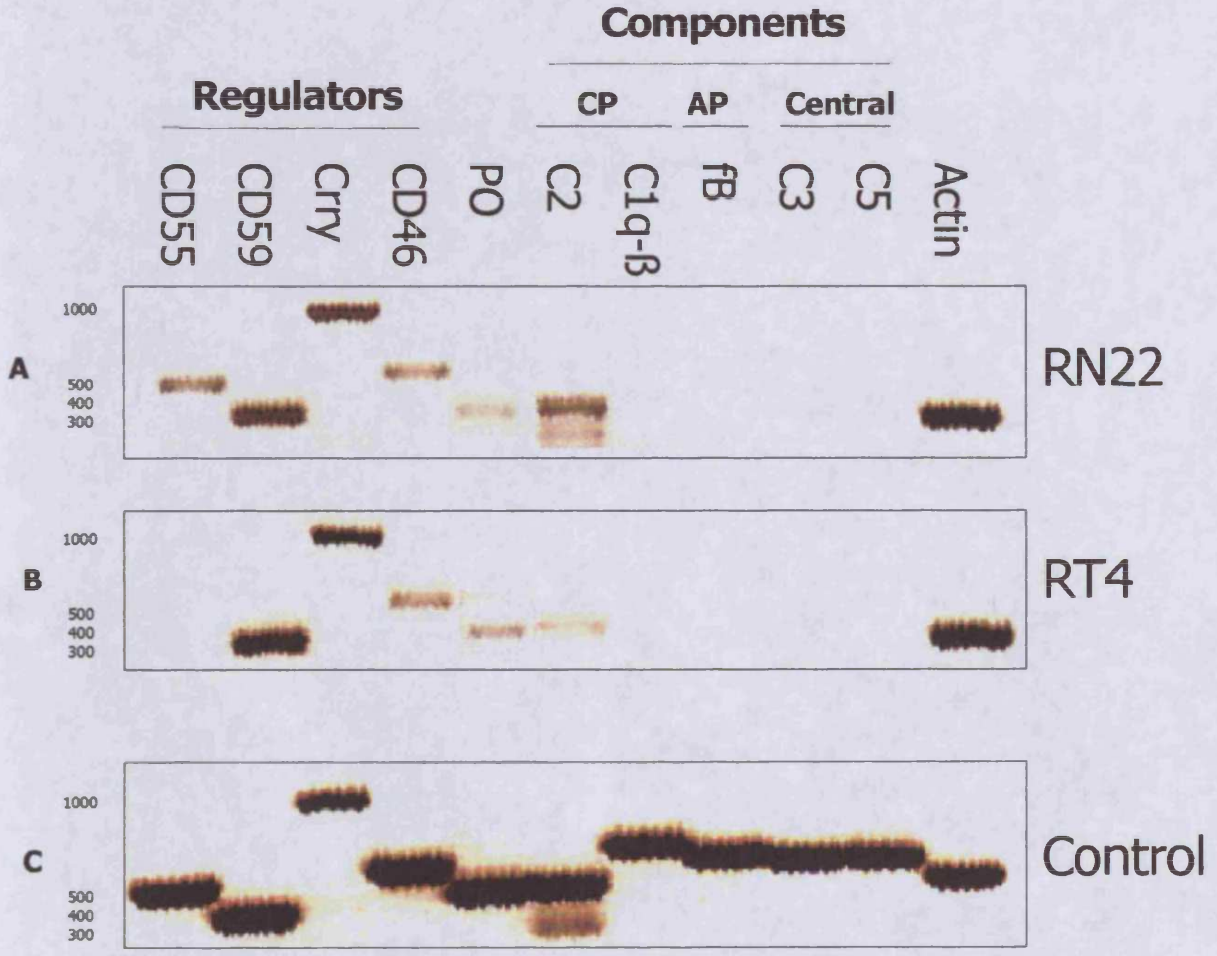

Figure 3

RT-PCR of cDNA from rat Schwann cell lines to determine presence or absence of mRNA for C reg and C components

cDNA was prepared from RNA isolated from cell lines RN22 (A) and RT4 (B), and probed with sequence-specific primers for all membrane-bound C regs, and C components spanning the entire cascade as described. cDNA from rat testis was used as a positive control for CD55, CD59, Crry and CD46.; rat liver cDNA was used as a positive control for all of the C components. pQE9-PO vector (refer Chapter 3) was used as a positive control for PO (C). Primers for actin were used as a control for RNA quality.

2.6 Immunostaining of rat Schwann cell lines, primary rat Schwann cell cultures and rat sciatic nerve sections

2.6.1 The search for a Schwann cell marker

2.6.1.2 Myelin basic protein as a marker of Schwann cells

Myelin basic protein (MBP) is a highly basic protein present at the cytoplasmic surface of compact myelin membranes, and represents between 5 and 15% of PNS myelin protein. By its highly charged nature, its is thought to contribute to myelin compaction together with PO via electrostatic interactions (Kursula 2001). This protein can be identified in benign and malignant Schwann cell tumors and granular cell tumors, and is useful to distinguish malignant schwannoma from malignant melanoma (Johnson, Glick et al. 1988). Recent work has tentatively divided Schwann cell markers into 3 distinct groups. Group 1 includes glial fibrillary acidic protein (GFAP), which is expressed temporally between immature Schwann cells and mature myelinating cells. Group 2 includes S-100 which is expressed during immature stages and continues into mature, myelinating Schwann cells. Group 3 includes MBP, which is only expressed in the mature, myelinating Schwann cells (Francis Pau and Wolf 2004).

2.6.1.3 S100 as a marker of Schwann cells

S100 is a group of closely related dimeric acidic calcium-binding proteins, first isolated from the CNS (Moore 1965). The group is composed of a dimer with alpha and beta subunits, able to combine in three isoforms S100ao (alpha dimer), S100a (alpha-beta isoform) and S100b (beta dimer). S100 has structural similarities to the calcium-binding domain of calmodulin, and the name derives from its solubility in 100% saturated ammonium sulphate. S100 is abundant in the brain, and Schwann cells within the PNS; S100a and S100b localise to glial cells, whereas S100ao has a neuronal localisation. S100 can be found in soluble as well as in membrane-bound form (Donato 1986). Immunocytochemical studies demonstrated that S100 protein is also produced by a wide variety of normal and neoplastic cells of mesodermal, neuroectodermal, and epithelial origin (Herrera, Turbat-Herrera et al. 1988).

Dako's Z311 rabbit anti-cow S100 antibody reacts with both the alpha and beta dimers of S100, cross-reacts strongly with human, chicken, kangaroo, mouse and rat S100, and staining is both nuclear and cytoplasmic.

S100 is most useful in distinguishing between several different tumours, for example brain glial cell and ependymal cell tumours as opposed to metastatic tumours originating from outside the brain; tumours with Schwann cell origin versus other soft tissues, and

particularly melanocytic tumours (DAKO 1994). It was necessary therefore to search for a more specific marker of the PNS, and in particular Schwann cells.

2.6.1.4 Peripheral myelin protein 22 (PMP22) as a marker of Schwann cells

PMP22 is a 22kDa transmembrane protein expressed by the Schwann cell and thus by compact myelin, and constitutes between 2 and 10% of total peripheral nerve myelin protein (Snipes, Suter et al. 1992). Duplication and deletion of the PMP22 gene is associated with Charcot-Marie-Tooth disease 1A (CMT1A) and Hereditary Neuropathy with Pressure Palsies (HNPP) respectively. Rats over-expressing a transgene for PMP22 exhibit a hypomyelinating phenotype (Sereda, Griffiths et al. 1996). Its function has been poorly understood, but suggestions to date have included control of Schwann cell growth cycle (Zoidl, Blass-Kampmann et al. 1995), Schwann cell-axon adhesion (Snipes, Suter et al. 1992), intercellular signalling (Snipes, Suter et al. 1993), and more recently PMP22 has been found to be a constituent of intercellular junctions in epithelia, in particular in association with tight junction protein occludin. PMP22 expression is highest in myelinating Schwann cells of peripheral nerves, although significant levels of mRNA for PMP22 have been detected in non-neural tissues, for example, rat liver and intestine (Notterpek, Roux et al. 2001). Work studying domain specific trans-interactions between PMP22 and myelin protein zero (P0) has suggested that PMP22 and P0 are involved in direct protein-protein binding, and so function to maintain and stabilise PNS myelin. Homophilic interactions (PMP22-PMP22, P0-P0) and heterophilic interactions (PMP22-P0) are evident in a model system, and any disruption through mutation had a direct effect on this binding (Hasse, Bosse et al. 2004).

2.6.5 Methods

Adult Lewis rats were euthanized and the sciatic nerves were removed, and snap-frozen in isopentane at -40^{0}C. Frozen tissues were embedded in OCT medium (Agar Laboratories, Stanstead, Essex, UK), and sectioned transversely in a cryostat at 8-10µm. Sections were fixed in neat acetone for 5 minutes. Fixed sections were incubated with primary antibodies (rabbit anti-cow S100 (DAKO, Cat. No. Z311); mouse anti-human MBP (Serotec Cat. No. MCA685S); rabbit anti-human PMP22 (AbCam, Cat. No. 15507)) at 10µg/ml or 1:200 dilution for the PMP22 antibody, for 1 hour at RT in a humid chamber. Following washing (x5) in PBS, sections were incubated with donkey α-rabbit-Ig-rhodamine (Jacksons 711-025-152) at 1:200 dilution, for 1 hour at RT in a humid chamber. Following washing (x5), slides were mounted in VectorShield (Vector Laboratories, UK), and analysed on an inverted fluorescence microscope. As a control for non-specific binding of Ig, staining with total Ig

appropriate for the species used was also included. No background staining was observed (data not shown).

2.6.5.1 Results: Identification of a Schwann cell marker

As a preliminary assessment, comparisons between the distribution of MBP, S100 and PMP22 were made using rat sciatic nerve sections (Figure 4). MBP staining was diffuse within the sciatic nerve, while S100 appeared both around the myelin sheath of the axon, as well as within the axon itself. PMP22 staining was more focussed, and appeared exclusively on Schwann cell bodies.

In light of this, it was concluded that PMP22 was a more specific marker of Schwann cells than MBP or S100, and therefore the PNS. Co-localisation studies of PMP22 and CReg on PNS-derived Schwann cell lines, primary cultures and tissues were performed. In addition, rat spinal cord and kidney were examined to determine cross-reactivity of the anti-PMP22 antibody against these tissues.

2.6.5.2 Examination of specificity of PMP22 staining for the PNS

Adult Lewis rats were euthanized and the spinal cord and kidney were removed, and snap-frozen in isopentane at -40^{0}C. Sections were processed as described in Section 2.6.5.

2.6.5.3 Results: PMP22 specificity testing

Expression of PMP22 was clearly restricted to peripheral nerve roots (PNR) adjacent to the spinal cord with no staining of cells observed within the white matter. Intense staining of the central canal was evident with PMP22, presumably on ependymal cells. Rat kidney sections were to be used as a negative control for this antibody; however, unexpectedly, highly focussed PMP22 staining was evident within the glomeruli of rat kidney (Figure 5). This non-neural expression of PMP22 has been described previously, and will be referred to in the discussion.

2.6.6 Coverslip culture: Rat Schwann cell lines and primary culture

2.6.4.1 Rat Schwann cell lines

RT4-D6P2T and RN22 rat Schwann cell lines were harvested and resuspended to 1x10^5 cells/ml. The suspension (50-100µl) was applied to 16mm diameter coverslips, and cells were grown overnight in DMEM-F5. Following washing in DMEM (no supplements), coverslips were fixed in neat acetone for 10s. Primary monoclonal antibodies against rat CD55 (RDIII7), CD59 (6D1), Crry (TLD1C11) and CD46 (MM.1) were diluted in 1% (w/v) BSA in PBS to 10µg/ml; polyclonal antiserum for PMP22 was diluted to 1:200 final dilution,

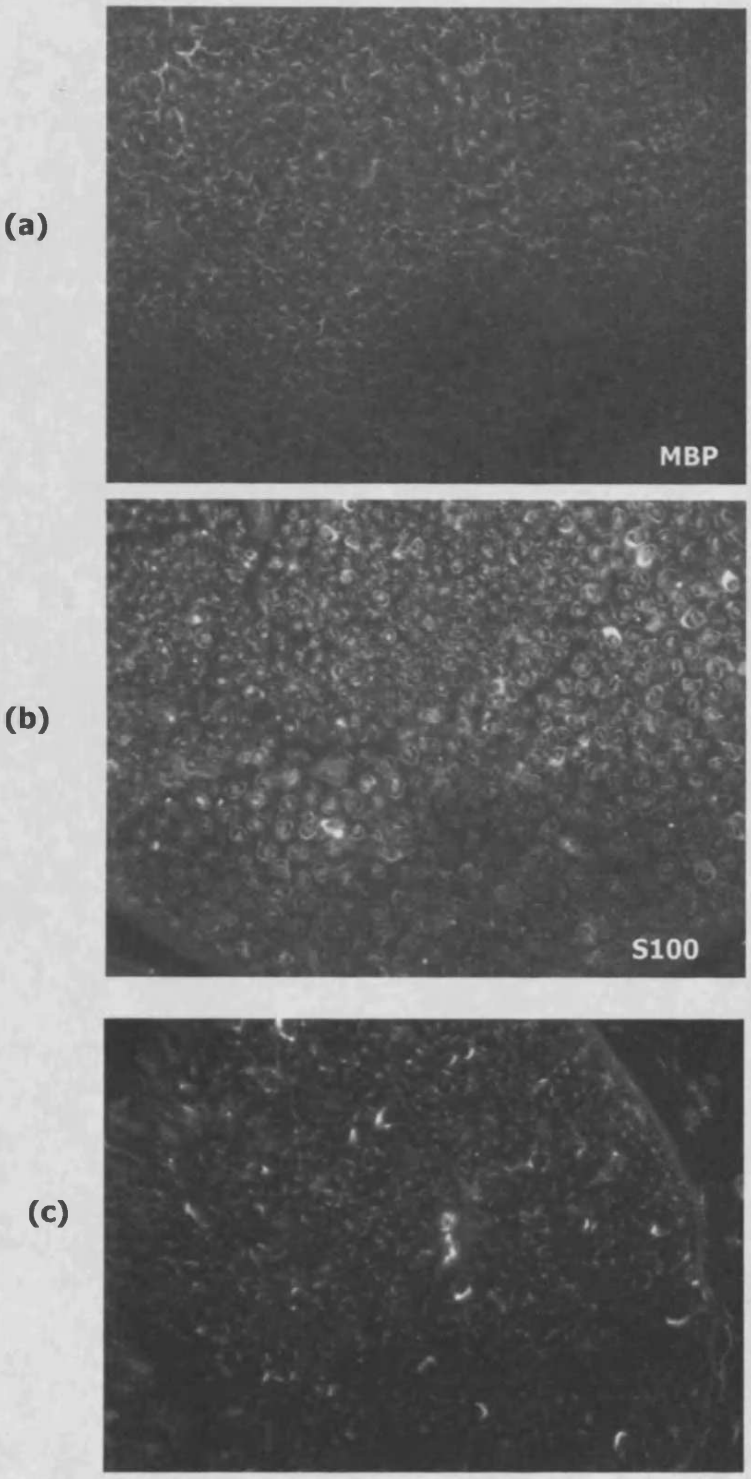

Figure 4

Comparison of rat Schwann cell markers by immunohistochemistry of rat sciatic nerve

Sections of rat sciatic nerve were stained with anti-MBP (a), anti-cow S100 (b) and anti-human PMP22 (c), detected using appropriate secondary antibodies, and analysed on an inverted fluorescent microscope.

Figure 5

Analysis of PMP22 expression in rat spinal cord and kidney

Rat spinal cord and kidney sections were stained for PMP22 and counter-stained with DAPI to visualise nuclei as described previously. Peripheral nerve roots (PNR) were visualised within the spinal cord sections, as well as the central canal and associated ependymal cells (PMP22, central canal, white arrow). Glomeruli (G) were visible in kidney sections. All images were taken at 200X magnification.

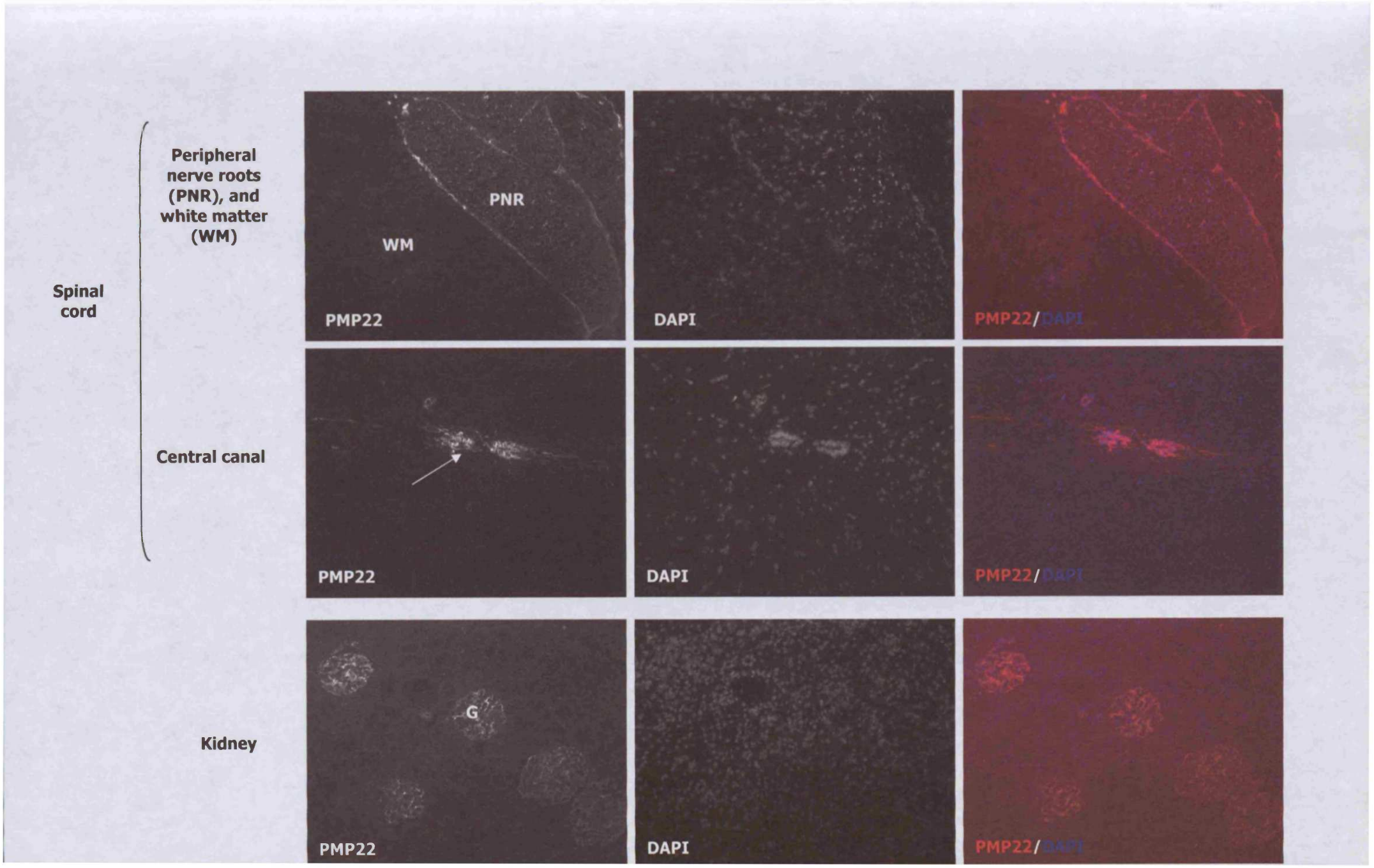
Spinal cord
Peripheral nerve roots (PNR), and white matter (WM)
PNR
WM
PMP22
DAPI
PMP22/DAPI
Central canal
PMP22
DAPI
PMP22/DAPI
Kidney
G
PMP22
DAPI
PMP22/DAPI

and applied to the coverslips for 1 hour at RT in a humid chamber. Coverslips were washed three times in PBS, and incubated with appropriate secondary antibodies (donkey antimouse Ig-FITC, Jackson, 715-095-151; donkey anti-rabbit-rhodamine, Jackson, 711-025-152) at 1/200 dilution in 1% (w/v) BSA in PBS) diluted in 1% (w/v) BSA in PBS containing DAPI at 100ng/ml, and incubated for 1 hour at RT in a humid chamber. Following further washing, coverslips were mounted in VectorShield and visualised using an inverted fluorescence microscope. Each figure shows staining of a particular cell line for a specific CReg together with PMP22 staining, and a merged image.

2.6.4.2 Results: RT4-D6P2T

PMP22 staining was focussed around the cell body in RT4-D6P2T; the cell line lacked expression of CD55, but had high relative expression of CD59 and Crry, though with a different distribution; CD59 had a smooth expression pattern on the cell body and processes while Crry appeared granular in its distribution. Crry was weakly distributed throughout the cell structure, but was focussed around the cell body (Figure 6). No expression of CD46 was evident in this cell line (data not shown). All images were taken at 400X objective magnification.

2.6.4.3 Results: RN22

PMP22 was again focussed around the cell body in this Schwann cell line. CD55 was weakly expressed by RN22, and its distribution was limited to the cell body. CD59 was highly expressed by RN22, specifically around the cell body, but also on elements radiating from the cell body. Crry expression was restricted to the cell body of RN22, and did not extend to the processes (Figure 7). CD46 was not expressed by the cell line (data not shown).

2.6.5 Primary rat Schwann cell culture

2.6.5.1 Methods

The protocol was adapted from that of Cole and de Vellis (Cole and de Vellis 1989). Sciatic nerves were dissected from five 3 day old Wistar pups, minced with a scalpel and transferred into DMEM (5ml, no supplements). The tissue was centrifuged at 350g and the pellet resuspended in collagenase at 2mg/ml final concentration in DMEM (5ml) and incubated at 37^0C for 30 minutes. Trypsin-EDTA (5g/l trypsin, 2g/l EDTA; 10X) was added to the collagenase at a 1:10 dilution and incubated at 37^0C for 15 minutes. The reaction was stopped with an equal volume of DMEM-F10 and incubated at room temperature (RT) for 10 minutes. The medium was carefully removed to leave approximately 1ml, and DNAse was added at 1:10 dilution and

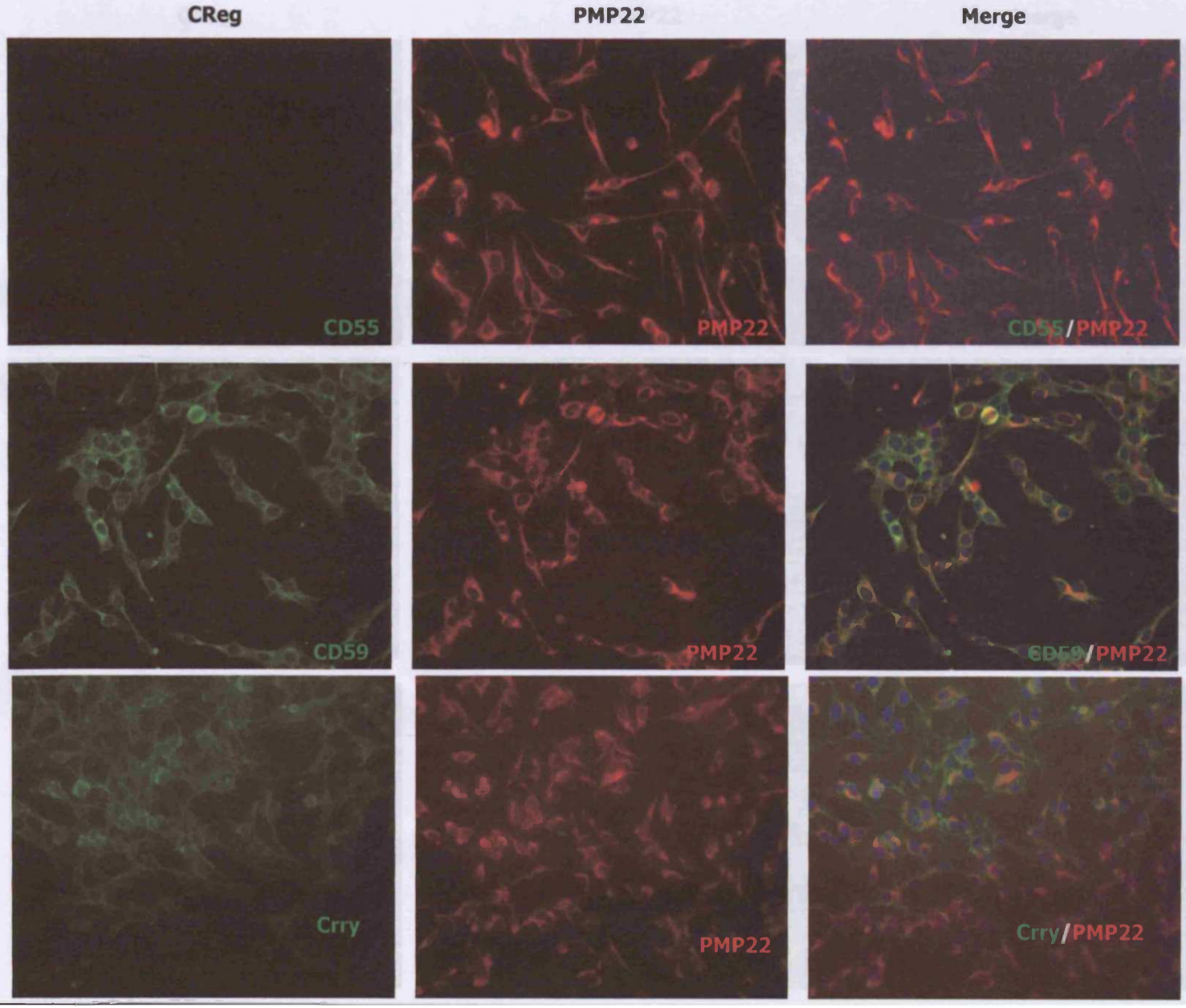

Figure 6

Analysis of membrane-bound C reg expression on rat Schwann cell line RT4

RT4 grown on coverslips were stained for membrane-bound C regs as described previously. Briefly, coverslips were incubated with anti-rat CD55 (RDIII7), anti-rat CD59 (6D1), anti-rat Crry (TLD1C11) and anti-rat CD46 (MM.1, not shown) at optimal pre-determined dilutions, for 1 hour at R.T in a humid chamber, and processed as described using FITC-conjugated secondary antibodies. Sections were double-stained for PMP22 as described. Images were merged to detect any co-localisation of expression. All images were taken at 400X magnification.

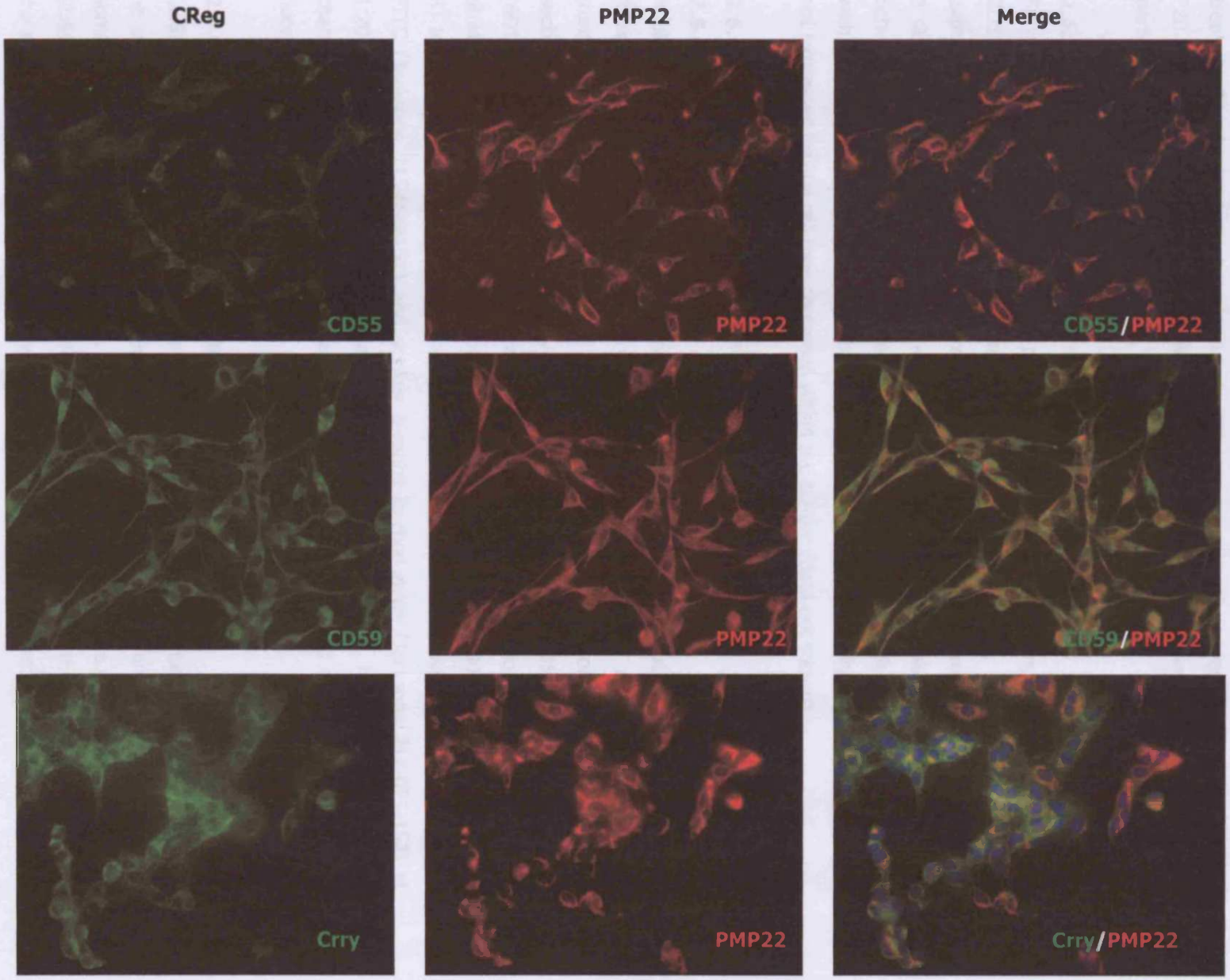

Figure 7

Analysis of membrane-bound CReg expression on rat Schwann cell line RN22

RN22 grown on coverslips were stained for membrane-bound CRegs as described previously. Briefly, coverslips were incubated with anti-rat CD55 (RDIII7), anti-rat CD59 (6D1), anti-rat Crry (TLD1C11) and anti-rat CD46 (MM.1, not shown) at optimal pre-determined dilutions, for 1 hour at R.T in a humid chamber, and processed as described using FITC-conjugated secondary antibodies. Sections were double-stained for PMP22 as described. Images were merged to detect any co-localisation of expression.

All images were taken at 400X magnification.

incubated for 10 minutes at RT. DMEM (5ml) was added to the tissue, mixed and left to stand for 5 minutes. The supernatant was removed and transferred to a clean tube. The tissue was gently homogenised using a Pasteur pipette, allowed to settle, and the supernatant was removed. The combined supernatants were centrifuged at 350g for 3 minutes. The pellet containing the Schwann cells was resuspended in a minimal volume of DMEM-F20 (approximately 500µl), and approx. 30-40µl was added to coverslips coated with poly-D-lysine at 10µg/ml in sterile water within a 12-well plate. Following 24 hr incubation, the cells were treated with 10µM cytosine arabinoside for 24 hours, and medium was replaced with DMEM-F20. Cells were left to proliferate for 3 days prior to staining. Immunocytochemistry was performed as in Section 2.6.6.

2.6.5.2 Results

Schwann cells were identified in the primary culture by positive staining for PMP22 (Figure 8). CD55 was not expressed on primary rat Schwann cells; however, CD59 was abundantly expressed throughout the Schwann cell, including the cell body and processes. There was also a degree of co-localisation evident with PMP22 staining. Crry was also highly expressed on Schwann cells, although it had a granular distribution around the cell body, and co-localised with PMP22 staining. Fibroblasts within the culture also expressed Crry (Figure 8). CD46 was not expressed by any cell type contained within the culture (data not shown).

2.6.6 Immunohistochemistry of rat sciatic nerve

2.6.6.1 Methods

Adult Lewis rats were euthanized and the sciatic nerve removed, cut into blocks and snap-frozen in isopentane at -40^{0}C. Frozen tissues were embedded in OCT medium, and sectioned transversely in a cryostat at 8-10µm. Sections were fixed in neat acetone for 5 minutes. Fixed sections were incubated with primary monoclonal antibodies (α-rat CD55 (RDIII7), α-rat CD59 (6D1), α-rat Crry (TLD1C11) and α-rat CD46 (MM.1) at optimal dilutions determined by prior titration experiments, and primary polyclonal antibody (α-PMP22, 1:200 dilution) for 1 hour at RT in a humid chamber. Sections were washed in PBS, and incubated with donkey α-mouse-Ig-FITC (Jacksons 715-096-151) and donkey α-rabbit-Ig-rhodamine (Jacksons 711-025-152) at 1:200 dilution, including DAPI staining for nuclei at 100ng/ml for 1 hour at RT in a humid chamber. Following washing, slides were mounted in VectorShield, and analysed on an inverted fluorescence microscope.

2.6.6.2 Results: CReg profile

CD55 displayed a focussed expression within the rat sciatic nerve, although this was unlikely to be on Schwann cells since staining was distinct from DAPI staining, and PMP22 staining, and some staining is likely to be vascular. CD55 was also expressed on the perineurium (Figure 9). CD59 was abundantly expressed, and appeared continuously around the axon, presumably on the myelin sheath, and possibly on the axon itself. Again, this is not exclusive, and a degree of

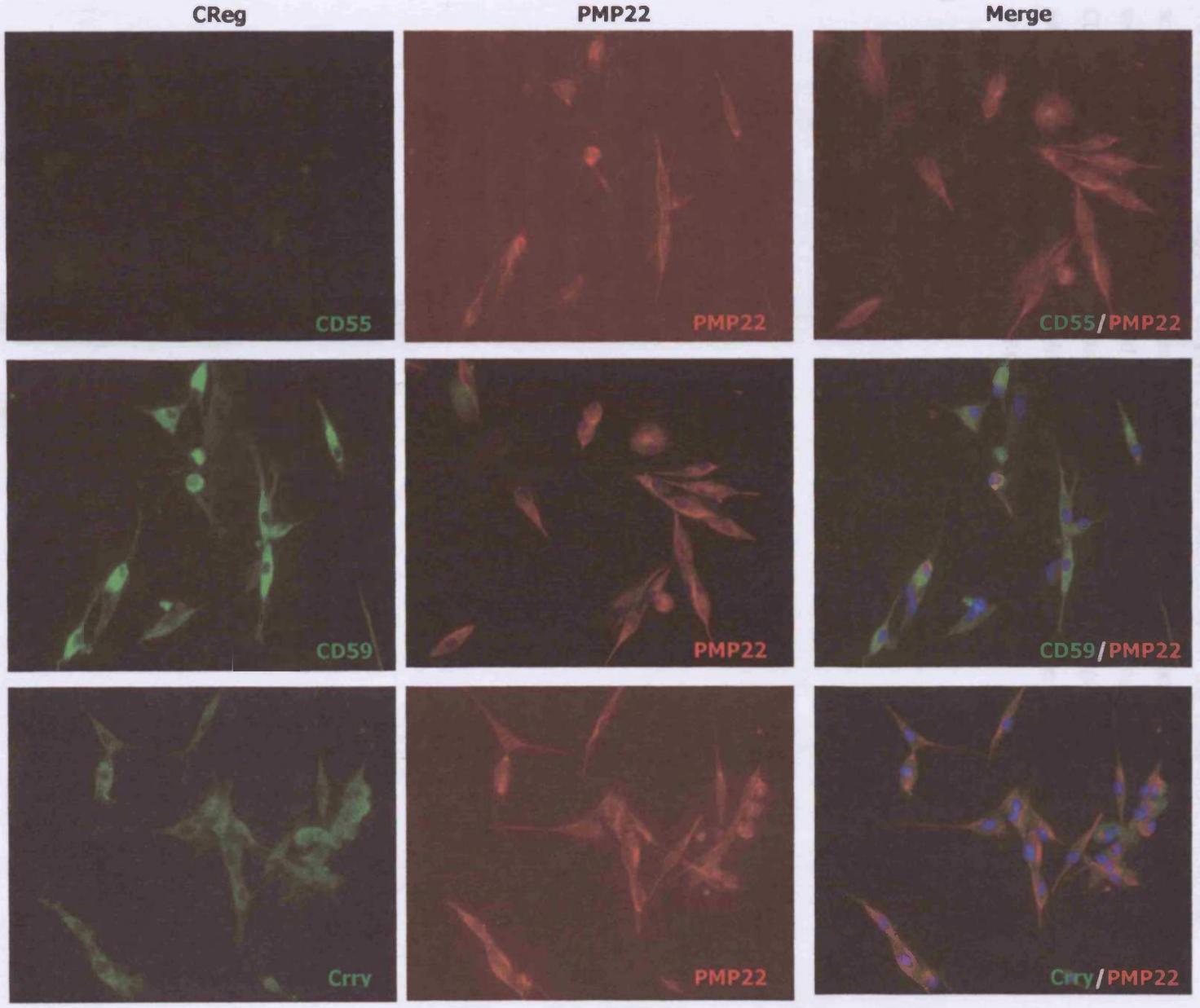

Figure 8

Analysis of membrane-bo CReg expression on primary Schwann cells

Primary rat Schwann cells were isol as described, and grown on cover for 3 days prior to staining. Cover were stained for membrane-boun regs as described previously. Bri coverslips were incubated with ant CD55 (RDIII7), anti-rat CD59 (6I anti-rat Crry (TLD1C11) and ant CD46 (MM.1, not shown) at opt pre-determined dilutions, for 1 hou R.T in a humid chamber, processed as described using F conjugated secondary antibo Sections were double-stained PMP22 as described. Images v merged to detect any co-localisatio expression.

All images were taken at 4 magnification.

co-localisation is evident with PMP22 suggesting some expression on the Schwann cell body. The perineurium was also positive for CD59 (Figure 9, CD59, white arrow). Crry had a focussed expression throughout the nerve which co-localised with DAPI and PMP22 staining, suggesting that at least some Crry is expressed on Schwann cells. In addition, the perineurium was positive for Crry, together with additional areas of staining, possibly on the vasculature. CD46 staining was absent on rat sciatic nerve as expected since it is now known to be testis-restricted in the rat (not shown). As a positive control for α-rat CD46 antibody (MM.1) staining, acetone fixed rat sperm were stained (not shown).

To identify whether CD55 and Crry were expressed additionally on the vasculature within the sciatic nerve, additional staining was performed using anti-CD93 antibodies (Figure 10). CD93 is expressed by endothelial cells, and thus serves as a good marker for the vasculature. Some CD55 and Crry expression was indeed localised to endothelial cells (white arrows, Figure 10), although not exclusively. Some CD55 staining was also evident on the perineurium surrounding the nerve bundle (arrow heads, Figure 10).

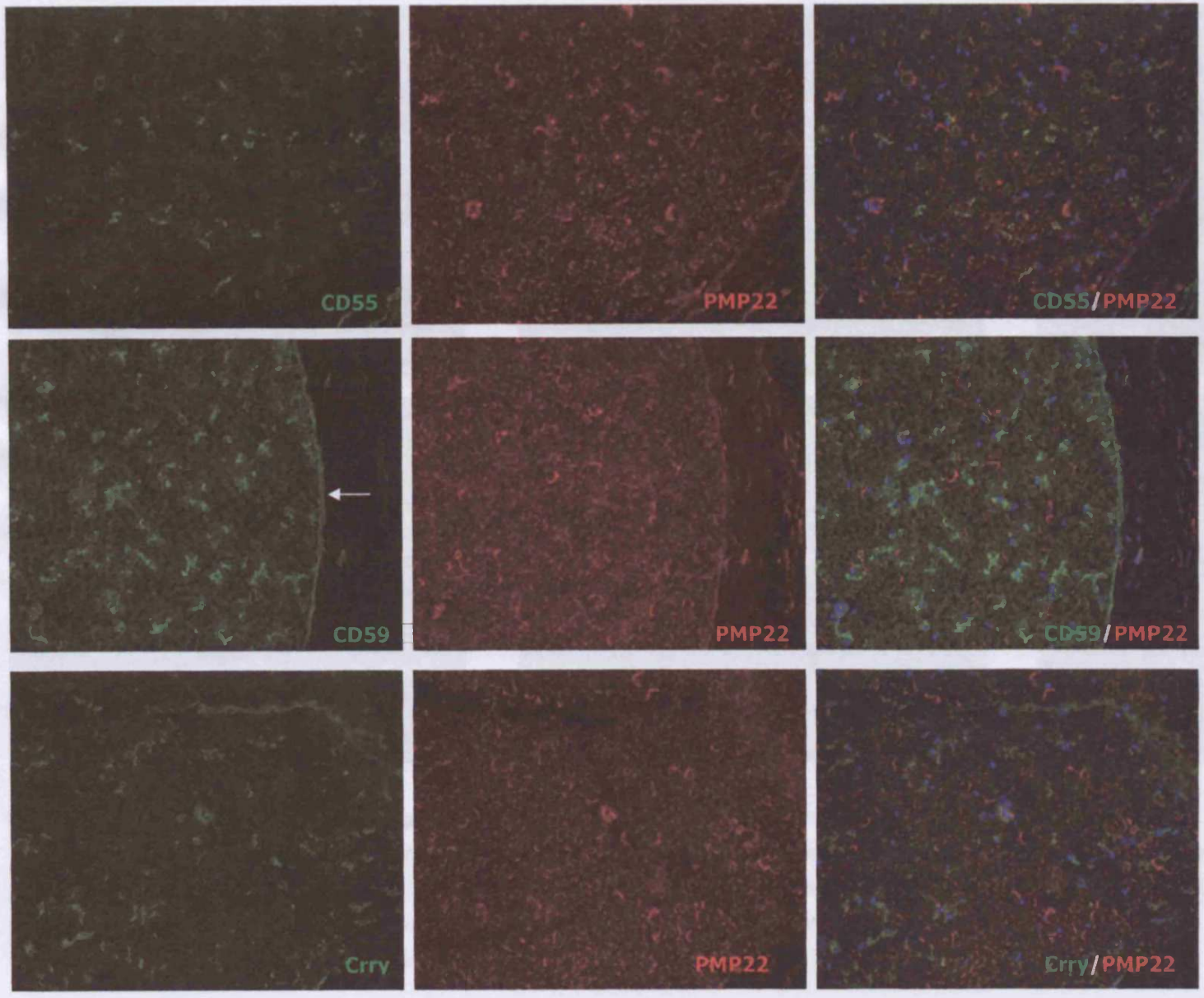

Figure 9

Analysis of CReg expression on adult rat sciatic nerve

Rat sciatic nerve sections were stained for membrane-bound CRegs as described previously. Briefly, sections were incubated with anti-rat CD55 (RDIII7), anti-rat CD59 (6D1), anti-rat Crry (TLD1C11) and anti-rat CD46 (MM.1, not shown) at optimal pre-determined dilutions, for 1 hour at R.T in a humid chamber, and processed as described using FITC-conjugated secondary antibodies. Sections were double-stained for PMP22 as described. images were merged to detect co-localisation between CReg and PMP22.

All images were taken at 400X magnification.

White arrow=perineurium

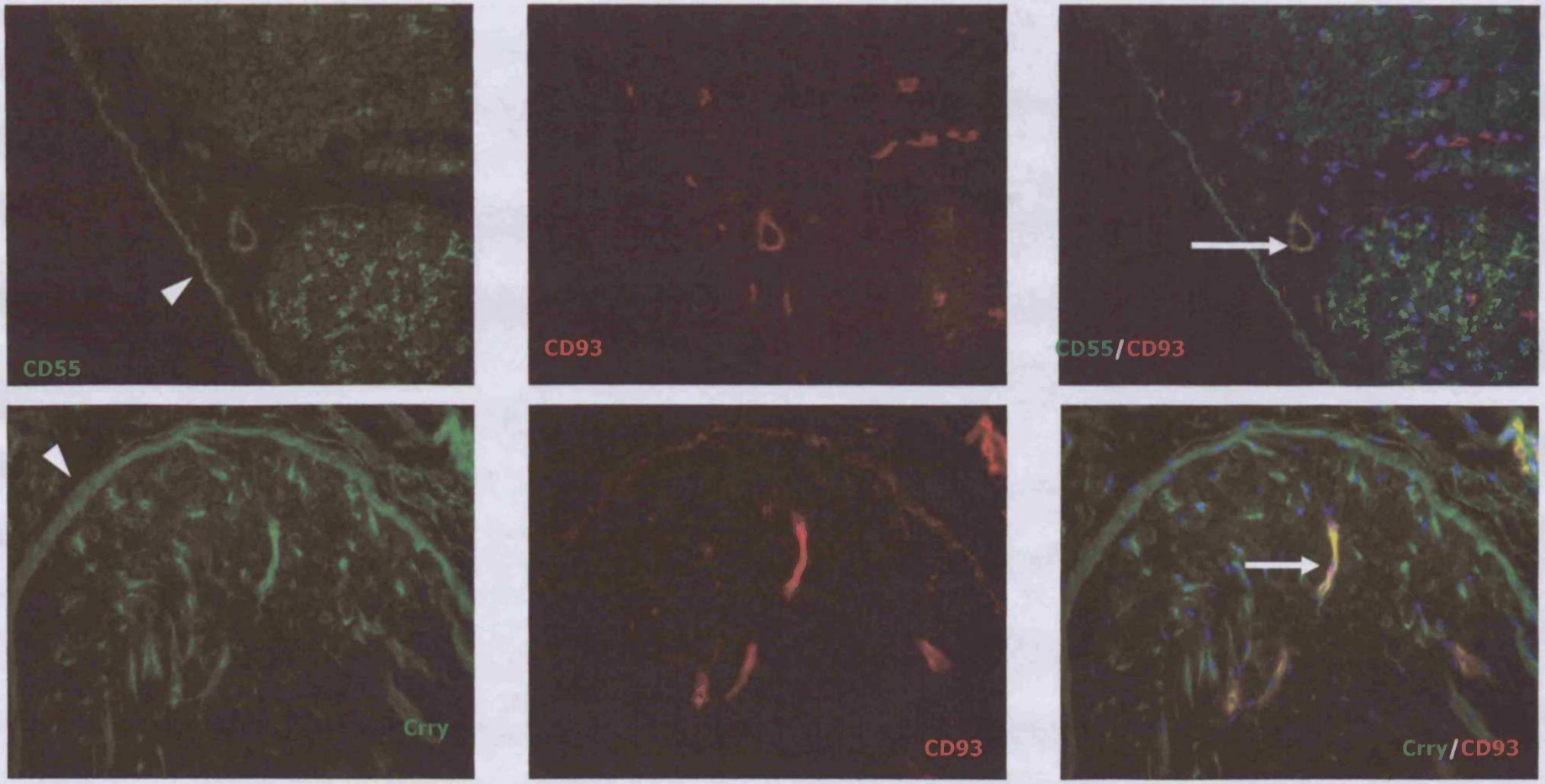

Figure 10

Analysis of location of CD55 and Crry expression in rat sciatic nerve

Rat sciatic nerve sections were stained for membrane-bound CRegs CD55 and Crry as described previously, and double stained with endothelial marker CD93. Briefly, sections were incubated with mouse anti-rat CD55 (RDIII7), and mouse anti-rat Crry (TLD1C11), and double-stained with rabbit anti-CD93 for 1 hour at R.T in a humid chamber, and processed as described using FITC/rhodamine-conjugated secondary antibodies. All images were taken at 400X magnification.

White arrow heads=perineurium staining; white arrows = co-localisation of CReg with CD93

2.7 Discussion

2.7.1 Summary

CD55 had a restricted expression within the rat PNS; both CD59 and Crry were widely expressed both *in vitro* and *in vivo*. CD46 was absent from all PNS-derived cells and tissues (Table 4)

Cell type	S100	PMP22	CD55	CD59	Crry	CD46
RT4-D6P2T	+	++	-	+++	++	-
RN22	+	++	+	+++	++	-
Primary Schwann cells	+	++	-	+++	++	-
Sciatic nerve	+	++	++	+++	++	-

Table 4

Summary of membrane-bound CReg expression within the PNS by immunocytochemistry, immunohistochemistry and flow cytometry

KEY: -= no staining; +=weak staining; ++=moderate staining; +++intense staining
All values refer to >90% of population stained. In the case of primary Schwann cell culture, values did not include fibroblasts within the cultures; Schwann cells accounted for approximately 70% of the total culture.

2.7.2 PMP22 expression

PMP22 expression was more focussed within the PNS than S100 or MBP, and so provided a useful tool for studying the PNS and associated cell types, including the Schwann cell. However, PMP22 was not restricted to the PNS; it was unexpectedly observed in this study that it was highly expressed in the kidney, and in the central canal within the spinal cord. Although the role of PMP22 remains largely undefined, it is well established that deletions, duplications or mutations in the gene encoding PMP22 account for the majority of heritable demyelinating peripheral neuropathies. PMP22 expression is highest in myelinating Schwann cells; however, a study in the mouse showed that high levels of PMP22 transcripts were present in non-neural tissues, namely in adult intestine. In addition, expression was observed in mesoderm-derived tissues, in particular connective tissues of the face region, bones, lung mesenchyme and muscle. Expression was also detected in ectoderm-derived tissues, such as epithelia of the lens and the skin (Baechner, Liehr et al. 1995). More recently, work has established that PMP22 is associated with markers of tight junction complexes including zonula occludens 1 (ZO-1) and occludin in the rat (Notterpek, Roux et al. 2001). To date, a comprehensive study of PMP22 expression in the rat has not been

performed, and it would be especially interesting to further analyse cell types stained within the kidney. Since the glomerulus was stained most strongly, it would be of benefit to further define the cell types expressing PMP22, for example, glomerular basement membrane, mesangial cells, or endothelial cells. Although it is out of the scope of this study, this remains an exciting possibility for the future.

2.7.3 CReg expression

2.7.3.1 CD55

Interestingly, CD55 expression has been shown in this study to have a restricted expression within the PNS, with little or no expression on Schwann cells, but expression on the whole sciatic nerve, on the vasculature and on the perineurium. CD55 is a known ligand for CD97, an activation-induced leucocyte antigen, and as such, may be involved in a novel adhesion pathway, primarily used by activated, but not quiescent T and B cells (Hamman, Vogel et al. 1996). CD55 upregulation associated with increased expression of CD97 has previously been demonstrated in inflammatory conditions, for example multiple sclerosis. In this study, CD97 expression was absent from normal white matter in the brain; however, in pre-active lesions defined by abnormalities of the white matter, infiltrating cells such as T cells, macrophages and microglia expressed CD97, while CD55 was highly expressed by endothelial cells. In active lesions concurrent with myelin degradation, both macrophages and microglia expressed CD55 and CD97, suggesting a critical involvement of CD55-CD97 interactions in inflammatory processes (Visser, de Vos et al. 2002). It would be interesting to investigate the expression of CD97 within the PNS, as a mechanism for T and B cells to bypass the blood-nerve-barrier and cause pathology, and investigate the role of CD55 expression within the limited vasculature of the sciatic nerve and on the perineurium in particular, may play. It would also be interesting to evaluate the expression of CD97 on auto-reactive T cells present in GBS patients. If present, docking of CD97 onto CD55 on the vasculature or the perineurium may provide a means of entry for activated T cells into the sciatic nerve. Perhaps it is an advantage for Schwann cells to express CD55 at such low levels, or not to express it at all, and effectively block this adhesion of leucocytes to the Schwann cell membrane, thus averting an inflammatory response. CD55 has also been implicated as a receptor for uropathogenic strains of *E. coli*, and enteroviruses of the Picornavirus family, and in a sub-group known as echoviruses (Harris and Morgan 2004).

2.7.3.2 CD59

CD59 has been demonstrated in this study to be widely expressed, on both Schwann cell lines and primary culture, and in the whole sciatic nerve. The PNS in this respect is well protected from MAC attack. However, the absence of such protection would lead to

increased susceptibility to induction of peripheral neuropathy, or other C-mediated diseases, and this work has thus identified a molecule for further study *in vivo*.

Cd59a-/- mice have been generated in our laboratory, and provide a target for investigation into the susceptibility of these mice to EAN induction, to firmly establish a role for MAC dysregulation in mediating disease.

2.7.3.3 Crry

Crry is ubiquitously expressed in the rat PNS; on Schwann cell lines and primary cultures, and within the sciatic nerve itself; within the vasculature, on Schwann cells, and on the perineurium. The PNS is therefore well protected from the deleterious effects of aberrant C activation. It is likely that Crry substitutes for CD55 and CD46 within the PNS since it encompasses the functions of both molecules, possibly allowing CD55 to perform other non-C-related roles within the PNS.

2.7.3.4 CD46

CD46 in the rat is known to have a restricted expression in the reproductive tract, in particular on spermatozoa and their precursors spermatids in sexually-mature rats (Mizuno, Harris et al. 2004), (Mizuno, Harris et al. 2005). It is therefore not surprising that CD46 was not detected at the protein level within the PNS. However, mRNA for CD46 was detected in both Schwann cell lines studied. Initial studies following the cloning of CD46 revealed mRNA expression of this CReg in brain, spleen, ileum, muscle, liver, heart, lung, kidney and testis (Mead, Hinchliffe et al. 1999). Although expression of mRNA within the PNS has not previously been reported, its presence in this study is not surprising. The relevance of this wide expression pattern remains undefined, but the lack of protein expression within the PNS suggests no functional significance of the expression in this system.

2.7.4 C components

In this study, Schwann cells were incapable of expressing the majority of C components, as identified by RT-PCR. With the exception of C2, no mRNA was detected for any component (C1q-β, fB, C3, or C5). The relevance of C2 detection remains unclear, and it would be interesting to see if this correlated with protein expression. C2 mRNA expression may be analogous to the CD46 expression described earlier, and have no functional significance. However, extrahepatic synthesis of C2 has previously been demonstrated in C6 deficient rats with a partial deficiency of C2 (Timmerman, Van Dixhoorn et al. 1997). Selective up-regulation of C2, at both the mRNA and protein levels, has been demonstrated by human mesangial cells in response to CMV infection, mediated likely by IFNs (Timmerman, Beersma et al. 1997). More recently, HIV-1 infection of human astrocytes has been shown to induce a

marked upregulation of both C2 and C3, while CReg expression was unchanged. However, human C2 may be alternatively spliced to give rise to a secreted (C2 long) protein, and an intracellular (C2 short) form in liver, macrophages and fibroblasts (Cheng and Volanakis 1994). Does rat C2 also have this feature?

It is likely that C2 expression in isolation has no functional significance. It would be important to determine whether, when appropriately stimulated, Schwann cells are capable of expressing a complete C pathway. This could provide a means of protection for the PNS against invading pathogens, or this may contribute towards the C-mediated attack on myelin in autoimmune disease such as GBS. Analysis of the effect of pro-inflammatory cytokine stimulation of Schwann cell lines would provide a starting point for this analysis, and could progress into an *in vivo* model. For example, following induction of EAN in the rat, Schwann cells could be harvested from affected animals, and examined for changes in expression profile with respect to C components and CRegs. Is C3 deposited on the surface of Schwann cells? Are Schwann cells capable of expressing a complete C system under these conditions? What happens to CReg expression? Following successful optimisation of EAN, the model could be used to investigate these questions.

Chapter 3
Generation of Antigens for Induction of Experimental Autoimmune Neuritis (EAN)

1 Introduction

In the PNS, myelin is formed by extension of the plasma membrane of Schwann cells, which, following differentiation, functions by wrapping itself around an axon. Following compaction, the membrane contains little water, has high lipid content and a set of specific proteins. PNS-specific proteins include MPZ or PO, MBP, P2, PMP-22, CNPase and the two isoforms of the MAG (Kursula 2001).

The extracellular inter-membrane space of non-compact myelin is 12-14nm whereas in compacted myelin it is only 2nm (Kursula 2001). Compaction results in protein and lipid being laid down in a series of concentric layers visible by electron microscopy. Both PO and MBP are believed to be key players in this process. In terms of myelin stabilisation, PO appears to be critical in maintaining the extracellular faces of two compact myelin membranes at a distance of 2nm from each other (Shapiro, Doyle et al. 1996), while MBP apparently plays a role in linking two cytoplasmic faces of myelin membranes via its strong positive charge. The myelin sheath itself also has sections composed of non-compact myelin, for example the Schmidt-Lanterman incisures, which express MAG and CNPase specifically.

Difficulty in studying these proteins lies in the fact that all myelin proteins are very well adapted to their environment, that is, they must maintain constant interactions with surrounding membranes, making them difficult to purify and study in solution (Kursula 2001).

1.1 Myelin Protein Zero (PO)

PO was first identified in 1973 by gel electrophoresis as a 28kDa integral glycoprotein present as the major protein component in peripheral nerve myelin (Greenfield, Brostoff et al. 1973), (Everly, Brady et al. 1973). PO is a 219 amino acid glycoprotein, and a member of the Ig superfamily, and accounts for over 50% of the protein in the PNS. It is composed of an extracellular domain (EC) with a single immunoglobulin (Ig)-like loop created by a disulphide bond between Cys21 and Cys98. It carries the HNK-1 carbohydrate epitope, a transmembrane region, and a basically-charged cytoplasmic domain, capable of forming electrostatic interactions with the apposing anionic bilayer. PO has been cloned from a variety of species and shown to be highly conserved. Relative to the amino acid sequence of

human PO, the rat, chicken and shark proteins are 94%, 75% and 50% identical respectively (Eichberg 2002).

1.2 PO as an adhesion molecule

X-ray diffraction studies on peripheral myelin structure from the mutant *shiverer* mouse which has deletions in the *mbp* gene, have suggested a role for PO in myelin compaction (Kirschner and Ganser 1980). This theory has been expanded by X-ray crystallographic studies that have demonstrated that PO exists as a protomer which assumes a fold similar to that of an Ig variable domain, containing 10 anti-parallel β strands organised as two β-sheets. Using analytical ultracentrifugation, such protomers were capable of dimerisation and then tetramerisation, forming a gel-like phase at high concentrations. Within a physiological context, PO extracellular domains at the intraperiod line of myelin are considered to be capable of forming homophilic interactions through tetrameric structures on apposing membrane surfaces either via hydrogen bonding or by intercalation of protruding hydrophobic tryptophan side chains, producing the regular intermembrane spacing observed in compact myelin (Shapiro, Doyle et al. 1996). Further evidence for PO as an adhesion molecule comes from studies on transfected cells. Non-adherent cells transfected with PO show aggregation, which can be blocked by addition of free PO or by anti-PO antibodies (Filbin and Tennekoon 1990).

A role for the carbohydrate moiety in adhesion has been suggested by the finding that antibodies to HNK-1 glycosyl chain were capable of partially inhibiting homophilic interaction of PO (Griffiths, Schmitz et al. 1992), and cells expressing unglycosylated PO even in the presence of wild type expressing cells were incapable of adhesion (Filbin and Tennekoon 1993).

The PO gene was cloned, characterised and mapped in 1993 by Hayasaka and colleagues, and was found to be around 7kb in length, and contained 6 exons corresponding to the functional domains; exon 1 contains the signal sequence, exons 2 and 3 contain the extracellular (EC) domain, while exon 4 encodes the TM region, and exons 5 and 6 encode the cytoplasmic domain (Hayasaka, Himoro et al. 1993a). Associations between mutations in the PO gene and specific forms of hereditary motor and sensory neuropathies such as CMT1B, Dejerine-Sotas syndrome and congenital hypomyelination, have been revealed by genetic linkage analyses (Kulkens, Bolhuis et al. 1993). PO is present on chromosome 1q22-q23, and at least 56 distinct mutations have been identified, with approximately 77% found in exons 2 and 3 encoding the extracellular domain (Pfend, Matthieu et al. 2001). CMT1B is characterised by distal muscular atrophy and weakness, hollow feet and reduced nerve conduction velocities (NCV), and signs of de- and remyelination can be demonstrated in peripheral nerve biopsies. The gene responsible has been genetically linked to the same

chromosomal location as the PO gene, and numerous mutations can be demonstrated. For example, deletion of the serine 34 codon in exon 2 results in defects in myelination and CMT1B, either by formation of abnormal homodimers, or processing anomalies leading to toxicity for the Schwann cell (Kulkens, Bolhuis et al. 1993). Also, a substitution of Ser63 for a cysteine residue leads to a severe conformational change in the EC domain since the cysteine may participate in disulphide bonding (Hayasaka, Himoro et al. 1993).

1.3 PO as a neuritogenic antigen

Acute EAN is an autoimmune disease that can be induced in susceptible animals by inoculation with various PNS antigens emulsified in FCA, and mirrors many morphological and electrophysiological aspects of GBS.

Waksman and Adams first demonstrated EAN in rabbits by active immunisation with homogenised PNS tissue (Waksman and Adams 1955). Since then, investigators have induced EAN with various PNS proteins; in rats, EAN may be induced by immunisation with purified bovine PNS myelin, with purified PO from bovine spinal nerve roots (Milner, Lovelidge et al. 1987), bovine P2 (Suzuki, Kitamura et al. 1980), (Kadlubowski, Hughes et al. 1980), recombinant human P2 protein (Weishaupt, Giegerich et al. 1995), PMP22 (Gabriel, Hughes et al. 1998) or peptides spanning the neuritogenic epitopes in both PO (Linington, Lassman et al. 1992) and P2 (Rostami and Gregorian 1991). Adoptive transfer of T cell lines reactive with P2 protein (Rostami, Burns et al. 1985) and PO protein have also been shown to transfer disease in rats (Linington, Lassman et al. 1992).

In mice, Taylor and Hughes demonstrated susceptibility in the SJL mouse by immunisation with bovine P2, but resistance in Balb/c and C57Bl/6 (Taylor and Hughes 1985). More recently, a more severe disease has been induced in the SJL mouse using bovine peripheral nerve myelin (BPNM) in combination with pertussis toxin and IL-12 (Calida, Kremlev et al. 2000). Initially disease could only be induced in C57Bl/6 mice using a complex immunisation schedule in CD4/CD8 knockout mice, but more recent work demonstrated successful EAN induction using the immunodominant PO peptide 180-199 in combination with pertussis toxin (Zou, Ljunggren et al. 2000).

1.4 Chapter Aim

Due to inaccessibility of bovine myelin following the bovine spongiform encephalopathy (BSE) crisis in the UK in 1992 (www.defra.gov.uk/animalh/bse/index), it became necessary to find a suitable alternative antigen for induction of EAN in both rats and mice. Work by Zhu and colleagues demonstrated successful induction of EAN in the Lewis rat using peptide 180-199 derived from the human PO amino acid sequence (Zhu, Pelidou et al. 2001). With regard to disease induction in the mouse, it was our initial aim to test the susceptibility to

EAN induction of a variety of C deficient and C reg knockout mice. Since the majority of these mice were available on a C57Bl/6 background, we used the work of Zou and colleagues described above as a tool for optimisation of the model (Zou, Ljunggren et al. 2000).

In addition, it was clear that the whole EC domain of PO played an important role in maintenance of myelin compaction. Work by Archelos in 1993 had demonstrated the presence of antibodies against the EC domain of PO (PO-EC) during active EAN induced by bovine spinal root myelin (Archelos, Roggenbuck et al. 1993). We were interested therefore in the ability of the EC domain to elicit a response in isolation, and used a bacterial expression system to generate sufficient quantities of the protein for testing.

This chapter describes the generation of antigens for EAN induction in both rats and mice; specifically generation of peptides derived from human PO amino acid sequence, the cloning, bacterial expression, purification and characterisation of the EC domain of human PO, and preparation of homogenates and peripheral nerve myelin from tissues.

2 Materials and Methods

All chemicals unless otherwise stated were from Sigma Aldrich Chemical Company, (Gillingham, UK).

2.1 Synthesis of peptides derived from the human PO sequence

2.1.1 Methods

The following peptides were synthesized by solid-phase stepwise elongation using an Applied Biosystems 433A peptide synthesizer. Numbering began at residue 1 of the mature protein.

A Human PO peptide amino acids 180-199
Sequence: ASKRGRQTPVLYAMLDHSR (refer to Figure 2)

B Human PO peptide amino acids 180-199 with amide modification at carboxy terminus
Sequence: ASKRGRQTPVLYAMLDHSR-amide

C Mouse PO peptide amino acids 106-125 (Miletic, Utermohlen et al. 2005)
Sequence: IVGKTSQVTLYVFEKVPTRY

2.1.2 Results

Mass spectrometry was used to confirm the identity and purity of the peptide preparations. Expected molecular weights of peptides were derived from the Peptide Molecular Weight Calculation Tool available online at www.genscript.com/ssl-bin/peptide_mw. The expected molecular weight of peptide A (human PO 180-199) was 2187Da (Figure 1). The major peak on the mass spectrometry trace for this peptide corresponded to 2186Da, most likely due to the normal isotopic distribution of ^{14}C, which contains 1% ^{13}C. Other peaks seen on the trace derive from incomplete chains of amino acids during synthesis. The expected molecular weight of peptide B (human PO 180-199-amide) was 2186Da, and the major measured peak obtained was at 2186Da (with minor peaks at 2185 and 2187Da), while for peptide C (mouse PO 1206-125) the predicted value was 2327Da, and the measured major peak was at 2329Da, with minor peaks at 2328 and 2330Da.

2.2 Cloning, expression, purification & refolding of the extracellular domain of human Myelin Protein Zero (PO-EC)

2.2.1 Cloning of cDNA for PO-EC domain into pQE9 vector

2.2.1.1 Methods

cDNA encoding the full length human PO gene was kindly provided by Prof. D. Kirschner (Department of Biology, Boston College, Chestnut Hill, Massachusetts 02467, USA). pQE9 vector (Figure 2a) containing sequence for mouse myelin oligodendrocyte glycoprotein (mMOG) in frame with a polyhistidine tag (x6) (pQE9-mMOG-His_6) (Figure2b), was kindly provided by Dr. Mark Griffiths (Dept. Medical Biochemistry & Immunology, Cardiff University [original source Dr. Hugh Reid, Dept. of Biochemistry and Molecular Biology, Monash University, Australia].

Peptide A

Human PO 180-199

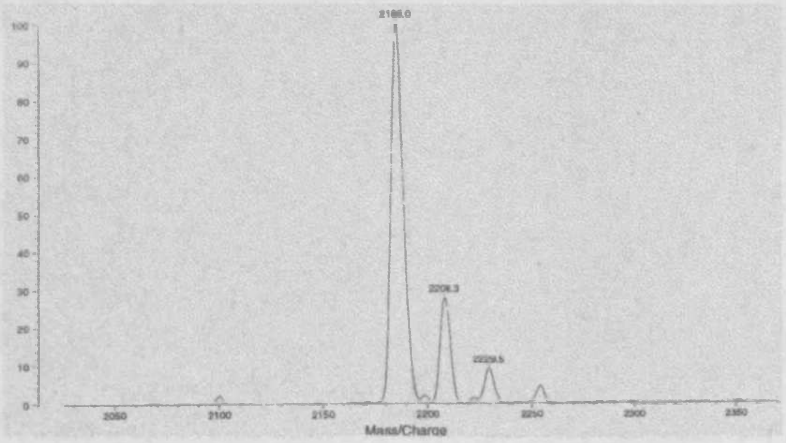

Peptide B

Human PO 180-199-amide

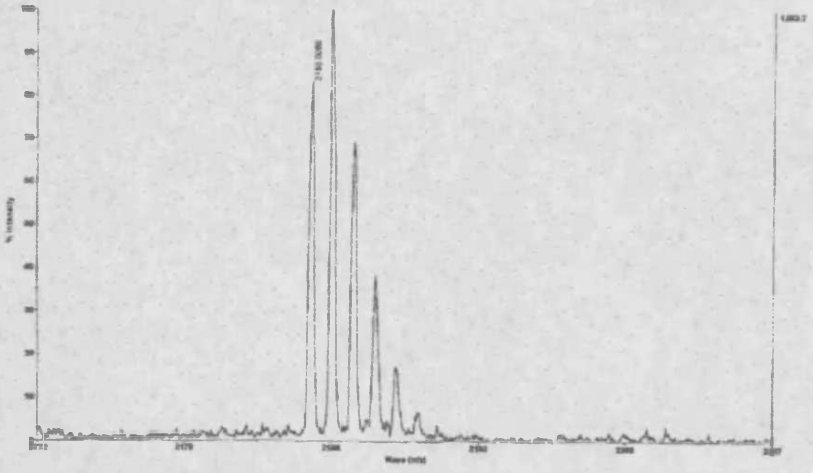

Peptide C

Mouse PO 106-125

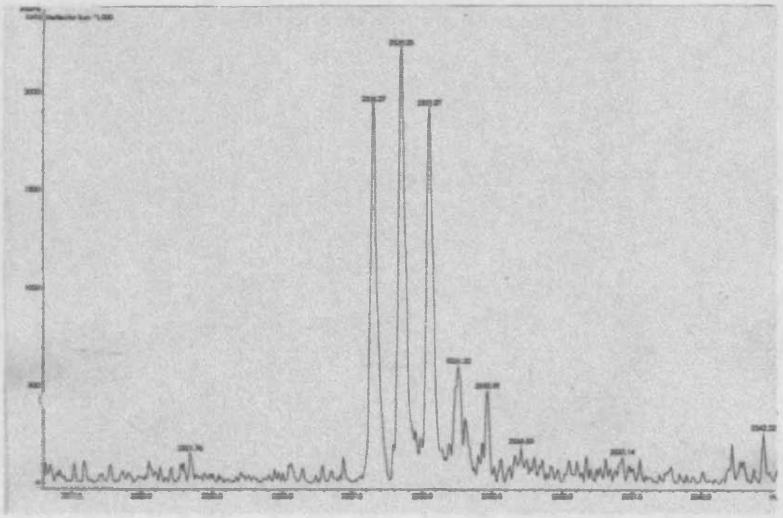

Figure 1

Mass spectrometry trace of peptides derived from PO

Each peptide (A, human PO 180-199; B, human PO 180-199-amide; C, mouse PO 106-125) was mixed with matrix (α-cyano-4-hydroxysinnamic acid) and analysed in the reflectron mode in a Bruker Reflex III MALDI-TOF mass spectrometer of which a trace was shown above. Intensity of signal was shown on the y axis, and mass/charge ratio on the x axis.

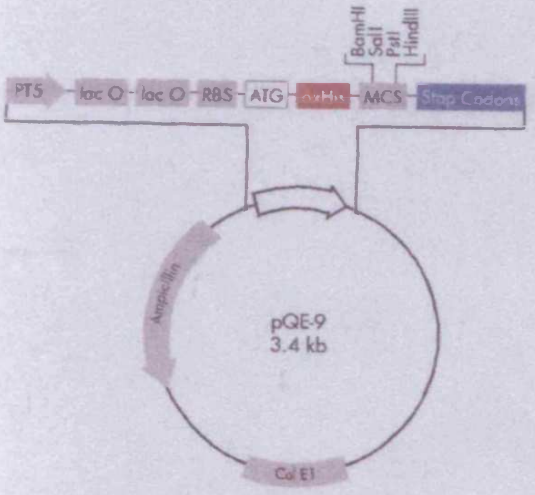

Figure 2a

pQE9 vector used for expression of PO-EC domain

The vector (Qiagen, Crawley, West Sussex), is 3.4kb, and contains a lac operator element, a 6XHis-tag coding sequence, a multiple cloning site (MCS) which contains restriction sites for BamH1, SalI, PstI and HindIII, and an ampicillin resistance gene. In this experiment, pQE9 was obtained which contained the sequence for mMOG cloned in BamH1 and HindII restriction sites within the MCS.

pQE9-mMOG-His_6

His tag **BamH1** **Mouse MOG**

M R G S H H H H H H G S G Q F R V I G P G Y P I

atg aga gga tcg cat cac cat cac cat cac gga tcc gga caa ttc aga gtg ata gga cca ggg tat ccc atc

R A L V G D E A E L P C R I S P G K N A T G M E

cgg gct tta gtt ggg gat gaa gca gag ctg ccg tgc cgc atc tct cct ggg aaa aat gcc acg ggc atg gag

V G W Y R S P F S R V V H L Y R N G K D Q D A E

gtg ggt tgg tac cgt tct ccc ttc tca aga gtg gtt cac ctc tac cga aat ggc aag gac caa gat gca gag

Q A P E Y R G R T E L L K E T I S E G K V T L R

caa gca cct gaa tac cgg gga cgc aca gag ctt ctg aaa gag act atc agt gag gga aag gtt acc ctt agg

I Q N V R F S D E G G Y T C F F R D H S Y Q E E

att cag aac gtg aga ttc tca gat gaa gga ggc tac acc tgc ttc ttc aga gac cac tct tac caa gaa gag

A A M E L K V E D - -

gca gca atg gag ttg aaa gtg gaa gat taa taa aag ctt ggg

HindIII

Figure 2b
Sequence of mMOG contained within pQE9 vector showing location of BamH1 and HindIII sites, and the location of the poly-histidine tag

Using a BamH1 and HindIII digest on pQE9-mMOG-His_6, the mouse MOG sequence could be removed, and human PO-EC domain sequence could be inserted, provided BamH1 and HindIII sites were included.

Forward and reverse primers were designed to span the extracellular domain of the human PO sequence (Entrez Pubmed Nucleotide NM_000530), and to include a BamH1 and HindIII restriction endonuclease sites. Enzyme spacer regions were also inserted to reduce any steric hindrance for restriction enzymes:

PO-EC Forward (NH_2 terminus)

GCG GGA TCC ATC GTG GTT TAC ACT GAC AGG

Spacer Bam H1 PO-EC domain

PO-EC Reverse (COOH terminus)

GGG AAG CTT TTA TTA GTA CCT AGT TGG CAC TTT TTC

Spacer HindIII Stop Stop PO-EC domain

The location of the primer sequence is shown in Figure 3. Primers were obtained from Invitrogen Life Technologies (Paisley, UK). PCR using PO-EC domain primers on cDNA encoding full length PO, was performed using standard protocols described in Chapter 2, Section 2.5.4, with a primer annealing temperature of 62°C to verify correct primer design.

2.2.1.2 Results

PCR products were separated on agarose gels and stained as described. The major band obtained corresponded to the expected PO-EC domain sequence of 392bp. The minor higher band was non-specific, and most likely a result of excess template (Figure 4).

2.2.2 Preparative PCR

2.2.2.1 Methods

2.2.2.1.1 VENT polymerase PCR

VENT polymerase was used in a preparative scale PCR since it has proof-reading capability, absent from Taq polymerase. The protocol for this PCR was as follows: 3µl each of PO-EC forward and reverse primers, 15µl 1mM dNTPs, 5µl 10x ThermoPol buffer, 1µl PO-full length plasmid, 1µl VENT polymerase and 22µl distilled water, giving a total volume of 50µl. Thermal cycling was started, consisting of a denaturation step at 94°C for 30 secs (s) followed by primer annealing at 62°C for 30s and extension at 72°C. A total of 30 cycles were performed followed by a final extension step at 72°C for 10min. Since VENT has exonuclease activity, PCR products were frozen immediately following termination of the program. PCR product (50µl) was loaded onto a 2% NuSieve (Cambrex Bioscience, Wokingham, UK) ethidium bromide agarose gel, and

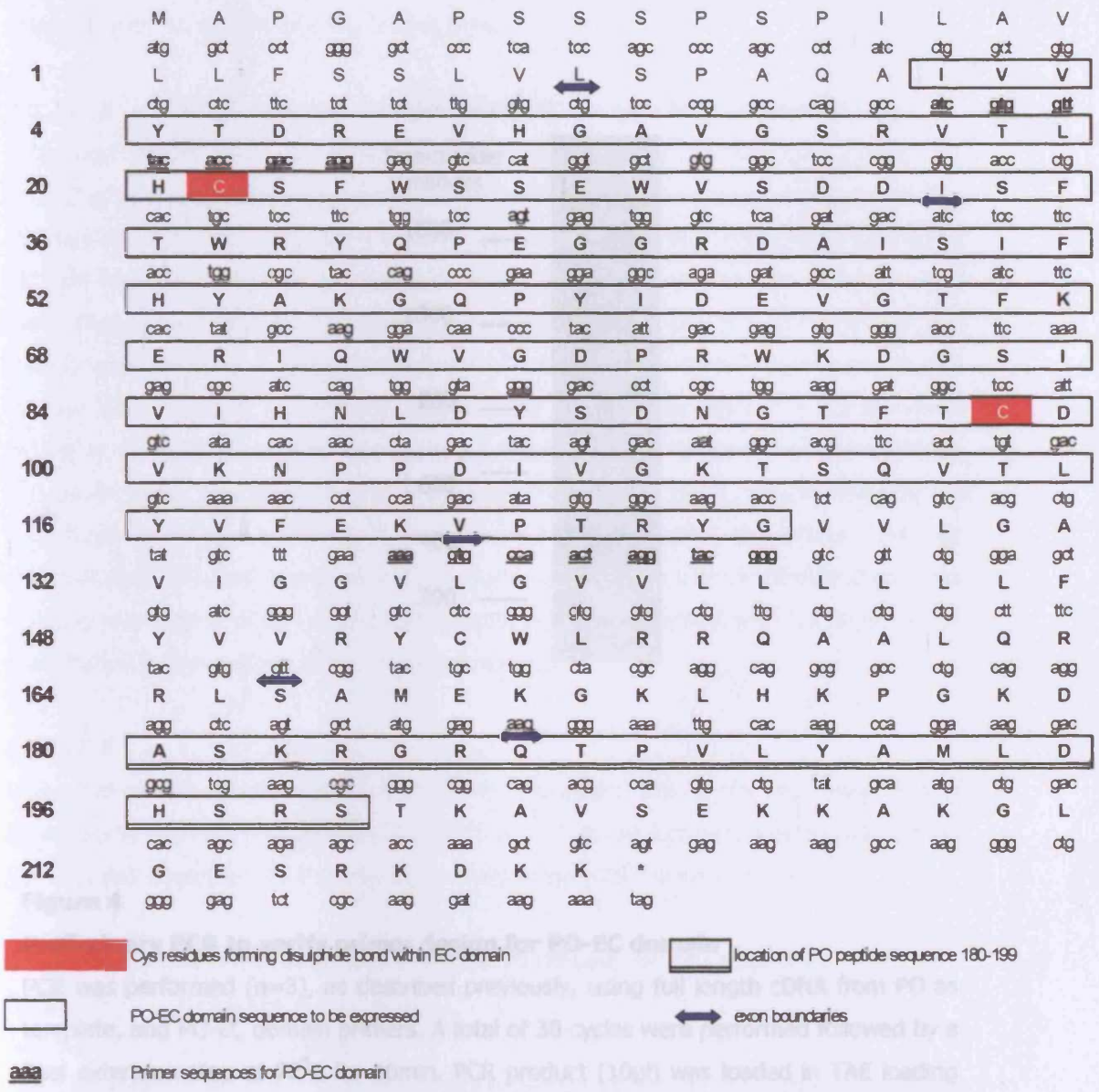

Figure 3

cDNA sequence of human PO and deduced amino acid sequence

Numbering of amino acid residues began from residue 1 of the mature protein. Shown are the location of the cysteine residues forming the disulphide bond within the EC domain, the sequence of PO-EC domain to be expressed, the location of primer sequences encoding this region, the location of PO peptide sequence 180-199, and the boundaries between the 6 exons within human PO. Adapted from (Hayasaka, Takada et al. 1993).

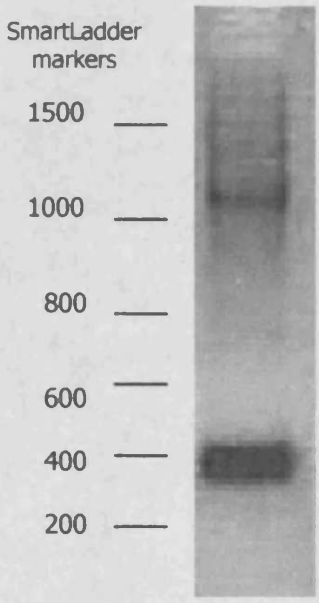

Figure 4

Preliminary PCR to verify primer design for PO-EC domain

PCR was performed (n=3), as described previously, using full length cDNA from PO as template, and PO-EC domain primers. A total of 30 cycles were performed followed by a final extension step at 72^0C for 10min. PCR product (10µl) was loaded in TAE loading buffer onto a 1% ethidium bromide agarose gel, and electrophoresed at 100V for 1 hour. Smartladder markers were included for accurate determination of size of bands. Bands were visualised under UV illumination and images captured with a digital camera using the Bio-Rad Gel Documentation system.

subjected to electrophoresis at 80V for 1 hour. Bands were visualised as described previously, although care was taken to minimise the product's exposure to UV illumination since exposure is capable of cross-linking DNA.

2.2.2.1.2 GeneClean purification of PO-EC domain PCR sequence

DNA was 'cleaned' using GeneCleanIII kit (QBiogene, supplied by Anachem, Luton, UK) according to the manufacturer's instructions. Briefly, the DNA band was excised from the ethidium-bromide stained NuSieve agarose gel with a clean razor blade using long wave UV light for visualisation for as short a time as possible. Appropriate eye protection was used. The excised band was weighed (0.1g=100µl) and NaI solution (concentration not stated) approximately 3 times the volume of the slice was added from a pre-diluted solution within the kit. To remove agarose, the mixture was placed in a water bath incubator at 45-55^{0}C until the agarose had melted. EZ glassmilk silica matrix was added (1µl binds 1-2µg DNA) and incubated at room temperature for 5 minutes, followed by centrifugation for approximately 30 seconds at 20,000g to pellet the matrix. DNA was eluted in distilled water. Samples of the products (1µl, 5µl) were electrophoresed on a 1% NuSieve low melting point gel to allow quantitation by comparison with 5µl SmartLadder quantitation markers (Eurogentec, Southampton, UK).

2.2.2.1.3 Results

Quantification of concentration of VENT PCR product was performed using 5µl of SmartLadder markers (Figure 5). Two quantities of PCR product were loaded onto the gel (1, 5µl), and corresponded to 80ng/µl, on comparison with markers.

2.2.3 Restriction digest of pQE9-mMOG to release mMOG sequence

2.2.3.1 Methods

2.2.3.2 BamH1 digest

The pQE9 vector obtained contained a sequence coding mMOG. To release the mMOG sequence to enable cloning of PO-EC sequence, a double restriction digest was performed on mini-prep prepared pQE9-mMOG. The reaction conditions were as follows: 5µg pQE9-mMOG, 7µl 10x BamH1 buffer (New England Biolabs (NEB), Herts UK), 5µl BamH1 and distilled water giving a total reaction volume of 70µl incubated at 37^{0}C for 2 hours.

2.2.3.3 QIAquick purification of digested DNA

Prior to digestion with the second enzyme, DNA was purified using the QIAquick purification system (Qiagen, UK) according to manufacturer's instructions. Briefly, 350µl of buffer PB (containing guanidine hydrochloride and isopropanol) was added to the reaction mixture, and transferred to a QIAquick column. Following centrifugation for 30 seconds at

20,000g, the flow through was removed and the column washed with buffer PE (containing ethanol). Following further centrifugation at 20,000g, the column was eluted in 60µl of distilled water.

2.2.3.4 HindIII digest

The reaction conditions for this second digest were as follows: 60µl QIAquick eluate, 7µl 10x HindIII buffer (NEB) and 5µl HindIII (NEB) incubated at 37°C for 20 hours. A 2% NuSieve gel was loaded with the product to allow visualisation of the digest.

2.2.3.5 Results

Successful removal of the mMOG sequence was evident following restriction enzyme digest of pQE9-mMOG (Figure 6). Two bands were visible following agarose gel electrophoresis, corresponding to mMOG at approximately 392bp, and digested pQE9 at 1.2kb. pQE9 was purified using the GeneClean system as described previously.

2.2.4 Generation of 'sticky ends' on PO-EC domain sequence by double digest with BamH1 and HindIII restriction enzymes

2.2.4.1 Methods

Following VENT-PCR of the PO-EC domain sequence, the product was subjected to GeneClean as for pQE9-mMOG, and double digests as outlined above. PO-EC domain sequence were subjected to final GeneClean and quantitated as described previously (data not shown).

2.2.5 'Sticky end' ligation of PO-EC domain and pQE9 vector

2.2.5.1 Cloning of PO-EC domain digested DNA into pQE9 vector

2.2.5.2 Methods

PO-EC domain restriction digest fragments were cloned into the pQE9 vector using T4 DNA ligase. Typically, the ligation mixture contained 100ng of vector DNA with a vector:insert ratio of 1:3, 1µl 10X ligase buffer (660mM Tris-HCl, (pH 7.6), 50mM $MgCl_2$, 100mM DTT, Bioline) 1µl T4 DNA ligase, in a total volume of 10µl using distilled water, and incubated at 16°C overnight.

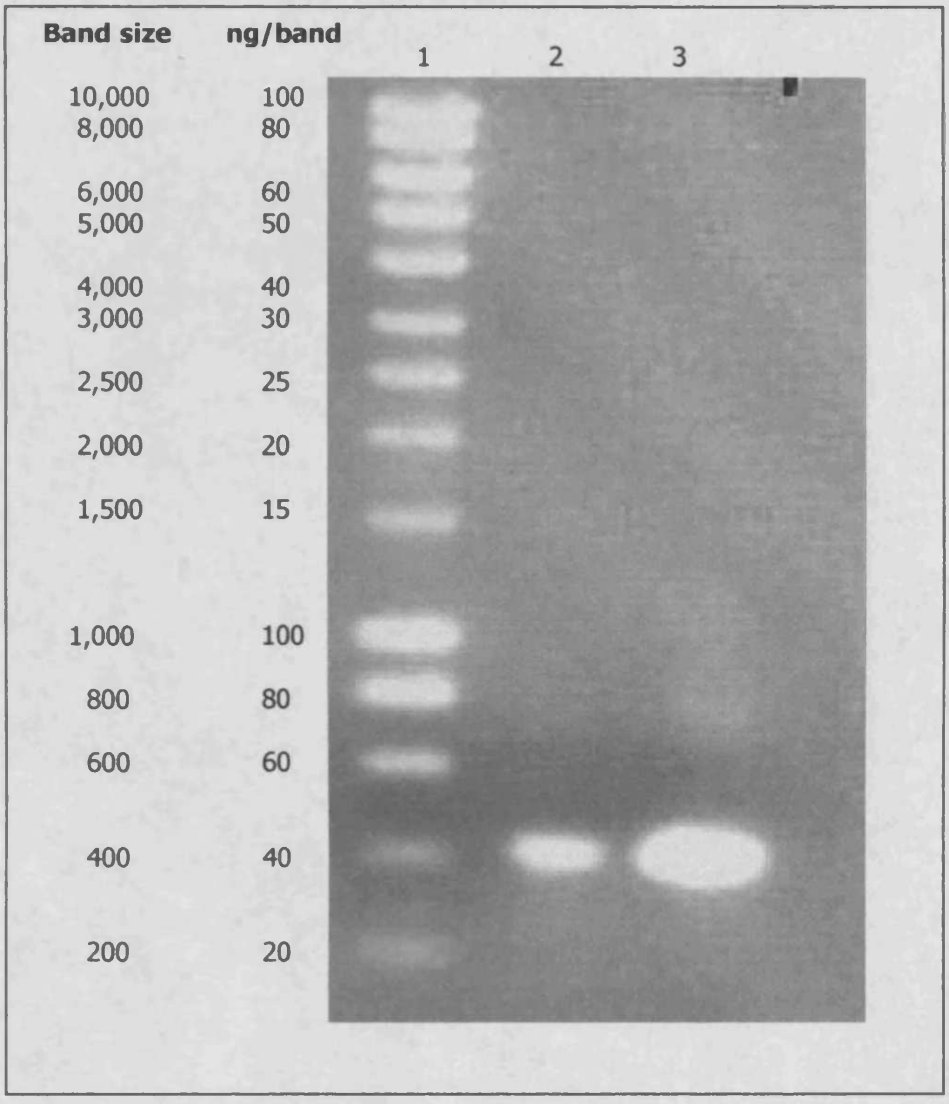

Figure 5

Quantitation of VENT PCR product following GeneClean using SmartLadder marker quantification (Eurogentec)

5µl of SmartLadder markers were applied to a 1% agarose gel. Different quantities of PCR product (1, 5µl) were applied to enable correct quantitation.

Lane 1: 5µl SmartLadder

Lane 2: 1µl GeneClean Product

Lane 3: 5µl GeneClean Product

The VENT PCR products corresponded to 80ng/µl

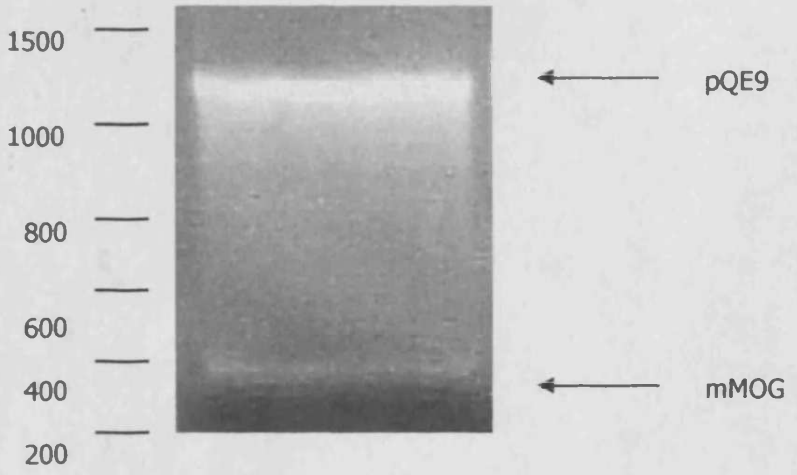

Figure 6

Agarose gel electrophoresis of double digested pQE9-mMOG to confirm successful release of mMOG sequence.

Briefly, pQE9-mMOg was subjected to BamH1 digest at 37^{0}C for 2 hours. Following purification of DNA using the QIAquick system, the DNA was subjected to HindIII digestion at 37^{0}C for 20 hours. The double digested product was visualised on a 2% NuSieve ethidium bromide stained gel. 2 bands were present; pQE9 empty vector at 1.2kb, and released mMOG at approximately 400bp. The band containing pQE9 was excised and purified using the QIAquick system.

A 1µl aliquot of ligation mixture was electroporated into DH5α electro-competent *Escherichia coli* (*E. coli*; in-house) at 2.5kV, 25µFD using a BioRad Genepulser. Pre-warmed Super Optimal Catabolite repression (SOC) medium (1ml; 0.5% (w/v) yeast extract, 2% (w/v) tryptone, 10mM NaCl, 2.5mM KCl, 10mM $MgCl_2$, 20mM $MgSO_4$, 20mM glucose; 700µl) was added immediately, incubated at 37^{0}C for 30min and spread on LB-Agar plates containing 100µg/ml ampicillin and 25µg/ml kanamycin (Sigma). The plates were incubated at 37^{0}C overnight. Colonies were picked and resuspended in 20µl distilled water. The suspension (1-2µl) was plated onto a reference plate with the remainder boiled for 10min in a PCR block to release and denature the vector, then cooled on ice for 5min. The denatured vector was used as a template in a PCR reaction using primers flanking the multiple cloning site (MCS) of the vector and the insert (pQE9 forward: GTGAGCGGATAACAATTATAA; pQE9 reverse: CGGCAACCGAGCGTTCTGAAC).

2.2.5.3 Results

Positive colonies with inserts of the correct size were identified using pQE9 flanking primers. Positive clones were detected in lanes 1, 4, 5, 7 and 9 (Figure 7, A). Colonies 1, 4 and 5 were selected for further analysis. Colonies were transferred from the reference plate into 10ml cultures of Luria-Bertani broth (LB broth; for 1 litre, 10g tryptone, 5g yeast extract, 10g NaCl in distilled water) containing 100µg/ml ampicillin and 25µg/ml kanamycin, and incubated overnight in an orbital shaker. Bacteria were pelleted by centrifugation (2000g, 30min) and plasmids were purified using Qiagen MiniPrep kit. Plasmids were used as templates for a PCR to confirm presence of the PO-EC sequence (Figure 7, B). Colonies 1, 4 and 5 contained PO-EC domain sequence.

2.2.6 Sequencing of positive clones

2.2.6.1 Methods

Clones 1, 4 and 5 were taken for sequencing to detect any sequence errors. The sequencing reaction was performed as follows. Cloned DNA was sequenced using the ABI Prism BigDye Terminator Cycle Sequencing Ready Reaction Kit, containing AmpliTaq DNA polymerase, on an ABI 377 DNA sequencer. Sequencing primers were those flanking the MCS and insert. The reaction mix consisted of 300ng template DNA, 1pmol primer, 3µl BigDye sequencing mix, and made up to 10µl with sterile water. The reaction mix was overlaid with mineral oil and heated to 95°C in a PCR block. Thermal cycling was performed as follows: 96^{0}C for 30s, 50^{0}C for 15s, 60^{0}C for 4min, with rapid thermal ramping between steps, for a total of 25 cycles. The resulting reaction mix was pipetted to a clean microcentrifuge tube avoiding transfer of oil, and extension products were precipitated by addition of 2µl 3M sodium acetate, pH 4.6 and 50µl of 95% (v/v) ethanol. The mixture was vortexed and left at room temperature for 15min, and centrifuged for

20min at 16,000g. The supernatant was aspirated, and the pellet was washed in 70% (v/v) ethanol and dried. Samples were sequenced on an ABI 377 DNA sequencer.

2.2.6.2 Results

Sequence data obtained was aligned with the published sequence for PO-EC domain. Clone 5 contained no sequence errors, and was taken forward for transformation of M15pREP4 *E. coli* (data not shown).

2.2.7 Transformation of M15pREP4 *E. coli*

2.2.7.1 Background

M15pREP4 are an *E. coli* strain containing low-copy plasmid pREP4 that confers kanamycin resistance and constituitively expresses the lac repressor protein encoded by *lacI* gene, permitting high expression of the protein (QIAexpressionist handbook for high-level expression of 6xHis-tagged proteins, June 2003).

2.2.7.2 Methods

DNA (50ng) was added to 100µl of non-transformed M15pREP4 and electroporated at 2.5kV, 25µFD using a BioRad Genepulser. Psi broth (L-broth, 4mM $MgSO_4$, 10mM KCl;, 500µl) was added and incubated for 60 minutes at 37°C with agitation. Bacteria were spread onto 2 LB-Agar plates containing 100µg/ml ampicillin and 25µg/ml kanamycin (plate 1: 150µl cells/plate undiluted, and plate 2: 150µl cells at 1:20 dilution). Plates were incubated at 37°C overnight. Colonies were PCR screened using PO-EC domain primers, as detailed in section 2.2.5.

2.2.7.3 Results

All colonies screened had successfully incorporated the sequence for PO-EC domain (data not shown).

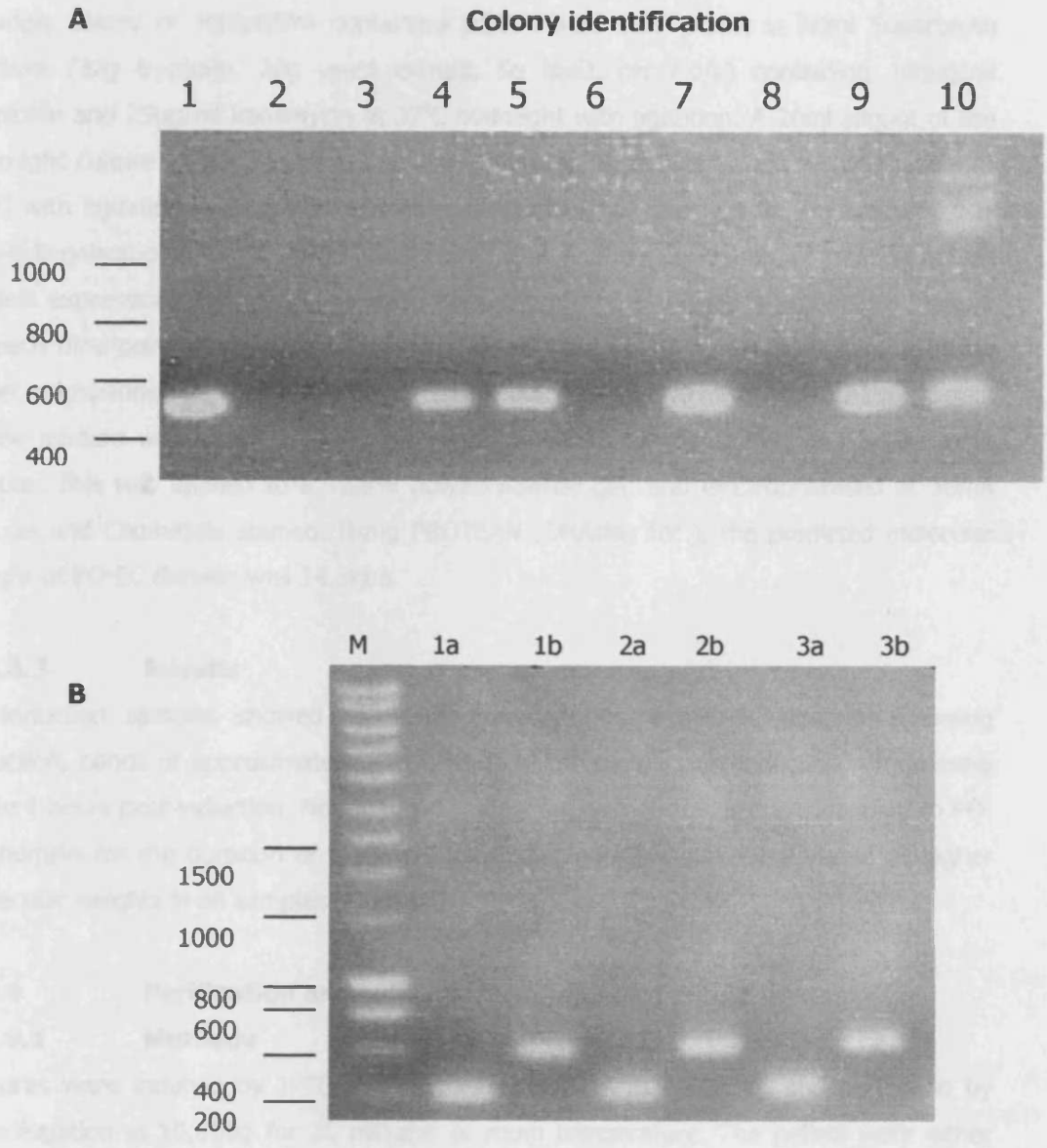

Figure 7

Identification of successfully transformed DH4-α bacteria with pQE9-PO-EC domain (A), and confirmation of insertion of PO-EC domain sequence

Following transformation of DH5α with pQE9-PO-EC domain, colonies were screened for successful transformation using pQE9 flanking primers (A). Positive colonies yielded a product of 590bp. Test colonies occupied lanes 1-9; lane 10 was untransformed pQE9 vector alone as a positive control. Colonies 1, 4 and 5 were taken forward for bulking and further testing to confirm correct incorporation of PO-EC domain sequence using PO-EC domain primers. Lanes 1a, 2a and 3a showed products from PO-EC primed PCR for colonies 1, 4 and 5 respectively; lanes 1b, 2b and 3b show products for pQE9 flanking primed PCR for colonies 1, 4 and 5 respectively.

2.2.8 Expression, purification and refolding of PO-EC domain

2.2.8.1 Induction of PO-EC expression in M15pREP4 *E. coli*

2.2.8.2 Methods

A single colony of M15pREP4 containing pQE9-PO-EC was grown in 50ml Superbroth medium (32g tryptone, 20g yeast extract, 5g NaCl, pH 7.0/L) containing 100µg/ml ampicillin and 25µg/ml kanamycin at 37°C overnight with agitation. A 20ml aliquot of the overnight culture was added to 1 litre of pre-warmed Superbroth medium, and grown at 37°C with agitation until optical density reading (OD_{600nm}) reached 0.5-0.7. Isopropyl-1-thio-β-D-galactopyranoside (IPTG) was added to a final concentration of 1mM to induce protein expression. Samples were taken at hourly intervals to assess protein expression. At each time-point, 1ml of the culture was centrifuged at 1000g for 2 minutes, and the pellet resuspended in 100µl of 9M Urea-Tris-Buffer (pH undetermined). A 10-15µl aliquot of the mixture was mixed 1:1 with reducing SDS-PAGE sample buffer, and boiled for 1 minute. This was applied to a 12.5% polyacrylamide gel, and electrophoresed at 30mA per gel and Coomassie stained. Using PROTEAN (DNAstar Inc.), the predicted molecular weight of PO-EC domain was 14.3kDa.

2.2.8.3 Results

Pre-induction samples showed no bands corresponding to PO-EC domain; following induction, bands of approximately 15kDa were visible by 1hr post-induction, progressing up to 4 hours post-induction. Non-induced sample showed no bands corresponding to PO-EC domain for the duration of the experiment. Bacterial proteins were visible at higher molecular weights in all samples (Figure 8).

2.2.9 Purification and solid phase refolding of PO-EC domain

2.2.9.1 Methods

Cultures were induced by IPTG for 4 hours at 37°C with agitation, and harvested by centrifugation at 10,000g for 20 minutes at room temperature. The pellets were either processed immediately or frozen at -80°C. For processing, pellets were resuspended in 5ml lysis buffer (6M guanidine hydrochloride, 0.5M NaCl, 10mM Tris, 5mM imidazole, pH 8.0) per gram of cells, and rotated for 1 hour at room temperature. The resulting lysate was sonicated using a probe sonicator for 3x10 seconds on ice. Insoluble material was removed by centrifuging at 10,000g for 30 minutes at room temperature.

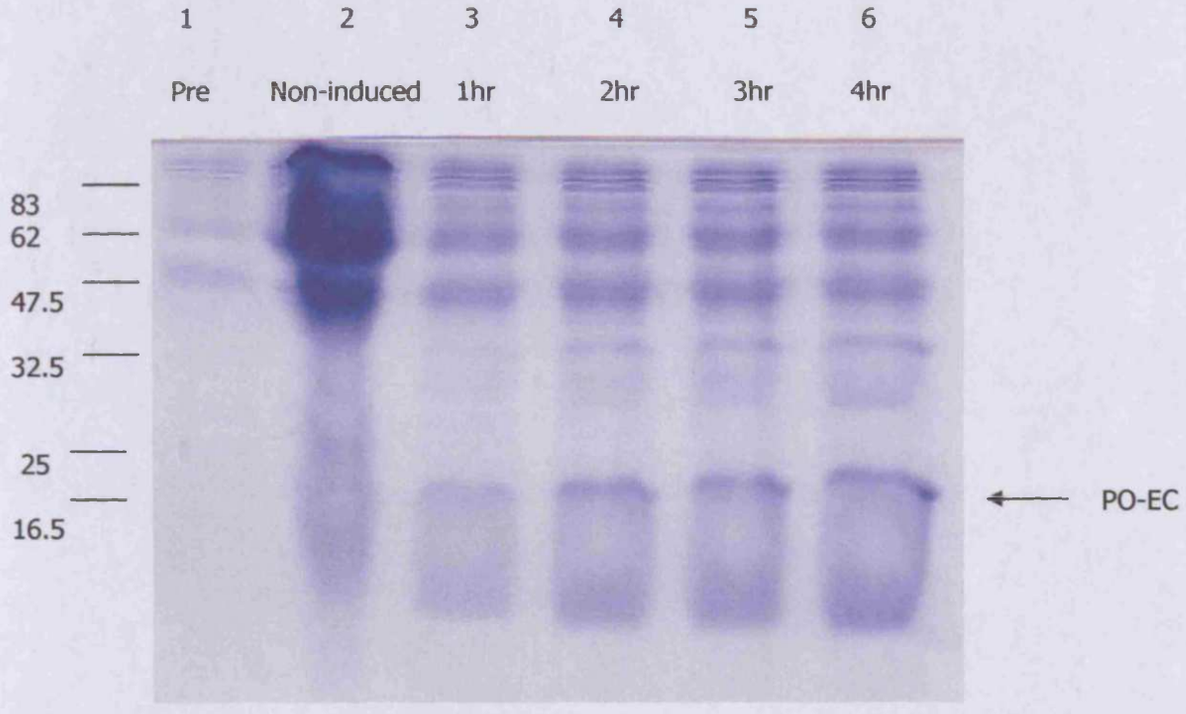

Figure 8

Confirmation of PO-EC domain protein expression in transformed M15pREP4 *E.coli* by SDS-PAGE and Coomassie staining

Samples (1ml) of pre-inoculated medium (Lane 1), non-induced inoculated medium (Lane 2), and 1hr, 2hr, 3hr and 4 hr post-IPTG induction (Lanes 3, 4, 5 and 6 respectively) were collected, centrifuged and resuspended in 100µl 9M UTB. Following centrifugation, 10µl of each sample was mixed 1:1 with non-reducing sample buffer, boiled for 5 minutes, and loaded onto a 12.5% SDS-PAGE gel. Electrophoresis was performed for 40 minutes at 30mA, and the gel was transferred to Coomassie blue staining solution for 1 hour at room temperature with gentle agitation. The gel was destained until bands were visible. Molecular weight markers were also run to allow determination of the size of bands.

A 10ml Nickel-NTA agarose column (Qiagen, UK) was pre-equilibrated with lysis buffer, and the cleared lysate containing the His-tagged PO-EC domain was applied directly to the column. All subsequent buffers were pH 8.0 unless otherwise stated (Table 1). The column was washed with 5 column volumes (CV) of Buffer A, followed by 5CV of Buffer B. The column was further subjected to 3 CV of A, C, D, C in that order, followed by a repeat of D and C. The column was washed in 5CV of Buffer A, and a linear gradient of Buffer A (+14mM 2-mercaptoethanol) versus Buffer E was set up over 16 hours. This was followed by a linear gradient of Buffer E versus Buffer F over 5 hours. His-tagged, refolded PO-EC domain was eluted with Buffer G containing 300mM imidazole, and extensively dialysed against PBS. The protein preparation was also subject to Amicon concentration, and final protein concentration was determined by absorbance at 280nm. Average yields for this protocol were approximately 1mg/litre of culture.

Buffer	Components
A	8M Urea, 100mM NaH_2PO_4, 10mM Tris, pH 8.0
B	8M Urea, 100mM NaH_2PO_4, 10mM Tris, pH 6.3
C	10mM Tris, pH 8.0
D	60% isopropanol, 10mM Tris, pH 8.0
E	100mM NaH_2PO_4, 10mM Tris, 2mM reduced glutathione, 0.2mM oxidised glutathione, pH 8.0
F	100mM NaH_2PO_4, 10mM Tris
G	100mM NaH_2PO_4, 10mM Tris, 300mM Imidazole, pH 8.0

Table 1 Identification of buffers used in the refolding protocol

2.2.10 Characterisation of refolded PO-EC domain

2.2.10.1 SDS-PAGE & Silver staining

2.2.10.2 Method

SDS-PAGE and silver staining were employed to determine the purity of the preparation from two separate runs through the expression and purification protocol. Briefly, 5-10µg of refolded protein was mixed 1:1 in non-reducing SDS-PAGE sample loading buffer, or reducing sample buffer, and heated to 99^0C for 5 minutes. Following cooling on ice for 5 minutes, samples were loaded onto a 12.5% SDS-PAGE gel, and electrophoresed at 30mA per gel for 40 minutes or until the loading buffer had migrated to the bottom of the gel. The gel was transferred to a staining tank, and subjected to Silver staining as detailed in Table 2.

Method	Time
50% (v/v) methanol, 10% (v/v) acetic acid	30 minutes
5% (v/v) methanol, 7% (v/v) acetic acid	30 minutes
Distilled water	Rinse
5% (v/v) glutaraldehyde	30 minutes
Distilled water (x3)	10 minutes each
0.1µg/ml dithiothreitol (DTT) in distilled water	30 minutes
Distilled water	Rinse
0.1% (w/v) silver nitrate	30 minutes
3% (w/v) Na_2CO_3	Rinse
3% (w/v) Na_2CO_3 + 25µl of 37% (v/v) formaldehyde in 50ml	Developing
Approx. 1g solid citric acid	Until reaction stops

Table 2 Silver staining protocol

2.2.10.3 Results

Silver staining was employed to characterise PO-EC domain from 2 refolding runs. It was clear that the major band detected corresponded to approximately 15kDa, the expected molecular mass of PO-EC domain (Figure 9, A). Higher molecular weight aggregates remained at approximately 40kDa and around 80kDa on non-reduced gels, but the majority of these reduced to one band of approximately 15kDa (Figure 9, B). It was evident that the purification protocol was robust and remained consistent between runs.

2.2.10.4 SDS-PAGE & Western blotting

2.2.10.5 Method

SDS-PAGE & Western blotting was employed to confirm the identity of PO-EC from 2 separate runs through the expression and purification protocol. Briefly, 1-5µg of refolded protein was mixed 1:1 in non-reducing sample loading buffer and electrophoresed as described in Chapter 2, Section 2.4.2. Mouse-anti-PO (kindly provided by Prof. Chris Linington, Dept. of Medicine and Therapeutics, University of Aberdeen, UK) was added to a solution of PBS-milk at 10µg/ml and incubated for 1 hour at room temperature on a roller, and developed using anti-mouse IgG-HRPO conjugate as described previously.

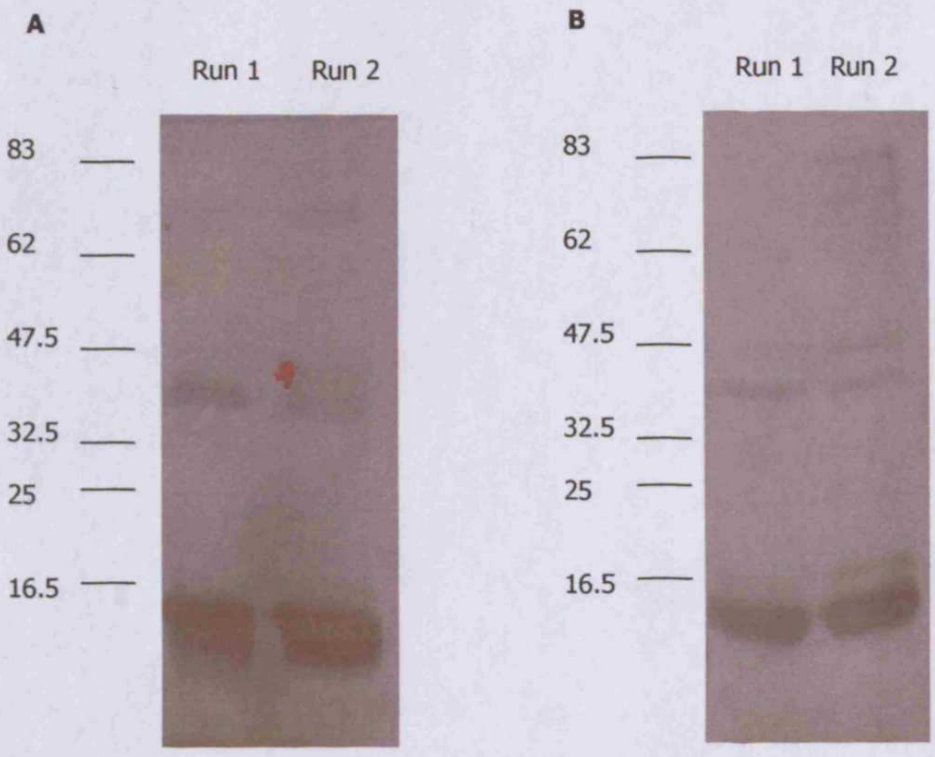

Figure 9

SDS-PAGE and Silver staining of recombinant refolded PO-EC domain from 2 separate runs

Cell lysate (10µl) from purification of runs 1 and 2 of the refolding protocol were mixed with an equal volume of either non-reducing (A) or reducing (B) sample buffer and boiled for 5 minutes. Samples were loaded onto a 12.5% SDS-PAGE gel and electrophoresed at 30mA per gel. Gels were subsequently Silver stained as described.

2.2.10.6 Results

Using the refolding procedure described, PO-EC domain was the major band detected at approximately 15kDa under non-reducing conditions with some higher molecular weight aggregates also detected (Figure 10, A). All of the higher Mr aggregates reduced down to approximately 15kDa (Figure 10, B). Consistency was seen between runs 1 and 2.

2.2.11 Non-refolding protocol for PO-EC domain expression and purification

2.2.11.1 Method

Protocol provided by Emily Mathey, Dept. of Medicine and Therapeutics, University of Aberdeen

Cultures of M15pREP4 were prepared as described in Section 3.2. Following IPTG induction for 4 hours, 1 litre cultures were harvested, and centrifuged at 10,000g for 20 minutes at room temperature. The pellets were pooled and resuspended in 5 times sonication buffer (sonibuffer, 300mM NaCl, 50mM PO_4, pH 7.4) and washed by centrifuging at 30,000g for 15 minutes. The pellet was frozen at -20^{0}C. To purify the inclusion bodies, the frozen pellet was resuspended in 10ml sonibuffer/litre of original culture and 0.5g of lysozyme was added. The suspension was sonicated on ice using a probe sonicator for 3 x 5 minutes with a one minute pause between each burst. The suspension was centrifuged at 30,000g for 20 minutes at 4^{0}C, and the supernatant discarded. The inclusion body-containing pellet was resuspended in wash buffer (0.5% (v/v) N, N-dimethyldodecylamine-N-oxide solution (LDAO) in sonibuffer), and washed four times. The subsequent pellet was resuspended in sonication buffer, homogenised and centrifuged at 30,000g for 20 minutes at 4^{0}C. The pellet was dissolved in 6M Guanidine hydrochloride, 50mM Tris, pH 8.0 at 10ml base buffer per gram of pellet. To the solution, 14µl/10ml β-mercaptoethanol was added. The dissolved pellet was left to stand at room temperature for 15 minutes, and diluted 1:10 with 6M guanidine hydrochloride base buffer.

Prior to loading the PO-EC domain-enriched solution to the column, the column was regenerated by passing 3 CV of regeneration buffer (1% EDTA (v/v), 0.05% (v/v) Tween 20), followed by 2CV of distilled water through. Two CV of 1% (w/v) $NiCl_2$ in distilled water was used to load the column with nickel, and it was equilibrated in 6M guandine hydrochloride base buffer. The protein-enriched solution was loaded at 1ml/minute, and passed through the column at least twice. The column was washed with 20CV of 6M guanidine hydrochloride

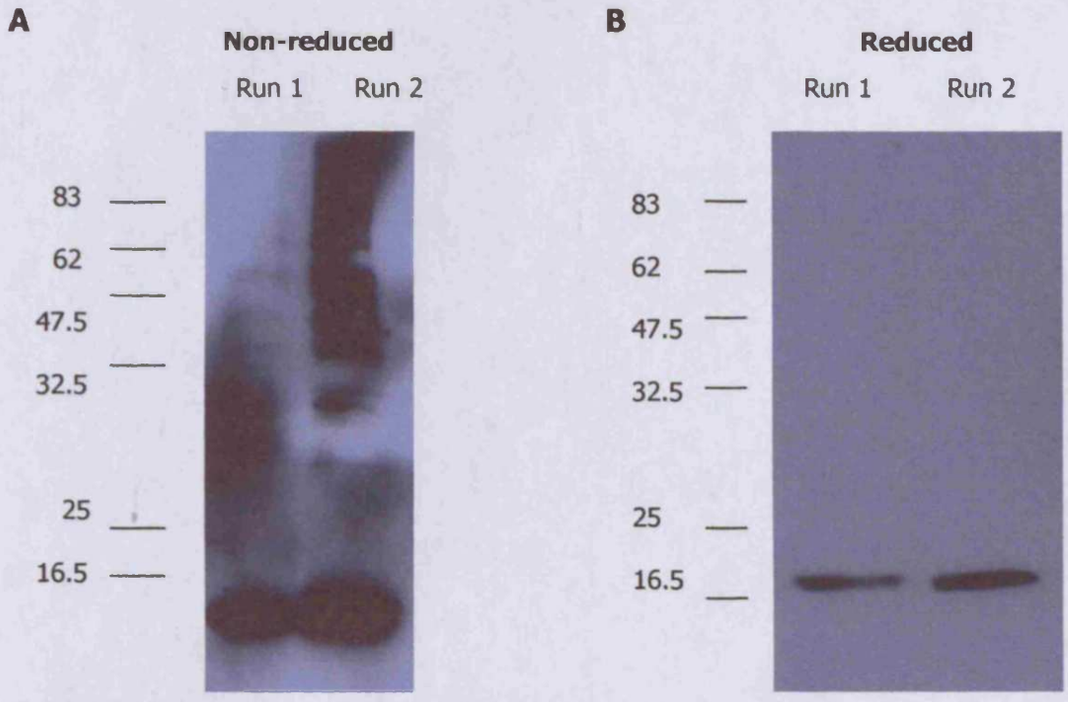

Figure 10

SDS-PAGE and Western blotting of recombinant *refolded* PO-EC

A 10µl sample of refolded, dialysed and concentrated protein solution from runs 1 and 2 was loaded 1:1 in non-reducing sample buffer (A) and reducing sample buffer (B) onto a 12.5% gel ,and blotted using mouse anti-PO (kindly provided by Prof. Linington, Aberdeen, UK) as described.

The position of the molecular weight markers were shown on the left in kDa.

base buffer containing 40mM imidazole. 6M guandine base buffer containing 0.5M imidazole, pH 6.0 was used to elute PO-EC domain. Fractions containing protein were identified by absorbance at 280nm, and positive fractions were dialysed into PBS overnight at 4^0C. Average yields obtained were approximately 8mg/litre of culture.

2.2.12 Characterisation of non-refolded PO-EC domain

2.2.12.1 SDS-PAGE & Coomassie staining

The non-refolding protocol resulted in aggregates of various sizes by SDS-PAGE and Coomassie staining under non-reducing conditions (Figure 11). The majority of these aggregates migrated to approximately 15kDa under reducing conditions, although a distinct band remained at approximately 60kDa, suggesting tetramer formation.

2.2.12.2 SDS-PAGE & Western blotting

Western blotting using mouse anti-PO mAb confirmed that all of the bands visualised by Coomassie staining corresponded to PO (Figure 12). Under non-reducing conditions, aggregates of various sizes were visualised, and corresponded to progressively higher molecular weight aggregates of PO-EC domain. Under reducing conditions, the majority of the aggregates migrated at approximately 15kDa, with another distinct band at approximately 60kDa, as seen previously following Coomassie staining of non-refolded PO-EC domain.

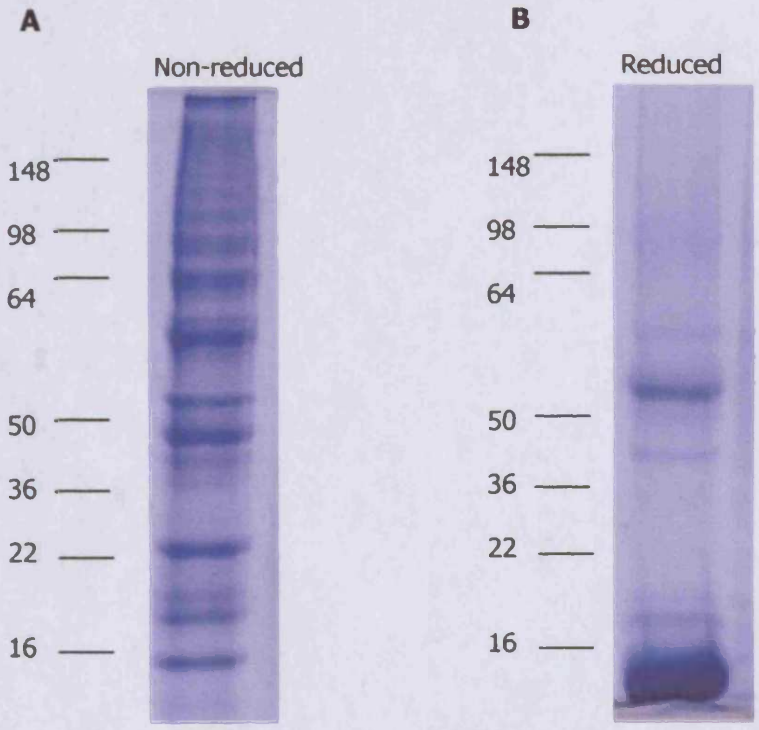

Figure 11

SDS-PAGE & Coomassie staining of non-folded PO-EC domain

10µg of protein was mixed 1:1 in either non-reducing (A) or reducing (B) loading buffer, and loaded onto a 12.5% SDS-PAGE gel. Following electrophoresis at 30mA per gel, the gel was Coomassie stained as described previously.

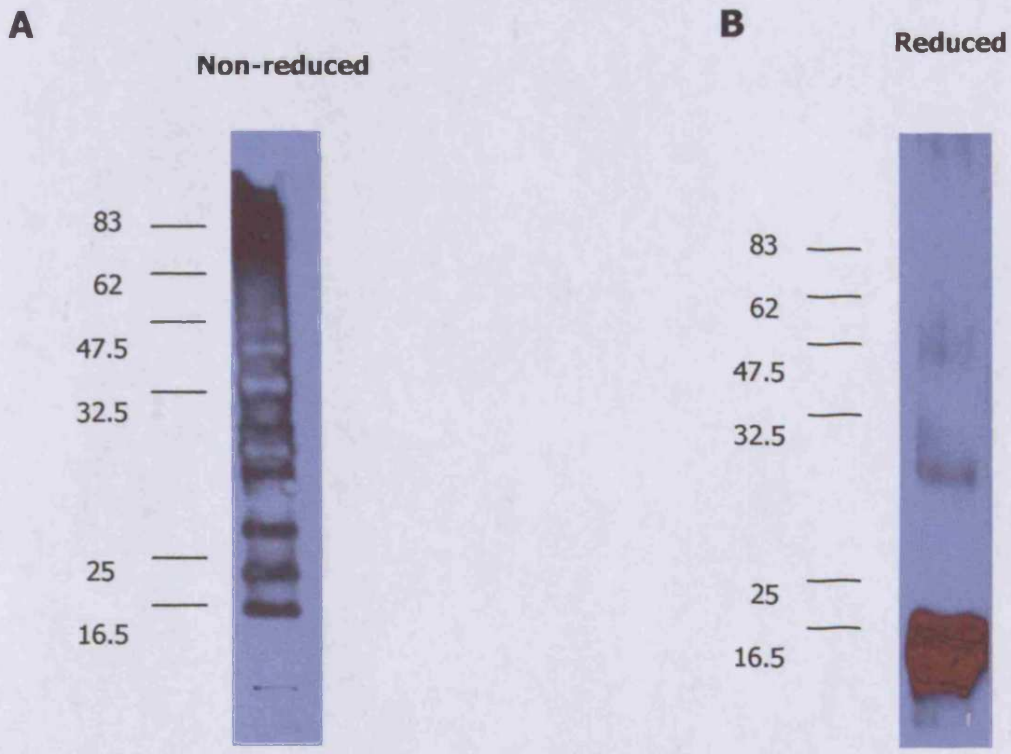

Figure 12

SDS-PAGE and Western blotting of non-refolded PO-EC

A 10µl sample of non-refolded, dialysed and concentrated protein solution from runs 1 and 2 was loaded 1:1 in non-reducing sample buffer (A) and reducing sample buffer (B) onto a 12.5% gel , and blotted using mouse anti-PO (kindly provided by Prof. Linington, Aberdeen, UK) as described.

The position of the molecular weight markers were shown on the left in kDa.

2.2.13 Circular Dichroism (CD) spectrum analysis of refolded versus non-refolded PO-EC domain

2.2.13.1 Principle

These studies were performed with the help of Dr. Konrad Beck, Matrix Biology and Tissue Repair Research Unit Dental School, Cardiff University. Circular dichroism spectroscopy (CD) can be used to determine whether a protein is correctly folded. CD depends on the sensitivity of far UV to the backbone conformation of proteins. Far UV (190-250nm) CD of a protein generally reflects the secondary structure content of the protein. At such wavelengths, the chromophore is the peptide bond, and a signal arises when it is located in a regular folded environment. Alpha-helix, beta-sheet, and random coil structures each give rise to a characteristic shape and magnitude of CD spectrum (Figure 13).

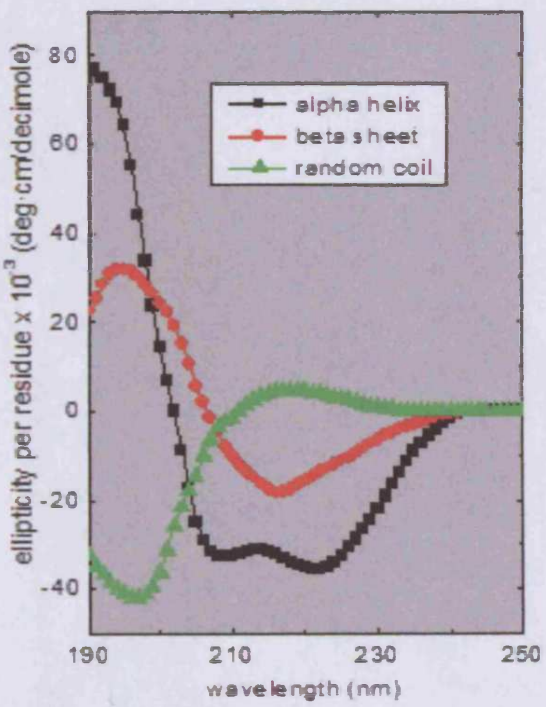

Figure 13 Principle of CD spectroscopy

The example above shows the characteristic spectrum of particular protein secondary structure; for example, beta sheet structures give rise to a signal at approximately 215nm if located in a properly folded environment.

Adapted from www.ap-lab.com/circular_dichroism.htm

2.2.13.2 Generation of a model template for PO-EC domain

To estimate the secondary structure content of the native protein, a model was derived using the X-ray structure of the rat homologue (PDB code 1neu) as a template (Kelly and Price 2000). The model was generated using SwissModel (Guex, Schwede et al. 2000). The secondary structure was derived from the model coordinates using the algorithms DSSP and STRIDE. The major difference is that DSSP assigns residues P76 to W78 and Y90 to D92 as a 3-10 helix whereas STRIDE does so only for the former residues. The overall secondary structure of the model is:

DSSP: 5.0% 3-10 helix, 47.9 β strands, 10.9 β turn, 36.2% others

STRIDE: 2.5% 3-10 helix, 47.9 β strands, 22.7 β turn, 26.9% others.

2.2.13.3 Measurement of CD spectra for refolded versus non-folded PO-EC domain

2.2.13.4 Method & Results

CD spectra were recorded on an AVIV 215 spectropolarimeter equipped with a thermostated cell holder. Spectra were recorded in 1mm Hellma QS strain free cells from 260nm to the minimum wavelength with an appropriate dynode voltage (> 500 V). Sample concentration was estimated from the absorption in the 280nm range using calculated absorption coefficients based on the amino acid composition assuming an oxidized state of the cysteine residues. Before measurements were taken, samples were extensively dialyzed against 100mM NaF (refolded PO-EC domain), or 8M urea (non-refolded PO-EC domain). The last dialysis buffer was used as a reference for both absorption and CD measurements. Before measurements, samples were centrifuged for 15min at 15,000g. Absorption spectra were recorded on a Beckman DU 800 spectrophotometer using a 100μl microcell at room temperature and corrected for light scatter using the method of Levine and Federici (Levine and Federici 1982) (refolded PO-EC domain, Figure 14). Analysis showed that both preparations were free from nucleic acid contamination (data not shown for non-refolded PO-EC domain). The CD spectra for refolded protein were measured in the 180 to 260nm range, while it was only possible to measure spectra for non-folded protein down to 213nm. As expected for a protein containing approximately 40% β-strand, absorption minima were recorded at 218nm for reference and refolded protein. It was clear that the non-folded protein did not share this characteristic (Figure 15). The helix content was estimated as 2-5%, β-strands: 36-44%, turns: 13-25% and random coil: 26-41%.

These values are in agreement with the assumption that the over-expressed and refolded PO-EC domain is in a fully folded conformation with respect to its secondary structure.

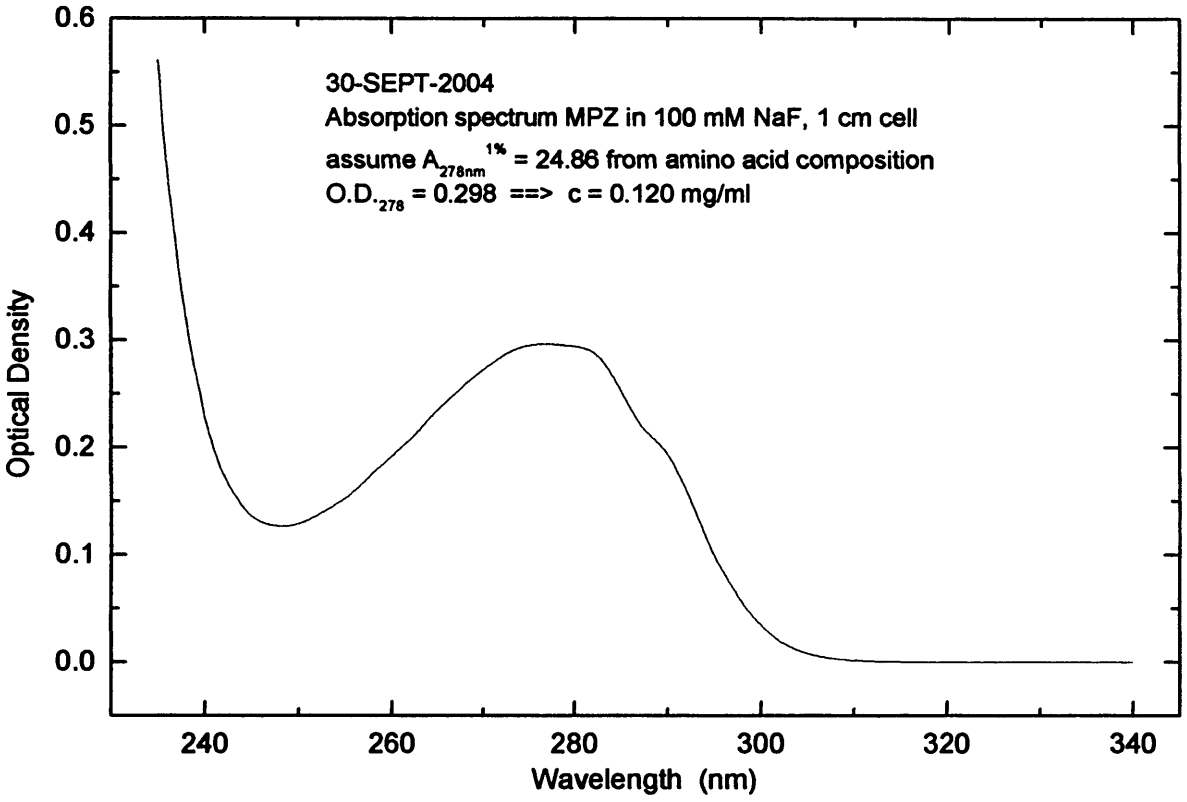

Figure 14

Absorption spectrum for refolded PO-EC domain

To assess whether the protein is free from nucleic acid contamination, and therefore the purity of the preparation, absorption spectra were recorded on a Beckman DU 800 spectrophotometer using a 100µl microcell at room temperature and corrected for light scatter. Protein solutions would give a high optical density reading at 280nm, while nucleic acids would give rise to a further signal at 260nm.

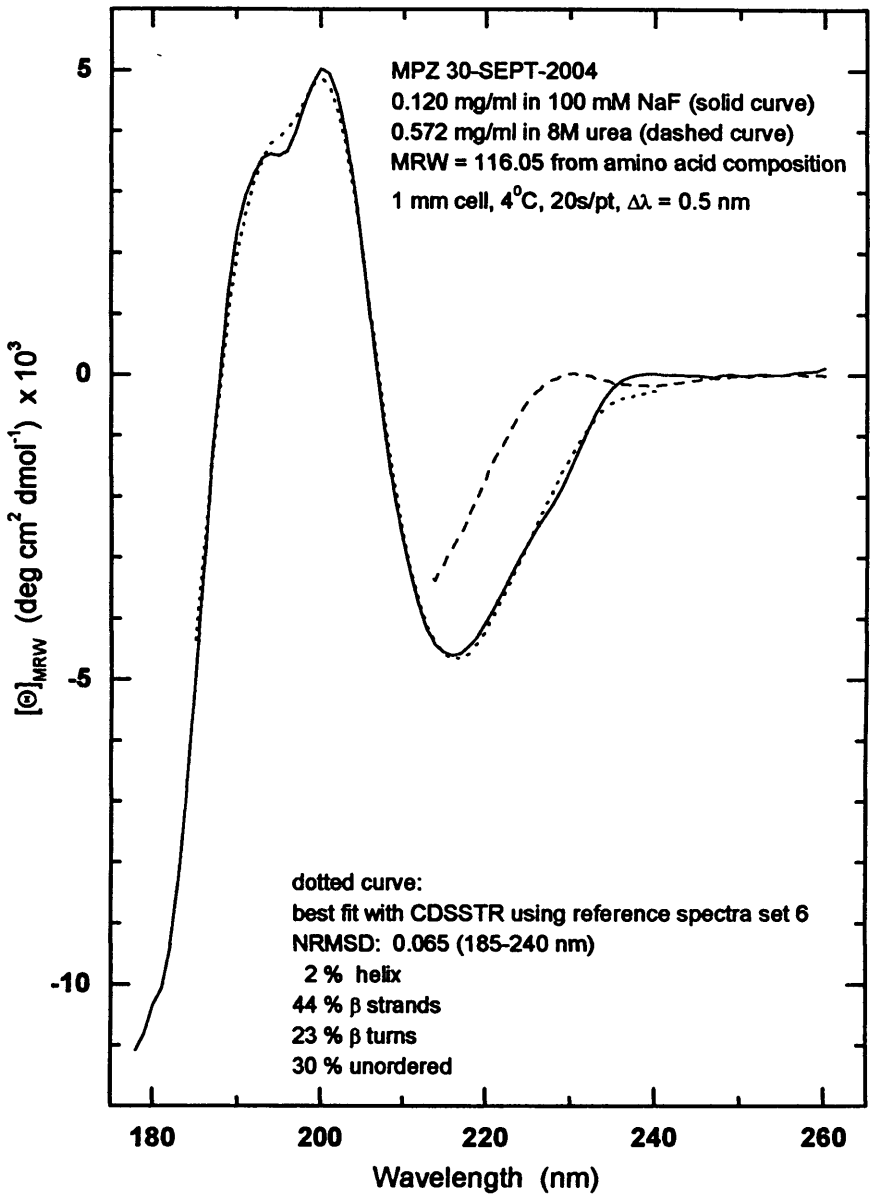

Figure 15

CD spectra of refolded versus non-refolded PO-EC domain

CD spectra were measured in the 180 to 260nm range for refolded protein (solid curve), non-folded protein as measured down to 213nm (dashed curve) and compared with a predicted spectrum for PO-EC domain (dotted curve).

2.2.14 Other myelin antigens

2.2.14.1 Sheep/Rat sciatic nerve homogenate

Sciatic nerve was isolated from a freshly butchered lamb (performed at Raglan abbatoir, Raglan, UK), and frozen in liquid nitrogen. The wet weight was 780mg. Following freeze-drying, a pestle and mortar was used to grind the tissue into a fine powder. A glass homogeniser was used to generate an emulsion in a minimal volume of saline (3.5ml), which corresponded to approximately 223mg/ml.

Similarly, sciatic nerves were isolated from 30 rats (performed at Biomedical Services Unit, Cardiff University), and frozen in liquid nitrogen. The wet weight was 540mg. The preparation was subjected to the same treatment as the sheep sciatic nerve homogenate.

2.2.14.2 Bovine peripheral nerve myelin

A pestle and mortar was placed in a -80^{0}C freezer overnight, while a 0.25M sucrose solution and a litre of distilled water was cooled in an ice bucket. The pestle was placed on a non-conducting surface, and 30-50ml of liquid nitrogen was added to cool the pestle, mortar and spatula. Following evaporation of the nitrogen, bovine cauda equina (supplied by Dr. Ian Gray, King's College London), was spread as thinly as possible with a spatula. The tissue was further cooled with liquid nitrogen and finely ground with the pestle and mortar following evaporation of the nitrogen. The powder was added into a cold beaker containing 150ml of 0.25M sucrose on ice to maintain coldness. A volume was transferred into a glass homogeniser, and homogenised; the resultant supernatant was poured into a pre-cooled beaker. This cycle was repeated until all tissue was homogenised. Connective tissue was removed using a strainer, and the supernatant was centrifuged at 1000g for 5 minutes at 4^{0}C. Floating tissue was discarded, and supernatants pooled. For maximum recovery, rotor buckets were rinsed with distilled water and included in the pooled material. The solution was centrifuged at 11,000g for 30 minutes at 4^{0}C twice. The pellets were pooled and weighed, and the resultant slurry was approximately 1:1 impure myelin:water. An equal volume of sterile saline was added, and the final product was freeze-dried overnight, and weighed.

3 Discussion

Peptides derived from human and mouse PO sequences were successfully prepared and characterised by mass spectroscopy, and will be used to induce EAN in both rats and mice in the subsequent chapter.

PO-EC domain was successfully cloned, expressed, purified and refolded using a bacterial expression system. Correct folding was demonstrated by CD spectroscopy. PO-EC domain was also prepared in bulk using a non-refolding protocol. Other myelin antigens were prepared, and will be tested for their capacity to induce disease in the next chapter. Overall yields from the refolding protocol were disappointing. From a 1 litre culture, it was usual to obtain only approximately 1mg of correctly refolded protein. This was primarily the reason for using the non-refolding protocol, since this protocol gave yields of between 8-10mg per litre of culture. Given that the refolding protocol had yielded respectable amounts (4-5mg/litre of culture) when applied to purification of mMOG (personal communication, Dr. Mark Griffiths, Cardiff University), which has a very similar structure to the EC domain of PO, being composed of single Ig loop, it became clear that this method required optimisation for this particular protein. However, due to time constraints, this was not possible. Heterologous expression of foreign genes in *E. coli* often leads to production of expressed protein within insoluble inclusion bodies; such inclusion bodies must then be solubilised and refolded into an active conformation. It is well established that refolding of inclusion body-derived proteins is not a straightforward process, and often requires an extensive 'trial and error' approach (Tsumoto, Ejima et al. 2003).

Recovering active proteins from inclusion bodies requires both solubilisation and refolding. Refolding is initiated by reducing the concentration of the denaturant used in the solubilisation. Protein refolding itself is not a single reaction, but rather competes with other reactions such as mis-folding and aggregation, which lead to inactive proteins. Unfolded proteins are generally disordered and flexible, while native protein is folded, rigid and compact. At high denaturant concentrations, proteins are unfolded; in aqueous solution they are folded. One would expect that transfer of a protein from denaturant to aqueous solution would cause the protein to fold; however, such a drastic process usually leads to mis-folding and aggregation, and in the absence of denaturant, these proteins lack the flexibility to adopt a native structure (Muralidhara and Prakash 2001). The poor yield obtained from the refolding of PO-EC domain is likely a result of a high proportion of misfolded and aggregated protein in the preparation resulting from a non-optimsed procedure.

There are various methods that could have been attempted to improve the efficiency of the refold protocol. One-step dialysis is one such method, where the protein in denaturant is dialysed against a refold buffer, thereby exposing it to descending concentrations of denaturant. Similar to this is a step-wise dialysis, using the same principle as above, but in a step-wise fashion, allowing equilibration at each step. Other methods include dilution of protein samples at high denaturant concentrations into a large volume of refolding buffer, and reverse dilution where refolding buffer is added to an unfolded protein containing

concentrated denaturant, such that denaturant and protein concentrations decrease simultaneously (Tsumoto, Ejima et al. 2003). Co-solute assistance may prove useful in facilitating refolding, and may be classified into 2 groups; folding enhancers which enhance protein-protein interactions, and aggregation suppressors, which reduce side chain associations. An example of a folding enhancer is sucrose (Lee and Timasheff 1981), while an example of an aggregation suppressor is polyethylene glycol (Cleland and Wang 2000).
Identifying the optimal refolding methodology is rate-limiting. However, the expansion of refolding methodologies is only likely to increase in this post-genomic era. To exploit the reservoir of knowledge that usually remains unpublished, a new web-accessible database has been devised which catalogues methods used in refolding over 300 proteins to date, named REFOLD (http://refold.med.monash.edu.au). The database can be interrogated using various parameters such as gene species, refolding protocol and structural family, and provides information in a spreadsheet format. To date, the most frequently used method for refolding is by simple dilution, reflecting the need for simplicity and cost-effectiveness in developing a refolding strategy (Buckle, Devlin et al. 2005).

On reflection, time may have been well spent on optimising this refolding protocol using the methods outlined above, to maximise yield, rather than repeating the same refolding protocol several times to obtain sufficient protein for subsequent animal studies.

Prokaryotic and eukaryotic expression systems are the two general categories of protein expression systems available to date. Although prokaryotic systems are often the systems of choice due to their ease of use and cost-effectiveness, their limitations should be considered for the production of eukaryotic proteins. Such proteins often undergo a variety of post-translational modifications, e.g. correct folding, glycosylation, phosphorylation and disulphide bridge formation, which require consideration (Rai and Padh 2001).
Bacterial expression systems command high growth rates, coupled with high protein expression rates. *E. coli* can grow rapidly and up to high density in relatively cheap media. Generation of fusion proteins, such as His-tags or maltose-binding protein (MBP) has greatly improved the efficiency of purification of such proteins (Maina, Riggs et al. 1988). However, distinct disadvantages exist. Common bacterial expression systems lack the capacity for post-translational modifications such as O- and N-linked glycosylation (Marston and Hartley 1990). In addition, over-expressed protein usually accumulates into inclusion bodies, and as mentioned earlier, requires solubilisation and subsequent refolding. Lysis to enable recovery of cytoplasmic proteins also often results in release of endotoxin, which must be removed from the final product (Rai and Padh 2001).

Yeast expression systems offer the advantage of lack of a toxic cell wall, such as in bacteria, and do not contain oncogenic or viral DNA, which may be present in mammalian systems. Yeast may be grown relatively rapidly, they secrete expressed proteins, their genome is already known, and they are able to glycosylated target proteins (Hitzeman, Hagie et al. 1981). However, it has been shown that both their O- and N-linked oligosaccharides have significantly different structures than their mammalian counterparts (Kornfeld and Kornfeld 1985). Hypermannosylation is also a feature of this system, which may hinder correct folding and therefore protein activity. Regardless, at this time, yeast offer a good compromise between bacterial and mammalian expression systems.

Insect systems have the capability for protein modifications, processing and transport systems present in higher eukaryotes, and use a helper-independent virus that may be propagated in high titre and facilitate production of large amounts of recombinant protein. Expressed protein is usually propagated in the correct cellular environment, e.g. membrane proteins are targeted to the membrane. However, some post-translational modifications are highly inefficient, and glycosylation capability is again limited (Kitts and Possee 1993).

For absolute product authenticity, mammalian expression systems offer all post-translational modifications, although oligosaccharide processing is species-dependent. Expressed proteins are correctly targeted, and most importantly, exist in a correctly folded configuration, with relevant post-translational modifications intact. However, mammalian cell culture is time-consuming and labour-intensive, and complex nutrient requirement coupled with low product concentrations, make this option less attractive for commercial applications (Kaufman 2000).

The EC domain of PO contains a HNK-1 carbohydrate epitope, also expressed by members of the Ig superfamily, integrins and proteoglycans. The HNK-1 epitope is found on the single N-glycan of PO, and its importance for function has been demonstrated by blocking of carbohydrate biosynthesis; this leads to a loss of adhesive properties of PO. Evidence also suggests that homophilic binding between PO molecules is mediated, in part, by lectin-like interactions between PO and HNK-1. Of particular note here is that autoantibodies present in patients with peripheral neuropathy, have been found to be reactive with the HNK-1 epitope (Voshol, van Zuylen et al. 1996). The lack of glycosylation within a bacterial expression system may therefore have consequences downstream with regard to the capability of PO-EC domain to elicit an auto-immune response, and lead to neuropathy. Perhaps in parallel to the bacterial expression system, yeast and mammalian systems could have been optimised, and their products tested for differences in disease induction.

Regardless of the points raised in this discussion, the aim of this chapter has been fulfilled. Various antigens derived from peripheral nerve proteins, and peripheral nerve tissues have been generated, and will be used to induce EAN in rats and mice.

Chapter 4

Part 1

Optimisation of acute Experimental Autoimmune Neuritis (EAN) in the Rat

1 Introduction

EAN is considered to be the best *in vivo* model of GBS, and as such, provides a valuable insight into the effector mechanisms of immune-mediated peripheral nerve demyelination.
EAN can be induced in susceptible animals by immunisation with various PNS antigens in FCA. EAN was first described in 1955 by Waksman and Adams, who immunised a rabbit with PNS homogenate (Waksman and Adams 1955). Since then, EAN has been successfully induced in rats, rabbits and mice (Maurer and Gold 2002). BPNM has been most widely used in this capacity (Feasby, Gilbert et al. 1987), (Archelos, Roggenbuck et al. 1993), (Vrisendorp, Flynn et al. 1995), (Jung, Toyka et al. 1995), (Gabriel, Gregson et al. 1997), (Bechtold, Yue et al. 2005), following the method of Kadlubowski and Hughes (Kadlubowski and Hughes 1979). In addition, peripheral myelin derived from other species has also been used in the induction of EAN in the rat, for example, porcine spinal root (Koh, Nakano et al. 1984), and horse sciatic nerve (Moon and Shin 2004).
Acute EAN in the rat is a monophasic disease, characterised clinically by progressive weakness initiated at the tail, progressing to hind limb weakness and wasting and resulting in hind limb paralysis. Histologically, the disease is characterised by massive inflammatory cell infiltration and demyelination of the peripheral nerves. Weakness generally begins around day 13 post-induction (p.i.), and reaches a maximum around day 16-18, after which a slow recovery may be made over several days.
The pathological mechanisms responsible for disease are thought to start in the lumbo-sacral nerve roots with nerve oedema due to disruption of the BNB at day 9-10, followed by perivenular lymphocyte infiltration at day 11-12. Large numbers of infiltrating macrophages are present, and demyelination of nerve fibres is evident. The disease spreads to the peripheral nerves forming multi-focal lesions (Vrisendorp 1997).
Individual protein components specific to PNM have been exploited in the induction of EAN. Peptide SP26 corresponding to the 53-78 amino acid sequence of bovine myelin P2 protein has been gaining favour in recent years (Vedeler, Conti et al. 1999), (Fujioka, Purev et al. 2000), (Beiter, Artelt et al. 2005). A few reports of PMP22 as an antigen for EAN induction have also been published (Gabriel, Hughes et al. 1998).

PO was first exploited in 1987 as an antigen to induce EAN in the Lewis rat. PO was prepared from bovine spinal root myelin, and in the presence of detergent, induced clinical disease with inflammatory infiltrates present in the sciatic nerve, and spinal roots, concurrent with a loss of myelin (Milner, Lovelidge et al. 1987). Work by Linington and co-workers in 1992 suggested that PO contains at least 2 neuritogenic T cell epitopes corresponding to peptides 56-71 and 180-199 of PO (Linington, Lassman et al. 1992). This was exploited by Zou and colleagues in 2001, where a comparison of neuritogenic activity of the peptides at different doses revealed different clinical courses, pathological changes and immune responses. Immunisation of Lewis rats with PO peptide 180-199 resulted in slightly earlier induction of clinical symptoms compared with 56-71, in a dose-dependent manner. Although both peptides resulted in a similar grade of inflammatory cell infiltration within the sciatic nerve, more severe demyelination was found with peptide 180-199 (Zhu, Pelidou et al. 2001).

1.1 Chapter Aim

The purpose of this chapter was to optimise the induction of EAN in both the rat and the mouse, and to compare the susceptibility of C deficient and C knockout animals to disease induction, in an effort to dissect out the role of C in disease pathogenesis. A literature review of EAN induction in the mouse revealed that the same PO peptide sequence (PO peptide 180-199) was capable of inducing EAN both in the C57Bl/6 mouse (Zou, Ljunggren et al. 2000) and the rat. This gave a starting point for the work.

BPNM has been the antigen of choice for EAN induction since the model was initially established. However, as mentioned earlier, the BSE crisis in the UK has obtaining bovine nervous tissue virtually impossible. Therefore, alternative strategies for disease optimisation had to be sought.

Several approaches have been used to date in the optimisation of EAN in the rat, and will be the focus of this chapter.

2 Materials and Methods

All chemicals unless otherwise stated were from Sigma Aldrich Chemical Company, (Gillingham, UK).

2.1 Animals

All animals used for preliminary optimisation experiments were obtained from Charles River Laboratories, UK, and were maintained according to Home Office guidelines within the

Biomedical Services Unit (BSU), University of Wales College of Medicine (UWCM), Cardiff. Male animals were used, and weighed between 160-250g at the start of each experiment.

2.2 Collection and processing of tissues for immunohistochemical analysis

All materials were obtained from Surgipath, Peterborough, UK, unless otherwise stated.

2.2.1 Paraffin wax embedded sections for light microscopy

2.2.1.1 Perfusion fixation of tissues

Animals were sacrificed by lethal injection of Euthatal (pentobarbitone; Rhone-Merieux, Harlow, UK). Animals were further perfused with 10% (v/v) formaldehyde in PBS via the aorta. Sciatic nerves, spinal cords and brains were removed and post-fixed in 10% (v/v) formaldehyde overnight at 4^0C. Tissues were paraffin-wax embedded by Dept. of Histology under the guidance of Dr. James Neal (Dept. of Pathology, UWCM, Cardiff).

2.2.1.2 Paraffin wax processing

Paraffin wax embedded tissue blocks were sectioned at 8µm using a Leitz 1512 rotary microtome. The sections were floated on a heated water bath, and picked up onto Snowcoat X-tra micro glass slides. Sections were dried slowly at room temperature for at least 1 hour, followed by overnight drying at 60^0C. Paraffin was removed from sections by placing in 100% xylene for 10 minutes followed by fresh xylene for 5 minutes. Sections were taken to water by sequential 5 minute incubations in absolute ethanol, 95% (v/v) ethanol and two changes of 70% (v/v) ethanol, followed by tap water. Following staining, sections were dehydrated by sequential incubations of 5 minutes in 70% (v/v) ethanol (x2), 95% (v/v) ethanol, cleared in xylene for 10 minutes (x2), and mounted with XAM neutral mounting medium (BDH).

2.2.2 Haematoxylin and Eosin (H&E) staining of paraffin wax embedded tissues

Sections were taken to water and stained with Harris's Haematoxylin for 5 minutes, 'blued' in Scott's tap water then washed in ordinary tap water. Haematoxylin staining was differentiated in 1% acid alcohol (70% (v/v) ethanol, 1% (v/v) conc. hydrochloric acid) for 1-2 seconds, and washed in tap water. Sections were further stained in Eosin for 2 minutes, washed in tap water, dehydrated, cleared in 100% xylene and mounted as above.

2.2.3 Luxol Fast Blue (LFB) staining of paraffin wax embedded tissues

Sections were taken to absolute ethanol and stained in 0.1% (w/v) luxol fast blue (solvent blue 38; Sigma) in 95% (v/v) ethanol for 16 hours at 37^0C. Sections were then washed in 70% ethanol (2x5min), rinsed in tap water, and differentiated with 0.05% (w/v) cresyl violet

acetate (Sigma) for 30 min, washed in tap water, dehydrated, cleared in xylene and mounted.

2.3 Collection and processing of tissues for electron microscopy (EM)

2.3.1 Tissue processing for EM

Rats were sacrificed by perfusion with 100ml 2% (v/v) formaldehyde, 0.3% (v/v) glutaraldehyde in phosphate buffer, pH 7.3, via the aorta while under terminal anaesthesia. Sciatic nerves were removed and post-fixed in the same buffer for 24 hours at room temperature.

To control for artefact, a rat was killed by a Schedule 1 method, and sciatic nerves were immersion fixed in the same buffer for 24 hours at room temperature.

2.3.2 Araldite embedding

The sciatic nerve was dissected away from any remaining muscle, and cut into 1-2mm^3 pieces in 0.1M phosphate buffer, pH 7.3. The tissue pieces were washed in phosphate buffer (4 x 60 mins) on a roller. The tissue was post-fixed in osmium tetroxide (OsO_4, 2% (v/v) in 0.1M veronyl acetate buffer) for 3 hours at 4^0C, and washed in 70% (v/v) ethanol (3 x 15 mins). The tissue can be stored at this point at -80^0C if desired. The tissue was fully dehydrated in ethanol gradients (90% (v/v) ethanol (2 x 10min), absolute ethanol (3 x 10min), and cleared in reactive intermediary propylene oxide (3 x 15min). Further processing into propylene oxide/Aradite 2:1 mixture for 30 minutes, followed by propylene oxide/Araldite 1:2 mixture for 30 minutes preceded Araldite impregnation (2 x 60min) at 50^0C. The tissue was embedded and polymerised at 65^0C for up to 48 hours in capsules containing paper labels.

2.3.3 Semi-thin sectioning

Semi-thin sections (0.5µm thickness) were cut on Reichert-Jung Ultracut E microtome (Leica, UK) using glass knives. Sections were picked up using an eyelash on a cocktail stick, and floated on a droplet of water on a glass slide. Droplets were dried on a hotplate at 50^0C for 2 minutes or at room temperature for 1 hour. The sections were stained with toluidine blue to identify areas suitable for further analysis.

2.3.4 Toluidine blue staining

Toluidine blue is a basic dye used as a quick stain for light microscopic orientation of sections for subsequent electron microscopy, and shows general structure, similar to that shown by H&E staining. A 0.5% (w/v) toluidine blue solution in 0.5% (v/v) di-sodium

tetraborate was prepared, mixed 1:1 with distilled water immediately prior to use, and filtered through a Whatman No. 1 filter paper. The section was flooded with this solution and heated on a hot-plate until the edges started to dry. Excess stain was washed off under running tap water. The sections were allowed to air-dry, and were mounted as described previously under a glass coverslip.

2.3.5 Ultra-thin sectioning

Having selected an area of interest from the semi-thin toluidine blue-stained sections, the relevant blocks were trimmed and sectioned at a thickness of 90-100nm, so that the tissue section appeared gold within the light spectrum. Sections were collected on the dull side of ethanol-washed, 200mesh, high transmission nickel grids by placing the grid underneath and removing the section on a droplet of water using fine forceps. Grids were air-dried at room temperature for at least 2 hours prior to staining.

2.3.6 Uranyl acetate staining of grids and EM

Uranyl acetate (4% saturated solution) was centrifuged to remove any un-dissolved crystals prior to use. A drop of uranyl acetate solution was placed onto a clean Petri dish, and the grid placed within the drop for 20-25 minutes. For each grid, three drops of double-distilled filtered water were used to wash the grid for 1 minute each. A small quantity of Reynolds (1963) lead citrate was withdrawn from beneath liquid paraffin (stored under paraffin since lead citrate will react with carbon dioxide to form a lead carbonate precipitate), and a drop placed into a Petri dish. The grid was transferred from the water to the lead citrate for 15 minutes, and washed as described previously. The grids were finally picked up using fine forceps and left to air-dry. Grids were examined with a Philips CM12 transmission EM at an accelerating voltage of 80kV. The EM was connected to a Link X-Ray detector with AN10K and the SIS MegaView III digital imaging system, linked to a Dual Athlon MP2000 PC.

2.4 Disease assessment

2.4.1 Clinical scoring

The rats were weighed daily, and evaluated clinically using the following scoring system: 0, no clinical features; 1, limp/ flaccid tail; 2, loss of co-ordination; 3, hind limb weakness and wasting; 4, hind limb paralysis (Schematic 1). Half-scores were applied for intermediate clinical signs. Animals were sacrificed by a Schedule 1 method upon reaching a clinical score of 4, or upon weight loss greater than or equal to 20% of original body weight.

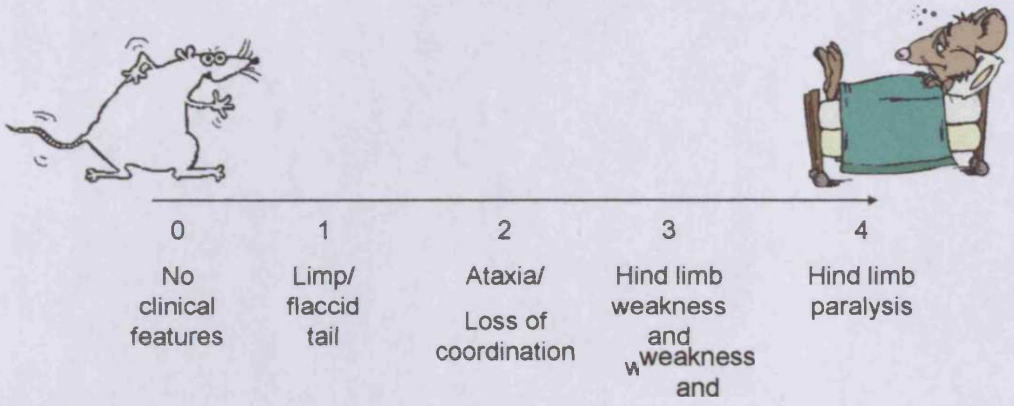

Schematic 1

Diagrammatic representation of the clinical scoring system implemented in EAN in the rat

3 Optimisation of EAN induction in the Rat

3.1 Induction of EAN in PVG/c rats using PO peptide 180-199 via footpad versus base of tail injection route

3.1.1 Aim

The overall aim of this project was to compare the susceptibility of various C deficient and knockout animals to disease induction. C6 deficiency was described in a colony of PVG/c rats in 1994, and provides a unique model for studying the importance of the MAC under experimental conditions (Leenaerts, Stad et al. 1994). Six male and six female PVG/c rats were obtained from this colony from Bantin and Kingman Universal Inc., (Freeman, CA, USA) and bred to establish a local colony. Initial experiments to establish EAN were therefore performed on wild type PVG/c rats.

As described previously, PO peptide 180-199 was used to successfully induce EAN in the Lewis rat (Zhu, Pelidou et al. 2001); efforts therefore concentrated on the susceptibility of PVG/c rats to EAN using this peptide. The efficacy of immunisation routes (footpad versus sub-cutaneous (s/c) base of tail) was also compared.

3.1.2 Induction protocol

Eleven male wild type PVG/c rats (120-200g) were obtained from Charles River Laboratories, and allowed to acclimatise for 1 week prior to disease induction. On day 0, Group A (n=6) received 200µg of PO peptide 180-199 (prepared by Severn Biotech, Kidderminster, UK), resuspended in 100µl sterile saline, and emulsified with 100µl of Freund's Incomplete

Adjuvant (FIA) containing 2mg *Mycobacterium tuberculosis* (*M. tuberculosis*) per animal in a Hamilton syringe, into the hind footpads. Hind footpads were thoroughly cleaned using antiseptic spray prior to injection to minimise infection.

Group B (n=5) received 200µg PO peptide 180-199 emulsified with 100µl of FIA containing 2mg *M. tuberculosis* per animal sub-cutaneously at the base of the tail. All animals were immunised under halothane inhalational anaesthesia. Animals were assessed daily for 21 days in terms of their weight, and clinical score as described previously.

3.1.3 Results

3.1.3.1 Assessment of weight and clinical score

All animals lost weight 24 hours following injection, and were given pre-wetted food daily. Normal weight gain was restored until day 13 to 19 whereafter Group A (Figure 1A, blue line) lost weight consistently. Group B continued to gain weight throughout the experiment (Figure 1A, pink line).

Unanticipated onset of inflammation at the site of the injection occurred in Group A (footpad-injected) animals at day 13, and all animals were given analgesic in drinking water to relieve pain. The scoring system was adjusted to account for tail and limb condition and to incorporate the symptoms from the inflammation as shown in Table 1. It was not possible to distinguish real neurological symptoms from local inflammation at this time.

Tail condition	
Clinical observation	***Score***
No clinical features	0
Moderate flaccid tail	0.5
Flaccid tail	1
Limb condition	
Clinical observation	***Score***
No clinical features	0
Slight swelling RHL/LHL	0.5
Moderate swelling RHL/LHL	1
Severe swelling RHL/LHL	1.5
No weight bearing RHL/LHL	2
Paralysis RHL/LHL	3
Swelling ALL limbs	3.5
Paralysis ALL limbs	4

Table 1

Adjusted scoring system to incorporate symptoms of inflammation around the injection site
A score was identified for tail and limb condition, and added together to give a final score.

All animals in Group A displayed progressive clinical symptoms at day 13 post-induction (B). One animal (ID 0) was sacrificed by a Schedule 1 method at day 16 with a clinical score of 4. Animals in Group B failed to display any clinical symptoms throughout the experiment. All animals were sacrificed at day 25, and tissue was harvested for histological analysis.

3.1.3.2 Histology

Following perfusion fixation of tissues and paraffin wax embedding (Section 2.2.1), sciatic nerve and spinal cord sections were stained by H&E. Spinal cord sections were additionally stained with LFB to detect changes in myelin. One animal from each group was shown for comparison; Group A (Figure 2, A-C); Group B (Figure 2, C- E).

Neither group displayed inflammatory cell infiltrates within the sciatic nerve (Figure 2: SN; A, D). It was possible to analyse the peripheral nerve roots (PNR) and the white matter (WM) within the spinal cord sections, firstly by H&E staining (Figure 2: B, D), and secondly by LFB staining to detect any evidence of demyelination (Figure 2: C, F). No inflammatory infiltrates were detected, and no changes in myelin architecture were evident in the PNR or WM within the spinal cord.

3.1.4 Discussion

PO peptide 180-199 failed to induce any specific clinical symptoms in either the footpad or base of tail-injected animals. The difference in clinical score between the 2 groups resulted from local inflammation at the footpad injection site, which was absent from the base of tail-injected animals. Histological analysis of the sciatic nerves and spinal cord revealed no difference between the 2 groups, and no inflammatory infiltrates or loss of myelin (Figure 2). The work used as a template for this experiment had no record of local inflammation at the footpad injection site (Zhu, Pelidou et al. 2001). To evaluate whether this response was due to the peptide or the adjuvant, adjuvant only controls would have been required. However, a literature search revealed it is likely to be adjuvant disease, since studies involving injection of heat-killed *M. tuberculosis* (used to supplement the FIA in this model) in paraffin into the footpad led to footpad swelling and adjuvant disease (Muir and Dumonde 1982). It is therefore critical to include adjuvant only controls in subsequent experiments.

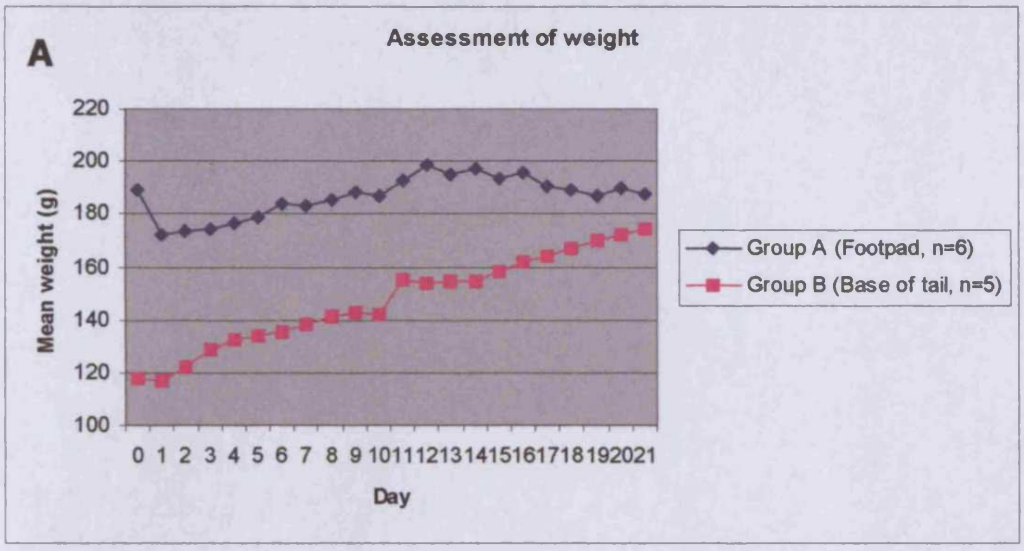

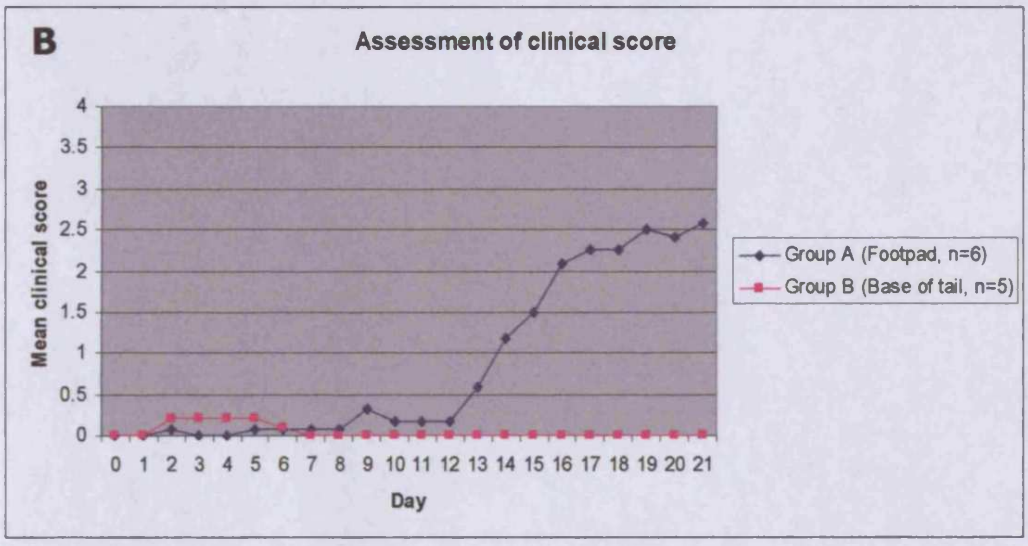

Figure 1 Induction of EAN using PO peptide 180-199

PVG/c rats were injected into hind footpads (Group A) or at the base of the tail (Group B) with an inoculum containing 200µg PO peptide 180-199 emulsified in FIA containing 2mg *M. tuberculosis* per animal at Day 0. Animals were assessed daily in terms of weight (A) and clinical score (B).

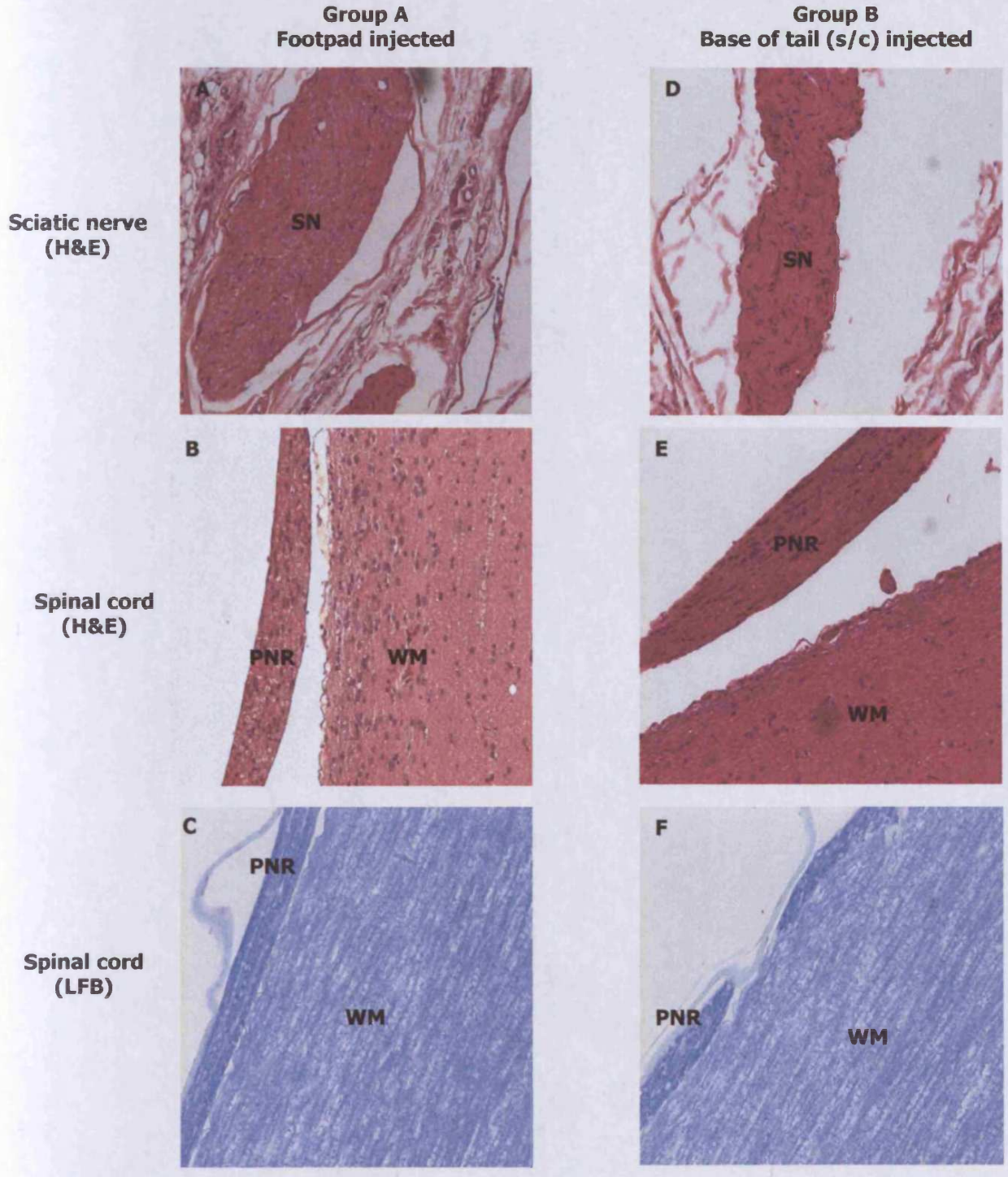

Figure 2

Histological analyses of sciatic nerve and spinal cord from footpad-injected versus base of tail-injected rats using PO peptide 180-199

Rats received PO peptide 180-199 emulsified in FIA containing 2mg *M. tuberculosis* either into the hind footpads (Group A), or sub-cutaneously at the base of the tail (Group B). Animals were assessed daily for changes in weight and clinical score, and followed for 25 days. Tissues were preserved by perfusion fixation and subjected to paraffin wax embedding as described. One animal for each group is shown for comparison; Group A (A, B, C); Group B (C, D, E). Sciatic nerve (SN, A, D) and spinal cord (SC, B, E) sections were stained by H&E for inflammatory infiltrate detection. SC was additionally stained for myelin with LFB (C, F). Peripheral nerve roots (PNR) were visible in the SC sections, and appeared healthy in both animals by H&E (B, E), and LFB staining (C, F).

3.2 Induction of EAN in PVG/c rats using bacterially expressed, refolded PO-extracellular domain (rPO-EC): Footpad versus base of tail injection route

3.2.1 Aim

Following the failure of PO peptide 180-199 to induce disease in PVG/c rats, alternative strategies were employed. Evidence in the literature suggested that recombinant forms of peripheral myelin proteins were capable of inducing EAN, for instance, PMP22, bacterially expressed as a glutathione-S-transferase (GST) fusion protein, had been used to induce a mild EAN in the Lewis rat (Gabriel, Hughes et al. 1998). However, the prevalence of peptides derived from PO in inducing disease in both rats and mice, made PO an attractive target for investigation into its capacity to induce EAN. Bond and co-workers had previously demonstrated the successful expression, purification and refolding of the extracellular domain of human PO in a bacterial expression system (Bond, Saavedra et al. 2001), and this was utilised as described in Chapter 3, Section 2.2.

3.2.2 Induction protocol

Sixteen male PVG/c rats (200-240g) were obtained from Charles River Laboratories, and allowed to acclimatise for 1 week. Eight groups of animals (n=2 per group) were set-up as shown below in Table 2.

Group	Antigen	Injection site
A	100µg rPO-EC*	Footpad
B	100µg rPO-EC	Base of tail
C	200µg rPO-EC	Footpad
D	200µg rPO-EC	Base of tail
E	400µg rPO-EC	Footpad
F	400µg rPO-EC	Base of tail
G	Adjuvant only	Footpad
H	Adjuvant only	Base of tail

*rPO-EC = recombinant PO-extracellular domain

Table 2

Identification of groups in terms of antigen and injection site

All groups received a dose of rPO-EC in saline emulsified in FIA containing 2mg *M. tuberculosis* in a total volume of 200µl or adjuvant only, either via the hind footpads or into the base of the tail sub-cutaneously. All animals were immunised under anaesthesia. Animals were assessed in terms of their weight and clinical score as described previously (Section 3.1.2). Due to the onset of inflammation around the injection site in the footpad-injected animals, the adjusted scoring system was implemented (Table 1).

3.2.3 Results

3.2.3.1 Assessment of weight and clinical score

All groups of animals lost weight 24 hours after immunisation, but normal weight gain was restored by day 3-4 p.i. Only animals from 200µg and 400µg rPO-EC dose footpad injected groups lost weight from day 13 p.i (Figure 3, A).

No clinical symptoms were evident in base of the tail injected groups, at any of the doses, while footpad injected animals displayed mild symptoms, seen previously (Section 3.1.3.1) in footpad-injected animals (Figure 3, B). No disease or inflammation was evident in adjuvant only controls, in either footpad or base of tail injected animals, suggesting that a component of the rPO-EC was responsible for the clinical symptoms seen in footpad injected animals.

All animals were sacrificed at day 21 p.i.

3.2.3.3 Histological analysis

Sections from representative animals of the highest dose rPO-EC-injected group and saline/adjuvant only controls are shown. Group E (rPO-EC injected into the hind footpads, Figure 4A) displayed white globular structures (G) surrounded by massive inflammatory cell infiltrates (IF) in the muscle (M) surrounding the sciatic nerve; however, the sciatic nerve (SN) remained unaffected (Figure 4A, inset). This was also seen in Group F (rPO-EC injected s/c at base of tail; Figure 4B) and again the SN remained unaffected. Limited inflammation was detected in Group G (adjuvant only into the hind footpad, Figure 4C) and Group H (adjuvant only, base of tail, Figure 4D); the SN in both groups remained unaffected.

3.2.3.4 Discussion

Immunisation of PVG/c rats with refolded rPO-EC, via the footpad resulted in a mild local inflammatory disease, accounting for the clinical score observed, (Figure 3, B). Immunisation at the base of the tail did not result in any clinical symptoms. Histologically, immunisation with refolded rPO-EC resulted in non-specific inflammatory infiltrates into the areas surrounding the sciatic nerve, regardless of the injection site (Figure 4). The sciatic nerve however remained unaffected. rPO-EC failed to induce any significant specific clinical disease. This experiment demonstrated that a component of rPO-EC was most likely responsible for the presence of massive inflammatory cell infiltrates seen in the muscle/connective tissue surrounding the sciatic nerve. Upon discussion with supervisors, it was concluded that the most likely source of contamination was from the bacterial expression system used to generate the antigen (refer Chapter 3, Section 2.2) and thus likely to be lipopolysaccharide (LPS)/ endotoxin-related. A method to remove LPS from insoluble protein was implemented, and the resulting protein was used to induce EAN in the Lewis rat in subsequent experiments.

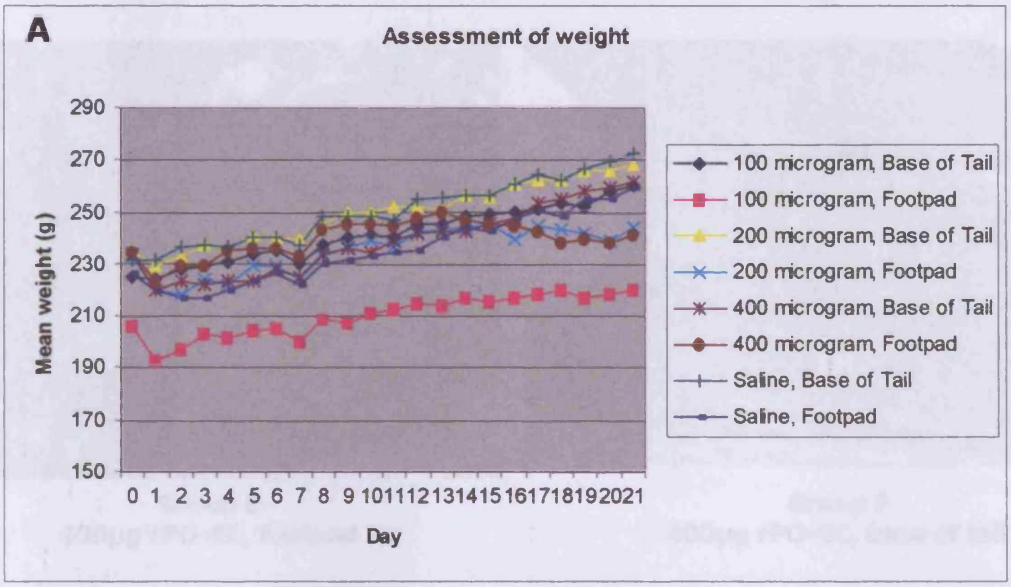

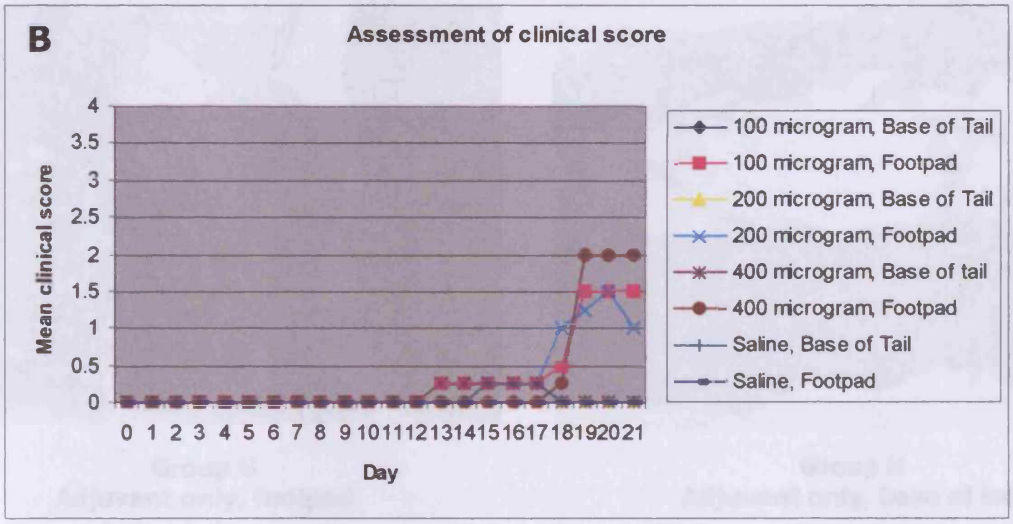

Figure 3

Assessment of weight and clinical score in rats injected with rPO-EC: Comparison of injection site and dose of antigen

On day 0, each animal received a dose response of rPO-EC (100, 200, 400µg) in saline emulsified in FIA containing 2mg M. tuberculosis in a total volume of 200µl or adjuvant only, either via the hind footpads or into the base of the tail sub-cutaneously. Animals were assessed daily in terms of their weight (A) and clinical score (B) as described previously.

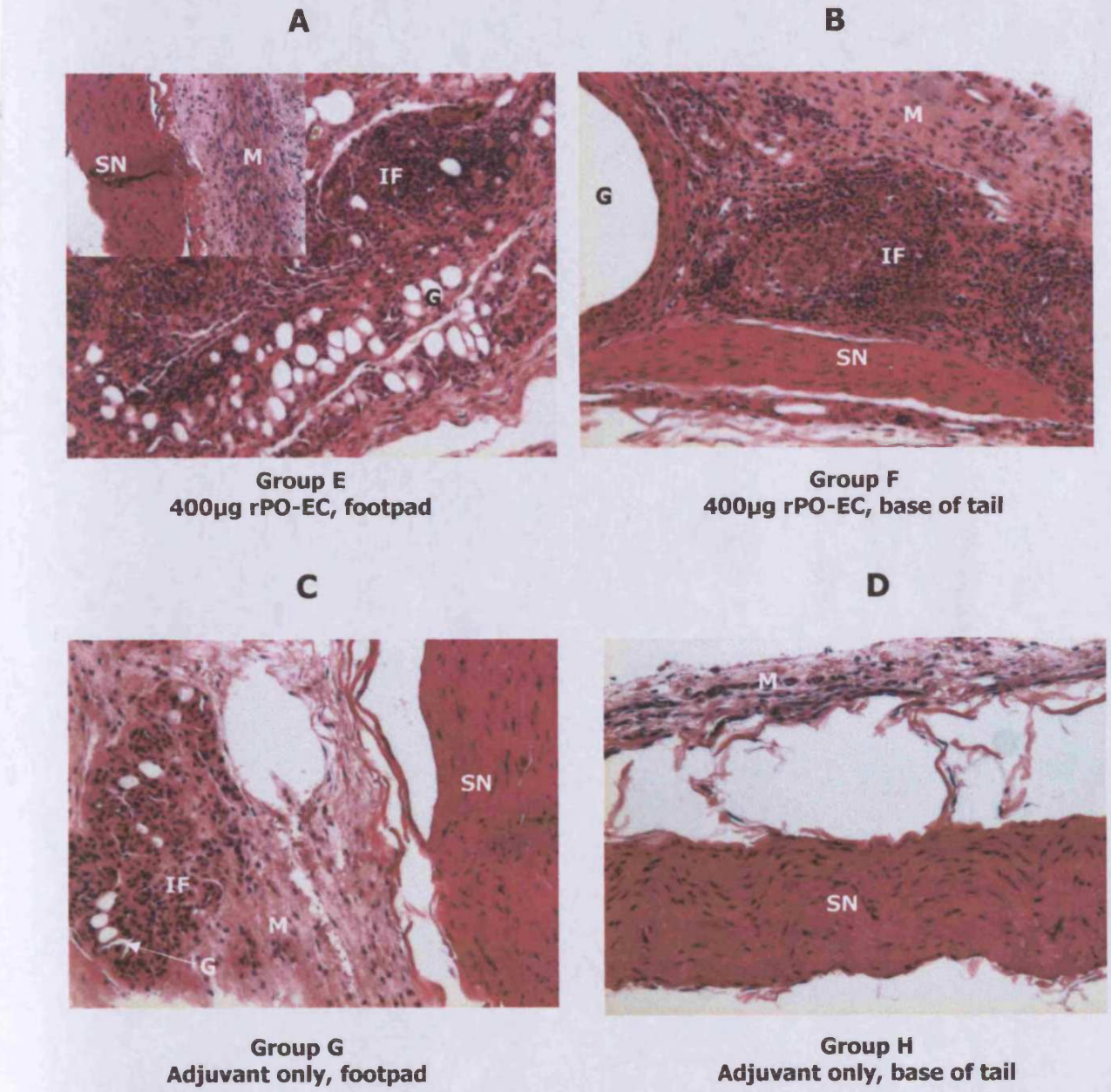

Figure 4

H&E staining of sciatic nerve sections from rPO-EC versus adjuvant only-injected animals

Rats were injected with a dose response of rPO-EC, either into the hind footpads or s/c at the base of the tail. At day 21, all animals were euthanized and tissues were perfusion fixed. Sections of sciatic nerve were stained by H&E to assess inflammatory cell infiltrates. Sections from representative animals of the highest dose rPO-EC-injected group and saline/adjuvant only controls are shown above (A; Group E (inset shows SN); B, Group F; C; Group G; D; Group H)

All images were taken at 100X magnification.

G=white globular structures; IF=inflammatory cell; SN=sciatic nerves; M=muscle/connective tissue

3.3 Experimental Modifications

3.3.1 rPO-EC as antigen

Due to the inefficiency of the refolding protocol for obtaining refolded PO-EC domain resulting in poor yields, non-refolded protein was be used for subsequent experiments since it was available in large quantities and would enable batch testing.

3.3.2 Animals

EAN had not been induced in the PVG/c rat using PO-derived antigens to date. PVG/c rats had previously been used successfully to assess the dependence of the terminal pathway in mediating EAE (Mead, Singhrao et al. 2002). However, upon discussion with colleagues, it was suggested that PVG/c rats are naturally relatively resistant to induction of autoimmune disease, and Lewis rats were significantly more susceptible. Susceptibility or resistance to autoimmune disease induction is associated with MHC (RT1 in the rat) class II gene products. This is not surprising given the key role of the MHC class II molecules in triggering CD4+ T cells by presenting restricted sets of peptides to the T cell receptor (TCR) (de Graaf, Barth et al. 2004). The C6 deficient PVG/c rats were undergoing backcrossing in-house onto the Lewis background, but were only on generation 6. It seemed prudent therefore, to optimise disease induction in the wild type Lewis rat in anticipation of the completion of the backcrossing at generation 10. Lewis rats were used in all subsequent experiments.

3.3.3 Assessment of coordination

Due to the subjective nature of assigning a clinical score of 2 (ataxia/ loss of coordination), and the commitment to reducing the number of animals used, refining procedures to minimise suffering, and replacing animal use as a condition of the personal animal licence (3Rs), a refinement was made to calculate and standardise measurement of the extent of coordination, by implementation of a balance beam test. The equipment consisted of a wooden beam 3cm in width and 1metre in length, suspended approximately 1 metre from the ground (Figure 5). Animals were trained to cross the beam to reach a darkened chamber. Animals were trained for 5 days prior to disease induction, and a coordination scoring system was designed and implemented (Table 4).; the higher the score, the less coordinated the rat.

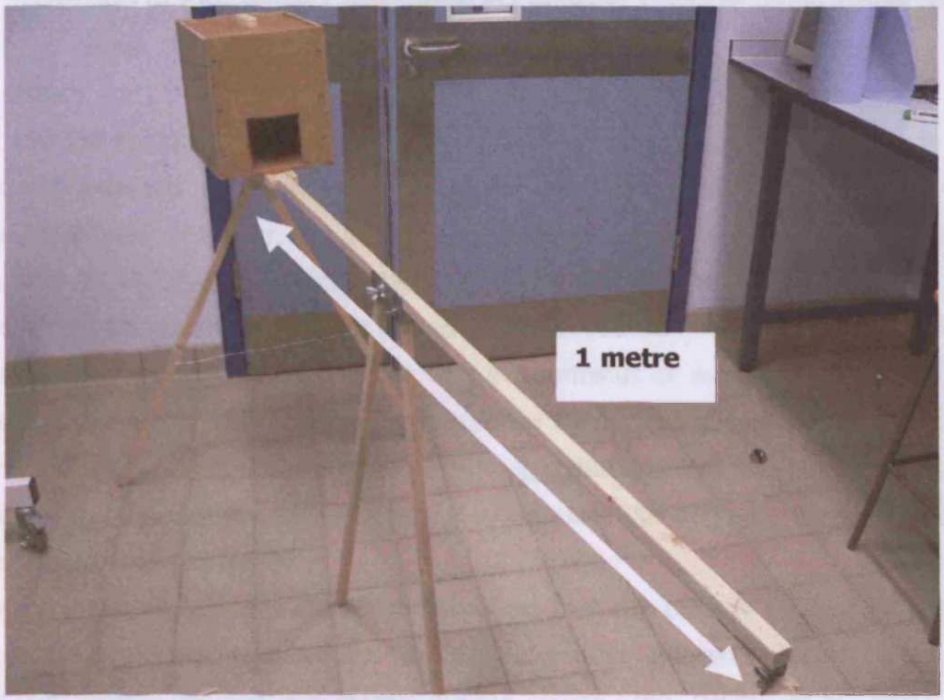

Figure 5

The balance beam as a tool to assess the extent of the coordination of the rat during EAN induction

Rats were placed 1 metre away from the dark chamber on the other side of the beam, and the time taken to cross the beam was recorded. A coordination score was awarded to each rat upon completion of the task.

Time taken (secs)	Coordination score
Less than 1 sec	0
1-5s	1
6-10s	2
11-15s	3
16-20s	4
21-60s	5
Unable to complete task in time allowed (60s)	6
Unable to complete task	7

Add 0.5 for each error; add 1 for each fall

Table 4 **Assessment of Coordination scoring system**

3.4 Induction of EAN using C-amidated PO peptide 180-199 using Lewis rats

3.4.1 Aim

Peptide 180-199 has been suggested to induce EAN in the Lewis rat (Zhu, Pelidou et al. 2001). After several attempts, we have been unable to repeat the induction protocol, and obtain reproducible disease. However, our original experiments were performed in PVG/c rats, which are now known to be resistant to many types of autoimmune disease induction.

Chemical modification of the peptide at N- and C- termini has been reported to enhance peptide presentation to T cells; either acetylation at the N-terminus or amidation of the C-terminus increases the lifetime of the free peptide in solution by protection from proteolysis (Maillere, Mourier et al. 1995). In addition, colleagues have suggested that amidation of the C-terminus of a peptide in this manner has been successful in inducing EAE in guinea pigs (Richard Mead, personal communication, 2004).

Previous reports using PO peptide 180-199 suggest that the dose of peptide delineates the clinical course of disease; for example, 50-100µg of peptide induced an acute clinical course, while 250µg peptide resulted in a chronic disease course (Zhu, Pelidou et al. 2001). A dose response of peptide was therefore examined in this experiment.

3.4.2 Peptide synthesis

Refer Chapter 3, Section 2.1 for details.

3.4.3 Induction protocol

Six wild type Lewis rats (160-200g) were obtained from Charles River, and allowed to acclimatise for 1 week before disease induction. On day 0 and day 7, animals were injected with a dose of PO 180-199-amide (100, 200 or 400µg), resuspended in 100µl sterile saline, and emulsified with 100µl of FIA containing 2mg/animal *M. tuberculosis* by sub-cutaneous injection into the base of the tail. All animals were immunised under anaesthesia.

Animals were assessed daily in terms of their weight, coordination, and clinical score as described previously.

3.4.3 Results

Animals were assessed daily for changes in weight, coordination and clinical score. All animals continued to increase in weight for the duration of the experiment (Figure 6, A). Following the training period from day-3 to day 0, all animals maintained their coordination throughout the experiment (Figure 6, B). No clinical symptoms were evident from any of the animals (Figure 6, C). Since no animals exhibited any pathological changes at any of the doses, all animals were combined for analysis (n=6).

3.4.4 Discussion

Although PO peptide 180-199 has been suggested to be immunodominant in the rat (Linington, Lassman et al. 1992), and a study using this peptide and a similar protocol to that described here, obtained significant clinical EAN (Zhu, Pelidou et al. 2001), we have been unable to reproduce the model in our laboratory. However, a recent study in C57Bl/6 mice suggested that PO peptide 180-199 resulted in a rather mild disease with poor reproducibility; but peptide 106-125 was found to be a neuritogenic epitope capable of inducing severe clinical EAN (Miletic, Utermohlen et al. 2005). This may have implications for disease induction in the rat, since only the Swedish group (Zhu, Pelidou et al. 2001) has published successful induction of EAN using this peptide.

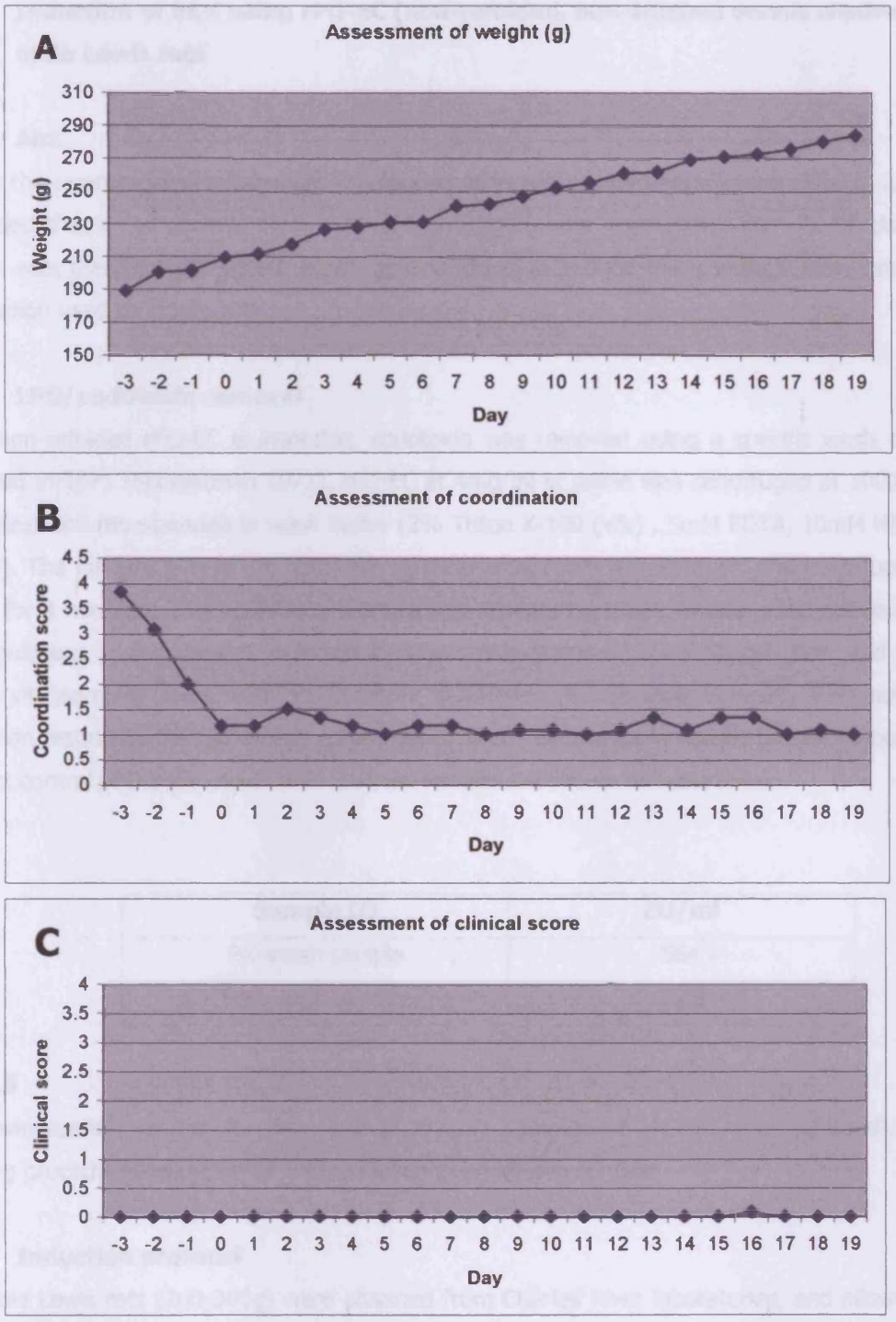

Figure 6

Assessment of weight and clinical score in PO peptide 180-199-amide-injected rats

Animals were injected on day 0 and day 7 with a dose response of PO peptide 180-199-amide in FCA as described. Animals were assessed daily for changes in weight (A), coordination (B), and clinical score (C) as described previously.

3.5 Induction of EAN using rPO-EC (non-refolded, non-washed versus washed) in male Lewis rats

3.5.1 Aim

Due to the unanticipated inflammatory response observed in rats injected with rPO-EC, it was concluded that a component, most likely LPS/endotoxin, was responsible. The rPO-EC domain protein was therefore subjected to stringent washing to reduce this contamination, and the preparation used to induce EAN.

3.5.2 LPS/endotoxin removal

Since non-refolded rPO-EC is insoluble, endotoxin was removed using a specific wash buffer identified in 1971 (Schnaitman 1971). rPO-EC at 4mg/ml in saline was centrifuged at 1000g for 4 minutes, and resuspended in wash buffer (2% Triton X-100 (v/v) , 5mM EDTA, 10mM HEPES, pH 7.4). The mixture was left to stand for 10 minutes at room temperature, and centrifuged at 1000g for 4 minutes. This washing procedure was repeated 4 times. Washing did not result in any significant protein loss as detected by Coomassie stained SDS-PAGE gel. Pre- and post-wash (x4) samples were sent to Cambrex (Cambrex Bio Science Verviers, Belgium) for endotoxin testing by the LAL kinetic chromogenic assay. Each sample was tested with a positive product control of 0.5 endotoxin unit (EU)/ml. Results are shown in Table 5:

Sample ID	EU/ml
Pre-wash sample	564
Post-wash sample	20.8

Table 5

Endotoxin testing results for pre- and post-wash samples of rPO-EC (non-refolded). The washing procedures lead to a 27-fold reduction in endotoxin content.

3.5.3 Induction protocol

Ten male Lewis rats (160-300g) were obtained from Charles River laboratories, and allowed to acclimatise for 1 week. Five days prior to induction (day -5), rats were trained on the balance beam in order to assess their coordination throughout the experiment.

On day 0, Group A (n=4) received 200µg rPO-EC (non-washed) in saline emulsified in FIA containing 2mg/animal *M. tuberculosis* in a total volume of 200µl via the hind footpads. Group B (n=6) received 200µg rPO-EC (washed to remove LPS/endotoxin) emulsified and injected as for Group A. All animals were immunised under anaesthesia. Animals were assessed in terms of their weight, coordination and clinical score as described previously.

NB It was noted that a weight discrepancy was evident between the 2 groups; however, these were the only animals available at this time.

3.5.4 Results

3.5.4.1 Assessment of weight and coordination

Animals from both groups showed an initial reduction in weight immediately following injection, but continued to increase weight steadily throughout the remainder of the experiment (Figure 7, A).

Animals from both groups scored high on the coordination score at the beginning of the training period (day -5), but became more adept at the task throughout the training period shown by a decrease in coordination score (day -5 to day 0) (Figure 7, B). Immediately following injection, there was an increase in score, most likely as a result of the trauma to the footpad during induction. There was maintenance of coordination until day 11, where both groups began to score high. Both groups showed a similar pattern in their coordination score reaching a maximum between days 15-17.

3.5.4.2 Assessment of clinical score and histological analysis

Since swelling of hind limbs was prevalent in these animals, the adjusted inflammation scoring system (Table 1) was employed.

Animals injected into the footpad with non-washed rPO-EC showed clinical symptoms from day 11 onwards, with severe swelling of the hind limbs, reaching a mean maximum score of 2 at the end of the experiment (Figure 8; A; Group A, blue line). Following LPS reduction by the washing procedure from rPO-EC in Group B, animals show a reduction in overall clinical score (Figure 8; A; Group B, pink line).

Sciatic nerves were isolated from each animal and embedded in paraffin wax. Sections were analysed by H&E staining for inflammatory infiltrates (Figure 8, B). Inflammatory cell infiltrates were evident in SN sections from Group A, although they were distinct from the SN within the connective tissue (inset). Reduction of LPS from rPO-EC using the washing protocol in Group B resulted in elimination of inflammatory infiltrates, but with no obvious specific neuropathy was detected, i.e. cellular infiltration or nerve fibre degeneration.

3.5.5 Discussion

In summary, it was clear that contamination of the bacterially expressed rPO-EC with LPS was causing significant morbidity to animals injected via the footpad. Reduction of LPS contamination using the washing procedure significantly reduced non-specific inflammatory cell infiltrates around the SN, but resulted in no specific EAN. It was clear therefore that rPO-EC was not able to induce EAN in the Lewis rat using the protocols described. It was unclear whether a defect in the T and B cell response to rPO-EC was involved in the failure to induce disease; therefore efforts were made to address this in the next experiment.

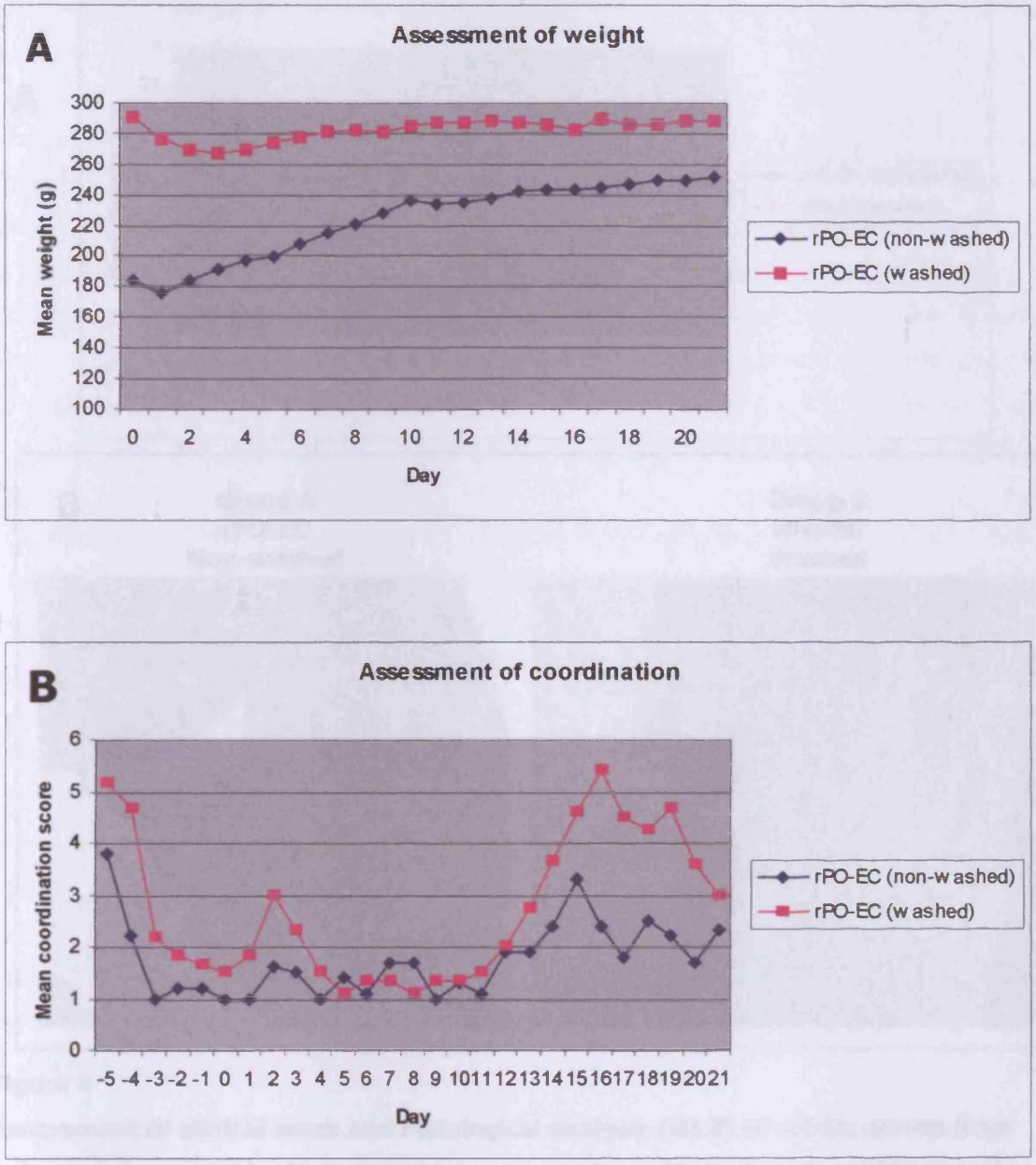

Figure 7

Assessment of weight and coordination of Lewis rats using rPO-EC washed versus non-washed to remove LPS to induce EAN

On day 0, each animal received 200µg rPO-EC, either washed or non-washed to remove LPS in saline emulsified in FIA containing 2mg M. tuberculosis in a total volume of 200µl or adjuvant only into the hind footpads. Animals were assessed daily in terms of their weight (A) and coordination (B) as described previously.

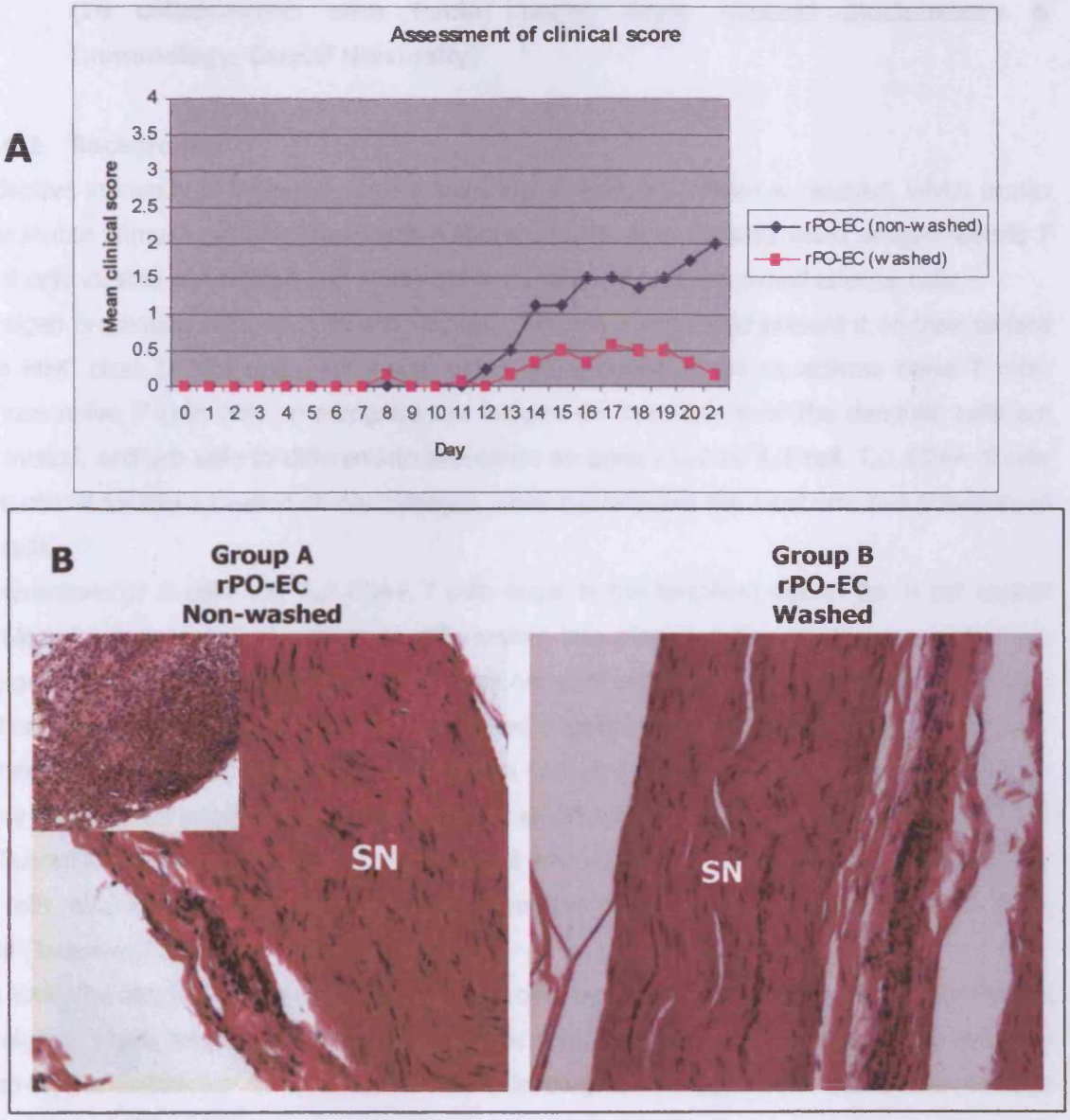

Figure 8

Assessment of clinical score and histological analysis (H&E) of sciatic nerves from animals injected with either washed or non-washed rPO-EC to induce EAN in male Lewis rats

Animals were assessed daily in terms of clinical score (A). Since swelling of hind limbs was prevalent in these animals, the adjusted inflammation scoring system was employed.

Following termination of the experiment at day 21, sciatic nerves were harvested, and H&E stained to assess inflammatory infiltration (B). Sciatic nerves in both groups of animals revealed no inflammatory cell infiltration, although extensive infiltration was evident in the muscle surrounding the sciatic nerve in Group A (B; Group A, inset).

3.6 Analysis of the T and B cell responses to the rPO-EC in the Lewis rat (In collaboration with Paula Longhi, Dept. Medical Biochemistry & Immunology, Cardiff University)

3.6.1 Background

Adaptive immunity is triggered when a threshold of dose of antigen is reached, which eludes the innate immune system. The adaptive immune response is initiated when antigen-specific T & B cells localise the antigen and proliferate in response to become armed effector cells.

Antigen presenting cells, such as dendritic cells, take up antigen and present it on their surface via MHC class II molecules, and enter secondary lymphoid tissue to activate naïve T cells. Those naïve T cells able to recognise the antigen on the surface of the dendritic cells are activated, and are able to differentiate into either an armed T_H1 or T_H2 cell. T_H1 CD4+ T cells are crucial for the activation of macrophages, while T_H2 cells are the most effective activators of B cells.

Interactions of B cells and T_H2 CD4+ T cells occur in the lymphoid tissue; the B cell cannot proliferate, form germinal centres or differentiate into plasma cells until they encounter the helper CD4+ T cell. B cells in contact with the helper T cell proliferate to form a primary focus where some isotype switching occurs. Activated B cell blasts then migrate to medullary cords where they divide and differentiate into plasma cells and secrete antibody. Other B cell blasts may migrate into primary lymphoid follicles and proliferate to form a germinal centre under the influence of antigen and helper T cells. Germinal centres are the site of selection of high affinity B cells, able to present antigen to T cells and receive positive signals such as IL-4 from the T cell (Janeway, Travers et al. 2001).

In EAN, the aim is to generate auto-reactive T cells by immunisation with various PNS-derived antigens, which become activated and cross the BNB. B cell activation is required to generate anti-myelin antibodies to drive C activation, leading to demyelination and axonal damage (Maurer and Gold 2002).

3.6.2 Aim

EAN is a CD4+ T cell mediated disease associated with inflammation and demyelination. The aim of this experiment was to test the effectiveness of CD4+ T cell responses in Lewis rats immunised with rPO-EC domain. CD4+ T cell responses were measured at two time points (14 and 39 days p.i.) by presenting purified T cells with various PO-derived antigens *in vitro* via antigen presenting cells (APCs). In addition, blood samples were taken at both time points to test the effectiveness of the B cell response by measuring Ab levels.

3.6.3 Induction protocol

Fourteen male Lewis rats (180-200g) were obtained from Charles River Laboratories, and split into 3 groups, as shown in Table 6:

Group	Antigen	No. animals
A	400µg rPO-EC (non-folded, washed)	6
B	Adjuvant only	6
C	None; naïve for APC generation	2

Table 6

Group identification, antigen and number of animals for experimental procedure

Animals in group A were injected at Day 0 with 400µg rPO-EC (non-refolded, washed) in saline emulsified in FIA supplemented with 2mg/animal *M. tuberculosis* into the hind footpads. Group B were subjected to the same immunisation protocol but injected with adjuvant only. Group C were naïve, and used for generation of antigen presenting cells (APC).

3.6.4 Methods

3.6.4.1 T cell proliferation assay

All manipulations were performed in a sterile environment where possible.

3.6.4.2 Isolation of CD4+ T cells

For selective isolation of CD4+ T cells, total leucocytes were obtained from spleens and lymph nodes at day 14 post-immunisation (p.i), and day 39 p.i. Each animal was sacrificed by a Schedule 1 method, and the spleen and popliteal lymph nodes were harvested with care taken to avoid harvest of fat, and transferred into a bijou tube containing RPMI wash medium (no supplements). The spleens and lymph nodes were transferred into a 6 well plate containing approximately 3ml fresh RPMI F5 medium. Using the end of a sterile syringe, the tissue was mashed, and the resulting mixture was put through a cell strainer to obtain a single cell suspension. An additional 10ml of RPMI-F5 was used to wash remaining cells from the plate.
Isolated leucocytes were incubated with anti-rat CD4 biotin-conjugated (no azide; W3/25, Caltag Laboratories, CA, USA) for 15 minutes on ice, and washed in magnetic cell sorting buffer (MACS buffer, 0.5% (w/v) BSA, 2mM EDTA in PBS) by centrifuging at 300g for 3 minutes. Ten microlitres of streptavidin-coated magnetic Dynabeads per 10^7 total cells (Miltenyi Biotec, UK) were added. Labelled cells were enriched using magnetic separation columns (Miltenyi Biotec).

3.6.4.3 Generation of APC

Spleens were harvested from freshly euthanized naïve rats, and processed by mashing as described above. Total cells were resuspended to $6x10^5$ cells/ml, and irradiated at 2400cGy to halt proliferation. This suspension was split into 4 groups, and pulsed with antigens of interest by incubating with antigen for 1 hour at 37^0C:

1 No antigen

2 PO peptide 180-199 @ 2mg/ml

3 rPO-EC (non-folded, autoclaved) @ 2mg/ml

4 rPO-EC (refolded) @ 50µg/ml

3.6.4.4 Lymphocyte proliferation assay

CD4+ T cells (100µl/well) were added to appropriate APC populations (100µl/well) in a 96 well round bottomed microtitre plate, and left to proliferate for 3 days. As a positive control for proliferation, triplicate wells were incubated with anti-rat CD3 antibody (G418, Pharmingen, BD Biosciences, Oxford, UK) to cross-link CD3 on the cell surface. After 3 days, cells were pulsed with [^{3}H]-methylthymidine (1µCi/well, Amersham Biosciences), and cultured for an additional 12 hours. [^{3}H]-methylthymidine incorporation was measured in a β-scintillation counter and results were expressed as counts per minute (cpm).

3.6.4.5 B cell response to rPO-EC domain

Two ELISA formats were designed to investigate the B cell response to rPO-EC domain, as shown in Schematic 2.

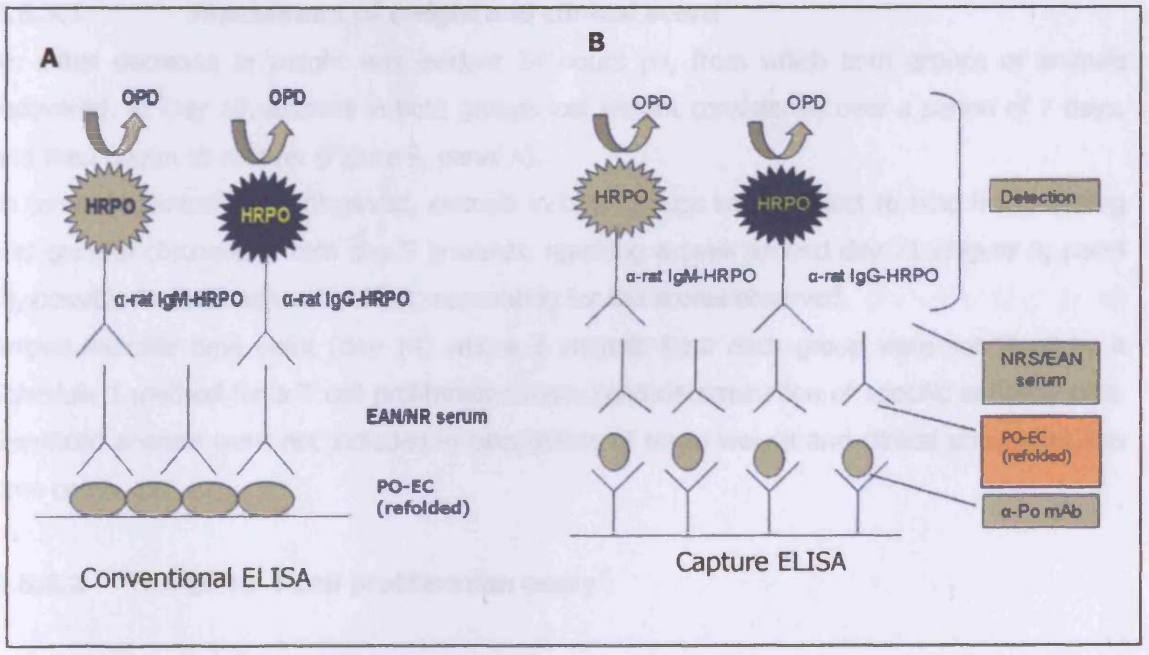

Schematic 2

Diagrammatic representation of ELISAs employed to determine the antibody response to rPO-EC

3.6.4.6 Conventional ELISA

rPO-EC (refolded) was coated at 10µg/ml on a 96 well microtitre plate for 1 hour at 37^{0}C, washed (x3) in wash buffer (PBS, 0.05% (v/v) Tween-20), and blocked in block buffer (PBS, 5% (w/v) BSA) for 1hour at 37^{0}C. Sera from rPO-EC and adjuvant only-injected rats at day 14

and day 39 were diluted in block buffer using a doubling dilution series starting at 2% (v/v) serum. Responses were amplified using both anti-rat IgM-HRPO (Binding Site, Cat No. 3080-05) and anti-rat IgG-HRPO (Jacksons, Cat. No. 712-035-150) conjugated antibodies, at 1:100 dilution in block buffer, and detected using *o*-Phenylenediamine dihydrochloride (OPD) (Sigma). Absorbance at 490nm was measured in a spectrophotometer. As a positive control, anti-PO mAb (kindly provided by Prof. Linington, University of Aberdeen, UK) was used at 10µg/ml, and a doubling dilution series was performed to test the ability of the antibody to recognise PO-EC domain.

3.6.4.7 Capture ELISA

Anti-PO monoclonal antibody was coated at 10µg/ml on a 96 well microtitre plate for 1 hour at 37^{0}C, washed (x3) in wash buffer, and blocked in block buffer for 1 hour at 37^{0}C. Refolded PO was added to the antibody-coated plate at 10µg/ml in PBS, and incubated for 1 hour at 37^{0}C. Sera from rPO-EC and adjuvant only-injected rats at day 14 and day 39 were analysed as described in section 3.6.4.6.

3.6.5 Results

3.6.5.1 Assessment of weight and clinical score

An initial decrease in weight was evident 24 hours p.i, from which both groups of animals recovered. At Day 13, animals in both groups lost weight consistently over a period of 7 days, and then began to recover (Figure 9, panel A).

In terms of clinical score observed, animals in both groups were subject to hind limb swelling and general discomfort from day 9 onwards, reaching a peak around day 21 (Figure 9, panel B), possibly from an adjuvant effect, accounting for the scores observed.

Arrows indicate time point (day 14) where 3 animals from each group were sacrificed by a Schedule 1 method for a T cell proliferation assay, and determination of specific antibody titre. Sacrificed animals were not included in calculations of mean weight and clinical score after this time point.

3.6.5.2 CD4+ T cell proliferation assay

Day 14

Three animals from each group were sacrificed at day 14 p.i., and subjected to CD4+ T cell proliferation assay as described.

Background proliferation was minimal (Figure 10, A, APC alone). No proliferation in response to PO peptide 180-199 was detected (Figure 10, B). Animal A0 from rPO-EC injected group responded to rPO-EC (non-folded), while no response was detected in any other animal (Figure 10, C). However, 2/3 animals (A0, A2) from the rPO-EC injected group were able to proliferate in response to refolded rPO-EC (Figure 10, D).

A summary chart represented average proliferative responses of the 3 animals from each group (Figure 10, E). It was clear that while CD4+ T cells were unable to respond to PO-peptide 180-199, they were able to respond in a limited fashion to non-folded rPO-EC. CD4+ T cells were able to respond to refolded rPO-EC with an approximately 2-fold greater efficiency than to the non-folded; however, the standard deviation observed was large, since 1 animal failed to respond.

As a positive control for proliferation, cells were incubated with cross-linking anti-rat CD3 mAb to give an estimation of total proliferation possible by the T cells. All populations were capable of a proliferative response (data not shown).

Day 39

Background proliferation was minimal (Figure 11, A). No proliferation in response to PO peptide 180-199 (Figure 11, B), to non-folded rPO-EC (Figure 11, C), or refolded rPO-EC (Figure 11, D) was detected. A summary chart (Figure 11, E) represented an average of the 3 animals from each group. It was clear that CD4+ T cells were unable to respond to any of the antigens tested.

As a positive control for proliferation, cells were incubated with cross-linking anti-rat CD3 mAb to give an estimation of total proliferation possible by the T cells. All populations responded (data not shown).

3.6.5.3 Analysis of B cell response

Conventional ELISA

As a positive control for this ELISA, monoclonal anti-PO antibody was titrated against 10µg/ml coating concentration of refolded rPO-EC domain. Results confirmed that this antibody was capable of recognising rPO-EC domain down to approximately 70ng (corresponding to an optical density reading of 1), underlining the sensitivity of the assay (Figure 12, panel A). However, when sera from rPO-EC domain-injected rats were compared to adjuvant only-injected rats, no specific response above background levels was detected (Figure 12, panel B).

Capture ELISA

Although no positive control antibody was available for this assay format, preliminary results suggested no specific antibody response against 'captured' rPO-EC domain (Figure 12, C).

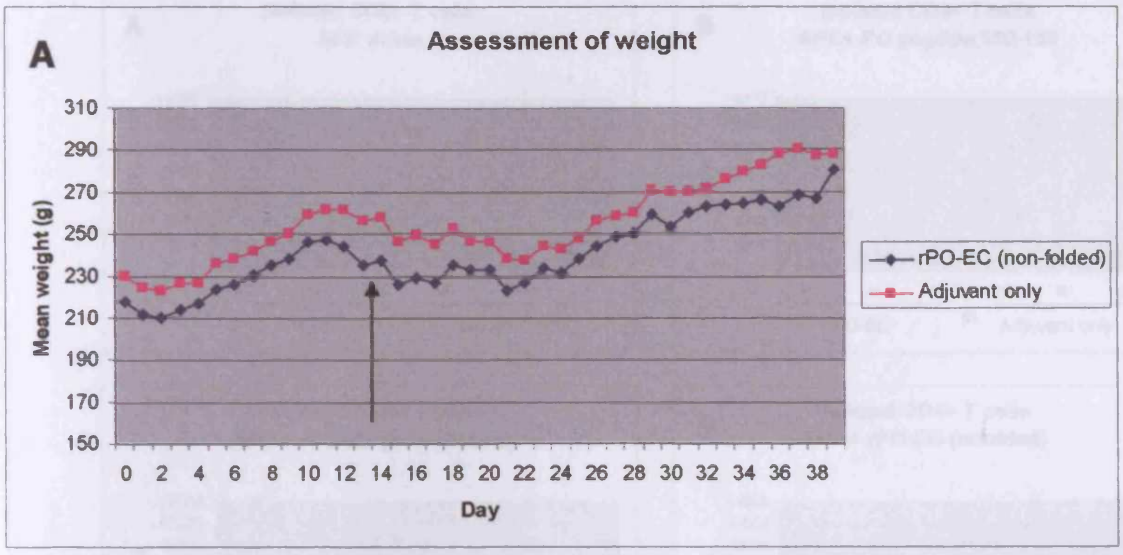

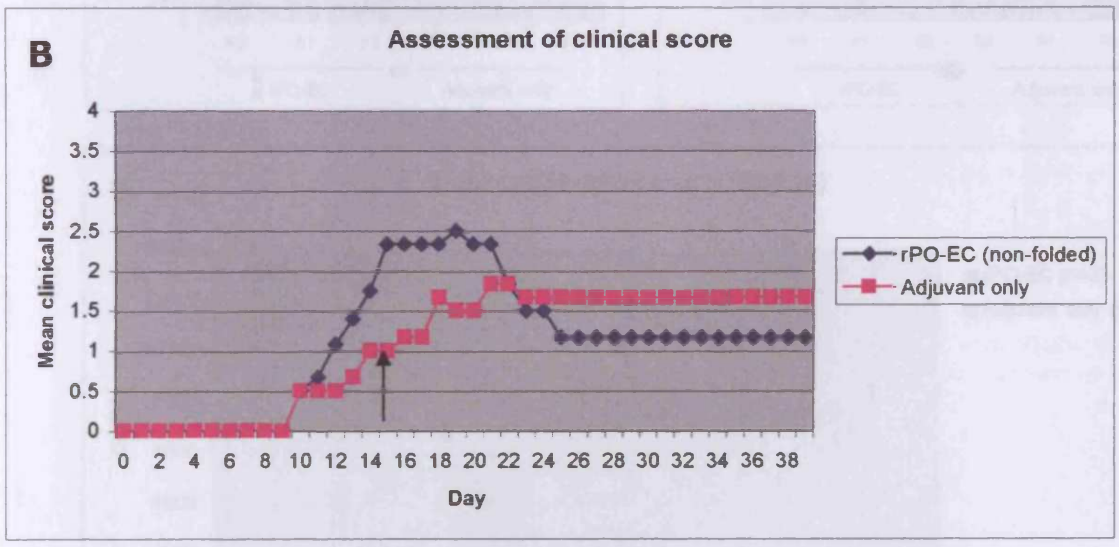

Figure 9

Assessment of weight and clinical score in rPO-EC versus adjuvant only Lewis rats

Following immunisation at day 0 with either rPo-EC domain (blue line) or adjuvant only (pink line), animals were assessed daily for changes in weight (panel A), and their clinical score (panel B).

Arrows indicate time point (day 14) where 3 animals from each group were sacrificed by a Schedule 1 method for a T cell proliferation assay, and determination of specific antibody titre. Sacrificed animals were not included in calculations of mean weight and clinical score after this time point.

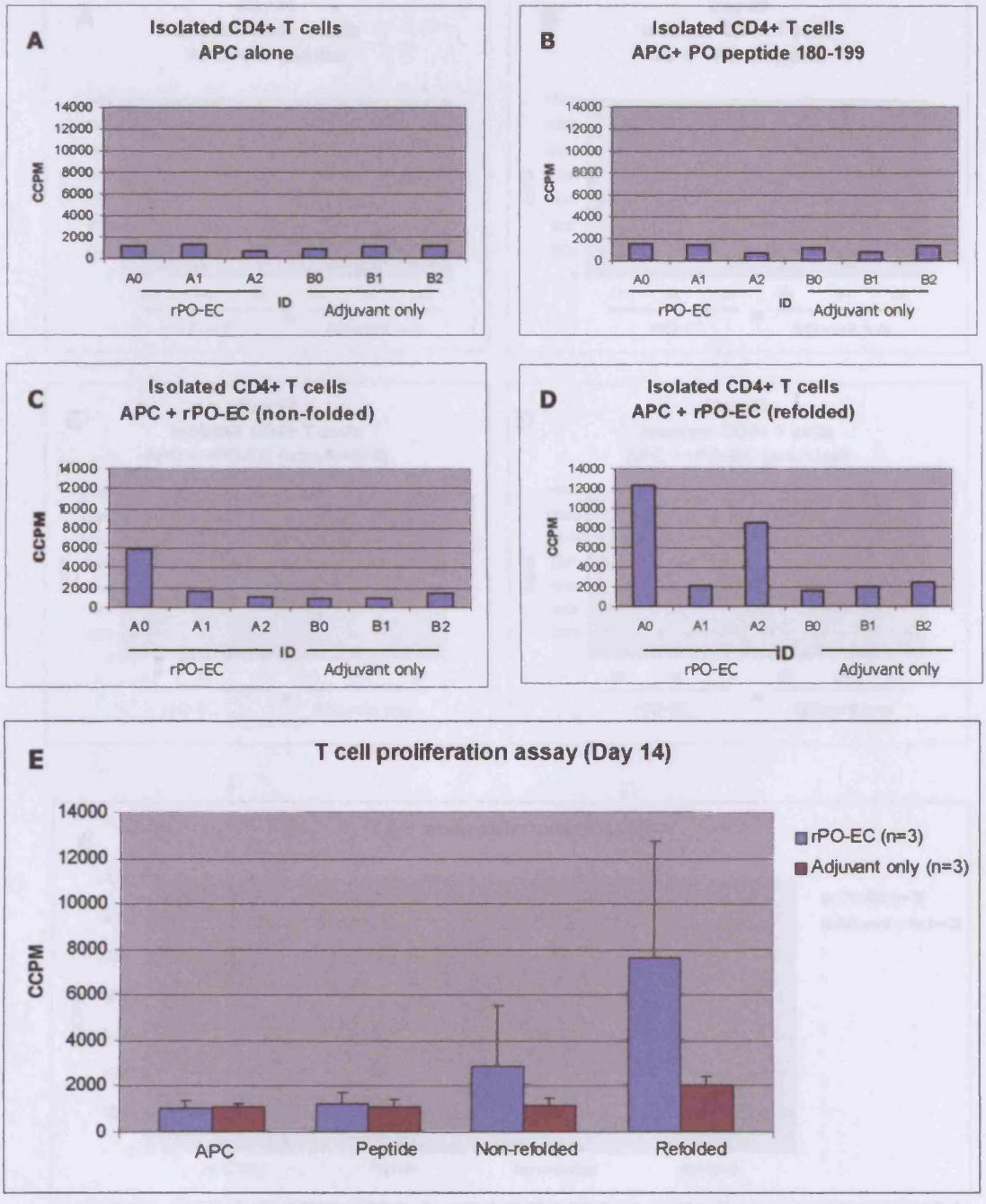

Figure 10 Day 14 CD4+ T cell proliferation assay results

Rats were injected with either rPO-EC or adjuvant only on Day 0. Three animals from each group were sacrificed on day 14, and CD4+ T cells were isolated, and subjected to proliferation assay as described. CD4+ T cells were analysed for proliferative response to various PO-derived antigens using APC alone (A), PO peptide 180-199 (B), rPO-EC (non-folded, C) and rPO-EC (refolded, D). Bars represent individual animals from the 2 groups. A summary of the data was presented in E. Bars represented an average of the 3 animals from each group. Error bars showed standard deviation.

As a positive control for proliferation, cells were incubated with cross-linking anti-rat CD3 mAb to give an estimation of total proliferation possible by the T cells. All populations were able to respond (data not shown).

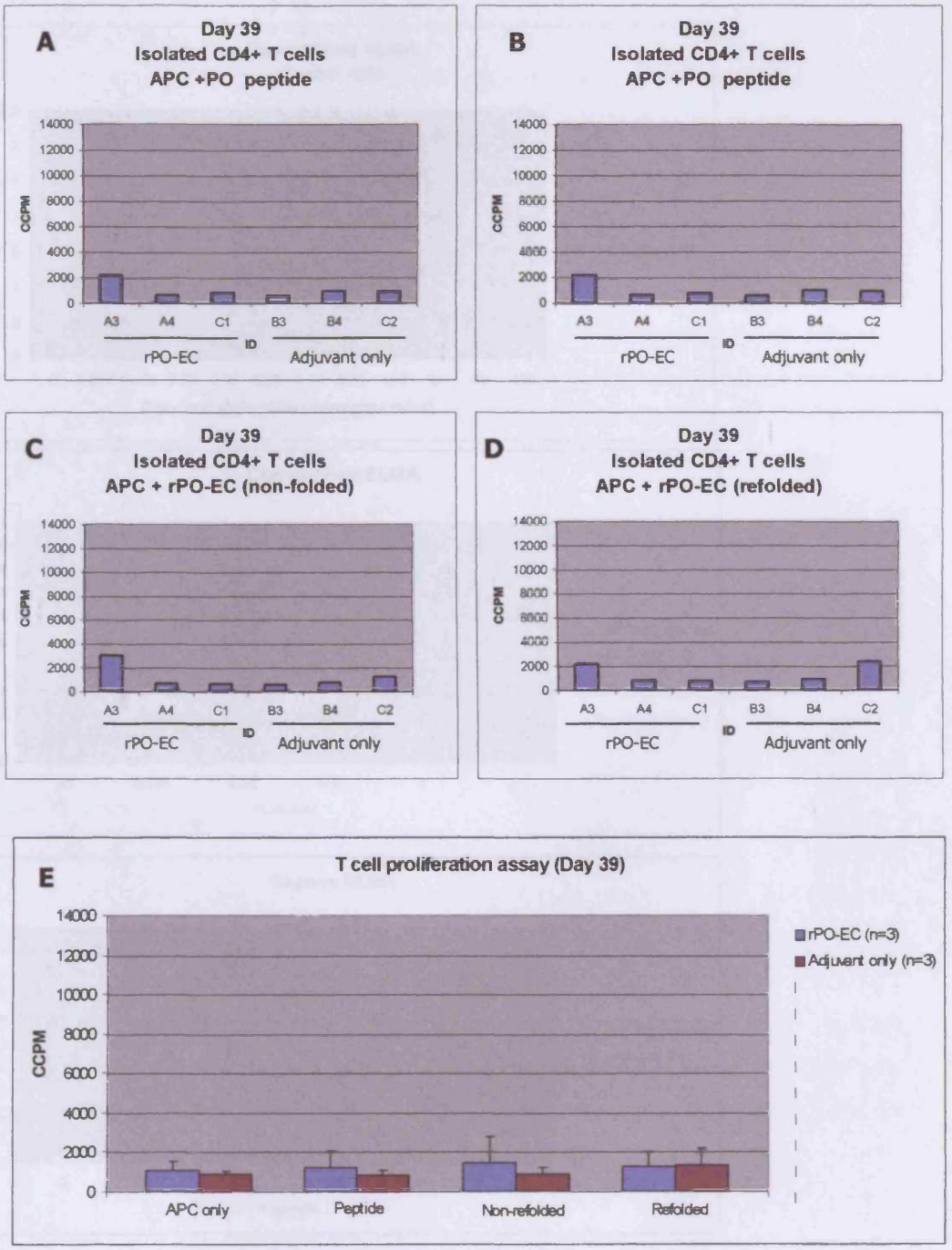

Figure 11 Day 39 CD4+ T cell proliferation assay results

Rats were injected with either rPO-EC or adjuvant only on Day 0. Three remaining animals from each group were sacrificed on day 39, and CD4+ T cells were isolated, and subjected to proliferation assay as described. CD4+ T cells were analysed for proliferative response to various PO-derived antigens using APC alone (A), PO peptide 180-199 (B), rPO-EC (non-folded, C) and rPO-EC (refolded, D). Bars represent individual animals from the 2 groups.

A summary of the data is presented in E. Bars represent an average of the 3 animals from each group. Error bars show standard deviation for each group.

As a positive control for proliferation, cells were incubated with cross-linking anti-rat CD3 mAb to give an estimation of total proliferation possible by the T cells. All populations were able to respond (data not shown).

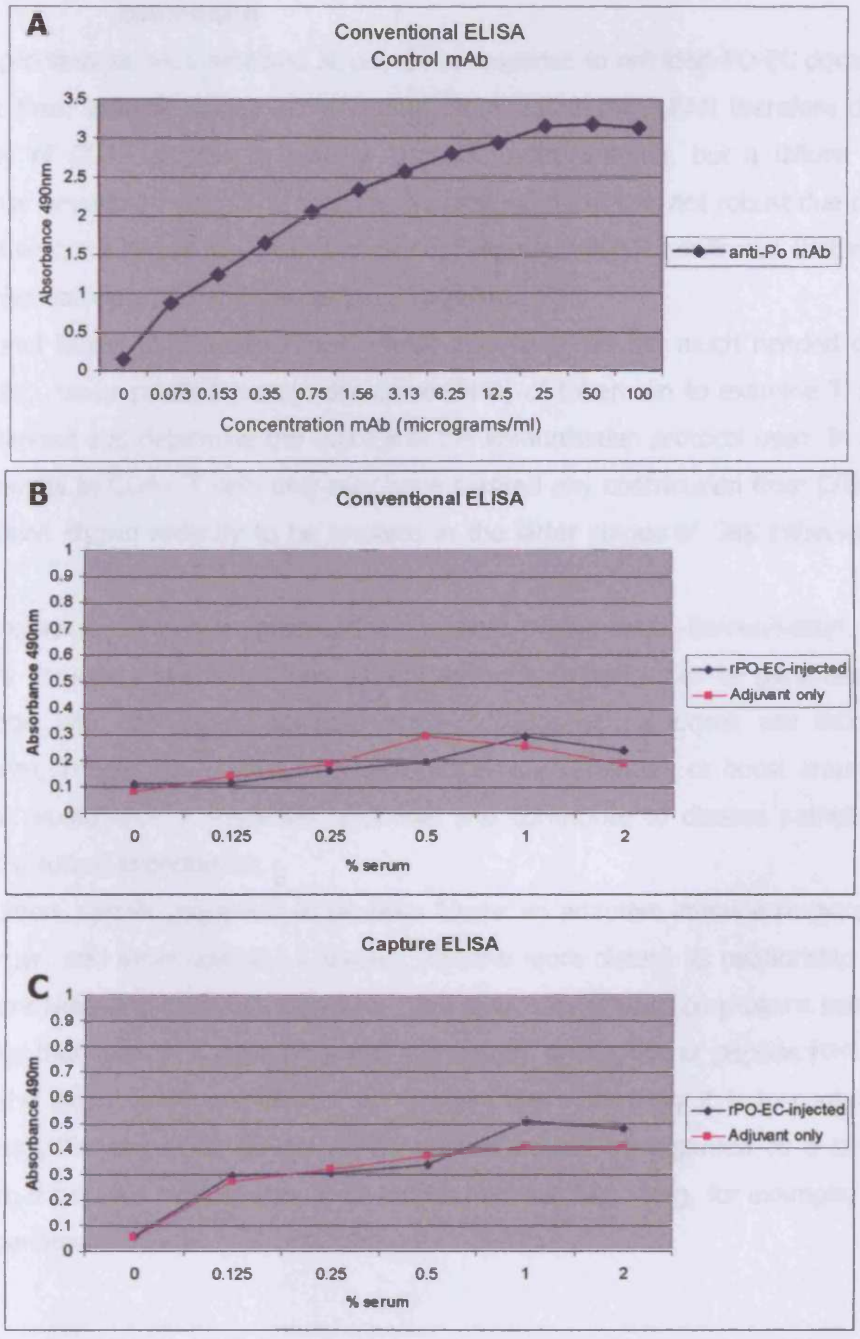

Figure 12

Conventional and Capture ELISAs to detect anti-PO antibodies following injection of rPO-EC domain

Conventional ELISA

As a positive control for this ELISA, monoclonal anti-PO antibody was titrated against 10µg/ml coating concentration of refolded rPO-EC (A). Sera from rPO-EC-injected animals were tested against sera from adjuvant only animals for reactivity against refolded rPO-EC (B).

Capture ELISA

Sera from rPO-EC-injected animals were tested against sera from adjuvant only animals for reactivity against refolded rPO-EC (C). No positive control antibody was available for this assay

3.6.6 Discussion

T cell proliferation was detected at day 14 in response to refolded PO-EC domain, but this was absent from animals at day 39. The difficulty in establishing EAN therefore did not lie in the inability of CD4+ T cells to initially respond to the antigen, but a failure to maintain the response beyond 14 days. The data for the capture ELISA was not robust due to the absence of a positive control, but the results of the conventional ELISA confirmed that no specific B cell response was detected at either of the time points.

Additional facets to this experiment would also have yielded much needed control data. For example, use of purified protein derivative (PPD) of tuberculin to examine T cell responses to the adjuvant and determine the success of the immunisation protocol used. In addition, limiting the analysis to CD4+ T cells only may have masked any contribution from CD8+ T cells, which have been shown recently to be involved in the latter stages of GBS (Wanschitz, Maier et al. 2003).

Immunological memory is produced as a result of the initial immunisation, which evokes a primary immune response. A more potent antibody response can be generated by subsequent challenge with the same antigen, where subsequent responses are increasingly intense (Janeway, Travers et al. 2001). Perhaps further immunisation, or boost around day 7-10 with antigen would elicit a sustained response, and contribute to disease pathology. This will be tested in future experiments.

In addition, certain properties of proteins favour an adaptive immune response. For example, the larger, and more complex a protein, and the more distant its relationship to self-antigens, the more likely it is to elicit a response. Such responses depend on proteins being degraded into peptides that bind MHC molecules, and subsequent recognition of peptide:MHC complexes by T cells; the larger and more distinct the protein, the more likely it is to contain such peptides (Janeway, Travers et al. 2001). PO-EC domain cannot be regarded as a large and complex protein; thus, EAN may be able to be induced successfully using, for example, peripheral nerve homogenates.

3.7 Induction of EAN using sheep sciatic nerve homogenate (SSNH)

3.7.1 Aim

Studies of the induction of EAN using isolated PNS proteins are limited in comparison to the volume of literature using bovine peripheral myelin, as stated in the introduction to this chapter. Due to the inaccessibility of bovine nervous tissue, alternatives were sought. Studies involving porcine (Koh, Nakano et al. 1984) and horse sciatic nerve homogenate-induction of EAN (Moon and Shin 2004) were limited, but remained an option. However, sheep sciatic nerve was in plentiful supply in Wales, and the possibility of it inducing EAN was examined.

3.7.2 Induction protocol

Six male Lewis rats (210-240g) were obtained from Charles River Laboratories and allowed to acclimatise for 1 week. On day 0 and 7, animals received a dose of SSNH in saline emulsified in FIA containing 2mg/animal *M. tuberculosis* in a total volume of 200µl, into the hind footpads, as shown in Table 7. All animals were immunised under inhalational anaesthesia. Animals were assessed in terms of their weight and clinical score as described previously.

Group	Antigen
A (n=2)	22.3mg SSNH
B (n-2)	10mg SSNH
C (n=2)	5mg SSNH

Table 7 Group identification and dose of SSNH

3.7.3 Results

3.7.3.1 Assessment of weight and clinical score

Following a small loss of weight 24 hours after the injection, animals continued to increase their weight regardless of dose of SSNH received (Figure 13, A).

No significant clinical symptoms were observed in any of the groups immunised (Figure 13, B).

No histological analysis was performed.

3.7.3.3 Discussion

SSNH failed to induce EAN in the Lewis rat. Early studies using purified PNS myelin from guinea pig, frog, rat, rabbit, cow and human in FCA to induce EAN in the Lewis rat found that rat, rabbit, cow and human PNS myelin was capable of eliciting clinical symptoms characteristic of EAN; frog PNS myelin failed to induce any clinical symptoms, while guinea pig PNS myelin caused superimposed symptoms of EAN and EAE (Smith, Forno et al. 1979). Therefore it would seem that induction of EAN is dependent on the species of the host animal and the source of antigen. To this end, rat sciatic nerve homogenate was used as a potential antigen to induce EAN in the Lewis rat in the next experiment.

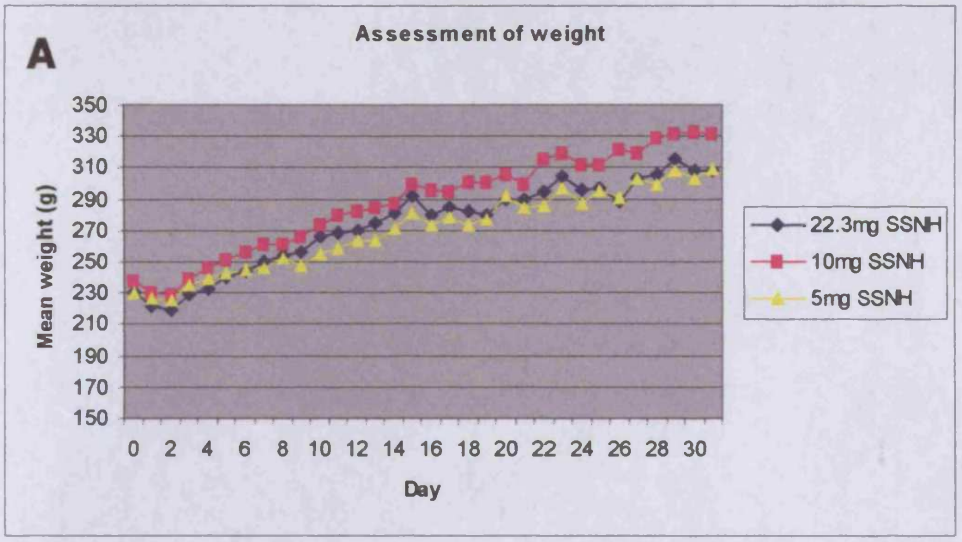

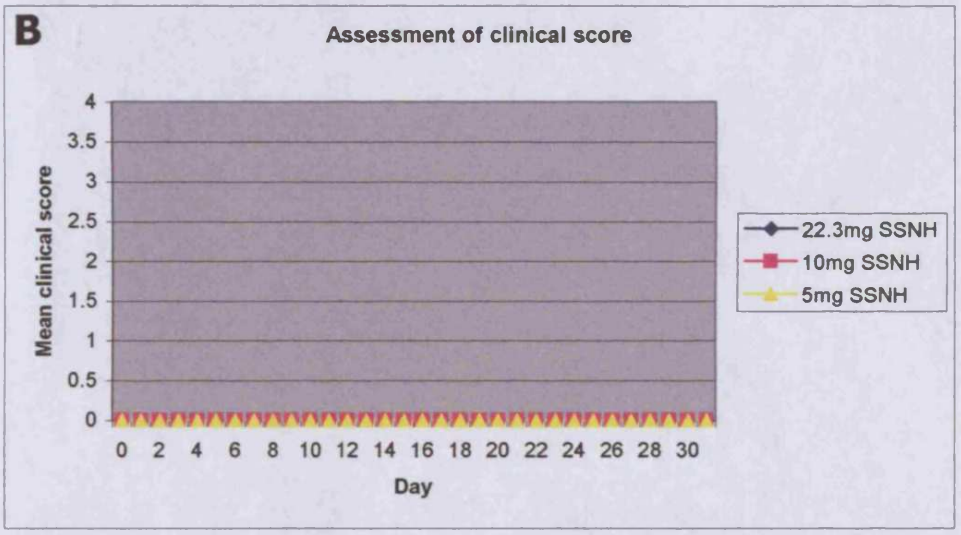

Figure 13

Assessment of weight and clinical score in SSNH-injected Lewis rats

Animals were injected with a dose response of SSNH (n=2 per dose) in saline emulsified in FIA containing 2mg/animal *M. tuberculosis* at day 0, and monitored in terms of weight (A) and clinical score (B) for 31 days.

3.8 Induction of EAN using rat sciatic nerve homogenate (RSNH) in the Lewis rat

3.8.1 RSNH preparation

Rats (30) were sacrificed by a Schedule 1 method, and sciatic nerves were harvested, and frozen on dry ice. Homogenates were prepared using a glass homogeniser in a minimal volume (5-10ml) of distilled water. Following generation of an emulsion, the sample was freeze-dried overnight, and the dry weight obtained.

For immunisation, a weight of powder was resuspended in a suitable volume of 0.9% (v/v) saline, and mixed with FCA in a Hamilton syringe

3.8.2 Induction protocol

Six wild type Lewis rats (160-210g) were obtained from Charles River Laboratories, and allowed to acclimatise for 1 week prior to disease induction. On day O, each animal received 20mg of RSNH, resuspended in 100µl sterile saline, and emulsified with 100µl of FIA containing 10mg/ml *M. tuberculosis* in a Hamilton syringe to form a stable emulsion. The emulsion was placed at 4^0C for 1 hour, and subsequently used for immunisation. All animals were immunised sub-cutaneously into the base of the tail, and under inhalational anaesthesia.

Animals were assessed daily in terms of their weight, and clinical score as described previously.

3.8.3 Results

3.8.3.1 Assessment of weight and clinical score

There was no change in weight throughout the course of the experiment (Figure 14, A) when all animals were taken together and values averaged (n=6) with the exception of a minor decrease seen at day 11-12. No specific clinical symptoms were evident when all animals were taken together (n=6), apart from mild disease after day 13 (Figure 14, B). However, 1/6 animals (animal A0) demonstrated a decrease in weight between day 11-14 compared with a representative animal (animal A1) (Figure 14, C). Clinical symptoms were observed in parallel with the loss in weight from day 13 onwards, with a maximum clinical score of 3 observed at day 15-16 p.i. (Figure 14, D). Animal A0 was sacrificed at day 17, together with a healthy animal A1.

Sciatic nerves were harvested from freshly perfused rats A0 and A1, and subjected to EM to detect any subtle changes in myelin morphology and to detect the presence of perivenular inflammation and macrophage-associated demyelination. Spinal cords were also removed for paraffin-wax embedding, and subsequent H&E staining (as described previously) to assess inflammatory cell infiltration.

All animals

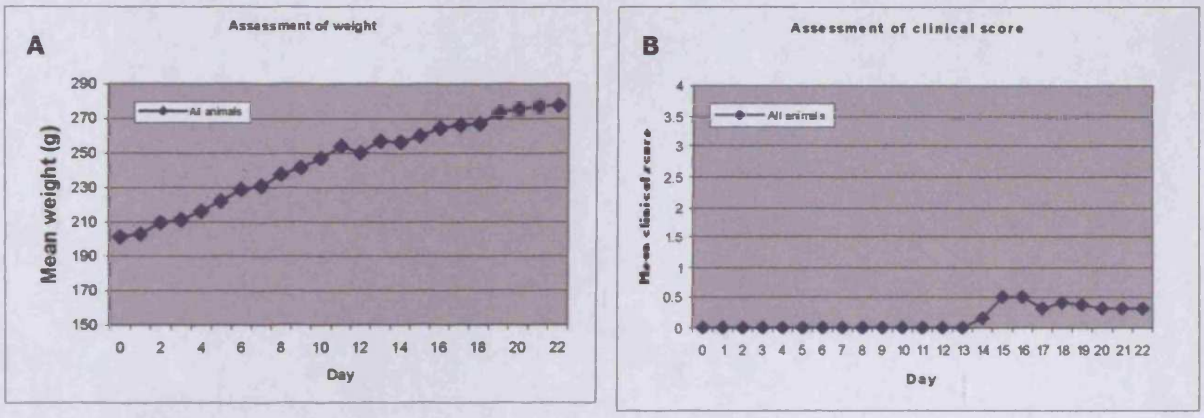

Animal 0 versus Animal 1

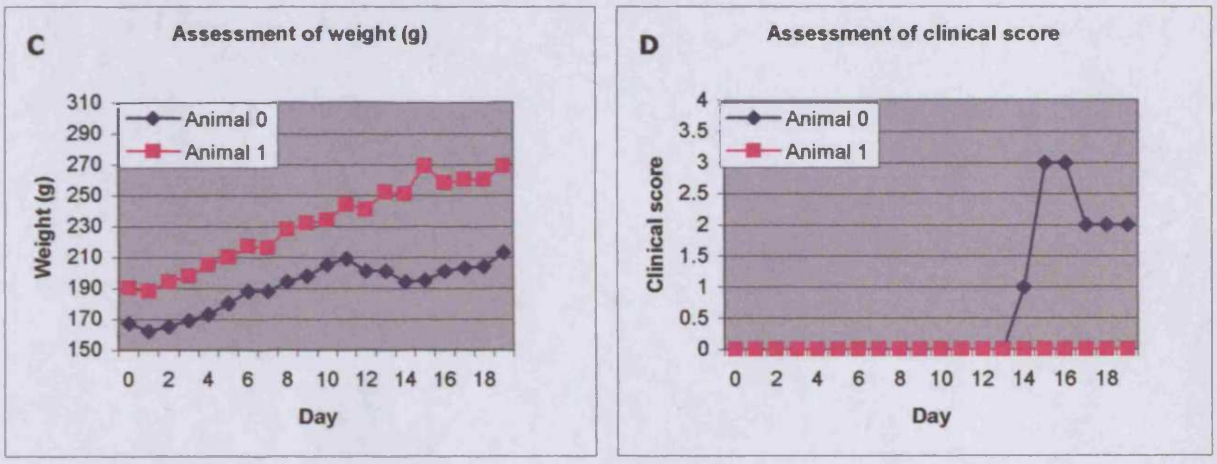

Figure 14

Induction of EAN using RSNH resulted in clinical disease in 1/6 animals

Six animals were injected sub-cutaneously at the base of the tail with 20mg RSNH on Day 0, and assessed daily in terms of weight and clinical score. Values for weight (A) and clinical score (B) were averaged for the 6 animals.

Animal 0 was the only animal to display any loss of weight (C) and clinical symptoms (D), and was compared separately to a healthy animal from the same experiment.

3.8.3.2 EM

3.8.3.2.1 Toluidine blue staining

Following semi-thin sectioning of processed sciatic nerve, sections were stained with toluidine blue to determine areas for subsequent analysis by EM. In addition, it was possible to detect any macro-changes in myelin architecture and evidence of inflammatory cells using light microscopy. Images were taken using a light microscope at 100X and 200X magnification of both clinically affected animal A0 (Figure 15, A and B), and healthy animal A1 (Figure 15, C and D). There was no evidence of myelin disruption (LFB) or inflammatory cell infiltrate (H&E) in the sciatic nerve of either animal (data not shown).

3.8.3.2.2 Electron microscopy

Following ultra-thin sectioning of processed sciatic nerve, sections were mounted onto nickel grids, and stained as described. No disruption of myelin architecture or inflammatory cells was evident in the sections from either clinically affected (Figure 16a) or healthy animals (Figure 16b).

Low power images of groups of axons were examined for disruption of myelin architecture (images A in both animals), while higher power images of myelinated versus non-myelinated axons were examined for clinically affected animal A0 (16a, panel B). Schwann cells surrounding axons were examined in both animals (images C in both animals), as well as blood vessels for evidence of migration of inflammatory cells (images D in both animals).

3.8.3.2.3 H&E staining of paraffin wax embedded spinal cord

Spinal cords were harvested following perfusion of animal A0 and control animal A1, and embedded in paraffin wax. Sections were stained by H&E to evaluate inflammatory cell infiltrates.

Within the low power images of spinal cord from clinically affected animal A0 (Figure 17, A, 50X, B, 100X), the white (WM) and grey matter (GM) were visible as well as the peripheral nerve root (PNR). Cellular infiltrates were evident in animal 0 within the white matter of the spinal cord, probably in the vicinity of the vasculature (arrows, A, B, C). Analysis of the PNR of the same animal revealed no pathology (Figure 17, A, B). However, this pathology was isolated, and was not representative of the entire section.

Analysis of spinal cord from healthy animal A1 revealed no cellular inflammation within either the spinal cord or the PNR (Figure 17, D, 50X; E, 100X).

3.8.4 Discussion

RSNH appeared to induce disease in Lewis rats, but at a very low frequency (1/6 animals). However, the histological analysis revealed that sciatic nerves remained unaffected, whilst minor inflammation was evident in the CNS.

Clinically affected animal A0 began the experiment weighing 167g, while the combined average of the remaining 5 animals totalled 208g.

The possibility that disease was dose-dependent existed, and the experiment was repeated in an effort to enhance reproducibility with lighter animals of approximately 160g in weight prior to induction. Six male Lewis rats with a combined average weight of 158g were obtained from Charles River, and subjected to the same immunisation protocol as for this experiment. No disease was seen (data not shown)

It remains a possibility that clinically-affected animal A0 was the runt of the particular litter, and as such, had some immunological dysfunction, which lead to the onset of neurological disease.

In conclusion, RSNH failed to consistently induce EAN in the Lewis rat.

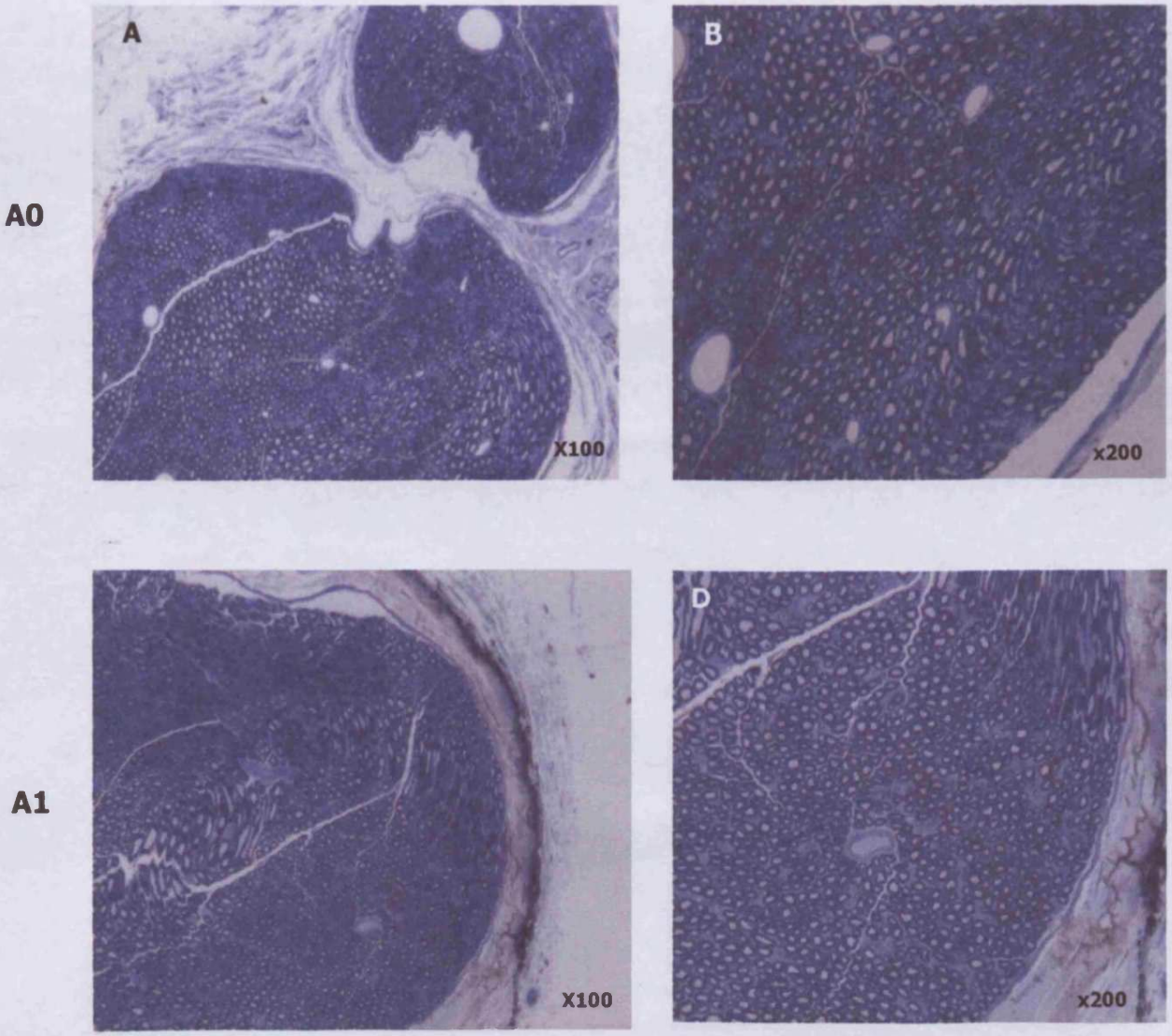

Figure 15

Toluidine blue staining of semi-thin sections of sciatic nerve from a clinically affected (A0) versus a healthy animal (A1)

Following processing of tissue as described, semi-thin sections (0.5µm) were cut, and stained with toluidine blue to determine areas of tissue for further analysis by EM.

Sections were analysed by light microscopy, and photographs were taken at 100X (A, C) and 200X B, D) magnification for each animal.

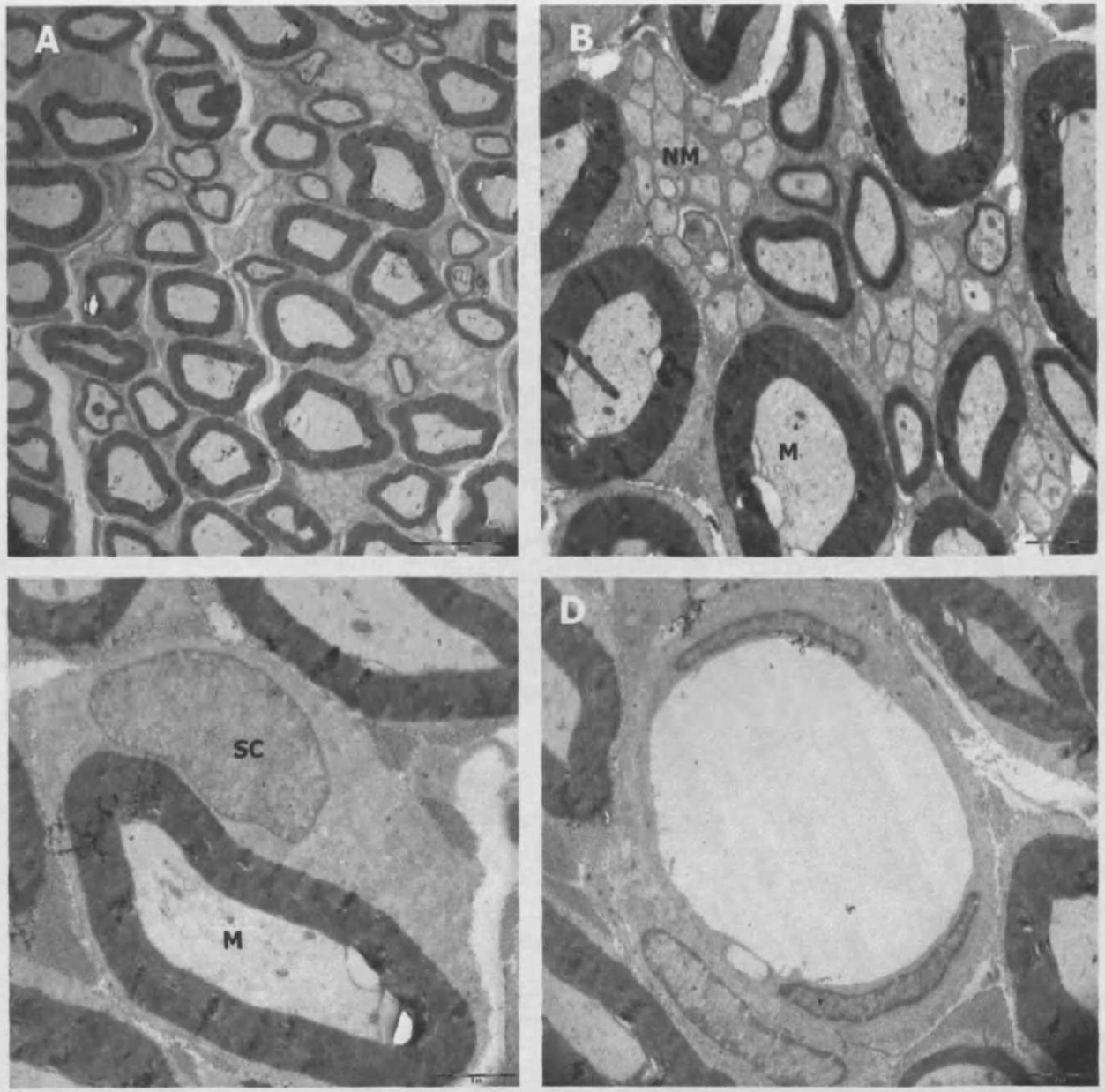

Figure 16a

Electron microscopy images of sciatic nerve sections from clinically affected animal A0

Ultra-thin sections of processed sciatic nerve were cut, mounted onto nickel grids and stained as described.

Grids were analysed on a Philips CM12 electron microscope, and images were captured using SIS MegaView III software.

No evidence of myelin disruption or inflammatory cell infiltration was present. Images captured include low power images showing groups of individual axons (A, scale bar = 10µm), higher power images showing a nerve bundle containing myelinated (M) and non-myelinated axons (NM) (B, scale bar = 2µm), a Schwann cell (SC) surrounding a myelinated axon (C, scale bar = 2µm) and a blood vessel surrounded by endothelial cells (EC) (D, scale bar = 2µm).

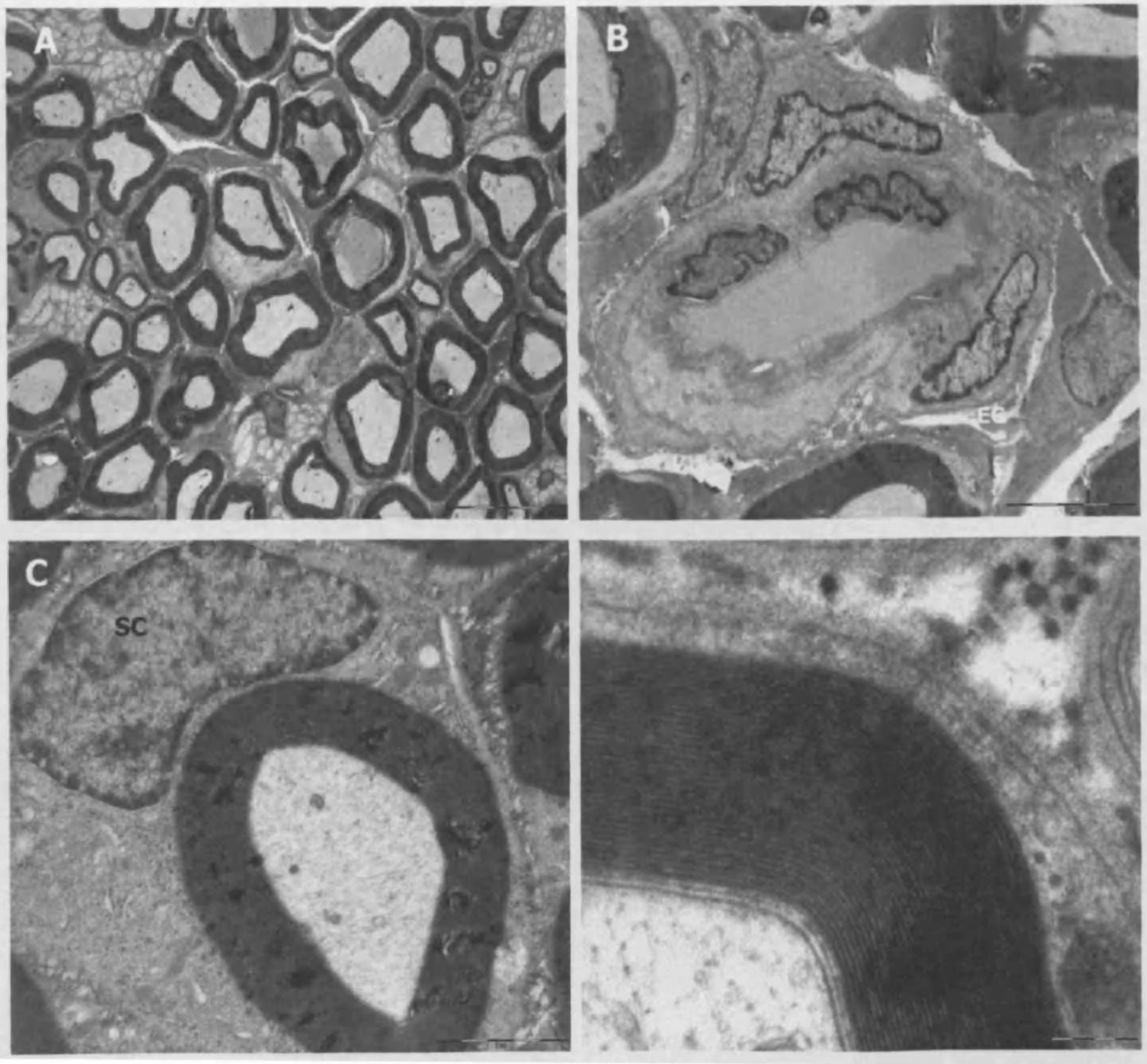

Figure 16b

Electron microscopy images of sciatic nerve sections from healthy animal A1

Ultra-thin sections of processed sciatic nerve were cut, mounted onto nickel grids and stained as described.

Grids were analysed on a Philips CM12 electron microscope, and images were captured using SIS MegaView III software. No evidence of myelin disruption or inflammatory cell infiltration was present. Images captured include a low power images showing groups of individual axons (A, scale bar = 10µm), a blood vessel surrounded by endothelial cells (EC) (B, scale bar = 5µm), a Schwann cell (SC) surrounding a myelinated axon (C, scale bar = 2µm), and a high power image capturing the individual layers of myelin surrounding an axon (D, scale bar = 200nm).

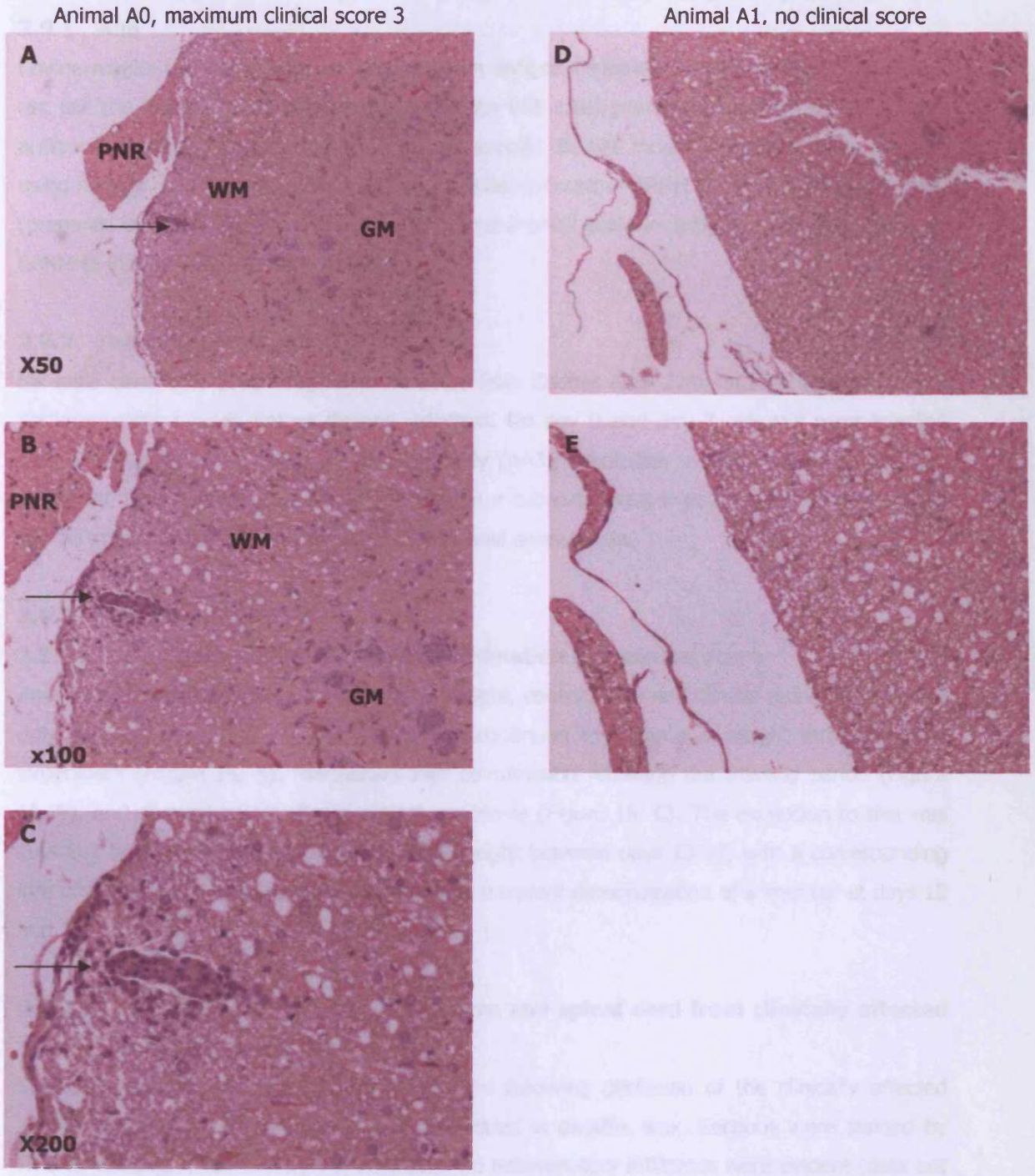

Figure 17

H&E staining of spinal cord sections from clinically affected animal A0 versus healthy animal A1

Spinal cords were harvested following perfusion of animal A0 and control animal A1, and embedded in paraffin wax. Sections were stained by H&E to evaluate inflammatory cell infiltrates.

Low power images of spinal cord sections (TS) from animal A0 showed the grey (GM) and white matter (WM) within the spinal cord and peripheral nerve roots (PNR) (A, B). A focussed inflammatory infiltrate within the white matter of the spinal cord was evident (arrow, A, B, C). The PNR of the same animal appeared healthy (A, B).

A parallel analysis was performed on healthy animal A1 (D, E, F).

3.9 Induction of EAN using bovine peripheral nerve myelin (BPNM) in Lewis rats

3.9.1 Aim

Bovine myelin has been long established as an antigen capable of inducing EAN in the Lewis rat, but the inaccessibility of tissue following the BSE crisis prompted a search for alternative antigens. As described earlier in this chapter, specific disease induction has not been possible using a range of other antigens. However, a limited amount of BPNM became available recently (prepared by Sarah Piddlesden, *circa* 1988), and a small scale investigation into the ability of BPNM to induce EAN was performed.

3.9.2 Induction protocol

Six male Lewis rats (180-200g) were obtained from Charles River Laboratories, and allowed to acclimatise for 1 week before disease induction. On day 0 and day 7, animals were injected with a 125µg of BPNM (n=3) or adjuvant only (n=3), emulsified in FIA containing 2mg per animal *M. tuberculosis* in a Hamilton syringe, in a sub-cutaneous injection into the base of the tail. All animals were immunised under inhalational anaesthesia.

3.9.3 Results

3.9.3.1 Assessment of weight, coordination and clinical score

Animals were assessed daily for changes in weight, coordination and clinical score. All adjuvant only animals, and 2/3 BPNM-injected animals continued to increase in weight throughout the experiment (Figure 18, A), maintained their coordination following the training period (Figure 18, B), and showed no significant clinical symptoms (Figure 18, C). The exception to this was animal 1 from BPNM group. This animal lost weight between days 13-17, with a corresponding loss of coordination between days 14-17, and a transient demonstration of a limp tail at days 15 and 16.

3.9.3.1 H&E staining of sciatic nerve and spinal cord from clinically affected animal BPNM 1

Sciatic nerves and spinal cords were harvested following perfusion of the clinically affected animal, and a non-affected animal, and embedded in paraffin wax. Sections were stained by H&E to evaluate inflammatory cell infiltrates. No inflammatory infiltrates were evident (data not shown).

3.9.4 Discussion

This preparation of BPNM was not able to induce reproducible disease in association with pathological changes in the peripheral nerves or the spinal cord. This may have been as a result of insufficient concentrations of myelin for induction. The state of the preparation was also unknown, since it had been stored at -20^{0}C since 1988.

Following this result, bovine cauda equina was obtained from Dr. Ian Gray (Dept. of Neuroimmunology, King's College, London). Bovine myelin was prepared as in Chapter 3,

Section 2.2.13.2. Lewis rats were injected with 2, 4 and 8mg of bovine myelin in FCA s/c at day 0, and assessed daily in terms of weight and clinical score. All animals remained healthy for the duration of the experiment.

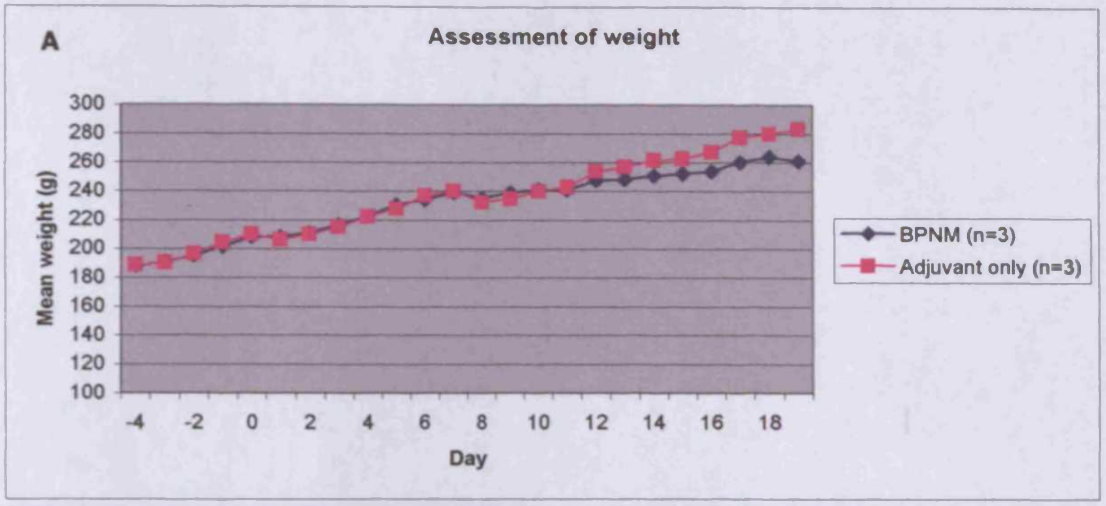

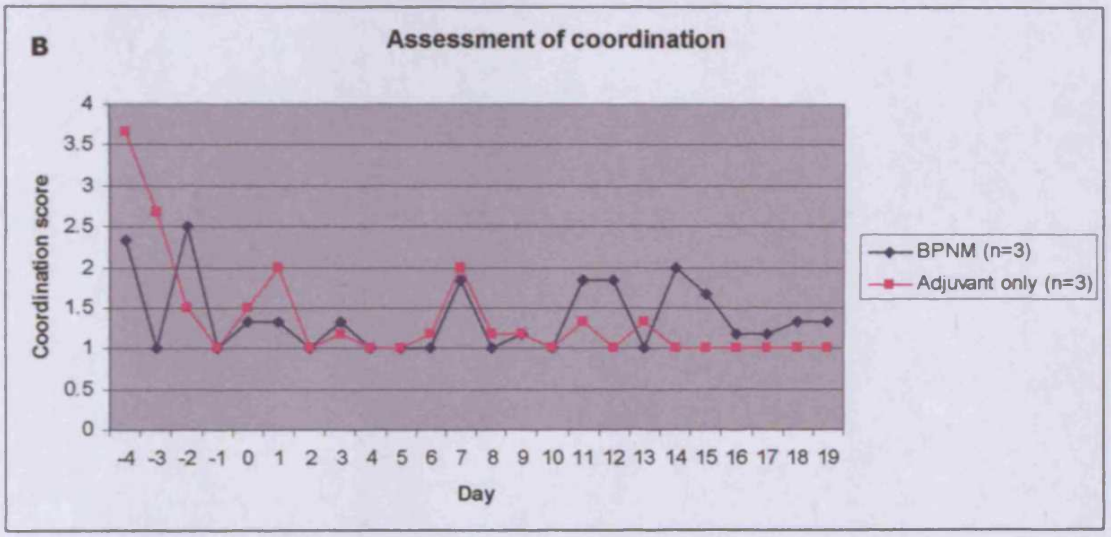

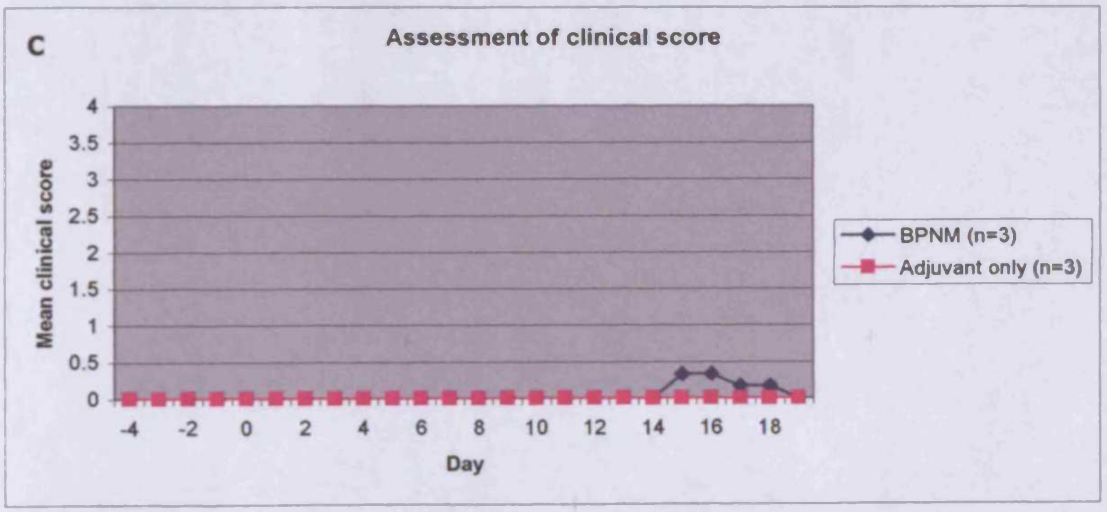

Figure 18

Assessment of weight, coordination and clinical score in BPNM–injected rats versus adjuvant only

Animals were injected on day 0 and day 7 with 125µg of BPNM in FCA as described. Animals were assessed daily for changes in weight (A), coordination (B), and clinical score (C) as described previously.

4 Summary and Discussion

A variety of different protocols have been used to date to optimise EAN induction in the rat, of which a summary is given in Table 8. No severe and reproducible disease has been able to be induced regardless of strain of rat, antigen used or site of injection.

Exp't	Strain	No. animals	Starting weight range (g)	Antigen	Site of injection	Outcome
3.1	PVG	11	120-200	PO peptide 180-199	Footpad versus base of tail	Unanticipated onset of inflammatory disease at site on injection in footpad-injected rats No pathology Adjuvant disease?
3.2	PVG	16	200-240	rPO-EC domain (refolded)	Footpad versus base of tail	Inflammatory disease at site of injection on footpad-injected rats Massive inflammatory cell infiltration at sites distinct from sciatic nerve irrespective of injection site
3.4	Lewis	6	160-200	PO peptide 180-199-amide	Base of tail	No disease
3.5	Lewis	10	160-300	rPO-EC domain (non-refolded; washed versus non-washed)	Footpad	Inflammatory infiltrates observed in rats injected with non-washed rPO-EC domain
3.6	Lewis	14	180-200	rPO-EC domain (non-refolded, washed)	Footpad	T and B cell responses examined; CD4+ T cells showed some response at day 14 but no response at day 39. No B cell response
3.7	Lewis	6	210-240	SSNH	Base of tail	No disease
3.8	Lewis	6	160-210	RSNH	Base of tail	1/6 rats demonstrated severe, but transient disease; runt of litter (probably as result of immunological dysfunction) No pathology
3.9	Lewis	6	180-200	BPNM	Base of tail	1/6 rats demonstrated transient limp tail No pathology

Table 8

Summary of approaches used to date in the induction of EAN in the rat

At this point, the reason for the failure of even the bovine myelin to induce EAN, since this is a well established protocol for disease induction was unknown. Initially, operator error seemed a likely explanation. However, upon discussion with Ian Gray (above), it appeared that the group were also experiencing difficulties in disease induction where previously, they had successfully

induced disease using a variety of antigens. It is their hypothesis that British Lewis rats have been bred for more general characteristics at the expense of their demyelinating properties. Lewis rats sourced from Germany or Italy are still susceptible to disease induction according to Dr. Gray, and tests are being performed in their laboratory on the different Lewis rats in a bid to obtain a working model of EAN (Ian Gray, personal communication, October 2005). If the British rats have indeed lost their susceptibility to peripheral demyelination, it would have a profound effect on the conclusions drawn to date from this chapter, and the work should be repeated. Until this matter is resolved, no conclusion regarding the ability of PO peptides, PO-EC, various homogenates, and bovine peripheral myelin to induce disease can be drawn.

Such resistance has previously been reported in Lewis rats with respect to EAE induction (Driscoll, Kies et al. 1985). Although sensitisation of these EAE-resistant Lewis (Le-R) rats with MBP induced cells capable of mounting a proliferative response to MBP in culture, such cells were incapable of transferring EAE to a naïve recipient. This genetic defect was demonstrated not to be linked to the RT1.B region of the MHC, and could be overcome by simultaneous transfer of LPS-activated antigen-nonspecific spleen cells.

Chapter 4

Part 2

The Mouse as a target species for acute Experimental Autoimmune Neuritis (EAN)

1 Introduction

A great advantage of establishing EAN in the mouse is the wide range of genetically engineered mutants that can be tested for susceptibility to disease. Efforts to establish a reproducible autoimmune neuritis in the mouse have either failed or have resulted in mild disease with poor reproducibility. The first studies involving active immunisation of mice was reported in 1985, in the SJL mouse, by immunisation with bovine myelin or bovine-derived P2 (Taylor and Hughes 1985). Of Balb/c, CBA, C57Bl/6 and SJL strains tested, the SJL mouse was the only strain found to develop a mild neurological deficit and histological lesions characteristic of EAN. Further studies using this model revealed that the SJL mouse suffered sub-clinical damage to the peripheral nerve myelin in association with electrophysiological dysfunction (Dieperink, O'Neill et al. 1991). More recently, this model has been used in combination with pertussis toxin (PT) to produce a more severe clinical disease, revealing severe demyelination, remyelination and obvious signs of inflammatory infiltration (Calida, Kremlev et al. 2000).

The majority of genetically engineered mice are backcrossed onto a C57Bl/6 background, thus development of EAN in this strain would offer an obvious advantage over the model previously described.

The first report of disease induction in this strain was in 1999. C57Bl/6 mice received bovine peripheral nerve myelin (BPNM)-primed lymph node cells, which were stimulated *in vitro* with P2 protein peptide 57-81. These mice were further challenged with BPNM in FCA together with PT, and developed EAN-specific clinical symptoms accompanied by extensive inflammatory infiltration and demyelination of the peripheral nerves (Zhu, Nennesmo et al. 1999).

A study by Linington and colleagues 1992 identified peptides derived from myelin protein zero (P0) as neuritogenic (Linington, Lassman et al. 1992). Zou and colleagues extended this work by demonstrating that the peptides, particularly P0 peptide 180-199, were capable of inducing EAN in the C57Bl/6 mouse, when immunised in association with PT (Zou, Ljunggren et al. 2000). However, disease incidence and severity was limited. Severity could be increased by immunisation with anti-mouse CTLA 4 antibody, known to exacerbate T cell-mediated autoimmune diseases (Zhu, Zou et al. 2001).

1.1 Chapter Aim

In our laboratory, various C deficient and knockout animals are available to enable a complete dissection of the C cascade, and assess the importance of each factor in disease initiation and progression (Figure 1). The majority of such animals are bred on a C57Bl/6 background, and as

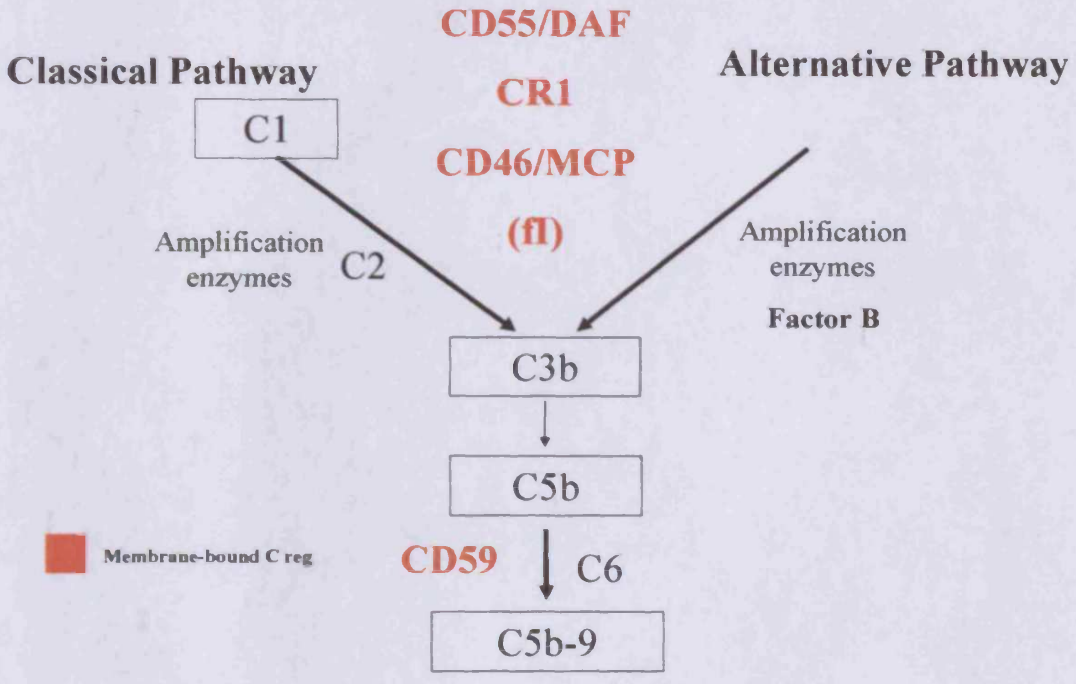

Figure 1

Summary of the C cascade demonstrating the scope of the genetically engineered mice available to evaluate the importance of each arm of the C system

Factor B/C2 -/- mice are available to assess the importance of C activation, C3-/- to realise the role of this central component, and C6 deficient mice to evaluate the terminal pathway. In addition, various C reg knockout animals are available, for example *Daf1-/-, Cd59-/-* and the *Daf1/Cd59a-/-* double knockout mice to assess the regulation of the activation and terminal pathway alone, and in combination.

a result, several approaches have been used to try to induce reproducible disease in the C57Bl/6 mouse. This is the focus of this part of the chapter.

2 Materials and methods

All chemicals unless otherwise stated were from Sigma Aldrich Chemical Company (Gillingham, UK).

2.1 Animals

All animals used were obtained from Charles River Laboratories, UK, and maintained according to Home Office guidelines within the Biomedical Services Unit (BSU), University of Wales College of Medicine, Cardiff.

2.2 Disease assessment

Animals were assessed daily for evidence of neurological dysfunction using a clinical scoring system: 0, no clinical features; 1, limp/flaccid tail; 2, ataxia; 3, hind limb weakness and wasting; 4, hind limb paralysis. Half scores were given for intermediate symptoms.

2.2 Collection and processing of tissues for immunohistochemical analysis

Refer Chapter 4 Section 2.2

3 Optimisation of EAN in the mouse

3.1 Induction of EAN in C57Bl/6 mice using PO peptide 180-199

3.1.1 Aim

PO peptide 180-199 had the potential to be used in both rats and mice and provided a suitable starting point for the optimisation of disease induction in both species.

Refer to Chapter 2, Section 2.1 for details on peptide synthesis.

3.1.2 Induction protocol

Six male C57Bl/6 mice (20-24g) were obtained from Charles River Laboratories, and allowed to acclimatise for 1 week. On the day prior to induction, mice were primed with 400ng/mouse of PT, injected intraperitoneally (IP). On Day 0, mice were injected sub-cutaneously (s/c) with various doses (50, 100 or 200µg/mouse) of PO peptide 180-199 (Severn Biotech Ltd, Kidderminster, UK) in 100µl saline emulsified 100µl with FIA containing 10mg/ml *M. tuberculosis*. Mice were further primed with 200ng/mouse PT (IP) on day 0, 1, 3 and 6, followed by a boost of peptide on Day 6.

Mice were assessed daily for changes in weight, and scored for clinical symptoms using the clinical scoring system described. Animals were sacrificed by a Schedule 1 method if clinical score reached 4 or if weight loss was greater than or equal to 20% of original body weight.

3.1.3 Results

3.1.3.1 Assessment of weight and clinical score

All animals lost weight between days 1 to 7, and again slightly between days 9-10 (Figure 2, A). No significant clinical symptoms were observed in any of the groups (Figure 2, B). No histological analysis was performed.

3.1.3.3 Discussion

PO peptide 180-199 failed to induce EAN in the C57Bl/6 mouse following the protocol of Zou and colleagues. However, some modifications of the protocol were forced; PT was given intra-peritoneally (IP) instead of intra-venously (IV) as reported due to a lack of appropriate expertise in the department.

Due to the previous resistance to disease induction seen in the C57Bl/6 mouse, it was decided to optimise EAN induction in immunologically-deficient animals such as the CD59a knockout animals (CD59a-/-) available in-house, in an attempt to provide a lower threshold for disease induction. A precedent for this exists following induction of EAE, the animal model of multiple sclerosis in CD59a-/-, where knockout animals exhibited greater disease severity, and demyelination compared to their wild type counterparts (Mead, Neal et al. 2004).

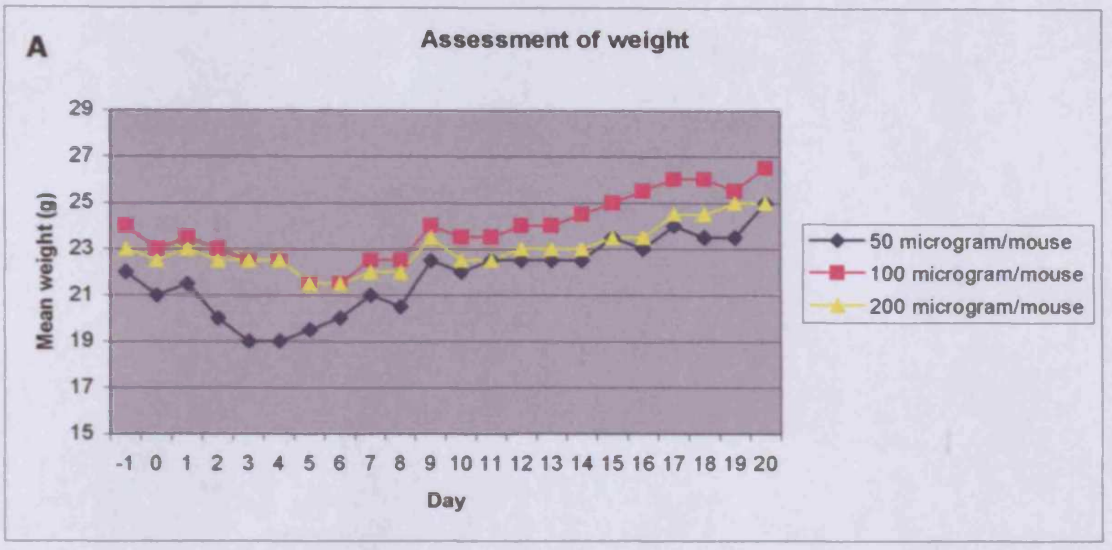

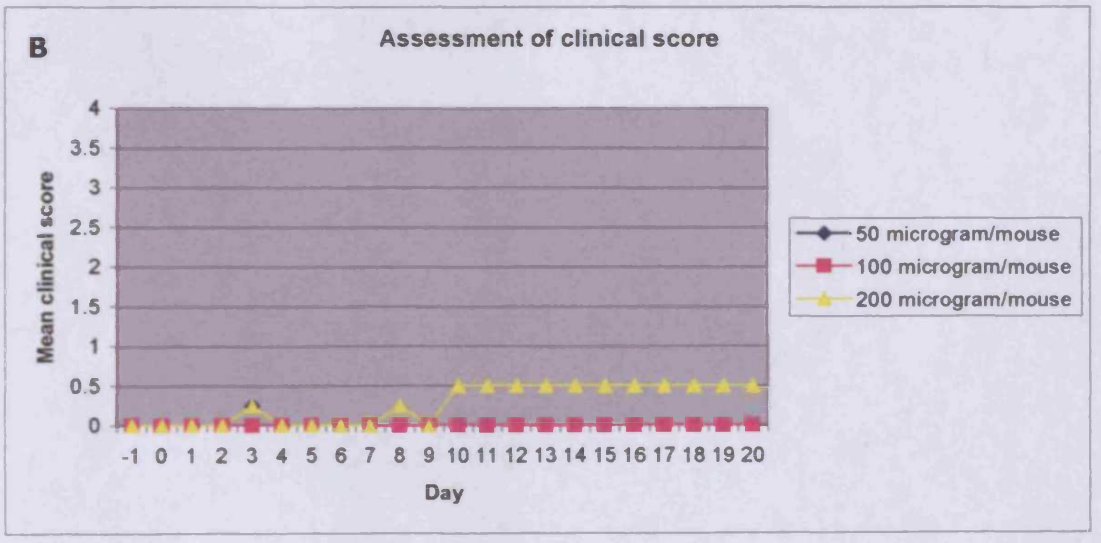

Figure 2

Assessment of weight and clinical score in PO peptide 180-199 and Pertussis toxin (PT)-injected C57Bl/6 mice

Mice were primed with 400ng PT (IP) on day-1 and 200ng PT on day 0, 1 and 3. Mice received PO peptide 180-199 in FCA on day 0 and day 6 (s/c)

Mice were assessed daily for changes in weight (A) and clinical score (B) as described.

3.2 Induction of EAN in *Cd59a -/-* mice with PO peptide 180-199

3.2.1 Aim

The lack of CD59a has been shown previously to enhance severity of disease in a variety of autoimmune models, by allowing unregulated MAC deposition. In a model of immune complex-mediated glomerulonephritis, lack of CD59a exacerbated renal injury (Turnberg, Botto et al. 2003), while in EAE, it was demonstrated that a lack of CD59a enhanced disease severity, demyelination and axonal injury (Mead, Neal et al. 2004).

It was postulated therefore that providing a lower threshold for disease induction would facilitate optimisation of the disease model.

3.2.2 Induction protocol

Nine male *Cd59a -/-* mice (21-23g) were obtained from Biomedical Services Unit (BSU), Cardiff University. On the day prior to induction, mice were primed with 400ng/mouse of Pertussis toxin (PT), injected IP. On Day 0, mice were injected s/c with various doses of PO peptide 180-199 (Severn Biotech Ltd, Kidderminster, UK) (150, 200, 250µg/mouse) in 100µl saline emulsified 100µl in FIA containing 10mg/ml *M. tuberculosis*. Mice were further primed with 200ng/mouse PT (IP) on day 0, 1, 3 and 6, followed by a boost of peptide on Day 6. Mice were assessed daily for changes in weight, and scored for clinical symptoms as described previously.

3.2.3 Results

3.2.3.1 Assessment of weight and clinical score

All animals showed decreased weight from day 2 post immunisation (p.i) up until day 7 p.i. Both the 150µg and 250µg groups increased weight after this period, while the 200µg group maintained their weight. At day 13, a small decrease in weight was evident in all 3 groups, followed by increased weight until the end of the experiment at day 22 (Figure 3, A). Animals in all 3 groups exhibited clinical signs:

150µg PO peptide 180-199 group

All 3 animals exhibited minimal clinical symptoms ranging from a clinical score of 0.5 to a maximum of 1 between day 13 and the end of the experiment at day 22. Animal 1L-1 was found dead at day 17 with minimal preceding clinical symptoms (maximum score 0.5), although had been noted to be 'agitated' at day 13.

200µg PO peptide 180-199 group

Two of three animals displayed clinical symptoms. Animal 1R-0 had a fully limp tail at day 16, but recovered by day 17. Animal 1R-2 had hind limb wasting in the absence of a limp tail, and was given a clinical score of 2. Animal 1R-1 displayed no clinical symptoms, but was found dead at day 10 before disease would have been expected at day 11-13.

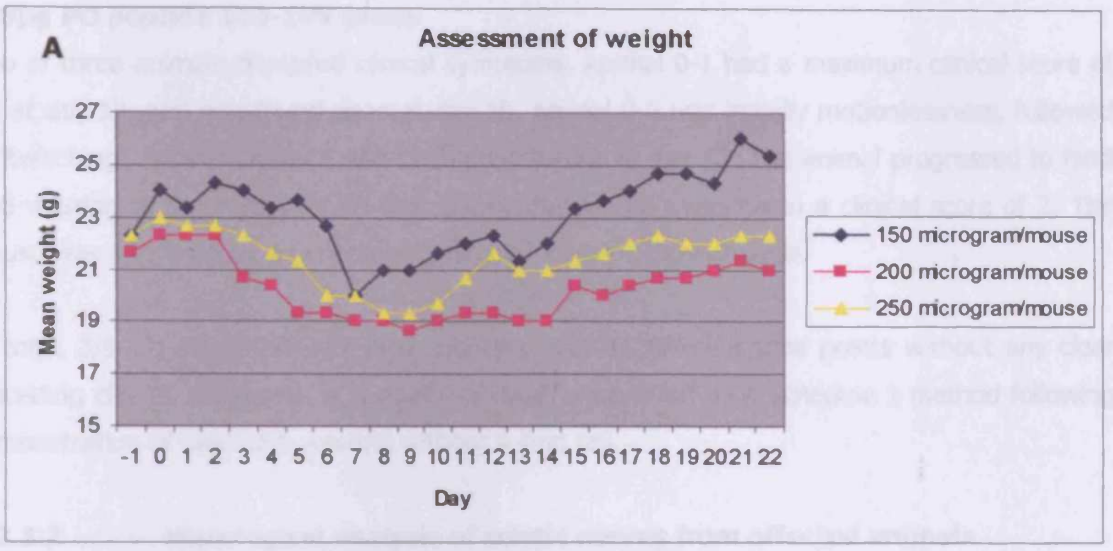

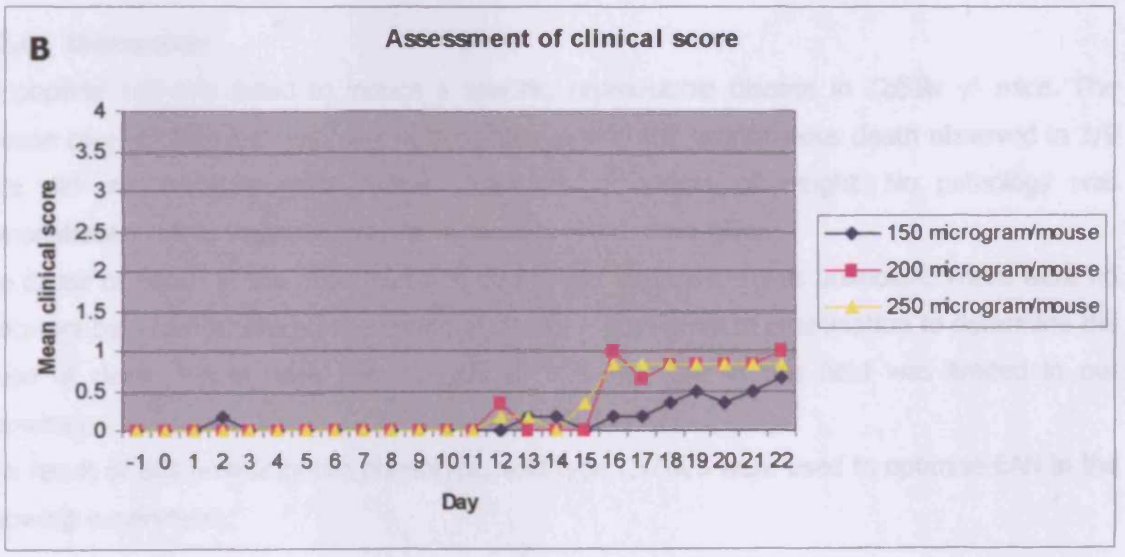

Figure 3

Assessment of weight and clinical score in *Cd59a-/-* mice immunised with PO peptide 180-199

Mice were primed with 400ng PT (IP) on day-1 and 200ng PT on day 0, 1 and 3. Mice received PO peptide 180-199 in FCA on day 0 and day 6 (s/c)

Mice were assessed daily for changes in weight (A) and clinical score (B) as described.

250µg PO peptide 180-199 group

Two of three animals displayed clinical symptoms. Animal 0-1 had a maximum clinical score of 0.5 at day 13, and was found dead at day 16. Animal 0-2 was initially motionlessness, followed by 'twitching', hyperventilation and circling behaviour at day 12. The animal progressed to hind limb wasting in the absence of a limp tail by day 16, and was given a clinical score of 2. The mouse was sacrificed by a Schedule 1 method for histological analysis.

In total, 3/9 *Cd59a -/-* animals died spontaneously at different time points without any clear preceding clinical symptoms. A further 2 animals were killed by a Schedule 1 method following demonstration of hind limb wasting without a limp tail.

3.2.3.2 Histological analysis of sciatic nerves from affected animals

Sciatic nerves were isolated from each animal and embedded in paraffin wax. Sections were analysed by H&E staining for inflammatory infiltrates by the Histology department and Dr. James Neal, UWCM.

No inflammatory infiltrates were present in sciatic nerves from 150µg (Figure 4, A), 200µg (Figure 4, B) or 250µg (Figure 4, C) groups, regardless of preceding clinical symptoms, thus nerves were not taken for further analysis for myelin by LFB staining.

3.2.4 Discussion

PO peptide 180-199 failed to induce a specific, reproducible disease in *Cd59a -/-* mice. The disease course observed was very heterogeneous, and the spontaneous death observed in 3/9 mice did not correlate with clinical symptoms, or a loss of weight. No pathology was demonstrated within the sciatic nerve, regardless of the dose given.

The cause of death in the mice that died during this experiment was unknown. There were no indicators by which to predict the timing of death. A post-mortem examination to determine the cause of death would have been beneficial, but expertise in this field was limited in our laboratory.

As a result of this unanticipated phenotype, wild type C57Bl/6 were used to optimise EAN in the following experiment.

150µg PO peptide 180-199
Animal 1L-1
Found dead at day 17
No preceding clinical symptoms

200µg PO peptide 180-199
Animal 1R-0
Limp tail at day 16 (transient)

250µg PO peptide 180-199
Animal 0-2
Hind limb wasting in absence of limp tail at day 16

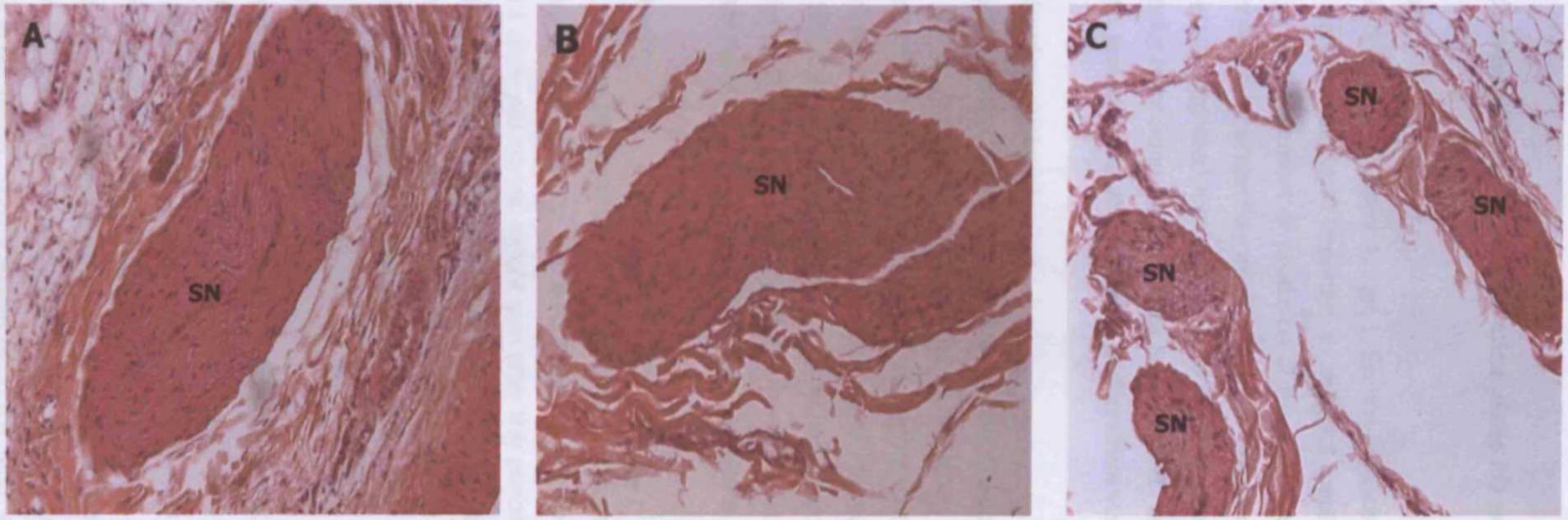

Figure 4 H&E staining of sciatic nerves from PO peptide 180-199-immunised *Cd59a-/-* animals

Sciatic nerves were isolated from animals at day 22, or during the experiment where indicated. Nerves were embedded in paraffin wax, and sections were cut and stained by H&E for detection of inflammatory infiltrates. Representative sections from each dose group are shown above; 150µg (A), 200µg (B) and 250µg (C).

All images were taken at 100X magnification.

3.3 Induction of EAN in C57Bl/6 mice using PO peptide 180-199-amide

3.3.1 Aim

As described previously (Chapter 4, Part 1, Section 3.4), chemical modification of the peptide at N- and C- termini has been reported to enhance peptide presentation to T cells; either acetylation at the N-terminus or amidation of the C-terminus increases the lifetime of the free peptide in solution by protection from proteolysis (Maillere, Mourier et al. 1995). In addition, colleagues have suggested that amidation of the C-terminus of a peptide in this manner has been successful in inducing EAE in guinea pigs (Richard Mead, personal communication, 2004). Expertise was also available at this time to perform intra-venous injection of PT (Paula Longhi).

3.3.2 Induction protocol

Six male C57Bl/6 mice (18-22g) were obtained from Charles River Laboratories, and allowed to acclimatise for 1 week. On the day prior to induction (day -1), mice were primed with 400ng/mouse of PT, injected IV at the tail vein under restraint. On Day 0, mice were injected s/c with a dose of 50, 100 and 200 micrograms of PO-peptide 180-199-amide in 100µl saline emulsified 100µl in FIA containing 10mg/ml *M. tuberculosis*. Mice were further primed with 200ng/mouse PT (IV) on day 0, 1, 4 and 6, followed by a boost of peptide on day 6. Mice were assessed daily for changes in weight, and scored for clinical symptoms as described previously.

3.3.3 Results

3.3.3.1 Assessment of weight and clinical score

Animals from each dose group lost weight consistently between day 0 and day 15 (Figure 5, panel A), but displayed normal weight gain after this period. No specific clinical symptoms were evident throughout the course of the experiment, with the exception of a mild, transient disease demonstrated by weakness of the tail tip, in all 3 groups between day 15 and 17 (Figure 5, panel B). No histological analysis was performed.

3.3.4 Discussion

Both PO peptide 180-199, and C-amidated PO peptide 180-199 failed to induce a reliable and specific EAN in the mouse, regardless of dose and strain of mouse used. The original paper suggested that PO peptide 180-199 alone resulted in a low incidence of disease (42.8%) associated with mild disease with a mean clinical score of 1. The authors suggested that using PT as an additional adjuvant increased the incidence of EAN to 93.7%, and resulted in a slightly more severe disease, with a mean score of 2 (Zou, Ljunggren et al. 2000). This was not reproducible in our hands. Several studies using the same immunisation schedule to induce EAN successfully have been reported in the literature (Zhu, Ljunggren et al. 2001), (Bao, Lindgren et al. 2002), (Yu, Duan et al. 2004), (Duan, Chen et al. 2004). However, the reports are all from the same group that published the original paper. In contrast, Miyamoto et al observed very mild disease in only one third of C57Bl/6 mice immunised with PO peptide 180-199. Disease

severity was only enhanced in mice with a heterozygous null mutation in PO (Miyamoto, Miyake et al. 2003).

A recent paper has challenged the neuritogenicity of PO peptide 180-199, suggesting that PO peptide 106-125 is capable of inducing a more severe disease, and inducing a 20-fold higher frequency of antigen-specific T cells (Miletic, Utermohlen et al. 2005). This was attempted in the following experiment.

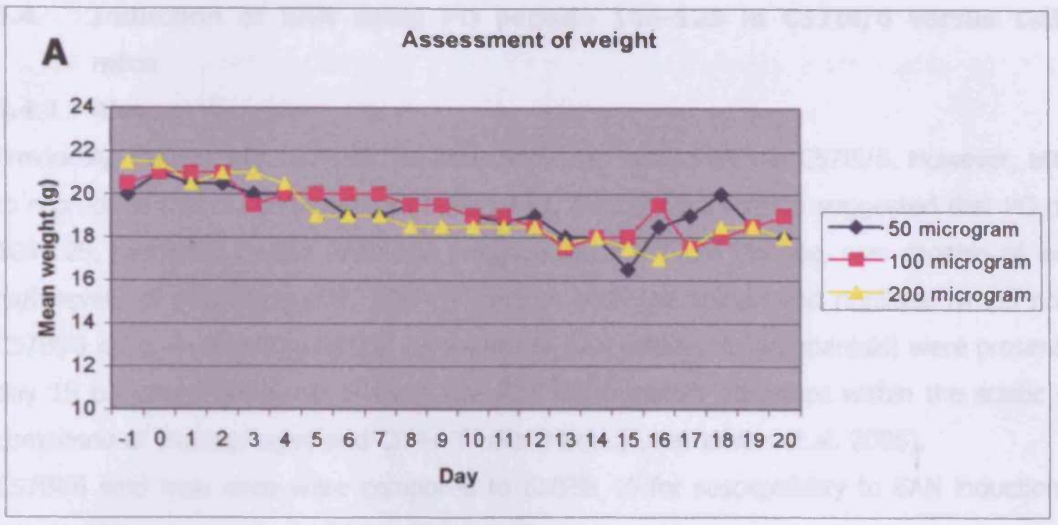

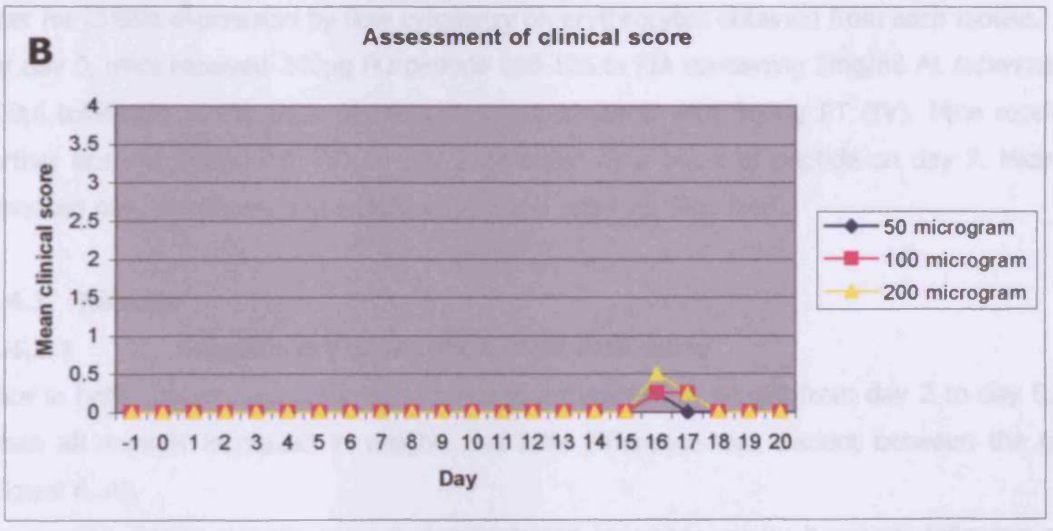

Figure 5

Assessment of weight and clinical score in C57Bl/6 mice immunised with PO peptide 180-199-amide

Mice were immunised with a dose response of PO peptide 180-199-amide on day 0 and 6, in conjunction with PT at day -1, 0, 1 and 3. Mice were assessed daily for changes in weight (A), and clinical score (B) as described.

3.4 Induction of EAN using PO peptide 106-125 in C57Bl/6 versus *Cd59a-/-* mice

3.4.1 Aim

Previously, PO peptide 180-199 has been shown to induce EAN in C57Bl/6. However, attempts to reproduce this in our laboratory have failed. A recent publication suggested that PO peptide 106-125, predicted by the RANKPEP program to be a T cell epitope, was capable of inducing high levels of peptide-specific CD4+ T cells in both the spleen and popliteal lymph nodes in C57Bl/6 mice. In addition, clinical symptoms of EAN (moderate paraparesis) were present up to day 15 p.i. and histological analysis revealed inflammatory infiltrates within the sciatic nerves composed of macrophages and CD4+ T cells (Miletic, Utermohlen et al. 2005).

C57Bl/6 wild type mice were compared to *Cd59a -/-* for susceptibility to EAN induction using this peptide.

3.4.2 Induction protocol

Six male *Cd59a -/-* mice (28-31g) were obtained from BSU. Five littermate controls were obtained by backcrossing *Cd59a -/-* mice onto C57Bl/6 through 1 generation, and screening the litter for CD59a expression by flow cytometry on erythrocytes obtained from each mouse.

On day 0, mice received 200µg PO peptide 106-125 in FIA containing 5mg/ml *M. tuberculosis* in 100µl total, s/c at the base of the tail, in combination with 500ng PT (IV). Mice received a further dose of 500ng PT (IV) on day 2, followed by a boost of peptide on day 7. Mice were assessed daily for changes in weight and clinical score as described.

3.4.3 Results

3.4.3.1 Assessment of weight and clinical score

Mice in both groups showed a trend towards a decrease in weight from day 2 to day 6, from when all animals increased in weight, and little difference was evident between the groups (Figure 6, A).

No specific clinical symptoms were demonstrated by either group; however, following careful monitoring, all animals appeared piloerected at day 4. *Cd59a -/-* mice displayed piloerection between day 8 and 11, while the littermate controls appeared healthy. Also at day 8, animal A3 of the *Cd59a -/-* group was vocalising, and remained isolated from the group as a whole, but recovered by day 9. On day 15, A2 (*Cd59a -/-*) and D0 (littermate control) both became extremely aggressive and difficult to handle. As a whole, *Cd59a -/-* mice appeared less healthy than their littermate controls. None of these observations led to any specific EAN-related clinical signs (Figure 6, B). No histological analysis was performed.

3.4.4 Discussion

PO peptide 106-125 failed to induce any specific clinical symptoms either in *Cd59a-/-* mice or littermate controls. A potential reason for this may be that in the study by Miletic et al, mice were first immunised via the footpad at day 0, followed by a s/c boost at day 7. Due to

restrictions imposed by the Home Office, the licence covering EAN induction does not allow the footpad route for immunisation in the mouse. The i.v. route for immunisation of PT did not enhance disease induction.

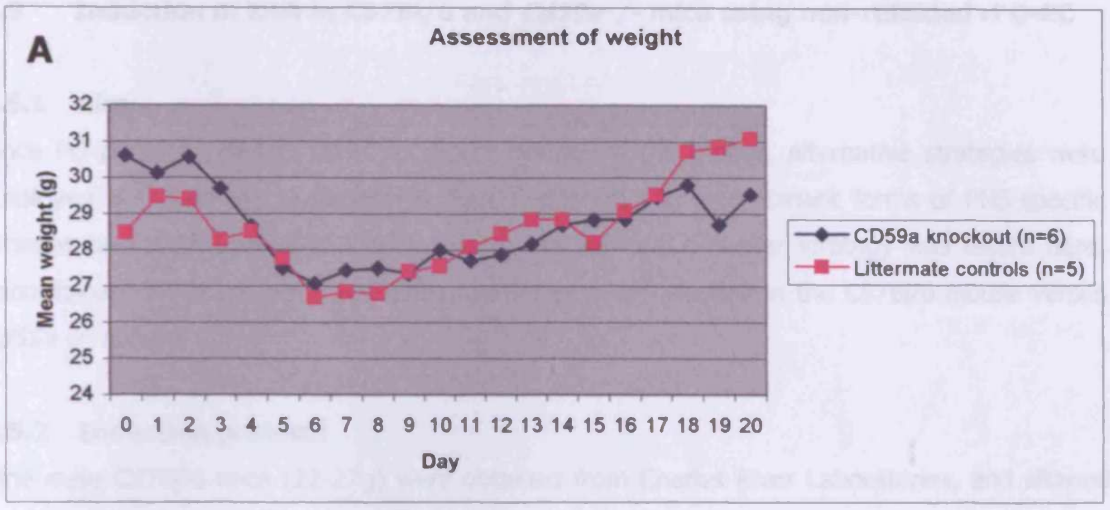

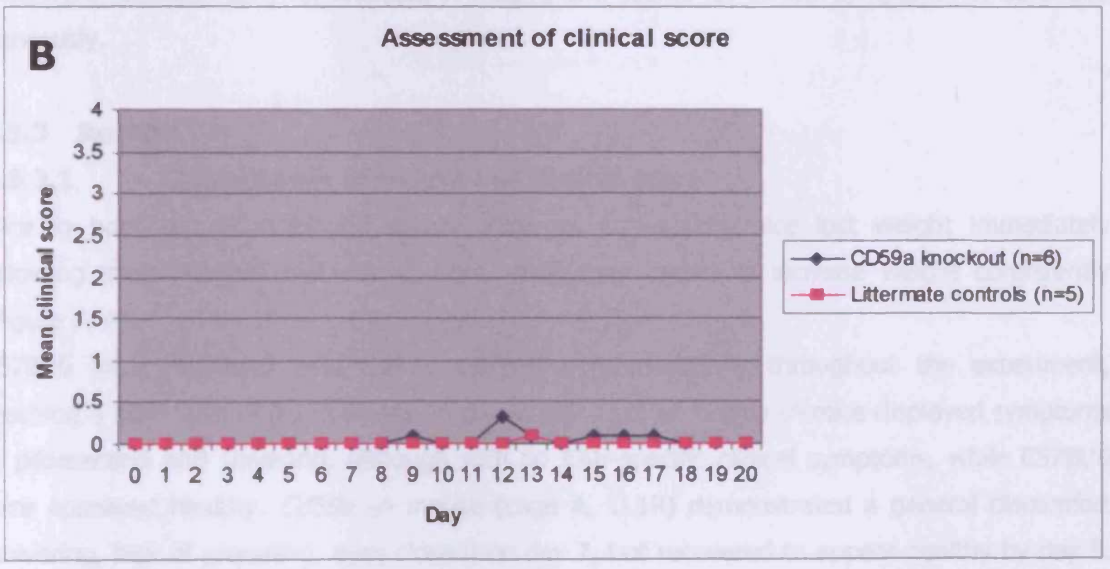

Figure 6

Assessment of weight and clinical score in CD59a knockout mice immunised with PO peptide 106-125

Mice were injected with 200µg PO peptide 106-125 in FIA containing 5mg/ml M. tuberculosis in a total volume of 100µl at day 0 and 7. In combination, PT (500ng/mouse, IV) was administered on day 0 and 2. Mice were assessed daily for changes in weight (A), and clinical score (B).

3.5 Induction of EAN in C57Bl/6 and *Cd59a-/-* mice using non-refolded rPO-EC

3.5.1 Aim

Since PO peptide 180-199 failed to induce disease in the mouse, alternative strategies were employed. As described in Chapter 4, Part 1, Section 3.2, recombinant forms of PNS-specific proteins had been utilised to induce EAN in the rat, and a similar strategy was tested here. Recombinant PO-EC domain, was used to attempt EAN induction in the C57Bl/6 mouse versus *Cd59a -/-* mouse.

3.5.2 Induction protocol

Nine male C57Bl/6 mice (22-27g) were obtained from Charles River Laboratories, and allowed to acclimatise for 1 week. Nine age-matched male *Cd59a -/-* mice were obtained from BSU at Cardiff University. On the day prior to induction (day -1), mice were primed with 400ng/mouse of PT, injected IP. On Day 0, mice were injected s/c with 200µg non-refolded rPO-EC in 100µl saline emulsified in 100µl FIA containing 10mg/ml *M. tuberculosis*. Mice were further primed with 200ng/mouse PT (IP) on day 0, 1, 3 and 6, followed by a boost of rPO-EC on Day 6.
Mice were assessed daily for changes in weight, and scored for clinical symptoms as described previously.

3.5.3 Results

3.5.3.1 Assessment of weight and clinical score

Mice in both groups displayed parallel changes in weight; mice lost weight immediately following immunisation until day 6, from when they began to increase weight consistently (Figure 7, A).

C57Bl/6 mice displayed mild clinical symptoms intermittently throughout the experiment, reaching a maximum of 0.167 at day 20 p.i. At day 2 p.i, all *Cd59a -/-* mice displayed symptoms of piloerection and shivering, although with no EAN-specific clinical symptoms, while C57Bl/6 mice appeared healthy. *Cd59a -/-* mouse (cage A, 1L1R) demonstrated a general discomfort (shivering, lack of grooming, eyes closed) on day 7, but recovered to appear healthy by day 8. Meanwhile, *Cd59a -/-* (cage B, 0) displayed a limp tail at day 8 (score 1), progressing to hind limb weakness and wasting at day 10 (score 3). However, the clinical symptoms were transient, and lasted only 24 hours (Figure 7, B). The mouse was sacrificed at day 12 for histological analysis. Remaining mice were sacrificed at the end of the experiment at day 23.

3.5.3.2 Histological analysis of sciatic nerves and spinal cord

It was suggested that inflammation of the PNS may occur up in the peripheral nerve roots leading from the spinal cord, and the reason for the lack of specific inflammatory cells detected

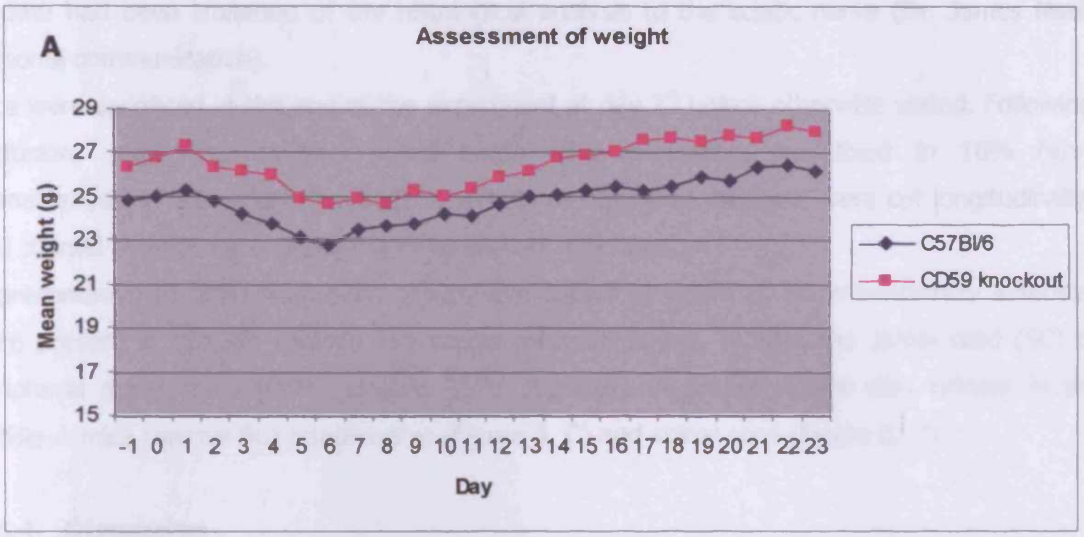

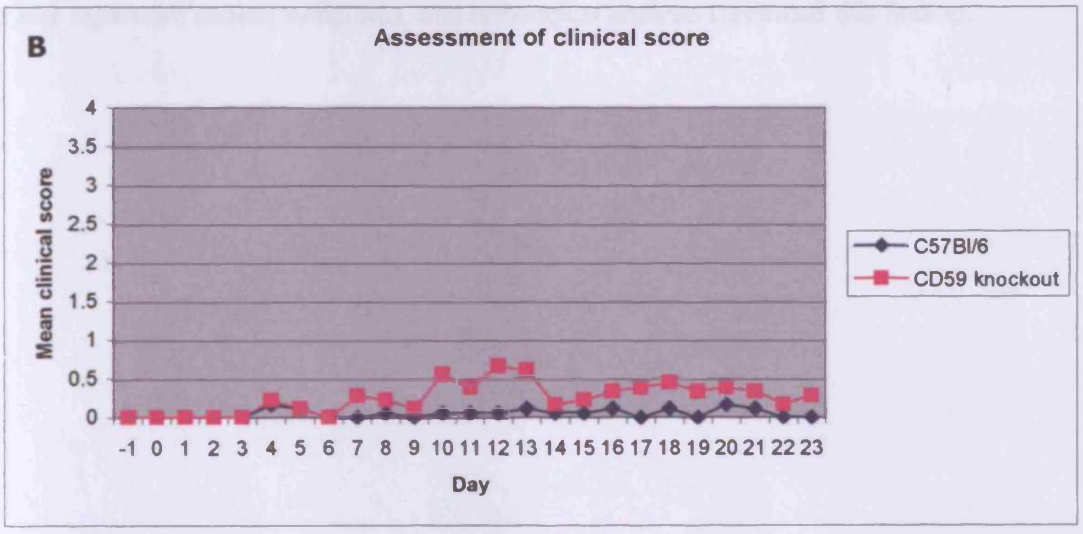

Figure 7

Assessment of weight and clinical score in C57Bl/6 and *Cd59a-/-* mice following immunisation with refolded rPO-EC

Mice were primed with 400ng PT (IP) on day-1 and 200ng PT on day 0, 1 and 3, and received PO peptide 180-199 in FCA on day 0 and day 6 (s/c)

Mice were assessed daily for changes in weight (A) and clinical score (B) as described.

to date had been limitation of the histological analysis to the sciatic nerve (Dr. James Neal, personal communication).

Mice were sacrificed at the end of the experiment at day 23 unless otherwise stated. Following perfusion, sciatic nerves and spinal cords were harvested, post-fixed in 10% (v/v) formaldehyde in PBS, and embedded in paraffin as described. Sections were cut longitudinally, and stained by H&E for detection of inflammatory infiltrates.

Representative sections from each group were shown in Figure 8. No inflammatory infiltrates were present in C57Bl/6 (animal 1R) sciatic nerve (Figure 8, A, SN), the spinal cord (SC) or peripheral nerve roots (PNR). (Figure 8, B, SC, PNR). A similar picture was evident in the *Cd59a-/-* mice (animal B0) sciatic nerve (Figure 8, C) and spinal cord (Figure 8, D).

3.5.4 Discussion

rPO-EC failed to induce EAN in either C57Bl/6 mice or *Cd59a -/-* mice. One out of nine *Cd59a-/-* mice displayed EAN-specific clinical signs at day 8, but symptoms were transient, and the mouse made a complete recovery by day 10. Histological analysis of sciatic nerve and spinal cord from the affected animal revealed no inflammatory infiltrates. None of the C57Bl/6 mice had any significant clinical symptoms, and histological analysis confirmed this finding.

C57Bl/6

Animal 1R

Max. clinical score 0.5

Sacrificed at day 23

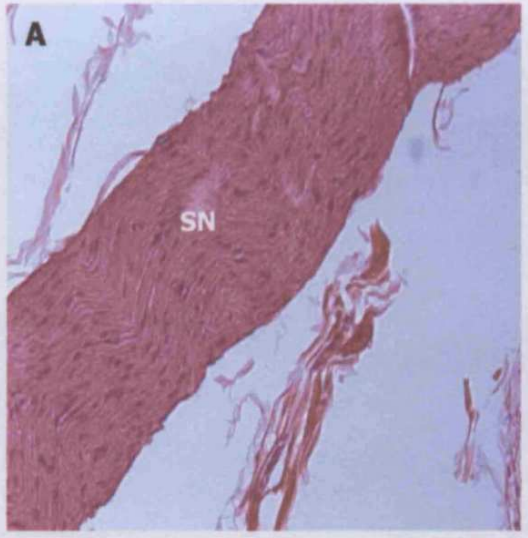

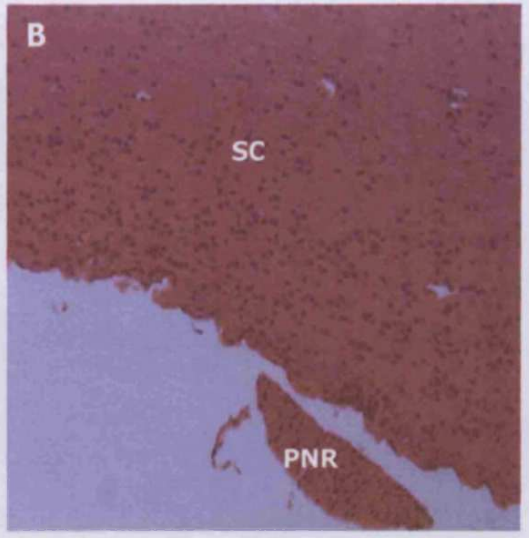

CD59a -/-

Animal B0

Clinical score 3 at day 8

Recovered by day 9

Sacrificed at day 12

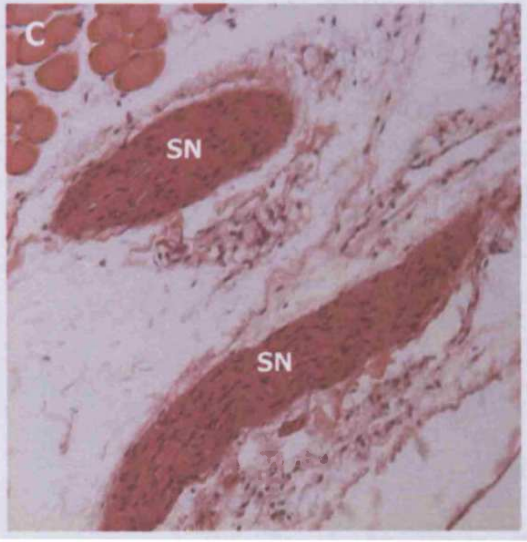

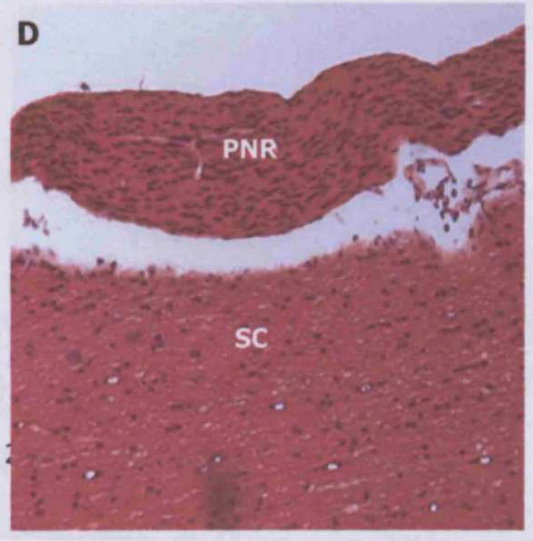

Figure 8

H&E staining of sciatic nerve and spinal cord sections from non-refolded rPO-EC-injected C57Bl/6 and CD59a-/-

Mice were sacrificed at the end of the experiment at day 23 unless otherwise indicated. Sciatic nerves (SN) and spinal cords (SC) were harvested, following fixation in 10% FA, embedded in paraffin wax. Sections were cut and stained with H&E as described.

Representative sections from each group are shown; C57Bl/6 (A, SN; B, SC where peripheral nerve roots (PNR) were visible); CD59a-/- (C, SN; D, SC showing PNR)

All images were taken at 100X magnification.

3.6 Induction of EAN in C57Bl/6 mice using rat sciatic nerve homogenate (RSNH)

3.6.1 Aim

Bovine peripheral myelin has previously been reported to be capable of inducing EAN in susceptible mouse strains, such as the SJL mouse, but not C57Bl/6 or Balb/c mice (Dieperink, O'Neill et al. 1991). A study of inhibition of chronic relapsing experimental allergic encephalomyelitis (CREAE) demonstrated that injection of 2mg of mouse sciatic nerve homogenate (MSNH) was able to induce EAN in the Biozzi AB/H mouse. Onset was at day 13, the mean clinical score observed was 1.8, and disease incidence was 100% (O'Neill, Baker et al. 1992). In addition, the authors included a sonication step in creating the emulsion of MSNH prior to immunisation, which may function to disrupt the proteins within the myelin sheath, and make them more accessible to the immune system.

Rat and mouse peripheral nerve proteins share a high degree of homology; for example, mouse PO shares 97.8% homology to rat PO at the amino acid level. Homology study was performed using MegAlign (DNAstar, Inc. USA). Rat RSNH had previously been prepared to test its ability to induce EAN in the rat, therefore it was also tested for its ability to induce EAN in the C57Bl/6 mouse.

3.6.2 Induction protocol

RSNH was prepared as described previously. Six male C57Bl/6 mice (19-21g) were obtained from Charles River Laboratories, and allowed to acclimatise for 1 week. On the day prior to induction (day -1), mice were primed with 400ng/mouse of PT, injected IP. On Day 0, mice were injected s/c with a dose response of 2.5, 5 and 10mg of RSNH in 100µl saline emulsified 100µl in FIA containing 10mg/ml *M. tuberculosis,* and sonicated for 20 minutes at 37^0C in a water bath sonicator. Mice were further primed with 200ng/mouse PT (IV) on day 0, 1, 3 and 6, followed by a boost of RSNH on Day 6.

Mice were assessed daily for changes in weight, and scored for clinical symptoms as described previously.

3.6.3 Results

3.6.3.1 Assessment of weight and clinical score

All animals lost weight between day 0 and day 10-11, after which 2.5mg and 10mg groups increased weight consistently; the 5mg group only maintained weight from day 12 onwards, with a slight decrease at day 18 (Figure 9).

All animals displayed piloerection and lack of grooming between days 7 and 8 p.i. On day 11, animal 1R (10mg RSNH group) displayed a hunched posture, but no specific clinical symptoms, and recovered the following day. On day 13, animal 2R displayed a similar hunched appearance, again with no specific clinical symptoms, but was found dead on day 14. Animal 0

was also found dead on day 17, with no preceding markers of disease. Histological analysis revealed no inflammatory infiltration (data not shown).

3.6.4 Discussion

RSNH failed to induce EAN in C57Bl/6 mice. Two out of 6 mice were found dead, with no preceding clinical symptoms. A thorough post-mortem should have been performed on these animals but as mentioned previously, expertise was not available at this time.

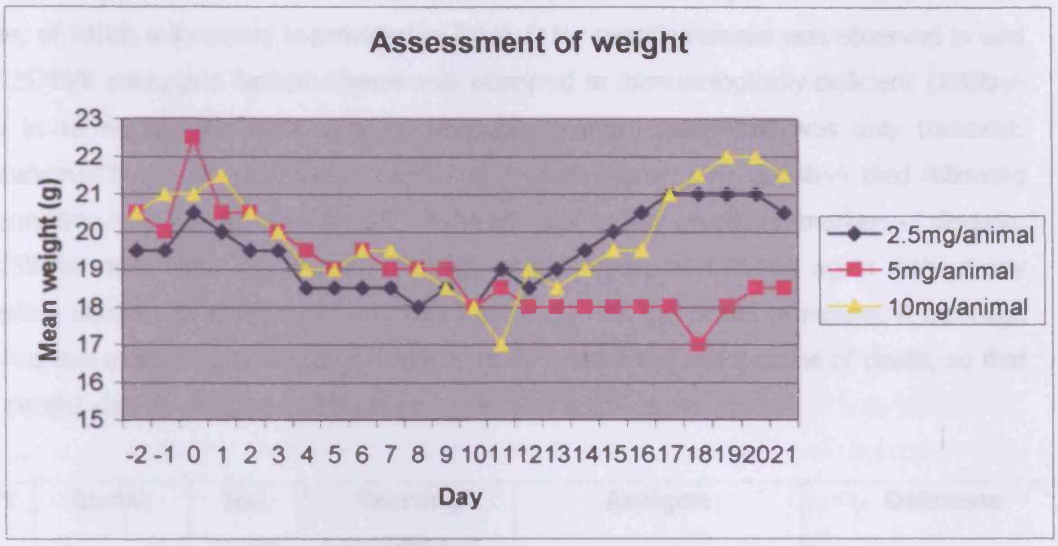

Figure 9

Assessment of weight in C57Bl/6 mice following immunisation with RSNH

Mice were immunised with 2.5, 5 and 10mg RSNH in FIA containing 10mg/ml M. tuberculosis on day 0 and day 6, in conjunction with PT at day -1, 0, 1 and 3.

Mice were assessed daily for changes in weight (above). No specific clinical symptoms were demonstrated.

4 Summary & Discussion

In conclusion, a number of different protocols were used in the optimisation of EAN in the mouse, of which a summary is provided in Table 1. No specific disease was observed in wild type C57Bl/6 mice, and limited disease was observed in immunologically-deficient *Cd59a-/-* mice, in terms of hind limb wasting, although in most cases this was only transient. Spontaneous death of mice was observed in 2 experiments; 3/9 *Cd59a-/-* died following immunisation with PO peptide 180-199, in the absence of any preceding markers of disease; 2/6 C57Bl/6 mice were found dead following immunisation with RSNH, again without any preceding markers of disease. This is very uncommon for this strain of mouse. A thorough post-mortem examination would be required to determine the exact cause of death, so that such deaths can be avoided in the future.

Exp't	Strain	No. used	Starting weight (g)	Antigen	Outcome
3.1	C57Bl/6	6	20-24	PO peptide 180-199	No disease
3.2	*Cd59a-/-*	9	21-23	PO peptide 180-199	3/9 spontaneous death 2/9 hind limb wasting in absence of limp tail No pathology
3.3	C57Bl/6	6	18-22	PO peptide 180-199-amide	No disease
3.4	C57Bl/6 versus *Cd59a-/-*	6	28-31	PO peptide 106-125	No specific disease CD59a-/- appeared less healthy
3.5	C57Bl/6 versus *Cd59a-/-*	9	22-27	rPO-EC domain (non-refolded)	1/9 CD59a-/- transient severe disease No pathology
3.6	C57Bl/6	6	19-21	RSNH	2/6 found dead No pathology

Table 1

Summary of approaches used to date in the optimisation of EAN in the mouse

The recent article published by Miletic et al has proven that PO peptide 180-199 is not capable of inducing severe and reproducible disease in the C57Bl/6 mouse. Their study showed that PO 180-199 in combination with PT injected i.v. induced disease in only 8/15 C57Bl/6 mice (Miletic, Utermohlen et al. 2005). This is not in agreement with the original paper published by Zou, Ljunggren at al, who suggested that PT injection increased disease incidence to 93.7% in the C57Bl/6 mouse injected with PO peptide 180-199 (Zou, Ljunggren et al. 2000). In our hands, neither protocol induced severe and/or reproducible disease in the C57Bl/6 mouse.

However, some modifications of the protocol of Miletic and colleagues were forced due to restrictions on the Home Office licence covering EAN induction in the mouse (30/1984). Footpad injections are not allowed on our current licence, and the first injection in the Miletic protocol was performed via the footpad. Such injections are necessary if isolating a draining lymph node as a primary site of action is necessary (Home Office website). This may be responsible for the lack of disease observed following injection of PO peptide 106-125 in the present study. An application for a modification of the licence should be submitted to the Home Office in the near future, citing this study as justification.

PO peptide 106-125 may well induce disease, but evidence of disease progression in histological analysis may be subtle, and H&E analysis alone is not sufficient to detect such changes. A more thorough histological analysis is required to encompass localisation of CD4+ T cells present in the sciatic nerve, as well as CD8+ T cells. Although GBS is recognised as primarily a CD4+ T cell-mediated disease, a recent report studying archival autopsy samples from GBS patients, demonstrated the presence of CD8+ T cells in peripheral nerve tissue at the later stages of GBS, which are thought to contribute to myelin damage by granzyme release (Wanschitz, Maier et al. 2003).

Specific analysis of macrophages using F4/80 marker would also be beneficial on frozen section of sciatic nerve, as well as analysis of expression of MHC class II molecules to detect antigen presenting cells.

In the PO peptide 106-125 model, there was an absence of active demyelination, although intraneural macrophages were observed in the sciatic nerve. Despite this, reduced nerve motor conduction was observed in PO peptide 106-125-injected mice compared with PBS-injected mice. Electrophysical examination has not been attempted throughout the course of these studies due to a lack of available expertise. For future successful evaluation of disease, particularly in mice, this should be included in routine disease assessment.

Enzyme-Linked Immunospot Assays (ELISPOT) also provided evidence for EAN induction in the mice in the study by Miletic. Interferon-gamma (IFN-γ)-producing T cells were detected in the popliteal lymph nodes (PLN) and spleen by day 9 p.i. in PO peptide 106-125-injected

mice. Further analysis revealed these cells were CD4+. This analysis was also performed on PO peptide 180-199-injected mice, and revealed a 20-fold lower frequency of antigen-specific T cells at day 9 in the PLN, which was undetectable by day 15 p.i.

In summary, for the future optimisation of this model in the C57/Bl6 mouse, the following parameters should be considered:

- assessment of weight and clinical score
- electrophysiological assessment
- ELISPOT assays to assess T cell activation
- histological assessment to encompass both the sciatic nerve and cauda equina: H&E, LFB staining for myelin, specific staining for CD4+ and CD8+ T cells, MHC class II expression

Although this more thorough analysis would require time invested in optimisation, the investigations may yield extremely useful data, and provide a means of testing the susceptibility of C deficient and knockout animals to disease induction.

Chapter 5

Part 1

Passive transfer Experimental Autoimmune Myasthenia Gravis (EAMG) in the Lewis rat

1 Introduction

MG is an autoimmune disease characterised by severe voluntary muscle weakness and excessive fatigue. The signs and symptoms result from an impairment of neuromuscular transmission caused by an auto-immune reaction against the nicotinic acetylcholine receptor (nAChR). Anti-nAChR antibodies bind the receptor, and target the post-synaptic membrane for C attack and subsequent lysis; this causes loss of the nAChR themselves and slows down neuromuscular transmission by disrupting the folded architecture of the post-synaptic membrane. Antibodies may also cross-link the nAChR, and increase their rate of internalisation (Lindstrom 2003). The animal model of the disease, EAMG can be induced either by immunisation with nAChR, or by passive transfer of anti-nAChR antibodies, and mimics many of the pathophysiological aspects of MG.

There is substantial evidence for a role for C in the pathogenesis of MG. Observations of changes in serum C levels in MG patients in the 1960s provided the first evidence for C involvement (Nastuk, Plescia et al. 1960). Numerous subsequent studies have identified IgG, C3, C9 and MAC deposits at the post-synaptic membrane in MG patients (Engel, Lambert et al. 1977; Sahashi, Engel et al. 1978; Sahashi, Engel et al. 1980; Fazekas, Komoly et al. 1986; Engel and Arahata 1987). Following on from this, a correlation between plasma C3c and disease severity was observed in MG patients (Kamolvarin, Hemachudha et al. 1991); in addition, sC5b-9 was detected in MG patient plasma, although this did not correlate with disease severity (Barohn and Brey 1993). The animal model of the disease EAMG has provided researchers with a tool to study the immune mechanisms responsible for mediating pathology. Decomplementation of rats with cobra venom factor (CVF) protected against passively or actively-induced EAMG (Lennon, Seybold et al. 1978; Tsujihata, Satoh et al. 2003). In parallel to the human studies, IgG and C3 were localised to the motor endplate in actively or passively-induced EAMG (Sahashi, Engel et al. 1978; Engel, Sakakibara et al. 1979). C deficient animals have also provided evidence on the role of C. C5 deficient mice were protected against development of actively induced EAMG despite having equal concentrations of anti-nAChR as their wild type controls (Christadoss 1988). Inhibition of the terminal pathway using polyclonal antiserum against C6 prevented development of passively

induced EAMG in rats (Biesecker and Gomez 1989); sCR1 delayed the onset and reduced disease severity of passively-induced EAMG in the rat (Piddlesden, Jiang et al. 1996). More recently, the advent of various knockout mice has provided material for studying complex immune interactions. For instance, IL-6 deficient mice showed a reduction in actively induced EAMG associated with reduced germinal centre formation and C3 production (Deng, Goluszko et al. 2002). Mice lacking C regulator CD55 (*Daf1-/-*) had enhanced susceptibility to passively induced EAMG (Lin, Kaminski et al. 2002), while C3-/- and C4-/- mice were resistant to actively induced EAMG, with heterozygotes demonstrating intermediate susceptibility (Tuzun, Scott et al. 2003).

However, testing of the importance of the terminal pathway is limited. This chapter aims to demonstrate the optimisation of passive transfer EAMG in the Lewis rat, and the use of the model to evaluate the role of the terminal pathway in meditating disease using the C6 deficient rat colony available. The passive transfer model was utilised since supply of nAChR is limited for actively induced disease. Passive transfer EAMG had also been optimised in our laboratory previously (Piddlesden, Jiang et al. 1996). The model was used to test various anti-C-therapeutics in acute autoimmune disease as seen in EAMG.

The second part of the chapter will describe the preliminary work in establishing passive transfer EAMG in the mouse, and the comparison of the susceptibility of various CReg knockout animals.

2 Materials and Methods

All chemicals unless otherwise stated were from Sigma Aldrich Chemical Company, Gillingham, UK, or Fisher Scientific UK Ltd, Loughborough, UK.

2.1 Animals

All animals used were obtained from Charles River Laboratories, UK, and maintained according to Home Office guidelines within the Biomedical Services Unit (BSU) at University of Wales College of Medicine, Cardiff.

2.2 Disease assessment

Animals were assessed daily for evidence of EAMG by analysis of weight loss, and a clinical scoring system. Animals were scored according to their ability to grasp and lift the lid of a mouse cage: 0, no disease; 1, reduced grip strength in front paws (can grip but cannot lift); 2, loss of grip in front paws; 3, loss of grip and hind limb weakness and wasting; 4, loss of grip and hind limb paralysis. Half scores were given for intermediate symptoms. Animals were sacrificed by a Schedule 1 method when weight loss was equal to, or exceeded 20% of

original body weight, or when clinical score reached 4. After the onset of clinical symptoms, rats were given pre-wetted food daily and assessed every 12 hours.

2.3 Collection and processing of tissues for immunohistochemical analysis

2.3.1 Paraffin wax embedded tissues for light microscopy

Refer to Chapter 4, Section 2.2

2.3.2 Frozen tissues for immunofluorescence light microscopy

Rats were euthanized by lethal injection of anaesthetic and the soleus muscle removed and snap-frozen in isopentane at -40^{0}C. Frozen tissues were embedded in OCT medium (Agar Scientific, Stanstead, Essex, UK), and sectioned longitudinally in a cryostat at 8-10µm. Sections were fixed in acetone for 5 minutes before storing at -20^{0}C.

3 Optimisation of passive transfer EAMG in the Lewis rat

3.1 Purification of rat anti-nAChR mAb35 from tissue culture supernatant

3.1.1 Background

mAb35 is a rat anti-*Electrophorus electricus* electric organ muscle-type nAChR antibody, of an IgG1 isotype (Tzartos, Rand et al. 1981). mAb35 binds the main immunogenic region (MIR) of the alpha subunit of muscle nAChR and cross-reacts with chicken, rat, mouse and human nAChR. It does not block their function, and has high affinity for native receptors, but low affinity for denatured receptors, thus limiting its use in Western blotting. The circulating half life is approximately 20 days (Prof. J. Lindstrom, personal communication, 2006). It is derived from hybridoma TIB-175 obtained from the American Tissue Culture Collection (ATCC, TIB-175), which was maintained in DMEM supplemented with 10% (v/v) foetal calf serum (FCS, heat inactivated), 2mM L-glutamine and 1mM sodium pyruvate.

3.1.2 Classical Prosep A affinity chromatography

A pre-column was prepared for removal of fine particles and non-specific sepharose binding contamination, by pouring sepharose 4B (Amersham Pharmacia) slurry into a column (approx. 2.5cm diameter, column bed height of approx. 3cm), which was washed with 10 CV of PBS to remove preservative. Cell culture supernatant was periodically collected, centrifuged at 1000g for 10minutes and sodium azide added as a preservative at 0.1% (w/v). The supernatant was stored at 4^{0}C until use. All purification was subsequently performed at 4°C. Following washing with 10 CV of PBS, the pre-column was connected in line with the Prosep A column (Amersham Pharmacia). The supernatant was passed through

both columns by gravity flow, which was then washed with PBS until no further protein was detected by Coomassie assay. Protein was eluted using 0.1M glycine, pH 2.5. The eluate was neutralised with 1M Tris-HCl, pH7 and dialysed overnight against PBS. The preparation was concentrated using an Amicon system, and protein concentration was determined by absorbance at 280nm.

3.1.3 Glycine-citrate Prosep A affinity chromatography

An alternative strategy for purification of mAb35 was attempted to eliminate bovine immunoglobulin (Ig) contamination remaining following classical methods.

The cell culture supernatant was centrifuged to remove cellular debris, and mixed 1:1 in glycine buffer (1M glycine, 0.15M NaCl, pH 8.6). The columns were pre-equilibrated in this buffer, and the mixed supernatant was applied. After loading, the column was washed in glycine buffer, and eluted in citrate buffer (0.1M citrate). A series of pH steps from 3-6 were used to determine the efficiency of elution, and a sample from each fraction was probed by dot blot for bovine Ig contamination, as well as for rat Ig. The dot blot revealed that most of the rat Ig was eluted at pH 5, while bovine Ig was preferentially eluted at pH 3.

Fractions containing mAb35 were pooled, concentrated and dialysed as described previously. SDS-PAGE and Western blotting was used to confirm the purity of mAb35.

3.1.4 Results

SDS-PAGE and Coomassie staining of mAb35 from classical prosep A runs revealed 3 major bands under non-reducing conditions at approximately 150kDa, which reduced to 2 bands at 50 and 25 kDa (Figure 1, Run 1), presumably corresponding to bovine Ig. Upon implementation of the glycine-citrate method, 1 band was detected at approximately 150kDa under non-reducing conditions following Coomassie staining. This reduced down to 50kDa and 25kDa corresponding to the heavy and light Ig chains (Figure 1, Run 2).

To confirm the identity of contaminants, SDS-PAGE and Western blotting of samples from both runs under non-reducing conditions was performed as described previously. Blots were probed with anti-bovine Ig-HRPO and anti-rat Ig-HRPO conjugates at 1:1000 in block buffer. Classical purification methods resulted in relatively high bovine Ig contamination (Figure 2, Run 1). Implementation of the glycine-citrate method virtually eliminated the bovine Ig contamination with only a faint bad detected at approximately 150kDa when probed with α-bovine-HRPO (Figure 2, Run 2).

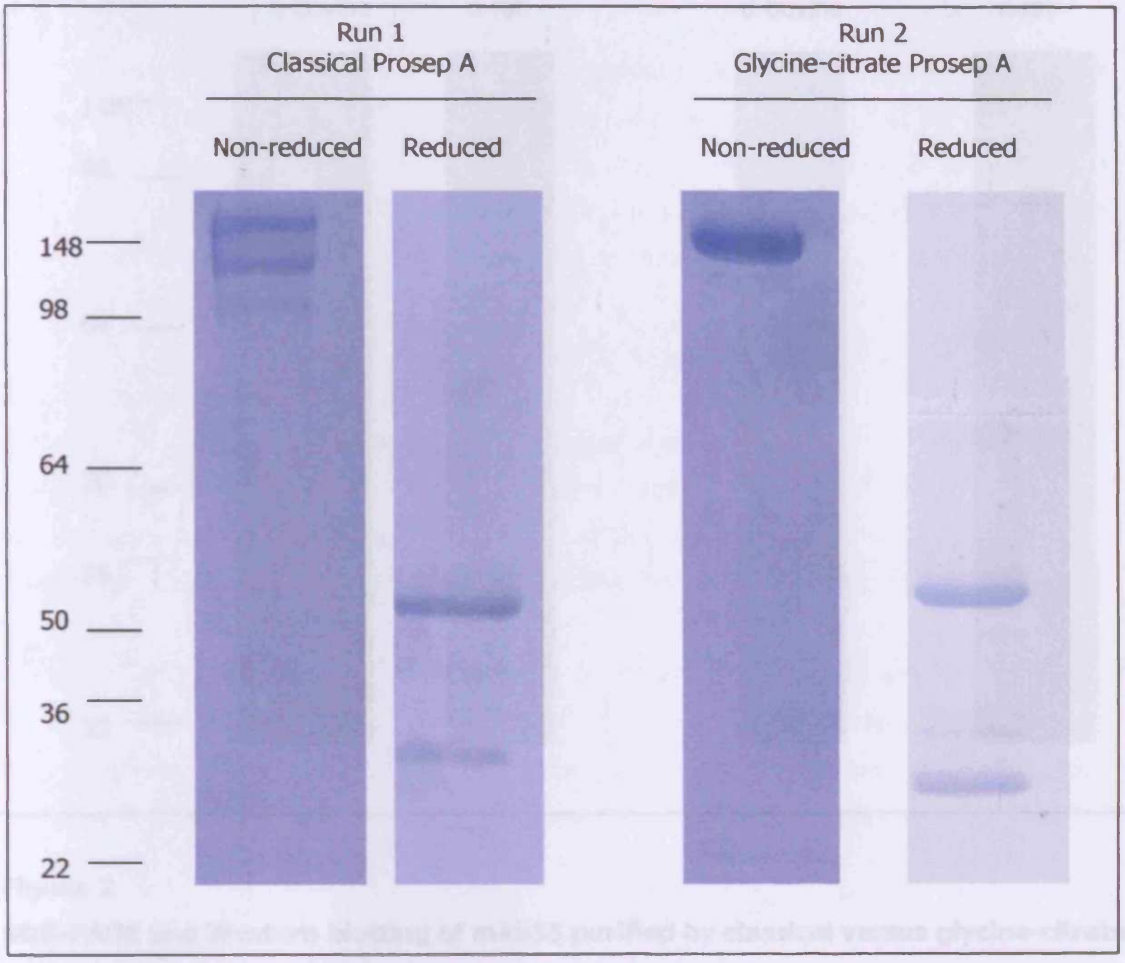

Figure 1

SDS-PAGE and Coomassie staining of mAb35 purified by Prosep A affinity purification versus glycine-citrate affinity purification

Samples of mAb35 from classical (run 1) and glycine-citrate Prosep A (run 2) were separated by SDS-PAGE on a 7.5% SDS-PAGE gel under non-reducing and reducing conditions, and Coomassie-stained as described.

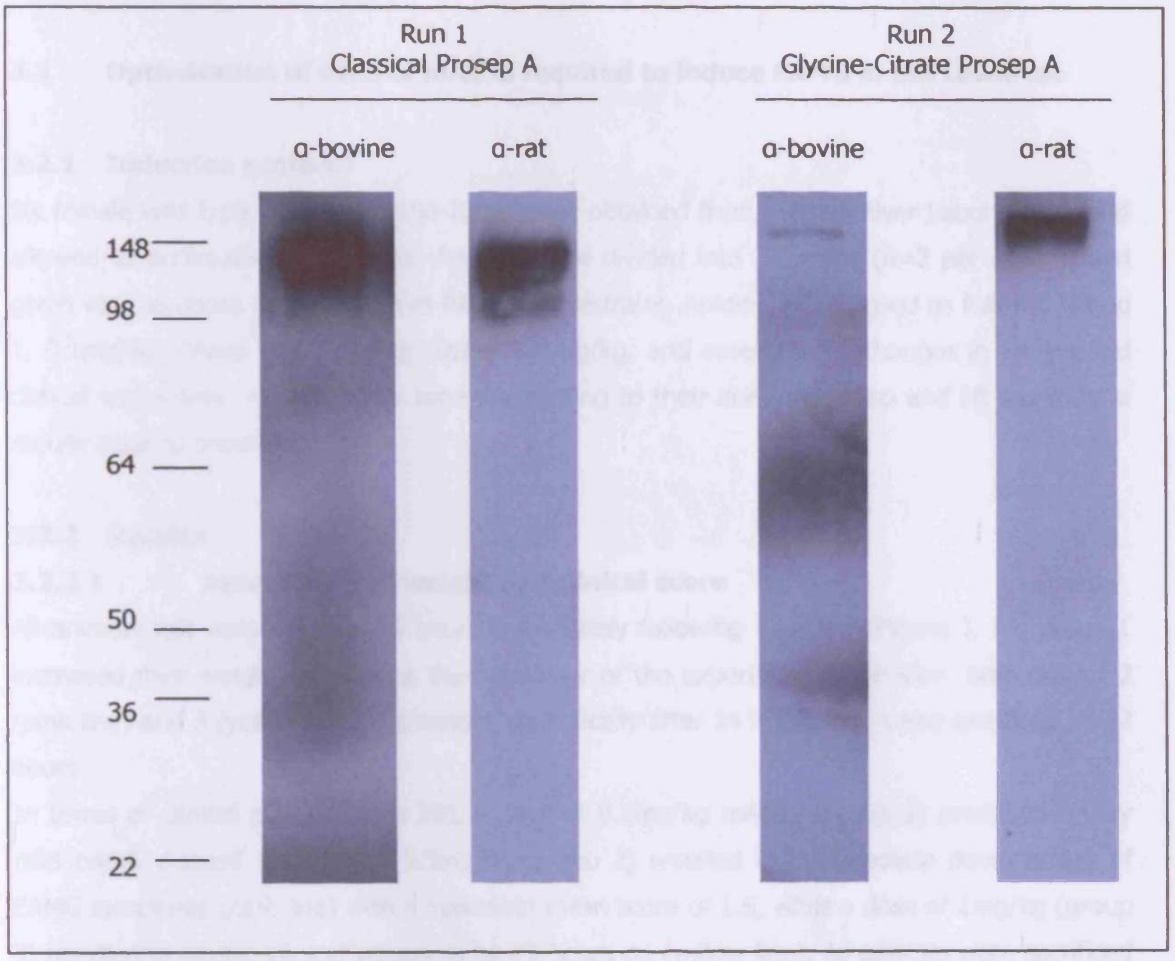

Figure 2

SDS-PAGE and Western blotting of mAb35 purified by classical versus glycine-citrate prosep A affinity chromatography

Samples of mAb35 from classical (run 1) and glycine-citrate Prosep A (run 2) were separated by SDS-PAGE on a 7.5% SDS-PAGE gel under non-reducing conditions, and transferred to nitrocellulose using standard methods. Blots were probed with anti-bovine Ig-HRPO or anti-rat Ig-HRPO conjugates at 1:1000 dilution in PBS, 5% (w/v) milk, and detected as described.

3.2 Optimisation of dose of mAb35 required to induce EAMG in the Lewis rat

3.2.1 Induction protocol

Six female wild type Lewis rats (160-200g) were obtained from Charles River Laboratories, and allowed to acclimatise for 1 week. Animals were divided into 3 groups (n=2 per group), and given various doses of mAb35 i.p in PBS under restraint. Animals were dosed as follows; Group 1, 0.1mg/kg; Group 2, 0.5mg/kg; Group 3, 1mg/kg, and assessed for changes in weight and clinical score daily. Animals were scored according to their ability to grasp and lift the lid of a mouse cage as described.

3.2.2 Results

3.2.2.1 Assessment of weight and clinical score

All animals lost weight in the 24 hours immediately following injection (Figure 3, A); group 1 increased their weight throughout the remainder of the experiment (blue line). Both groups 2 (pink line) and 3 (yellow line) lost weight dramatically after 24 hours, and were sacrificed by 72 hours.

In terms of clinical score (Figure 3B), a dose of 0.1mg/kg mAb35 (group 1) produced a very mild EAMG disease (blue line); 0.5mg/kg (group 2) resulted in intermediate development of EAMG symptoms (pink line) with a maximum mean score of 1.5, while a dose of 1mg/kg (group 3) resulted in severe clinical weakness by 72 hours p.i (yellow line). All animals were sacrificed at 72 hours p.i.

3.2.3 Discussion

A dose of 1mg/kg was deemed sufficient to induce severe clinical EAMG in subsequent experiments.

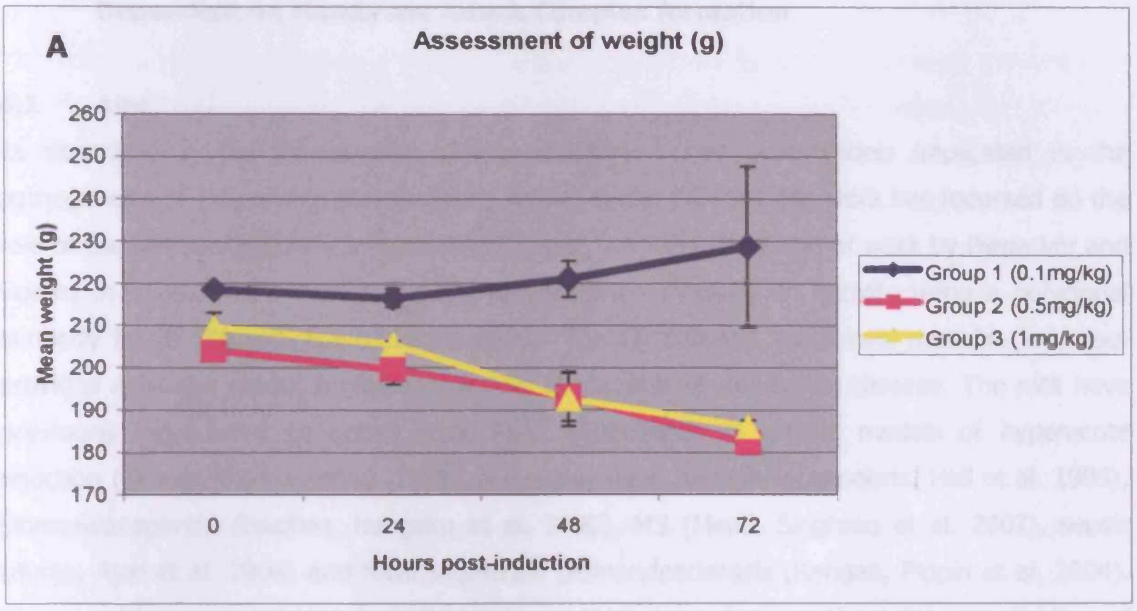

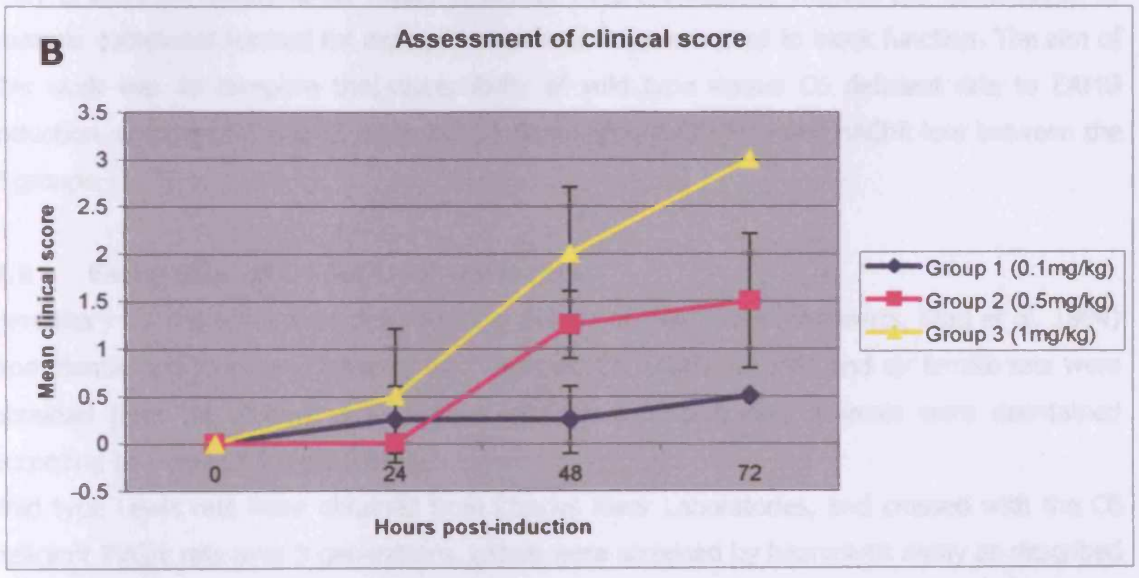

Figure 3

Assessment of weight and clinical score in dose response of mAb35

Female Lewis rats (160-200g) were subjected to a dose response of mAb35 in PBS (IP), and assessed daily in terms of weight (A), and clinical score (B). Data shown were the mean values (n=2) for each dose group, and error bars indicated the standard deviation.

4 Experimental Autoimmune Myasthenia Gravis (EAMG) in the Rat is Dependent on Membrane Attack Complex formation

4.1 Aim

As described in the introduction to this chapter, C has been widely implicated in the pathogenesis of MG, and in its associated animal model EAMG. Little work has focussed on the role of the terminal pathway in mediating disease, with the exception of work by Biesecker and Gomez in 1989. EAMG was completely prevented by blocking C6 activity using a polyclonal antibody to C6 (Biesecker and Gomez 1989). The C6 deficient rat colony available in-house, provides a unique model to assess the role of the MAC in mediating disease. The rats have previously been used to demonstrate MAC dependence in animal models of hyperacute rejection (Brauer, Baldwin et al. 1993), active Heymann nephritis (Leenaerts, Hall et al. 1995), glomerulonephritis (Hughes, Nangaku et al. 2000), MS (Mead, Singhrao et al. 2002), sepsis (Buras, Rice et al. 2004) and focal segmental glomerulosclerosis (Rangan, Pippin et al. 2004). They provide an experimental model to assess MAC dependence without the complication of immune complexes formed for example when antibodies are used to block function. The aim of this work was to compare the susceptibility of wild type versus C6 deficient rats to EAMG induction, compare C3 and C9 deposition, inflammatory infiltration and nAChR loss between the 2 groups.

4.2 Generation of C6 deficient Lewis rats

Hereditary C6 deficiency was described in a colony of PVG/c rats (Leenaerts, Stad et al. 1994) from Bantin and Kingman Universal Inc (Fremont, CA, USA). Six male and six female rats were obtained from this colony and bred to establish a local colony. Animals were maintained according to Home Office guidelines.

Wild type Lewis rats were obtained from Charles River Laboratories, and crossed with the C6 deficient PVG/c rats over 8 generations. Litters were screened by haemolytic assay as described previously, and a local colony was established. It is not known if Lewis C6 deficient rats are egentically identical to wild type Lewis with the exception of that locus. However, the functional role of C6 will be tested by reconstitution of Lewis C6 deficient rats with human C6.

4.3 Induction protocol

Six female Lewis rats (160-200g) were obtained from Charles River Laboratories, and allowed to acclimatise for 1 week. Five female C6 deficient Lewis rats (160-200g) were obtained from BSU. All animals were injected with 1mg/kg mAb35 in PBS (IP) on day 0, and assessed for changes in weight and clinical score as described previously.

4.4 Results

4.4.1 Assessment of weight and clinical score

There was a dramatic difference in the clinical manifestations of disease between the wild type and C6 deficient Lewis rats. Wild type animals began to lose weight consistently by 20 hours post-induction (Figure 4A, blue line), while C6 deficient animals, following a brief reduction in weight at 24 hours post-induction, continued to gain weight for the remainder of the experiment (pink line).

Wild type animals began to display clinical symptoms by 20 hours post-induction, resulting in severe clinical weakness by 41 hours p.i. (Figure 4B, blue line). In contrast, all C6 deficient animals were protected from any clinical manifestations of EAMG for the duration of the experiment (pink line).

The striking differences in clinical manifestation of EAMG were illustrated by photographs taken at 32 hours p.i. (Figure 5). The wild type animal displayed a limp tail, extreme pilo-erection, an inability to grip and lift the lid of a mouse cage, progressing to hind limb weakness, and partial paralysis of the hind limbs, and was given a score of 3.5 (photograph A). In complete contrast, the C6 deficient animal was protected from clinical disease, and remained healthy throughout the course of the experiment. The coat remained glossy, and ability to grip and lift the lid of a mouse cage was unaffected (photograph B). Wild type rats were sacrificed when clinical score reached 3-4 (41 hours p.i.; n=4).

4.4.1.1 Time points for tissue analysis

Wild type animals were sacrificed at 41 hours p.i. One representative C6 deficient rat, demonstrating no clinical symptoms, was also sacrificed at this time to for histological comparison. Remaining C6 deficient rats were sacrificed at the end of the experiment at day 7.

4.4.2 Quantification of bungarotoxin-reactive nAChR

4.4.2.1 Method

Soleus muscle was isolated from freshly euthanized rats following lethal injection, subjected to flash freezing in isopentane cooled on dry ice, and stored at -80^{0}C. Ten micrometer thin sections were cut on a cryostat, and transferred to Superfrost slides (Surgipath, UK). Sections were fixed in neat acetone for 5 minutes, and stored at -20^{0}C until use.

BuTx-rhodamine conjugate (T-1175, Molecular Probes, Invitrogen, Paisley, UK) was used to identify the nAChR, and provided a tool with which to evaluate the numbers of BuTx-reactive nAChR from comparable sections from each animal.

Briefly, BuTx-rhodamine was diluted to 1:200 in block buffer (PBS, 1% (w/v) BSA), and incubated for 40 minutes at room temperature in a humid chamber. Following 3 washes in PBS, sections were mounted using VectorShield, and analysed under a fluorescent microscope.

The density slicing function of the Openlab software (Improvision) was used to calculate the number of areas occupied by Bu-Tx-reactive nAChR in each section. Twenty fields were

captured from soleus muscle sections of each sample at the same exposure and magnification. Conditions imposed to ensure reproducibility were that fields were taken from a comparable area from within the soleus muscle in each animal, and that each field contained at least 2 Bu-Tx-reactive areas. Intensity limits were optimised, and density slicing was employed to identify the number of BuTx-reactive areas (Figure 6).

4.4.2.2 Results

Wild type animals had fewer BuTx-reactive nAChR compared with C6 deficient animals (Figure 7), and this difference was highly significant (Student's unpaired t test $p < 0.0001$). Statistical analysis was performed using InStat (GraphPad software, Inc.). No significant differences were observed in numbers of BuTx-reactive AChR between the C6 deficient animal sacrificed at 41 hours p.i. compared to those sacrificed at the end of the experiment at day 7, thus all animals were included in analysis regardless of time point at which sacrificed.

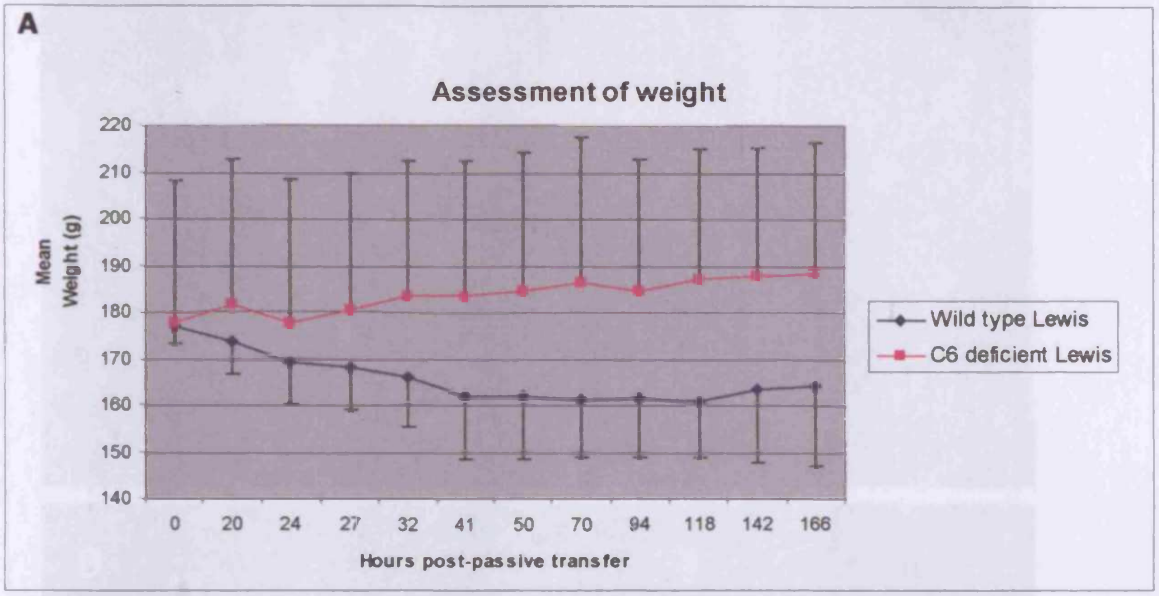

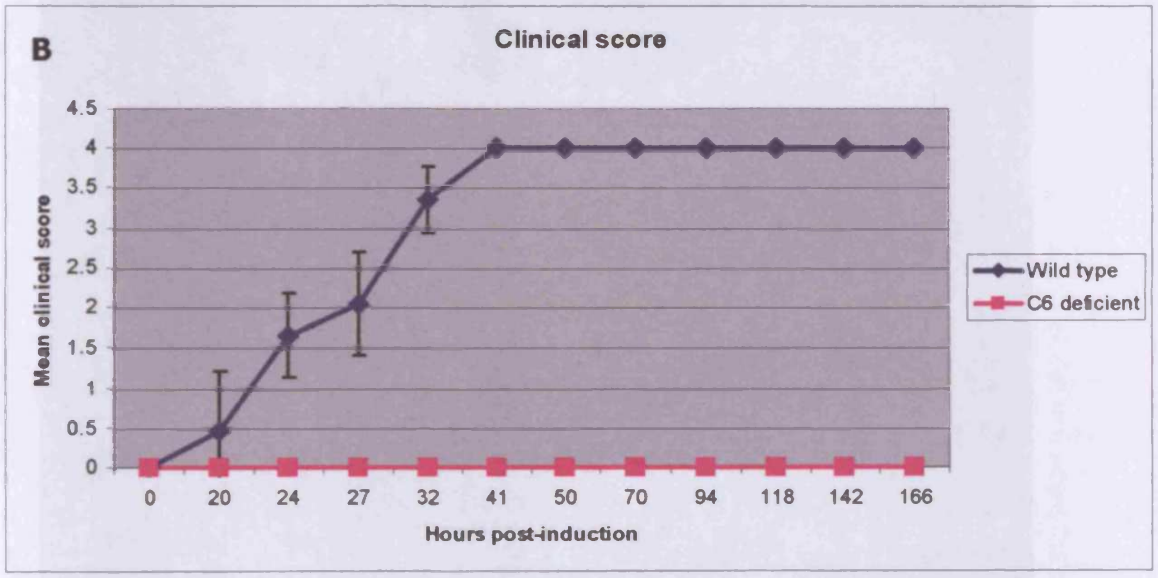

Figure 4

Assessment of weight and clinical in wild type versus C6 deficient Lewis rats following induction of EAMG

Wild type female Lewis rats (160-200g) and C6 deficient Lewis rats were injected with 1mg/kg mAb35 in PBS (IP), and assessed daily in terms of weight (A), and clinical score (B). Data presented represent mean values. Error bars represent standard deviation.

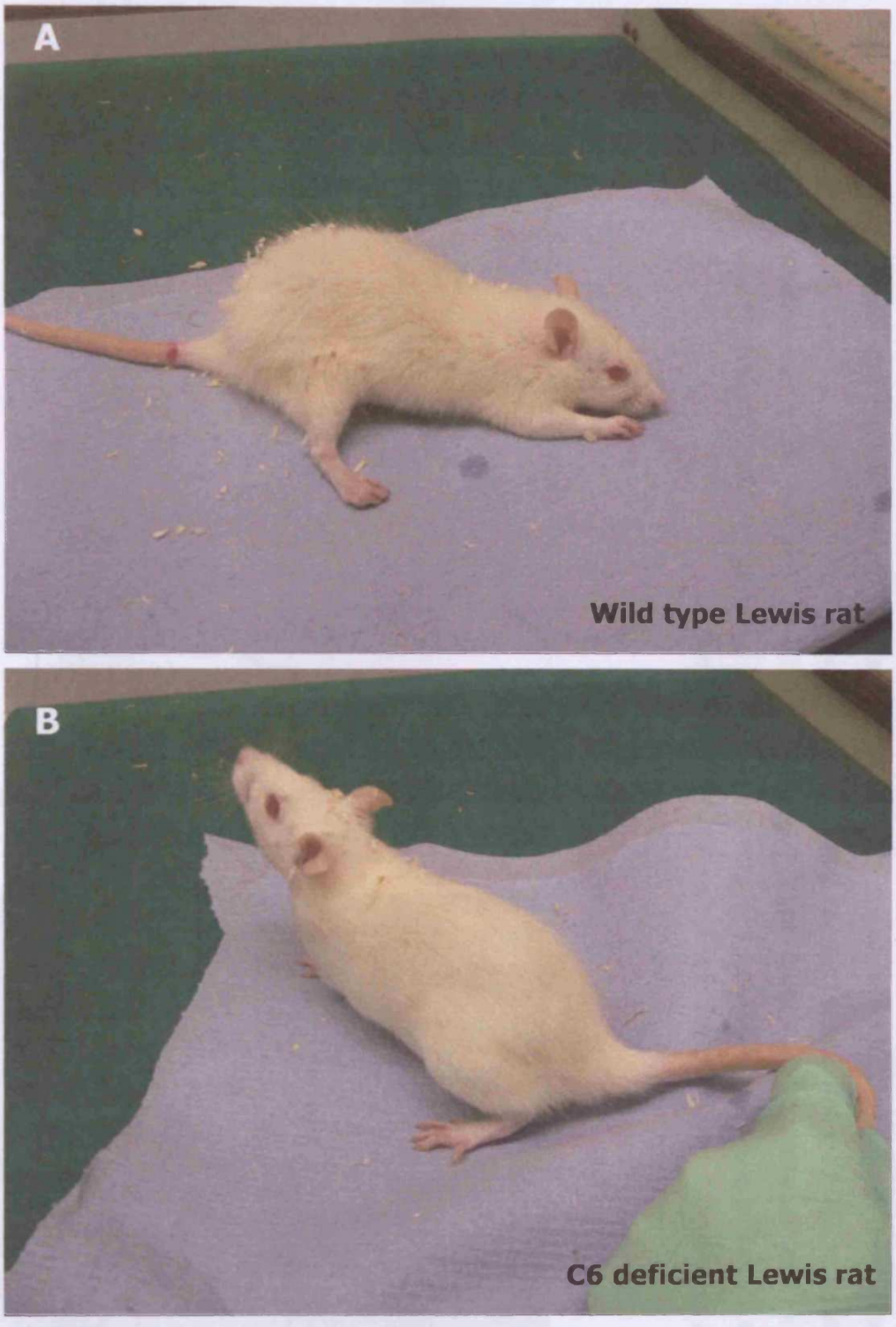

Figure 5

Clinical manifestation of passively induced EAMG in wild type versus C6 deficient Lewis rats

Following injection of mAb35, wild type animals begin to display clinical symptoms of EAMG; at 32 hours p.i., wild type animal 1 showed extreme piloerection and wasting, an inability to grip and lift the lid of a mouse cage, followed by hind limb weakness with partial hind limb paralysis as demonstrated in photograph A, and given a score of 3.5.

In contrast, C6 deficient rats did not show any clinical manifestations of disease; coats remained glossy, the ability to grip and lift the lid of a mouse cage was unaffected (photograph B).

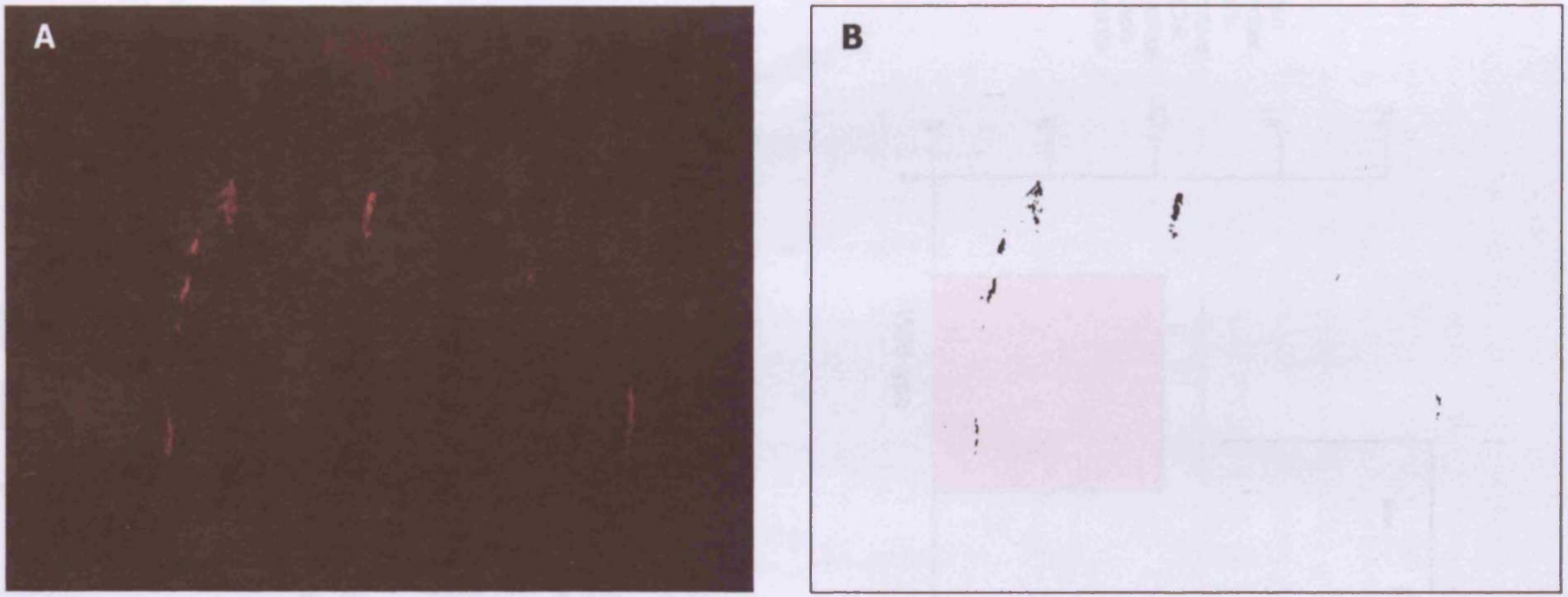

Figure 6

Evaluation of numbers of BuTx-reactive nAChR in rat soleus muscle using density slicing

Soleus muscle sections were cut from each rat, and stained with BuTx-rhodamine to identify nAChR as described (A). Using OpenLab software by Improvision, intensity limits were set, corresponding to positively stained nAChR, and the image was density-sliced (B). Measurements were made on the sliced image, of numbers of discrete areas identified. Twenty fields from each rat were analysed. Inclusion of a field for measurement required at least 2 BuTx-reactive areas to allow comparison between animals. The mean number of discrete areas was obtained for each rat, and subjected to statistical testing using InStat (GraphPad software, Inc.)

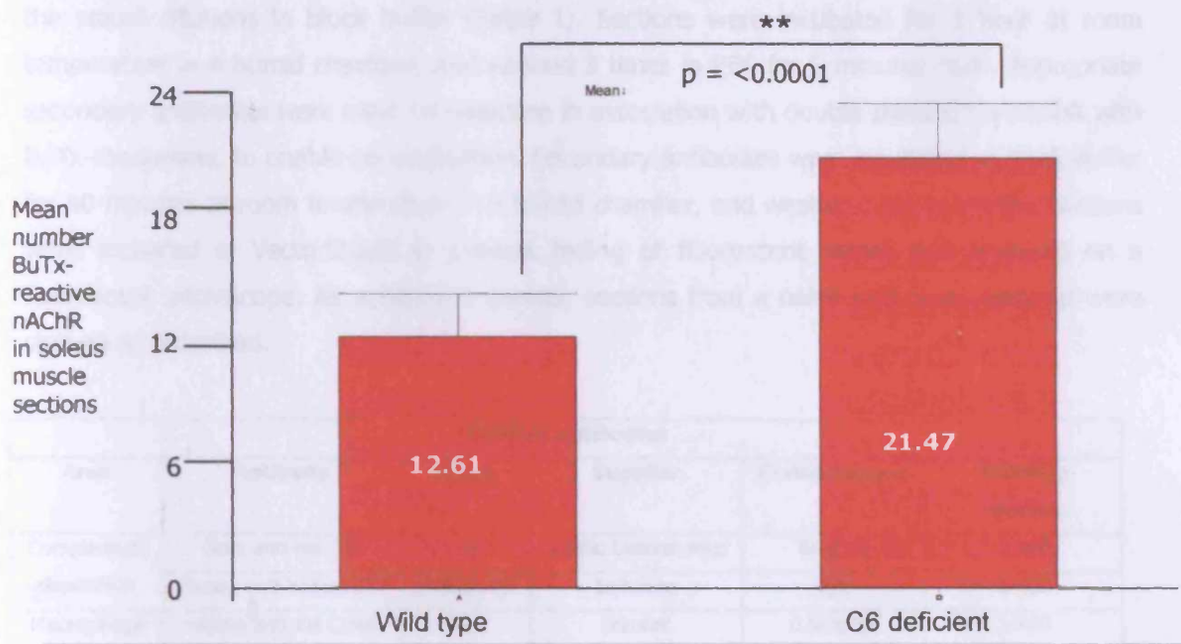

Figure 7

Assessment of total numbers of BuTx-reactive nAChR in wild type versus C6 deficient Lewis rats following EAMG induction

Soleus muscles were harvested, and sections were prepared as described. BuTx-rhodamine was used to label nAChR as described, and density slicing was performed to assess the total number of BuTx-reactive nAChR in wild type (n=6, 12.61) versus C6 deficient (n=5, 21.47) rats using Openlab software. Statistical tests were used to determine the significance of differences observed between the means of the 2 groups (Student's unpaired t test) using InStat software. Error bars represent standard deviation.

4.4.3 Visualisation of C deposition at the nAChR

4.4.3.1 Method

Frozen sections were prepared as described previously, and stained with the listed antibodies at the stated dilutions in block buffer (Table 1). Sections were incubated for 1 hour at room temperature in a humid chamber, and washed 3 times in PBS for 5 minutes each. Appropriate secondary antibodies were used for detection in association with double staining for nAChR with BuTx-rhodamine, to enable co-localisation. Secondary antibodies were incubated in block buffer for 40 minutes at room temperature in a humid chamber, and washed 3 times in PBS. Sections were mounted in VectorShield to prevent fading of fluorescent signal, and analysed on a fluorescent microscope. As a negative control, sections from a naive wild type Lewis rat were stained as described.

Primary antibodies					
Area	**Antibody**	**Clone**	**Supplier**	**Concentration**	**Working dilution**
Complement deposition	Goat anti-rat C3c	C3c	Nordic Laboratories	8mg/ml	1:400
	Sheep anti-human C9	Human C9	In-house	n/a	1:400
Macrophage infiltration	mouse anti-rat CD68	ED1	Serotec	0.5mg/ml	1:400
Complement regulators	Mouse anti-rat CD55	RDIII7	In-house	4.5mg/ml	1:100
	Mouse anti-rat CD59	6D1	In-house	5mg/ml	1:100
	Mouse anti-rat Crry	TLD1C11	In-house	2.8mg/ml	1:100
	Mouse anti-rat CD46	MM.1	In-house	2mg/ml	1:200
Secondary antibodies					
	Donkey anti-mouse Ig-FITC	715-096-151	Jacksons	1.4mg/ml	1:200
	Donkey anti-goat/sheep Ig-FITC	713-096-147	Jacksons	1.5mg/ml	1:200

Table 1

Identification of primary and secondary antibodies used for histological examination of soleus muscles from EAMG-induced rats

4.4.3.2 Results

C3 deposition

BuTx-reactive nAChR were visible in all animals (Figure 8; wild type A; C6 deficient D; naïve G). However, C3 deposition was only detected in animals subjected to induction of EAMG (white arrows, wild type panel B; C6 deficient panel E), and not in the naïve wild type animal (panel H). Merged images showed complete co-localisation of C3 deposition, if present, at the nAChR (wild type panel C; C6 deficient panel F).

Figure 8

Assessment of C3 deposition at the nAChR in wild type, C6 deficient and naïve Lewis rats

Soleus muscle from wild type (A-C) and C6 deficient (D-F) Lewis rats induced for EAMG, and a naïve rat (G-I) were harvested, and flash frozen in isopentane as described. Ten micrometer thin sections were cut and stained for nAChR (A, D, G) using rhodamine-conjugated BuTx. Sections were double-stained for activated C3 (C3c; B, E, H) using goat anti-rat C3c, and detected with donkey anti-goat-Ig-FITC conjugate. Sections were mounted in VectorShield, and analysed under an inverted fluorescent microscope. Images were merged for detection of colocalisation (C, F, I).

All images were taken at 400X magnification.

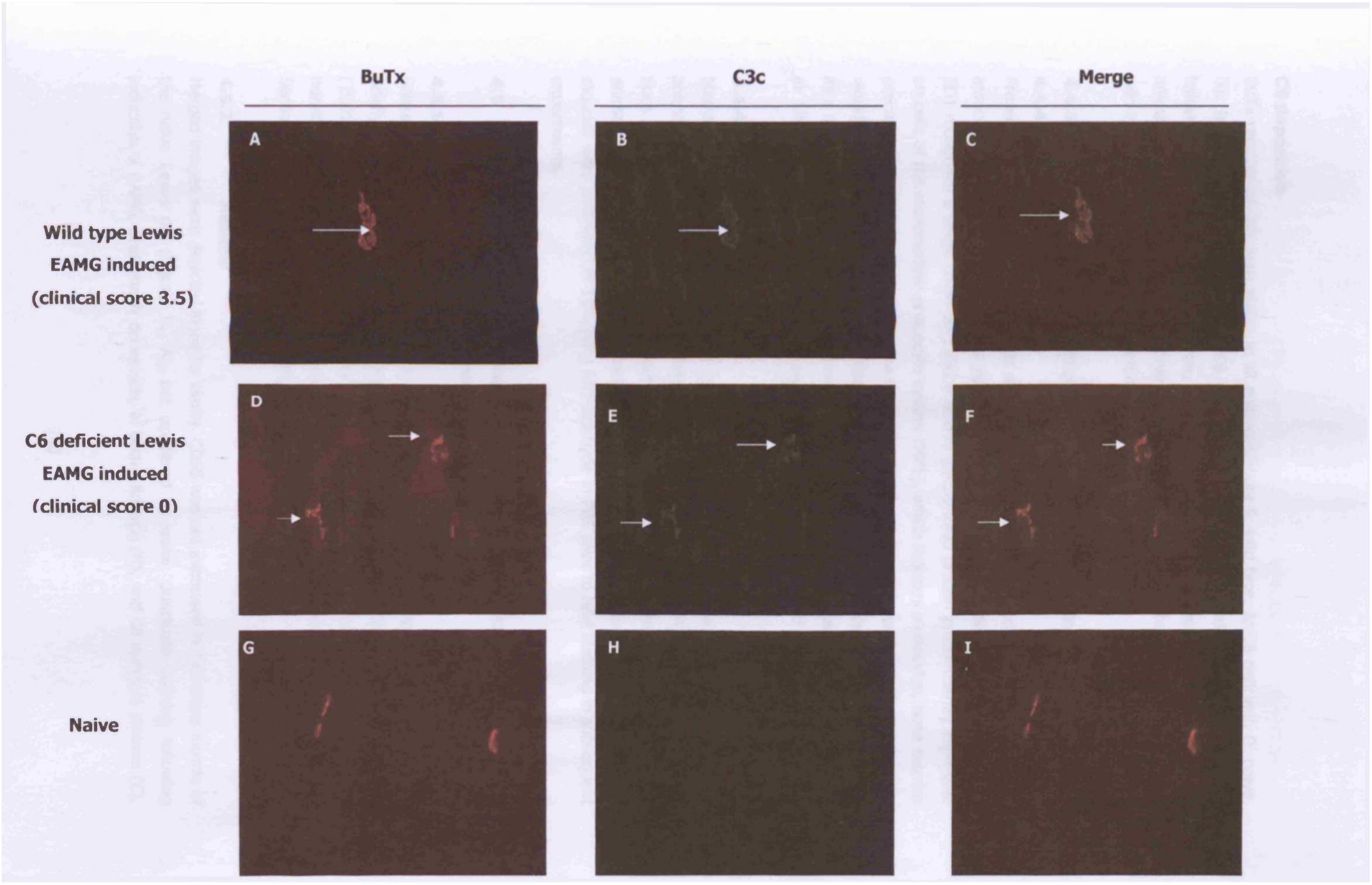
BuTx
C3c
Merge
Wild type Lewis
EAMG induced
(clinical score 3.5)
C6 deficient Lewis
EAMG induced
(clinical score 0)
Naive
A
B
C
D
E
F
G
H
I

C9 deposition

BuTx-reactive nAChR were visible in all animals (Figure 9; wild type, A; C6 deficient, D; naïve, G). In contrast to C3 deposition, C9 was only evident at the nAChR in wild type animals following EAMG induction (white arrow, B). No C9 positive staining was present in C6 deficient animals following EAMG induction either at the nAChR or throughout the muscle (E). The naïve wild type animals were also negative for C9 (H).

4.4.4 Detection of inflammatory cell infiltration within the soleus muscle

4.4.4.1 Methods

Frozen sections from soleus muscle were stained for CD68 using clone ED1 (Table 1) in association with BuTx-rhodamine as described, and analysed on a fluorescence microscope. ED1 recognises a single chain 90-110kDa heavily glycosylated protein predominantly expressed on cells of the mononuclear phagocyte system (MPS), which includes monocytes, bone marrow precursors and most free and tissue-fixed macrophages. Granulocytes and fibroblasts may weakly express ED1 upon activation (Serotec datasheet, MCA 341). However, it is widely used as a marker of rat macrophages, and numerous studies support this use (Damoiseaux, Dopp et al. 1994). In addition, frozen sections were stained by H&E as described previously.

4.4.4.2 Results

Massive macrophage infiltration was evident throughout the soleus muscle of the wild type animal confirmed by ED1 staining by immunofluorescence (Figure 10, A) and H&E staining (B). Such infiltration was minimal in C6 deficient animals (C,D), and absent from naïve wild type animals (E, F). It was clear that frozen sections did not give good quality H&E staining, and muscles were post-fixed in 10% (v/v) formaldehyde in PBS prior to H&E staining in subsequent experiments.

4.5 Analysis of CReg expression following induction of EAMG in wild type, C6 deficient and naïve Lewis rats

4.5.1 Method

Soleus muscle sections were stained for membrane-bound CRegs as described previously. Briefly, sections were incubated with anti-rat CD55 (RDIII7), anti-rat CD59 (6D1), anti-rat Crry (TLD1C11) and anti-rat CD46 (MM.1) at optimal pre-determined dilutions, for 1 hour at R.T in a humid chamber, and processed as described using FITC-conjugated secondary antibodies. Sections were double-stained for nAChR with Bu-Tx-rhodamine.

4.5.2 Results

Merged images were depicted alone for clarity. CD55 was not expressed in the soleus muscle of the naïve Lewis rat (Figure 11, A), but appeared as weak, punctuate staining following induction of EAMG, presumably on vessels, in both wild type (B), and C6 deficient animals (C).

CD59 was highly expressed within the naïve muscle (D), and remained so in both wild type (E) and C6 deficient animals following disease induction (F). A degree of co-localisation existed with the nAChR in all sets of animals (white arrows, D, E, F) suggesting the presence of CD59 at the endplate. Crry was weakly expressed in naïve muscle (G), and no differences were detected in wild type muscle (H) and C6 deficient (I) animals following EAMG induction. CD46 was not expressed in the soleus muscle of naïve (J), wild type (K) or C6 deficient (L) animals.

Figure 9

Assessment of C9 deposition at the nAChR in wild type, C6 deficient and naïve Lewis rats

Soleus muscle from wild type (A-C) and C6 deficient (D-F) Lewis rats induced for EAMG, and a naïve rat (G-I) were harvested, and flash frozen in isopentane as described. Ten micrometer thin sections were cut and stained for nAChR (A, D, G) using rhodamine-conjugated BuTx. Sections were double-stained for C9 (C3c; B, E, H) using sheep anti-human C9, and detected with donkey anti-goat-Ig-FITC conjugate. Sections were mounted in VectorShield, and analysed under an inverted fluorescent microscope. Images were merged for detection of colocalisation (C, F, I).

All images were taken at 400X magnification.

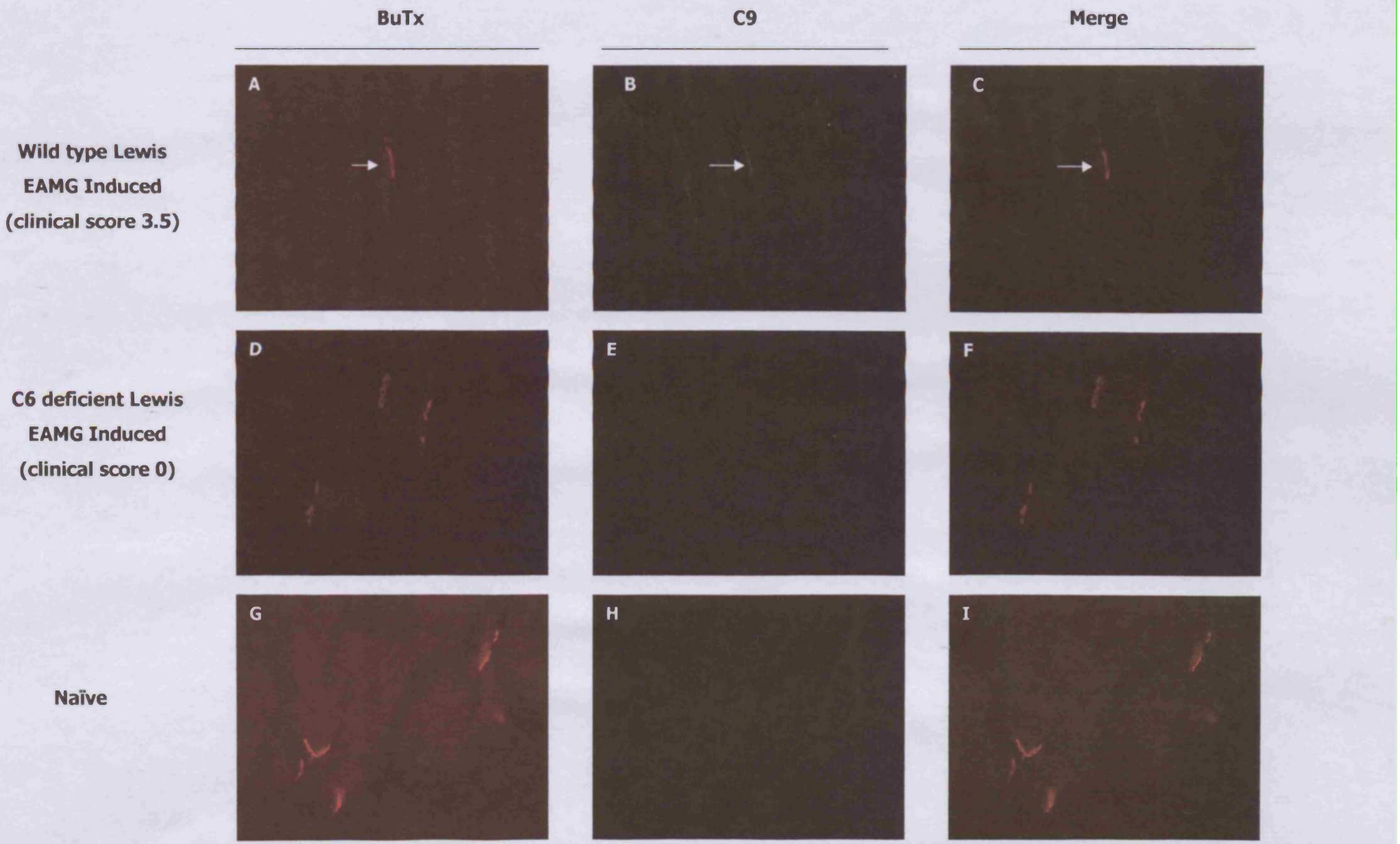
BuTx
C9
Merge
Wild type Lewis
EAMG Induced
(clinical score 3.5)
C6 deficient Lewis
EAMG Induced
(clinical score 0)
Naïve
A
B
C
D
E
F
G
H
I

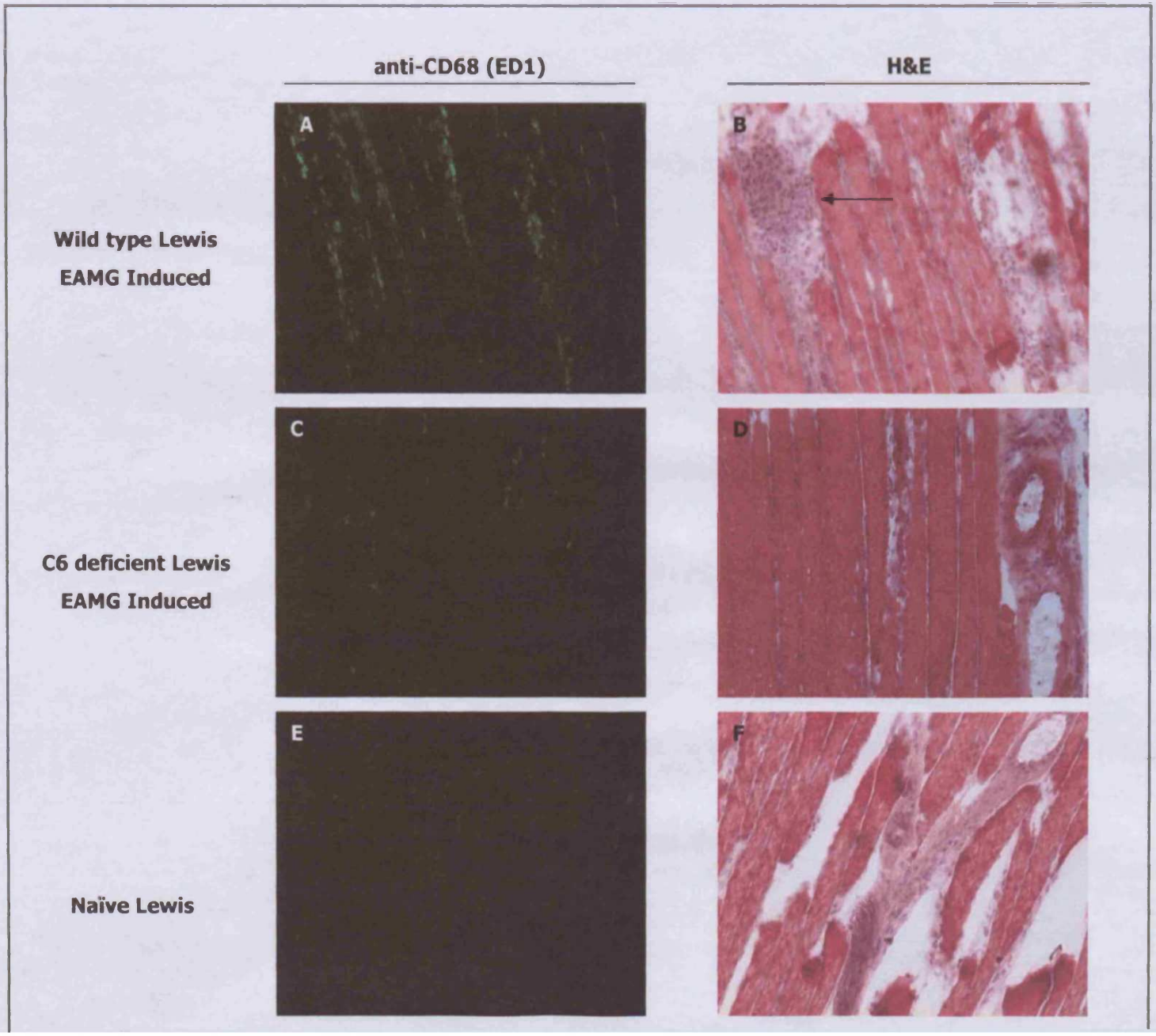

Figure 10

Assessment of inflammatory cell infiltration in wild type, C6 deficient and naïve Lewis rats

Frozen soleus muscle sections were stained with mouse anti-rat CD68 (ED1, wild type panel A; C6 deficient panel C; naïve panel E), and H&E stained (wild type panel B, arrow=inflammatory infiltrate; C6 deficient panel D; naïve panel F) to confirm the presence of macrophages within the muscle.

All images were taken at 200X magnification

Figure 11

Analysis of CReg expression in naive soleus muscle and wild type versus C6 deficient soleus following EAMG induction

Soleus muscle sections were stained for membrane-bound CRegs as described previously. Briefly, sections were incubated with anti-rat CD55 (RDIII7), anti-rat CD59 (6D1), anti-rat Crry (TLD1C11) and anti-rat CD46 (MM.1) at optimal pre-determined dilutions, for 1 hour at RT in a humid chamber, and processed as described using FITC-conjugated secondary antibodies. Sections were double-stained for nAChR with Bu-Tx-rhodamine as described to detect expression of CReg at the endplate. Merged images only were depicted in Figure 10.

All images were taken at 400X magnification.

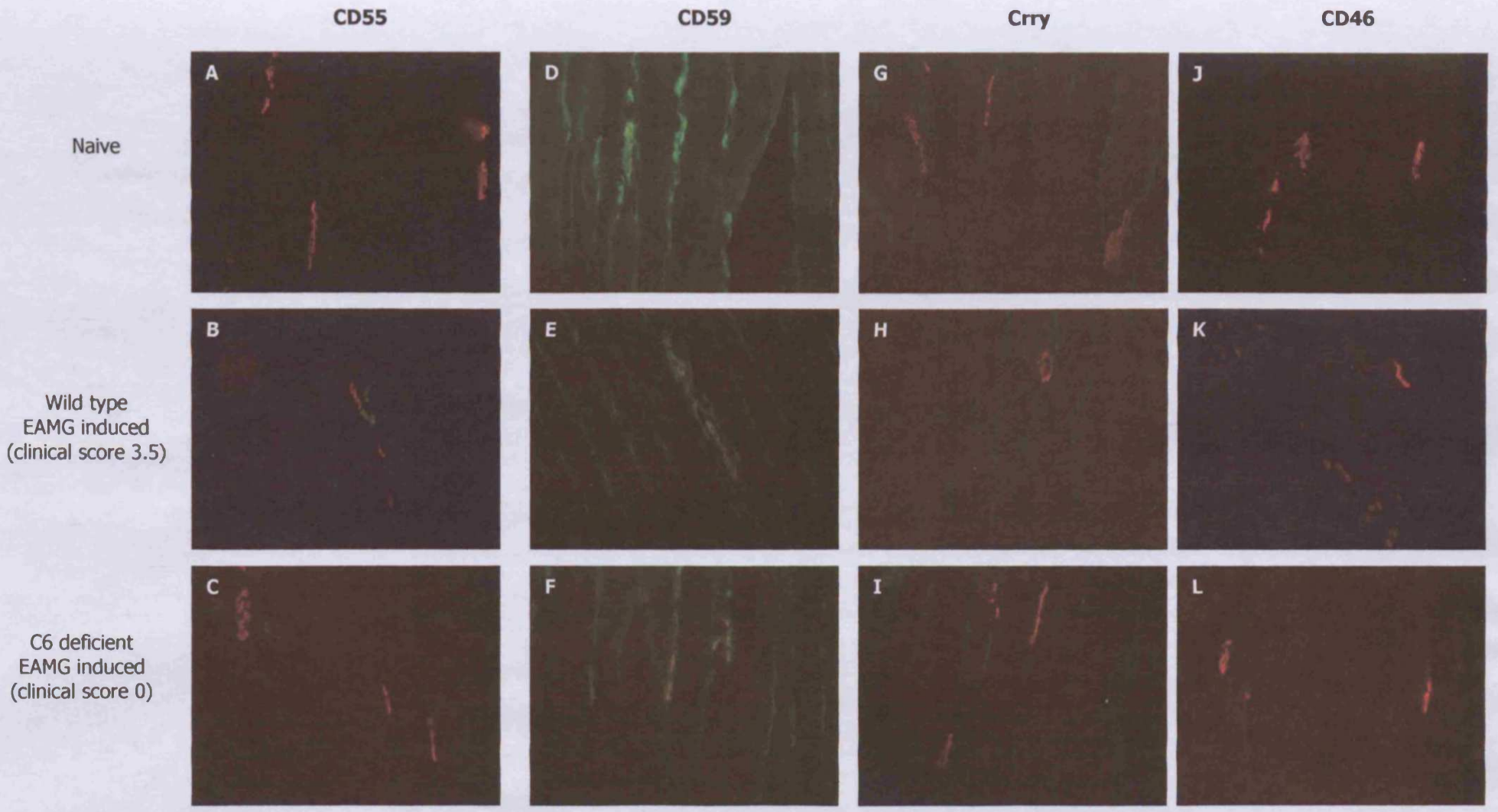
CD55
CD59
Crry
CD46
Naive
Wild type
EAMG induced
(clinical score 3.5)
C6 deficient
EAMG induced
(clinical score 0)
A
B
C
D
E
F
G
H
I
J
K
L

4.6 Reconstitution of C6 restores clinical manifestations of disease in C6 deficient Lewis rats following induction of EAMG

4.6.1 Aim

To confirm that C6 is the factor directly responsible for susceptibility of wild type rats to EAMG induction, human C6 was purified by affinity chromatography, and reconstituted to C6 deficient rats, thereby restoring to them a fully functional C system.

4.6.2 Purification of human C6

4.6.2.1 Preparation of anti-human C6 (FG-1) affinity column

Anti-human C6 mAb FG-1 (mouse IgG1), generated by Dr. Fiona Gagg (Dept. of Medical Biochemistry & Immunology) was purified from tissue culture supernatant using the glycine-citrate method described in Section 3.3. Purified antibody was dialysed into coupling buffer (0.1M $NaCO_3$, 0.5M NaCl, pH 8.3) overnight at 4^0C. CNBr-activated sepharose 4B (Amersham Pharmacia) was swollen and washed for 15 minutes on a sintered glass funnel with 300ml of 1mM HCl. One gram of sepharose is capable of binding 5-10mg of mAb. The swollen gel was mixed with antibody in coupling buffer and placed on a roller mixer for 1 hour at room temperature. The gel was placed in a column, and unbound antibody was removed with at least 5 CV of coupling buffer. Remaining active groups were blocked by washing the gel in 5 CV of block buffer (0.1M Tris, pH8) and standing in this solution for 2 hours at room temperature.

4.6.2.2 Purification of human C6 by affinity chromatography

All manipulations were performed at 4^0C unless otherwise stated.

Human plasma (270ml) was obtained from the blood bank, and PMSF (1mM) was added and stirred for 30 minutes at 4^0C. Polyethylene glycol (PEG-4000) was added to give a final concentration of 5% (w/v) PEG, and further stirred for 30 minutes. The mixture was centrifuged at 15,000g for 20 minutes, the pellet discarded, and the resulting supernatant adjusted to 16% (w/v) PEG by addition of 11g PEG-4000 per 100ml supernatant. Following stirring for 30 minutes, the mixture was centrifuged at 15,000g for 20 minutes, and the pellet re-dissolved in PBS overnight with stirring.

Following a pre-elution of the affinity column with glycine (0.1M, pH 3), the column was equilibrated in PBS. The C6-enriched solution was passed twice through a pre-column connected to the affinity column. The column was washed in PBS, 0.5M NaCl, and C6 was eluted in glycine (0.1M, pH 3) into 5ml fractions containing 300µl 1M Tris for neutralisation. Fractions containing C6 were identified by haemolytic assay, pooled and concentrated using an Amicon series 8000 stirred ultrafiltration cell (Millipore, UK) with a 30kDa cut-off membrane (Millipore, UK). C6 was dialysed into PBS overnight, assessed for purity by SDS-PAGE and Coomassie staining and Western blotting, and frozen at -80^0C.

Samples (10µg for Coomassie staining; 5µg for Western blotting) were run on 7.5% SDS-PAGE gels under non-reducing and reducing conditions, and electrophoresed using standard methods. Following transfer, blots were probed with sheep anti-human C6 (Binding Site, UK) at 1:1000 dilution in PBS, 5% milk (w/v), and detected using anti-goat-Ig-HRPO-conjugate (Jackson ImmunoResearch, West Grove, PA), known to cross-react with sheep Ig.

4.6.3 Results

Purification of human C6 using the FG-1 affinity column was successful. Analysis by SDS-PAGE and Coomassie staining revealed a major band under non-reducing conditions at 98-100kDa (Figure 12, A, non-reduced), which upon reduction, migrated to approximately 110-120kDa (Figure 12, A, reduced). This phenomenon has been reported previously for C6 since reduction of disulphide bonds present cause unfolding of the protein, and reduce its rate of migration. A band was also present at approximately 150kDa under non-reducing conditions (Figure 12, A, non-reduced), which reduced to 50kDa (antibody heavy chain), corresponding to antibody leaching from the column. A second band at 25kDa (antibody light chain) would have also been visible if a higher percentage gel was run.

Western blotting confirmed that the major band detected at 98-100kDa was C6 under non-reducing and reducing conditions (Figure 12, B, non-reduced, reduced).

4.7.1 Reconstitution of C6 to C6 deficient rats

4.7.1.1 Induction protocol

Six female wild type Lewis rats (150-160g) were obtained from Charles River Laboratories. Twelve C6 deficient female Lewis rats were obtained from BSU. Animals were split into 3 groups:

Group	Genotype	Reconstituted with
A	Wild type Lewis	PBS (IP)
B	C6 deficient Lewis	PBS (IP)
C	C6 deficient Lewis	8mg/kg C6 (IP)

In a previous study of the role of the MAC in mediating EAE and associated axonal injury, C6 was reconstituted to C6 deficient PVG/c rats at 8mg/kg (Mead, Singhrao et al. 2002), thus this concentration was used in this experiment. On day 0, all animals were injected with 1mg/kg mAb35 (IP). In addition, animals were injected with PBS, or C6 as detailed above. Animals in group C were bled by tail tipping to assess their haemolytic activity at time 0, and 24 hours p.i. All animals were assessed in terms of weight and clinical score as described previously.

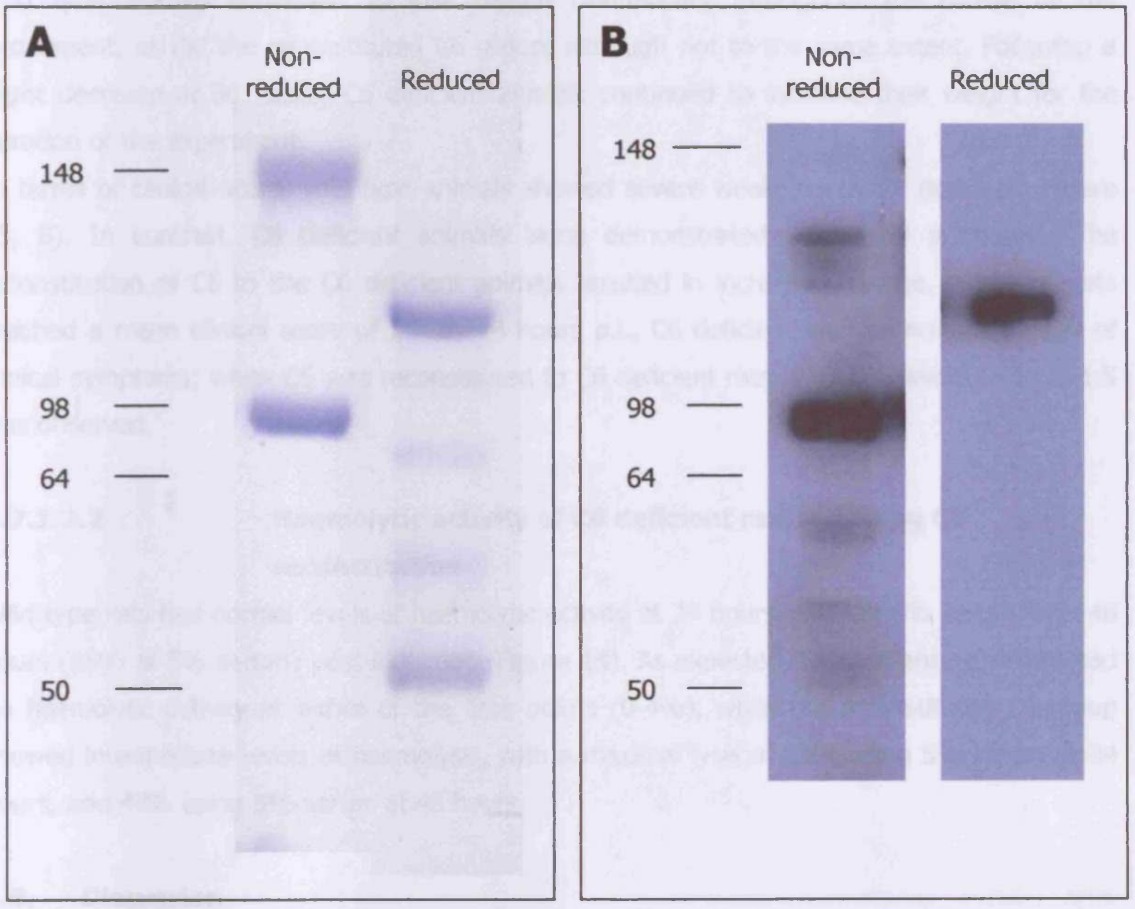

Figure 12

SDS-PAGE/ Coomassie staining and Western blotting of C6 purified by affinity chromatography

C6 was purified from human plasma as described. To assess purity, samples were subjected to SDS-PAGE and Coomassie staining (A). Ten micrograms of protein was loaded onto a 7.5% gel under non-reducing and reducing conditions, electrophoresed and Coomassie stained using standard methods.

Five micrograms of protein was loaded onto a 7.5% gel, under non-reducing and reducing conditions, and subjected to Western blotting as described. The blot was probed with sheep anti-human C6 (Binding Site, UK) at 1:1000 in PBS, 5% (w/v) milk, and detected using anti-goat-HRPO (Jacksons) at 1:1000 (B).

4.7.1.2 Results

4.7.1.2.1 Assessment of weight and clinical score

Both wild type animals and reconstituted C6 groups lost weight 24 hours p.i., (Figure 13, A). Wild type animals continued to lose weight dramatically throughout the course of the experiment, as did the reconstituted C6 group, although not to the same extent. Following a slight decrease at 30 hours, C6 deficient animals continued to increase their weight for the duration of the experiment.

In terms of clinical score, wild type animals showed severe weakness by 24 hours p.i.(Figure 13, B). In contrast, C6 deficient animals alone demonstrated no clinical symptoms. The reconstitution of C6 to the C6 deficient animals resulted in increased disease. Wild type rats reached a mean clinical score of 2.7 by 48 hours p.i., C6 deficient animals remained clear of clinical symptoms; when C6 was reconstituted to C6 deficient rats, a mean clinical score of 1.5 was observed.

4.7.1.2.2 Haemolytic activity of C6 deficient rats following C6 reconstitution

Wild type rats had normal levels of haemolytic activity at 24 hours (86% at 5% serum) and 48 hours (85% at 5% serum) post-induction (Figure 14). As expected, C6 deficient rat serum had no haemolytic activity at either of the time points (0-4%), while the reconstituted C6 group showed intermediate levels of haemolysis, with a maximal lysis of 53% using 5% serum at 24 hours, and 48% using 5% serum at 48 hours.

4.8. Discussion

C6 deficiency confers protection against development of passively transferred EAMG in the Lewis rat. Wild type animals exhibited severe weakness, wasting and weight loss from 24 hours p.i. and had to be sacrificed at 48 hours p.i. C6 deficient animals were protected from any disease manifestations for the duration of the experiment.

Activated C3b deposition was similar in wild type and C6 deficient animals and limited to the nAChR, suggesting that C3 deposition is not sufficient for disease progression. However, C9 deposition (used as an indicator of MAC attack) was limited to wild type animals, and presented at the nAChR, as identified by BuTx-rhodamine staining. No deposition was evident in C6 deficient animals, since they lack the ability to form lytic MAC. Therefore MAC deposition is associated and required for disease progression, and the weakness associated with it. In addition, nAChR loss is dependent on MAC formation since wild type animals had significantly lower numbers of receptors as identified by BuTx-rhodamine staining and density slicing, than their C6 deficient counterparts. Massive inflammatory cell infiltration was evident in wild type

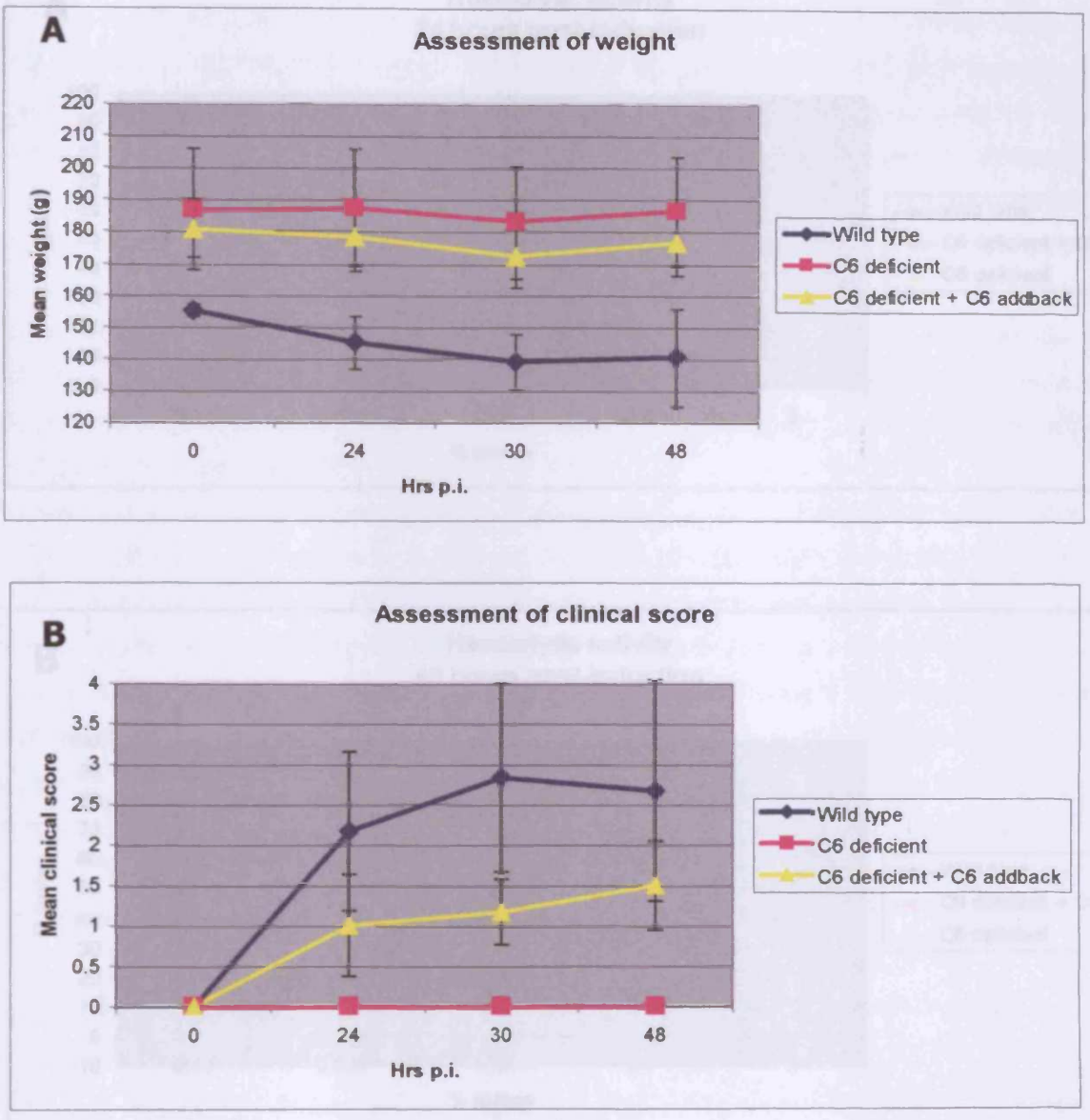

Figure 13

Assessment of weight and clinical score in wild type, C6 deficient and C6 deficient + C6 rats following EAMG induction

All rats were injected with 1mg/kg mAb35 (IP) at day 0. In addition, a group of C6 deficient animals were given human C6 at 8mg/kg (IP) at day 0, while remaining groups received PBS (IP). Animals were assessed daily in terms of weight (A), and clinical score (B). Data shown represent mean values for each group; errors represent standard deviation.

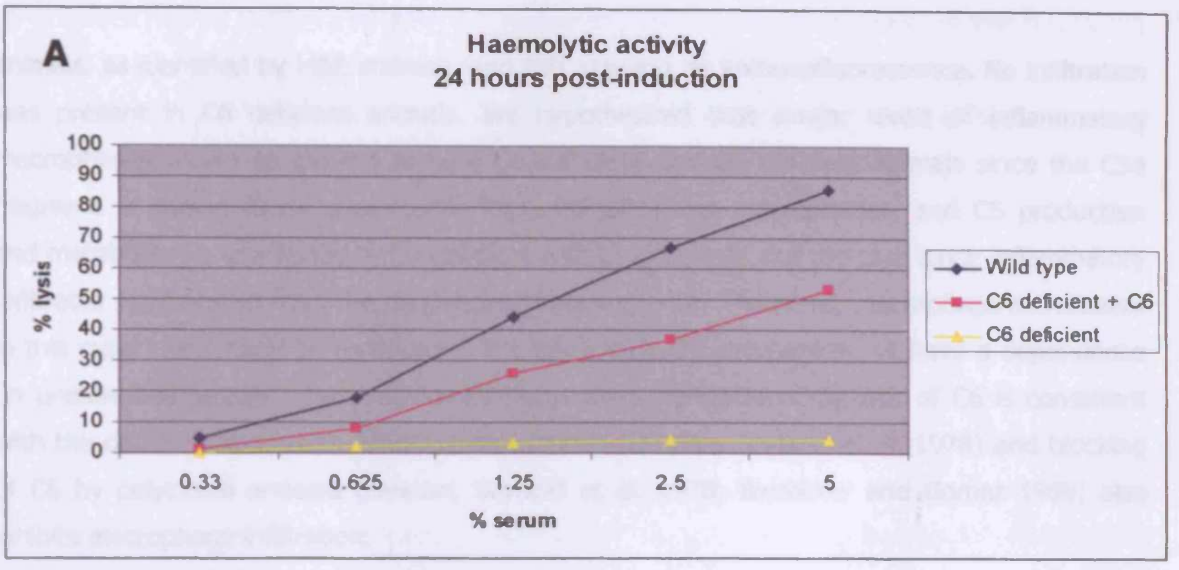

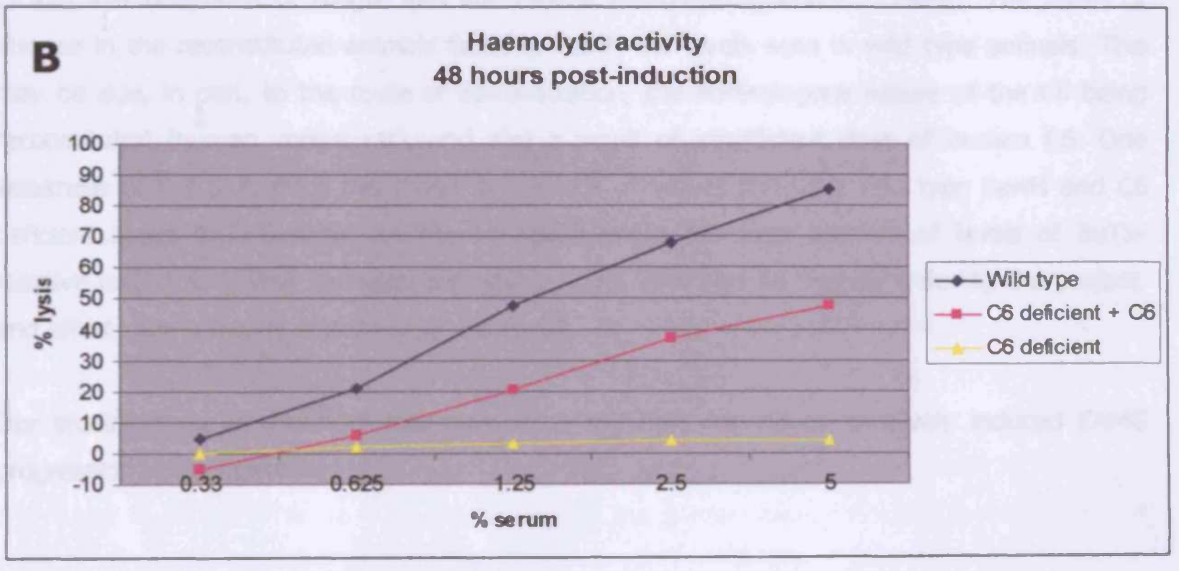

Figure 14

Assessment of haemolytic activity of serum obtained from wild type, C6 deficient, and C6 deficient + C6 rats following EAMG induction

Rats were immunised with mAb35 (1mg/kg, IP) on day 0. C6 deficient rats were additionally given either purified human C6 (8mg/kg, IP) or PBS (IP) on day 0. Animals were bled at 24 (A) and 48 (B) hours post-induction, and the serum used to assess lytic ability on sheep erythrocytes as described. Percentage lysis was calculated using: A_{415} (Test) – A_{415} (min) / A_{415} (Max) – A_{415} (min) X 100, and plotted against percentage serum used.

animals, as identified by H&E staining, and ED1 staining by immunofluorescence. No infiltration was present in C6 deficient animals. We hypothesized that similar levels of inflammatory macrophages would be evident in both C6 sufficient and C6 deficient animals since the C5a fragment is known to be chemotactic for neutrophils and macrophages, and C5 production and metabolism is unaffected in C6 deficient animals. This was not the case since inflammatory infiltrates were absent from the C6 deficient soleus muscle. Therefore, macrophage recruitment in this experiment must be functioning through a different mechanism, or have a dependence on unidentified factors. The inhibition of macrophage recruitment by lack of C6 is consistent with the demonstration that CVF-treatment of rats (Lennon, Seybold et al. 1978) and blocking of C6 by polyclonal antisera (Lennon, Seybold et al. 1978; Biesecker and Gomez 1989) also inhibits macrophage infiltration.

Reconstitution of C6 deficient rats with human C6, to approximately 50% of normal physiological levels was sufficient to enhance the susceptibility of the C6 deficient rats to the clinical manifestations of weight loss and clinical weakness observed in EAMG. The levels of disease in the reconstituted animals failed to reach the levels seen in wild type animals. This may be due, in part, to the route of administration, the heterologous nature of the C6 being reconstituted (human versus rat), and also a result of insufficient dose of human C6. One weakness of the data from this model is the lack of values for naïve wild type Lewis and C6 deficient Lewis BuTx-reactive nAChR, to enable more thorough analysis of levels of BuTx-reactive nAChR following immunisation with mAb35. This was an oversight during the project, and efforts are currently underway to rectify this.

Our studies show an absolute dependence on the MAC for clinical passively induced EAMG progression in the Lewis rat.

5 Testing of efficacy of anti-C therapy in passive transfer EAMG in the Lewis rat

(In association with Natalie Hepburn (Dept of Medical Biochemistry & Immunology, Cardiff University), Anwen Williams (Dept of Rheumatology, Cardiff University) and Miles Nunn (Centre for Ecology and Hydrology, Oxford)

5.1 Aim

The C system plays a vital role in host protection from foreign organisms. Anaphylatoxins C3a and C5a generated during C activation mimic the action of chemokines, and attract and activate phagocytes, while C3 fragments (C3b, iC3b) together with C4 fragments (C4b, iC4b) act as opsonins to target infecting organisms for phagocytosis. In addition, the pore-forming activities of the MAC result in lysis of target cells. These factors together, confer protection from infection. However, the discriminating power of the C system is lacking, and under conditions of inappropriate C activation, self cells may be seen as targets. To protect self-tissues, nature has evolved a battery of C regulators, both in plasma (for example, C1 esterase inhibitor, C4b binding protein, factor H), and on cell membranes, (for example CD55, CD46, CD59) and an additional regulator, exclusive to rodents termed Crry (Mizuno and Morgan 2004). Blocking of these regulators using neutralising antibodies has been shown to induce inflammatory disease, for example, systemic inhibition of Crry induced a marked transient shock reaction (Matsuo, Ichida et al. 1994).

The association of C in acute and chronic inflammatory diseases has previously been demonstrated, for example, in GBS (Hartung, Schwenke et al. 1987), (Koski, Sanders et al. 1987), in multiple sclerosis (Storch, Piddlesden et al. 1998), (Morgan, Campbell et al. 1984) and rheumatoid arthritis (Morgan, Daniels et al. 1988), (Jose, Moss et al. 1990), and their associated animal models, EAN (Vrisendorp, Flynn et al. 1995), experimental autoimmune encephalomyelitis (Mead, Singhrao et al. 2002), and collagen-induced arthritis (Mizuno, Nishikawa et al. 2001). While C itself is not always the primary cause of such diverse disease, it may act to sustain the inflammatory response, and perpetuate tissue damage. Taken together, it is clear that controlling C would have a clear therapeutic effect in a variety of inflammatory diseases.

C therapeutics to date have taken a variety of forms; neutralising antibodies, synthetic antagonists, soluble forms of existing CRegs, and gene therapy strategies to deliver C regs to sites of uncontrolled C activation (Mizuno and Morgan 2004).

Although systemic CVF treatment produces complete decomplementation by forming a stable C3/C5 convertase leading to consumption of C, its therapeutic use is limited due to its immunogenicity, short half-life and risk of infection from loss of opsonic function. Therefore, the focus of research in recent times has been in specific inhibition of pathological C processes, or local inflammatory-site-specific inhibition. Administration of soluble forms of membrane-bound CRegs at therapeutic dosages should, in theory, alleviate the effects of deleterious C activation. A soluble form of human C receptor 1 (sCR1) has been shown to be effective in a number of animal models of disease (Piddlesden, Storch et al. 1994; Piddlesden, Jiang et al. 1996).

However, long-term usage is limited due to short half-life, immunogenicity and high cost. sCR1 was rapidly cleared from the circulation, treatment was restricted due to development of anti-human CR1 antibodies, and costs were high due to the size and complexity of the molecule.
Natalie Hepburn and Claire Harris (Dept. Medical Biochemistry & Immunology, Cardiff University) have implemented a strategy to overcome these drawbacks. To extend the half life of these molecules, fusion protein technology has been exploited; the fusion of an antibody moiety to an active C reg dramatically increases the half-life of the molecule *in vivo*, the principle of which has been described previously (Ashkenazi, Capon et al. 1993; Harris, Williams et al. 2002). To address immunogenicity questions, and to provide proof of principle in animal models, the target molecule was Crry. This regulator is found in rodents, and therefore, theoretically lacks immunogenicity in the same species. It is anticipated that these proteins can be made in high yield and easily purified to overcome cost issues. A soluble form of Crry (Crry-4 SCR) was compared to Crry-Ig for ability to prevent onset of passive transfer EAMG in the rat.
In addition, the effectiveness of blocking C5 activation was also explored in this study. Previously, neutralising antibodies to C5 have been utilised in various models of disease, and have reached clinical trials (Fleisig and Verrier 2005). Specifically inhibiting the terminal pathway has advantages over systemic inhibition in that opsonic activities of earlier components could exist unhindered, thus overcoming the negative consequences of systemic C inhibition, such as recurrent bacterial infections. rEV576 is a novel 17kDa C regulatory protein from the soft tick *Ornithodoros moubata (O. moubata)*. Recent characterisation has demonstrated the ability of the protein to abolish production of C5a by both human classical and alternative C5 convertases. Addition of excess C5 competed away this activity, and direct binding of rEV576 to C5 was demonstrated by Western blotting (Nunn, Sharma et al. 2005). As a direct inhibitor of C5, this protein also provided an invaluable tool to re-assess the dependence of the terminal pathway on EAMG progression.

5.2 Materials and Methods

5.2.1 Generation of anti-C therapeutics

Both soluble rat Crry and Crry-Fc fusion protein were generated by Natalie Hepburn

5.2.1.1 Soluble rat Crry (4 SCR)

Soluble rat Crry (4SCR) protein was generated by cloning the 4 amino terminal SCRs of rat Crry from a plasmid containing 5SCRs of rat Crry previously made in house (Natalie Hepburn). The cloned cDNA was digested and ligated into the pDR2 vector. This vector was used to transfect CHO cells using lipofectamine. Crry proteins were purified from cell culture supernatant using a monoclonal anti-Crry affinity column (TLD1C11).

5.2.1.2 Rat Crry-Fc fusion protein

The 4 SCRs of Crry were cloned as above; the Fc was cloned from a plasmid already containing the Fc of rat IgG2a. The vector was transfected into CHO cells as described, and expressed protein was purified using affinity chromatography as described.

5.2.1.3 rEV576

The protein was a kind gift from Dr. Miles Nunn. Briefly, mRNA was isolated from the third and fourth nymphal salivary glands of *O. moubata*. Degenerate primers were used to amplify cDNA encoding the C inhibitor, and rEV576 coding region was ligated into pMETα C transfer vector. The yeast *Pichia methnaolica* strain pMAD11 was transformed, and protein purified using anion exchange chromatography and gel filtration (Nunn, Sharma et al. 2005).

5.2.2 EAMG Induction protocol

Twenty four female Lewis rats (160-200g) were obtained from Charles River Laboratories, and allowed to acclimatise for 1 week. The animals were split into 4 groups of 6 animals, according to the treatment received (Table 2)

Group Identification	Treatment
A	PBS only, 1ml/animal
B	Crry (4 SCR), 1ml/animal at 2mg/ml
C	Crry-Fc, 1ml/animal at 4mg/ml
D	rEV576, 1ml/animal at 3.25mg/ml

Table 2 Identification of groups according to treatment received

All animals were injected with 1mg/kg mAb35 in PBS (IP) on day 0, together with appropriate therapeutic as detailed in Table 2 (IV, into the tail vein). A pre-bleed was taken from each rat by tail tipping just prior to injection. Further bleeds were taken at 2, 4 and 6 hours p.i., and daily thereafter. Animals were assessed for changes in weight and clinical score as described previously.

5.3 Results

5.3.1 Assessment of weight and clinical score

All animals lost weight immediately following injection. PBS controls lost weight dramatically over the course of the experiment, and were sacrificed 52 hours p.i (Figure 15 A, dark blue line). Animals injected with Crry (4SCR) also showed a decrease in weight although they had recovered by 52 hours p.i. and began to gain weight (A, pink line). By contrast, both the Crry-Fc (A, yellow line) and rEV576 (A, light blue line) injected animals generally increased their weight throughout the experiment.

These changes were also reflected in the clinical scoring. PBS control animals displayed clinical symptoms at 24 hours p.i., reaching a maximum at 72 hours p.i (Figure 15 B, blue line). Crry

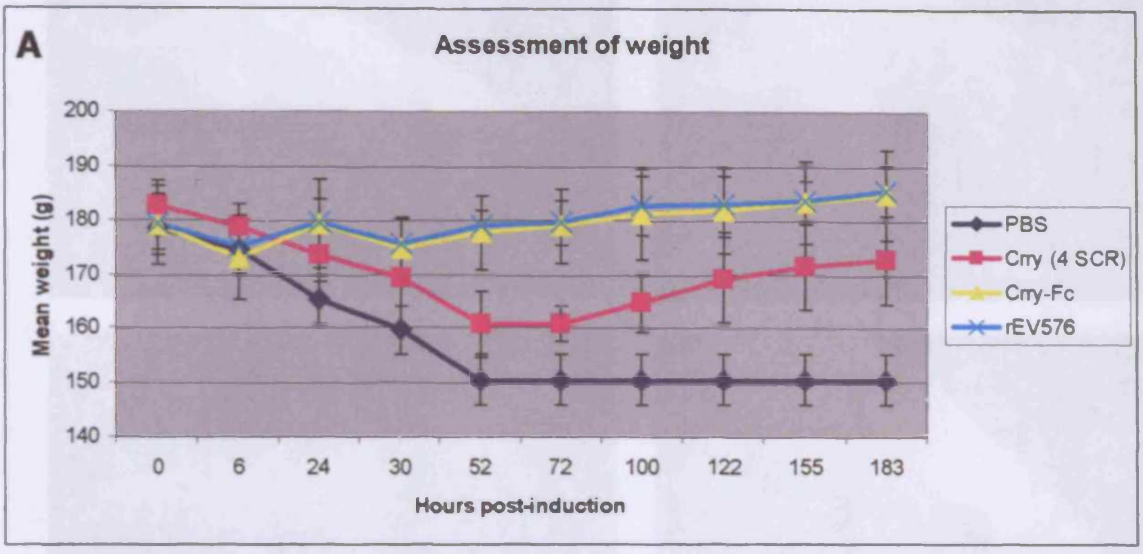

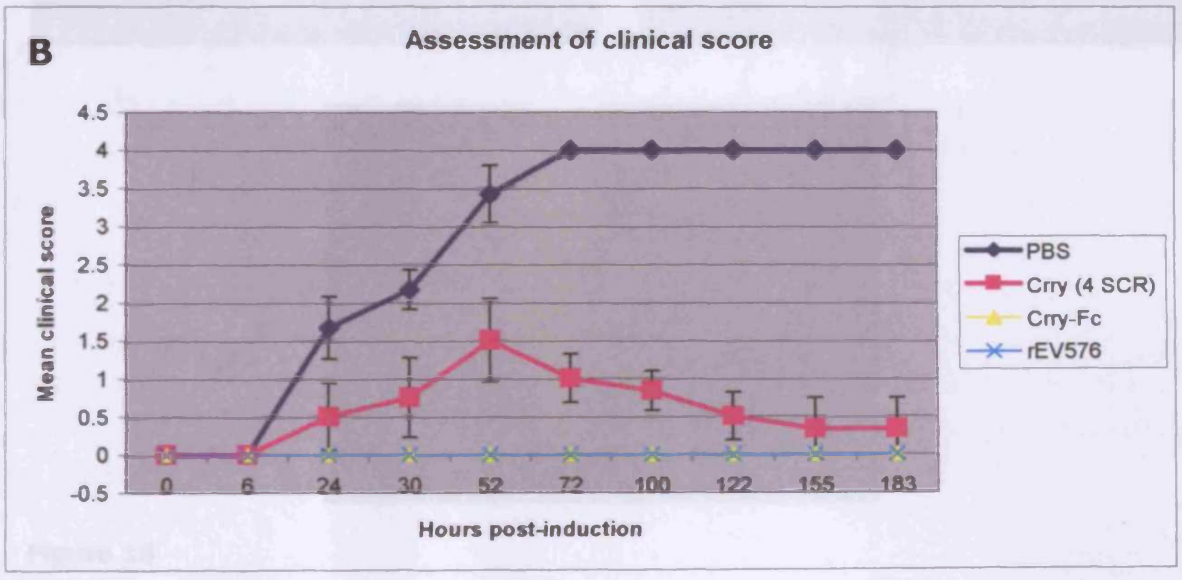

Figure 15

Assessment of weight and clinical score following EAMG induction +/- therapeutic intervention

Wild type female Lewis rats (160-200g) were injected with 1mg/kg mAb35 in PBS (IP), +/- anti-C therapeutics as listed in the figures; PBS only (dark blue line), Crry (4 SCR, pink line), Crry-Fc (yellow line) or rEV576 (turquoise line) as described, on day 0. Animals were assessed daily in terms of weight (A), and clinical score (B). Data represent mean values for each group (n=6) +/- standard deviation.

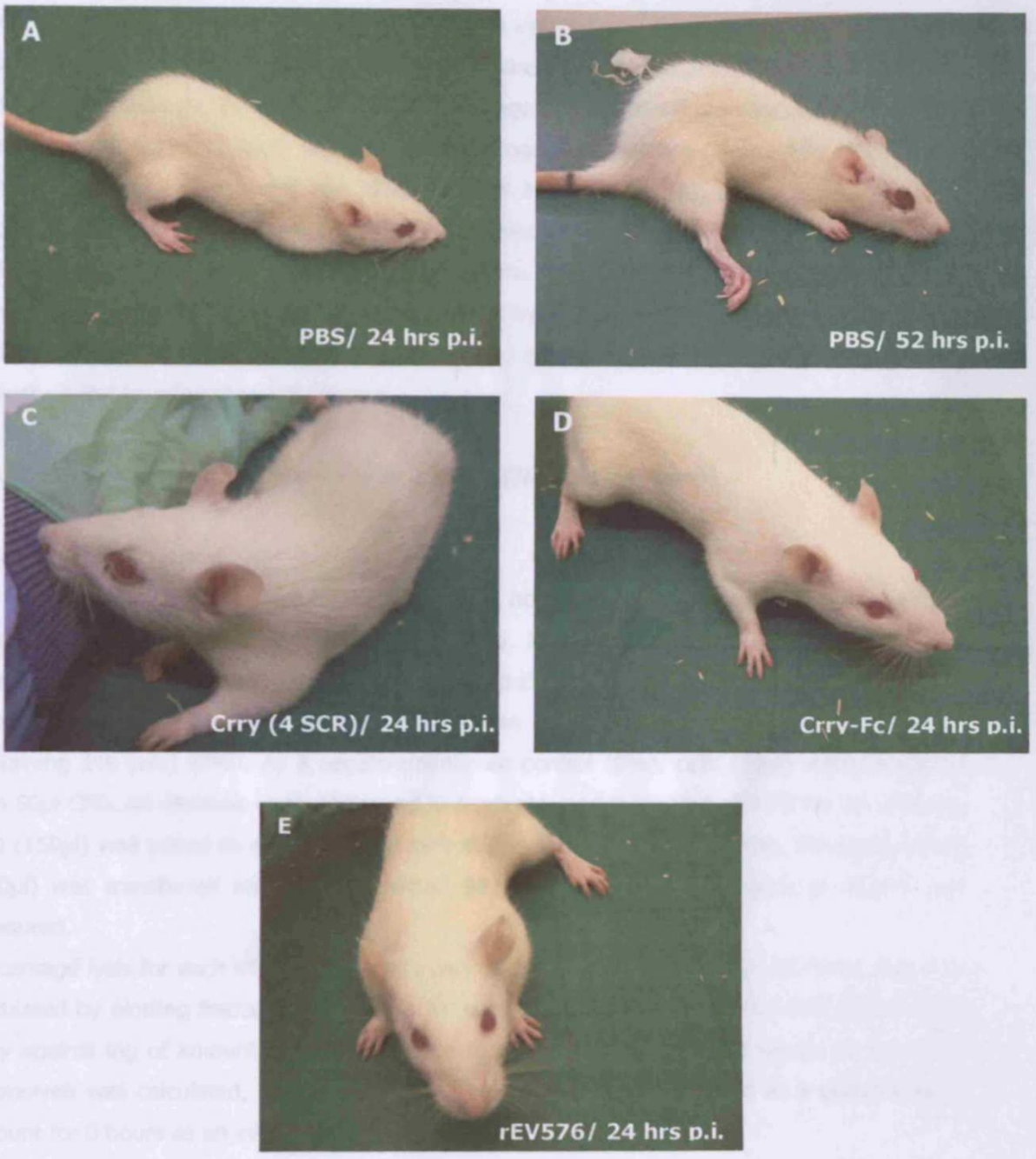

Figure 16

Clinical manifestation of passively induced EAMG in wild type Lewis rats +/- therapeutic intervention 24hrs p.i.

Twenty four hours following injection of mAb35, PBS-injected animals displayed clinical symptoms of EAMG; animals appeared with a flaccid tail, splayed hind limbs resulting from hind limb weakness, and piloerection (A), which progressed to hind limb paralysis by 52 hours p.i. (B). Crry (4 SCR)-injected rats showed mild clinical symptoms of slight pilo-erection, and fore limb weakness, reaching a maximum mean score of 1.5 by 52 hours p.i, and resolved by the end of the experiment (C). In contrast, both the Crry-Fc (D), and rEV576-injected (E) groups displayed no clinical symptoms at 24 hours and remained healthy for the duration of the experiment.

(4SCR)-injected animals demonstrated mild clinical symptoms, reaching a maximum of 1.5 at 52 hours p.i., but subsequently recovered (B, pink line). Crry-Fc (B, yellow line) and rEV576 (B, light blue line) both conferred complete protection against the clinical manifestations of EAMG. These changes are additionally highlighted by photographic evidence (Figure 16). PBS-injected animals displayed a flaccid tail, and piloerection at 24 hours p.i. (A), and progressed to hind limb weakness and wasting demonstrated by splayed hind limb by 52 hours p.i. (B). Crry (4 SCR)-injected rats showed mild clinical symptoms of slight pilo-erection, and fore limb weakness, reaching a maximum mean score of 1.5 by 52 hours p.i, which resolved by the end of the experiment (C). By contrast, Crry-Fc (D) and rEV576 (E) conferred complete protection against clinical manifestations of disease.

5.3.2 Measurement of C haemolytic activity (Natalie Hepburn)

5.3.2.1 Method

Tail bleeds were taken pre-induction, 2, 4 and 6 hours post-induction, and daily thereafter. Serum dilutions were performed in CFD at 1/10, 1/5, 1/4, 1/2, 1/1, 2/1, 3/1, 4/1, 5/1, 10/1 in a total volume of 50µl, and incubated with 50µl sheep EA (2%, v/v) in a round-bottomed 96-well plate. For maximum lysis, sheep EA (50µl) were incubated with 50µl of distilled water containing 1% (v/v) NP40. As a negative/minimum control (0%), cells (50µl) were incubated with 50µl CFD. All dilutions were performed in duplicate, and incubated at 37^0C for 30 minutes. CFD (150µl) was added to each well, and centrifuged at 1000g for 5 minutes. The supernatant (150µl) was transferred into a flat-bottomed 96 well plate, and absorbance at 415nm was measured.

Percentage lysis for each of the time points was calculated using the serum dilutions. This was calculated by plotting fractional haemolysis for each dilution =(average A415-0%)/(100%-0%) on y against log of amount of serum used on the x axis. The amount of serum to give 50% haemolysis was calculated, and the amount of serum was then expressed as a percentage of amount for 0 hours as an indication of the lytic activity of each serum.

5.3.2.2 Results

PBS controls exhibited increased plasma C activity (demonstrated by enhanced lytic ability of serum) likely due to an acute phase response, immediately following EAMG induction (Figure 17, dark blue line), which persisted throughout the experiment. Animals from this group were sacrificed at 72 hours p.i. due to onset of severe clinical symptoms. Crry (4 SCR)-injected animals showed no significant increase in C activity above 100% as seen in PBS control animals following an acute phase response (Figure 17, pink line). It was unclear whether the reason for the difference was a direct result of EAMG causing increased C activity in PBS control animals, or inhibition, albeit transient, of C by Crry (4 SCR). The fact that Crry (4 SCR) had less disease, and made a recovery from EAMG would suggest that Crry (4 SCR) was inhibiting C at the early time points. In contrast, Crry-Fc effectively inhibited C activity down to approximately 50% of

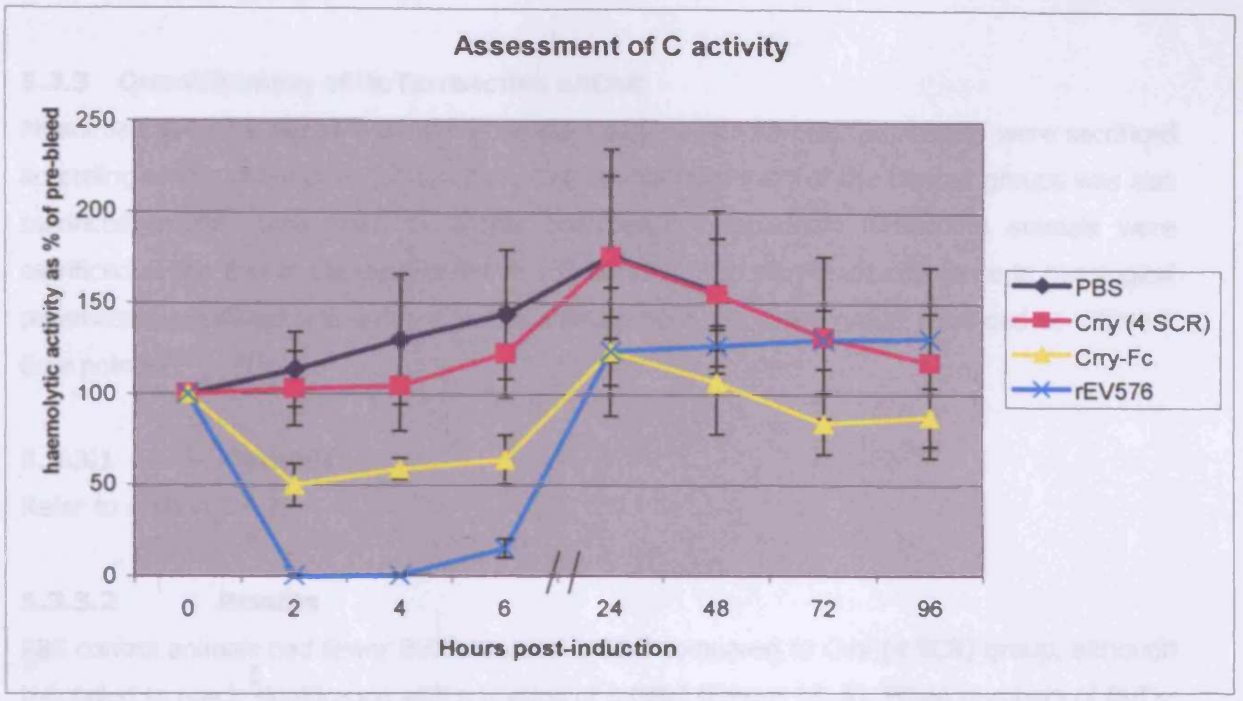

Figure 17

Assessment of C activity following EAMG induction +/- anti-C therapy

Rats were bled prior to induction of EAMG, and the C activity measured represented 100% haemolytic activity. Bleeds were also taken at 2, 4, 6, 24, 48, 72 and 96 hours post-induction where available. Percentage lysis for each of the time points was calculated using the serum dilutions. This was calculated by plotting fractional haemolysis for each dilution =(average A415-0%)/(100%-0%) on y against log of amount of serum used on the x axis. The amount of serum to give 50% haemolysis was calculated, and the amount of serum was then expressed as a percentage of amounts for 0 hours as an indication of the lytic activity of each serum, and plotted on a graph.

Data represent means for each group (n=6) +/- standard deviation.

normal, and maintained it at or around that level until around 24 hours p.i.(yellow line); rEV576 completely inhibited C activity until around 6 hours post-induction, but were back to normal levels at 24 hours (turquoise line).

5.3.3 Quantification of BuTx-reactive nAChR

All animals were sacrificed if clinical score reached 3-4. All PBS-injected animals were sacrificed according to this criterion at 72 hours p.i. One animal from each of the treated groups was also sacrificed at this time point to enable histological comparison. Remaining animals were sacrificed at the end of the experiment at 183 hours p.i. No significant difference in histological parameters examined was evident in the animals from the same group sacrificed at different time points.

5.3.3.1 Methods

Refer to section 4.4.2.

5.3.3.2 Results

PBS control animals had fewer BuTx-reactive nAChR compared to Crry (4 SCR) group, although this failed to reach significance with a p value of 0.0963 (Figure 18, A). When numbers of BuTx-reactive nAChR were compared between PBS and Crry-Fc group, again there were fewer nAChR in the PBS group, but this did reach significance (B, p=0.0382). This was also true for PBS versus rEV576 group, and the difference was very significant (C, p=0.005).

5.3.4 Visualisation of C deposition at the nAChR

5.3.4.1 C3 deposition

Soleus muscle from PBS-injected (Figure 19a, A-C; Figure 19b, A-C), Crry (4 SCR, Figure 18a, D-F) and Crry-Fc (Figure 19a, G-I) Lewis rats induced for EAMG, were harvested, and flash-frozen in isopentane as described. nAChR were identified by BuTx-rhodamine labelling (A, D, G). C3 deposition was evident at the nAChR in PBS-injected animals (Figure 19a, B), and Crry (4 SCR)-injected animals (Figure 19a, E). Deposition was limited to the nAChR as demonstrated by the co-localised images (C, F). In contrast, Crry-Fc-injected animals had much reduced C3 deposition at the nAChR (G-I).

rEV576-injected animals also displayed reduced C3 deposition at the nAChR, when compared with the PBS and Crry (4 SCR) groups (Figure 19b, D-F). This was unexpected since rEV576 is a potent inhibitor of C5. However, it is likely that in PBS and Crry (4 SCR)-treated groups, that occurrence of extensive tissue damage also contributed to C activation, which would have been less marked in the rEV576 group.

5.3.4.2 C9 deposition

Soleus muscle from PBS-injected (Figure 20a, A-C; Figure 20b, A-C), Crry (4 SCR, Figure 20a D-F), Crry-Fc (Figure 20a, G-I) and rEV576-injected (Figure 20b, D-F) Lewis rats induced for EAMG, were harvested, and flash frozen in isopentane as described

BuTx-reactive nAChR were visible in all animals. In contrast to C3 deposition, C9 was only evident in PBS and Crry (4 SCR) animals following EAMG induction. No C9 positive staining was present on nAChR from Crry-Fc-injected rats. Trace C9 deposition was evident on sections from rEV576-injected animals nAChR. C9 staining was limited to the nAChR in all cases.

5.3.4.3 Inflammatory cell infiltration

Soleus muscle from all animals were flash-frozen in isopentane, sections were cut as described previously, and stained with mouse anti-rat-CD68 (Figure 20, A, C, E, G). In addition, the other soleus muscle from each animal was post-fixed in 10% (v/v) formaldehyde in PBS to allow better preservation of structures for H&E staining (B, D, F, H). A scoring system for inflammatory cell

infiltration was designed in association with Dr. James Neal, Neuropathologist, UWCM, Cardiff; 0, no inflammation; 1; up to 20% of whole muscle infiltrated; 2, up to 40% of whole muscle infiltrated; 3, up to 60% of whole muscle infiltrated; 4, over 80% of muscle fibres infiltrated.

Massive cellular infiltration was evident in PBS-injected animals following EAMG induction (A, B). A lesser extent of infiltration was apparent in Crry (4 SCR)-injected animals (C, D), while no infiltration occurred in Crry-Fc (E, F) or rEV576-injected (G, H) animals. A summary table showing average scores for infiltration is shown in Table 3.

Group	IF (anti-rat CD68)	H&E
PBS	2.67	2.67
Crry (4 SCR)	2.67	2.16
Crry-Fc	0.34	0.83
rEV576	1	0.83

Table 3

Assessment of inflammatory cell infiltration in EAMG animals +/- therapy

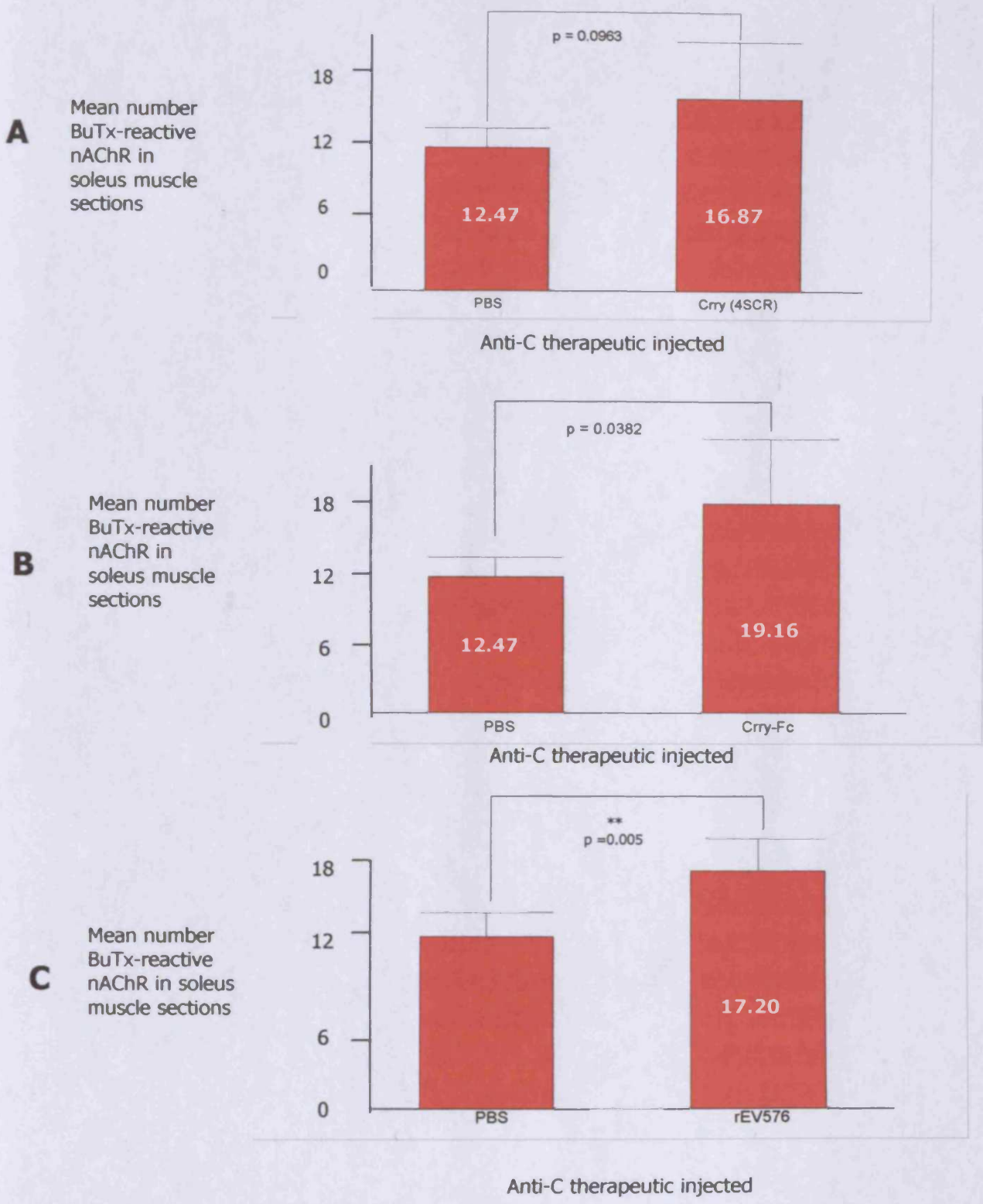

Figure 18 Statistical analysis of BuTx-reactive nAChR numbers

Soleus muscles from each animal were harvested, sectioned and stained for nAChR as described previously. Twenty fields from each animal from a comparable area within the soleus muscle were taken, and subjected to density slicing using pre-determined intensity limits. Total numbers were calculated and a mean for each group was plotted against the PBS control, and subjected to a two-tailed t test using InStat. PBS versus Crry (4 SCR, A); PBS versus Crry-Fc (B), PBS versus rEV576 (C). Data represents mean for each group +/- standard deviation.

Figure 19a

Assessment of C3 deposition at the nAChR in PBS, Crry (4 SCR) and Crry-Fc treated Lewis rats

Soleus muscle from PBS-injected (A-C), Crry (4 SCR, D-F) and Crry-Fc (G-I) Lewis rats induced for EAMG, were harvested, and flash frozen in isopentane as described. Briefly, 10 micrometer thin sections were cut and stained for nAChR (A, D, G) using rhodamine-conjugated BuTx. Sections were double-stained for activated C3 (C3c; B, E, H) using goat anti-rat C3c, and detected with donkey anti-goat-Ig-FITC conjugate. Sections were mounted in VectorShield, and analysed under an inverted fluorescent microscope. Images were merged for detection of colocalisation (C, F, I).

All images were taken at 400X magnification.

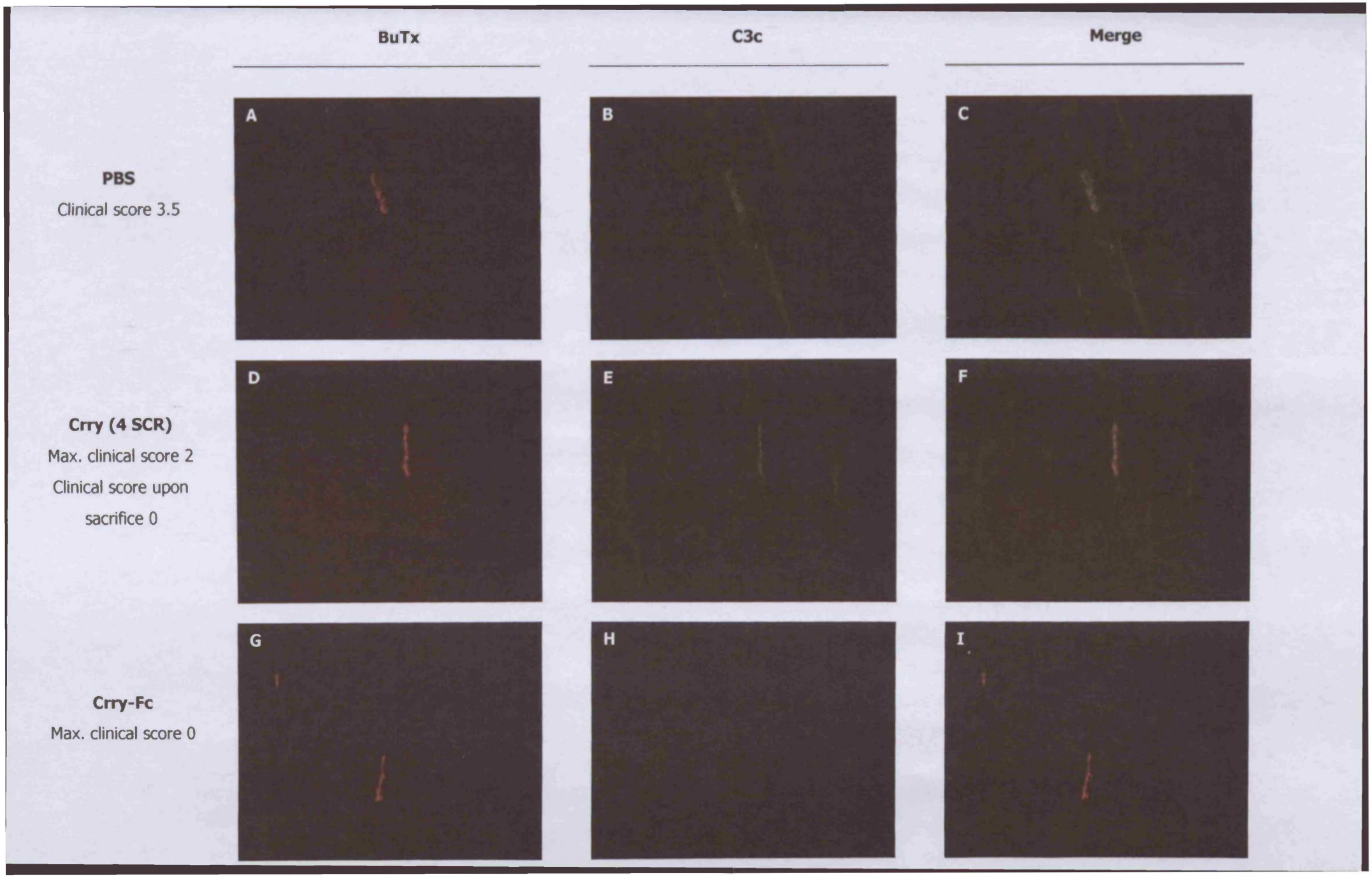
BuTx
C3c
Merge
PBS
Clinical score 3.5
A
B
C
Crry (4 SCR)
Max. clinical score 2
Clinical score upon
sacrifice 0
D
E
F
Crry-Fc
Max. clinical score 0
G
H
I

Figure 19b

Assessment of C3 deposition at the nAChR in PBS and rEV576 treated Lewis rats

Soleus muscle from PBS-injected (A-C) and rEV576-injected (D-F) Lewis rats induced for EAMG, were harvested, and flash frozen in isopentane as described. Briefly. 10 micrometer thin sections were cut and stained for nAChR (A, D) using rhodamine-conjugated BuTx. Sections were double-stained for activated C3 (C3c; B, E) using goat anti-rat C3c, and detected with donkey anti-goat-Ig-FITC conjugate. Sections were mounted in VectorShield, and analysed under an inverted fluorescent microscope. Images were merged for detection of colocalisation (C, F).

All images were taken at 400X magnification.

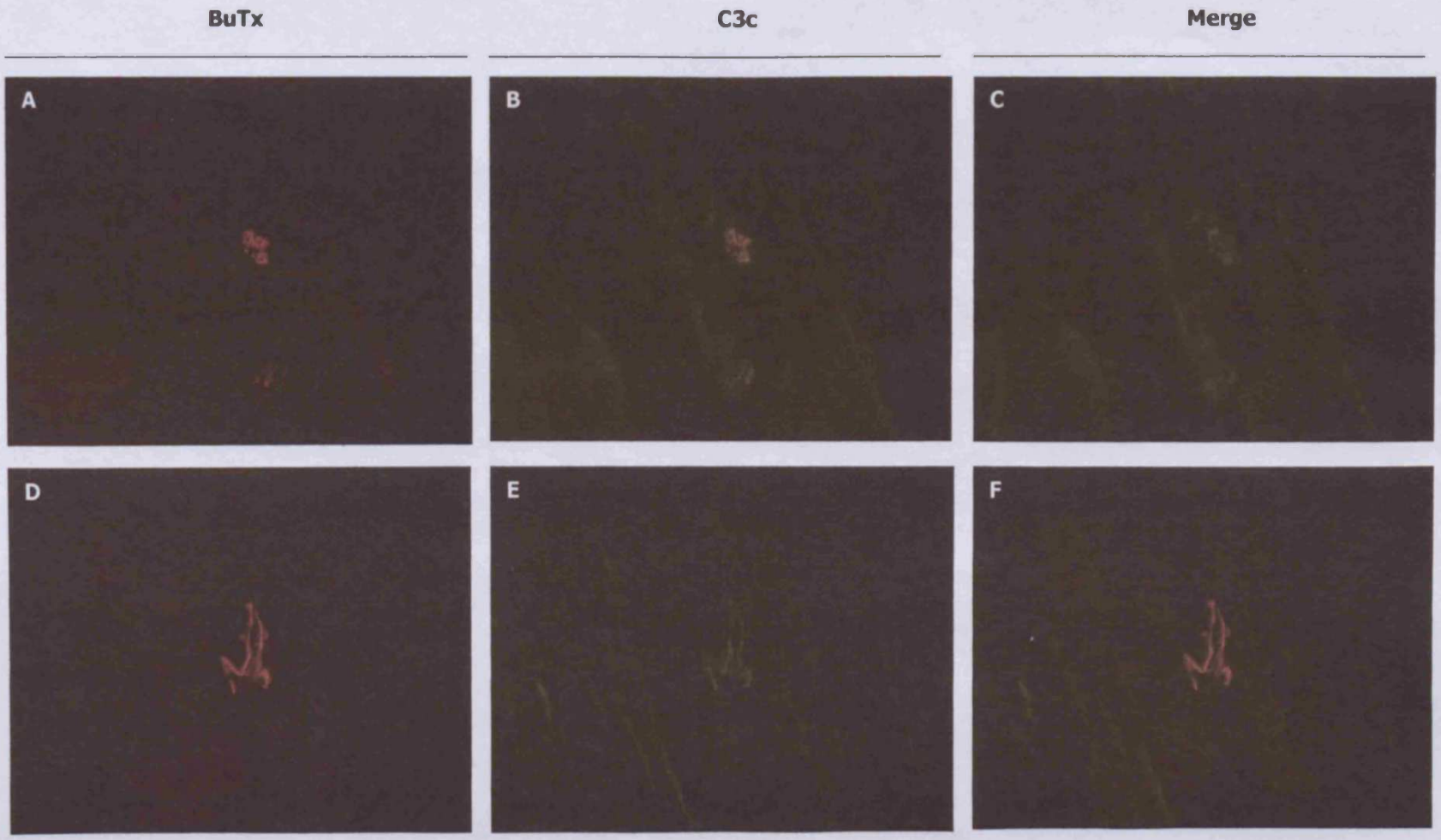
BuTx
C3c
Merge
A
B
C
PBS
Clinical score 3
D
E
F
rEV576
Max. clinical
score 0

Figure 20a

Assessment of C9 deposition in PBS versus Crry (4 SCR) and Crry-Fc-injected rats following EAMG induction

Soleus muscle from PBS (A-C), Crry (4 SCR, D-F) and Crry-Fc (G-I)-injected Lewis rats induced for EAMG were harvested, and flash frozen in isopentane as described. Ten micrometer thin sections were cut and stained for nAChR (A, D, G) using rhodamine-conjugated BuTx. Sections were double-stained for C9 (B, E, H) using sheep anti-human C9, and detected with donkey anti-goat-Ig-FITC conjugate. Sections were mounted in VectorShield, and analysed under an inverted fluorescent microscope. Images were merged for detection of co-localisation (C, F, I).

All images were taken at 400X magnification.

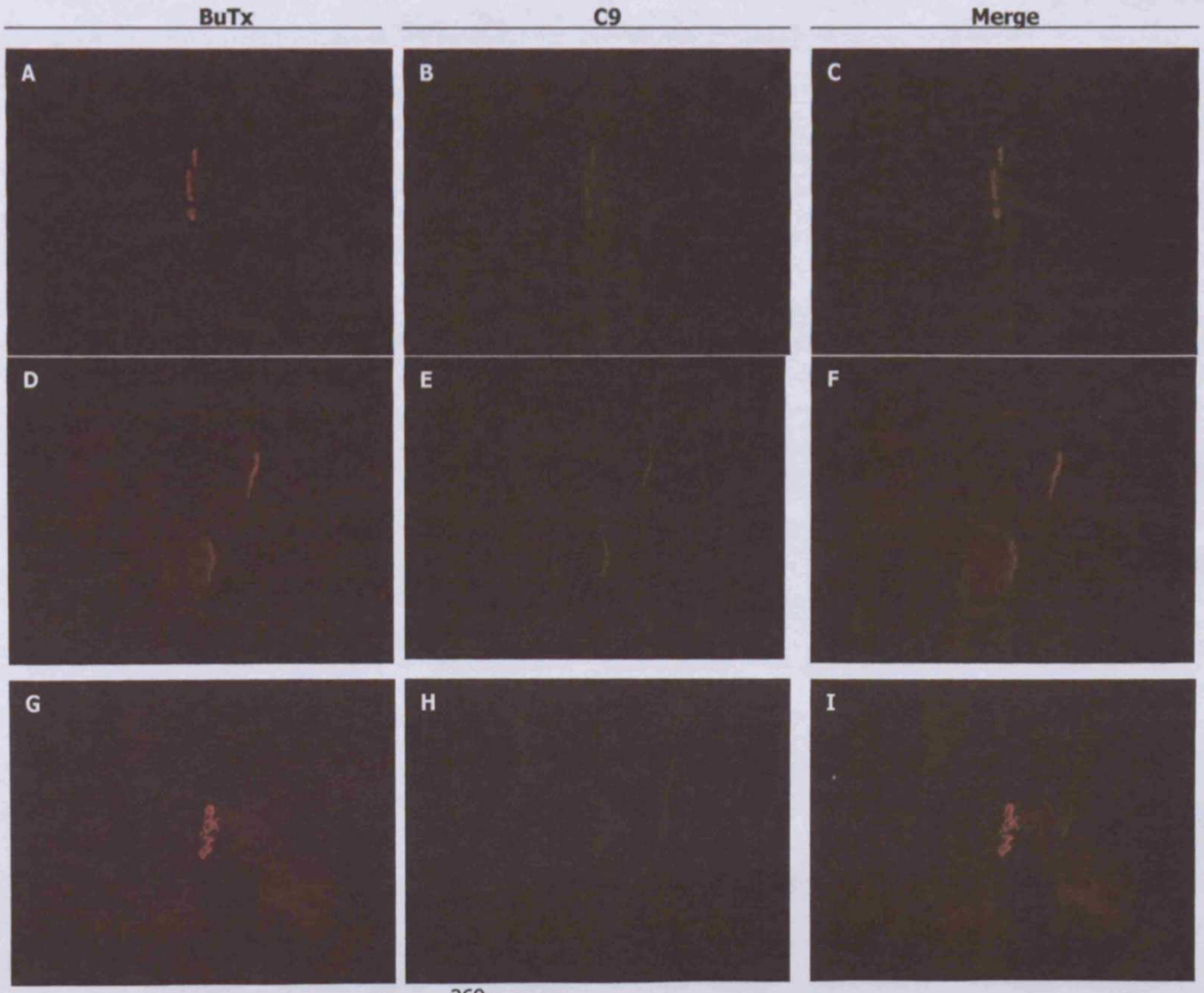
BuTx
C9
Merge
A
B
C
PBS
Clinical score 3.5
D
E
F
Crry (4 SCR)
Max. clinical score 2
Clinical score upon sacrifice 0
G
H
I
Crry-Fc
No clinical score

Figure 20b

Assessment of C9 deposition in PBS versus rEV576-injected rats following EAMG induction

Soleus muscle from PBS (A-C) and rEV576 (D-F)-injected Lewis rats induced for EAMG were harvested, and flash frozen in isopentane as described. Ten micrometer thin sections were cut and stained for nAChR (A and D) using rhodamine-conjugated BuTx. Sections were double-stained for C9 (B and E) using sheep anti-human C9, and detected with donkey anti-goat-Ig-FITC conjugate. Sections were mounted in VectorShield, and analysed under an inverted fluorescent microscope. Images were merged for detection of co-localisation (C and F).

All images were taken at 400X magnification.

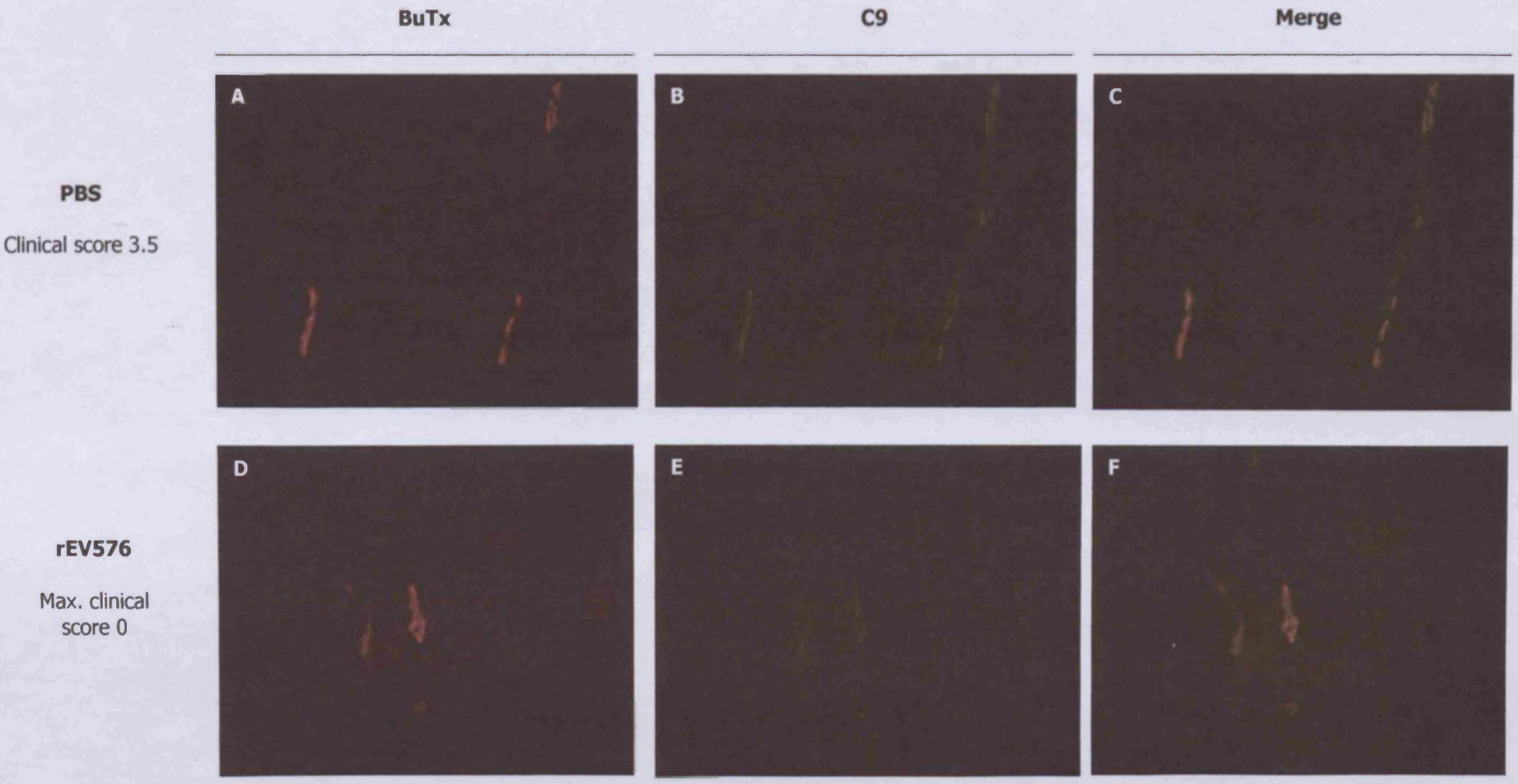
BuTx
C9
Merge
A
B
C
PBS
Clinical score 3.5
D
E
F
rEV576
Max. clinical score 0

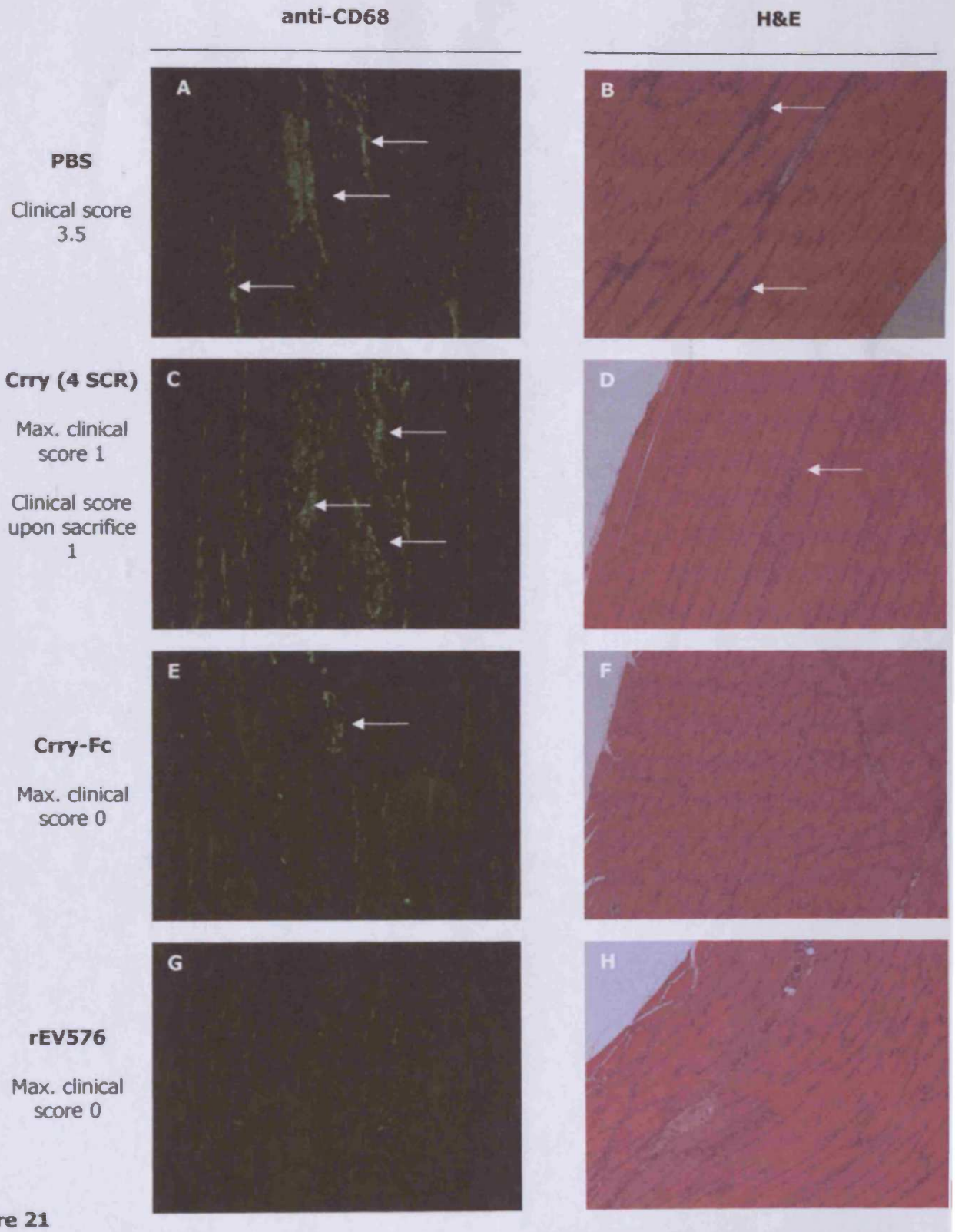

Figure 21

Assessment of inflammatory cell infiltration in treated animals following EAMG induction

Frozen soleus muscle sections were stained with mouse anti-rat CD68 (ED1, A, C, E, G). Soleus muscles were also post-fixed in 10% formaldehyde in PBS, embedded in paraffin wax as described previously and H&E stained (B, D, F, H) to detect inflammatory cell infiltration. PBS (A, B); Crry (4 SCR; C, D); Crry-Fc (E, F); rEV576 (G, H). Arrow point to areas of dense infiltration.

All immunofluorescence images were taken at 200X magnification. All H&E sections were taken at 50X magnification.

5.4 Discussion

The passive transfer model of EAMG in rats has provided an opportunity to test the efficacy of two novel anti-C therapeutic strategies. Contrary to expectations, soluble Crry (4 SCR), although not delaying the onset of clinical symptoms, did reduce the severity of EAMG seen in the rat, presumably by inhibiting C activation during the very early stages of disease onset. This remains unconfirmed, although further CH50 studies are being conducted presently on non-diseased animals at early time-points to address this issue. A degree of protection from nAChR loss was also demonstrated, although this did not reach significance ($p=0.0963$). C3 and C9 deposition were observed at the nAChR, and similar levels of inflammatory infiltrates to those animals injected with PBS alone were observed throughout the muscle.

Crry-Fc failed to completely inhibit C activity, but reduced it to 50% of normal levels, which was sufficient to confer protection from the clinical manifestations of EAMG in the rat. This was also reflected in a significant protection from nAChR loss ($p=0.0382$). Crry-Fc also inhibited C activity at the nAChR, and no C3b or C9 deposition was detected. Protection against excessive inflammatory infiltration was also evident following treatment with Crry-Fc.

rEV576 completely inhibited C activity for the first 6 hours p.i. Levels returned to normal following 24 hours, though this was sufficient to confer complete protection from weight loss and clinical symptoms of EAMG. Significant protection from nAChR loss was also observed ($p=0.005$). C3b deposition was still evident although this was not sufficient for disease progression. Trace C9 deposition was observed, although this was not sufficient to cause weakness.

Chapter 5

Part 2

Preliminary study of Experimental Autoimmune Myasthenia Gravis in the Mouse

1 Introduction

The first studies involving EAMG induction in mice were described in 1975 by Toyka and colleagues, who demonstrated that passive transfer of ammonium sulphate-fractionated MG serum was capable of inducing EAMG in mice. Although mice did not display any obvious clinical symptoms of disease, they showed reduced amplitude of m.e.p.p.s and reduced numbers of nAChRs at NMJs (Toyka, Drachman et al. 1975). Further to this work, monoclonal antibodies, raised in rats against nAChR from the electric organ of *Torpedo californica* (*T. californica*) (McAb1, 2 and 3) were shown to be capable of inducing disease in mice, rats and guinea pigs. Passive transfer of these antibodies into rats and guinea pigs induced clinical, electrophysical and biochemical evidence of EAMG; however, mice again failed to display any signs of clinical weakness, although their m.e.p.p. amplitude was reduced by 50%; this reflects their high safety factor for neuromuscular transmission (Lennon and Lambert 1980). In an elegant study, thymus tissue fragments from MG patients were transplanted into severe combined immunodeficient (SCID) mice, able to tolerate xenografts, and shown to induce EAMG. Measurements included detection of human anti-nAChR antibodies at levels typically seen in patients with severe MG and human Ig deposits at the nAChR (Schonbeck, Padberg et al. 1992).

EAMG is routinely induced in mice either by repeated active immunisation with purified nAChR from electric organs of *T. californica* or *Electrophorus electricus* (*E. electricus*) (Tuzun, Scott et al. 2003), or by passive transfer of monoclonal antibodies against the nAChR (Lin, Kaminski et al. 2002).

1.1 C in EAMG in the mouse

A study by Christadoss in 1988 demonstrated that C5 deficient mice were protected from development of actively induced EAMG, despite having concentrations of anti-nAChR antibodies in their serum similar to their C5 sufficient counterparts (Christadoss 1988). A reduction in actively induced disease was also demonstrated in IL-6 deficient mice, which was shown to correlate with reduced germinal centre formation and C3 production (Deng, Goluszko et al. 2002). Subsequent studies have demonstrated resistance to actively induced disease in C3-/- and C4-/- mice, with heterozygotes displaying intermediate susceptibility (Tuzun, Scott et al. 2003).

Using the passive transfer model in C regulator knockouts, enhanced susceptibility to EAMG was demonstrated in *Daf1-/-* mice. Following administration of McAb3 (rat IgG), *Daf1-/-* mice

displayed severe clinical weakness exemplified by reduced hang-time, flattening of post-synaptic membranes and widening of the synaptic cleft, a marked reduction in nAChR levels (33% of normal compared to 55% of normal in *Daf1*+/+), and C3 deposition at the NMJ, compared to littermate controls. Normally, the hang-time test requires sensitisation with pancuronium bromide, but the weakness displayed by *Daf1*-/- was so severe, that this proved unnecessary. The authors suggested that DAF plays a critical role in protecting the NMJ and surface nAChR molecules against C-mediated damage (Lin, Kaminski et al. 2002).

The same group also examined mRNA levels of membrane-bound CRegs on extra-ocular muscles in passively induced EAMG. They showed decreased levels of mRNA for *Daf1*, *Cd59* and Crry following disease onset (Kaminski, Li et al. 2004).

Mice provide a unique opportunity for studying the pathogenesis of MG as a result of the availability of mutant, congenic, transgenic and various knockout mice. In our laboratory, gene knockout, or deficient mice encompassing all aspects of the C cascade are available; in terms of C components, C1q-/-, C2/fB, C3-/-, C5 and C6 deficient mice have been generated; in terms of C regulation, *Daf1*-/- and *Cd59a*-/- mice are available. Taken together, these mice provide a valuable resource with which to explore the role of C in mediating EAMG.

1.2 Aim

Due to the limited supply of nAChR, passive transfer EAMG was used to optimise disease induction using a rat anti-nAChR antibody obtained from Prof. Vanda Lennon, Mayo Clinic, USA, which has been used successfully in previous studies of EAMG induction in C57Bl/6 mice (Lin, Kaminski et al. 2002; Kaminski, Li et al. 2004).

Although an assessment of the susceptibility of *Daf1*-/- mice has previously been undertaken, this is lacking for *Cd59a*-/-. The availability of both strains of mice provide a unique opportunity for examining regulation in C activation and in the terminal pathway by backcrossing *Cd59a*-/- with *Daf1*-/-, resulting in double knockout *Cd59a*/*Daf1*-/- strain.

In mice, the genes encoding CD55 (DAF), CD59, C1s and C1r have been duplicated and demonstrate differential expression in tissues, with one form restricted to reproductive tissues (Baalasubramanian, Harris et al. 2004). *Daf1* is expressed in almost all tissues, and considered to be the mouse counterpart of human DAF, whereas *Daf2* is constitutively expressed only in the testis and in dendritic cells of the spleen. Studies have shown that neuromuscular DAF protein derives from the *Daf1* gene, (Lin, Fukuoka et al. 2001), thus *Daf1*-/- mice provide a suitable tool to examine the importance of DAF regulation in EAMG.

Mouse CD59a was identified and characterised in our laboratory and exhibited a wide expression pattern which paralleled human CD59 expression (Powell, Marchbank et al. 1997). Following this, *Cd59a*-/- mice were generated in our laboratory in 2001. Despite the complete absence of CD59a, mice were healthy and fertile. However, erythrocytes showed spontaneous intravascular haemolysis, which increased following treatment with cobra venom factor (CVF) to trigger sustained C activation (Holt, Botto et al. 2001). Later, the *Cd59* gene was found to have

been duplicated, with a second form designated *Cd59b*, encoding a second protein CD59b, which was eventually shown to be testis restricted (Baalasubramanian, Harris et al. 2004). Although the *Cd59a-/-* mice exhibit a mild phenotype, they have been used successfully to test their susceptibility to MAC-mediated injury in a variety of animal models of disease. *Cd59a-/-* mice were shown to have enhanced disease severity, demyelination and axonal injury in murine EAE (Mead, Neal et al. 2004), and exacerbated tubular injury and interstitial leucocyte infiltration following ischemia-reperfusion injury (Turnberg, Botto et al. 2003).

The aim of this preliminary work was to establish the model and assess the susceptibility of C regulator knockout mice *Cd59a-/-, Daf1-/-* and *Cd59a/Daf1-/-* to induction of passive transfer EAMG.

2 *Daf1/Cd59a-/-* mice are more susceptible to passively induced EAMG than their single knockout counterparts

2.1 Materials & Methods

2.1.1 Animals

Daf1-/- mice were obtained from Prof. Wenchao Song (Dept. Pharmacology, Centre for Experimental Therapeutics, University of Pennsylvania, PA, USA), and were backcrossed onto C57Bl/6 for 10 generations.

Cd59a-/- mice were generated in our laboratory on a C57Bl/6 background (Holt, Botto et al. 2001), bred within isolation containers in BSU, and released into conventional cages following weaning.

2.1.2 Induction protocol

Six male *Cd59a-/-* mice, 2 male *Daf1-/-* mice and 3 male *Cd59a/Daf1-/-* mice (21-31g) were obtained from BSU, Cardiff University, and kept in conventional cages according to Home Office guidelines. Wild type mice were omitted from this study since they do not show signs of EAMG induced by passive transfer due to their high safety factor for neuromuscular transmission. On day -1 prior to injection, mice were assessed for their hang-time ability, by measuring the time taken to fall 3 times from a grid (Figure 1). A maximum hang-time of 10 minutes was allowed for each mouse. McAb3 was obtained as crude lyophilised ascites fluid in 0.02% (v/v) azide at approximately 50mg/ml. The preparation was reconstituted with 1ml distilled water, and absorbance at 280nm of a diluted sample gave an indication as to the protein concentration. On day 0, mice were injected intraperitoneally (IP) with 50µl of McAb3 (rat anti-mouse nAChR, IgG) corresponding to approximately 25µg specific antibody, and were observed daily in terms of their weight and hang-time. In addition, a clinical scoring system was implemented as follows; 0, no clinical score; 1, reduced grip strength in front paws; 2, loss of grip in front paws; 3, hind limb weakness; 4, hind limb paralysis. Animals having lost greater than or equal to 20% of their original body weight, or having reached a clinical score of 4 were sacrificed by a Schedule 1 method, according to Home Office regulations. Animals exhibiting any clinical symptoms were given pre-wetted food, and observed twice daily for deterioration.

2.2 Results

2.2.1 Assessment of weight

Animals in all 3 groups lost weight immediately following injection on day 0 (Figure 2A).

Cd59a/Daf1-/- showed the most dramatic change in weight (yellow line), followed by *Daf1-/-* (pink line), then *Cd59a-/-* (blue line).

2.2.2 Hang-time measurement

Cd59a/Daf1-/- demonstrated severe clinical symptoms by day 1 p.i., and their hang-time was reduced substantially from a mean of 365 seconds on day -1 to 13 seconds by day 1 (Figure

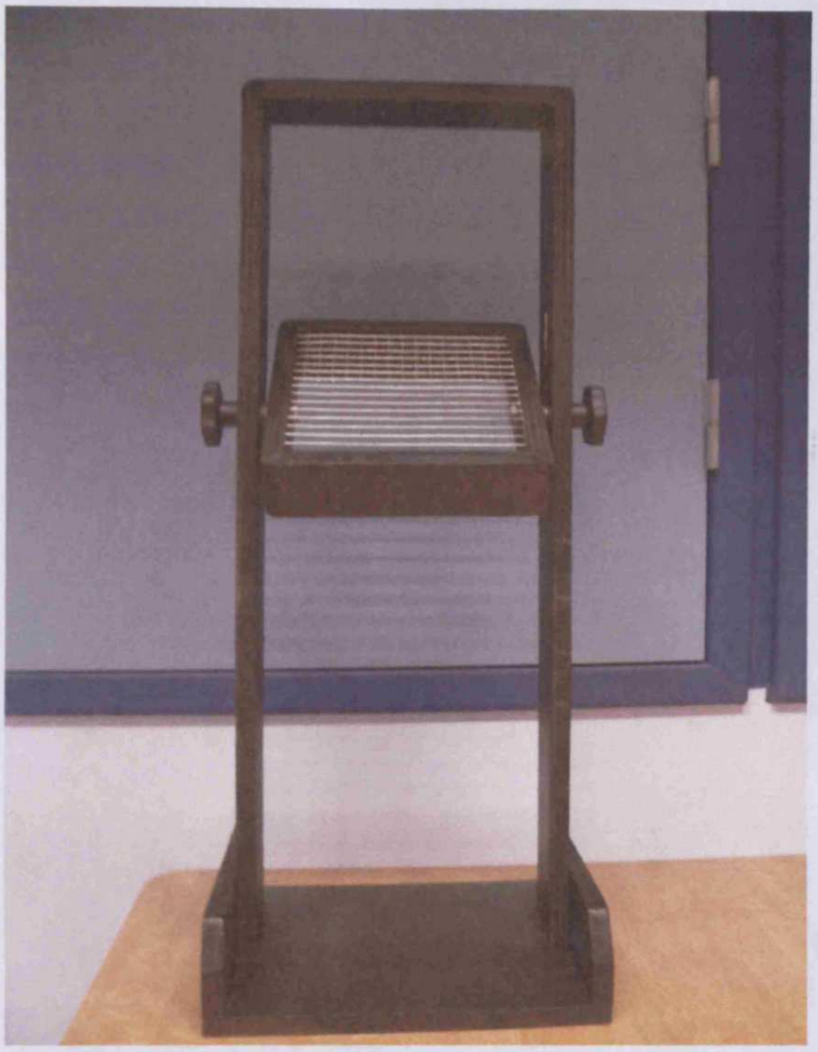

Figure 1

Hang-time measurement in mice following EAMG induction

On day -1, mice were assessed for muscle weakness following repeated exercise, by hanging upside down on a grid. The hang-time measurement measures the total time taken for a mouse to fall three times from the grid. Following fall 1, the timer was paused, the apparatus was re-set, and the mouse was replaced on the grid, and the timer was re-started. This was repeated a further 2 times, and the total time taken was recorded.

2B). All animals in this group were sacrificed by a Schedule 1 method on day 1. There was little change in hang-time measurement in *Cd59a-/-* throughout the course of the experiment; *Daf1-/-* showed a reduced hang-time measurement from 600 seconds on day -1 to 196.5 seconds by day 3.

2.2.3 Assessment of clinical score

Cd59a/Daf1-/- mice displayed severe clinical symptoms 24 hours p.i., consisting of a flaccid tail, hind limb paralysis, intense piloerection, and an inability to lift their heads (Figure 3A, yellow line; photo C). All mice in this group reached a clinical score of 4, and were sacrificed by a Schedule 1 method. No specific clinical symptoms were present in *Daf1-/-* (Figure 3A, pink line, photo A), or *Cd59a-/-* mice (Figure 3A, blue line; photo B) at the same time-point, although all *Cd59a-/-* animals displayed slight piloerection.

2.2.4 Histological analysis

2.2.4.1 Methods

Soleus muscles were isolated from freshly euthanized mice sacrificed by cervical dislocation, and flash-frozen in isopentane as described previously. Ten micrometer thin sections were cut on a cryostat, and acetone-fixed for 5 minutes. BuTx-rhodamine conjugate was used to identify the nAChR. C deposition was also analysed; goat anti-rat C3c at 1:400 dilution was used to identify C3b staining at the nAChR. No specific antibody was available to determine MAC deposition at the nAChR. To visualise inflammatory infiltrates, rat anti-mouse CD11b-FITC directly conjugated antibody was utilised. CD11b antigen is part of the CD11b/CD18 heterodimer (Mac-1), which is also known as the C3 C receptor. The monoclonal antibody recognizes human as well as mouse CD11b antigen. In mouse, the CD11b antigen is expressed on macrophages, granulocytes, NK cells, B1 cells and a subset of dendritic cells. Antibodies and BuTx were incubated in block buffer for 40 minutes at room temperature in a humid chamber, and washed 3 times in PBS. Sections were mounted in VectorShield to prevent fading of fluorescent signal, and analysed on a fluorescent microscope.
In addition, soleus muscles were post-fixed in formaldehyde (10% (v/v) in PBS), and subjected to H&E staining as described previously.

2.2.4.2 Results

2.2.4.3 C3b deposition

BuTx-reactive nAChR were visible in all animals (Figure 4; *Cd59a-/-*, A; *Daf1-/-*, D; *Cd59a/Daf1-/-*,G). However, C3 deposition was only detected in single knockout *Cd59a-/-* (B), and *Daf1-/-* (E) animals, and absent from *Cd59a/Daf1-/-* mice (E). Merged images showed complete co-localisation of C3 deposition, if present, at the nAChR (*Cd59a-/-*, C; *Daf1-/-*, F; *Cd59a/Daf1-/-*, I).

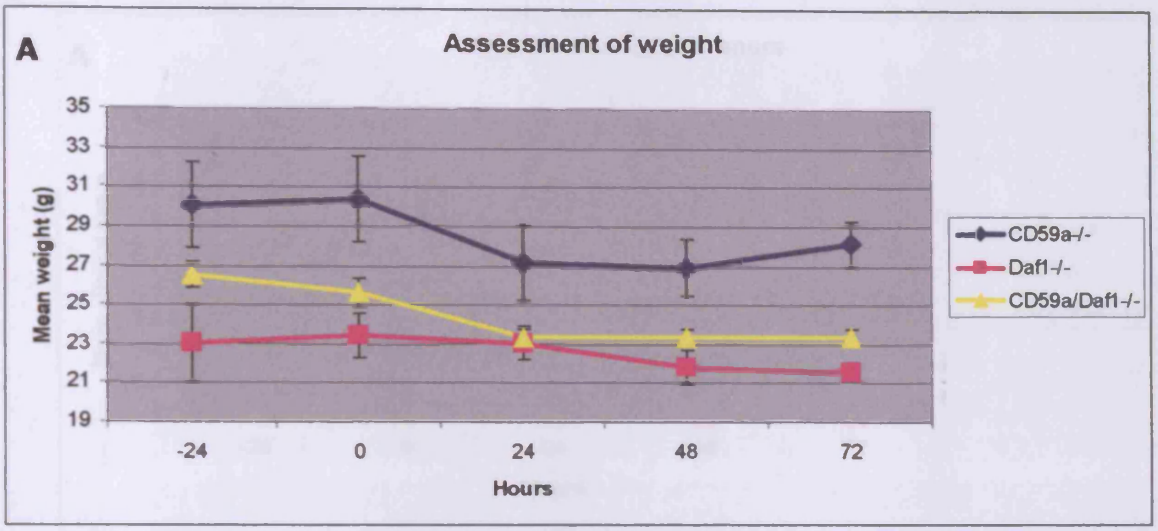

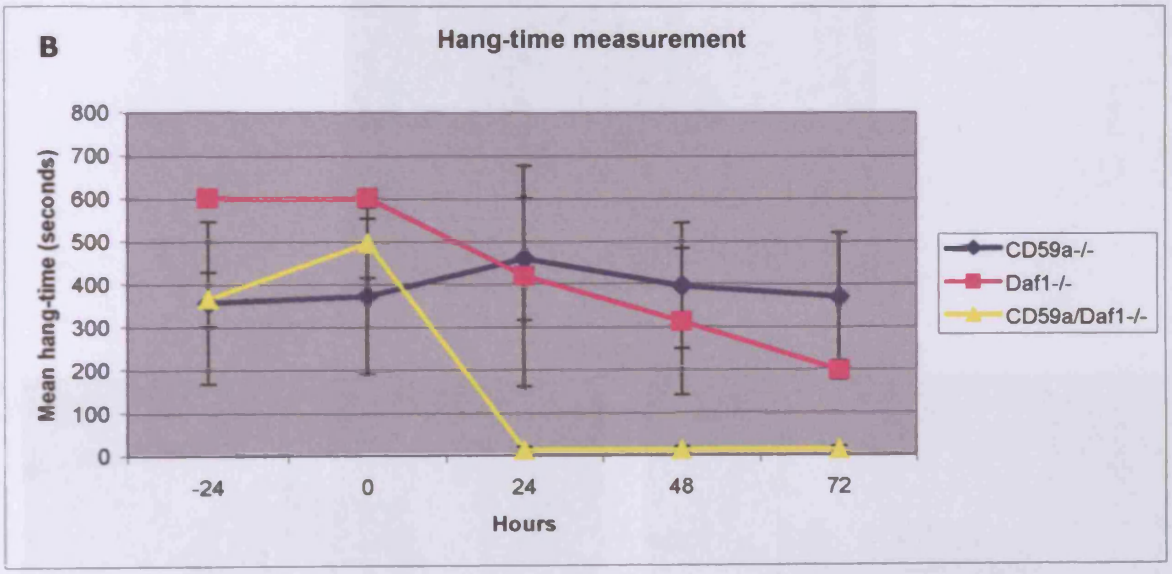

Figure 2

Assessment of change in weight and hang-time measurement for all groups of animals

*Cd59*a -/- (n=6), *Daf1*-/- (n=2) and *Cd59a/Daf1*-/- (n=3) were immunised with mcAb3 on Day 0, and assessed daily in terms of weight (A) and hang-time (B) as described. Data represents mean values in each group +/- standard deviation.

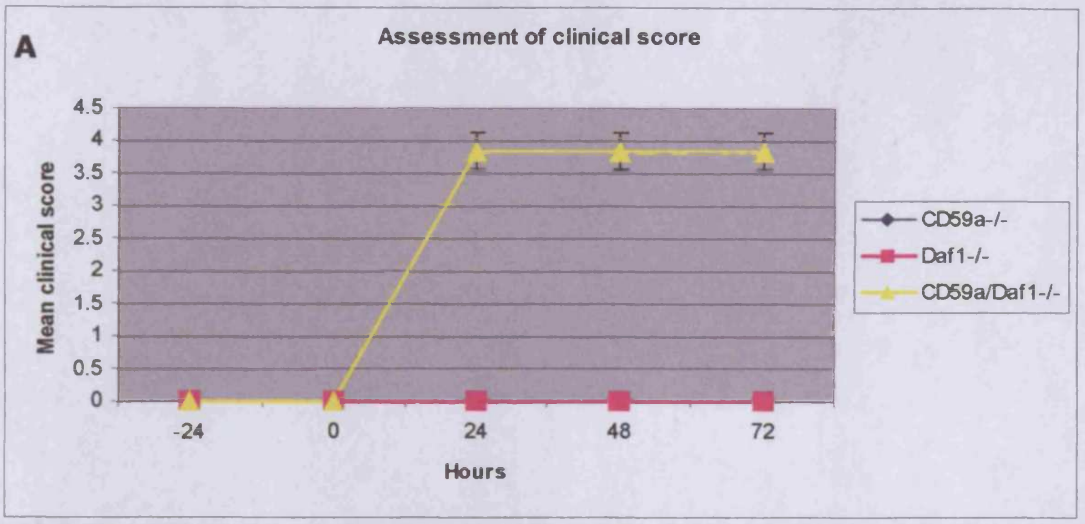

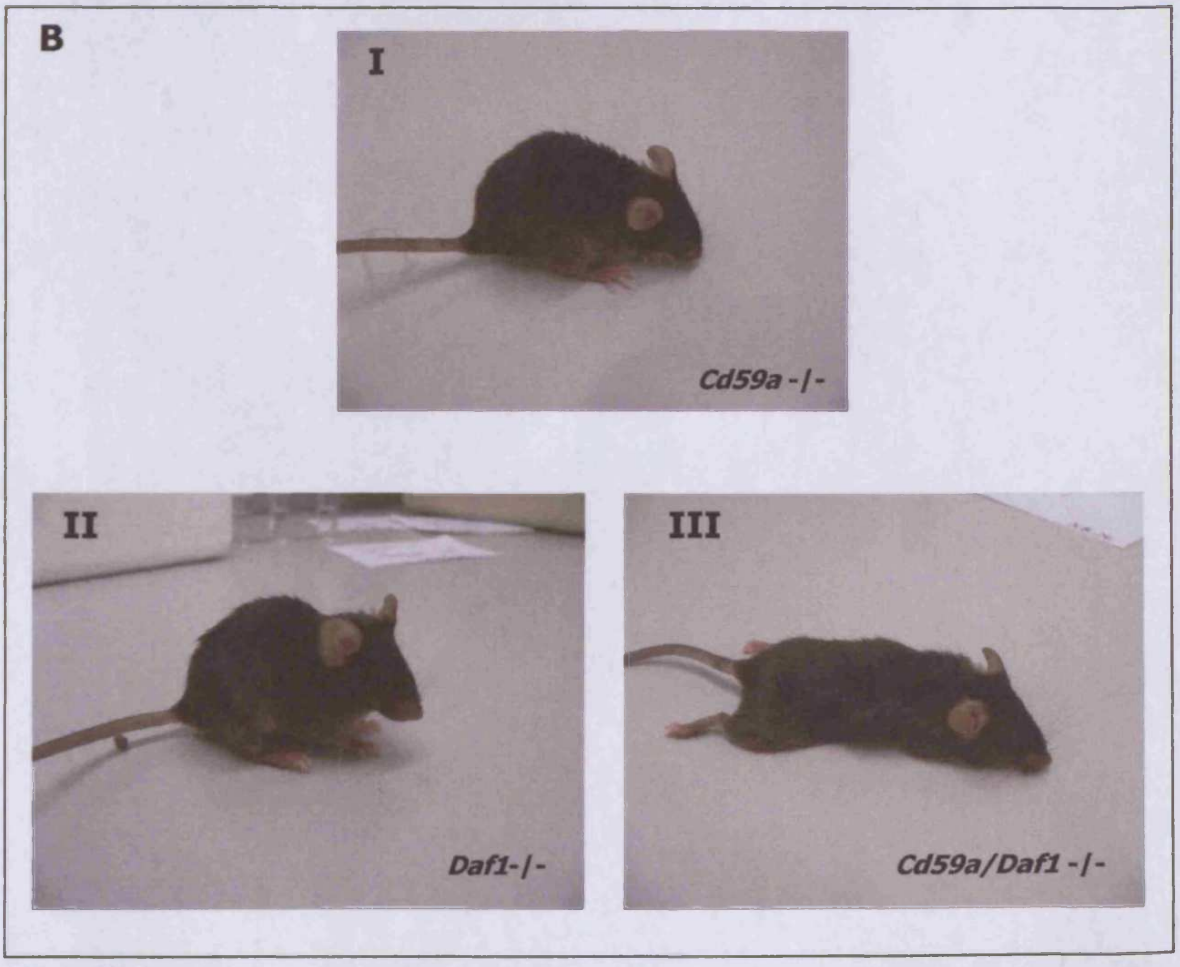

Figure 3

Assessment of clinical score in *Cd59a-/-, Daf1-/-, and Cd59a/Daf1-/-* following EAMG induction

Cd59a -/-, Daf1-/- and *Cd59a/Daf1-/-* were immunised with mcAb3 on Day 0, and assessed daily for changes in clinical score as described (A). Data represent mean values for each group +/- standard deviation. Data points for *Cd59a-/- and Daf1-/-* overlayed each other.

On day 1, *Cd59a-/-* mice (panel I) and *Daf1-/-* mice (panel II) displayed no clinical symptoms, while *Cd59a/Daf1-/-* mice displayed hind limb paralysis (panel III), reaching a clinical score of 4, and were sacrificed by a Schedule 1 method.

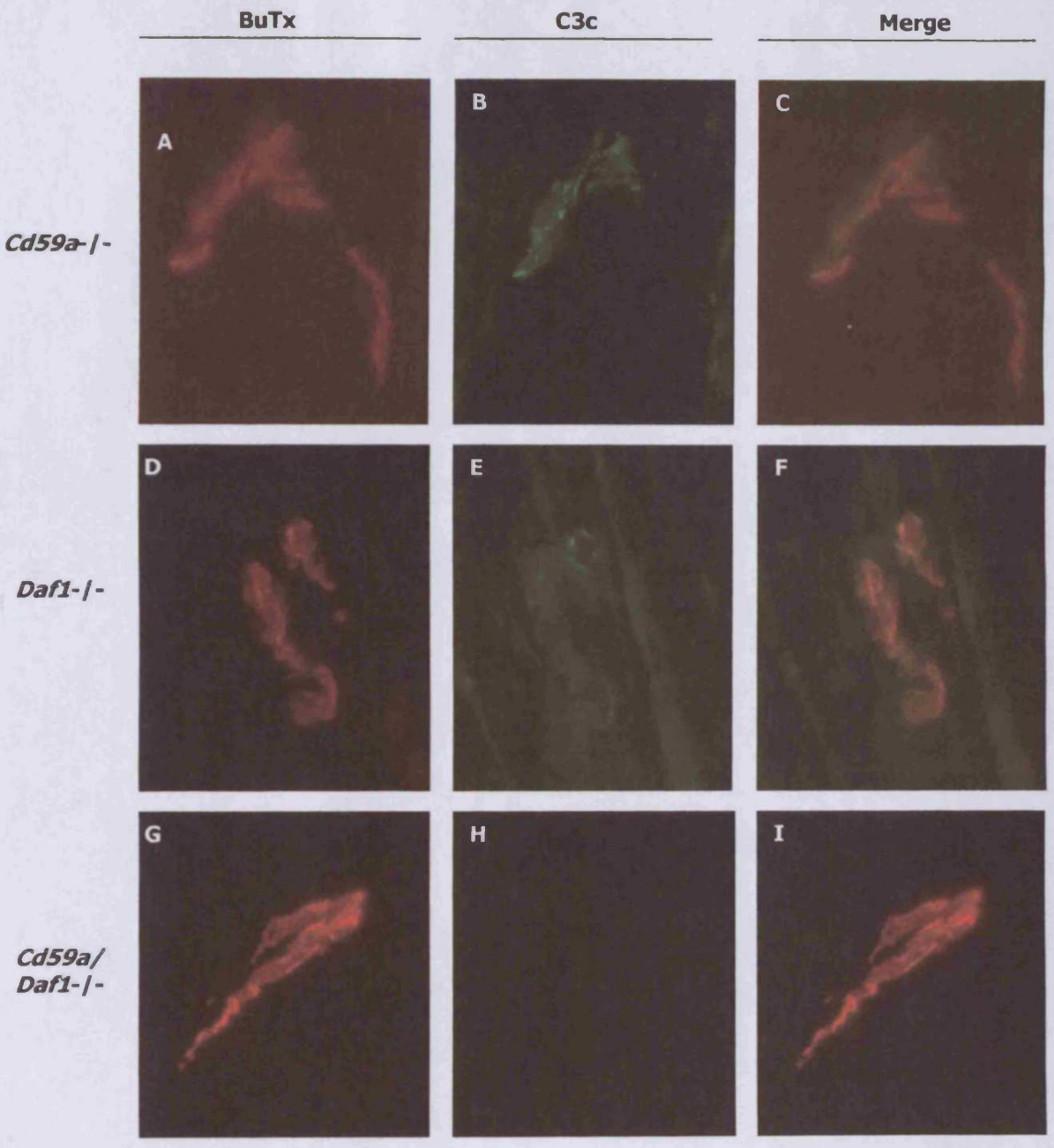

Figure 4

Assessment of C3 deposition at the nAChR in *Cd59a-/-*, *Daf1-/-* and *Cd59a/Daf1-/-* mice following EAMG induction

Soleus muscles from *Cd59a-/-* (A-C), *Daf1-/-* (D-F) and *Cd59a/Daf1-/-* (G-I) mice were harvested following induction of EAMG, and flash frozen in isopentane as described. Sections were stained with BuTx-rhodamine to identify nAChR (A, D, G), and double-stained with goat anti-rat C3c, detected with donkey anti-goat-Ig-FITC conjugate (B, E, H). Sections were mounted in VectorShield, and analysed under an inverted fluorescence microscope. Images were merged to detect co-localisation of C deposition at the nAChR (C, F, I). All images were taken at 400X magnification, magnified by 100%, and cropped to isolate the staining.

2.2.4.4 Inflammatory cell infiltration

Massive macrophage infiltration was evident in the soleus muscle of the *Cd59a-/-* mice confirmed by CD11b staining by immunofluorescence (Figure 5, A) and H&E staining (B). Such infiltration was minimal in *Daf1-/-* mice (C, D), and *Cd59a/Daf1-/-* (E, F).

2.3 Discussion

Cd59a/Daf1-/- displayed the most severe phenotype following EAMG induction, with most pronounced weight loss, severe weakness (as measured by the hang-time test), and clinical score. The animals were sacrificed 24 hours post-induction. Both single knockout groups of animals also displayed weight loss, although not as pronounced as for the double knockout animals, with *Daf1-/-* displaying the least weight loss. No weakness was detected using the hang-time test for *Cd59a-/-,* but *Daf1-/-* showed a trend towards a decrease in hang-time for the duration of the experiment (72 hours). Neither single knockout groups showed any clinical weakness, which was reflected in an absent clinical score. However, histologically, both *Cd59a-/-* and *Daf1-/-* showed C3 deposition at the nAChR, which was completely absent from the most severely affected group, the *Cd59a/Daf1-/-* mice. With a lack of regulation in both the activation and terminal pathways, it may be the case that C was completely depleted from these animals following EAMG induction, i.e. 'burn-out', accounting for the lack of C3 deposition observed. In terms of inflammatory cell infiltration, the most severe infiltration was detected in *Cd59a-/-,* with limited infiltration in both the *Daf1-/-* and *Cd59a/Daf1-/-* mice. It would appear that the lack of CD55 correlates with a lack of inflammatory cell infiltration.

Passive transfer EAMG has previously been described in the *Daf1-/-* mouse (Lin, Kaminski et al. 2002). The authors report that *Daf1-/-* displayed a severe weakness following induction of EAMG by 24 hours p.i., measured by the hang-time test, as compared to *Daf1+/+* littermate controls. The authors performed 3 experiments in the *Daf1-/-* mice, using either ascites fluid, or purified IgG from the ascites fluid. In either case, severe weakness was displayed by these animals by 24 hours p.i. This was not reproducible in our hands. However, in agreement with our data, they did report C3 deposition at the nAChR, although inflammatory cell infiltration was not measured. A number of parameters were performed by the authors that were not performed in this experiment. A measurement of nAChR levels, and electron microscopy demonstrated lower levels of nAChR in *Daf1-/-,* and NMJ gave a flattened appearance, consistent with EAMG induction.

The numbers of animals used in our experiments were small as a result of a limited supply of the inducing antibody. To substantiate our data, higher numbers of animals (n=6 per

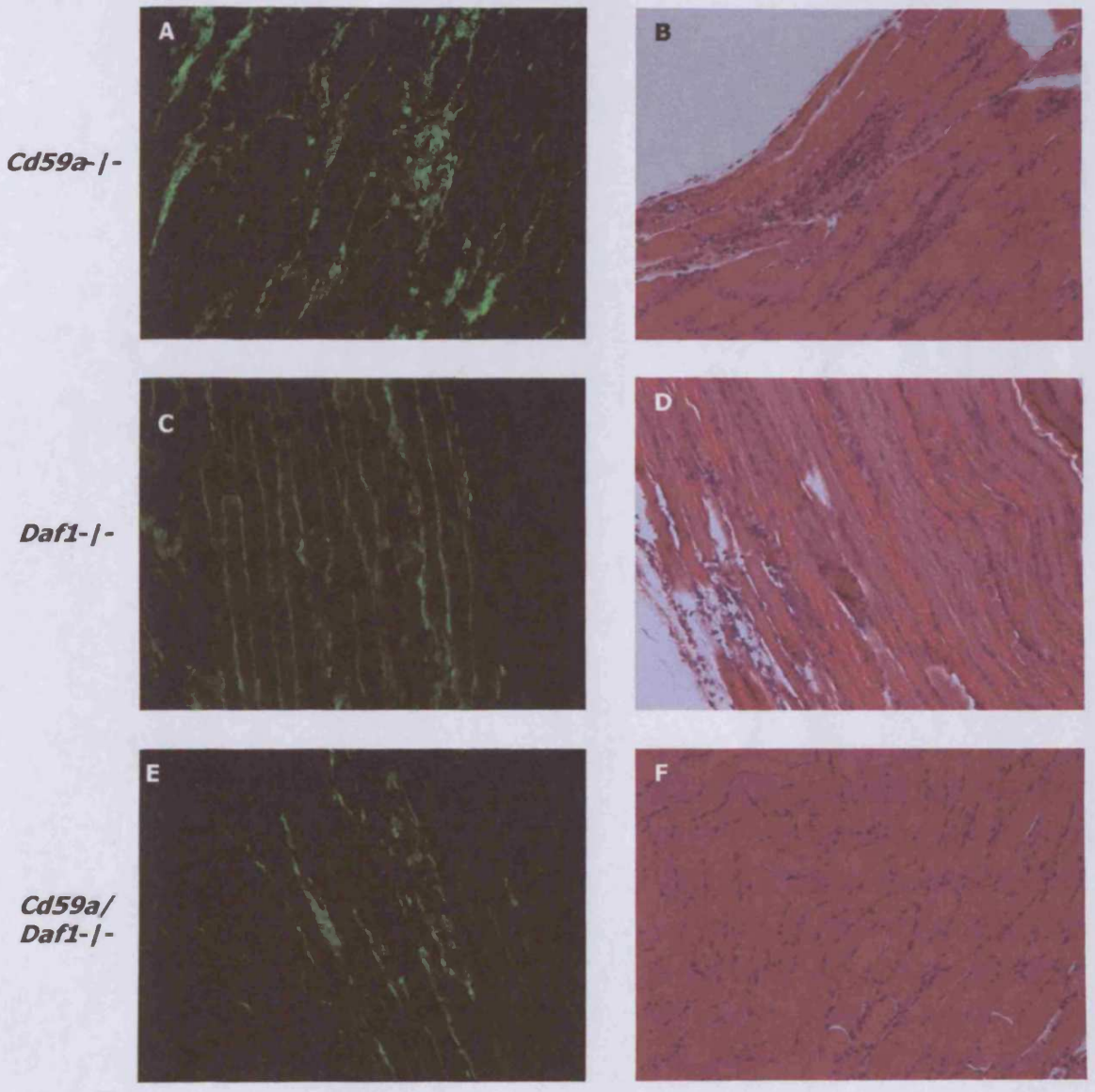

Figure 5

Assessment of inflammatory cell infiltration in *Cd59a-/-*, *Daf1-/-* and *Cd59a/Daf1-/-* mice following EAMG induction

Frozen soleus muscle sections from *Cd59a-/-* (A, B), *Daf1-/-* (C, D) and *Cd59a/Daf1-/-* (E, F) were stained with rat anti-mouse CD11b-FITC conjugate (A, C, E), and H&E stained (B, D, F) to confirm the presence of inflammatory cell infiltrates within the muscle.

All IF images were taken at 200X magnification; H&E images were taken at 100X magnification.

group) will be required, as well as *Cd59a+/+* and *Daf1+/+* littermates to be used as controls. In addition, a measure of nAChR would shed light on the true extent of nAChR loss, and further histological analyses of the NMJ by electron microscopy would provide direct evidence of flattening of post-synaptic folds and widening of the synaptic cleft.

It would be unwise to conclude anything from this limited study, although the data does suggest perhaps an alternative role for CD55 in mediating disease, possibly in mediating macrophage infiltration since a lack of CD55 correlates with a lack of macrophage infiltration, and warrants further study.

Chapter 6

General Discussion, Future Work and Conclusions

1 Project Aim

The primary aim of this project was to fully evaluate the role of C in peripheral neuropathy, using cell lines and animal models of human peripheral neuropathy. The secondary aim was to evaluate the role of C in a neuromuscular disorder, such as MG, where C has already been strongly implicated in disease pathogenesis.

1.1 C in GBS

Initial studies in Chapter 2 focussed on the characterisation of the C components and CRegs within the PNS. It was my aim to determine the level of protection conferred by CRegs on Schwann cells and sciatic nerve, and to assess the ability of Schwann cells to synthesize C components. From our studies, we demonstrated that the ability of the rat PNS to synthesize C components is extremely limited under normal conditions. However, only expression of C2 was detected under normal conditions. The relevance of this observation is unclear, although it is unlikely that C2 has a functional relevance in isolation. In humans, studies have shown that *in vitro* cultured fibroblasts and Schwann cells in isolation also do not show high expression of C components, but by IHC, showed immunoreactivity for C1s, C1r and C3 (de Jonge, van Schaik et al. 2004). It is likely that the environment the Schwann cells find themselves in plays a role in determining their expression profile. Perhaps the system used in this study for analysing expression of C component was too artificial; Schwann cells are never found in isolation, thus a co-culture system would have allowed examination of Schwann cell expression profiles relevant to the environment in which they normally find themselves. Similar studies have been performed previously, for example co-cultures of dorsal root ganglia (DRG) and peritoneal macrophages from the rat have been used to determine the presence of MAC on demyelinating fibres (Bruck, Bruck et al. 1995), studies analysing demyelination have used co-cultures of rat Schwann cells and embryonic DRG (Zanazzi, Einheber et al. 2001) and studies examining dysmyelination induced by IgM antisulphatide mAb have also applied similar systems (Rosenbluth and Moon 2003).

Characterisation of CReg expression in my study showed that CD55 had a restricted expression within the rat PNS, while both CD59 and Crry were widely expressed. CD46 was absent from all PNS-derived cells and tissues.

CD55 had a restricted expression in the PNS, with little or no expression on Schwann cells, but expression on whole sciatic nerve, on the vasculature and perineurium, some of which

co-localised with CD93 staining on endothelial cells. As mentioned previously, this restricted expression may have functional relevance in regard to the reported interaction with CD97 in a novel adhesion pathway (Hamman, Vogel et al. 1996). Increased CD55 and CD97 expression has also been implicated in inflammatory disease (Visser, de Vos et al. 2002). Had the EAN model been successfully established, the T cell-dependence and inflammatory component of the disease could have been examined in terms of the CD55-CD97 interaction, and provided an interesting avenue for future investigation.

CD59 was particularly highly expressed on Schwann cells both *in vitro* and *in vivo*, primarily on the myelin sheath, and possibly on the axon itself, as well as the perineurium of the sciatic nerve. This means that the sciatic nerve is well protected from MAC attack, but does this expression have a functional significance? To address this question, my aim was to examine the susceptibility of *Cd59a-/-* mice to EAN induction. One would expect that a dysregulation of MAC would lead to greater demyelination and tissue damage. However, since the tested method of inducing EAN in the mouse failed to induce specific disease, this question remains unanswered.

Crry was also highly expressed within the PNS, on Schwann cells both *in vitro* and *in vivo*, and on the perineurium. Some of this expression co-localised with CD93 staining, again suggesting expression on the endothelium. The functional significance of this expression is difficult to test *in vivo* since Crry-/- mice are embryonic lethal, and can only be rescued following backcrossing onto a C3-/- background (Xu and Mao 2000). However, since Crry is exclusively found in rodents, its relevance to human studies is limited.

It would be beneficial to assess whether observations made in the rat would have any relevance for extrapolation to the human situation. Limited studies on expression of CReg and C component biosynthesis in human PNS have been performed. A study in 2004 described expression of C components in the axons, whereas expression of CRegs was observed in the perineurium. CD59 expression was not observed on the Schwann cell, but was present on the myelin sheath, endoneurium, epineurium, blood vessels and perineurium, which is in direct contradiction from my observations in the rodent. In agreement with my studies, CD46 was not expressed in PNS tissues, while CD55 was weakly expressed on the Schwann cells and endoneurium and perineurium (de Jonge, van Schaik et al. 2004). CR1 expression was not examined in our study. To date only CR2 has been identified, and a molecule of 200kDa (C3bR-200) which is likely to be the rat immune adherence receptor, has been partially characterised and found to be analogous to CR1 (Quigg and Holers 1995). CR1 has been shown previously to be expressed in human

peripheral nerve. Extracts from myelinated and unmyelinated human nerves were shown to contain functional and non-functional CR1 respectively, though to be due to differences in glycosylation (Vedeler, Matre et al. 1989). CR1 therefore could provide a marker for myelinating Schwann cells in humans.

PMP22 was identified in this study as a target for further investigation due to the surprising observation that its expression was NOT restricted to PNS-derived tissues. I found high levels of expression in the kidney, specifically the glomeruli, and in the CNS, specifically within the central canal (Chapter 2). The fine localisation of expression of PMP22 within the kidney remains to be investigated, and may include the glomerular basement membrane, mesangial cells, or endothelial cells (Young and Heath 2000). PMP22 has previously been used to induce EAN in the rat, although this resulted in only a mild neuropathy (Gabriel, Hughes et al. 1998). However, effects elsewhere were not examined, and it may be the case that immunisation with PMP22 causes a glomerulonephritis rather than a neuropathy, although this remains untested. A thorough examination of the expression of PMP22 in the rat is urgently required to identify potential tissue targets for auto-immune disease. The study would entail RT-PCR analysis to identify where mRNA is expressed, Western blot analysis of tissue lysates, and IHC localisation, together with specific cellular markers to localise protein expression.

Chapter 3 described the successful production of a variety of antigens for the induction of EAN in both rats and mice. Due to the inaccessibility of bovine myelin following the BSE crisis, it became necessary to seek alternative antigens with which to actively induce EAN. A literature search revealed that peptides derived from PO, were being used to successfully induce disease in both species, thus PO was identified as a target for antigen generation for EAN. PO peptide 180-199 was first identified by Linington and Lassman as a neuritogenic epitope within PO, capable of inducing T cell-mediated EAN in the Lewis rat (Linington, Lassman et al. 1992).

Peptides corresponding to human PO 180-199, PO 180-199-amide and mouse PO 106-125 were synthesized as described. PO-EC domain was bacterially expressed and refolded successfully, as determined by CD spectroscopy (Chapter 3), although yields obtained were poor compared to mMOG EC domain, due to a lack of optimisation of the refold procedure. The discussion in Chapter 3 highlighted the requirement for an extensive 'trial and error' approach for the refolding of different proteins, as it should not be assumed that a protocol that works well for one protein will necessarily be suitable for another, regardless of similarities in size and structure. Given that the immunogenicity of the HNK-1 carbohydrate

moiety on PO has previously been demonstrated by the observation that GBS patients have antibodies in their serum specifically against this epitope (Voshol, van Zuylen et al. 1996), the bacterial expression system used in the generation of PO-EC domain, with its lack of post-translational modifications, may have been responsible for the lack of immunogenicity of this recombinant molecule observed in our studies. PO-EC domain, either refolded or non-refolded, failed to induce peripheral neuropathy in both rats and mice, and also failed to elicit specific polyclonal rabbit antiserum (unpublished data from this study). If other expression systems, with post-translational modification capability, had been used in parallel to this expression system, the question of the immunogenicity of the carbohydrate moiety on PO-EC domain could have been addressed.

Chapter 4 described attempts at inducing EAN in rats (Part 1), and mice (Part 2). Although numerous protocols were used for the optimisation of disease induction, all attempts failed. Many possible reasons exist for this failure.

The majority of autoimmune diseases are associated with certain MHC class II haplotypes, mostly due to presentation of auto-antigenic peptides on certain MHC class II molecules. For development of autoimmunity, a self-reactive T cell repertoire reactive with the presented peptide fragments must be available. Differential distribution of HLA-DQb/DRb epitopes has been observed in different forms of GBS; AMAN and AIDP (Magira, Papaioakim et al. 2003), as well as in MS, which is strongly associated with HLA-DR2a, DR2b and DQ6 in US Americans and Northern Europeans. As with humans, susceptibility or resistance in models of disease is also associated with MHC class II gene products (RT1 in the rat) (de Graaf, Barth et al. 2004). Previous studies examining the influence of HLA haplotypes in GBS have often given conflicting results, most likely as a result of low numbers of patients studied. However, more recently, the susceptibility to EAN had been shown to differ between various inbred rat strains (Dahlman, Wallstrom et al. 2001), underlining that disease susceptibility in rats is also genetically determined. A recent study has definitively proven that MHC class II genes are major susceptibility genes in EAN (de Graaf, Wallstrom et al. 2004). The study examined the influence of the MHC phenotype and non-MHC phenotype on disease induction following immunisation of rats with BPNM or P2 peptide 58-81, using a variety of inbred, MHC congenic and intra-MHC congenic rat strains. However, it was observed that non-MHC genes also determine susceptibility since only Lewis, DA, PVG and COP genomes were susceptible while BN, WF, F344 and ACI genomes were protective.

These data suggest a powerful reason as to why no disease was induced in preliminary experiments performed in the PVG rats. PVG ($RT1^c$) as used in my experiments, were protected from disease induction in the de Graaf study, while PVG ($RT1^{av1}$) developed monophasic EAN following immunisation with BPNM. However, the Lewis rat genome was

generally highly susceptible to disease induction using both BPNM and P2 peptide, with the exception of LEW.1.N, which was resistant to P2-induced EAN. The susceptibility of 2 further strains was also not tested (LEW.1NR1 and LEW.1.LR1) with respect to induction of disease with BPNM, and showed differential susceptibility to P2-induced EAN.
Despite attempts at interrogating the Charles River website, it remains unclear as to the particular substrain supplied, and used in these experiments. It remains a possibility therefore that a more resistant substrain of Lewis rat was used.

A second reason for the lack of disease seen in rats and mice may be due to the heterologous nature of the antigens used in the preliminary optimisation studies. We used the human PO sequence as a template on which to base our peptide synthesis and bacterial expression. This was because the extracellular domain of human PO had previously been successfully expressed, purified and refolded (Bond, Saavedra et al. 2001). We also believed that since T (Khalili-Shirazi, Hughes et al. 1992) and B cell (Khalili-Shirazi, Atkinson et al. 1993) responses to human PO had been detected in patients with GBS, that human PO was sufficiently immunogenic for subsequent animal studies. However, the failure of human PO peptides 180-199, and human PO-EC domain to induce disease may stem from the fact that there are small differences in the amino acid sequences between human and rodent, which may have been critical to initiate a sustained immune response (Figure 6.1). The neuritogenic PO peptide 180-199 previously determined by Linington and colleagues (Linington, Lassman et al. 1992) was derived from the rat sequence, in which there is one amino acid change from alanine in the human sequence to serine in the rodent sequence (Figure 1). As examined in the Introduction (Section 1.7.1.1), single amino acid substiutions may have profound effects on the ability of peptides to induce autoimmune reactions on account of TCR avidity for certain MHC class II/peptide complexes. The studies performed by Zhu and colleagues on EAN induction using PO peptide 180-199 (Zhu, Pelidou et al. 2001), successfully used the rat sequence to generate the peptide, and thus the serine substitution may have great significance for disease induction.

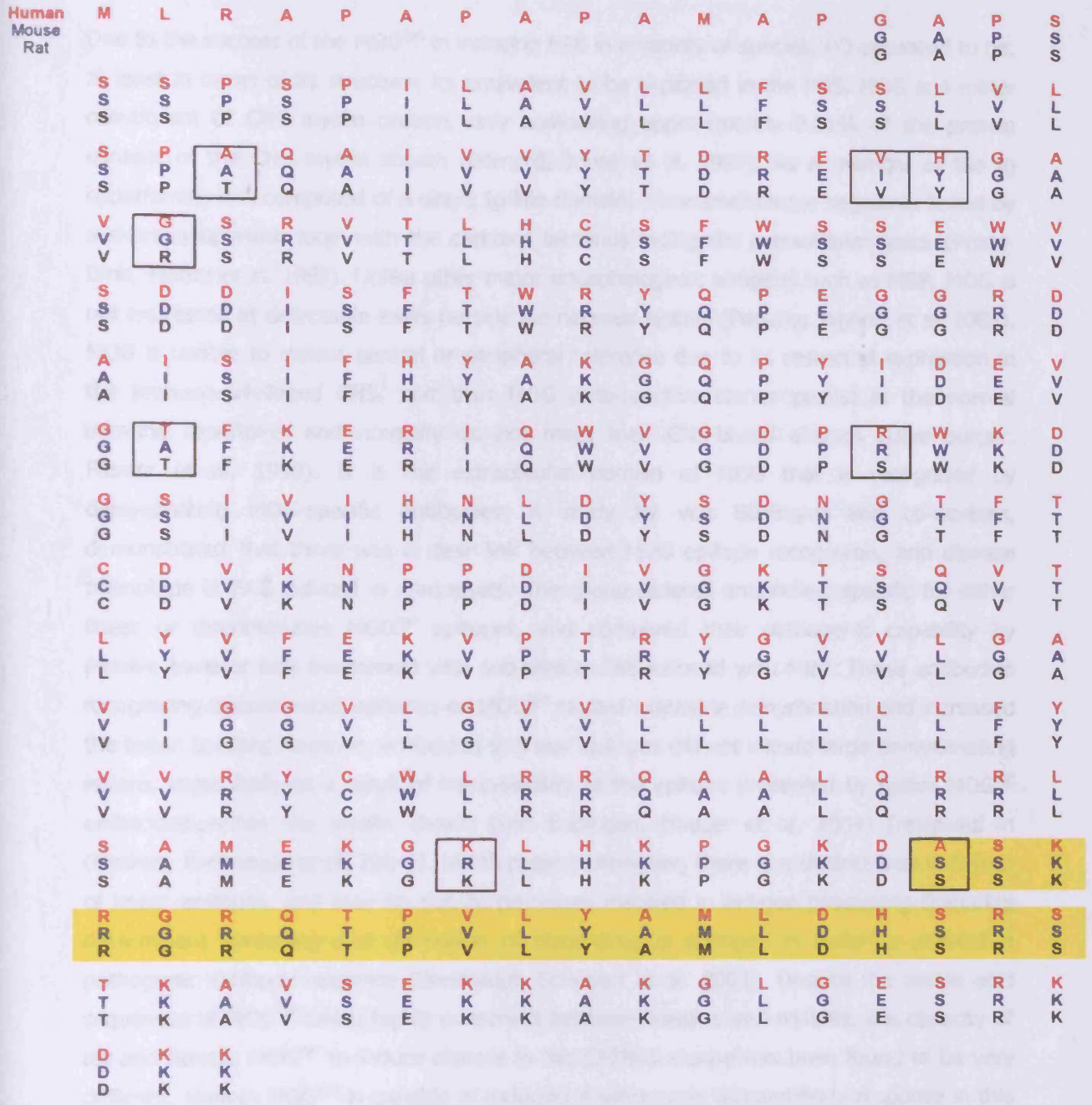

Figure 1 **Alignment of amino acid sequences of PO from human, mouse and rat**

Amino acid sequences were obtained from Entrez Pubmed (human, NM_000530, red; mouse, NM_008623, blue; rat, NM_017027, black), and aligned using MegAlign (DNAstar, Inc.). Variations between sequences were highlighted by a border. Yellow shaded area corresponded to PO peptide sequence 180-199.

Due to the success of the MOG^{Igd} in inducing EAE in a variety of species, PO appeared to be, at least in terms of its structure, its equivalent to be exploited in the PNS. MOG is a minor constituent of CNS myelin protein, only composing approximately 0.01% of the protein content of the CNS myelin sheath (Bernard, Johns et al. 1997). As a member of the Ig superfamily, it is composed of a single Ig-like domain, 2 transmembrane segments linked by a short cytoplasmic loop, with the carboxyl terminus facing the extracellular space (Pham-Dinh, Mattei et al. 1993). Unlike other major encephalogenic antigens such as MBP, MOG is not expressed at detectable levels outside the nervous system (Pagany, Jagodic et al. 2003). MOG is unable to induce central or peripheral tolerance due to its restricted expression in the immuno-privileged CNS, and thus MOG auto-reactive clones persist in the normal immune repertoire, and normally do not meet their CNS-based antigen (Litzenburger, Fassler et al. 1998). It is the extracellular domain of MOG that is recognised by demyelinating MOG-specific antibodies. A study by von Büdingen and co-workers, demonstrated that there was a clear link between MOG epitope recognition, and disease phenotype in EAE induced in marmosets. The group isolated antibodies, specific for either linear or discontinuous MOG^{Igd} epitopes, and compared their pathogenic capability by passive transfer into marmosets with sub-clinical EAE induced with MBP. Those antibodies recognising discontinuous epitopes on MOG^{Igd} caused extensive demyelination and increased the lesion burden; however, antibodies to linear epitopes did not initiate large demyelinating lesions, most likely as a result of inaccessibility of the epitope presented by native MOG^{Igd} embedded within the myelin sheath (von Budingen, Hauser et al. 2004) [reviewed in (Mathey, Breithaupt et al. 2004)]. In MS patients however, there is a distinct bias in favour of linear epitopes, and may be due to proteases involved in antigen processing favouring determinant spreading and disruption of discontinuous epitopes in order to prevent a pathogenic antibody response (Breithaupt, Schubart et al. 2003). Despite the amino acid sequences of MOG^{Igd} being highly conserved between humans and rodents, the capacity of rat and human MOG^{Igd} to induce disease in the C57Bl/6 mouse has been found to be very different. Human MOG^{Igd} is capable of inducing a pathogenic autoantibody response in this mouse strain (Lyons, Ramsbottom et al. 2002), while rat MOG^{Igd} is not (Bourquin, Schubart et al. 2003). This dramatically demonstrates the impact that small differences in amino acid sequence may have on the relative importance of arms of the immune system in autoimmune disease, and underlines again the need to use autologous antigens when studying autoimmunity (Mathey, Breithaupt et al. 2004).

The capacity of PO protein to induce EAN in susceptible animals has been shown previously. Milner et al demonstrated that whole PO, prepared from bovine spinal root myelin, was

capable of inducing clinical EAN in Lewis rats with severe histological lesions, but only in the presence of lysophosphatidylcholine (LPC). It was thought that LPC allows proteins to adopt their native conformations following purification, thus exposing immunogenic epitopes. EAN induced with purified bovine P2 protein was also enhanced by addition of LPC (Milner, Lovelidge et al. 1987). Addition of LPC may also have enhanced the ability of our PO-EC domain to induce an immune response. Clearly native purified PO is capable of inducing disease, as is PO within a myelin preparation. Whole PO, and PO within myelin sheaths would also contain the TM and cytoplasmic regions of the protein. Since neuritogenic PO peptide 180-199 is located within the cytoplasmic region of PO, is the cytoplasmic domain a requirement for autoimmune disease initiation?

T cell responses to PO and P2 have previously been demonstrated in GBS and chronic inflammatory demyelinating polyneuropathy (CIDP) patients (Khalili-Shirazi, Hughes et al. 1992). Various studies have also demonstrated the presence of antibodies to peripheral nerve proteins in the sera of GBS patients, with the most common antibodies directed against PO (Khalili-Shirazi, Atkinson et al. 1993; Yan, Archelos et al. 2001; Allen, Giannopoulos et al. 2005) although these responses are only detected in a minority of patients.

This has also been mirrored in EAN in the Lewis rat (Archelos, Roggenbuck et al. 1993), where induction of disease using purified bovine myelin resulted in specific antibody responses to PO detected at day 13, almost concurrent with symptoms of EAN, while antibody responses to P2 lagged behind by 1-3 days, and did not correlate with disease activity. The antibody responses to PO were measured using bacterially expressed, refolded extracellular domain of PO in an ELISA format. The mystery lies in why this PO was not used to induce disease. Had it been tried and failed to induce disease? No single report is available on the ability of bacterially expressed EC domain of PO to induce EAN.

EAN may also be induced with bacterially expressed PMP22 in the rat (Gabriel, Hughes et al. 1998). However, the disease severity was limited to mild weakness of the tail tip which although persisted throughout the experiment, showed no histological features in the sciatic nerve, and only isolated demyelinated fibres in the spinal root in 7 out of 21 animals. The reason for such a mild neuropathy may be due to the unrestricted nature of PMP22 expression in the Lewis rat, as demonstrated by these studies, with high expression detected in the kidney (Chapter 2). Perhaps a more severe response would have been elicited in the kidney, which is infinitely more accessible than the PNS.

The expression of PO in the rat remains unclear. It is possible that PO too has an unrestricted expression pattern, and neuropathy would not be expected to necessarily be a primary sign of an autoimmune response against this protein. The lack of a commercially

available antibody which recognises native PO has so far hampered efforts to examine PO localisation, although it would be possible to examine expression at the mRNA level using primers designed already for this project (Chapter 3), in all tissues in the rat.

Discussion with Dr. Neil Robertson (Dept. of Neurology, University Hospital of Wales, Cardiff) revealed that some patients with CIDP may benefit from treatment with the anti-CD52 (CAMPATH-1H) antibody, currently used in clinical trials for lymphoid malignancy (Lundin, Porwit-MacDonald et al. 2004) and rheumatoid arthritis (RA) (Issacs, Manna et al. 1996). CAMPATH-1H functions to deplete T cells, which express the CD52 antigen, via a C-mediated pathway (Rowan, Hale et al. 1995), and therefore effectively eliminates the T cell component of an autoimmune disease. Current treatment regimes in CIDP utilise IVIg and plasma exchange, which although ameliorates symptoms during the relapse, has been documented as extremely debilitating for the patient (since most patients receive treatment every 3 months, and require a hospital stay) (Bersano, Carpo et al. 2005). CAMPATH-1H treatment was evaluated in 1 patient, and the response was remission which was sustained for at least 1 year (Dr. Robertson, personal communication). It would be extremely beneficial for the success of future therapy to have a working model of CIDP, in which the mechanism of action of CAMPATH-1H, and any downstream effects could be further interrogated. The studies on MHC class II susceptibility in EAN revealed that COP and LEW.1AV1 rats strains developed severe chronic disease following immunisation with BPNM (de Graaf, Wallstrom et al. 2004), and could therefore provide a working model of CIDP.

C57Bl/6 mice are known to be resistant to EAN induction using P2 protein (Taylor and Hughes 1985), and BPNM (Zhu, Nennesmo et al. 1999). Attempts at establishing reliable and severe disease have either failed or resulted in a mild disease with poor reproducibility. Using the immunodominant peptide 180-199 from human PO, Zou and colleagues (Zou, Ljunggren et al. 2000) described successful induction of EAN in this resistant strain, enhanced by addition of PT. However, these findings have not been confirmed by any other group, although Zou and colleagues have published extensively using this model (Zhu, Ljunggren et al. 2001; Bao, Lindgren et al. 2002; Zhu, Bao et al. 2002; Bao, Lindgren et al. 2003; Duan, Chen et al. 2004; Yu, Duan et al. 2004), I have been unable to successfully induce disease. Earlier in 2005, Miletic and co-workers (Miletic, Utermohlen et al. 2005) published data using a peptide derived from mouse PO capable of inducing severe and highly reproducible EAN in the C57Bl/6 mouse. This failed to induce severe and reliable disease in my hands (Chapter 4, Part 2). As mentioned in the discussion of that chapter, a wider-ranging analysis of histology from the animals to encompass not only H&E staining, but also specific staining for macrophages, CD4+ and CD8+ T cells and B cells should have

been performed. In addition, T cell proliferation experiments should have been conducted to assess the ability of T cells to respond to PO peptide 106-125, as well as testing of generation of antibodies to the peptide, i.e. a B cell response. Electrophysiological assessments may also have been performed. Perhaps disease obtained was mild in our hands, and a more through analysis would have revealed a degree of neuropathy.

The studies previously performed in both EAN (de Graaf, Wallstrom et al. 2004) and EAE in the rat (de Graaf, Barth et al. 2004) with respect to MHC class II association with susceptibility to disease, would be highly beneficial in this mouse model. Given the inherent resistance of the C57Bl/6 mouse to disease induction, it would be extremely beneficial to see if patterns emerge regarding susceptibility and resistance to disease induction, to enable design of better models in the future.

1.2 C and MG

Although C is widely implicated in the pathology of MG, analysis of individual components was lacking. EAMG mimics many of the pathological changes at the NMJ seen in MG patients, albeit, in a more acute manner.

Chapter 5 described the successful induction of passively transferred EAMG in the rat (Part 1) and mouse (Part 2). In the rat, following optimisation of dose of antibody against the nAChR (mAb35, 1mg/kg), subsequent experiments evaluated the role of the MAC in mediating disease, using wild type rats versus animals deficient in the terminal pathway component C6. PVG rats were backcrossed onto Lewis background for 8 generations, with the intention of utilising the same strain for passively and actively induced EAMG. Following injection with mAb35, animals were assessed in terms of weight loss and weakness as described. Wild type animals exhibited a severe clinical weakness and paralysis 36 hours post-induction in parallel to severe weight loss, while C6 deficient animals were protected from clinical manifestations of disease. Histological examination revealed C3 deposition at the nAChR, and therefore the NMJ in both wild type and C6 deficient animals, but MAC deposition was only evident in wild type animals. Inflammatory cell infiltration was extensive in wild type animals, but absent from C6 deficient animals, corresponding to a decreased number of BuTx-positive nAChR in the wild type animals.

To confirm that the presence of C6 was required for disease induction, human C6 was purified from plasma by affinity chromatography, and reconstituted to C6 deficient rats. Reconstitution of C6 to the C6 deficient rat resulted in enhanced susceptibility to disease. These data demonstrate conclusively that MAC is the major drive to NMJ destruction in EAMG.

Passive transfer EAMG was also utilised in the testing of 3 anti-C therapeutic strategies; a soluble form of Crry (4 SCR), a Crry-Fc fusion protein and a C5 inhibitor (rEV576). All therapies were administered in parallel to disease induction. Contrary to expectations, soluble Crry reduced severity of EAMG, from which animals were able to recover, but addition of an Fc tail markedly enhanced this capacity, and completely protected animals from any clinical manifestations. This was also true for the C5 inhibitor rEV576, and may provide a mechanism by which to selectively inhibit the terminal pathway.
Taken together, these data confirm conclusively that the MAC is key in mediating EAMG in the Lewis rat, and C5a is not required for disease initiation or progression. Similar results have previously been obtained in EAE, where blockade of the C5a receptor using a small molecule antagonist failed to protect against EAE in the rat (Morgan, Griffiths et al. 2004).

Although current treatments for patients with MG are effective (IVIg, plasma exchange, steroid treatments), patients exist that fail to respond to such treatments, so-called refractory MG, for which alternative therapies must be sought (Wylam, Anderson et al. 2003). Anti-C therapy may therefore provide a means of treating such patients. Our studies have highlighted the importance of the MAC in mediating disease, and thus identified a target for future immunotherapeutic strategies. The benefit of using a therapy selective for the terminal pathway is appealing since it would not interfere with the activation pathways of C which have important biological roles in immune complex processing and bacterial clearance. It should be noted that systemic inhibition of the terminal pathway may increase susceptibility to *Neisseria* infections (Morgan and Walport 1991). However, the immunogenicity of rEV576 in the rat has not been addressed, and may provide an obstacle to its effective use in therapy. Soluble forms of classical CRegs have already been utilised in clinical trials, with sCR1 (TP10) receiving the most attention (Lazar, Bokesch et al. 2004; Li, Sanders et al. 2004). Membrane-addressed forms of human CD59 has also been proven to be effective in antigen-induced arthritis (Linton, Williams et al. 2000) and in Miller Fisher syndrome (Halstead, Humphreys et al. 2005). Targeting of CD59 to the endplate using a CD59-BuTx fusion protein would provide a highly specific targeting mechanism for anti-C therapy in EAMG. However, its inherent toxicity could be by-passed by means of fusion of antibody fragments containing an antigen binding site (possibly against the main immunogenic region (MIR) of the nAChR), which would not block its function, and still allow efficient targeting of the CReg. The anti-nAChR mAb, mAb35, used in for EAMG induction in my studies, could provide a template for testing of this hypothesis in the rat model and could then be extrapolated to the human condition. This has previously been tested using CD55-based fusion proteins, with an antibody fragment targeted to the hapten dansyl (Zhang, Lu et al. 2001).

While acute EAMG mimics the pathology seen in MG, MG is generally considered a chronic disease and thus this model has limited relevance for extrapolation to the human situation. Actively induced EAMG more closely mimics a chronic disease, and will be considered for future experiments. In addition, perhaps it would be possible to induce a more chronic disease using a lower dose of mAb35, with repeated immunisations. This remains to be proven but provides a useful avenue for further investigation. Future work could also examine the efficacy of anti-C therapy following established disease; this may be more relevant to the human situation.

Passive transfer EAMG was also established in the mouse, using a monoclonal antibody (mcAb3) kindly provided by Prof. Vanda Lennon. Only preliminary work has been performed to date, but has yielded some interesting observations. *Daf1/Cd59a-/-* mice were more susceptible to passively induced EAMG than their single knockout counterparts (Chapter 5, Part 2). These mice showed severe clinical weakness characterised by complete hind limb paralysis at 24 hours post-induction. Paradoxically, histological findings demonstrated no C3 deposition, and minimal inflammatory cell infiltration in the soleus muscle of these severely affected animals, while *Cd59a-/-* mice, demonstrating no clinical symptoms, showed C3 deposition at the nAChR, as well as extensive inflammatory infiltrates in sections of soleus muscle. *Daf1-/-* mice also showed no clinical symptoms, but did show C3 deposition, but with minimal inflammatory infiltration. It appeared that a lack of CD55 correlated with a reduced inflammatory infiltration. It would be interesting to evaluate the expression of CD97 in the *Cd59a-/-* animals, and see if this co-localised with CD11b staining for macrophages. A mechanism for inflammatory cell infiltration may therefore be mediated by CD55 in these mice, and the lack of the regulator protects muscle in *Daf1-/-* and the double knockouts *Daf1/Cd59a-/-* from infiltration. Analysis of lymphocytes derived from whole blood of histologically affected mice for CD97 expression may also yield a further insight into this mechanism. However, C deposition and inflammatory cell infiltration was clearly not sufficient to drive clinical weakness in the *Cd59a-/-* mice, thus clinical symptoms must be derived from another source in these animals. Possibly a lack of regulation in both the activation and terminal pathways of C in the double knockout mice, may have lead to complete depletion of C in the early stages of disease, providing an explanation for lack of C deposition at the nAChR. This experiment has recently been repeated while this thesis was being written, with statistically significant numbers of animals. Preliminary analysis has revealed extensive inflammatory infiltration in 7 out of 8 *Daf1/Cd59a-/-* mice. The lack of inflammatory infiltration observed in my experiments was likely an artefact of small numbers of animals used, and underlines the importance of using statistically significant numbers of

animals. The system of quantification of receptor loss used in the rat will also be included in this latest analysis.

CD55 had a restricted expression within the PNS (Chapter 2), and also in soleus muscle (Chapter 5). In the rat, no expression of CD55 was detected at the NMJ or elsewhere in the soleus muscle in the naïve rat; however, following EAMG induction, weak, punctuate staining, presumably on vessels, was observed in wild type animals that were susceptible to disease, but this staining was absent from C6 deficient animals that were protected from disease. Although the MAC has been established as the primary cause for the destruction of the NMJ, other mechanisms may also be at play, regarding inflammatory cell recruitment. Sections could be examined for identification of inflammatory cells as macrophage, T cells or B cells in MG. Future work would focus on identifying the structures expressing CD55 following EAMG induction, and examining expression of CD97, perhaps at the NMJ. CD97 expression has previously been shown to be absent from normal white matter in the brain, but present on T cells, macrophages and microglia, in pre-active lesions in MS (Visser, de Vos et al. 2002). Is this also true in MG? Is there a lack of CD97 expression in the normal endplate, and does expression increase following disease onset? CD55 expression did show some co-localisation with CD93 expression in my experiments in Chapter 2, providing evidence for expression on the endothelium, but the expression of CD97 was not analysed.

1.3 Conclusions

The data presented in this thesis has increased our understanding of the expression of C components and regulators in the PNS in the rat. Characterisation of the ability of the PNS to protect against C attack yielded interesting observations, and allowed me to target my research to areas of relevance, such as functional analysis of high expression of CD59 in and around the PNS, the interaction of CD55 and its ligand CD97, and further analysis on the expression of PMP22.

C has been widely implicated in disease pathogenesis in GBS, and in its corresponding animal model EAN. Unfortunately, no further evidence of C involvement has been generated during this project using published methods and modifications of disease induction. There remains a great deal of work to complete to further our understanding of the interplay between the innate and adaptive arms of the immune system in determining susceptibility to disease, and in mediating disease pathogenesis, and we have the tools with which to explore this fields, just not the model as yet.

As a result of the data presented in this thesis, the role of the MAC in mediating neuromuscular disease in the rat has been defined, and the terminal pathway identified as a target for future immunotherapy. I have also established a model of EAMG in the rat, and its application to testing of various anti-C therapeutics has been validated. In addition, interesting preliminary observations have also been obtained in a mouse model of EAMG, the findings of which are providing a platform for current research.

Chapter 7
References

Abromson-Leeman, S., R. Bronson, et al. (1995). "Experimental autoimmune neuritis induced in Balb/C mice by myelin basic protein-specific T cell clones." Journal of Experimental Medicine 182: 587-592.

Adelmann, M. and C. Linington (1992). "Molecular mimicry and the autoimmune response to the peripheral nerve myelin PO glycoprotein." Neurochemical Research 17: 887-891.

Aegerter-Shaw, M. J., J. L. Cole, et al. (1987). "Expansion of the complement receptor gene family. Identification in the mouse of two new genes realted to the CR1 and CR2 gene family." Journal of Immunology 138(10): 3488-94.

Alajouanine, T., R. Thurel, et al. (1936). "La polyradiculonevrite aigue generalisee avec diplegie faciale et paralusie terminale des muscles respiratoires et avec dissociation albuminocytologique: etude anatomique." Rev Neurol (Paris) 65: 681-697.

Alberts, B., D. Bray, et al. (1994). Molecular Biology of the Cell. New York, Garland Publishing, Inc.

Allen, D., K. Giannopoulos, et al. (2005). "Antibodies to peripheral nerve myelin proteins in chronic inflammatory demyelinating polyradiculoneuropathy." Journal of Peripheral Nervous System 10(2): 174-180.

Anderson, D. J., A. F. Abbott, et al. (1993). "The role of complement component C3b and its receptors in sperm-oocyte interaction." Proc. Natl. Acad. Sci. USA 90: 10051-10055.

Archelos, J. J., M. Maurer, et al. (1993). "Suppression of experimental allergic neuritis by an antibody to the intracellular adhesion molecule ICAM-1." Brain 116(5): 1043-1058.

Archelos, J. J., K. Roggenbuck, et al. (1993). "Detection and quantification of antibodies to the extracellular domain of PO during experimental allergic neuritis." Journal of Neurological Science 117: 197-205.

Asbury, A. K. and P. K. Thomas (1995). Peripheral Nerve Disorders 2. Oxford, Butterworth Heineman.

Ashkenazi, A., D. J. Capon, et al. (1993). "Immunoadhesins." International Reviews in Immunology 10(2-3): 219-227.

Astrom, K. E. and B. H. Waksman (1962). "The passive transfer of experimental allergic encephalomyelitis and neuritis with living lymphoid cells." Journal of Pathology and Bacteriology 83: 89.

Baalasubramanian, S., C. L. Harris, et al. (2004). "CD59a is the primary regulator of membrane attack complex assembly in the mouse." Journal of Immunology 173: 3684-3692.

Baechner, D., T. Liehr, et al. (1995). "Widespread expression of the peripheral myelin protein-22 gene (PMP22) in neural and non-neural tissues during murine development." Journal of Neuroscience Research 42(6): 733-741.

Bansal, R. and A. N. Malaviya (1984). "Isolation and characterisation of C1q from human serum." Asian Pac J Allergy Immunol 2(2): 217-221.

Bansal, R. and S. E. Pfeiffer (1987). "Regulated galctolipid synthesis and cell surface expression in Schwann cell line D6P2T." Journal of Neurochemistry 49(6): 1902-1911.

Bao, L., J. U. Lindgren, et al. (2002). "The critical role of IL-12p40 in initiating, enhancing and perpetuating pathogenic events in murine experimental autoimmune neuritis." Brain Pathol 12(4): 420-429.

Bao, L., J. U. Lindgren, et al. (2003). "Exogenous soluble tomour necrosis factor receptor type 1 ameliorates murine experimental autoimmune neuritis." Neurobiology of Disease 12(1): 73-81.

Barohn, R. J. and R. L. Brey (1993). "Soluble terminal complement components in human myasthenia gravis." Clin. Neurol. Neurosurg. 95(4): 285-290.

Basta, M., I. Illa, et al. (1996). "Increased in vitro uptake of the complement C3b in the serum of patients with Guillain-Barre syndrome, myasthenia gravis and dermatomyositis." Journal of Neuroimmunology 71(1-2): 227-229.

Baumann, N. and D. Pham-Dinh (2001). "Biology of oligodendrocyte and myelin in the mammalian central nervous system." Physiological Reviews 81(2): 871-927.

Bechtold, D. A., X. Yue, et al. (2005). "Axonal protection in Experimental Autoimmune Neuritis by the sodium channel blocking agent flecanide." Brain 128: 18-28.

Beiter, T., M. R. Artelt, et al. (2005). "Experimental Autoimmune Neuritis induces differential microglia activation in the rat spinal cord." Journal of Neuroimmunology 160: 25-31.

Bernard, C. C., T. G. Johns, et al. (1997). "Myelin oligodendrocyte glycoprotein: a novel candidate autoantigen in multiple sclerosis." Journal of Molecular Medicine 75: 77.

Bersano, A., M. Carpo, et al. (2005). "Long-term disability and social status change after Guillain-Barre Syndrome." Journal of Neurology Epub ahead of print.

Biesecker, G. and C. M. Gomez (1989). "Inhibition of acute passive transfer experimental autoimmune myasthenia gravis with Fab antibody to complement C6." Journal of Immunology 142(8): 2654-2659.

Bolotin, C., S. Morris, et al. (1977). "Purification and structural analysis of the fourth component of human complement." Biochemistry 16(9): 2008-2015.

Bond, J. P., R. A. Saavedra, et al. (2001). "Expression and purification of the extracellular domain of human myelin protein zero." Protein Expression and Purification 23: 398-410.

Bongrazio, M., A. R. Pries, et al. (2003). "The endothelium as physiological source of properdin: role of wall shear stress." Molecular Immunology 39(11): 669-675.

Bourquin, C., A. S. Schubart, et al. (2003). "Selective unresponsiveness to confirmational B cell epitopes of the myelin oligodendrocyte glycoprotein in H-2b mice." Journal of Immunology 171: 455-461.

Bradbury, K., S. R. Aparicio, et al. (1984). "Role of complement in demyelination in vitro by multiple sclerosis serum and other neurological disease sera." Journal of Neurological Science 65(3): 293-305.

Brauer, R. B., W. M. r. Baldwin, et al. (1993). "Use of C6-deficient rats to evaluate the mechanism of hyperacute rejection of discordant cardiac xenografts." Journal of Immunology 151(12): 7240-7248.

Breithaupt, C., A. S. Schubart, et al. (2003). "Structural insights into the antigenicity of myelin oligodendrocyte glycoprotein." Proc. Natl. Acad. Sci. USA 100: 9446-9451.

Bruck, W., Y. Bruck, et al. (1995). "The membrane attack complex of complement mediates peripheral nervous system demyelination in vitro." Acta Neuropathol 90: 601-607.

Bruck, W. and R. L. Friede (1991). "The role of complement in myelin phagocytosis during PNS wallerian degeneration." Journal of Neurological Science 103(2): 182-7.

Buckle, A. M., G. L. Devlin, et al. (2005). "The matrix refolded." Nature Methods 2(3).

Buras, J. A., L. Rice, et al. (2004). "Inhibition of C5 or absence of C6 protects from sepsis mortality." Immunobiology 209(8): 629-635.

Calida, D. M., S. G. Kremlev, et al. (2000). "Experimental allergic neuritis in the SJL/J mouse: induction of severe and reproducible disease with bovine peripheral nerve myelin and pertussis toxin with or without interleukin-12." Journal of Neuroimmunology 107(1): 1-7.

Caras, I. W., M. A. Davitz, et al. (1987). "Cloning of decay-accelerating factor suggestd novel use of splicing to generate two proteins." Nature 325(6104): 545-549.

Chakravarti, D. B. and H. J. Muller-Eberhard (1988). "Biochemical characterisation of the human complement protein C6." Journal of Biological Chemistry 263(34): 18306-18312.

Cheng, J. and J. E. Volanakis (1994). "Alternatively spliced transcripts of the human complement C2 gene." Journal of Immunology 152(4): 1774-1782.

Childs, L. A., R. Harrison, et al. (1985). "Complement-dependent toxicity of serum from myasthenic patients to muscle cells in culture." Journal of Neuroimmunology 9(1-2): 69-80.

Choy, L. N., B. S. Rosen, et al. (1992). "Adipsin and an endogenous pathway of complement from adipose cells." Journal of Biological Chemistry 267: 12736-41.

Christadoss, P. (1988). "C5 gene influences the development of murine myasthenia gravis." Journal of Immunology 140(8): 2589-2592.

Cleland, J. L. and D. I. C. Wang (2000). "Cosolvent assisted protein refolding." Biotechnology 8: 1274-1278.

Cole, R. and J. de Vellis (1989). "Preparation of astrocytes and oligodendrocyte cultures from primary rat glial cultures. A dissection and tissue culture." Manual of the Nervous System Chapter 26: 121-131.

Compston, D. A. S., A. Vincent, et al. (1980). "Clinical, pathological, HLA antigen and immunological evidence for disease heterogeneity in myasthenia gravis." Brain 103(579-601).

Cooper, N. R. and H. J. Muller-Eberhard (1970). "The reaction mechanism of human C5 in immune hemolysis." Journal of Experimental Medicine: 775-793.

Curman, B., L. Sandberg-Tragardh, et al. (1977). "Chemical characterisation of human factor B of the alternative pathway of complement activation." Biochemistry 16(24): 5368-5375.

Dahlback, B. and E. R. Podack (1985). "Characterisation of human S protein, an inhibitor of the membrane attack complex of complement. Demonstration of a free reactive thiol group." Biochemistry 24(9): 2368-2374.

Dahlman, I., E. Wallstrom, et al. (2001). "Polygenic control of autoimmune peripheral nerve inflammation in rat." Journal of Neuroimmunology 119: 166-174.

DAKO (1994). Rabbit anti-cow S-100, Code No. Z311: Specification sheet.

Damoiseaux, J. G., E. A. Dopp, et al. (1994). "Rat macrophage lysosonal membrane antigen recognised by monoclonal antibody ED1." Immunology 83(1): 140-147.

Davies, A., D. L. Simmons, et al. (1989). "CD59, and Ly-6-like protein expressed in human lymphoid cells, regulates the action of the complement membrane attack complex on homologous cells." Journal of Experimental Medicine 170: 637-654.

de Graaf, K., S. Barth, et al. (2004). "MHC Class II isotype- and allel-specific attentuation of Experimental Autoimmune Encephalomyelitis." Journal of Immunology 173: 2792-2802.

de Graaf, K., E. Wallstrom, et al. (2004). "MHC and non-MHC gene regulation of disease susceptibility and disease course in experimental inflammatory peripheral neuropathy." Journal of Neuroimmunology 155: 73-84.

de Jonge, R. R., I. N. van Schaik, et al. (2004). "Expression of complement components in the peripheral nervous system." Human Molecular Genetics 13(3): 295-302.

Demberg, T., B. Pollok-Kopp, et al. (2002). "Rat Complement factor H: molecular cloning, sequencing and quantification with a newly established ELISA." Scandinavian Journal of Immunology 56(2): 149-160.

Deng, C., E. Goluszko, et al. (2002). "Resistance to experimental autoimmune myasthenia gravis in IL-6 deficient mice is associated with reduced germinal centre formation and C3 production." Journal of Immunology 169(2): 1077-1083.

Dieperink, M. E., A. O'Neill, et al. (1991). "Experimental allergic neuritis in the SJL/J mouse: dysfunction of peripheral nerve without clinical signs." Journal of Neuroimmunology 35(1-3): 247-59.

Donato, R. (1986). "S-100 proteins." Cell Calcium 7(3): 123-145.

Donev, R., S. Baalasubramanian, et al. (2005). Soluble CD59 binds specifically to fibroblasts and other cell types and triggers enhanced proliferation. 10th Meeting on Complement in Human Disease, Heidelberg, Germany, Molecular Immunology.

Dragon-Durey, M. A., V. Freemeaux-Bacchu, et al. (2003). "Restricted genetic defects underlie human complement C6 deficiency." Clin. Exp. Immunol. 132(1): 87-91.

Driscoll, B. F., M. W. Kies, et al. (1985). "The nature of the defect in experimental allergic encephalomyelitis (EAE)-resistant Lewis (Le-R) rats." Journal of Immunology 134(3): 1567-70.

Duan, R. S., Z. Chen, et al. (2004). "CCR5 deficiency does not prevent PO peptide 180-199 immunised mice from experimental autoimmune neuritis." Neurobiology of Disease 16(3): 630-637.

Eichberg, J. (2002). "Myelin PO: New knowledge and new roles." Neurochemical Research 27(11): 1331-1340.

Engel, A. G. and K. Arahata (1987). "The membrane attack complex at the endplate in myasthenia gravis." Annals of New York Academy of Sciences 505: 326-332.

Engel, A. G., E. H. Lambert, et al. (1977). "Immune complexes (IgG and C3) at the motoe end-plate in myasthenia gravis:ultrastructural and light microscopic localisation and electrophysiologic correlations." Mayo Clin. Proc. 52(5): 267-280.

Engel, A. G., H. Sakakibara, et al. (1979). "Passively transferred experimental autoimmune myasthenia gravis. Sequential and quantitative study of the motor end-plate fine structure and ultrastructural localisation of immune complexes (IgG an C3)." Neurology 29(2): 179-188.

Everly, J. I., R. O. Brady, et al. (1973). "Evidence that the major protein in rat sciatic nerve myelin is a glycoprotein." Journal of Neurochemistry 21(21): 329-334.

Fazekas, A., S. Komoly, et al. (1986). "Myasthenia gravis: demonstration of membrane attack complex in muscle end-plates." Clin. Neuropathol. 5(2): 78-83.

Fearon, D. T. (1995). "The CD19/CR2/TAPA-1 complex pf B lymphocytes: linking natural to acquired immunity." Annual Review of Immunology 13: 127.

Fearon, D. T., K. F. Austen, et al. (1974). "Properdin factor D: characterisation of its active site and isolation of the precursor form." Journal of Experimental Medicine 139(355-366).

Feasby, T. E., J. J. Gilbert, et al. (1987). "Complement depletion suppresses Lewis rat experimental allergic neuritis." Brain Research 419: 97-103.

Filbin, M. T. and G. I. Tennekoon (1990). "High level of expression of the myelin protein PO in Chinese hamster ovary cells." Journal of Neurochemistry 55(500-505).

Filbin, M. T. and G. I. Tennekoon (1993). "Homophilic adhesion of the myelin PO protein requires glycosylation of both molecules in the homophilic pair." Journal of Cell Biology 122: 451-459.

Fisher, M. (1956). "Syndrome of opthalmoplegia, ataxia and areflexia." New England Journal of Medicine 255: 57-65.

Fleisig, A. J. and E. D. Verrier (2005). "Pexelizumab - a C5 complement inhibitor for use in both acute myocardial infarction and cardiac surgery with cardiopulmonary bypass." Expert Opinion Biol. Ther. 5(6): 833-839.

Francis Pau, K. Y. and D. P. Wolf (2004). "Derivation and characterization of monkey embryonic stem cells." Reproductive Biology and Endocrinology 2: 41.

Fross, R. D. and J. Daube (1987). "Neuropathy in the Miller-Fisher Syndrome: clinical and electrophysiologic findings." Neurology 37: 1493-1498.

Fujioka, T., E. Purev, et al. (2000). "Flow cytometric analysis of infiltrating cells in the peripheral nerves in Experimental Allergic Neuritis." Journal of Neuroimmunology 108: 181-191.

Fujita, N., A. Kemper, et al. (1998). "The cytoplasmic domain of the large myelin associated glycoprotein isoform is needed for proper CNS but not peripheral nervous system myelination." Journal of Neuroscience 18: 1970-1978.

Gabriel, C. M., N. A. Gregson, et al. (1997). "Human immunoglobulin ameliorates rat experimental autoimmune neuritis." Brain 120: 1533-1540.

Gabriel, C. M., R. A. Hughes, et al. (1998). "Induction of Experimental Autoimmune Neuritis with peripheral myelin protein-22." Brain 121: 1895-1902.

Giese, K. P., R. Martini, et al. (1992). "Mouse PO gene disruption leads to hypomyelination, abnormal expression of recognition molecules, and degeneration of myelin and axons." Cell 71(4): 565-76.

Graus, Y. M., J. J. Verschurren, et al. (1993). "Age-related resistance to experimental autoimmune myasthenia gravis in rats." Journal of Immunology 150(9): 4093-4103.

Greenfield, S., S. Brostoff, et al. (1973). "Protein composition of the peripheral nervous system." Journal of Neurochemistry 20(1207-1216).

Griffiths, L. S., B. Schmitz, et al. (1992). "L2/HNK-1 carbohydrate and protein-protein interactions mediate the homophilic binding of the neural adhesion molecule PO." Journal of Neuroscience Research 33: 639-648.

Guex, N., T. Schwede, et al. (2000). Current protocols in Protein Science. Protein tertiary structure modelling. J. E. Coligan, B. M. Dunn, H. L. Ploegh, D. W. Speicher and P. T. Wingfield. New York, John Wiley & Sons, Inc. Unit 2.8: 1-17.

Guillain, G., J. A. Barre, et al. (1916). "Sur un syndrome de radiculonevrite avec hyperalbuminose du liquide cepharachidien sans reaction cellulaire: remarques sur les caracteres cliniques et graphiques des reflexes tendineux." Bull Soc Med Hop Paris 40: 1462-1470.

Hadden, R. D., N. A. Gregson, et al. (2002). "Accumulation of immunoglobulin across the 'blood-nerve-barrier' in spinal roots in adoptive transfer experimental autoimmune neuritis." Neuropathol Appl Neurobiol 28(6): 489-497.

Hahn, A. F. (1998). "Guillain-Barré syndrome." Lancet 352: 635-41.

Hai, M., N. Muja, et al. (2002). "Comparative analysis of Schwann cell lines as model systems for myelin gene transcription studies." Journal of Neuroscience Research 69: 497-508.

Halstead, S. K., P. D. Humphreys, et al. (2005). "Complement inhibition abrogates nerve terminal injury in Miller Fisher syndrome." Ann. Neurol 58(2): 203-210.

Halstead, S. K., G. M. O'Hanlon, et al. (2004). "Anti-disialoside antibodies kill perisynaptic Schwann cells and damage motor nerve terminals via membrane attack complex in a murine model of neuropathy." Brain 127(9): 2109-23.

Hamman, J., B. Vogel, et al. (1996). "The seven-span transmembrane receptor CD97 has a cellular ligand (CD55, DAF)." Journal of Experimental Medicine 184(September): 1185-1189.

Harris, C. L., S. M. Hanna, et al. (2003). "Characterisation of the mouse analogues of CD59 using novel monoclonal antibodies: tissue distribution and functional comparison." Immunology 109: 117-126.

Harris, C. L. and B. P. Morgan (1999). Complement Regulatory Proteins. San Diego, London, Boston, New York, Sydney, Toronto, Academic Press.

Harris, C. L. and B. P. Morgan (2004). The many faces of the membrane regulators of complement.

Harris, C. L., O. B. Spiller, et al. (2000). "Human and rodent decay-accelerating factors (CD55) are not species restricted in their complement-inhibiting activities." Immunology 100(4): 462.

Harris, C. L., A. S. Williams, et al. (2002). "Coupling complement regulators to immunoglobulin domains generates effective anti-complement reagents with extended half-life in vivo." Clin. Exp. Immunol. 129: 198-207.

Harrison, R. A. (1983). "Human C1 inhibitor: improved isolation and preliminary structural characterisation." Biochemistry 22(21): 5001-5007.

Hartung, H. P., B. C. Kieseier, et al. (2001). "Progress in Guillain-Barre syndrome." Current Opinion in Neurology 14: 597-604.

Hartung, H. P., B. Schafer, et al. (1987). "Ciclosporin A prevents P2 cell line-mediated experimental autoimmune neuritis (AT-EAN) in rat." Neuroscience Letters 83(1-2): 195-200.

Hartung, H. P., C. Schwenke, et al. (1987). "Guillain-Barre Syndrome: Activated complement components C3a and C5a in CSF." Neurology 37: 1006-1009.

Hartung, H. P., H. J. Willison, et al. (2002). "Acute immunoinflammatory neuropathy: update on Guillain-Barre syndrome." Current Opinion in Neurology 15: 571-577.

Hasse, B., F. Bosse, et al. (2004). "Peripheral myelin protein 22kDa and protein zero: domain specific trabs-interactions." Molecular and Cellular Neuroscience 27: 370-378.

Hattori, N., M. Yamamoto, et al. (2003). "Demyelinating and axonal features of Charcot-Marie-Tooth disease with mutations of myelin-related proteins (PMP22, MPZ and Cx32): a clinicopathological study of 205 Japanese patients." Brain 126(1): 134-51.

Hawkins, B. R., W. Y. Chan-Lui, et al. (1984). "Strong association of HLA-BW46 with juvenile onset myasthenia gravis in Hong Kong Chinese." Journal of Neurol. Neurosurg. Psychiatry 47(5): 555-557.

Hayasaka, K., M. Himoro, et al. (1993). "De novo mutation of the myelin P0 gene in Dejerine-Sottas disease (hereditary motor and sensory neuropathy type III)." Nature Genetics 5(Nov): 266-268.

Hayasaka, K., M. Himoro, et al. (1993a). "Structure and chromosomal localisation of the gene encoding the human myelin protein zero." Genomics 17(3): 1993.

Hayasaka, K., G. Takada, et al. (1993). "Mutation of the myelin PO gene in Charcot-Marie-Tooth neuropathy type 1B." Human Molecular Genetics 2(9): 1369-.

Haymaker, W. and J. W. Kernohan (1949). "The Landry-Guillain-Barre syndrome: a clinical pathologic report of 50 fatal cases and a review of the literature." Medicine 28: 59-141.

Hays, A. P., N. Latov, et al. (1987). "Experimental demyelination of nerve induced by serum of patients with neuropathy and an anti-MAG IgM M-protein." Neurology 37(2): 242-256.

Heininger, K., G. Stoll, et al. (1986). "Conduction failure and nerve conduction slowing in expeirmental allergic neuritis induced by P2-specific T-cell lines." Ann. Neurol 19(1): 44-49.

Herrera, G. A., E. A. Turbat-Herrera, et al. (1988). "S-100 protein expression by primary and metastatic adenocarcinomas." American Journal of Clinical Pathology 89(168-176).

Hill, J., T. F. Lindsay, et al. (1992). "Soluble complement receptor type 1 ameliorates the local and remote organ injury after intestinal ischemia-reperfusion in the rat." Journal of Immunology 149(5): 1723-1728.

Hillarp, A., H. Wiklund, et al. (1997). "Molecular cloning of rat C4b binding protein alpha- and beta-chains: structural and functional relationships among human, bovine, rabbit, mouse and rat proteins." Journal of Immunology 158(3): 1315-1323.

Hinchliffe, S. J., O. B. Spiller, et al. (1998). "Molecular cloning and functional characterisation of the rat analogue of human decay accelerating factor (CD55)." Journal of Immunology 161: 5695-5703.

Hitzeman, R. A., F. E. Hagie, et al. (1981). "Expression of a human gene for interferon in yeast." Nature 293(5835): 717-722.

Hoch, W., J. McConville, et al. (2001). "Auto-antibodies to the receptor tyrosine kinase MuSK in patients with myasthenia gravis without acetylcholine receptor antibodies." Nature Medicine 7: 365-8.

Hoedemaekers, A., J.-L. Bessereau, et al. (2001). "Role of the target organ in determining susceptibility to experimental autoimmune myasthenia gravis." Journal of Neuroimmunology 89: 131-141.

Hoedemaekers, A., Y. M. Graus, et al. (1997). "Macrophage infiltration at the neuromuscular junction does not contribute to AChR loss and age-related resistance to EAMG." Journal of Neuroimmunology 75: 147-155.

Holt, D. S., M. Botto, et al. (2001). "Targeted deletion of the CD59 gene causes spontaneous intravascular haemolysis and haemoglobinuria." Blood 98(2): 442-9.

Horiuchi, T., K. J. Macon, et al. (1989). "cDNA cloning and expression of human complement component C2." Journal of Immunology 142: 2105-2111.

Hourcade, D. E., L. Mitchell, et al. (2002). "Decay-accelerating factor (DAF), complement receptor 1 (CR1) and factor H dissociate the complement AP C3 convertase (C3bBb) via sites on the type A domain of Bb." Journal of Biological Chemistry 277(2): 1107-1112.

Hughes, J., M. Nangaku, et al. (2000). "C5b-9 membrane attack complex mediates endothelial cell apoptosis in experimental glomerulonephritis." American Journal of Renal Physiology 278: F747-F757.

Hughes, R. A. C., P. Atkinson, et al. (1992b). "Sural nerve biopsies in Guillain-Barre syndrome: axonal degeneration and macrophage-mediated demyelination and absence of cytomegalovirus genome." Muscle Nerve 15: 568-575.

Hughes, T. R., S. J. Piddlesden, et al. (1992). "Isolation and characterisation of a membrane protein from rat erythrocytes which inhibits lysis by the membrane attack complex of rat complement." Biochemical Journal 284((Pt 1)): 169-76.

Hugli, T. E., C. Gerard, et al. (1981). "Isolation of three separate anaphylatoxins from complement-activated human serum." Mol Cell Biochem 41: 59-66.

Isenman, D. E. (1983). "The role of the thioester bond in C3 and C4 in the determination of the conformational and functional states of the molecule." Annals of New York Academy of Sciences 421: 277-290.

Issacs, J. D., V. K. Manna, et al. (1996). "CAMPATH-1H in rheumatoid arthritis-an intravenous dose-ranging study." British Journal of Rheumatology 35(3): 231-240.

Jacobs, B. C., R. W. Bullens, et al. (2002). "Detection and prevalence of alpha-latrotoxin-like effects of serum from patients with Guillain-Barre syndrome." Muscle Nerve 25(4): 549-558.

Jacobs, B. C., P. H. Rothbarth, et al. (1998). "The spectrum of antecedent infections in Guillain-Barre syndrome. A case control study." Neurology 51: 1110-1115.

Janeway, C. A., P. Travers, et al. (2001). Immunobiology: The Immune System in Health and Disease. New York, Garland Publishing.

Johnson, M. D., A. D. Glick, et al. (1988). "Immunohistochemical evaluation of Leu-7, myelin basic-protein, S100-protein, glial-fibrillary acidic-protein, and LN3 immunoreactivity in nerve sheath tumors and sarcomas." Arch Pathol Lab Med 112(2): 155-160.

Jones, T. A., T. Bergfors, et al. (1988). "The three-dimensional structure of P2 myelin protein." EMBO 7: 1597-604.

Jose, P. J., I. K. Moss, et al. (1990). "Measurement of the chemotactic complement fragment C5a in rheumatoid synovial fluids by radioimmunoassay: role of C5a in the acute inflammatory phase." Ann. Rheum. Dis. 49(10): 747-752.

Jung, S., K. V. Toyka, et al. (1995). "Soluble complement receptor 1 inhibits experimental autoimmune neuritis in Lewis rats." Neuroscience Letters 200(3): 167-170.

Kadlubowski, M. and R. A. Hughes (1979). "Identification of the neuritogen for Experimental Allergic Neuritis." Nature 277: 140-141.

Kadlubowski, M., R. A. Hughes, et al. (1980). "Experimental allergic neuritis in the Lewis rat: characterization of the activity of peripheral myelin and its major basic protein,P2." Brain Research 184(2): 439-454.

Kaminski, H. J., Z. Li, et al. (2004). "Complement regulators in extraocular muscle and experimental autoimmune myasthenia gravis." Experimental Neurology 189: 333-342.

Kamolvarin, N., T. Hemachudha, et al. (1991). "Plasma C3c in immune-mediated neurological diseases: a preliminary report." Acta Neurol Scand 83(6): 382.

Kaufman, R. J. (2000). "Overview of vector design for mammalian gene expression." Mol Biotechnol 16(2): 151-160.

Kelly, S. M. and N. C. Price (2000). "The use of circular dichroism in the investigation of protein structure and function." Current Protein and Peptide Science 1: 349-384.

Kerr, M. A. (1981). "The second component of human complement." Methods Enzymology 80(54-64).

Khalili-Shirazi, A., P. Atkinson, et al. (1993). "Antibody responses to PO and P2 myelin proteins in Guillain-Barre Syndrome and chronic idiopathic demyelinating polyradiculoneuropathy." Journal of Neuroimmunology 46: 245-251.

Khalili-Shirazi, A., R. A. C. Hughes, et al. (1992). "T cell response to myelin proteins in Guillain-Barre syndrome." Journal of Neurological Science 111: 200-203.

Kim, Y. U., T. Kinoshita, et al. (1995). "Mouse complement regulatory protein Crry/p65 uses the specific mechanisms of both human decay-accelerating factor and membrane cofactor protein." Journal of Experimental Medicine 181(1): 151-9.

Kirschner, D. A. and A. L. Ganser (1980). "Compact myelin exists in the absence of myelin basic protein in the *shiverer* mutant mouse." Nature 283: 207-210.

Kirshfink, M. (2001). "Targeting complement in therapy." Immunological Reviews 180: 177-89.

Kirszbaum, L., J. A. Sharpe, et al. (1989). "Molecular cloning and characterisation of the novel human complement-associated protein, SP-40,40: a link between the complement and reproductive systems." EMBO 8(3): 711-718.

Kitts, P. A. and R. D. Possee (1993). "A method for producing recombinant baculovirus expression vectors at high frequency." Biotechniques 14(5): 810-817.

Klickstein, L. B., T. J. Bartow, et al. (1988). "Identification of distinct C3b and C4b recognition sites in the human C3b/C4b receptor (CR1, CD35) by deletion mutagenesis." Journal of Experimental Medicine 168: 1699-1717.

Koh, C. S., T. Nakano, et al. (1984). "Detection of immune complexes in Experimental Allergic Neuritis." Journal of Neurological Science 63: 229-239.

Kornfeld, R. and S. Kornfeld (1985). "Assembly of asparagine-linked oligosaccharides." Annual Review of Biochemistry 54: 631-634.

Koski, C. L. (1990). "Characterisation of complement-fixing antibodies to peripheral nerve myelin in Guillain-Barre Syndrome." Annual Neurology 27(suppl): S44-S47.

Koski, C. L., A. E. Estep, et al. (1996). "Complement regulatory molecules on human myelin and glial cells: differential expression affects the deposition of activated complement proteins." Journal of Neurochemistry 66: 303-312.

Koski, C. L., M. E. Sanders, et al. (1987). "Activation of terminal components of complement in patients with Guillain-Barre syndrome and other demyelinating neuropathies." Journal of Clinical Investigation 80: 1492-1497.

Koski, C. L., P. Vanguri, et al. (1985). "Activation of the alternative pathway of complement by human peripheral nerve myelin." Journal of Immunology 134: 1810-1814.

Koski, C. L., P. Vanguri, et al. (1985a). "Anti-peripheral myelin antibody in patients with demyelinating neuropathy: Quantitative and kinetic determination of serum antibody by complement component 1 fixation." Proc. Natl. Acad. Sci. USA 82: 905-910.

Kristensen, T., R. T. Ogata, et al. (1987). "cDNA structure of murine C4b-binding protein, a regulatory component of the serum complement system." Biochemistry 26(15): 4668-4674.

Kristensen, T., R. A. Wetsel, et al. (1986). "Structural analysis of human complement protein H: homology with C4b binding protein, beta 2-glycoprotein I, and the Ba fragment of B2." Journal of Immunology 136(9): 3407-3411.

Kuhn, S., C. Skerka, et al. (1995). "Mapping of the complement regulatory domains in the human factor H-like protein 1 and in factor H1." Journal of Immunology 155(12): 5663-5670.

Kulkens, T., P. A. Bolhuis, et al. (1993). "Deletion of the serine 34 codon from the major peripheral myelin protein Po gene in Charcot-Marie-Tooth disease type 1B." Nature Genetics 5: 35-39.

Kursula, P. (2001). "The current status of structural studies on proteins of the myelin sheath (Review)." International Journal of Molecular Medicine 8: 475-79.

Kvarnstrom, M., E. Sidorova, et al. (2002). "Myelin protein P0-specific IgM producing monoclonal B cell lines were established from polyneuropathy patients with monoclonal gammopathy of undetermined significance (MGUS)." Clin. Exp. Immunol. 127(2): 255-262.

Lambris, J. D. and H. J. Muller-Eberhard (1984). "Isolation and characterisation of a 33,000-dalton fragment of complement Factor B with catalytic and C3b binding activity." Journal of Biological Chemistry 259(20): 12685-12690.

Lang, T. J., T. C. Badea, et al. (1997). "Sublytic terminal complement attack on myotubes decreases the expression of mRNAa encoding muscle-specific proteins." Journal of Neurochemistry 68(4): 1581-1589.

Lassman, H., W. Fierz, et al. (1991). "Chronic relapsing experimental allergic neuritis induced by repeated transfer of P2-protein reactive T cell lines." Brain 114(Pt 1B): 429-42.

Latov, N. (1995). "Pathogenesis and therapy of neuropathies associated with monoclonal gammopathies." Ann. Neurol 37(Suppl 1): S32-S42.

Lazar, H. L., P. M. Bokesch, et al. (2004). "Soluble human complement receptor 1 limites ischemic damage in cardiac surgery patients at high risk requiring cardiopulmonary bypass." Circulation 110(11 Suppl 1): II274-279.

Lee, J. C. and S. N. Timasheff (1981). "The stabilisation of proteins by sucrose." Journal of Biological Chemistry 256: 7193-7201.

Leenaerts, P. L., B. M. Hall, et al. (1995). "Active Heymann nephritis in complement component C6 deficient rats." Kidney International 47(6): 1604-1614.

Leenaerts, P. L., R. K. Stad, et al. (1994). "Hereditary C6 deficiency in a strain of PVG/c rats." Clinical & Experimental Immunology 97(3): 478-482.

Lennon, V. A. and E. H. Lambert (1980). "Myasthenia gravis induced by monoclonal antibodies to acetylcholine receptors." Nature 285: 238-240.

Lennon, V. A., J. Lindstrom, et al. (1975). "Experimental autoimmune myasthenia: a model of myasthenia gravis in rats and guinea pigs." Journal of Experimental Medicine 141(6): 1365-1375.

Lennon, V. A., M. E. Seybold, et al. (1978). "Role of complement in the pathogenesis of experimental autoimmune myasthenia gravis." Journal of Experimental Medicine 147(4): 973-83.

Levine, R. L. and M. M. Federici (1982). "Quantitation of aromatic residues in proteins: model compounds for second-derivative spectroscopy." Biochemistry 21(11): 2600-2606.

Levine, R. P. and A. W. Dodds (1990). "The thioester bond of C3." Curr Top Microbiol Immunol 153: 73-82.

Li, J. S., S. P. Sanders, et al. (2004). "Pharmacokinetics and safety of TP10, soluble complement receptor 1, in infants undergoing cardiopulmonary bypass." American Heart Journal 147(1): 173-180.

Lin, F., Y. Fukuoka, et al. (2001). "Tissue distribution of products of the mouse decay-accelerating factor (DAF) genes. Exploitation of a Daf1 knock-out mouse and site-specific antibodies." Immunology 104(2): 215-225.

Lin, F., H. J. Kaminski, et al. (2002). "Markedly enhanced susceptibility to experimental autoimmune myasthenia gravis in the absence of decay-accelerating factor protection." Journal of Clinical Investigation 110: 1269-1274.

Lindstrom, J. (2000). "Acetylcholine receptors and myasthenia." Muscle Nerve 23(4): 453-477.

Lindstrom, J. (2003). "Nicotinic acetylcholine receptors of muscles and nerves. Comparison of their structures, functional roles and vulnerability to pathology." Annals of New York Academy of Sciences 998: 41-52.

Lindstrom, J., B. L. Einarson, et al. (1976). "Pathological mechanisms in experimental autoimmune myasthenia gravis I Immunogenicity of syngeneic muscle acetylcholine receptor and quantitative extraction of receptor and antibody-receptor complexes from muscles of rats with experimental autoimmune myasthenia gravis." Journal of Experimental Medicine 144: 726-738.

Lindstrom, J., A. G. Engel, et al. (1976). "Pathological mechanisms in experimental autoimune myasthenia gravis II Passive transfer of experimental autoimmune myasthenia gravis in rats with anti-acetylcholine receptor antibodies." Journal of Experimental Medicine 144: 739-753.

Linington, C., S. Izumo, et al. (1984). "A permanent rat T cell line that mediates experimental allergic neuritis in the Lewis rat in vivo." Journal of Immunology 133(4): 1946-1950.

Linington, C., H. Lassman, et al. (1992). "Cell adhesion molecules of the immunoglobulin supergene family as tissue-specific autoantigens: induction of experimental allergic neuritis." Journal of Neuroimmunology 22: 1813-17.

Linton, S., A. S. Williams, et al. (2000). "Therapeutic efficacy of a novel membrane-targeted complement regulator in antigen-induced arthritis in the rat." Arthritis Rheum 42(11): 2590-2597.

Litzenburger, T., R. Fassler, et al. (1998). "B lymphocytes producing demyelinating autoantibodies: development and function in gene-targeted transgenic mice." Journal of Experimental Medicine 188: 169-180.

Longhi, M. P., B. Sivasankar, et al. (2005). Modulation of CD4+ T cell activation by CD59. 10th Meeting on Complement in Human Disease, Heidelberg, Germany, Molecular Immunology.

Lublin, D. M., M. K. Liszewski, et al. (1988). "Molecular cloning and chromsomal localisation of human membrane cofactor protein (MCP)." Journal of Experimental Medicine 168(181-194).

Lundin, J., A. Porwit-MacDonald, et al. (2004). "Cellular immune reconstitution after subcutaneous alemtuzumab (anti-CD52 monoclonal antibody, CAMPATH-1H) treatment as first-line therapy for B-cell chronic lymphocytic leukaemia." Leukaemia 18(3): 484-490.

Lyons, J. A., M. J. Ramsbottom, et al. (2002). "Critical role of antigen-specific antibody in experimental autoimmune encephalomyelitis induced by recombinant myelin oligodendrocyte glycoprotein." European Journal of Immunology 32: 1905-1913.

Magira, E. E., M. Papaioakim, et al. (2003). "Differential distribution of HLA-DQ beta/DR beta epitopes in the two forms of Guillain-Barre syndrome, acute motor axonal neuropathy and acute inflammatory demyelinating polyneuropathy (AIDP): identification of DQ beta epitopes associated with susceptibility to and protection form AIDP." Journal of Immunology 170: 3074-3080.

Maillere, B., G. Mourier, et al. (1995). "Fine chemical modifications at the N- and C-termini enhance peptide presentation to T cells by increasing the lifespan of both free and MHC-complexed peptides." Molecular Immunology 32(17-18): 1377-85.

Maina, C. V., P. D. Riggs, et al. (1988). "An Escherichia coli vector to express and purify proteins by fusion to and separation from maltose-binding protein." Gene 74(2): 365-373.

Marston, F. A. and D. L. Hartley (1990). "Solublisation of protein aggregates." Methods Enzymology 182: 264-276.

Martin, P. E. M., J. Steggles, et al. (2000). "Targeting motifs and functional parameters governing the assembly of connexins into gap junctions." Biochemical Journal 349: 281-87.

Martini, R., J. Zielasek, et al. (1995). "Protein zero (PO)-deficient mice show myelin degeneration in peripheral nerves characteristic of inherited human neuropathies." Nature Genetics 11(3): 281-86.

Mathers, L. H. (1985). The Peripheral Nervous System: Structure, Function, and Clinical Correlations, Addison-Wesley Publishing Company, Inc.

Mathey, E., C. Breithaupt, et al. (2004). "Sorting the wheat from the chaff: identifying demyelinating components of the myelin oligodendrocyte glycoprotein (MOG)-specific autoantibody repertoire." European Journal of Immunology 34: 2065-2071.

Matsunami, N., B. Smith, et al. (1992). "Peripheral myelin protein-22 maps in the duplication in chromosome 17p11.2 associated with Charcot-Marie-Tooth 1A." Nature Genetics 1: 176-9.

Matsuo, S., S. Ichida, et al. (1994). "In vivo effects of monoclonal antibodies that functionally inhibit Complement regulatory proteins in rats." Journal of Experimental Medicine 180: 1619-1627.

Maurer, M. and R. Gold (2002). "Animal models of immune-mediated neuropathies." Current Opinion in Neurology 15: 617-622.

Maves, K. K. and J. M. Weiler (1993). "Properdin: approaching four decades of research." Immunology Research 12: 233-243.

McCombe, P. A., J. D. Pollard, et al. (1987). "Chronic inflammatory demyelinating polyradiculoneuropathy." Brain 110: 1617-1630.

Mead, R. J., S. J. Hinchliffe, et al. (1999). "Molecular cloning, expression and characterisation of the rat analogue of human membrane cofactor protein (MCP/CD46)." Immunology 98: 137-143.

Mead, R. J., J. W. Neal, et al. (2004). "Deficiency of the complement regulator CD59a enhances disease severity, demyelination and axonal injury in murine acute experimental allergic encephalomyelitis." Lab Investig 84(1): 21-28.

Mead, R. J., S. K. Singhrao, et al. (2002). "The membrane attack complex of complement causes severe demyelination associated with acute axonal injury." Journal of Immunology 168(1): 458-465.

Medicus, R. G., J. Melamed, et al. (1983). "Role of human factor I and C3b receptor in the cleavage of surface-bound C3bi molecules." European Journal of Immunology 13(6): 465-470.

Meier, C., R. Dermietzel, et al. (2004). "Connexin32-containing gap junctions in Schwann cells at the internodal zone of partial myelin compaction and in Schmidt-Lanterman incisures." Journal of Neuroscience 24(13): 3186-98.

Midroni, G. and J. M. Bilbao (1995). Chapter 5: Schwann cells and myelin in the peripheral nervous system. Biopsy diagnosis of peripheral neuropathy. S. M. Cohen. Butterworth-Heinemann, Reed Elsevier.

Miletic, H., O. Utermohlen, et al. (2005). "PO 106-125 is a neuritogenic epitope of the peripheral myelin protein PO and induces autoimmune neuritis in C57BL/6 mice." Journal of Neuropathology & Experimental Neurology 64(1): 66-73.

Milner, P., C. A. Lovelidge, et al. (1987). "PO myelin protein produces experimental allergic neuritis in Lewis rats." Journal of Neurological Science 79: 275-285.

Minta, J. O., M. J. Wong, et al. (1996). "cDNA cloning, sequencing and chromosomal assignment of the gene for mouse complement factor I (C3b/C4b inactivator): identification of a species specific divergent segment in factor I." Molecular Immunology 33(1): 101-112.

Miwa, J. M., I. Ibanez-Tallon, et al. (1999). "Lynx1, an endogenous toxin-like modulator of nicotinic acetylcholine receptors in the mammalian CNS." Neuron 23: 105-114.

Miwa, T., M. Nonaka, et al. (1998). "Molecular cloning of rat and mouse membrane cofactor protein (MCP, CD46): preferential expression in testis and close linkage between the mouse Mcp and Cr2 genes on distal chromosome 1." Immunogenetics 48: 363-371.

Miwa, T., N. Okada, et al. (2000). "Alternative exon usage in the 3' region of a single gene generates glycophosphatidylinositol-anchored and transmembrane forms of rat decay-accelerating factor." Immunogenetics 51: 129-137.

Miyamoto, K., S. Miyake, et al. (2003). "Heterozygous null mutation of myelin PO protein enhances susceptibility to autoimmune neuritis targeting PO peptide." European Journal of Immunology 33(3): 656-665.

Mizuno, M., C. L. Harris, et al. (2004). "Rat membrane cofactor protein (MCP; CD46) is expressed only in the acrosome of developing and mature spermatozoa and mediates binding to immobilised activated C3." Biology of Reproduction 71: 1374-1383.

Mizuno, M., C. L. Harris, et al. (2005). "Expression of CD46 in developing rat spermatozoa: ultrastructural localisation and utility as a marker of the various stages of the seminiferous tubuli." Biology of Reproduction 72: 908-915.

Mizuno, M. and B. P. Morgan (2004). "The possibilities and pitfalls for anti-Complement therapies in inflammatory diseases." Current Drug Targets - Inflammation & Allergy 3: 87-96.

Mizuno, M., K. Nishikawa, et al. (2002). "Soluble complement receptor type 1 protects rats from lethal shock induced by anti-Crry antibody following lipopolysaccharide priming." International Archives of Allergy and Immunology 127: 55-62.

Mizuno, M., K. Nishikawa, et al. (2001). "Membrane complement regulators protect against the development of type II collagen-induced arthritis in rats." Arthritis Rheum 44(10): 2425-2434.

Molina, H., I. Kinoshita, et al. (1990). "A molecular and immunochemical characterisation of mouse CR2. Evidence for a single gene model of mouse complement receptors 1 and 2." Journal of Immunology 145(9): 2974-2983.

Molina, H., W. Wong, et al. (1992). "Distinct receptor and regulatory properties of recombinant mouse complement receptor 1 (CR1) and Crry, the two genetic homologues of human CR1." Journal of Experimental Medicine 175(1): 121-129.

Molina, H., W. W. Wong, et al. (1992). "Distinct receptor and regulatory properties of recombinant mouse complement receptor 1 (CR1) and Crry, the two genetic homologues of human CR1." Journal of Experimental Medicine 175(1): 121-9.

Moon, C. and T. Shin (2004). "Increased expression of osteopontin in the spinal cords of Lewis rats with Experimental Autoimmune Neuritis." Journal of Veterinary Science 5(4): 289-293.

Moore, B. W. (1965). "A soluble protein characteristic of the nervous system." Biochemical and Biophysical Research Communications 19: 739-744.

Morgan, B. P., A. K. Campbell, et al. (1984). "Terminal component of complement (C9) in cerecrospinal fluid of patients with multiple sclerosis." Lancet 2(8397): 251-254.

Morgan, B. P., R. H. Daniels, et al. (1988). "Measurement of terminal complement complexes in rheumatoid arthritis." Clin. Exp. Immunol. 73(3): 473-478.

Morgan, B. P. and P. Gasque (1997). "Extrahepatic complement biosynthesis: where, when and why?" Clin. Exp. Immunol. 107: 1-7.

Morgan, B. P., P. Gasque, et al. (1997). "The role of complement in disorders of the nervous system." Immunopharmacology 38: 43-50.

Morgan, B. P., M. R. Griffiths, et al. (2004). "Blockade of the C5a receptor fails to protect against experimental autoimmune encephalomyelitis in rats." Clin. Exp. Immunol. 138(3): 430-438.

Morgan, B. P. and M. J. Walport (1991). "Complement deficiency and disease." Immunology Today 12(9): 301-306.

Muir, V. Y. and D. C. Dumonde (1982). "Different strains of rats develop different clinical forms of adjuvant disease." Annals of the Rheumatic Disease 41: 538-543.

Muralidhara, B. K. and V. Prakash (2001). "Molten globule state of human serum albumin." Curr. Sci. 72: 831-834.

Nagasawa, S., C. Kobayashi, et al. (1985). "Purification and characterisation of the C3 convertase of the classical pathway of human complement system by size ezclusion high-performance liquid chromatography." Journal of Biochem (Tokyo) 97(2): 493-499.

Nakano, S. and A. G. Engel (1993). "Myasthenia gravis: quantitative immunocytochemical analysis of inflammatory cells and detection of complement membrane attack complex at the end plate in 30 patients." Neurology 43(6): 1167-1172.

Nardelli, E., A. Bassi, et al. (1996). "Systemic passive transfer studies using IgM monoclonal antibodies to sulfatide." Journal of Neuroimmunology 64(2): 221.

Nastuk, W. L., O. J. Plescia, et al. (1960). "Changes in serum complement activity in patients with myasthenia gravis." Proc. Soc. Exp. Biol. Med. 105: 177-184.

Newsom-Davis, J., A. J. Pinching, et al. (1978). "Function of circulating antibody to acetylcholine receptor in myasthenia gravis: investigation by plasma exchange." Neurology 28(3): 266-272.

Nicholson-Weller, A. and C. E. Wang (1994). "Structure and function of decay-accelerating factor CD55." J Lab Clin Med 123(4): 485-491.

Notterpek, L., K. J. Roux, et al. (2001). "Peripheral myelin protein 22 is a constituent of intercellular junctions in epithelia." Proceedings National Academy of Sciences 98(25): 14404-14409.

Nunn, M. A., A. Sharma, et al. (2005). "Complement inhibitor of C5 activation from the soft tick Ornithodoros moubata." Journal of Immunology 174(4): 2084-2091.

Nyland, H., R. Matre, et al. (1981). "Immunological characterisation of sural nerve biopsies from patients with Guillain-Barre Syndrome." Annals of Neurology 9(Suppl): 80-6.

O' Leary, C. P. and H. J. Willison (2000). "The role of antiglycolipid antibodies in peripheral neuropathies." Current Opinion in Neurology 13: 583-588.

O'Bryan, M. K., H. W. G. Baker, et al. (1990). "Human seminal clusterin (SP-40, 40)." Journal of Clinical Investigation 85: 1477-1486.

Omidvar, N., E. C. Wang, et al. (2005). GPI-anchored CD59 on target cells enhances human natural killer cell-mediated cytotoxicity. 10th Meeting on Complement in Human Disease, Heidelberg, Germany, Molecular Immunology.

O'Neill, J. K., D. Baker, et al. (1992). "Inhibition of chronic relapsing experimental allergic encephalomyelitis in the Biozzi AB/H mouse." Journal of Neuroimmunology 41: 177-188.

Oosterhuis, H. J. G. H. (1989). "The natural course of myasthenia gravis: a long term follow up study." Journal of Neurol. Neurosurg. Psychiatry 52: 1121-1127.

Pagany, M., M. Jagodic, et al. (2003). "Genetic variation in myelin oligodendrocyte glycoprotein expression and susceptibility to experimental autoimmune encephalomyelitis." Journal of Neuroimmunology 139: 1-8.

Pangburn, M. K., R. D. Schreiber, et al. (1981). "Formation of the initial C3 convertase of the alternative complement pathway." Journal of Experimental Medicine 154: 856-867.

Paparounas, K., G. M. O'Hanlon, et al. (1999). "Anti-ganglioside antibodies can bind peripheral nerve nodes of Ranvier and activate the complement cascade without inducing acute conduction block in vitro." Brain 122: 807-816.

Patrick, J. and J. Lindstrom (1973). "Autoimmune response to acetylcholine receptor." Science 180: 871-2.

Perkins, S. J. and A. S. Nealis (1989). "The quaternary structure in solution of human complement subcomponent $C1r_2C1s_2$." Biochemical Journal 263: 463-469.

Petersen, I., G. Baatrup, et al. (1985). "Complement-mediated solubilisation of immune complexes and their interaction with complement C3 receptors." Complement 2(2-3): 97-110.

Petranka, J., J. Zhao, et al. (1996). "Structure-function relationships of the complement regulatory protein CD59." Blood Cells, Molecules and Diseases 22(23): 281-296.

Pette, H. and S. Kornyey (1930). "Zur histologie und Pathogenese der akutentzundlichen Formen der Landryschen Paralyse." Z. Gesamte Neurol Psychiatr 128: 390-412.

Pfeiffer, S. E. and W. Wechsler (1972). "Biochemically differentiated neoplastic clone of Schwann cells." Proc. Natl. Acad. Sci. USA 69(10): 2885-2889.

Pfend, G., J. Matthieu, et al. (2001). "Implication of the extracellular disulfide bond on myelin protein zero expression." Neurochemical Research 26(5): 503-510.

Pham-Dinh, D., M. G. Mattei, et al. (1993). "Myelin/oligodendrocyte glycoprotein is a member of a subset of the immunoglobulin superfamily encoded within the major histocompatibility complex." Proc. Natl. Acad. Sci. USA 90: 7990-7994.

Philbrick, W. M., R. G. Palfree, et al. (1990). "The CD59 antigen is a strcuctural homologue of murine Ly-6 antigens but lacks interferon inducibility." European Journal of Immunology 20(1): 87-92.

Piddlesden, S. J., S. Jiang, et al. (1996). "Soluble complement receptor 1 (sCR1) protects against experimental autoimmune myasthenia gravis." Journal of Neuroimmunology 71: 173-177.

Piddlesden, S. J., M. K. Storch, et al. (1994). "Soluble recombinant complement receptor 1 inhibits inflammation and demyelination in antibody-mediated demyelinating experimental allergic encephalomyelitis." Journal of Immunology 152(11): 5477-5484.

Pilartz, M., T. Jess, et al. (2002). "Adoptive transfer experimental allergic neuritis in newborn Lewis rats results in inflammatory infiltrates, mast cell activation and increased Ia expression with only minor nerve fibre degeneration." Acta Neuropathol (Berl) 104(5): 513-524.

Pillemer, L., L. Blum, et al. (1954). "The properdin system and immunity. I. Demonstration of a new serum protein, properdin, and its role in immune phenomena." Science 120: 279-285.

Plomp, J. J., P. C. Molenaar, et al. (1999). "Miller Fisher anti-GQ1b antibodies: alpha-latrotoxin-like effects on motor end plates." Annual Neurology 45: 189-199.

Post, T. W., M. K. Liszewski, et al. (1991). "Membrane cofactor protein of the complement system: Alternative splicing of serine/threonine/proline-rich

isoforms that correlate with protein phenotype." Journal of Experimental Medicine 174: 93-102.

Poulas, K., T. Tsouloufis, et al. (2000). "Treatment of passively transferred experimental autoimmune myasthenia gravis using papain." Clin. Exp. Immunol. 120: 363-368.

Powell, M. B., K. J. Marchbank, et al. (1997). "Molecular cloning, chromosomal localisation and functional characterisation of the mouse analogue of human CD59." Journal of Immunology 158(4): 1692-702.

Preissner, K. T., E. R. Podack, et al. (1985). "The membrane attack complex of complement: relation of C7 to the metastable membrane binding site of the intermediate complex C5b-7." Journal of Immunology 135(1): 445-451.

Prineas, J. W. (1972). "Acute idiopathic polyneuritis: an electron microscope study." Lab Investig 26: 133-147.

Prineas, J. W. (1981). "Pathology of the Guillain-Barre syndrome." Annual Neurology 9(suppl): S6-S19.

Pruitt, S. K. and R. R. Bollinger (1991). "The effect of soluble complement receptor type 1 on hyperacute allograft rejection." J Surg Res 50(4): 350-355.

Qian, Y. M., X. Qin, et al. (2000). "Identification and functional characterisation of a new gene encoding the mouse terminal pathway complement inhibitor CD59." Journal of Immunology 165: 2528.

Qin, X., N. Krumrei, et al. (2003). "Deficiency of the mouse complement regulatory protein mCd59b results in spontaneous hemolytic anemia with platelet activation and progressive male infertility." Immunity 18: 217-227.

Qin, X., T. Miwa, et al. (2001). "Genomic structure, functional comparison, and tissue distribution of mouse Cd59a and Cd59b." Mammalian Genome 12: 582-589.

Quigg, R. J., M. L. Galishoff, et al. (1993). "Isolation and characterisation of complement receptor type 1 from rat glomerular epithelial cells." Kidney International 43(3): 730-736.

Quigg, R. J. and V. M. Holers (1995). "Characterisation of rat complement receptors and regulatory proteins. CR2 and Crry are conserved, and the C3b receptor of neutrophils and platelets is distinct from CR1." Journal of Immunology 155(3): 1481-1488.

Quigg, R. J., C. F. Lo, et al. (1995). "Molecular characterisation of rat Crry: widespread distribution of two alternative forms of Crry mRNA." Immunogenetics 42(5): 362-7.

Rai, M. and H. Padh (2001). "Expression systems for production of heterologous proteins." Current Science 80(9): 1121-1128.

Rangan, G. K., J. W. Pippin, et al. (2004). "C5b-9 regulates peritubular myofibroblast accumulation in experimental focal segmental glomerulosclerosis." Kidney International 66(5): 1838-1848.

Ratnoff, O. D. and I. Lepow, H. (1957). "Some properties of an esterase derived from preparations of the first component of complement." Journal of Experimental Medicine 106(2): 327-343.

Romi, F., E. K. Kristoffersen, et al. (2005). "The role of complement in myasthenia gravis: serological evidence of complement consumption in vivo." Journal of Neuroimmunology 58(1-2): 191-194.

Romi, F., G. O. Skeie, et al. (2005). "Striational antibodies in myasthenia gravis: reactivity and possible clinical significance." Arch Neurol 62(3): 442-446.

Romi, F., G. O. Skeie, et al. (2000). "Complement activation by titin and ryanodine receptor autoantibodies in myasthenia gravis. A study of IgG

subclasses and clinical correlations." Journal of Neuroimmunology 111(1-2): 169-176.

Rosenbluth, J. and D. Moon (2003). "Dysmyelination induced in vitro by IgM antisulphatide and antigalactocerebroside monoclonal antibodies." Journal of Neuroscience Research 71(1): 104-109.

Rostami, A., J. B. Burns, et al. (1985). "Transfer of experimental allergic neuritis with P2-specific T cell lines." Cell Immunology 91(2): 354-361.

Rostami, A. and S. K. Gregorian (1991). "Peptide 53-78 of myelin P2 protein is a T cell epitope for the induction of experimental autoimmune neuritis." Cell Immunology 132(2): 433-441.

Rowan, W. C., G. Hale, et al. (1995). "Cross-linking of the CAMPATH-1 antigen (CD52) triggers activation of normal human T lymphocytes." International Immunology 7(1): 69-77.

Rushmere, N. K., R. Harrison, et al. (1994). "Molecular cloning of the rat analogue of human CD59: structural comparison with human CD59 and identification of a putative active site." Biochemical Journal 304: 595-601.

Rushmere, N. K., S. Tomlinson, et al. (1997). "Expression of rat CD59: functional analysis confirms a lack of species selectivity and reveals that glycosylation is not required for function." Immunology 90(4): 640-646.

Sahashi, K., A. G. Engel, et al. (1980). "Ultrastructural localisation of the terminal and lytic ninth compliment component (C9) at the motor endplate in myasthenia gravis." Journal of Neuropathology & Experimental Neurology 39(2): 160-172.

Sahashi, K., A. G. Engel, et al. (1978). "Ultrastructural localisation of immune complexes (IgG and C3) at the endplate in experimental autoimmune myasthenia gravis." Journal of Neuropathology & Experimental Neurology 37(2): 212-223.

Sakurada, C., H. Seno, et al. (1994). "Molecular cloning of rat complement regulatory protein, 5I2 antigen." Biochemical and Biophysical Research Communications 198(3): 819-26.

Sanders, M. E., C. L. Koski, et al. (1986). "Activated terminal complement in cerebrospinal fluid in Guillain-Barre syndrome and multiple sclerosis." Journal of Immunology 136: 4456-4459.

Sawada, R., K. Ohashi, et al. (1990). "Isolation and expression of the full length cDNA encoding CD59 antigen of human lymphocytes." DNA Cell Biology 9(3): 213-220.

Sawant-Mane, S., S. J. Piddlesden, et al. (1996). "CD59 homologue regulates complement-dependent cytolysis of rat Schwann cells." Journal of Neuroimmunology 69: 63-71.

Schlaf, G., E. Rothermel, et al. (1999). "Rat complement factor I: molecular cloning, sequencing and expression in tossues and isolated cells." Immunology 98(3): 464-474.

Schmid, C. D., M. Stienekemeier, et al. (2000). "Immune deficiency in mouse models for inherited peripheral neuropathies leads to improved myelin maintenance." Journal of Neuroscience 20(2): 729-35.

Schnaitman, C. A. (1971). "Effect of ethylenediaminetetraacetic acid, Triton X-100, and lysozyme on the morphology and chemical composition of isolate cell walls of Escherichia coli." Journal of Bacteriology 108(1): 553-563.

Schonbeck, S., F. Padberg, et al. (1992). "Transplantation of thymic autoimmune microenvironment to severe combined immunodeficiency mice." Journal of Clinical Investigation 90: 245-250.

Sereda, M., I. Griffiths, et al. (1996). "A transgenic model of Charcot-Marie-Tooth disease." Neuron 16(5): 1049-1060.

Seya, T., M. Okada, et al. (1990). "Regulation of proteolytic activity of complement factor I by pH: C3b/C4b receptor (CR1) and membrane cofactor protein (MCP) have different pH optima for factor I-mediated cleavage of C3b." Journal Biochem (Tokyo) 107(2): 310-315.

Shapiro, L., J. P. Doyle, et al. (1996). "Crystal structure of the extracellular domain from PO, the major structural protein of peripheral nerve myelin." Neuron 17: 435-449.

Smith, M. E., L. S. Forno, et al. (1979). "Experimental Allergic Neuritis in the Lewis rat." Journal of Neuropathology & Experimental Neurology 38(4): 377-391.

Snipes, G. J., U. Suter, et al. (1993). "Human peripheral myelin protein-22 carries the L2/HNK-1 carbohydrate adhesion epitope." Journal of Neurochemistry 61: 1961-4.

Snipes, G. J., U. Suter, et al. (1992). "Characterisation of a novel peripheral nervous system myelin protein (PMP-22/SR13)." Journal of Cell Biology 117: 225-38.

Spies, J. M., J. D. Pollard, et al. (1995). "Synergy between antibody and P2-reactive T cells in experimental allergic neuritis." Journal of Neuroimmunology 57(1-2): 77-84.

Stanley, K. K. (1989). "The molecular mechanism of complement C9 insertion and polymerisation in biological membranes." Curr Top Microbiol Immunol 140: 49-65.

Stoll, G., B. Schmidt, et al. (1991). "Presence of the terminal complement complex (C5b-9) precedes myelin degradation in immune-mediated demyelination of the rat peripheral nervous system." Annual Neurology 30: 147-155.

Storch, M. K., S. J. Piddlesden, et al. (1998). "Multiple sclerosis: in situ evidence for antibody- and complement-mediated demyelination." Ann. Neurol 43(4): 465-471.

Suzuki, M., K. Kitamura, et al. (1980). "Neuritogenic activity of peripheral nerve myelin proteins in Lewis rats." Neuroscience Letters 19(3): 353-358.

Takisawa, H., N. Okada, et al. (1994). "Complement inhibitor of rat cell membrane resembling mouse Crry/p65." Journal of Immunology 152(6): 3032-8.

Tamura, N., A. Shimada, et al. (1972). "Further evidence for immune cytolysis by antibody and the first eight components of complement." Immunology 22: 131-140.

Taylor, W. A. and R. A. Hughes (1985). "Experimental Allergic Neuritis induced in SJL mice by bovine P2." Journal of Neuroimmunology 8(2-3): 153-7.

Tenner, A. J. and D. B. Volkin (1986). "Complement subcomponent C1q secreted by cultured human monocytes has subunit structure identical to that serum C1q." Biochemical Journal 233: 451-458.

Thiel, S., T. Vorup-Jensen, et al. (1997). "A second serine protease associated with mannan-binding lectin that activates complement." Nature 386(6624): 506-510.

Timmerman, J. J., M. F. Beersma, et al. (1997). "Differential effects of cytomegalovirus infection on complement synthesis by human mesangial cells." Clin. Exp. Immunol. 109(3): 518-525.

Timmerman, J. J., M. G. A. Van Dixhoorn, et al. (1997). "Complement C6 and C2 biosynthesis in syngeneic PVG/c- and PVG/c+ rat strainsq." Scandinavian Journal of Immunology 46(4): 366-372.

Tomozawa, Y. and N. Sueoka (1978). "In vitro segregation of different cell lines with neuronal and glial properties from a stem cell line of rat neurotumour RT4." Proc. Natl. Acad. Sci. USA 75(12): 6305-6309.

Toyka, K. V., D. B. Drachman, et al. (1977). "Myasthenia gravis. Study of humoral immune mechanisms by passive transfer to mice." New England Journal of Medicine 296(3): 125-131.

Toyka, K. V., D. B. Drachman, et al. (1975). "Myasthenia gravis: passive transfer from man to mouse." Science 190: 397-399.

Trapp, B. D., M. Dubois-Dalcq, et al. (1984). "Ultrastructural localisation of P2 protein in actively myelinating rat Schwann cells." Journal of Neurochemistry 43: 944-48.

Tsiftsoglou, S. A., A. C. Willis, et al. (2005). "The catalytically active serine protease domain of human complement factor I." Biochemistry 44(16): 6239-6249.

Tsujihata, M., A. Satoh, et al. (2003). "Effect of myasthenic immunoglobulin G on motor end-plate morphology." Journal of Neurology 250: 75-82.

Tsujihata, M., T. Yoshimura, et al. (1989). "Diagnostic significance of IgG, C3 and C9 at the limb muscle motor end-plate in minimal myasthenia gravis." Neurology 39(10): 1359-1363.

Tsumoto, K., D. Ejima, et al. (2003). "Practical considerations in refolding proteins from inclusion bodies." Protein Expression and Purification 28: 1-8.

Turnberg, D., M. Botto, et al. (2003). "CD59a deficiency exacerbates accelerated nephrotoxic nephritis in mice." Journal od American Society Nephrology 14(9): 2411-2413.

Tuzun, E., B. J. Scott, et al. (2003). "Genetic evidence for involvement of classical complement pathway in induction of experimental autoimmune myasthenia gravis." Journal of Immunology 171: 3847-3854.

Tzartos, S. J., S. Hochschwender, et al. (1987). "Passive transfer of experimental autoimmune myasthenia gravis by monoclonal antibodies to the main immunogenic region of the acetylcholine receptor." Journal of Neuroimmunology 15(2): 185-194.

Tzartos, S. J., D. Rand, et al. (1981). "Mapping of surface structures of Electrophorus acetylcholine receptor using monoclonal antibodies." Journal of Biological Chemistry 256(16): 8635-8645.

Valentijn, L. J., P. A. Bolhuis, et al. (1992). "The peripheral myelin gene PMP-22/GAS-3 is duplicated in Charcot-Marie-Tooth disease type 1A." Nature Genetics 1(3): 166-170.

Vanguri, P., C. L. Koski, et al. (1982). "Complement activation by isolated myelin: Activation of the classical pathway in the absence of myelin-specific antibodies." Proc. Natl. Acad. Sci. USA 79: 3290-94.

Vedeler, C. A. (2000). "Inflammatory neuropathies: update." Current Opinion in Neurology 13: 305-309.

Vedeler, C. A., G. Conti, et al. (1999). "The expression of CD59 in experimental allergic neuritis." Journal of Neurological Sciences 165: 154-159.

Vedeler, C. A., N. E. Gilhus, et al. (1990). "Expression of complement C3b/C4b receptors (CR1) on erythrocytes from patients with myasthenia gravis." Acta Neurol Scand 82(4): 259-262.

Vedeler, C. A. and R. Matre (1988). "Complement receptors CR1 on human peripheral nerve fibres." Journal of Neuroimmunology 17: 315-322.

Vedeler, C. A., R. Matre, et al. (1989). "Isolation and characterisation of complement receptors CR1 from human peripheral nerve." Journal of Neuroimmunology 23: 215-221.

Vedeler, C. A., E. Ulvestad, et al. (1994). "The expression of CD59 in normal human nervous tissue." Immunology 82: 542-547.

Vedeler, C. A., E. Wik, et al. (1997). "The long-term prognosis of Guillain-Barre syndrome. Evaluation of prognostic factors including plasma exchange." Acta Neurol Scand 95(5): 298-302.

Vik, D. P., P. Munoz-Canoves, et al. (1990). "Identification and sequence analysis of four complement factor H-related transcripts in mouse liver." Journal of Biological Chemistry 265(6): 3193-3201.

Vincent, A., J. McConville, et al. (2004). "Seronegative myasthenia gravis." Seminars in Neurology 24(1): 125-133.

Vincent, A., J. Palace, et al. (2001). "Myasthenia gravis." The Lancet 357: 2122-2128.

Vincent, A. and N. Willcox (1999). "The role of T cells in the initiation of autoantibody responses in thymoma patients." Pathol Res Pract 195(8): 535-540.

Visser, L., A. F. de Vos, et al. (2002). "Expression of the EGF-TM7 receptor CD97 and its ligand CD55 (DAF) in multiple sclerosis." Journal of Neuroimmunology 132: 156-163.

Volanakis, J. E., R. E. Schrohenloher, et al. (1977). "Human Factor D of the alternative complement pathway: purification and characterisation." Journal of Immunology 119(1): 337-342.

von Budingen, H. C., S. L. Hauser, et al. (2004). "Epitope recognition on the myelin/oligodendrocyte glycoprotein differentially influences disease phenotype and antibody effector functions in autoimmune demyelination." European Journal of Immunology 34: 2072-2083.

Voshol, H., C. W. E. M. van Zuylen, et al. (1996). "Structure of the HNK-1 carbohydrate epitope on bovine peripheral myelin glycoprotein PO." The Journal of Biological Chemistry 271(38): 22957-22960.

Vrisendorp, F. J. (1997). "Insights into Campylobacter jejuni-induced Guillain-Barre Syndrome from the Lewis rat model of Experimental Allergic Neuritis." Journal of Infectious Diseases 176(Suppl 2): S164-8.

Vrisendorp, F. J., R. E. Flynn, et al. (1998). "Systemic complement depletion reduces inflammation and demyelination in adoptive transfer experimental allergic neuritis." Acta Neuropathol 95: 297-301.

Vrisendorp, F. J., R. E. Flynn, et al. (1997). "Soluble complement receptor 1 (sCR1) is not as effective as cobra venom factor in the treatment of experimental allergic neuritis." International Journal of Neuroscience 92(3-4): 287-298.

Vrisendorp, F. J., R. E. Flynn, et al. (1995). "Complement depletion affects demyelination and inflammation in experimental allergic neuritis." Journal of Neuroimmunology 58: 157-165.

Waksman, B. H. and R. D. Adams (1955). "Allergic neuritis: an experimental disease of rabbits induced by the injection of peripheral nervous tissue and adjuvants." Journal of Experimental Medicine 102: 213-236.

Walport, M. J. (2001). "Complement: First of two parts." New England Journal of Medicine 344(14): 1058-1066.

Wanschitz, J., H. Maier, et al. (2003). "Distinct time pattern of complement activation and cytotoxic T cell response in Guillain-Barre Syndrome." Brain 126(9): 2034-42.

Warner, L. E., M. J. Hilz, et al. (1996). "Clinical phenotypes of different MPZ (PO) mutations may include Charcot-Marie-Tooth type 1B, Dejerine-Sottas and congenital hypomyelination." Neuron 17(3): 451-460.

Watling, K. J. (1998). The RBI Handbook of Receptor Classification and Signal Transduction, RBI.

Watts, M. J., J. R. Dankerts, et al. (1990). "Isolation and characterisation of a membrane attck complex inhibting protein present in human serum and other biological fluids." Biochemical Journal 265: 471-477.

Weishaupt, A., G. Giegerich, et al. (1995). "T cell antigenic and neuritogenic activity of recombinant human peripheral myelin P2 protein." Journal of Neuroimmunology 63(2): 149-156.

Wells, C. A., R. A. Saavedra, et al. (1993). "Myelin PO glycoprotein: Predicted structure and interactions of extracellular domain." Journal of Neurochemistry 61(6): 1987-95.

Wong, W. W. (1990). "Structural and functional correlation of the human complement receptor type 1." J Invest Dermatol 94(6 Suppl): 64S-67S.

Wong, W. W. and D. T. Fearon (1985). "p65: a C3b-binding protein on murine cells that shares antigenic determinants with the human C3b receptor (CR1) and is distinct from murine C3b receptor." Journal of Immunology 134(6): 4048-56.

Wylam, M. E., P. M. Anderson, et al. (2003). "Successful treatment of refractory myasthenia gravis using rituximab: a paediatric case report." Journal of Pediatrics 143(5): 674-677.

Xu, C. and D. Mao (2000). "A critical role for murine complement regulator Crry in fetomaternal tolerance." Science 287: 498-501.

Yamashina, M. E., T. Ueda, et al. (1990). "Inherited complete deficiency of 20 kilodalton homologous restriction factor (CD59) as a cause of paroxysmal nocturnal haemoglobinuria." New England Journal of Medicine 323: 1184-

Yan, W. X., J. J. Archelos, et al. (2001). "PO protein is a target antigen in chronic inflammatory demyelinating polyradiculoneuropathy." Ann. Neurol 50(3).

Yeh, C. G., H. C. J. Marsh, et al. (1991). "Recombinant soluble human complement receptor type 1 inhibits inflammation in the reversed passive arthus reaction in rats." Journal of Immunology 146(1): 250-256.

Yokoyama, I. and F. Waxman (1994). "Differential susceptibility of immune complexes to release from the erythrocyte CR1 receptor by Factor I." Molecular Immunology 31(3): 227-240.

Yoon, S. H. and D. T. Fearon (1985). "Characterisation of a soluble form of the C3b/C4b receptor (CR1) in human plasma." Journal of Immunology 134(5): 3332-3338.

Young, B. and J. W. Heath (2000). Wheater's Functional Histology, Churchill Livingstone, An imprint of Harcourt Publisher's Limited.

Young, J. D. E., C. C. Liu, et al. (1986). "The pore forming protein (perforin) of cytolytic T lymphocytes is immunologically related to the components of membrane attack complex of complement through cysteine-rich domains." Journal of Experimental Medicine 164: 2077-2082.

Yu, S., R. S. Duan, et al. (2004). "Increased susceptibility to experimental autoimmune neuritis after upregulation of the autoreactive T cell response to peripheral myelin antigen in apolipoprotein E-deficient mice." Journal of Neuropathology & Experimental Neurology 63(2): 120-128.

Yuki, N. (1997). "Molecular mimicry between gangliosides and lipopolysaccharides of Campylobacter jejuni from patiemts with Guillain Barre Syndrome and Miller Fisher Syndrome." Journal of Infectious Diseases 176(Suppl 2): S150-3.

Yuki, N., M. Yamada, et al. (2001). "Animal model of axonal Guillan Barre syndrome induced by sensitisation with GM1 ganglioside." Annals of Neurology 49(6): 712-20.

Zanazzi, G., S. Einheber, et al. (2001). "Glial growth factor/neurogulin inhibits Schwann cell myelination and induces demyelination." Journal of Cell Biology 152(6): 1289-1299.

Zhang, G., P. H. Lopez, et al. (2004). "Anti-ganglioside antibody-mediated neuronal cytotoxicity and its protection by intravenous immunoglobulin: implications for immune neuropathies." Brain 127(5): 1085-100.

Zhang, H. F., S. Lu, et al. (2001). "Targeting of functional antibody decay-accelerating factor fusion proteins to a cell surface." Journal of Biological Chemistry 276(29): 27290-27295.

Zheng, X., T. L. Saunders, et al. (1995). "Vitronectin is not essential for normal mammalian development and fertility." Proc. Natl. Acad. Sci. USA 92(26): 12426-12430.

Zhu, J., H. Link, et al. (1994). "The B cell repertoire in experimental allergic neuritis involves multiple myelin proteins and GM1." Journal of Neurological Science 125(2): 132-137.

Zhu, J., I. Nennesmo, et al. (1999). "Induction of experimental autoimmune neuritis in CD4-8-C57BL/6J mice." Journal of Neuroimmunology 94(1-2): 196-203.

Zhu, J., S. H. Pelidou, et al. (2001). "P0 glycoprotein peptides 56-71 and 180-199 dose-dependently induce acute and chronic experimental autoimmune neuritis in Lewis rats associated with epitope spreading." Journal of Neuroimmunology 114(1-2): 99-106.

Zhu, J., L. Zou, et al. (2001). "Cytotoxic T lymphocyte-associated antigen 4 (CTLA-4) blockade enhances incidence and severity of experimental autoimmune neuritis in resistant mice." Journal of Neuroimmunology 115(1-2): 111-7.

Zhu, Y., L. Bao, et al. (2002). "CD4 and CD8 T cells, but not B cells, are critical to the control of murine experimental autoimmune neuritis." Experimental Neurology 177(1): 314-320.

Zhu, Y., H. G. Ljunggren, et al. (2001). "Suppression of autoimmune neuritis in IFN-gamma receptor-deficient mice." Experimental Neurology 169(2): 472-478.

Ziccardi, R. J., B. Dahlback, et al. (1984). "Characterisation of the interaction of human C4b-binding protein with physiological ligands." Journal of Biological Chemistry 259(22): 13674-13679.

Zoidl, G., S. Blass-Kampmann, et al. (1995). "Retroviral-mediated gene transfer of the peripheral myelin protein PMP22 in Schwann cells: modulation of cell growth." EMBO 14: 1122-8.

Zou, L. I., H. G. Ljunggren, et al. (2000). "P0 protein peptide 180-199 together with pertussis toxin induces experimental autoimmune neuritis in resistant C57BL/6 mice." Journal of Neuroscience Research 62: 717-721.